REPORT UAG - 28

PART III

WORLD DATA CENTER A
for
Solar-Terrestrial Physics

COLLECTED DATA REPORTS
ON
AUGUST 1972 SOLAR - TERRESTRIAL EVENTS

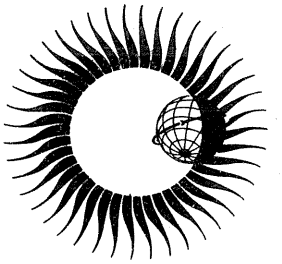

JULY 1973

WORLD DATA CENTER A

National Academy of Sciences
2101 Constitution Avenue, N. W. Washington, D. C. U.S.A., 20418

World Data Center A consists of the Coordination Office

and eight subcenters:

World Data Center A
Coordination Office
National Academy of Sciences
2101 Constitution Avenue, N.W.
Washington, D. C., U.S.A. 20418
Telephone (202) 961-1478

Solar and Interplanetary Phenomena, Ionospheric Phenomena, Flare-Associated Events, Geomagnetic Variations, Magnetospheric and Interplanetary Magnetic Phenomena, Aurora, Cosmic Rays, Airglow:
World Data Center A
for Solar-Terrestrial Physics
National Oceanic and Atmospheric Administration
Boulder, Colorado, U.S.A. 80302
Telephone (303) 499-1000 Ext. 6467

Geomagnetism, Seismology, Gravity (and Upper Mantle Project Archives):
World Data Center A:
Geomagnetism, Seismology and Gravity
Environmental Data Service, NOAA
Boulder, Colorado, U.S.A. 80302
Telephone (303) 499-1000 Ext. 6311

Glaciology:
World Data Center A:
Glaciology
U. S. Geological Survey
1305 Tacoma Avenue South
Tacoma, Washington, U.S.A. 98402
Telephone (206) 383-2861 Ext. 318

Longitude and Latitude:
World Data Center A:
Longitude and Latitude
U. S. Naval Observatory
Washington, D. C., U.S.A. 20390
Telephone (202) 698-8422

Meteorology (and Nuclear Radiation):
World Data Center A:
Meteorology
National Climatic Center
Federal Building
Asheville, North Carolina, U.S.A. 28801
Telephone (704) 254-0961

Oceanography:
World Data Center A:
Oceanography
National Oceanic and Atmospheric Administration
Rockville, Maryland, U.S.A. 20852
Telephone (202) 426-9052

Rockets and Satellites:
World Data Center A:
Rockets and Satellites
Goddard Space Flight Center
Code 601
Greenbelt, Maryland, U.S.A. 20771
Telephone (301) 982-6695

Tsunami:
World Data Center A:
Tsunami
National Oceanic and Atmospheric Administration
P.O. Box 3887
Honolulu, Hawaii, U.S.A. 96812
Telephone (808) 546-5698

Notes:

(1) World Data Centers conduct international exchange of geophysical observations in accordance with the principles set forth by the International Council of Scientific Unions. WDC-A is established in the United States under the auspices of the National Academy of Sciences.
(2) Communications regarding data interchange matters in general and World Data Center A as a whole should be addressed to: World Data Center A, Coordination Office (see address above).
(3) Inquiries and communications concerning data in specific disciplines should be addressed to the appropriate subcenter listed above.

WORLD DATA CENTER A
for
Solar-Terrestrial Physics

REPORT UAG - 28 PART III

COLLECTED DATA REPORTS
ON
AUGUST 1972 SOLAR - TERRESTRIAL EVENTS

Helen E. Coffey, Editor

WDC-A for Solar - Terrestrial Physics

Boulder, Colorado U.S.A.

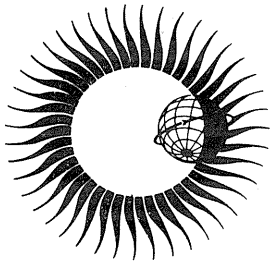

Prepared by World Data Center A for
Solar-Terrestrial Physics, NOAA, Boulder, Colorado
and published by

U.S. DEPARTMENT OF COMMERCE
NATIONAL OCEANIC AND ATMOSPHERIC ADMINISTRATION

ENVIRONMENTAL DATA SERVICE
Asheville, North Carolina, USA 28801

July 1973

SUBSCRIPTION PRICE: $9.00 a year; $2.50 additional for foreign mailing; single copy price varies.* Checks and money orders should be made payable to the Department of Commerce, NOAA. Remittance and correspondence regarding subscriptions should be sent to the National Climatic Center, Federal Building, Asheville, NC 28801, Attn: Publications.

*PRICE THIS ISSUE $1.50

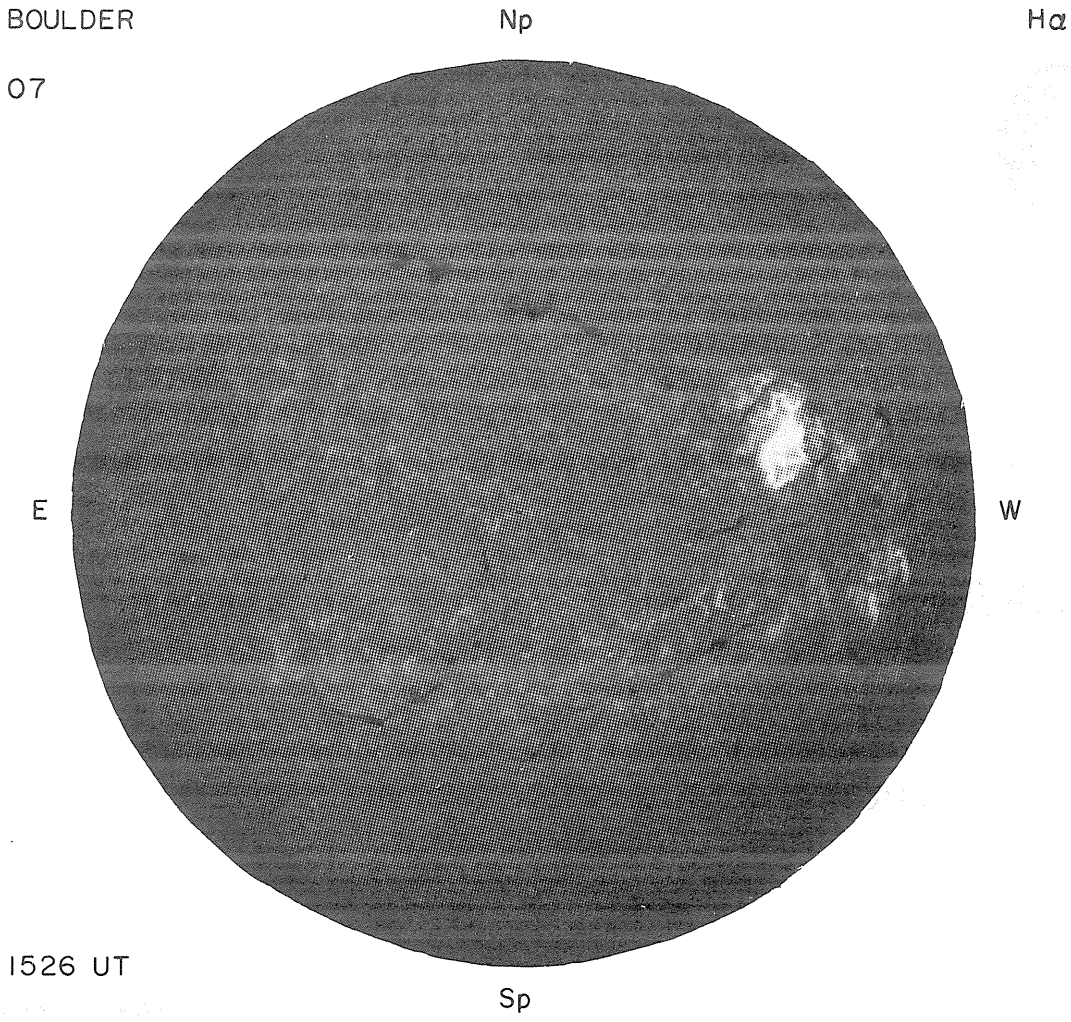

FLARE OF 07 AUGUST 1972

SUMMARY TABLE OF CONTENTS

PART I

FOREWORD

1. SUMMARIES OF AUGUST 1972 EVENTS
2. SOLAR OPTICAL DATA
3. SOLAR RADIO DATA

PART II

4. SPACE OBSERVATIONS
5. COSMIC RAYS
6. IONOSPHERE

PART III

6. IONOSPHERE (continued)
7. GEOMAGNETISM
8. AERONOMY AND MISCELLANEOUS

APPENDIX I: Miscellaneous Data and Information from WDC-A
APPENDIX II: Other References
APPENDIX III: Explanation of Solar Radio Chart and Table

ALPHABETICAL INDEX

AUTHOR INDEX

TABLE OF CONTENTS FOR PART III

	Page
6. IONOSPHERE (continued)	587
"Ionospheric and Whistler Activity Observed at the Panská Ves and Průhonice Observatories, 26 July - 14 August 1972" (F. Jiricek, J. Lastovicka and P. Triska)	588
"SCL and SEA Associated with Solar Events July 29 to August 10, 1972" (S. N. Mitra)	595
"Midlatitude D-region Response to the August 2, 1972 Event" (Ward J. Helms)	601
"Ionizing Radiation and After Effects of Solar Proton Flares on August 4 and 7, 1972" (G. T. Nestorov and E. M. Apostolov)	603
"Ionospheric Observations at Kiruna during July 26 - August 14, 1972" (H. Borg and R. Lundin)	609
"Effects of the Solar Activity in August 1972 on the Circuit Kalundborg - Lindau (245 kHz, 456 km)" (Chr. Timpe)	616
"Corpuscular Effects in the Night Ionosphere during the Period July 26 - August 14, 1972" (P. Velinov and G. Nestorov)	618
"Simultaneous Measurement of LF Wave Intensities and Phase at Hiraiso" (N. Wakai, C. Ouchi and S. Fujii)	622
"Effects on Transequatorial VLF Propagation for Retrospective World Interval July 26 - August 14, 1972" (Y. Sahai and M. A. O. Sales)	627
"Measurements at the AFCRL Geopole Observatory during August 1972" (S. M. Silverman, R. F. K. Krassa and J. P. Turtle)	630
"The Retrospective World Interval July 26 to August 14, 1972 as Observed at the RWC Darmstadt (FTZ)" (B. Beckmann, R. Eyfrig, P. Suessmann and H. Wegener)	635
"HF Radio Propagation Disturbances August 1-9, 1972" (Rikio Maeda)	640
"14 MHz Fieldstrength Observations on the Transequatorial Path Tsumeb/ S.W. Africa - Lindau (Darmstadt)/W. Germany" (R. Eyfrig and J. Röttger)	643
"Events of July 26 - August 14, 1972 as Recorded by the A_3-Type Absorption in the Lower Ionosphere" (Syed Ziauddin)	645
"Polar Cap Absorption Event of 3-10 August, 1972 by the Riometer Data" (V. M. Driatsky and V. A. Ulyev)	647
"Ground Based Ionospheric Observations from the Danish Geophysical Observatories in Greenland during the Period August 1-16, 1972" (J. Taagholt, P. Stauning and V. Neble Jensen)	651
"Polar Riometer Observations during August 1972" (Raymond J. Cormier)	666
"Polar Cap Disturbances of August 1972 Observed on Transpolar VLF Phase Measurements" (Y. Hakura, T. Ishii, T. Asakura and Y. Terajima)	668
"Polar Observations during the August 1972 Solar Cosmic Ray Events" (A. J. Masley and M. B. Baker)	672
"Characteristics of the August 1972 Solar Particle Events as Observed Over the Earth's Polar Caps" (J. B. Reagan, W. L. Imhof and V. F. Moughan)	676
"VLF Observations at Halley Bay, August 1972" (W. R. Piggott and T. W. Thomas)	684
7. GEOMAGNETISM	685
"Auroral Electrojet Indices for August 1972" (J. H. Allen, C. A. Abston and L. D. Morris)	686
"Hourly Equatorial Dst Values (Provisional)" (M. Sugiura and D. J. Poros)	699
"Geomagnetic Disturbances of August 4-9, 1972" (K. Kawasaki, Y. Kamide, F. Yasuhara and S.-I. Akasofu)	702
"On the Geo-Activity of the Solar Flares of 2, 4, 7 and 11 August 1972" (I. N. Odintsova, L. N. Leshchenko, K. N. Vasiliev and G. V. Givishvili)	708

Page

7. GEOMAGNETISM (continued)

"Report on the Geomagnetic and Ionospheric Changes Recorded At Ahmedabad during the August 1972 Events" (S. S. Degaonkar, T. S. G. Sastry and R. G. Rastogi) 717
"The Development of Current Vortices in the Polar Cap Preceding the Large Magnetic Storms of August 4-5 and August 9, 1972" (E. I. Loomer and G. Jansen van Beek) 722
"Normal Magnetic Field, Micropulsation and Riometer Observations at Auroral Station Murmansk" (B. E. Brunelli, G. A. Loginov, G. A. Petrova and L. T. Afanasyeva) 727
"Morphological Classification of a Geomagnetically Disturbed Period in the Retrospective World Interval 26 July - 14 August 1972 Carried Out Using the Standard Magnetograms of the Budkov Observatory" (Jaroslav Halenka) 731
"On the Magnetospheric Storm of August 1972" (M. Bossolasco, A. Elena and A. Caneva) 733
"Substorm Components of the Geomagnetic Storms 4 - 9 August 1972" (E. Selzer and J. Roquet) 737
"Low Latitude Observations of the Geomagnetic Field for the Retrospective World Interval July 26 - August 14, 1972" (B. N. Bhargava) 743
"Total Magnetic Field Variation at Thumba during 3 - 10 August 1972" (P. D. Agarwal) 744
"The Behavior of the Geomagnetic Pulsations during Two Magnetic Storms of August 1-10, 1972" (O. V. Bolshakova, A. L. Kalisher, E. T. Matveyeva and R. V. Shchepetnov) 745
"Spectral Structure of Storm-Associated Geomagnetic Pulsations Observed at Onagawa during the Period of August 4-11, 1972" (Takao Saito, Tohru Sakurai, Minoru Kondo, Tadyoshi Tamura and Masaei Abe) 747
"Storms between August 4 and 11, 1972" (Bohumila Bednářová-Nováková) 752
"Discussion of the Geomagnetic Data Recorded at Hyderabad, India during July 26 - August 14, 1972" (B. J. Srivastava) 754
"On the Giant Pulsations of the 04-06 August 1972 Geomagnetic Storm Observed at Manila" (J. E. Salcedo) 762
"Observations of Storm-Associated Pc5 Magnetic Oscillations at the Geosynchronous Orbit: August 9, 1972" (Joseph N. Barfield) 764
"Southern Polar Region Micropulsation Activity Associated with the 11976 Event" (H. Robert Willard, Ward J. Helms and Harold B. Liemohn) 766
"Magnetic Micropulsations Observed at Several Ground Stations August 3 - 14, 1972" (R. R. Heacock, V. P. Hessler, M. Kivinen, J. S. Reid and J. K. Olesen) 772
"Observations of Geomagnetic Micropulsations at a Midlatitude Station" (J. W. Münch) 780

8. AERONOMY AND MISCELLANEOUS 783

"Atmospheric Densities at Heights between 300 and 900 km Obtained from the Drag of Five Satellites during the Interval 22 July to 16 August 1972" (L. G. Jacchia and J. W. Slowey) 784
"Discontinuous Change in the Terrestrial Length of Day After Great Solar Flare of August 1972" (S. H. Plagemann and J. Gribbin) 792
"Photometric Observations of Mid-Latitude Aurora during the August 1972 Solar-Geophysical Event" (E. G. Mullen and D. J. Davis, Jr.) 795
"Aurora Backscatter Observations from August 3 to August 10, 1972" (P. Czechowsky) 796
"Simultaneous Pulsations in Radio Aurora, Magnetic Field, and Absorption Observed during the August 1972 Storms" (J. G. Keys) 799

TABLE OF CONTENTS FOR PART III (continued)

Page

8. AERONOMY AND MISCELLANEOUS (continued)

"Ground-Based Measurements of the 6300A OI Airglow Intensity and Temperature during Period 4-14 August 1972" 802
(R. E. Smith and G. R. Swenson)
"Airglow Observations from Southern Africa during the Interval 4 August - 7 August 1972" 805
(E. H. Carman and M. P. Heeran)
"Atmospheric Electric Data during August 4th - 12th, 1972" 809
(R. Muhleisen and R. Reiter)
*"Recurrence of the Solar Corpuscular Events" 811
(Maria Torelli)

NOTE: Three additional contributions were received for this compilation. They are given here only by title because there was not time for interaction between the editors and authors to clarify some points. The papers are deposited in WDC-A archives.

"Geophysical Effects on Pupal Weights on An Insect during Retrospective World Interval July 26 - August 14, 1972"
(Howard W. Smith, Department of Entomology, University of Idaho, Moscow, Idaho, U.S.A.)
"Unusual Magnetic Activity during 4-10 August 1972 and Some of Its Biological Consequences"
(B. J. Srivastava and D. S. Bhaskara Rao, National Geophysical Reseach Institute, Hyderabad-500007, India)
"Solar-Induced Effects on the Lower Troposphere as Observed in Early August 1972"
(Nicholas L. Rosner, New York, New York U.S.A.)

APPENDIX I. Miscellaneous Data and Information from WDC-A.

1. Reprint of Table of Contents and Introduction for UAG-21 ("Preliminary Compilation of Data for Retrospective World Interval July 26 - August 14, 1972", J. Virginia Lincoln and Hope I. Leighton, November 1972") 813

2. Supplementary Information on Solar Data:

Culgoora Hα flare patrol film held at WDC-A 817

Charts of flare observations for August 1, 2, 4, 7 and 11, 1972 818

3. Analog Recording of Selected Solar Noise Bursts (Toyokawa) 824

4. Supplementary Information on Cosmic Ray Data
List of Tables and Graphs held at WDC-A 828

5. Ionospheric Data

Tables of hourly foF2 from 64 stations for the period August 1-11, 1972 reprinted from "Ionospheric Data", FA-344, U.S. Department of Commerce, (Boulder, Colorado, 80302, U.S.A.) 832

"Hourly Values of Ionospheric Data from Eight Locations for the period July 26 through August 14, 1972" by S. M. Ostrow (reprinted from UAG-21) 857

6. Supplementary Information on Geomagnetic Data

Magnetograms specially prepared for the August events and held at WDC-A 860

High-Resolution Geomagnetic Micropulsation Records from the United Kingdom for the August 1972 Events 861

* Paper received too late to put in proper section (Solar Optical Data).

Page

APPENDIX II. Other references 862

APPENDIX III. Explanation of Solar Radio Summary Charts and Table 872

Alphabetical Index 877

Author Index 885

Summary on page 8.

For basic data and indices for this section and others, see Appendix I for Table of Contents to Report UAG-21.

For data papers presented or published elsewhere which contain additional information on ionospheric observations and the other categories included in this report, see Appendix I.

For Tables of hourly foF2 from 64 stations covering the period August 1-11, 1972, see Appendix I.

For plots of hourly foF2 and fmin from 8 stations covering the period July 26 - August 14, 1972, see Appendix I.

Ionospheric and Whistler Activity Observed at the Panská Ves and Průhonice Observatories, 26 July - 14 August 1972

by

F. Jiříček, J. Laštovička, and P. Tříska
Geophysical Institute, Czechoslovak Academy of Sciences
Prague, Czechoslovakia

This brief note consists of three parts: the multifrequency observations of SID events, general characteristics of the lower ionosphere based on A3 absorption measurements, and the results of whistler and VLF emission observations.

Multifrequency Observations of SID Events

The SID activity was observed at the Panská Ves Observatory (N50.52, E14.57) of the Geophysical Institute, Prague. Table 1 gives a list of SID-monitoring measurements; they cover the whole lower ionosphere.

Table 1

List of SID-monitoring measurements made at the Panská Ves Observatory. L = McIlwain parameter.

method type	f(kHz)	reflection point	distance (km)
SWF A3	6090	50°04′N 10°20′E L = 2.2	610
	2775	52°27′N 12°27′E L = 2.4	518
	2614	52°08′N 11°00′E L = 2.4	610
SFA	164	49°00′N 08°01′E L = 2.1	999
	155	48°13′N 20°20′E L = 2.0	981
SEA	27		

Note:

SFA .... Sudden Field Anomaly observed as an interference effect of the LF ground wave and 1-hop sky wave provides information on the sky wave amplitude and phase variation.

Usual SID activity was observed during the period in question - 14 events in 20 days. Table 2 contains all the SID events observed from 26 July to 14 August. The following scale of importances is used: SWF - 1, 2, 3, 3+; SEA - 1, 2, 3, 3+; SFA - 0, 1, 2, 3, 3+. Solar X-ray data are taken from "Solar-Geophysical Data" [1972], as are lists of SID, PCA, etc.

The two SID events occurring in July and the three on 1 August are typical and consistent with X-ray data ["Solar-Geophysical Data," 1973]. The second event on 1 August is associated with a strong X-ray burst.

The 2 August event was caused by a relatively weaker X-ray burst ["Solar-Geophysical Data", 1972] exciting only an SFA event.

The SID on 4 August corresponded to a very strong X-ray burst. The 6090 kHz frequency was not totally absorbed, and it indicated that this event consisted of two clearly distinct events; the 27 kHz SEA accompanied the first one.

Of the three SID's observed on 7 August the third event was relatively strong and showed two clearly distinct events on 6090 kHz. This is shown in Figures 1a - 1c.

Table 2

List of SID events between 26 July - 14 August, 1972. Time in UT
C - evaluation impossible for technical reasons; D - very small or no effect;
E - large enhancement of absorption throughout sunlit period; N - no effect;
T - total absorption lasting several hours and starting early in the morning.

date	SWF					SFA					SEA				Remarks
	f(kHz)	start	max.	end	imp.	f(kHz)	start	max.	end	imp.	start	max.	end	imp.	
28 Jul	2614	1323		1343	2	164	1324	1331	1346	1	1324		1345	1	
	2775	1324		1346	2	155	1324	1331	1347	1					
	6090	1324	1330	1344	2										
31 Jul	2614	1103		1218	2	164	1112	1120	1150	2		D			
	2775	1105		1218	2	155	1112	1120	1217	1					
	6090	1114	1120	1144	2										
1 Aug	2614	0659		0742	2	164	0700		0743	0		N			
	2775	0659		0741	2	155	0702		0750	1					
	6090	0702		0731	1										
1 Aug	2614	0842		1025	3	164	0842	0929	1007	2	0850	0855	0953	2	
	2775	0842		1028	3	155	0843	0929	1015	2					
	6090	0905	0927	1016	3										
1 Aug	2614		C			164	1138	1155	1217	1		N			
	2775	1138		1215	2	155	1140		1213	1					
	6090	1138		1218	2										
2 Aug	2614		T			164	1045	1048	1127	1		N			
	2775		T			155	1046	1051	1131	1					
	6090		E, N												
4 Aug	2614	0620		1329	3+	164	0623	0636		3	0624	0632	0742	3+	two clearly distinct events on 6090 kHz
	2775	0620		1258	3+	155	0623	0636		3					
	6090	0620		0847	3+										
	6090	0942		1057	3										
7 Aug	2614	1054		1135	2	164	1054		1138	1	1058		1141	1	
	2775	1054		1135	2	155	1057		1134	0					
	6090	1057	1108	1130	2										
7 Aug	2614	1200		1223	2	164	1203	1206	1227	1	1203	1210	1234	1	
	2775	1200		1218	2	155		D							
	6090	1203	1208	1223	2										
7 Aug	2614	1508		1729	3	164	1509	1525	1645	3		C			two clearly distinct events on 6090 kHz
	2775	1508		1728	3	155	1510	1525	1647	3					
	6090	1509	1637	1618	3										
9 Aug	2614	1001		1049	2	164		N				N			optical subflare N15, W62
	2775	1002	1014	1038	2	155		N							
	6090		N												
11 Aug	2614		C			164	1217			2		N			the second event started before the end of the first event
	2775		C			155	1217			2					
	6090	1217	1223		2	164	1236	1245	1340	2					
	6090	1234		1332	3	155	1235	1246	1351	2					
12 Aug	2614	0739	0750	0759	1	164	0740		0810	0	0740	0746	0818	1	
	2775	0738		0759	1	155	0742	0747	0808	1					
	6090		N												
12 Aug	2614	1433		1505	2	164		C			1433	1445	1507	2	
	2775	1433		1508	2	155	1433		1513	1	1433	1445	1507	2	
	6090	1433	1439	1453	1										

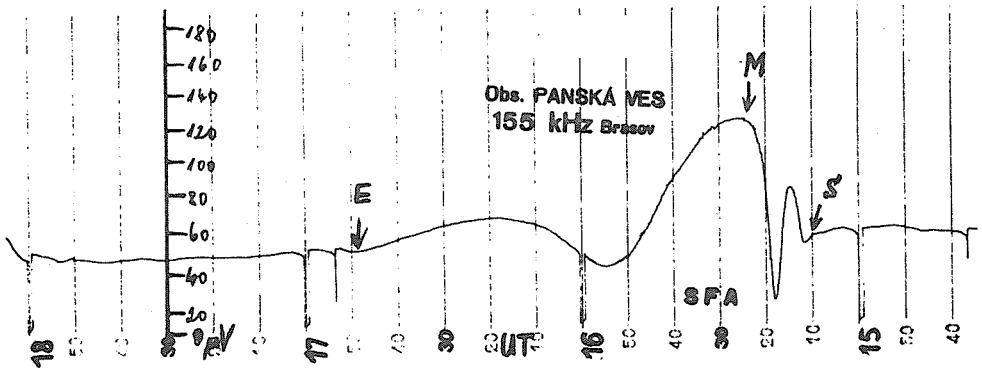

Fig. 1a. SFA on 155 kHz, 7 August 1972.

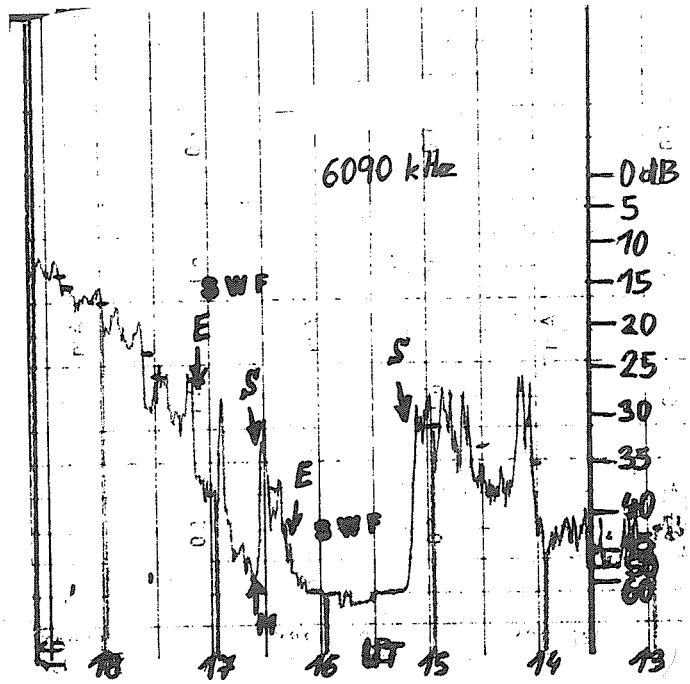

Fig. 1b. SWF on 6090 kHz, 7 August 1972.

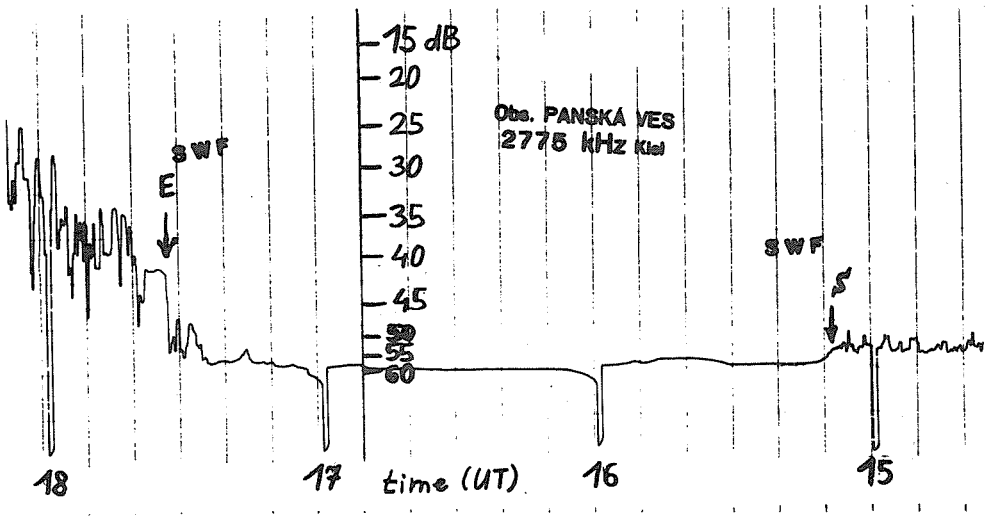

Fig. 1c. SWF on 2775 kHz, 7 August 1972.

An interesting and non-typical event was observed on 9 August. It is associated with a small subflare; the world-wide list of SID's report three SWF's and one SCNA ["Solar-Geophysical Data," 1972]. Solar X-ray data are not available. ["Solar-Geophysical Data", 1972]. The presence of considerably pronounced SWF's on 2614 and 2775 kHz and not on other frequencies resembles an SID event observed on 17 June 1970 [Laštovička and Fedorova, 1972]. This event seems likely to be an event of corpuscular origin, possibly in connection with the sharp narrow maximum of the geomagnetic storm observed simultaneously at that time. The SWF's observed are shown in Figures 2a and 2b.

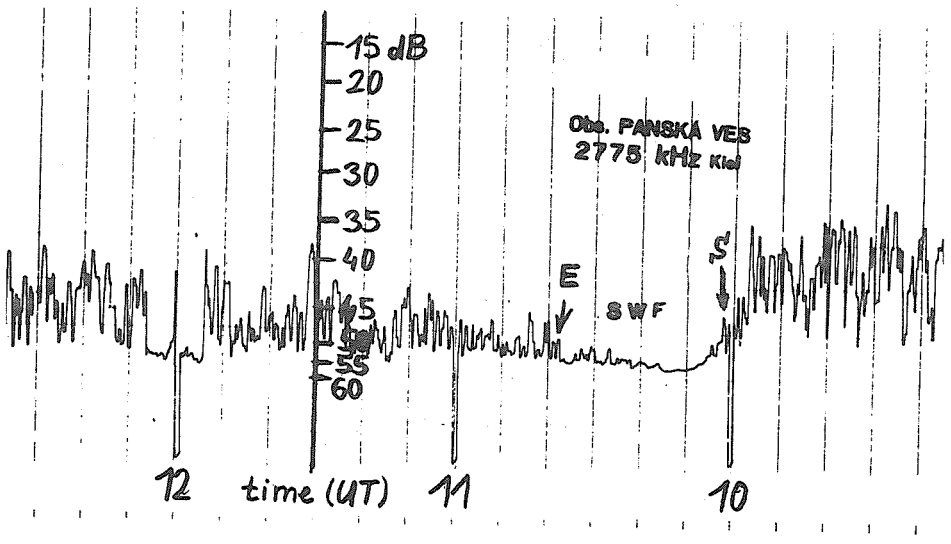

Fig. 2a. SWF on 2775 kHz, 9 August 1972.

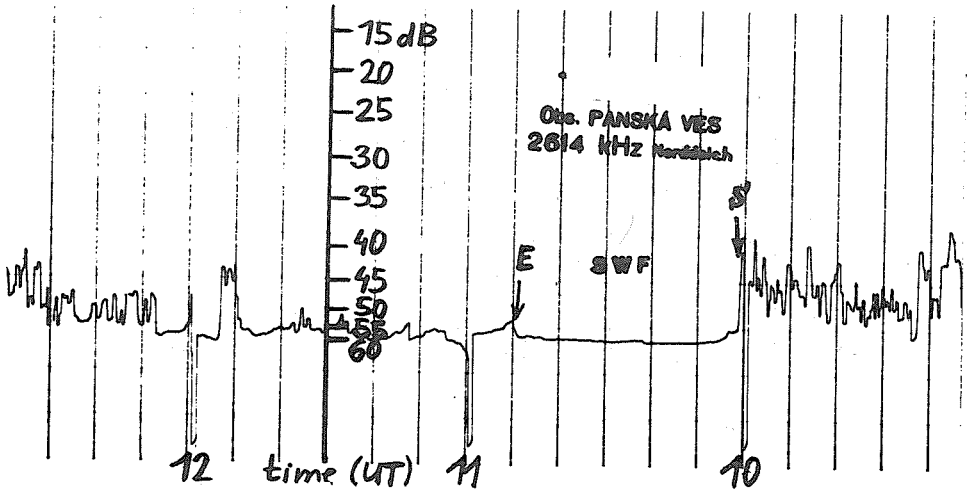

Fig. 2b. SWF on 2614 kHz, 9 August 1972.

The SID observed on 11 August is a well-developed example of two overlapping events. We can see the start of the second event before the end of the first event. An example is given in Figures 3a - 3b.

Both SID's observed on 12 August are typical events and they correlate quite well with X-ray data.

General Characteristics of the Lower Ionosphere Based on A3 Absorption Measurements

HF A3 absorption data are suitable for studying the daytime lower ionosphere, and LF data give some information on the nighttime conditions.

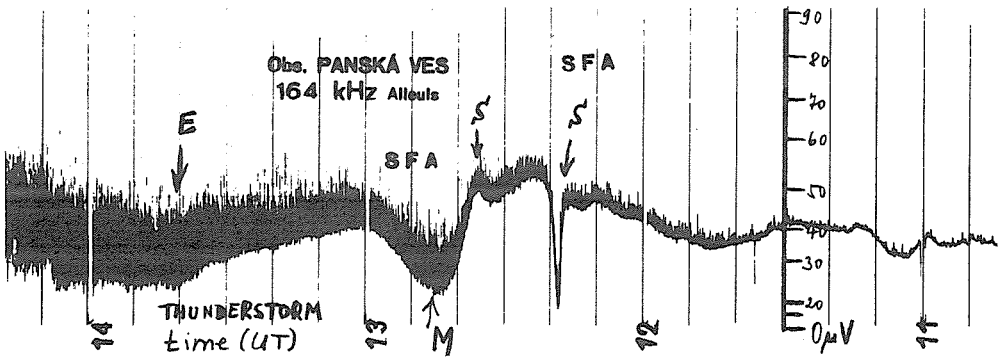

Fig. 3a. SFA on 164 kHz, 11 August 1972.

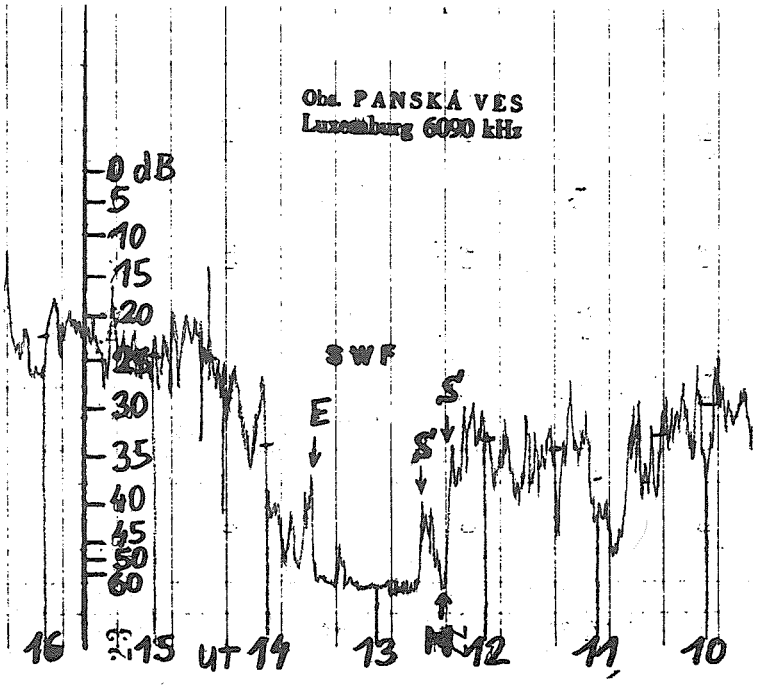

Fig. 3b. SWF on 6090 kHz, 11 August 1972.

The daytime absorption measured on 2775 kHz (Table 1) was enhanced by more than 5 dB during the following periods: 27 - 29 July, 1 - 4 August, 6 - 8 August, and 10 - 11 August, while a total absorption of non-flare origin was observed at 0500 - 1130 UT 2 August, 1000 - 1030 UT 6 August, 1400 - 1430 UT 7 August, and 0800 - 1400 UT 8 August. Similar results were found on 2614 and 6090 kHz (Table 1). The great absorption observed on 8 August can probably be attributed to PCA maximum on that day. The total absorption observed on 2 August, however, cannot be linked with any particle event and may be attributed to a very high level of X-ray flux observed.

The nighttime lower ionosphere was studied by the use of the LF A3 absorption data measured on 272 kHz (reflection point N49.56, E16.1, L = 2.1; d = 236 km) at the Průhonice Observatory. Two groups of anomalous enhancements of nighttime absorption for the period in question are summarized in Table 3, both being connected with geomagnetic storms. The 26 - 27 July group represents the after effect of a geomagnetic storm with SSC at 1856 UT 24 July, while the 4 - 7 August group represents mainly the after effect of the strong geomagnetic storm with SSC at 0119 UT 4 August. This supports the connection between a geomagnetic storm and the appearance of a significant nighttime absorption enhancement [Jiříček et al., 1972]. The bay-like absorption disturbance observed on 7 August 2030-2200 UT can be regarded as one of the manifestations of the strong geomagnetic storm mentioned above.

Table 3

Anomalous nighttime enhancements of abscrption on 272 kHz. SR - sunrise; SS - sunset; N - night (=100° till 2300 UT). The scale A_o-A_3 is routinely used.

date	26	27	28	29	30	31	1	2	3	4	5	6	7	8	9	10	11	12
SR		A_o						A_o										
SS		A_o								A_o								
N	A_o	A_2				A_o				A_o	A_1	A_2	A_1		A_o			

Results of Whistler and VLF Emission Observations

Routine whistler observations from the Panská Ves Observatory are available. This is a typical mid-latitude station where under normal conditions ducted whistlers and VLF emissions propagating along paths between L = 1.6 - 3.2 are observed [Jiříček, 1970]. The whistler activity shows a minimum in summer months (August - September); during this time, whistlers normally occur only during the night [Jiříček, 1972]. Their occurrence before sunset or during daylight hours in summer months is often associated with minor or moderate geomagnetic disturbances. Accordingly, the VLF activity in the period 26 July to 14 August 1972 (see Table 4) can be considered as enhanced with a disturbed interval between 4 - 8 August. The occurrence of VLF discrete emissions (chorus) at Panská Ves is also an indication of disturbed conditions. These occurred for the first time in early morning hours

Table 4

PANSKÁ VES 50°32′N, 14°34′E **WHISTLERS** 26 July - 14 August 1972

UT / Date	00 50	01 50	02 50	03 50	04 50	05 50	06 50	07 50	08 50	09 50	10 50	11 50	12 50	13 50	14 50	15 50	16 50	17 50	18 50	19 50	20 50	21 50	22 50	23 50
26			3		1				-											1				2
27	1	1	1	6	1	1											2	1	2			1	2	5
28	2	12	3	24	13	16	6	6		4										1	3	7	2	
29																								1
30		11	16	6	7	-	-	-	-	-										2	1	1	4	28
31	42	24	3	-												6	11		4	2				
1		1	1	1											3			7	12	2	5	6	5	5
2	4	15	14	8															3				1	1
3																						2	4	5
4	7	7	8	8E	4E	6						4	3	16	19	33	63	50	52	48	30	7	6	2
5	3	1	2				E											3		2				
6	5	1	E	E	E		E										1			4	1E			
7	10	5			E															2		2	2	2
8	10	8	3E	9																	1	1	1	2
9	10	4	9																	7	6	10	-	-
10	4		1	2						-	-	-							2	1	3	3	2	7
11	7	11	25	26	1	-	-	-	-	-	1	1		-	-					2	14	23	4	15
12	15	6	2	39	1												1						1	
13	1		2			1	1	5							1			1						
14																								

Figure - number of whistlers observed from 50 to 52 min.
- - no observations
E - VLF emissions

of 4 August and persisted until the early morning hours of 8 August. The strong whistler activity on 4 August began about noon and attained a maximum before sunset. Only one-hop whistlers were observed. The high whistler rate in the late afternoon indicates favorable conditions for the formation of whistler ducts. This is also indicated by the occurrence of 3-hop whistler echoes in the runs at 1850 and 1950 UT. Unfortunately, the very diffuse whistler traces and the lack of knowledge of the initial atmospherics prevented the determination of L-values of the propagation paths so that electron density within the plasmasphere could not be estimated.

REFERENCES

JIŘÍČEK, F. 1970 On the Determination of Propagation Paths of Mid-Latitude Whistlers for Purposes of Estimating the Magnetospheric Electron Density. Studia geoph. et geod., 14, 402 - 413.

JIŘÍČEK, F. 1972 Whistler Activity in Central Europe during the Period of Increasing Solar Activity from 1964 to 1968. Trav. Inst. Géoph. Tchécosl. Acad. Sci. No. 313, Academia, Praha.

JIŘÍČEK, F., J. LAŠTOVIČKA, and P. TŘÍSKA 1972 Report on Ionospheric and Whistler Activity at the Panská Ves and Průhonice Observatories on September 1, 1971, World Data Center A, Upper Atmospheric Geophysics Report UAG-12, Part II, 430 - 431.

LAŠTOVIČKA, J. and N. I. FEDOROVA 1972 On an SID of the Corpuscular Origin. Manuscript (to be published).

1972 Solar-Geophysical Data, 337 Part I, 338 Part I, U. S. Department of Commerce, (Boulder, Colorado, U.S.A. 80302).

1973 Solar-Geophysical Data, 341 Part II, 342 Part II, U. S. Department of Commerce, (Boulder, Colorado, U.S.A. 80302).

SCL and SEA Associated with Solar Events July 29 to August 10, 1972

by

S. N. Mitra
4, Kotla Lane
New Delhi-1, India

Introduction

The author set up in August 1958 an experimental arrangement for continuous recording at Delhi (N28.6°, E77.2°) of the field strength of Radio Tashkent on 164 kHz with a view to studying D-region phenomena. The experimental arrangement has been published [Mitra, 1964]. The analysis of results indicated that all types of solar flares gave well-defined indications in the recording of field strength. Sudden changes associated with solar optical and X-ray flares were named SCL by the author [Mitra, 1970] as a distinctive flare phenomenon on the amplitude of the sky wave field intensity of long wave propagation. In recent years the scope of the investigation has been extended to include another distant U.S.S.R. long wave station, Radio Alma Ata transmitting on 182 kHz. In addition, recordings of SEA are also in progress following the experimental technique of Krivsky et al. [1963].

We present in this note some of the phenomena we observed in our field strength recordings of 164 kHz, 182 kHz and atmospherics on 27 kHz during the period July 29 to August 10, 1972.

Experimental Observations

August 1, 1972:

We observed an SCL on both 164 and 182 kHz between 0855 and 0950 UT. Although a 1B (Hα) optical flare was reported on this day between 0841 and 1101 UT, we prefer to associate this SCL with the X-ray flare which began at 0855E UT and ended at 0954D UT. We did not observe any SEA on 27 kHz. Figure 1 shows the actual recordings of SCL.

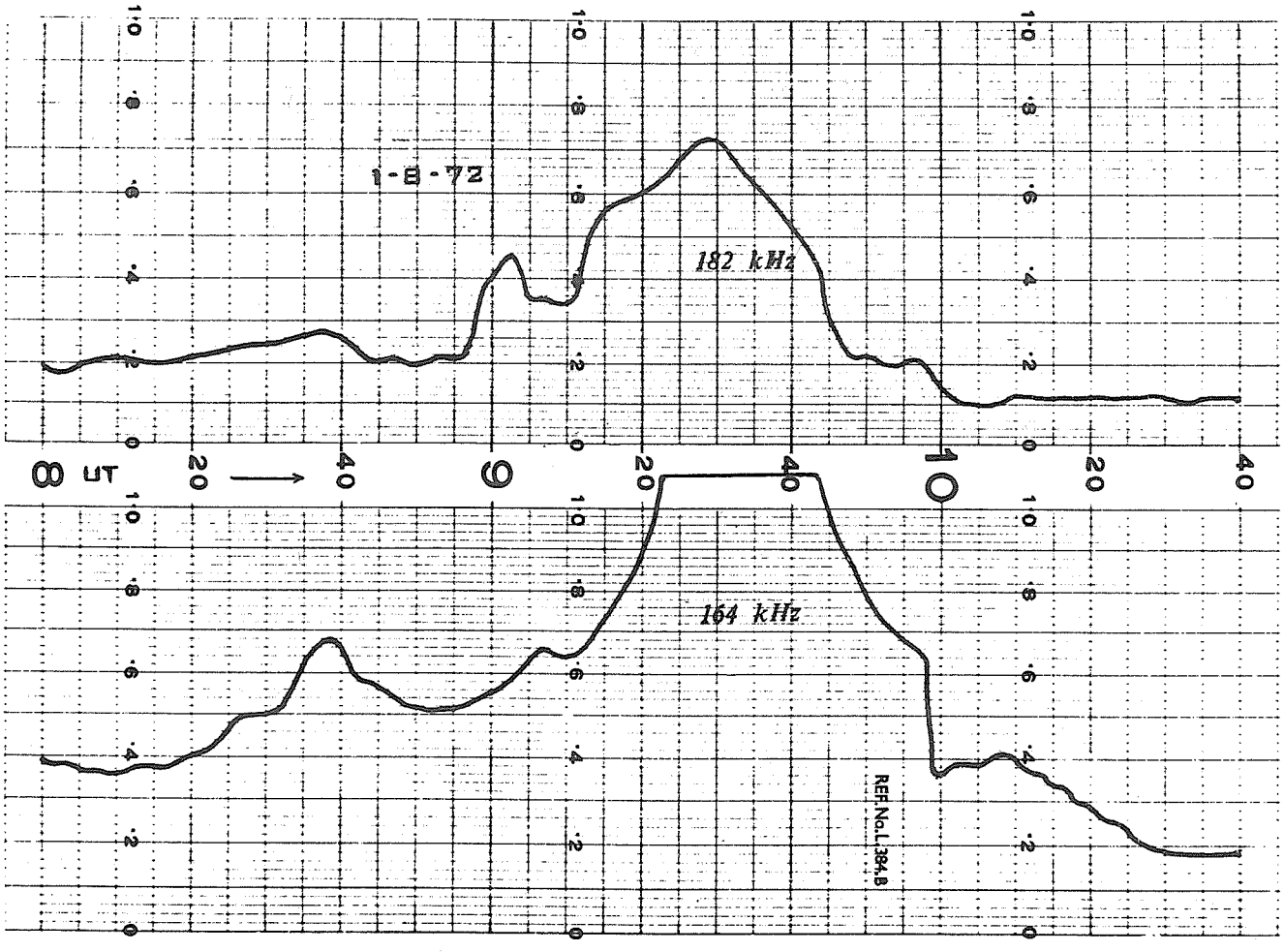

Fig. 1. August 1, 1972 recording of SCL on 164 and 182 kHz.

August 2, 1972:

We observed an SCL on 164 kHz and an SEA on 27 kHz between 0313 and 0405 UT. A 1B optical flare was reported beteen 0316 and 0506D UT and an X-ray flare at 0254 UT. Figures 2 and 3 show the actual recordings of SCL and SEA, respectively.

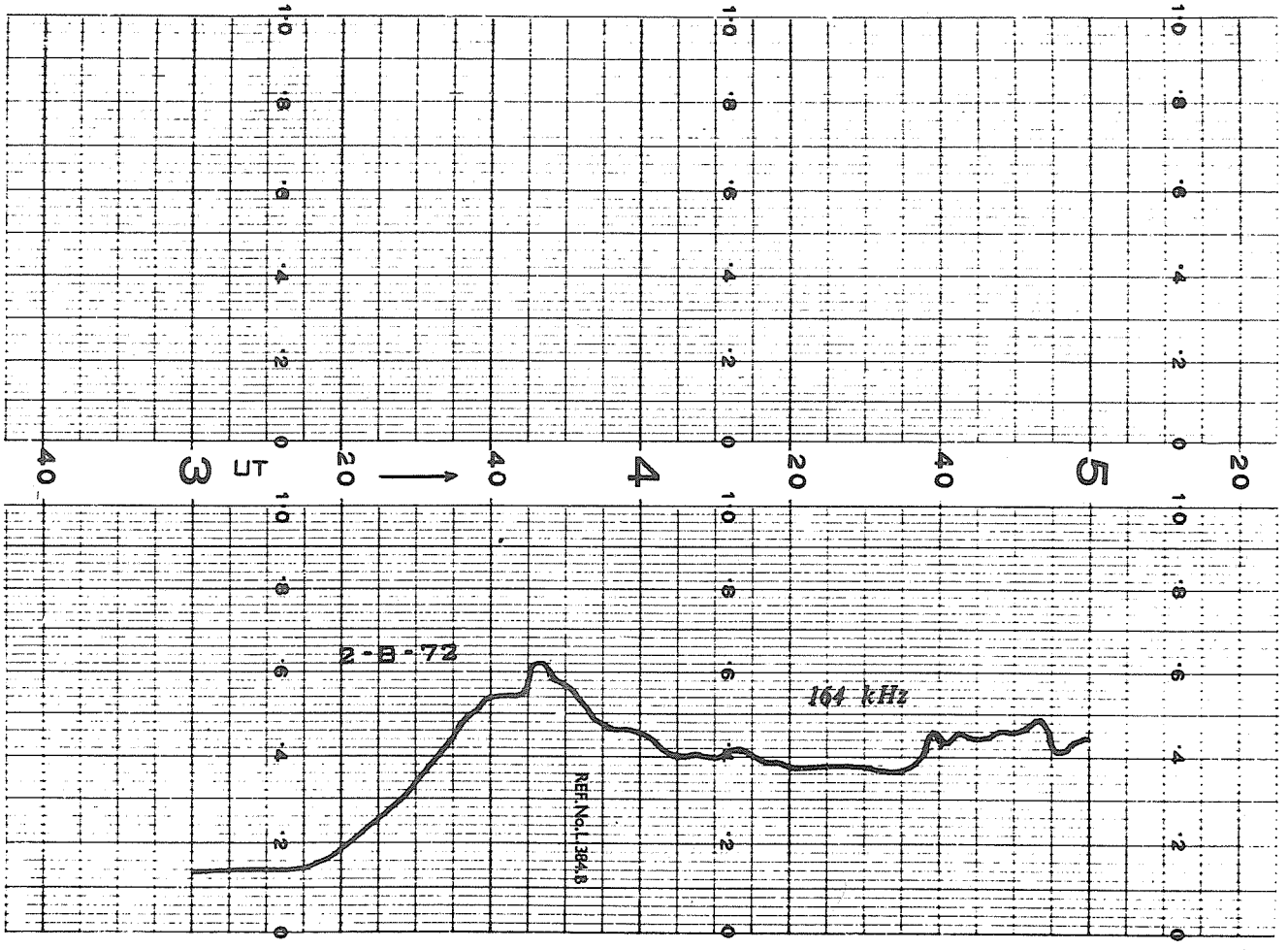

Fig. 2. August 2, 1972 recording of SCL on 164 kHz

August 3, 1972:

In our recording of 164 kHz we observed a peculiar phenomenon between 0950 and 1130 UT. No solar flare was reported at that time. However, there was an incidence of solar protons with speeds of 350 to 585 km/sec monitored by Pioneer 9. The protons have been associated with the August 2 flare between 0313 - 0506 UT. On some earlier occasions also, we have found similar increases of field strength associated with the incidence of high energy protons. Figure 4 shows the actual recording of this event.

August 4, 1972:

We observed a series of sudden changes in our recordings on 164 and 182 kHz between 0530 and 0730 UT. These are rare type records, usually associated with proton flares. An important feature of this observation is that the variations of field strength of 164 kHz were found to be opposite to those of 182 kHz. Such phenomena are extremely rare, especially during sunlit periods when the two variations follow each other closely. An X-ray flare was reported between 0527 and 1359 UT. Figure 5 shows the actual recording of the event.

August 7, 1972:

A type-B SCL [Mitra, 1970] was observed in our recording of 182 kHz between 0245 and 0325 UT. An X-ray flare has been observed between 0253E and 0308 UT. Another type-A SCL was observed on 182 kHz between 0335 and 0440 UT. An X-ray flare occurred between 0348 and 0442 UT and a 1 B optical flare between 0348E and 0450 UT. Figure 6 shows the actual recording.

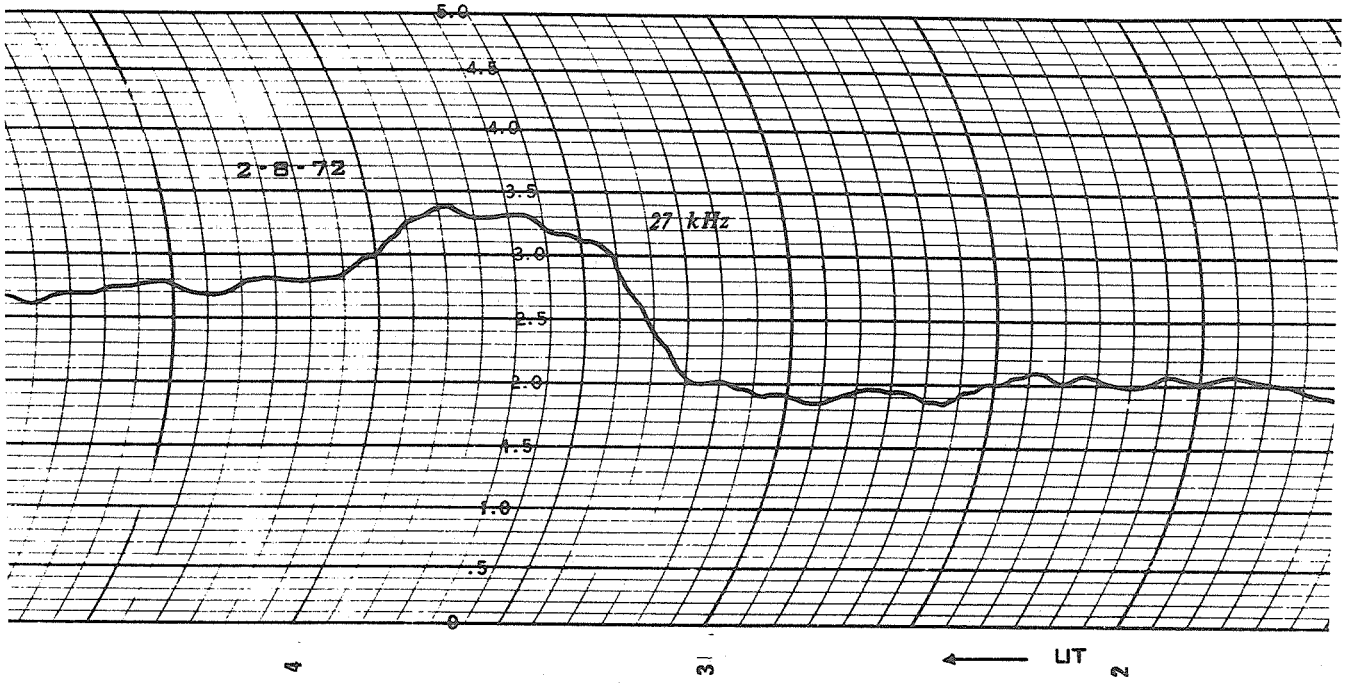

Fig. 3. August 2, 1972 recording of SEA on 27 kHz.

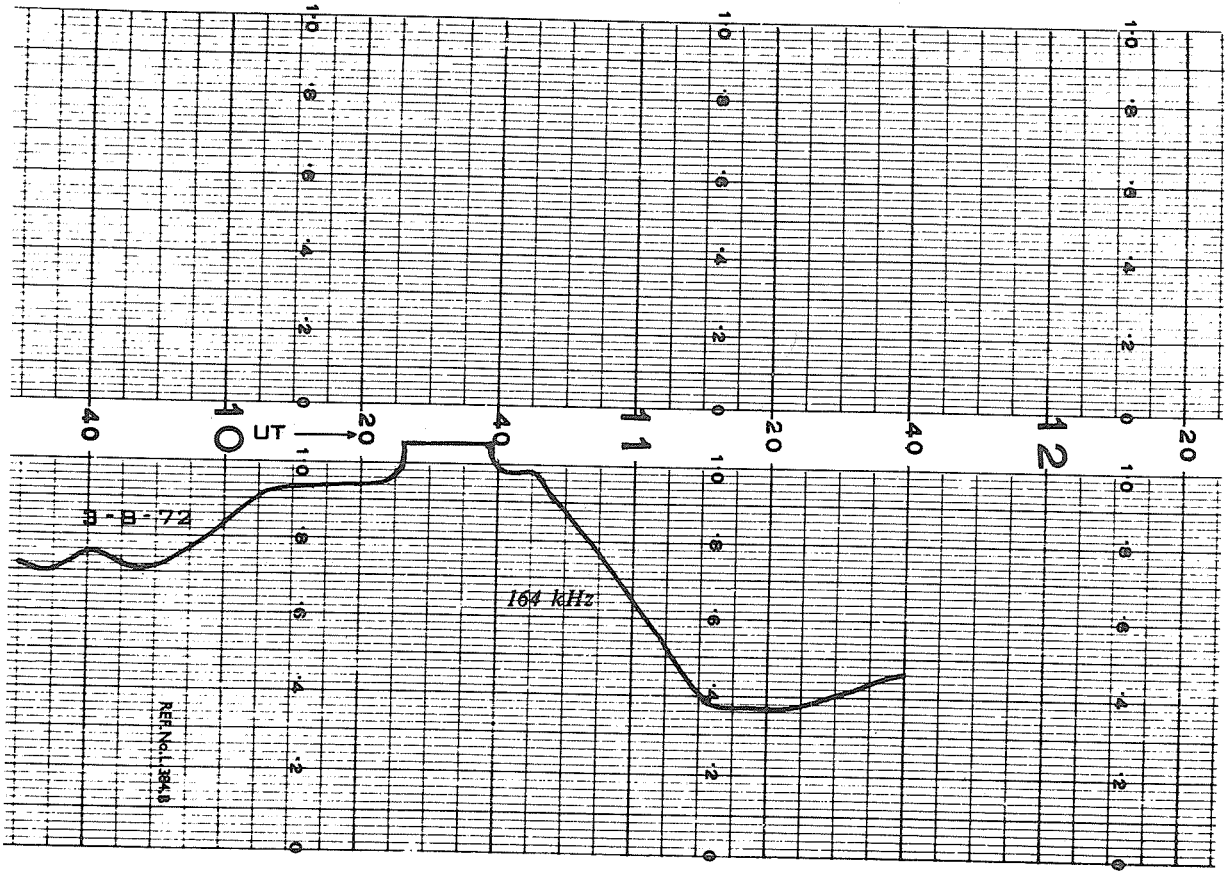

Fig. 4. August 3, 1972 recording of SCL on 164 kHz (presumably associated with proton flare of August 2, 0313 - 0506 UT).

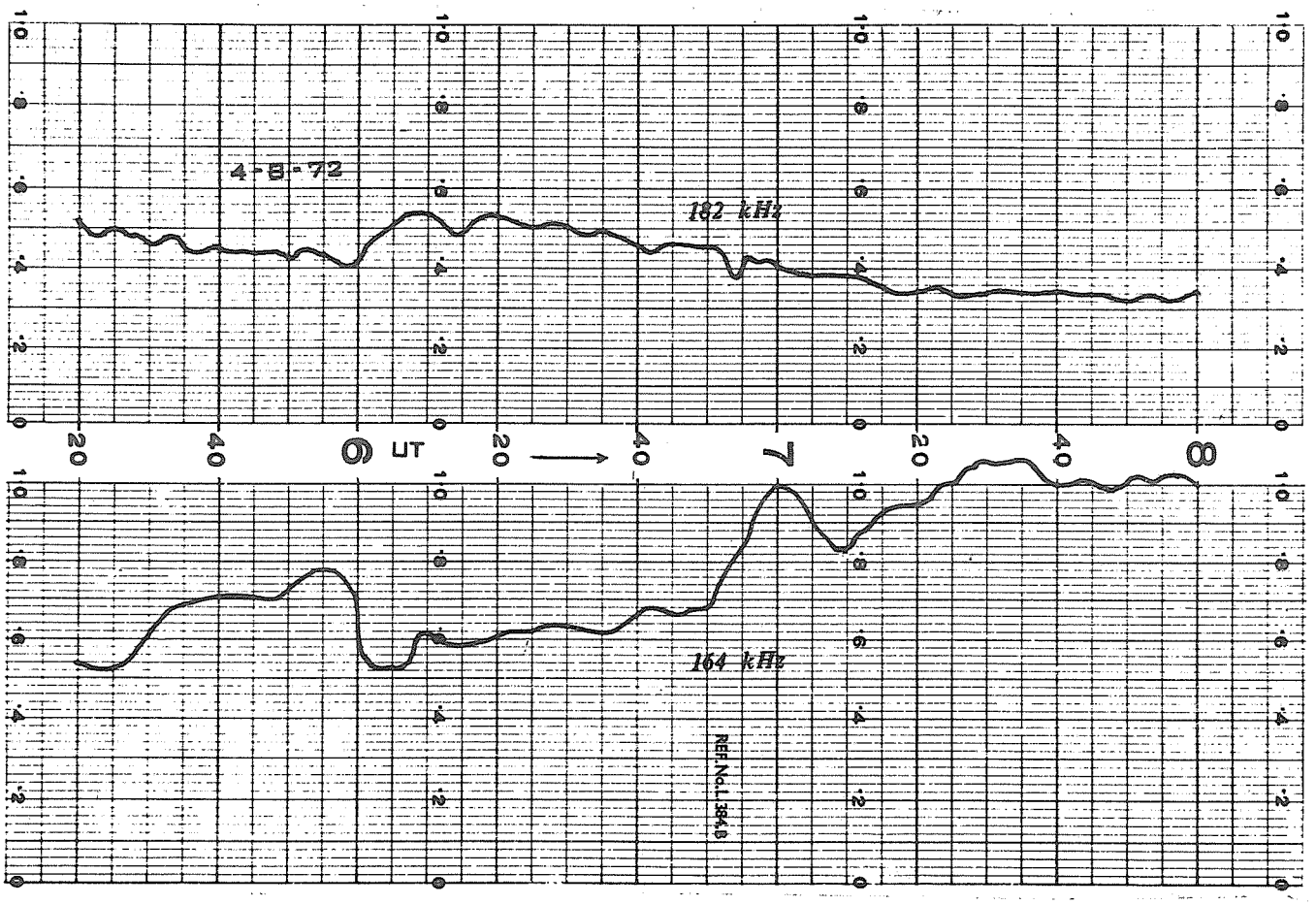

Fig. 5. August 4, 1972 recording of SCL on 164 and 182 kHz (presumably associated with proton flares).

Table 1 gives the summary of observations of SCL and SEA by the author and the corresponding flares, both optical and X-ray, and associated SID's.

Data on optical and X-ray flares and SID's have been taken from the "SGD" [1972, 1973] .

REFERENCES

KRIVSKY, L., et al.	1963	Bull. Astronom. Inst. (Czechoslovakia), 14, 5.
MITRA, S. N.	1964	J. Atm. Terr. Phys., 26, 375.
MITRA, S. N.	1970	Solar Physics., 15, 249.
	1972 1973	Solar Geophysical Data, 338 Part I, 342 Part II, U.S. Department of Commerce (Boulder, Colorado, U.S.A. 80302)

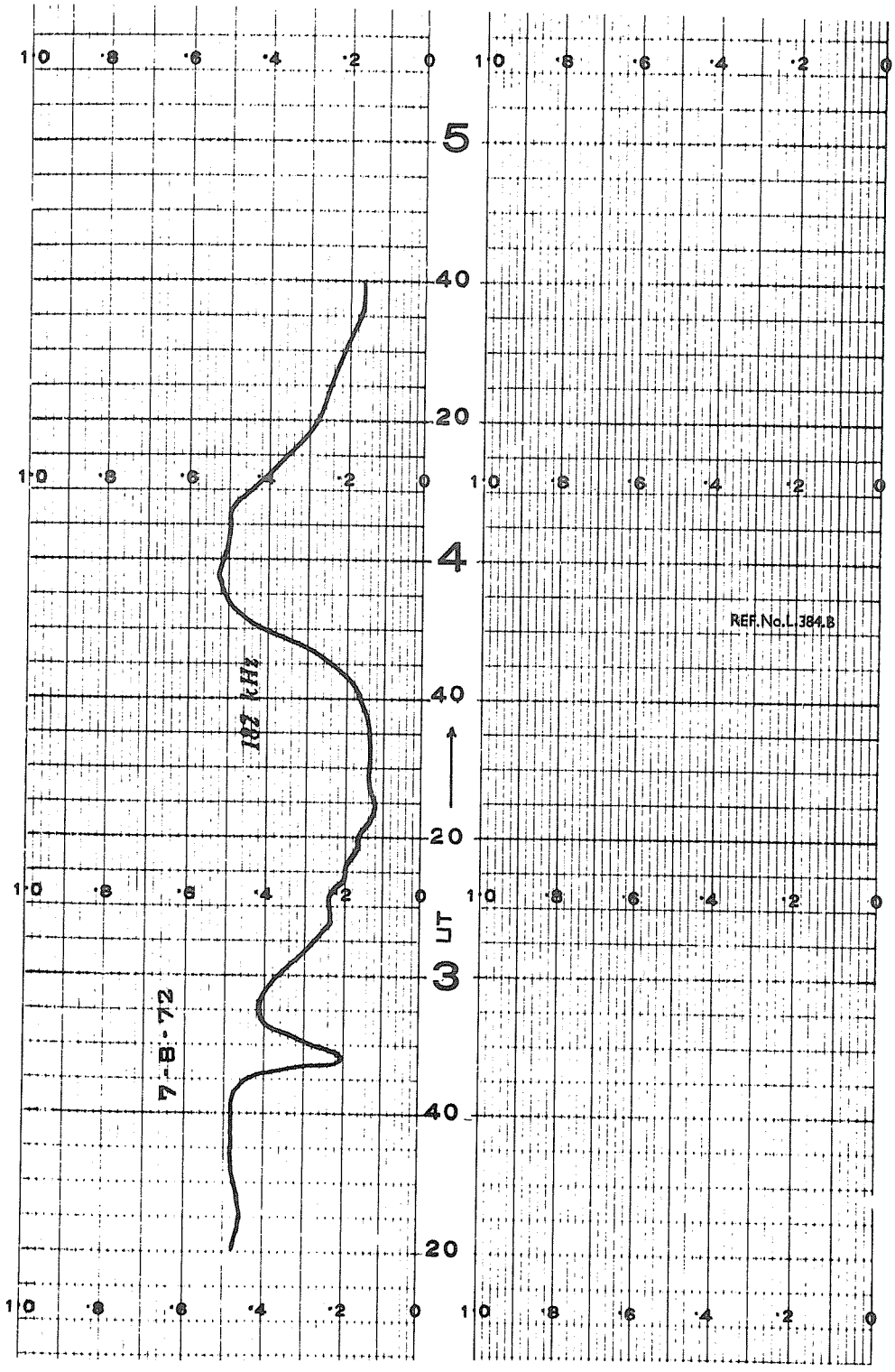

Fig. 6. August 7, 1972 recording of SCL on 182 kHz.

Table 1

	SOLAR FLARE (OPTICAL)				X-RAY OUTSTANDING EVENTS									SID'S		SCL (DELHI-Mitra)				SEA (DELHI-Mitra)		
Date Aug. 1972	Beg. UT	Max. UT	End UT	Imp.	Start UT	0.5-3A Flux	Peak Time UT	1-8A Flux	Peak Time UT	8-20A Flux	Peak Time UT	End UT	Beg. UT	Events	Freq. kHz	Beg. UT	Max. UT	End UT	Beg. UT	Max. UT	End UT
1	0841	0915	1101	1B	0855E	169	0921	326	0921D	178	0929	0954D	0842	SWF-1	182	0855	0930	0950	-	-	-
															164	0855	-	0950D			
2	0316	0410U	0506D	1B	0254	712	0402	1790	0358	429	0357E	1601	0312	SWF-5	164	0313	0346	0405	0316	0348	0406
														SCNA-2							
														SEA-1							
														SPA-2							
														LF-SPA-4							
														SES-4							
3															164	0947	-	1115			
4	0617	0640	0855	3B	0527	7460	0642	4560	0642	429	0642	1359	0528	SPA-2	182	0530	-	0730	-	-	-
7	-	-	-	-	0253E	169	0253	326	0253	118	0254	0308	0252	SWF-2	182	0245	0255	0325			
														SCNA-1							
														SPA-2							
														LF-SPA-3							
														SES-3							
7	0348E	0355	0450	1B	0348	26.3	0350	114	0428	148	0429	0442	0350	SWF-3	182	0335	0357	0440			
														SCNA-1							
														SEA-2							
														LF-SPA-3							
														SES-4							

Midlatitude D-region Response to the August 2, 1972 Event

by

Ward J. Helms
University of Washington
Department of Electrical Engineering
Seattle, Washington

ABSTRACT

D-region phase height and conversion coefficient magnitude are presented for a near vertical incidence path near Seattle, Washington during the period July 28 to August 16, 1972. The response of the D-region to a large X-ray flux at nearly grazing incidence is also shown. The electron density perturbation is seen to decrease well before the flare maximum indicating occultation by the atmosphere of the earth.

During August 1972 measurements of the phase and amplitude of the near normal incidence conversion reflection coefficient $_{\parallel}R_{\perp}$ at 18.6 kHz were made at the University of Washington. These measurements are made with a carefully constructed and adjusted shielded loop antenna of the type described by Belrose [1962]. The baseline of this experiment is 67.46 kilometers over relatively level earth, essentially normal to a magnetic meridian. Normally both the groundwave (plus some residual skywave) and the skywave signals are recorded, so that absolute phase measurements may be maintained. However, during this event the groundwave recording system was inoperative, so only relative phase measurements are presented here. The receiving equipment consists of two phase-locked VLF receivers with effective bandwidths of approximately 3 milliHertz [Allyn, 1969]. The output phase of these receivers is compared to a reference, derived from a Varian R-20 Rubidium frequency standard, at 18.6 kHz with a digital phase meter and is presently written on digital magnetic tape.

However, during the August event the skywave phase and amplitude were recorded on a two-channel brush chart recorder and have been hand-scaled.

Figure 1 shows the phase and amplitude records obtained over the period between July 28 and August 16, 1972. The dotted portions are times at which the D-region phase height was fluctuating so rapidly that the phase lock receiver could not track it. Therefore, the phase reading is an averaged value. During these periods it is possible for the receiver to lose or gain a cycle. The data as presented in Figure 1 represent our best estimate of relative phase height. However, ambiguities of 2π are possible at the dotted portion of the record.

The amplitude scale on this Figure has been calibrated in magnitude of $_{\parallel}R_{\perp}$ referred to 75 kilometers. At the time that these records were taken the amplitude measurement system became non-linear at a value of 0.2, therefore where the record is constant at this value we can only infer that $_{\parallel}R_{\perp} \geq 0.2$.

Figure 2 presents the response of the D-region to a solar X-ray burst during local sunset. SOLRAD 10 data indicate that the X-ray flux peaked a few minutes past 0400 UT. As seen in Figure 2 the maximum deviation from the normal sunset phase height occurred at 0330 UT. We attribute this difference to occultation of the X-ray flux by the earth's atmosphere.

REFERENCES

ALLYN, J. D. 1969 VLF Approach to Synchronous Timing at Two Remote Locations. Master's Thesis, Department of Electrical Engineering, University of Washington, Seattle, Washington.

BELROSE, J. S. 1962 The Use of a Screened Loop Antenna for Reception of Low Frequency Radio Waves. R.P.L. Report No. 10-0-1, D.R.T.E., Ottawa, Canada, June 1962.

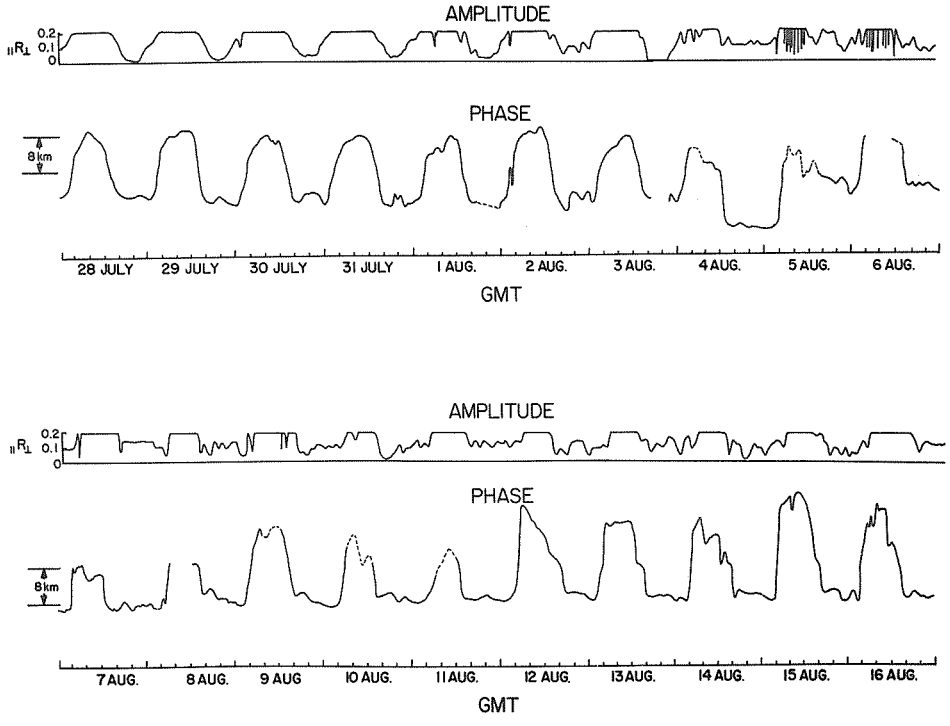

Fig. 1. NPG skywave phase and amplitude records for the period July 28 to August 16, 1972.

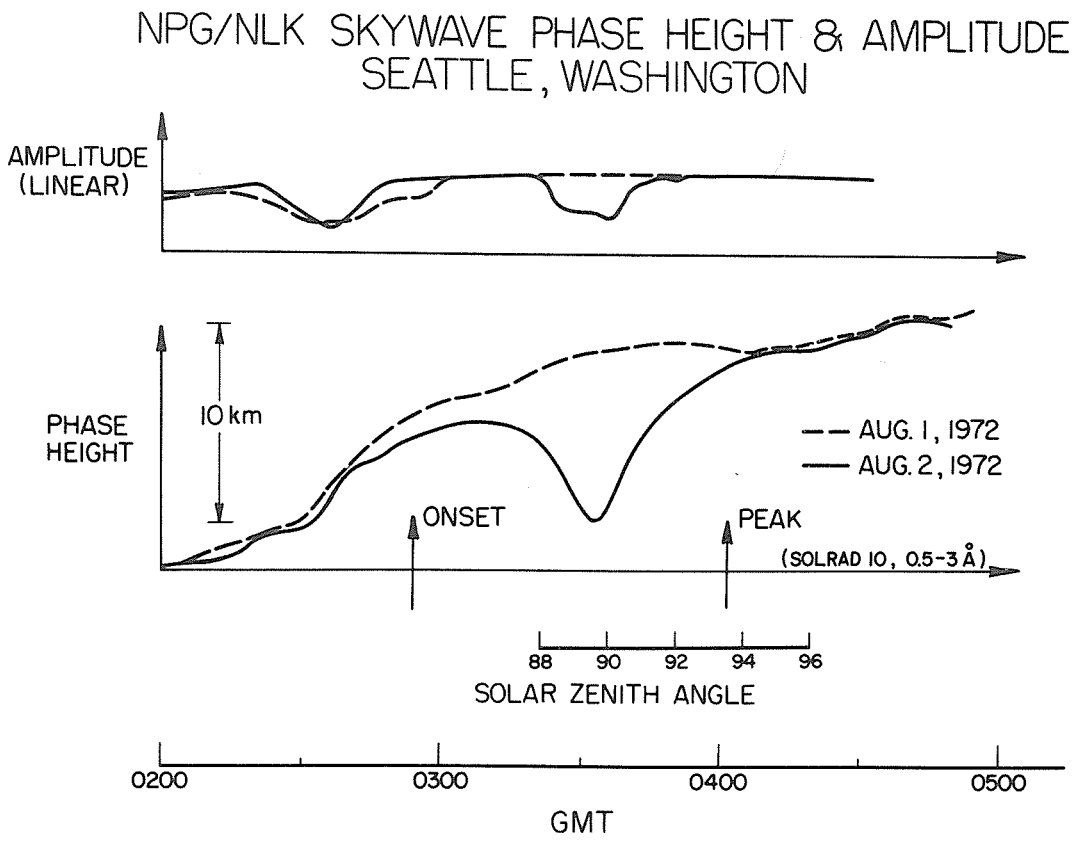

Fig. 2. NPG/NLK skywave phase height and amplitude records for local sunset on August 1 and 2, 1972.

Ionizing Radiation and After Effects of Solar Proton Flares on August 4 and 7, 1972

by

G. T. Nestorov and E. M. Apostolov
Geophysical Institute of the
Bulgarian Academy of Sciences
Moskovska 6, Sofia, Bulgaria

Introduction

During the period of increased solar activity July 25 to August 15, 1972 the absorption in the low ionosphere was measured by the A3 method on 6.06 MHz (Kaltanizetta - Sofia, path length 950 km). At the same time, phase height measurements on 182 kHz, (850 km path), field-strength measurements on 164 kHz, (1720 km path), and atmospheric recordings on 27 kHz were taken.

Measurements shown in Figure 1 were recorded at the Ionospheric Observatory at Sofia (N42.6, E23.4). Figure 1 shows the August 4 event.

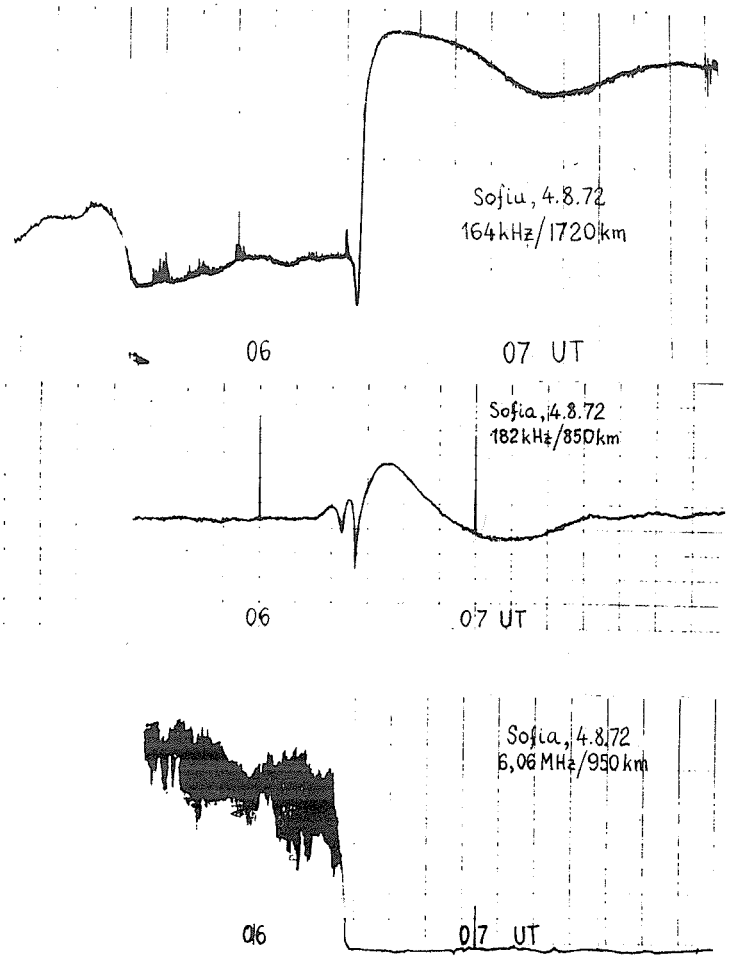

Fig. 1. August 4, 1972 records from Sofia for 164 kHz, 182 kHz and 6.06 MHz.

On the basis of these measurements, it is shown that absorption in the D-region is not only a qualitative indicator of heliophysical processes, but also a suitable instrument for quantitative estimates of solar ionizing radiation.

Energy Spectra of X-rays on August 4 and 7, 1972 Deduced from Ionospheric Data

Here, a method of aeronomic analysis of the D-region is applied by a representation of the vertical electron density distribution by an exponential law [Nestorov, 1970, a,b,c]. The nondeviative absorption, L, of a radio wave for a double pass of the ray through the ionosphere is

$$L = C \int_{h_0}^{h_{rE}} \frac{N(h)\,\mu(h)}{\omega^2_{eff} + \mu^2(h)}\,dh \qquad C = \frac{4\pi e^2}{mc} \qquad (1)$$

where h_0 = base height of the ionosphere, h_{rE} = reflection height of the signal, $\omega_{eff} = \omega_i + \omega_L'$ is an effective frequency for a given path, $N(h)$ = profile of the electron concentration, $\mu(h)$ = profile of the collision frequency. By means of a double gradient model of the D-region; namely, $N_a = \exp\,[b_1(h_a - h_0)]$ and $N_{rE} = \exp\,[b_2(h_{rE} - h_a)]$ where h_a = 65 km, from an experimental determination of the nondeviative absorption L and by means of the unchangeability of the CR-layer, from equation (1) we determine the profile of the electron concentration up to the beginning of the flare (see Figure 2).

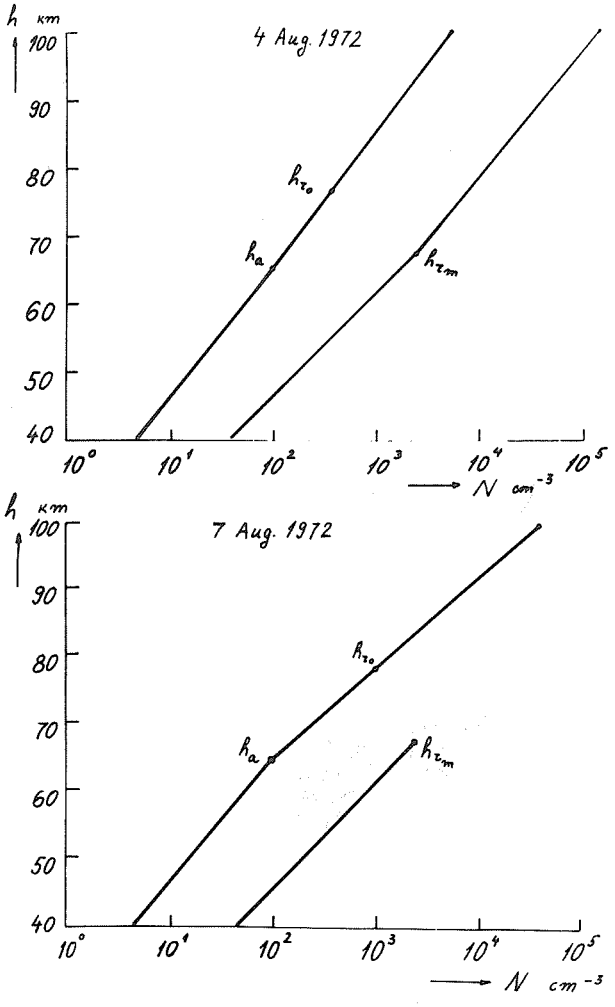

Fig. 2. Theoretically determined profile of the electron concentration prior to the beginning and at maximum of the major solar flares on August 4 and 7, 1972.

Under conditions of quasi-equilibrium we determine the electron production at a given height

$$q_0 = \alpha_0' N^2 \qquad (2)$$

where $\alpha_0' = 1/2\tau N$, τ = relaxation time. The form of the differential energy spectrum [Nestorov, 1969] for $\lambda = 2 - 7$ Å , under calm conditions and increased solar activity, can be described by the power function

$$I_\infty(\lambda) = K\lambda^n \quad , \quad n = 4 \, , \qquad (3)$$

whence the q(h) profile

$$q(h) = \text{const} \quad \lambda^4 \, . \qquad (4)$$

The general electron production in a column of 1 cm^2 cross-section between the values λ_1 and λ_2, corresponding to unit optical depth at heights h_1 and h_2 will be

$$Q = \int_{h_1}^{h_2} q(h)dh \approx \text{const}\ \lambda^4 \Delta h \qquad (5)$$

The corresponding integral flux of ionizing radiation at the boundary of the ionosphere is

$$I\ (\leq \lambda) = 5.15 \times 10^{-11} . \ Q \ . \ \sec \chi \qquad (6)$$

In this way, the integral X-ray flux $I_\infty\ (\leq\lambda)$ is obtained prior to the solar flare on August 4, 1972 (Figure 3), to the beginning of the SID at 0624 UT.

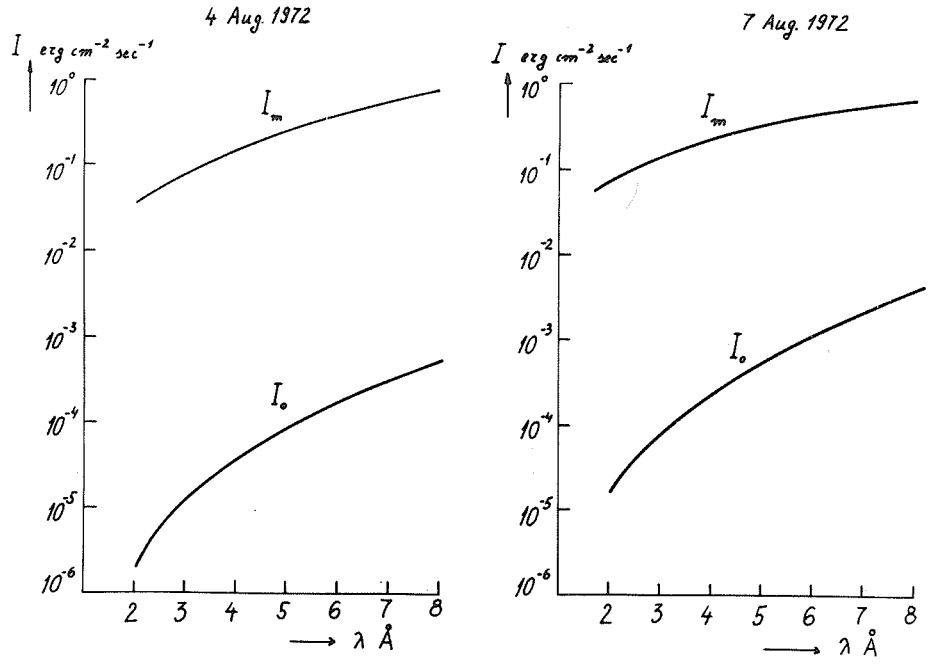

Fig. 3. Theoretically determined integral flux of ionizing radiation prior to the beginning (I_0) and at maximum (I_m) of the major solar flares on August 4 and 7, 1972.

Under highly disturbed conditions, the exponent n in the power law of the differential energy spectrum (equation 3) is highly variable. It may be determined from the solar radio emission flux density (in units of $10^{-22}Wm^{-2}Hz^{-1}$) data [Apostolov, 1973]. Up to the beginning of the solar flare at 1502 UT on August 7, 1972, the level of I_∞ (≤ 8 Å) is high and $n = 4.3$, derived from the 2800 MHz - Ottawa solar radio noise data ["Solar-Geophysical Data", 1972, 1973]. The results of I_∞ ($\leq \lambda$) are given in Figure 3.

At the maximum of the SID effect, at 0638 UT during the solar flare on August 4, 1972, according to the vertical sounding data at Sofia, fmin = 3.5 MHz, whence we find the electron concentration at the reflection point for the 6.06 MHz, (950 km) path. The extreme point of the N(h) profile at the maximum of the SID effect is found by means of the decreasing of the reflection height $\Delta h = h_{ro} - h_{rm}$ of the long waves (182 kHz, 850 km).

Thus we obtain the gradient of the electron concentration under flare conditions, b_{2m} for a height above h_{rm}.

The gradient of electron concentration under flare conditions, b_{1m}, at a height below h_{rm} is found by the relative change of the field strength of atmospherics [Budden, 1961]

$$\frac{Em}{E_o} = \exp\left[\frac{2\omega_i}{C}\left(\frac{1}{C_1}\arctan\frac{\mu o}{\omega_i} - \frac{1}{C_{1m}}\arctan\frac{\mu m}{\omega_i}\right)\right] \qquad (7)$$

For the SID maximum at 1522 UT on August 7, 1972, fmin data are lacking. But for the calculation, obtaining the profile for heights below h_{rm} (i.e., the gradient b_{1m}) of equation (7) is sufficient.

The N(h) profile obtained in this way and for the SID maximum (Figure 2) renders it possible for us to find the increase in electron production [Nestorov, 1967] under non-equilibrium conditions:

$$\frac{q_m}{q_o} = \frac{1}{\alpha'_o N_o C_1}\cdot\frac{d(N_m/N_o)}{dt} + \frac{C_2}{C_1}\cdot\left(\frac{N_m}{N_o}\right)^2 \qquad (8)$$

$$C_1 = \frac{1+C_o^-}{1+C_m^-} \qquad C_2 = \frac{\alpha'_m}{\alpha'_o}$$

During strong proton flares the flux density of solar radio emission greatly increases. From this increase [Apostolov, 1973], the exponent n of the X-ray differential flux ($\lambda < 8$ Å) can be determined. From data [Solar-Geophysical Data, 1973], [Apostolov, 1973], for the maxima of the solar flares on August 4 and 7, 1972, $n = 1.3$.

After obtaining q_m by the above method (equations 3 - 6), we obtain the integral X-ray flux at the boundary of the atmosphere at a solar flare maximum. The results are given in Figure 3.

In Table 1 the values of the X-ray flux deduced from ionospheric data and by SOLRAD 10 measurements are given.

Table 1

Date	Time UT	SID	Ionospheric Data		SOLRAD 10	
			I($\leq$ 3 Å)	I($\leq$ 8 Å)	I(0.5-3 Å)	I(1-8 Å)
			erg $cm^{-2}sec^{-1}$		erg $cm^{-2}sec^{-1}$	
4 Aug. 1972	0600	begin	1.12×10^{-5}	5.68×10^{-4}		6×10^{-4}
	0638	max.	9.20×10^{-2}	8.87×10^{-1}	7.46×10^{-2}	4.56×10^{-1}
7 Aug. 1972	1500	begin	7.03×10^{-5}	4.80×10^{-3}		5×10^{-3}
	1522	max.	1.4×10^{-1}	6.36×10^{-1}	8.95×10^{-2}	4.56×10^{-1}

After Effects of Proton Flares

In Figure 4 the average daily variation of E_{164} for the Allouis transmitter is given by a thick line. The monthly median is shown by a dot-dash line. In the upper part of Figure 4, dashes show the geomagnetic index A_p. It can be observed that while up to August 7, 1972, the daily field strength is near the median value, from August 8 the field strength E_{164} increases greatly, with three definite maxima on August 9, 12 and 14. It is clear that these are after effects of the proton flares of August 4 and 7, and of the greatly disturbed geomagnetic field during this period. For a better illustration of the first maximum, the diurnal variation of the field strength is given by a thick line in Figure 5. The diurnal variation of the monthly medians is given by a dashed line. The great increase of E_{164} can be seen clearly after 1000 UT on August 8, 1972, which continues on August 9 as well. On August 10 the field is normal. Similar diagrams may be made for the remaining two maxima as well.

Such after effects on the investigated path are observed in other cases of powerful solar flares [Nestorov, 1967].

The most probable mechanism of these effects is a weakening of the CR-layer as a consequence of the shading of the cosmic radiation by an abundance of energetic particle floods around the earth during the studied period (modulation processes). Another reason for the increase of E_{164} may be the increase of the electron concentration gradient in the reflection region as a consequence of the additional ionizing source.

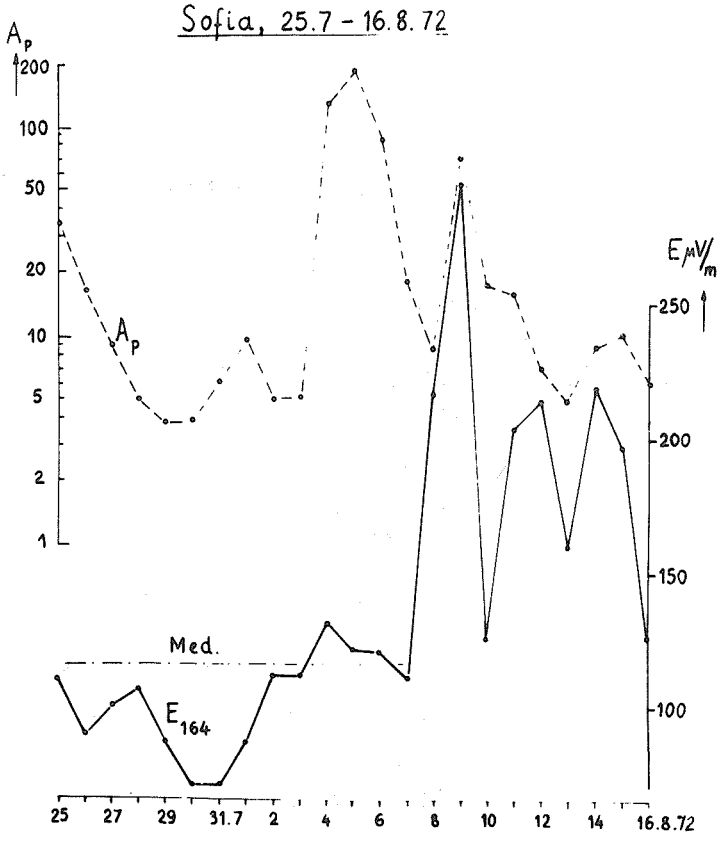

Fig. 4. Average daily variation of E_{164} (thick line), monthly median (dot-dash line), and geomagnetic A_p indices (dashed line) are shown for the period July 25 - August 16, 1972.

The Contribution of X-rays (1 - 8 Å) in the Ionization of the D-region

The increase in X-rays on August 4, 1972 and its slow decrease after the flare is a good basis for investigating its influence on the ionization of D-region. Figure 6 shows part of the record of field strength on 6.06 MHz on August 4, 1972. In the concluding period of the SID the field strength begins to recover after 1300 UT, while at 1400 UT the absorption is still quite large compared to the pre-flare period. From data ["Solar-Geophysical Data", 1973], the flux I(1-8 Å) before

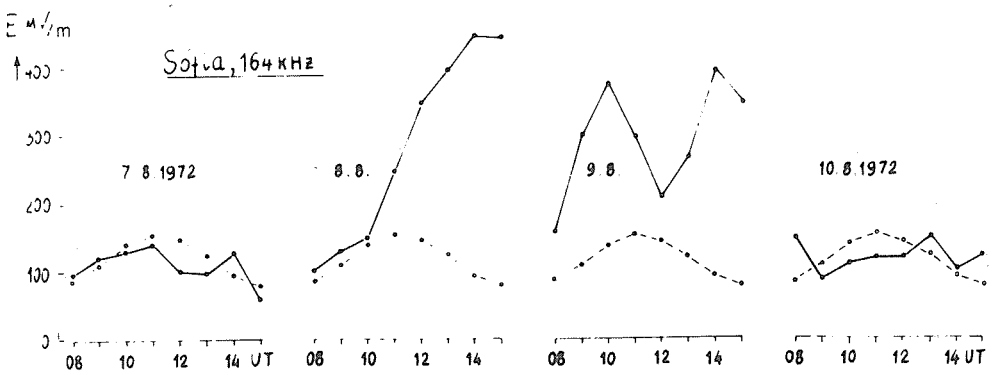

Fig. 5. Average daily variation of E_{164} (thick line) and monthly medians (dashed line) for the period 0800-1400 UT August 7-10, 1972 are shown.

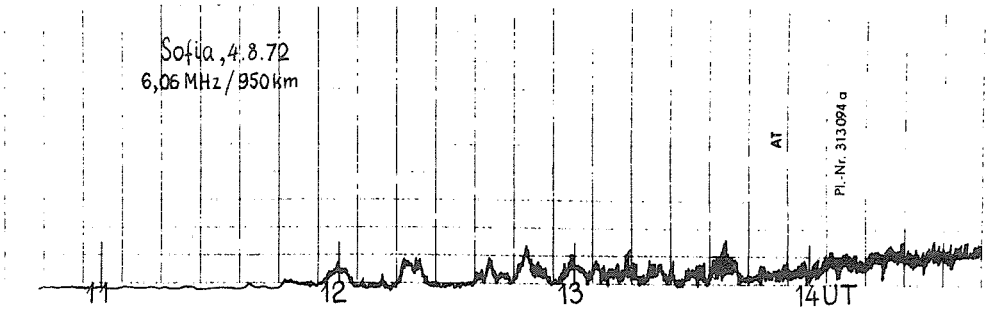

Fig. 6. Field strength variations on 6.06 MHz are shown for the period 1100 - 1400 UT August 4, 1972.

the proton flare is about 1×10^{-3}erg cm^{-2}sec^{-1}. At 1400 UT, I(1-8 Å) $\approx 6 \times 10^{-3}$erg cm^{-2}sec^{-1} and, as seen in the record, this flux is the reason for the considerable absorption in the D-region. This shows the essential influence of X-rays on the ionization of the lower ionosphere.

REFERENCES

APOSTOLOV, E. M.	1973	Differential Spectrum of Solar X-ray and its Relation with the Solar Radio-Emission (unpublished).
BUDDEN, K. G.	1961	Radio Waves in the Ionosphere, Cambridge University Press.
NESTOROV, G. T.	1967	Vremenni Variacii na Electronnata Productia v Oblasta D pri SHE, Izv. Geoph. Inst. BAN, 10, 13.
NESTOROV, G. T.	1969	Physica na Niskata Ionosphera, BAN, Sofia
NESTOROV, G. T.	1970a	Exponential Model of Ionospheric D region, Compt. rend. Acad. bulg. Sci., 23, No. 8, 939.
NESTOROV, G. T.	1970b	Experiment with Exponential Model for Ionospheric D-region, Compt. rend. Acad. bulg. Sci., 23, No. 9, 1079.
NESTOROV, G. T.	1970c	Aeronomic Characteristics of D-region and Energetic Spectra of Ionizing Radiation, Compt. rend. Acad. bulg. Sci., 23, No. 10, 1207.
NESTOROV, G. T.	1971	Solar X-ray and Particle Radiation in Connection with the Geomagnetic Storm in Late September 1969, Compt. rend. Acad. bulg. Sci., 24, No. 10, 1317.
	1972	Solar-Geophysical Data, 388, Part I, U.S. Department of Commerce, (Boulder, Colorado, U.S.A. 80302).
	1973	Solar-Geophysical Data, 342, Part II, U.S. Department of Commerce, (Boulder, Colorado, U.S.A. 80302).

Ionospheric Observations at Kiruna during July 26 - August 14, 1972

by

H. Borg and R. Lundin
Kiruna Geophysical Observatory
S-981 01 Kiruna 1, Sweden

Introduction

Ionospheric observations from Kiruna during the outstanding solar activity in August 1972 and the associated geomagnetic events are collected and presented in a synoptic figure (Figure 1). Reproductions of magnetometer and riometer records are given in separate figures. Ionosonde records from Lycksele Ionospheric Observatory, south of Kiruna, have been included in the synoptic figure to show the latitudinal variations.

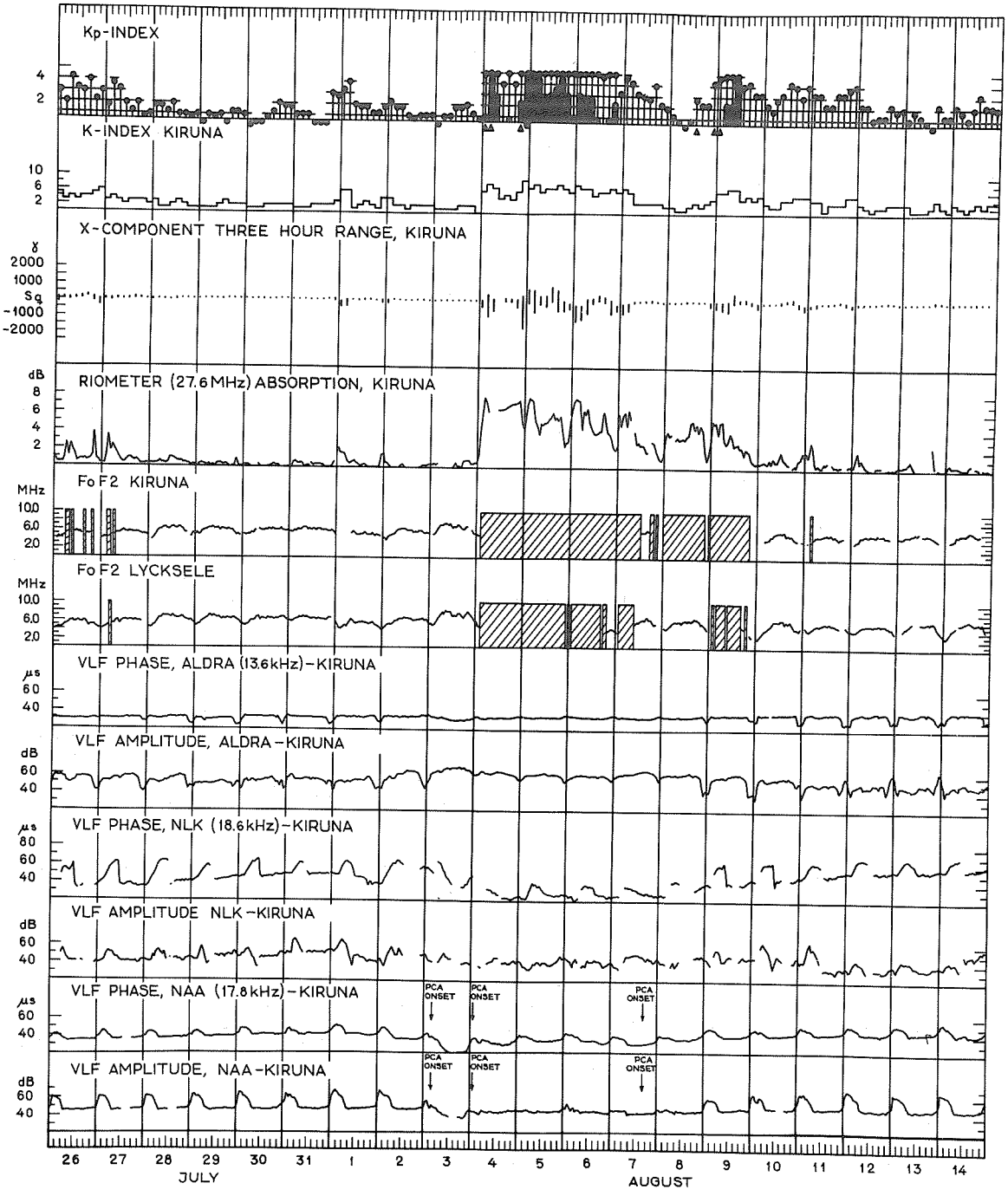

Fig. 1. Survey of ionospheric effects as recorded in Kiruna and nearby observatories. Empty areas in the plots correspond to periods of no recordings.

The coordinates of the two stations are given in the table below:

	Geographic		Corrected geomagnetic*	
	latitude	longitude	latitude	longitude
Kiruna	N67.8	E20.4	N64.8	E104.2
Lycksele	N64.6	E18.7	N61.7	E100.6

* [Gustafsson, 1970]

The ionosonde data used are reproduced from the bulletins published by the Research Institute of National Defence, Stockholm, Sweden. The geographic coordinates of the transmitters of the VLF signals received in Kiruna and shown in this data report are as follows:

NAA (17.8 kHz) N44.6 W 67.3
NLK (18.6 kHz) N48.2 W121.9
ALDRA (13.6 kHz) N66.4 E 13.2

The NLK-Kiruna path crosses the central polar cap while the NAA-Kiruna and ALDRA-Kiruna paths are tangential to the auroral zone.

VLF recordings

In terms of phase advance and amplitude decrease on the VLF signal, three PCA events were observed: (0415 UT August 3; 0115 UT August 4; 1610 UT August 7). Similarily, two minor PCA's were detected on 19 and 22 July and might possibly be related to the same flare regions causing the August events.

Riometer recordings

A very strong cosmic radio noise absorption at 27.6 MHz occurred during the period 3 to 10 August. The absorption was in fact so heavy that the diurnal variation normally seen was not as pronounced. The absorption during 4 August was constantly above the 6 dB level. For further details see Figures 2, 3 and 4.

Ionosonde recordings

The absorption is manifested in the plots of the critical frequency of the F2-layer as black-outs and are shown in Figure 1 as crosshatched areas. A period of almost continuous black-out was observed in Kiruna between 4 (0300 UT) and 9 (1900 UT) August and in Lycksele during 4 (0300 UT) and 6 (2000 UT) August.

Magnetometer recordings

A large geomagnetic storm started with an sc at 0120 UT on 4 August after a period of relative quietness. The storm period ending on 7 August is characterized by quite intense disturbances, often with extended periods of pulsations. On 4 August at 2150 UT the X-component deviated by -1100γ from the Sq value and the Z-component by 940γ, indicating an auroral electrojet located south of Kiruna. The maximum deviation of the X-component (-1750γ) seen during the period occurred at 2248 UT 4 August.

The second moderate storm appeared during the period 8 to 12 August with an onset time just before midnight.

Remarks

Except for the fact that the ionospheric effects are very pronounced in the data, no unexpected effects are seen. With the variety of flares occurring in the period it is difficult to relate the ionospheric events to any specific flare. Evidently the strong geomagnetic storm and the period of heavy absorption, both starting almost simultaneously, must be due to particles released from the sun at different times.

REFERENCES

G. GUSTAFSSON 1970 Arkiv für Geofysik, 5, 595

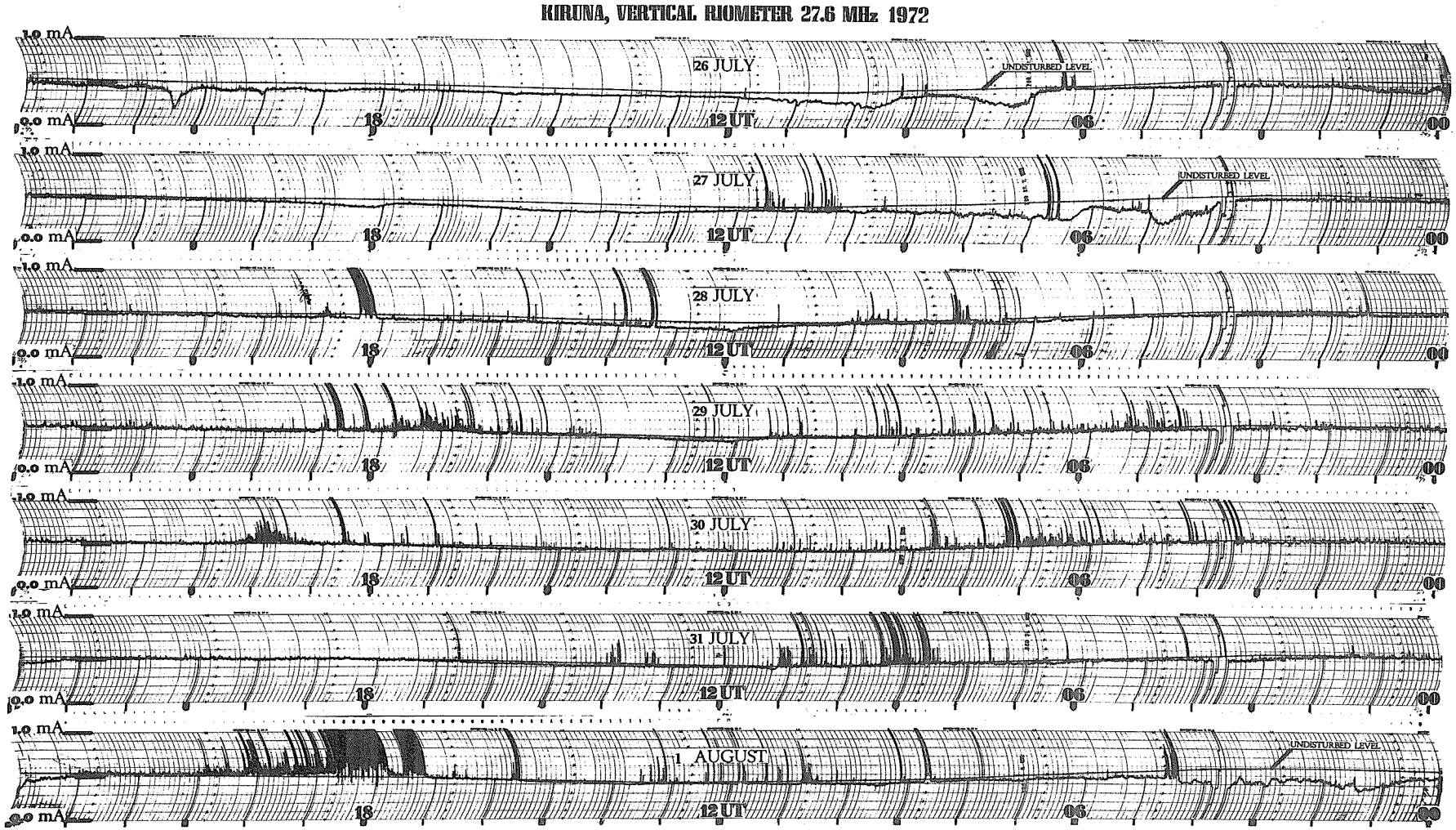

Fig. 2. Riometer records from Kiruna on 27.6 MHz.

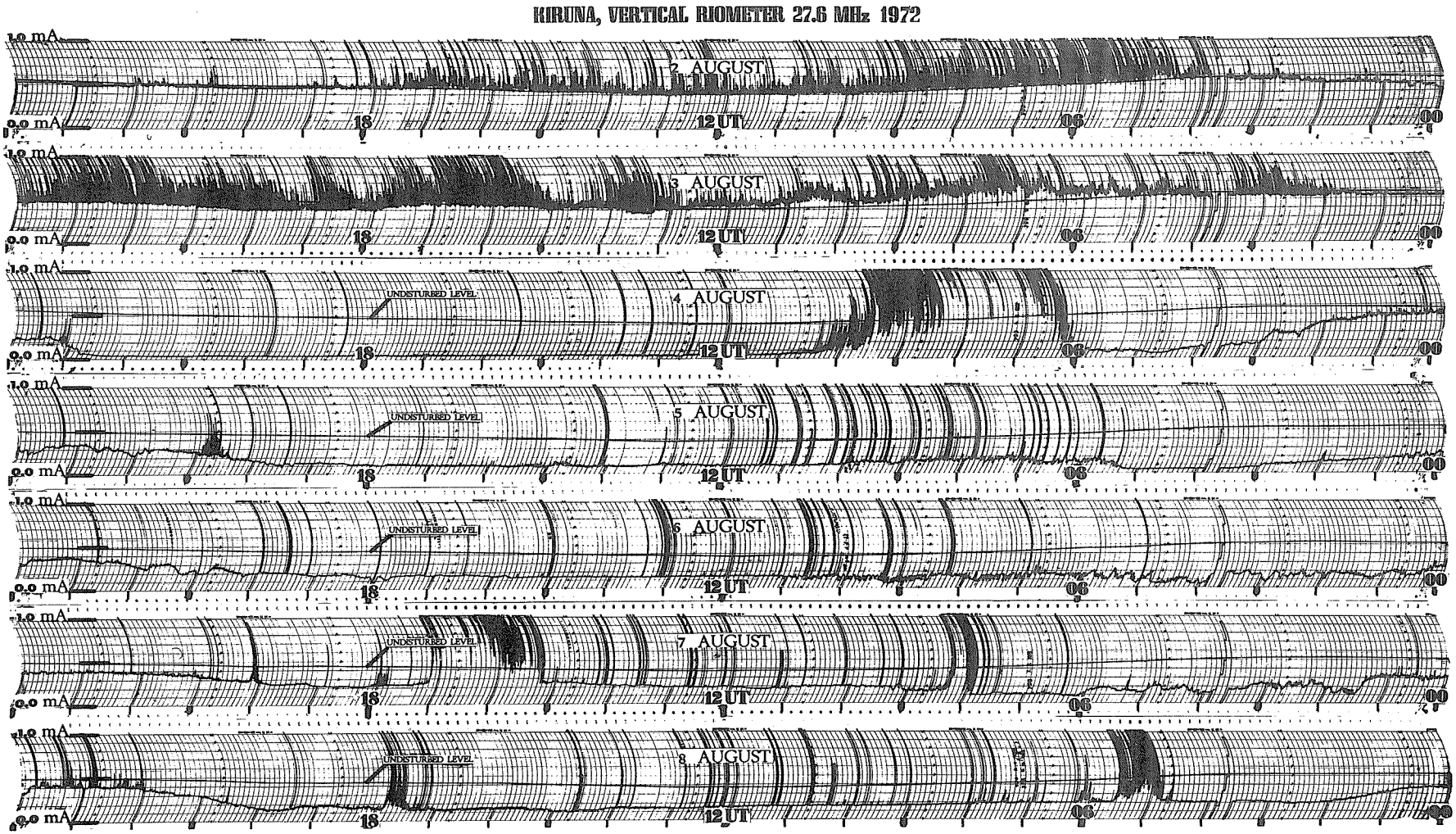

Fig. 3. Riometer records from Kiruna on 27.6 MHz.

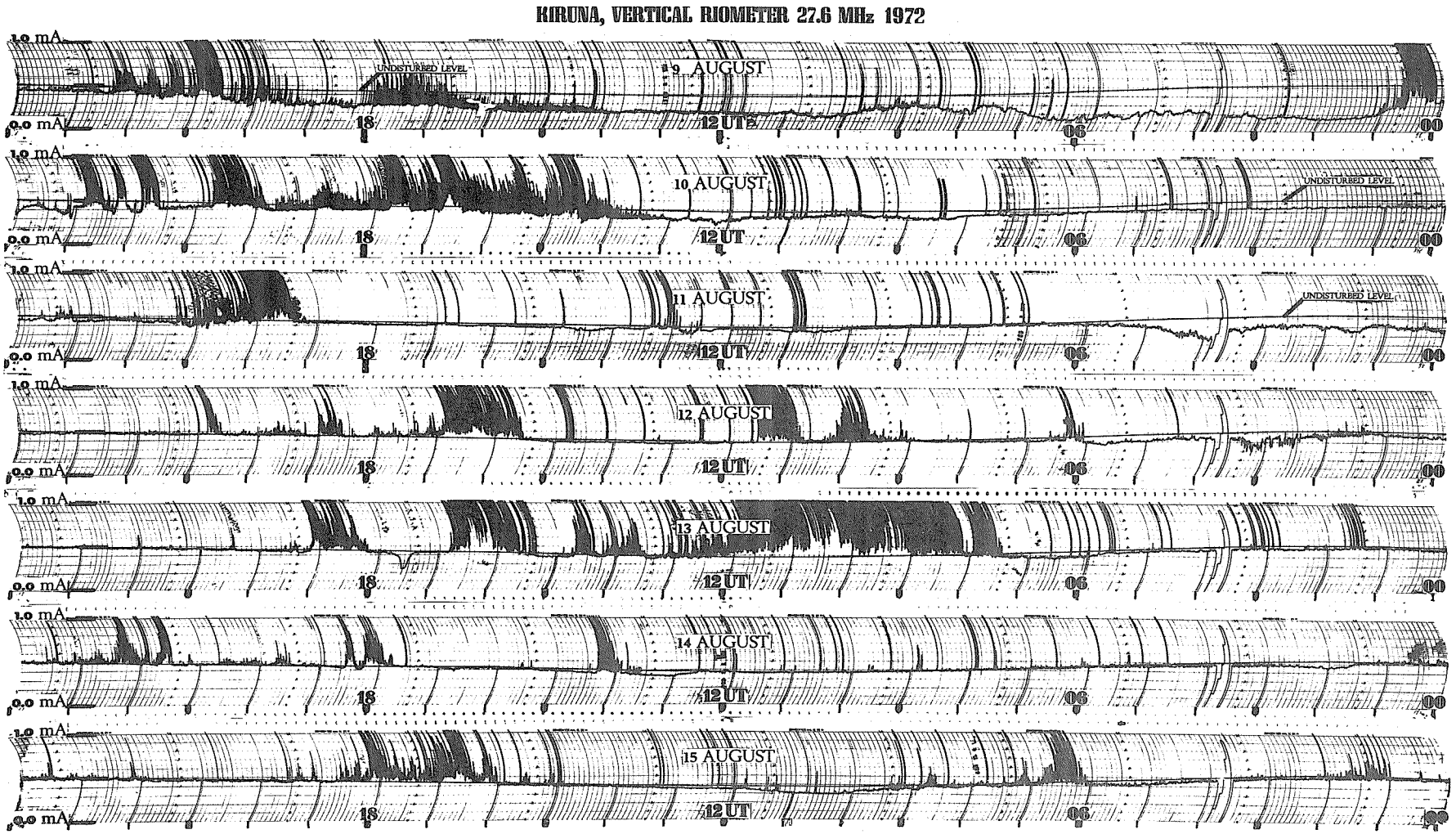

Fig. 4. Riometer records from Kiruna on 27.6 MHz.

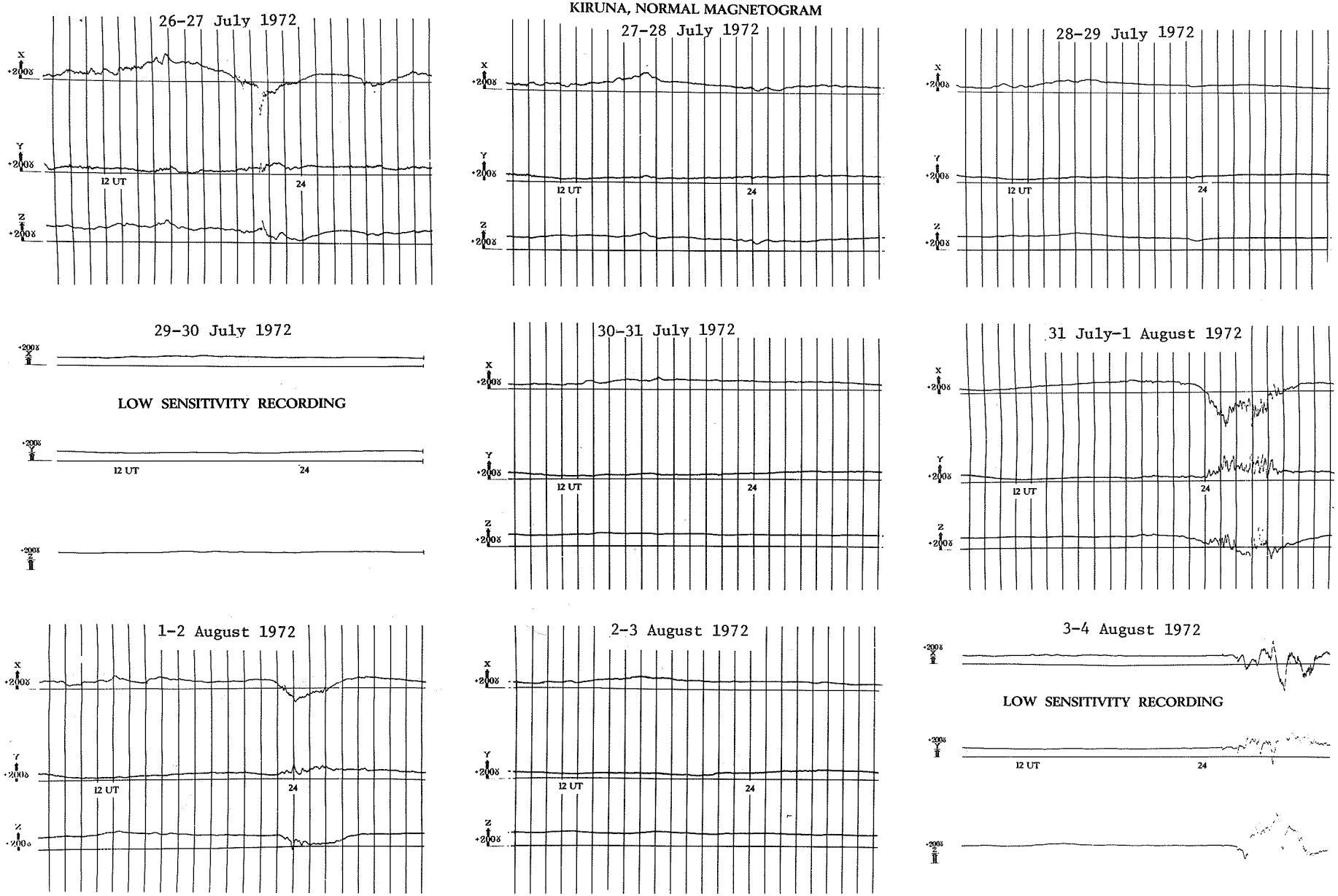

Fig. 5. Kiruna normal magnetograms. The reproductions are extracted from "Kiruna Geophysical Data". Note the low-sensitivity recordings.

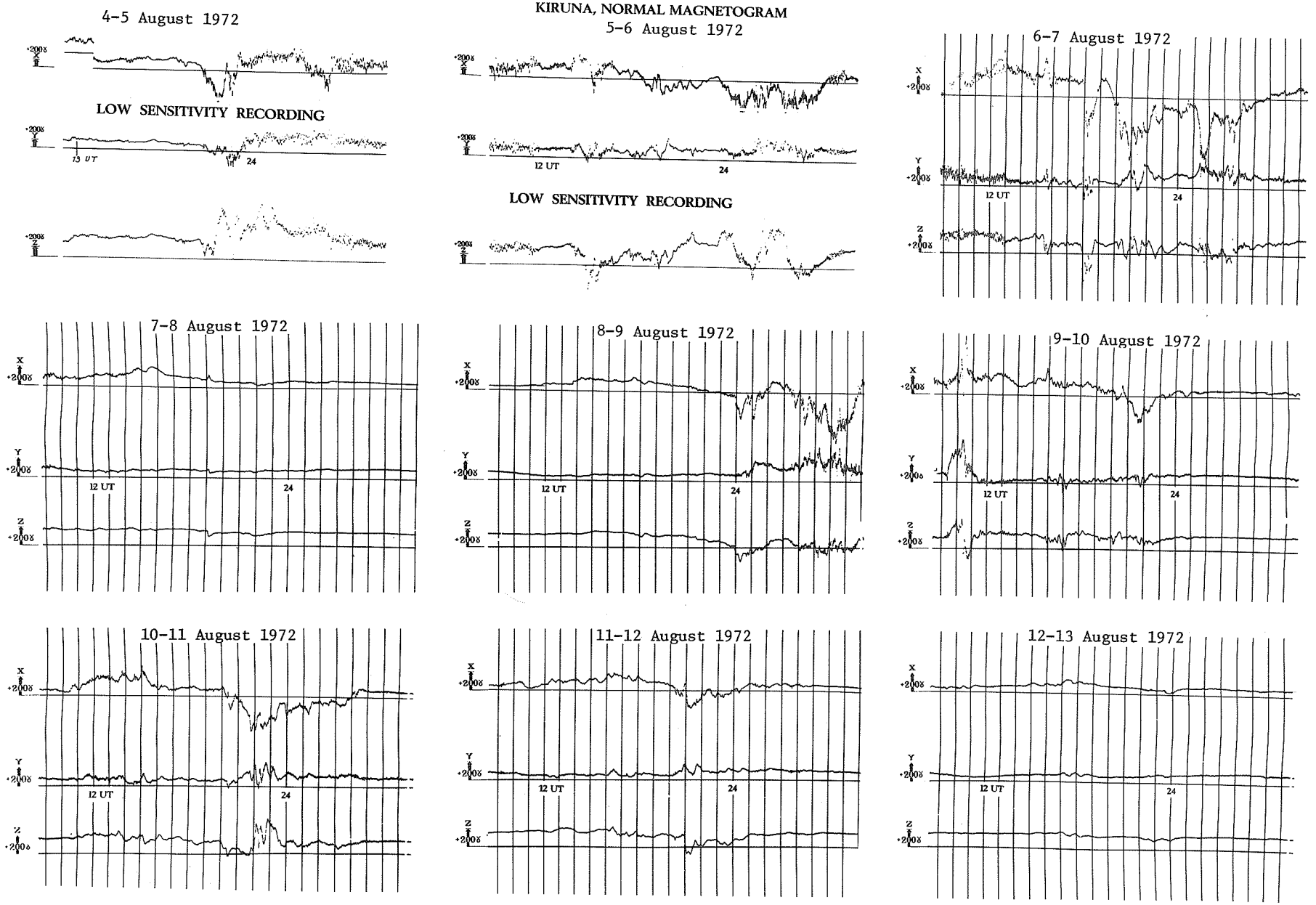

Fig. 6. Kiruna normal magnetograms. The reproductions are extracted from "Kiruna Geophysical Data". Note the low-sensitivity recordings.

Effects of the Solar Activity in August 1972 on the Circuit Kalundborg - Lindau (245 kHz, 456 km)

by

Chr. Timpe
Max-Planck-Institut für Aeronomie
Institut für Ionosphärenphysik
3411, Lindau, Federal Republic of Germany

ABSTRACT

The long wave Kalundborg - Lindau circuit is not useful for the determination of solar flare effects, and even in August 1972 no effect could be detected. But between August 4 and 12 during evening hours, an enhancement of absorption occurred, probably due to solar particles. It is shown how this additional absorption can be explained by an increase of ionization in the D-region.

The Long Wave Circuit Kalundborg - Lindau

Since 1971 at Lindau (E10.1, N51.6) the Danish long wave transmitter Kalundborg has been recorded on 245 kHz to determine absorption in the lower ionosphere. The principle of the antenna and receiving system is the same as described by Sprenger and Lauter [1966]. By means of a loop antenna perpendicular to the direction of propagation, the ground wave is suppressed completely while the field strength of the sky wave (which, in general, is very much less than the field strength of the ground wave) can still be measured. It was possible to calculate simple exponential electron density profiles for the height-range from about 75 km to about 95 km using pairs of absorption values measured simultaneously on the Kalundborg - Lindau circuit and the short-wave (2.775 MHz) Kiel - Lindau circuit [Timpe, 1973].

It seems remarkable that the Kalundborg - Lindau circuit is not useful for the determination of solar flare effects. At no time during the running of this equipment could any effect be clearly detected. Only the beginnings of some effects could be identified, provided they were known from other measurements. It seems therefore that during a flare the increasing electron density in the D-region not only causes a stronger absorption but also a better reflection of the long wave.

Particular Effects in August 1972

Even the strongest solar flare effects in August 1972 were not detectable on the long wave circuit. But on August 2 in the morning and from August 4 to 12 in the evening the absorption on 245 kHz was abnormally high Figure 1 shows the absorption values between July 26 and August 14, 1972 for 1900 MET (1800 UT, solar zenith angle $\cos\chi = 0.1$) and 2000 MET (near sunset). Especially on August 4, when the largest solar flare effect was recorded, the absorption was extremely high even two hours after sunset. It should be mentioned that the enhancement of absorption on each of the short wave circuits, e.g. Kiel - Lindau (2.775 MHz), was of the same order, with the exception of August 4, when the absorption on 2.775 MHz was only a little higher than normal (compare the distribution by Schwentek, elsewhere in this compilation). Unfortunately, the transmitter in Kalundborg is switched off between midnight and 0600 MET, so there are no absorption values from the early morning.

The enhancement of absorption is probably due to solar particles and it is equivalent to an increase of ionization in the D-region of the ionosphere. Figure 2 shows several electron density profiles for 1900 and 2000 MET which were computed from the absorption values at 245 kHz and 2.775 MHz according to the method described by Timpe [1973]. The profiles (a) hold for normal conditions and are computed from median values between July 26 and August 3, 1972. The profiles (b) and (c) are computed from the values of August 4 and August 5 to 12, respectively. The Figure shows that at 1900 MET in the height range 80 to 90 km the electron densities of profiles (b) and (c) are about twice as great as that of profile (a). On August 4 the same rate still appears at 2000 MET, while on the other days (August 5-12) the electron density is increased by the factor 1.4 on the average. So the solar particle influx led to a rather high ionization in the D-region even on the night-side of the earth.

REFERENCES

SPRENGER, K., and E. A. LAUTER (1966): Verfahren zur Messung der ionosphärischen Absorption (A3-Methode) im Lang-und Mittelwellenbereich, Veröffentlichungen des Nationalkomitee für Geodäsie und Geophysik der Deutschen Akademie der Wissenschaften zu Berlin, Nr. II/1, 47 - 66.

TIMPE, CHR. 1973

Ein Verfahren zur Bestimmung angenäherter Elektronendichte-profile der unteren Ionosphäre aus Absorptionsmessungen bei 245 kHz, 2.775 MHz und 27.6 MHz, (Approximate electron-density profiles of the lower ionosphere from measurements of absorption at 245 kHz, 2.775 MHz and 27.6 MHz) to be published in Z. Geophys.

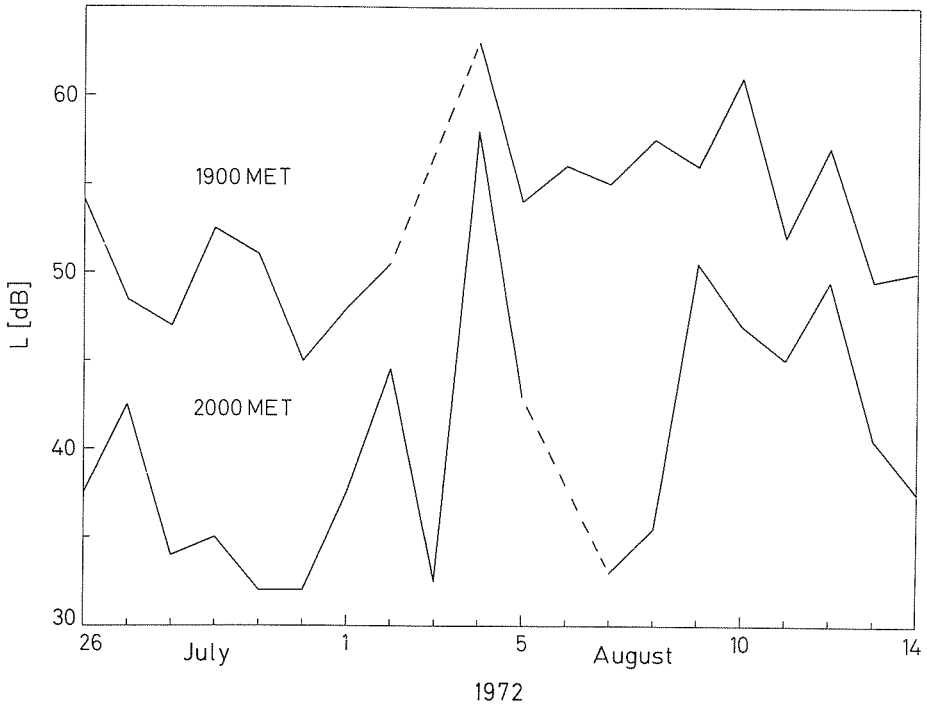

Fig. 1. Absorption L (dB) for the period July 26 to August 14, 1972 at 1900 MET (1800 UT, sun's zenith angle $\cos\chi = 0.1$) and 2000 MET (near sunset).

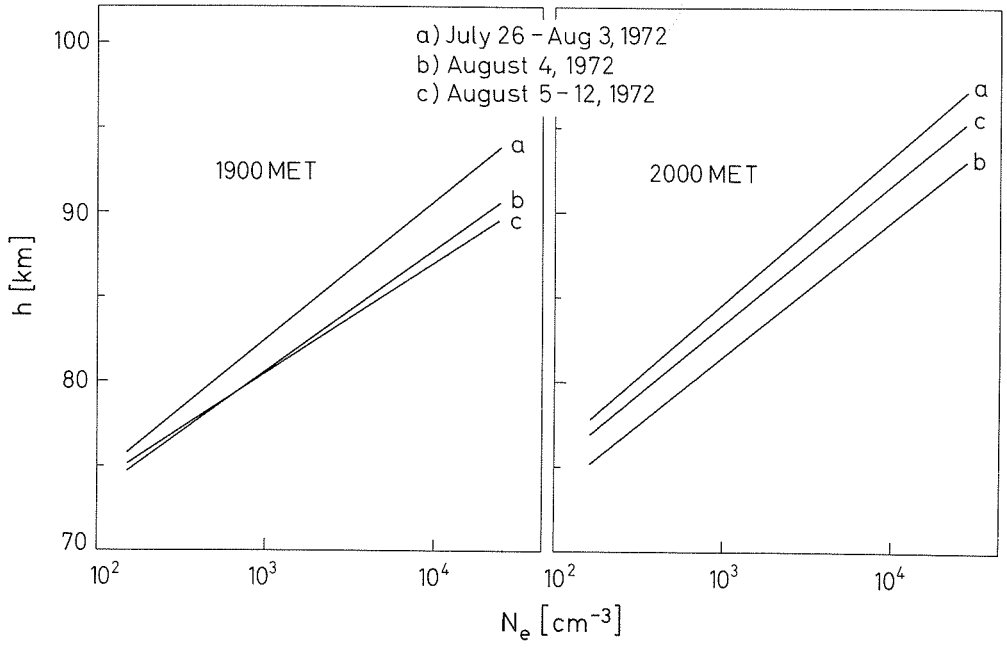

Fig. 2. Exponential electron density profiles computed from absorption values at 245 kHz and 2.775 MHz.

Corpuscular Effects in the Night Ionosphere during the Period July 26 - August 14, 1972

by

P. Velinov and G. Nestorov
Geophysical Institute
Bulgarian Academy of Sciences
Sofia, Bulgaria

This paper deals with some effects in the night ionosphere which have occurred as a consequence of the penetration of energetic particles into the high atmosphere during the period of unusual solar activity July 26 - August 14, 1972 associated with the transit of McMath Plage Region 11976. This period is connected also with the strongest geomagnetic storm during the current solar cycle [Lincoln et al., 1972].

The analysis was done on the basis of absorption measurements by the A3-method in the LF, MF, and HF ranges at the ionospheric observatory in Sofia (N42.6, E23.4) as shown in Table 1. The information from these measurements refers to the altitude interval from 80 to 200 km depending on the frequency of the observation. The angle of incidence of the wave on the reflective region is denoted by i.

Table 1

Station	Frequency f (kHz)	Distance d(km)	f cos(i) (kHz)
Brašov	155	370	75
Allouis	164	1720	25
Krajova	557	180	420
Pleven	593	140	480
Vakarel	827	35	820
Pristina	1412	170	1200

The variations in the absorption L_{155}, L_{164}, L_{557}, L_{593}, L_{827}, and L_{1412} on July 27 and 28, 1972 (Figs. 1-3) are aftereffects of particle precipitation when the geomagnetic activity on July 25 had increased and A_p index reached 33. The aftereffect arises 2 or 3 days after the zero day, which agrees with our theoretical results [Nestorov and Velinov, 1972].

The absorption effect on July 30 (weak increase of L_{557}, L_{593}, L_{1412}, L_{155}, and L_{164} and decrease of L_{827}) may be associated with the increase of the proton flux recorded by Explorer 41 (1969-53 A) during the night of July 28-29 when protons with energies greater than 10 Mev reached the value $\approx 10^4$/ster cm^{2}sec, but after that quickly dropped on the same day.

The weak increase in geomagnetic activity (A_p=10) on August 1 gives a weak precipitation of particles which leads to some increase of the absorption L_{827} and L_{155} on August 1, and L_{593}, L_{1412}, and L_{164} on August 2. The fact that the effect is more significant on paths 827 and 1412 kHz shows that these particles are comparatively soft.

The strong geomagnetic storm on August 4-5 (A_p = 132-182), whose effect on the lower ionosphere is discussed later in detail, has its main influence on L_{164} and L_{557} on August 5 and on L_{593}, L_{1412}, and L_{827} on August 6. Here the aftereffect appears on August 8, the two types of corpuscular events on the high atmosphere being commensurable in magnitude. Although the particle flux penetrating the ionosphere during the first half of August 1972 is significant, it is just on August 6 and 8 that the largest hourly averages flux particles are recorded by ATS - 1, sometimes attaining 680 to 491 particles cm^{-2}sec^{-1}, respectively, in the energy level 21 - 70 Mev. As is well known, the solar proton flux measured by ATS -1 is representative of the flux in interplanetary space and over the polar caps; and so the effects in the whole ionosphere on 6 and 8 August support the PCA influence on the middle latitude ionosphere. Since a strong PCA occurs as early as August 3 it is worth investigating its influence more in detail, especially on the lower ionosphere (see Fig. 4).

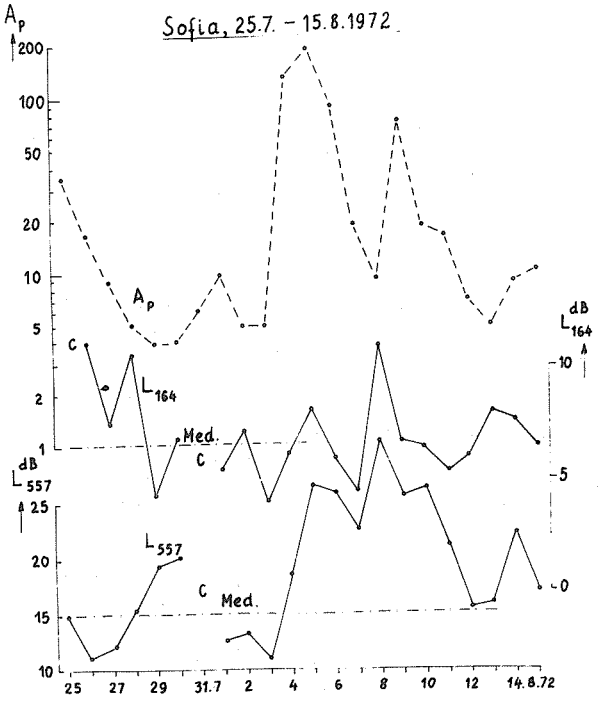

Fig. 1. Variation of A_p and absorption L_{164} and L_{557} for the period July 25 - August 15, 1972.

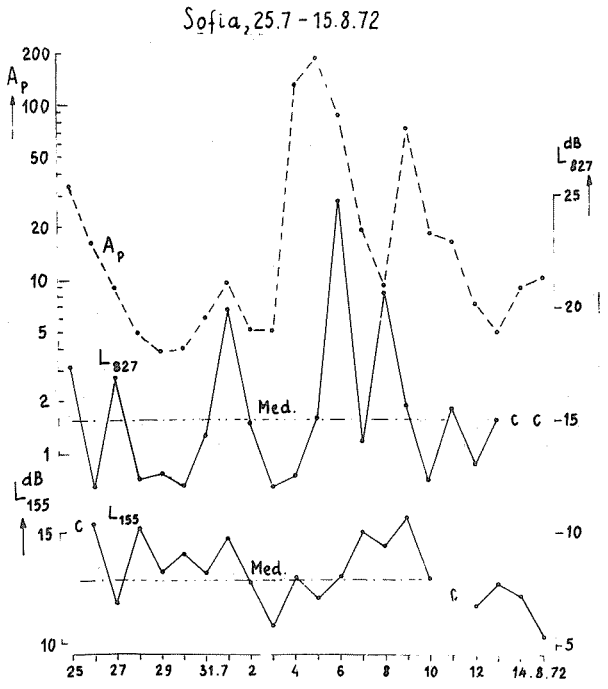

Fig. 2. Variation of A_p and absorption L_{827} and L_{155} for the period July 25 - August 15, 1972.

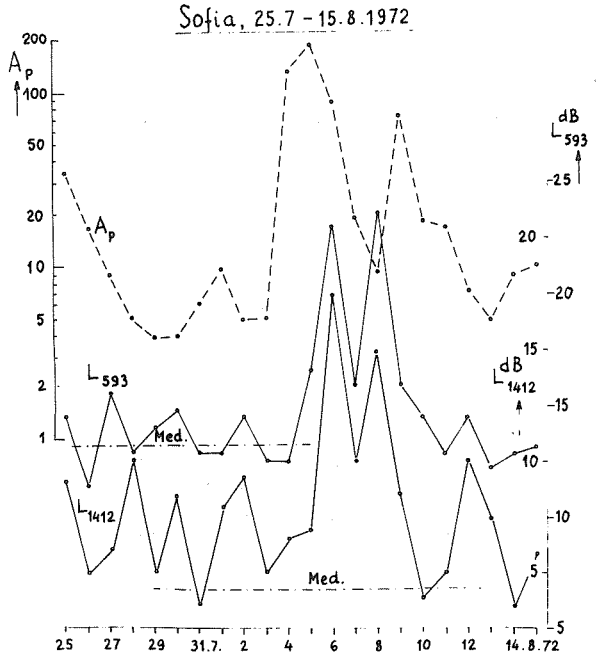

Fig. 3. Variation of A_p and absorption L_{593} and L_{1412} for the period July 25 - August 15, 1972.

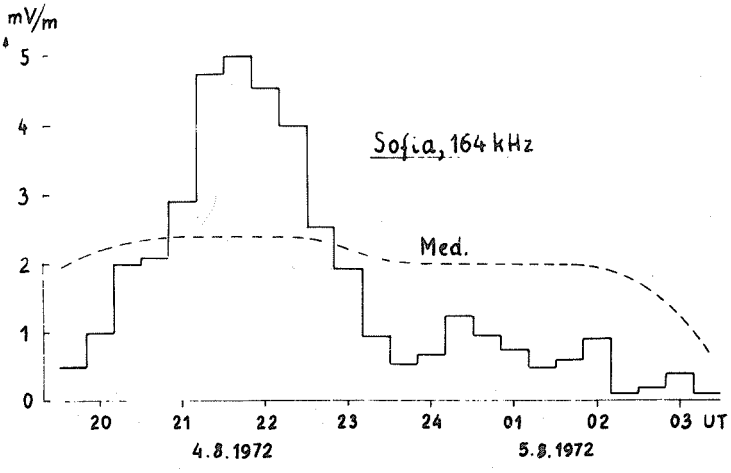

Fig. 4. Variation of field strength on 164 kHz during the night of August 4-5, 1972.

The new increase in geomagnetic activity on August 9 (A_p=74) has some effect on L in the ionosphere on August 11 and 12, which is associated with the weak increase of the proton flux recorded by ATS - 1 on the same days.

In Figure 4 we present the variation of field strength on 164 kHz during the night of August 4-5, i.e. during the main effect when there has been a strong Forbush effect provoked by the strong geomagnetic storm. In such cases we usually observe an ionization increase in the lower ionosphere independent of the galactic cosmic ray flux because of the geomagnetic threshold as well [Velinov, 1971]. However, from Figure 4 it is seen that in the interval 2100-2300 UT a very high field strength is observed which significantly surpasses the monthly median value L_m = 6 dB. For about 30 minutes in the indicated interval the absorption drops down to $L \simeq 0$ dB, which indicates strong increase of the electron concentration gradient in the reflection region, probably caused by the particle precipitation, whose main part causes a powerful PCA effect at the same time. Indeed, comparing the records in Figure 4 and riometer data from McMurdo, a coincidence of the maximum effects in the interval 2100-2200 UT is seen. The maximum phase of the powerful geomagnetic storm develops during this interval; that is why it is probable that the increased ionization produced by the particle precipitation, together with the sudden sharp increase in the system of currents in the night E-layer from the geomagnetic storm, contribute to the formation of a steep ionization gradient which reflects the radio waves almost ideally, i.e. with a reflection coefficient $\rho \simeq 1$. The gradual decrease in the amplitude of the geomagnetic field variations, as well as the strong Forbush-effect increase after 2200, lead to a decrease in field strength at 164 kHz, which is caused by the increase of the deviative absorption as a consequence of the high gradient layer dissolution (i.e. the reflection is diffusive, which is confirmed by the record character after 2200 UT), as well as by the increase in nondeviative absorption as a consequence of the increased cosmic ray flux in the high atmosphere. This is also the traditional influence of Forbush-effects on the ionization condition of the cosmic layer in the lower ionosphere.

From the above it is seen that the behavior of the lower ionosphere the night of August 4-5, is really unusual. This is due to the coincidence of several factors (geomagnetic storm PCA effect and its influence on the middle latitude ionosphere, Forbush-decrease of the galactic cosmic rays, etc.). Here some estimates will be made for comparison of the contribution of the different factors in the complex. On the basis of the record from Figure 4 after 2300 UT, when the absorption begins to approach $L \simeq 18$ dB from a monthly median value (for 2300-0300 UT) $L_m \simeq 8$ dB, the increase of the electron production rate can be estimated by using the equation for its relative increase

$$\frac{\Delta q}{q} = \frac{\Delta L}{L}\left(2+\frac{\Delta L}{L}\right), \qquad (1)$$

where q and L are the mean or median values in the quiet period, and Δq and ΔL the respective deviations. Hence at ΔL=10 dB and L_{med} = 8 dB we obtain

$$\frac{\Delta q}{q} \simeq 400\%.$$

However, from this additional ionization only an insignificant part is determined by the Forbush effect, which is easily established by the variation equation of q from the galactic cosmic rays at a height h in the high atmosphere [Velinov, 1971].

$$\frac{\delta q(h)}{q(h)} = \frac{\delta \rho(h)}{\rho(h)} - \delta R_c W_q(R_c) + \int_{R_c}^{\infty} W_q(R)\,\frac{\delta n(R)}{N(R)}\,dR,$$

where the first term on the right-hand side represents the change due to atmospheric density variation, the second one as that due to the geomagnetic threshold variation R_c (i.e. resulting from the geomagnetic variation) and the third one as that due to the variation of the primary cosmic ray spectrum. In strong geomagnetic storms the second term is very important; from it and for R_c=5 BV, we can determine

$$\frac{\Delta q}{q} = 30\%$$

for the present geomagnetic storm and at middle latitudes, where the reflection point of the 964 kHz signal is situated. A relative increase of the absorption corresponds to this additional ionization from equation (1)

$$\frac{\Delta L}{L} = \sqrt{1+\frac{\Delta q}{q}} - 1$$

or

$$\frac{\Delta L}{L} \simeq 14\%, \text{ i.e. } \Delta L \simeq 1 \text{ dB},$$

which is an order of magnitude less than the general ΔL during the period under investigation. Therefore, the remaining 9 dB from the general ΔL are determined by high energy solar particle penetration. It is very probable that, under the conditions of the strong geomagnetic storm and the powerful PCA event, an insignificant part of the solar cosmic rays also penetrate the area of the middle latitudes. This effect could be called a middle-latitude influence of PCA.

On the basis of equation (1) and the values of L_{557} in Figure 1, the flux of precipitating particles on August 8 can be estimated in the interval 80-110 km in the manner indicated by Nestorov and Velinov [1972]. At L_{med}=15 dB and ΔL=15 dB, $\Delta q/q$=3 is obtained -- for this additional ionization a flux 3.10^{-4}erg cm^{-2} sec^{-1} is necessary.

Thus, we see the number of unusual phenomena which have arisen during the period of July 26 - August 14. For example, the main influence of the strong geomagnetic storm from August 4 appears on the day zero as well as 2 and 4 days after it, i.e. the influence is in three stages, while the mean statistical picture of the geomagnetic storms influence on the ionization state of the night ionosphere so far was the effect on the zero day and the aftereffect on two days after it.

All this speaks of the complexity and peculiarity of the processes in the solar-terrestrial relationships during the unusual solar activity in the period under investigation.

REFERENCES

NESTOROV, G. and P. VELINOV — 1972 — Ionospheric Effects from Solar Particles during January 24 - February 3, 1971, World Data Center A for Solar-Terrestrial Physics, Report UAG-24, Part I, 240.

LINCOLN, J. V. and H. I. LEIGHTON — 1972 — Preliminary Compilation of Data for Retrospective World Interval July 26 - August 14, 1972, World Data Center A for Solar-Terrestrial Physics, Report UAG-21.

VELINOV, P. — 1971 — On Variations of the Cosmic Ray Layer in the Lower Ionosphere, J. Atmos. Terr. Phys., 33, 429.

Simultaneous Measurement of LF Wave Intensities and Phase at Hiraiso

by

N. Wakai, C. Ouchi and S. Fujii
Hiraiso Branch, Radio Research Laboratories
Japan

Loran-C pulse signals (Northwest Pacific chain, SS-3, 100 kHz) from four transmitters have been recorded at Hiraiso (36° 22' N, 140° 38' E) since 1970. Details of the observation are described in the paper by Wakai et al. [1973].

Outline of Loran-C transmitters necessary to comprehend the meaning of data presented herein is shown in Table 1.

Table 1. Function and position of Loran-C station, and great circle distance and azimuthal angle of path.

Transmitter	Position (degree) (Lat. N, Long. E)	Distance (km)	Azimuth* (degree)	Power (MW)
Master (Iwojima)	24.8 141.33	1287	176.8	4
W-Slave (Marcus)	24.28 153.98	1852	132.76	4
X-Slave (Hokkaido)	42.75 143.72	757	19.51	0.6
Y-Slave (Okinawa)	26.6 128.15	1602	230.87	0.6

*angle of arrival at the receiver from transmitters (measured clockwise from north)

Figures 1 to 4 show unusual variations of amplitude and phase of Loran-C signals associated with distinctive solar X-ray bursts during August 2 to 9, 1972. In those figures, the ordinate of amplitude records is scaled in dB above a relative level for four signals (M, solid; W, dashed; X, dotted; and Y, dash-dot lines). The phase record is given just for M station signal, being scaled in microseconds. As the carrier frequency is 100 kHz, 10 microseconds corresponds to 360° in phase angle.

The tracking point of phase was placed at the eighth cycle behind the start of pulse (80 microseconds delayed). In the propagation path between Iwojima and Hiraiso, the first and second hop E-modes arrive at the receiver with about 50 and 120 microseconds delay, respectively. Accordingly, the phase measured refers to that of the resultant vector of the ground wave and the first hop sky wave components.

The phase record in the figures always shows the advance associated with the flare as indicated by arrows marked at the onset of SID's, while the amplitude shows complex variations with sudden drop or enhancement, depending upon the solar zenith angle, path length and the magnitude of X-ray burst.

REFERENCES

WAKAI N., S. FUJII and C. OUCHI 1973 SID effects as observed in intensities of LF radio waves, J. Rad. Res. Labs. (Japan), 20, (in press).

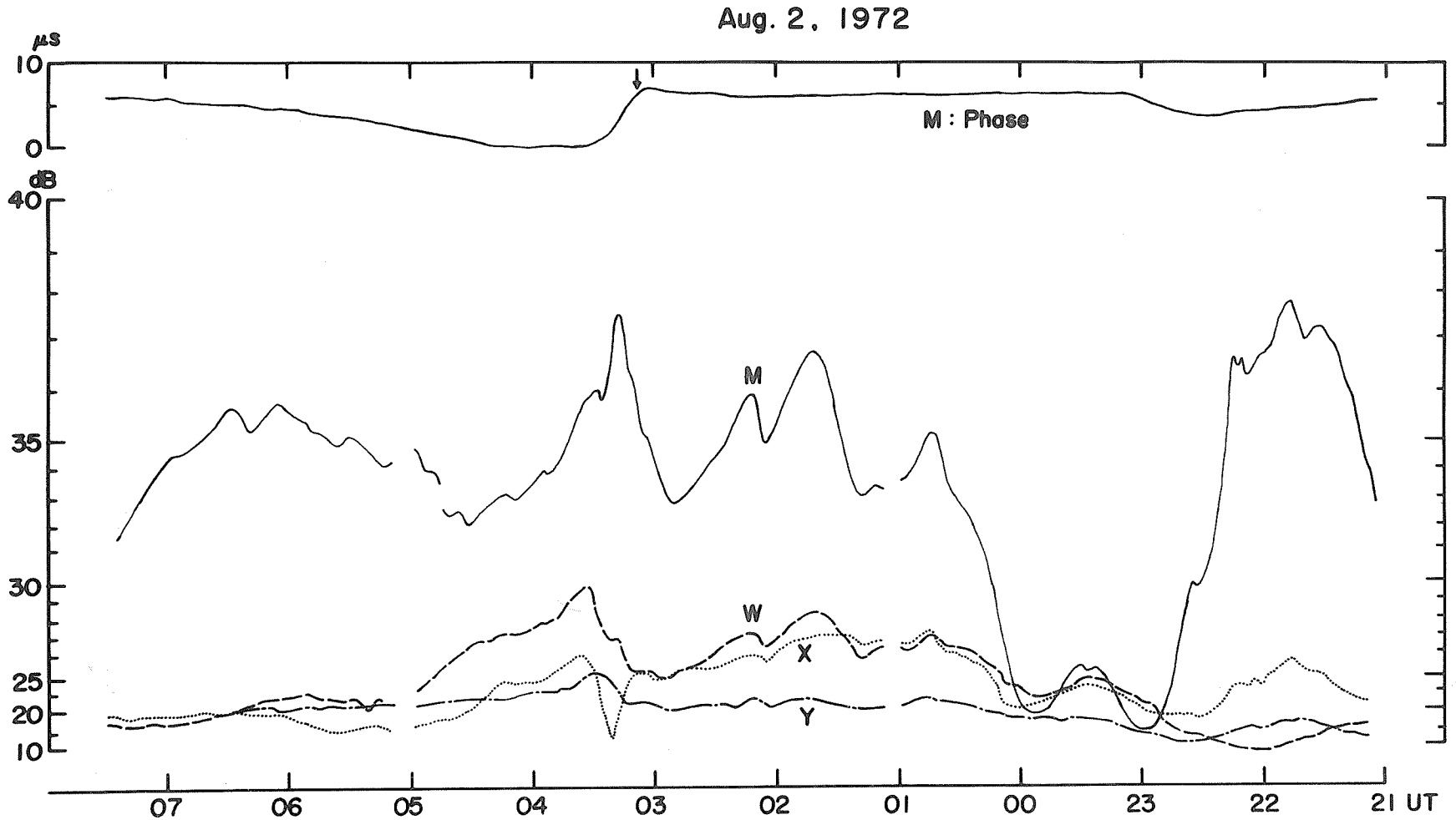

Fig. 1. Variation of amplitudes and phase of Loran-C signals for August 2, 1972. Ordinate of amplitude is scaled in dB above a relative level (M, solid; W, dashed; X, dotted; Y, dash-dot lines). Phase is given for M only.

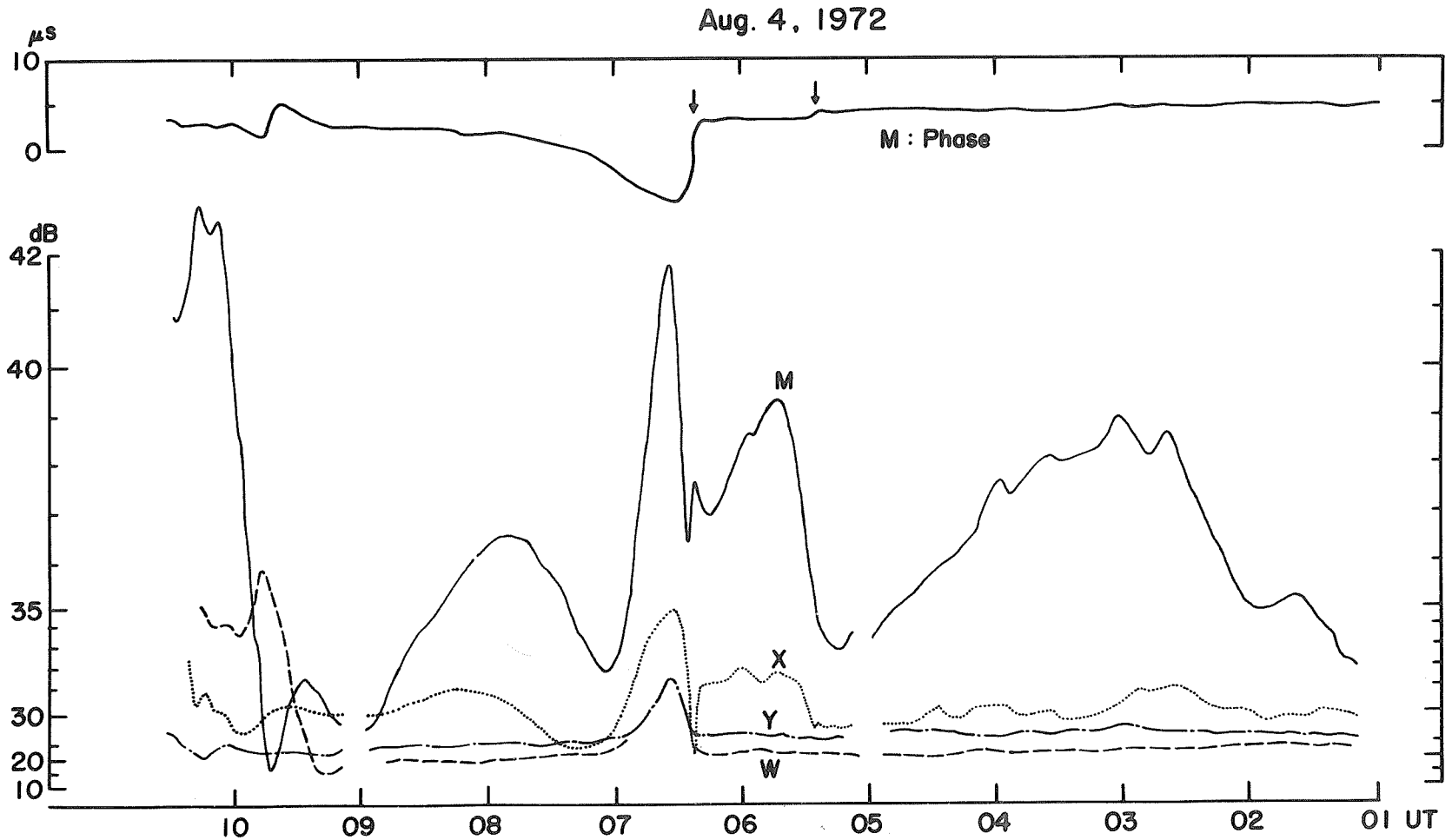

Fig. 2. Same as Figure 1 for August 4, 1972.

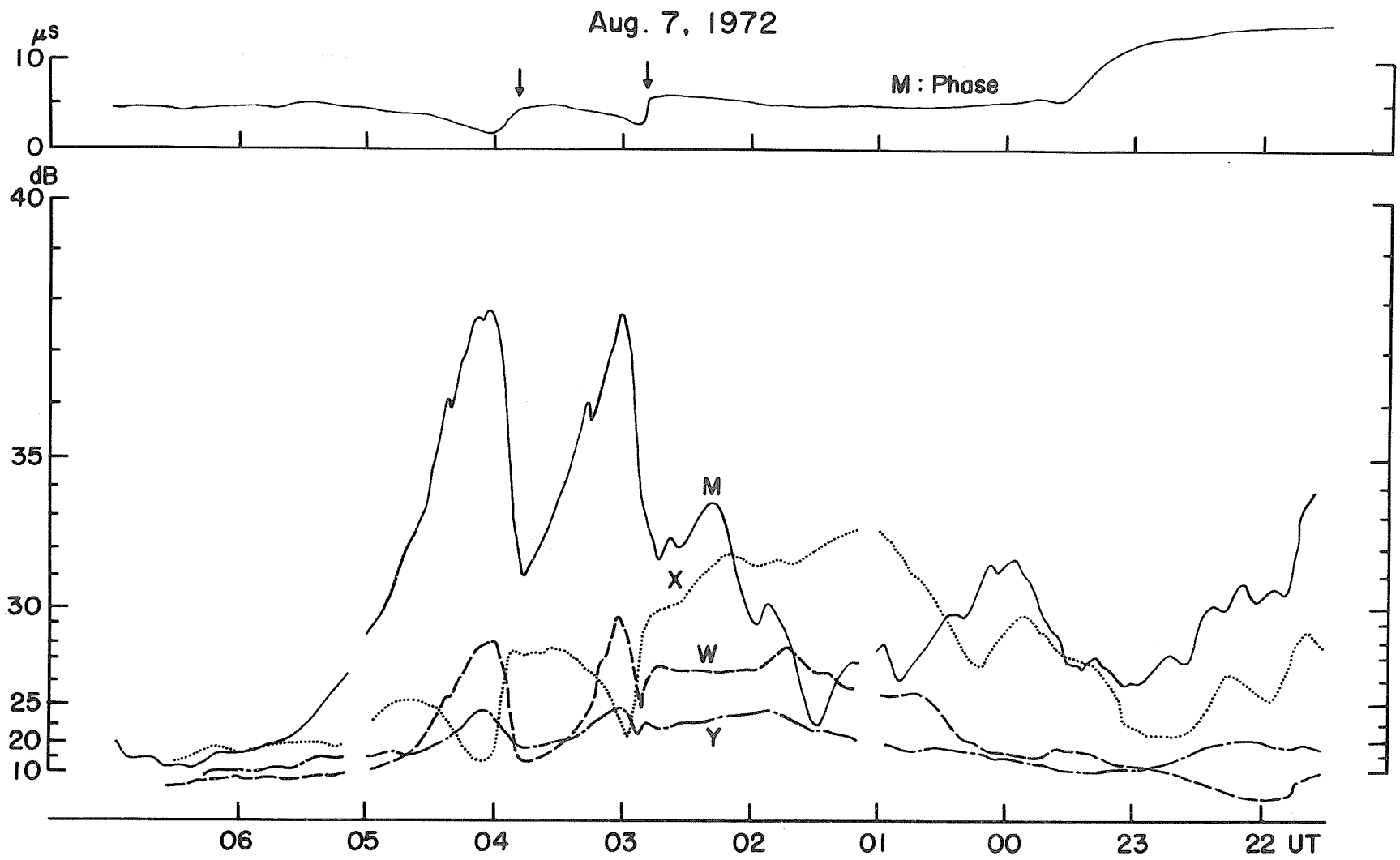

Fig. 3. Same as Figure 1 for August 7, 1972.

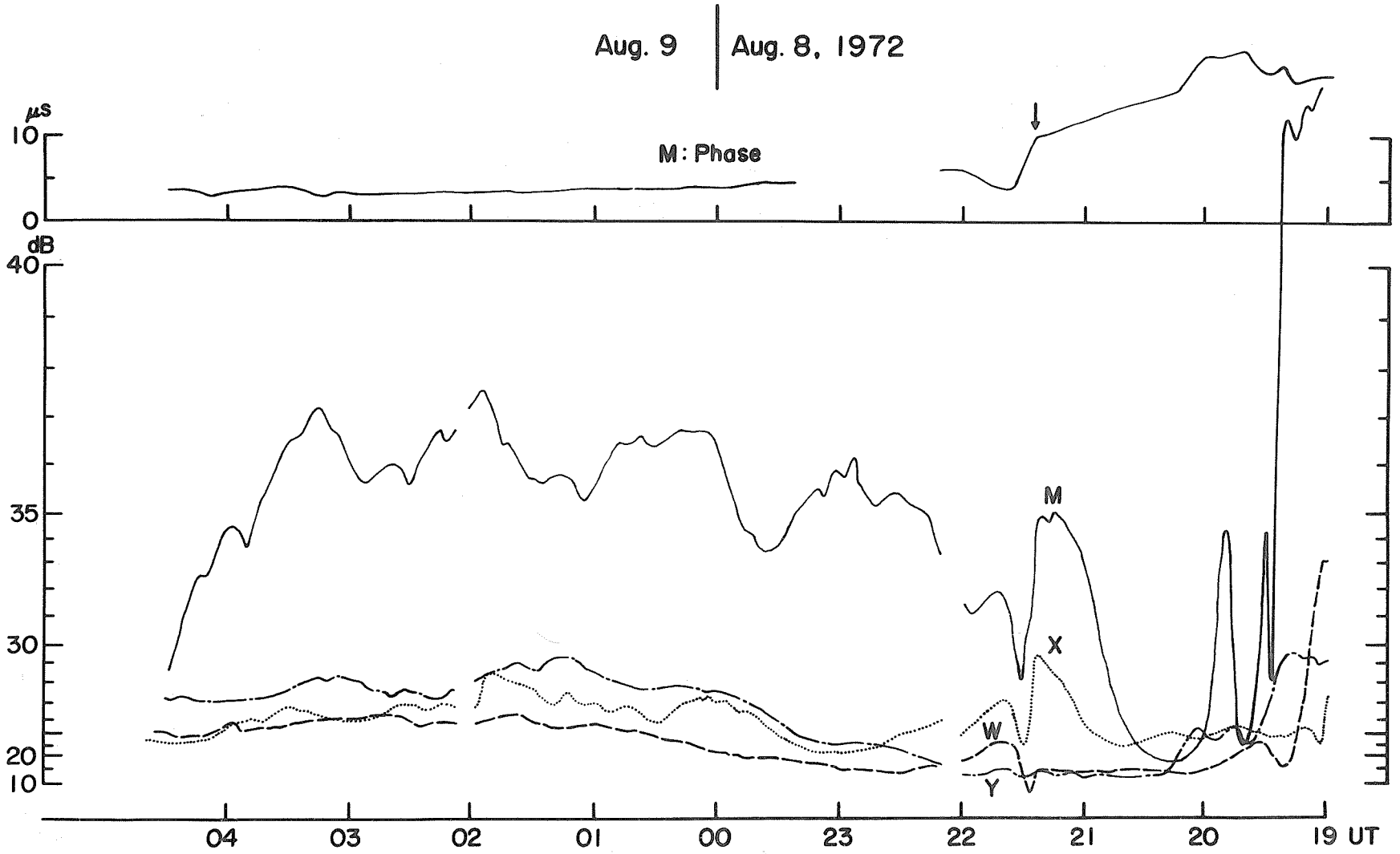

Fig. 4. Same as Figure 1 for August 8-9, 1972.

Effects on Transequatorial VLF Propagation for Retrospective World Interval July 26 - August 14, 1972

by

Y. Sahai and M. A. O. Sales
Instituto de Pesquisas Espaciais
Sao Jose dos Campos - SP - Brasil

This report presents the effects observed on the transequatorial, NAA (Cutler, Maine, U.S.A.) - Sao Jose dos Campos, Brazil, VLF propagation path for Retrospective World Interval July 26 - August 14, 1972, the period of unusual solar activity associated with transit of McMath Plage Region 11976.

The data presented were obtained with a VLF receiving station installed at this Institute (Lat. S23.3, Long. W45.8). The tracking station comprises a "TRACOR" model 599J VLF/LF tracking receiver, a shielded loop antenna (TRACOR model 599-603D) and a "Hewlett-Packard" Cesium Beam Frequency Standard model 5061A. Phase tracking is obtained with a receiver gain of 70 dB and time constant of 50 seconds. The phase and amplitude are recorded on strip-chart recorders and variations can be scaled to an accuracy of $\pm$ 1 μsec and 0.7 dB, respectively.

Tables 1 and 2 give details of the Sudden Phase Anomalies (SPA) and Sudden Enhancements of VLF signals (SES) observed during this period, respectively.

Sahai and Rai [1973] have discussed the effects of the magnetic storm of August 4 - 5, 1972 on this VLF propagation path. The magnetic storm was observed at Sao Jose dos Campos on August 4, 1972 with sudden commencement at 2050 UT, followed by another larger sudden commencement at 2240 UT. The main phase of the storm began at about 2330 UT; a partial recovery occurred at 0400 UT on August 5, but the disturbance continued on subsequent days also. The VLF phase and amplitude records for the NAA - SJC path, along with the magnetogram obtained at Sao Jose dos Campos for August 4 - 5, 1972 are shown in Figure 1a. The corresponding records for August 1 - 2, 1972 (a quiet day) are shown in Figure 1b for comparison. The phase records for August 4 - 5 show a phase advance at 2330 UT, and thereafter the phase continues to be disturbed throughout the night. There is no effect seen on the phase in association with the first sudden commencement at 2050 UT, as during that period NAA - SJC path was going through the sun-set transition. The VLF amplitude record for August 4 - 5, 1972 shows marked amplitude variations. It may also be mentioned that VLF records for several nights following the magnetic storm were disturbed.

REFERENCE

SAHAI, Y. and D. B. RAI 1973 "VLF propagation effects associated with magnetic storms on a transequatorial path passing through Brazilian Magnetic Anomaly," communicated for publication in Jour. Atmos. Terr. Phys.

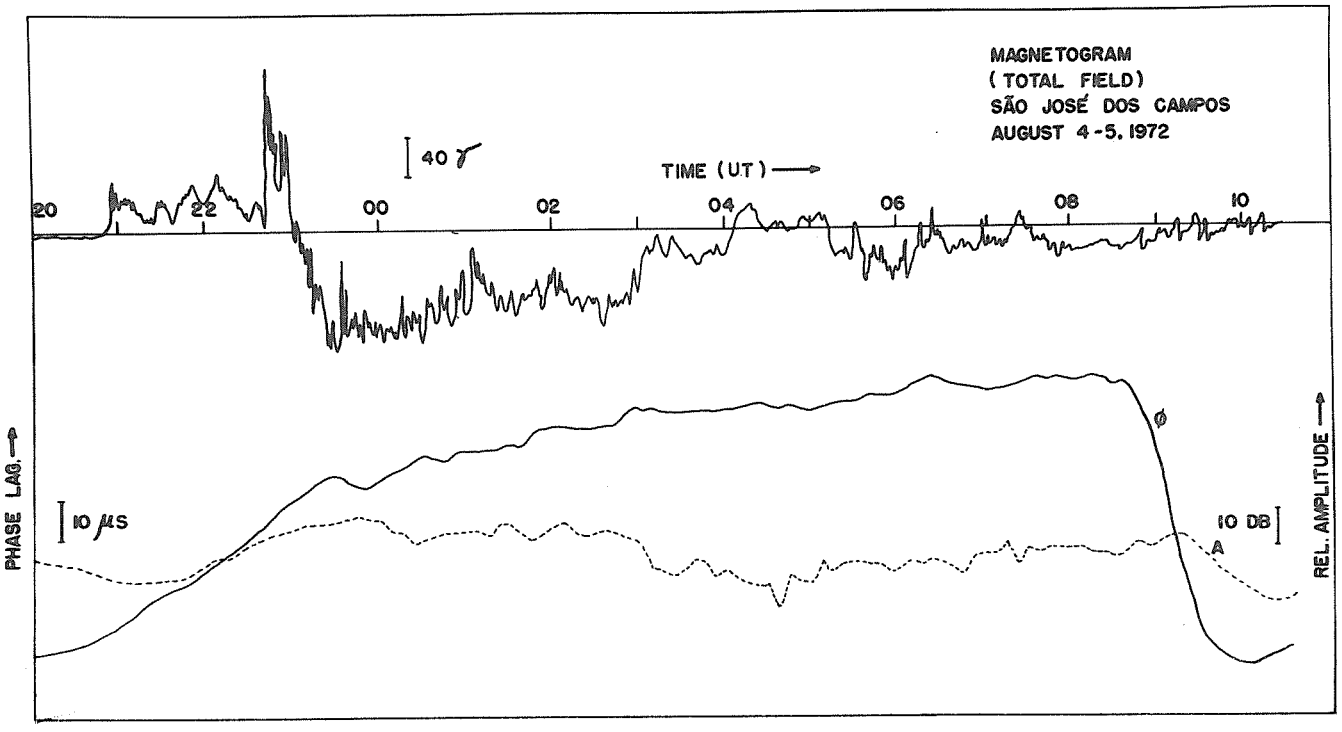

Fig. 1a. Magnetogram along with VLF phase (ϕ) and Amplitude (A) records for NAA-SJC on August 4-5, 1972.

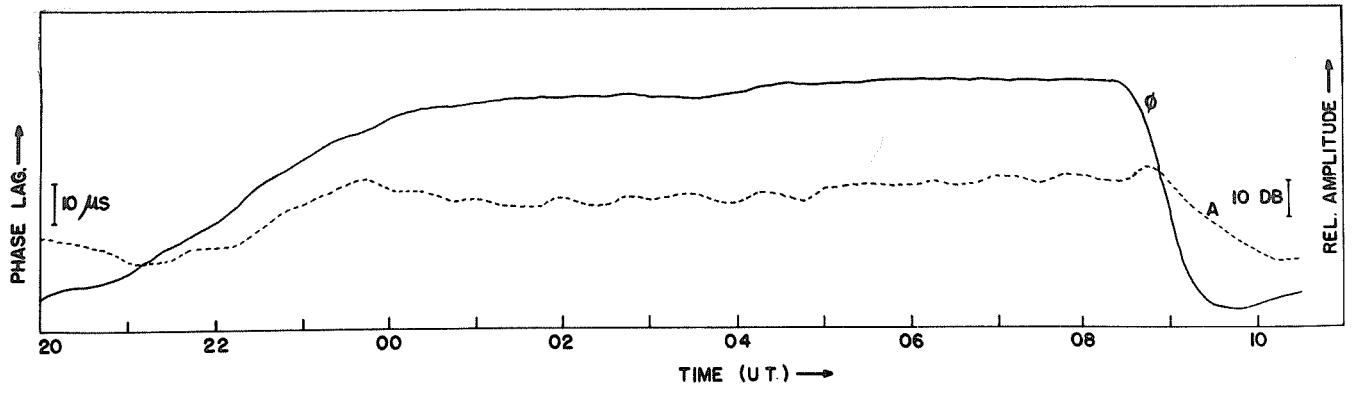

Fig. 1b. Corresponding VLF records for NAA-SJC on a quiet day August 1-2, 1972.

Table 1

Sudden Phase Anomalies - SPA
July - August 1972

Observing Station: Lat. S23.3, Long. W45.8
Sao Jose dos Campos - Brazil
Transmitter: Cutler (NAA) 17.8 kHz

Chart Speed: 1 inch per hour
Time Constant: 50 sec

DATE 1972	START UT	END UT	MAX UT	PHASE SHIFT AT MAX (μsec)
July 28	1322	*	1329	8
July 29	1857	1932	1901	2
July 30	1600	1631	1602	2
July 31	1106	*	1111	2
	1117	*	1122	8
	1201	1230	1210	10
August 1	1145	*	1152	4
	1308	1339	1313	2
	1529	1610	1535	2
	1651	1735	1653	2
	1758	1840	1806	2
August 2	1036	1120	1040	2
	1842	*	1848	14
	2004	*	2018	6
August 3	1505	1550	1510	3
August 7	1028	*	1049	4
	1138	*	1144	5
	1500	1920	1528	42
August 9	1622	1735	1630	8
August 11	1200	*	1207	4
	1223	*	1233	22
	1240	*	1247	29
August 12	1421	1610	1431	15

Table 2

Sudden Enhancements of VLF Signals - SES
July - August 1972

Observing Station: Lat. S23.3, Long. W45.8
Sao Jose dos Campos - Brazil
Frequency: 17.8 kHZ

Chart Speed: 1 inch per hour
Time Constant: 50 sec

DATE 1972	START UT	END UT	MAX UT	SES IMPT	DEFINITENESS
July 28	1319	*	1324	1 +	5
July 29	1857	1920	1900	1 -	2
July 31	1114	*	1118	2 +	4
August 1	1307	1330	1311	-	1
August 2	1045	*	1052	1 +	5
	1840	*	1845	2	5
	2001	*	2015	2	5
August 3	1500	*	1509	1 +	2
August 7	1507	1528	1512	3 +	3
August 11	1200	*	1209	2 -	1
August 12	1421	1500	1432	2	5

Measurements at the AFCRL Geopole Observatory during August 1972

by

S. M. Silverman, R. F. K. Krassa and J. P. Turtle
AFCRL Geopole Observatory
Air Force Cambridge Research Laboratories
Bedford, Massachusetts 01730

The AFCRL Geopole Observatory carries out a number of measurements of upper atmosphere parameters. These include cosmic ray, optical, magnetic, and ionospheric measurements. During the great PCA of August 1972 the optical equipment for studying atmospheric emission was not operating, the sun being above the horizon for 24 hours a day during the entire period. Riometer data from Thule will be presented elsewhere in this report together with data from other stations [Cormier, 1973]. Here we present the magnetic, micropulsation, VLF, and cosmic ray data. No analysis is attempted.

Magnetic Measurements

The magnetic activity as shown by the horizontal and vertical components of the Schonstedt Fluxgate magnetometer are shown in Figures 1 and 2. The figures have been plotted from readings made every 15 minutes. The sudden storm commencement at about 0115 UT on August 4 is evident. A second sudden storm commencement, of greater range, has occurred by 2100 UT of August 4. The onset of another storm is evident at midnight of August 8.

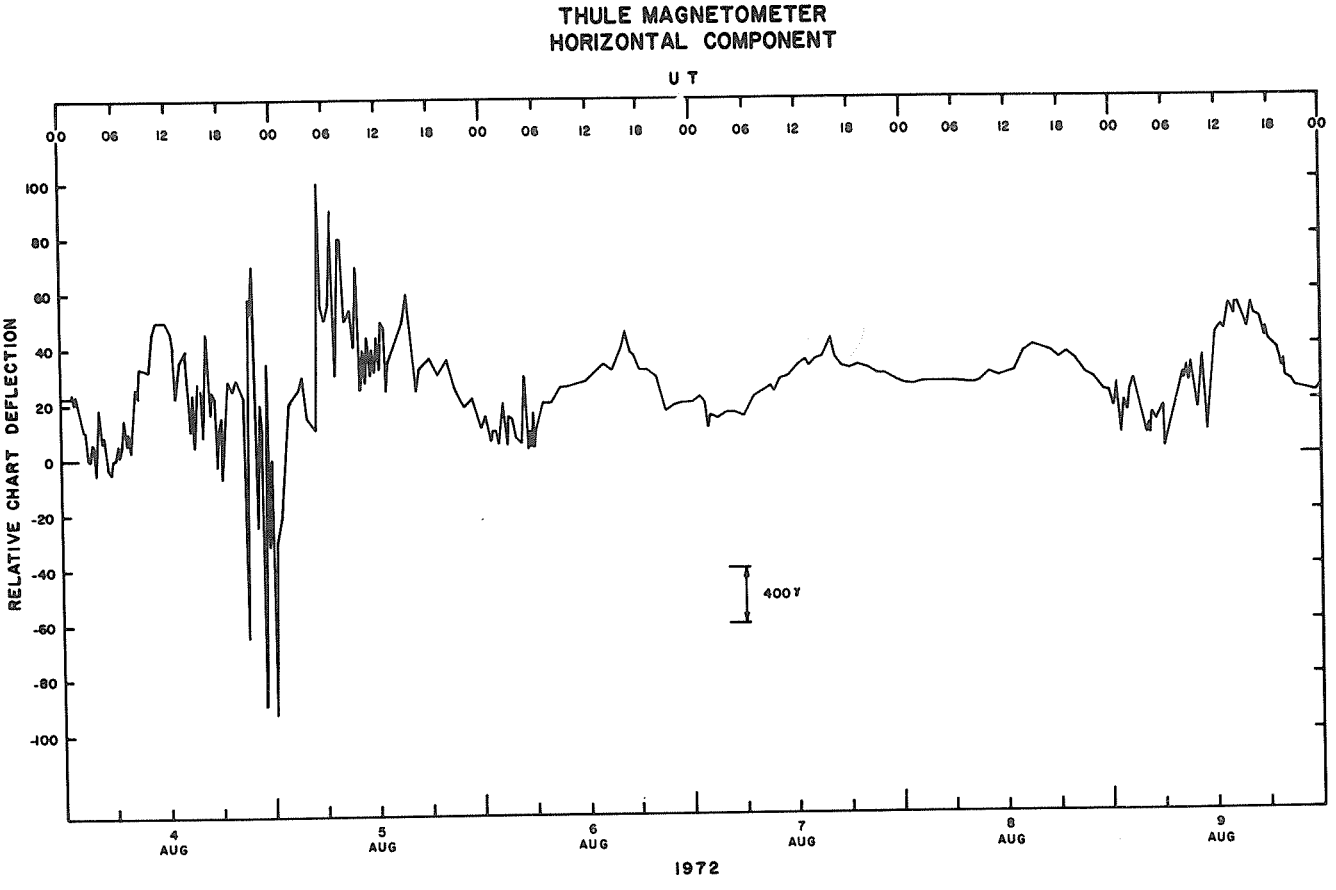

Fig. 1. Horizontal component of the magnetic field, recorded by the Thule magnetometer August 4-9, 1972.

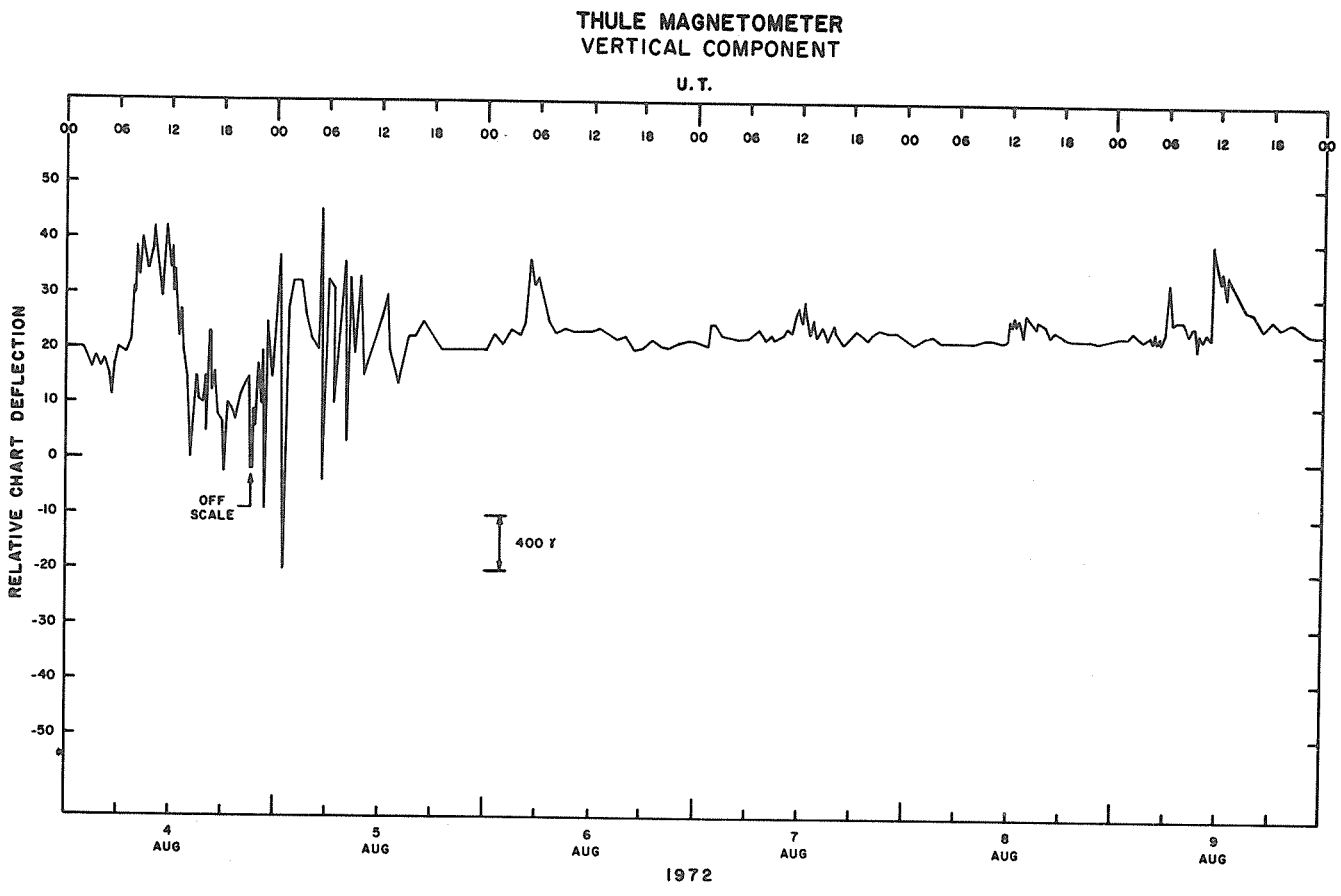

Fig. 2. Vertical component of the magnetic field, recorded by the Thule magnetometer August 4-9, 1972.

Micropulsation data in the range from 0.003 to 5 Hz are collected for the Geomagnetism Laboratory of NOAA. Thse data for the period from August 4-10 are shown in Figure 3. A major disturbance becomes evident at 2053 UT August 4, corresponding to the sudden storm commencement producing the maximum magnetometer excursions during the August 4-9 period.

Cosmic Rays

The nucleonic intensity is shown in Figure 4. A description of these events using data from a number of stations is given by Pomerantz and Duggal [1973] of the Bartol Research Foundation, the responsible experimenters for the Geopole equipment. Here I shall only briefly summarize the highlights. The Forbush decrease which reached its maximum early on August 5 was the largest recorded in some forty years of observations. It had the additional distinction of doing this in about 24 hours, which may be compared to its nearest competitor in July 1959 where the maximum reduction occurred after a seven day period. During the August 1972 period a total of three Forbush decreases occurred, two on August 4 and 5, and one on August 9. In addition, two intensity increases occurred, one on August 4 and one on August 7. The increase on August 4 seems most likely to be due to the arrival of solar particles of relativistic energies. The entire sequence of events seems to be one of the most interesting since observations of cosmic rays began.

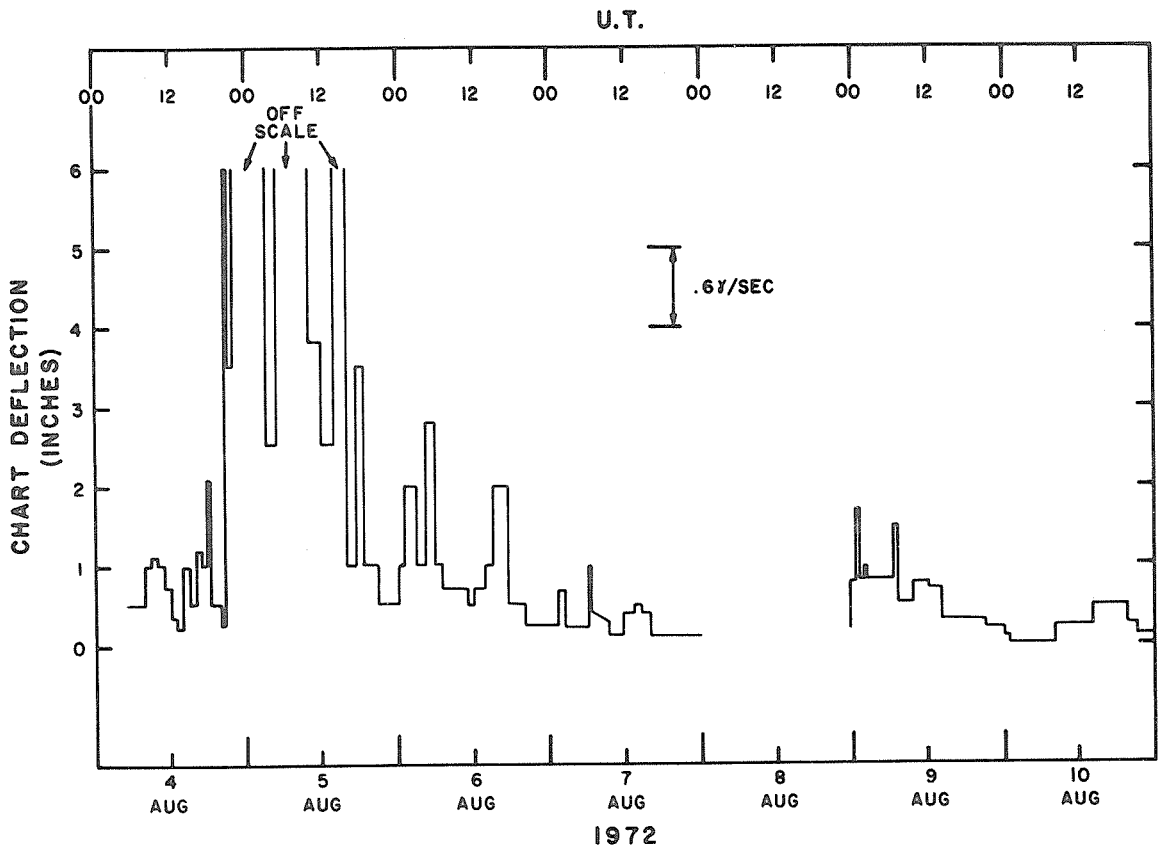

Fig. 3. Micropulsation data in the range 0.003-5 Hz for August 4-10, 1972.

VLF

VLF phase and amplitude data for the period July 26 through August 14 for the reception at Thule of the NLK/NPG transmitter in Jim Creek, Washington at 18.6 kHz are shown in Figure 5. The times of major solar flares are indicated by arrows. The data indicate that there was a small particle precipitation disturbance beginning late on July 27 and continuing through the end of July 30. For the major August event initial particle precipitation effects on VLF propagation become evident following sunrise on August 2. The particle precipitation effects reached a maximum on August 4 and were followed by a gradual recovery through August 7. Additional particle effects were produced after the flare on August 7. The recovery from disturbed propagating conditions on August 9 to almost normal conditions on August 10 was unusually rapid.

Solar Flare Effect on VLF

In the period July 26 - August 14 three solar-flare-produced SIDs were noted on the NPG-Thule records. These are shown on Figure 6. The flare at 2003 UT August 2 showed a slow development from start to maximum, and this is reflected in the effects recorded in the VLF data. The other important flares of this sunspot region occurred at times when the lower latitude portion of the path was in darkness, and therefore they did not register on the charts. A flare at 1742 UT August 15 was not from spot group 331 and is thus not included in this report but may be noted here because a flare effect was evident on the records even though the flare is listed in the Prompt Report of "Solar-Geophysical Data" [1972] only as a subflare. It appears from this that it would be of interest to compare X-ray and optical effects of flares.

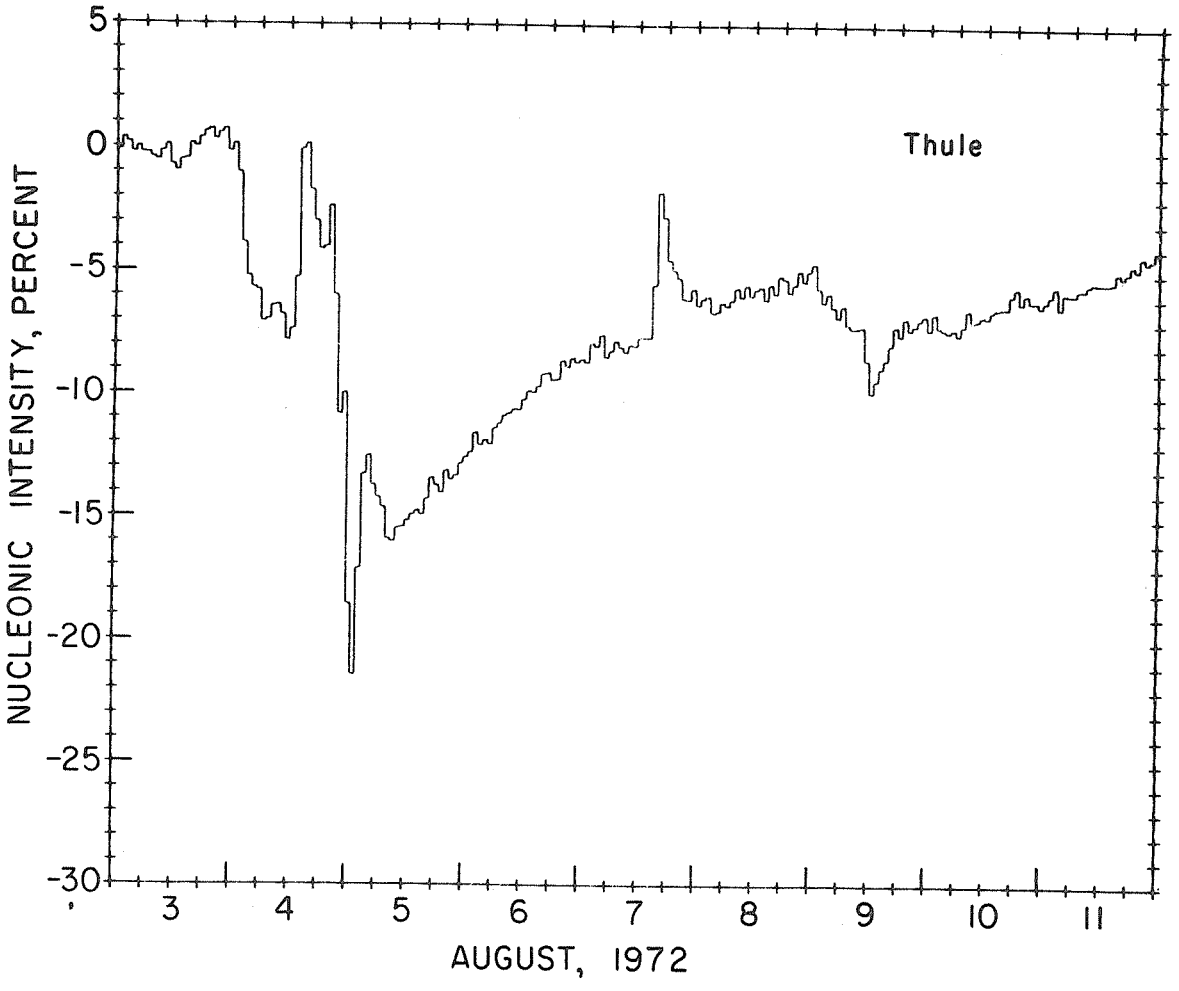

Fig. 4. Nucleonic component of the cosmic radiation observed at Thule, August 3-11, 1972.

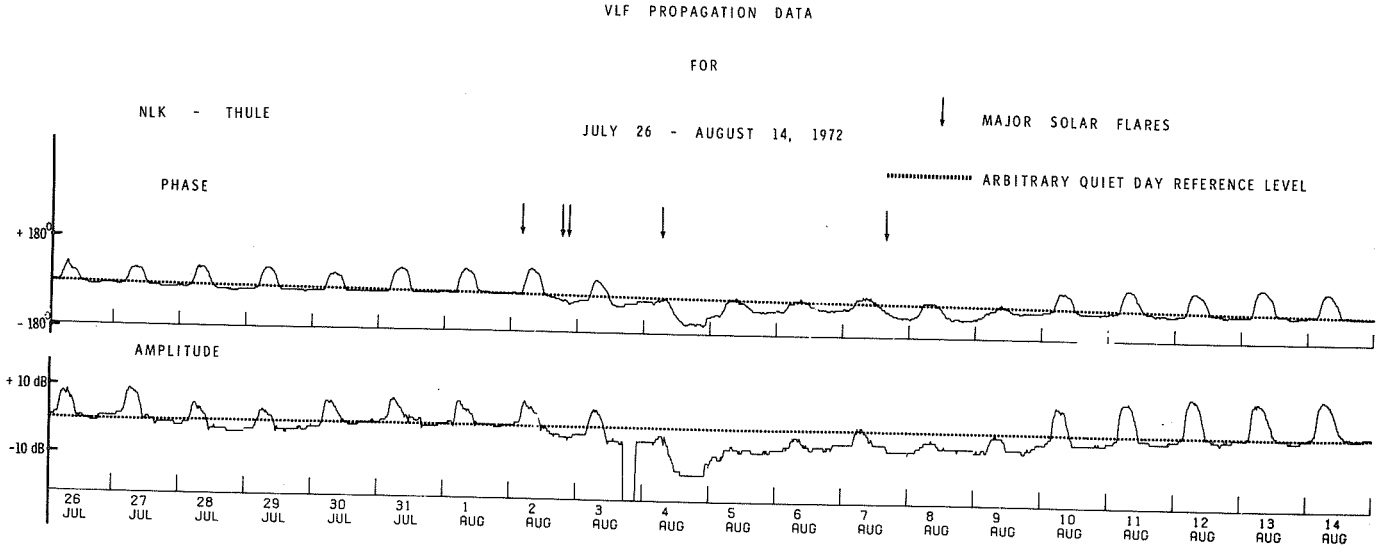

Fig. 5. VLF propagation data for the path NLK-Thule, July 25 - August 14, 1972.

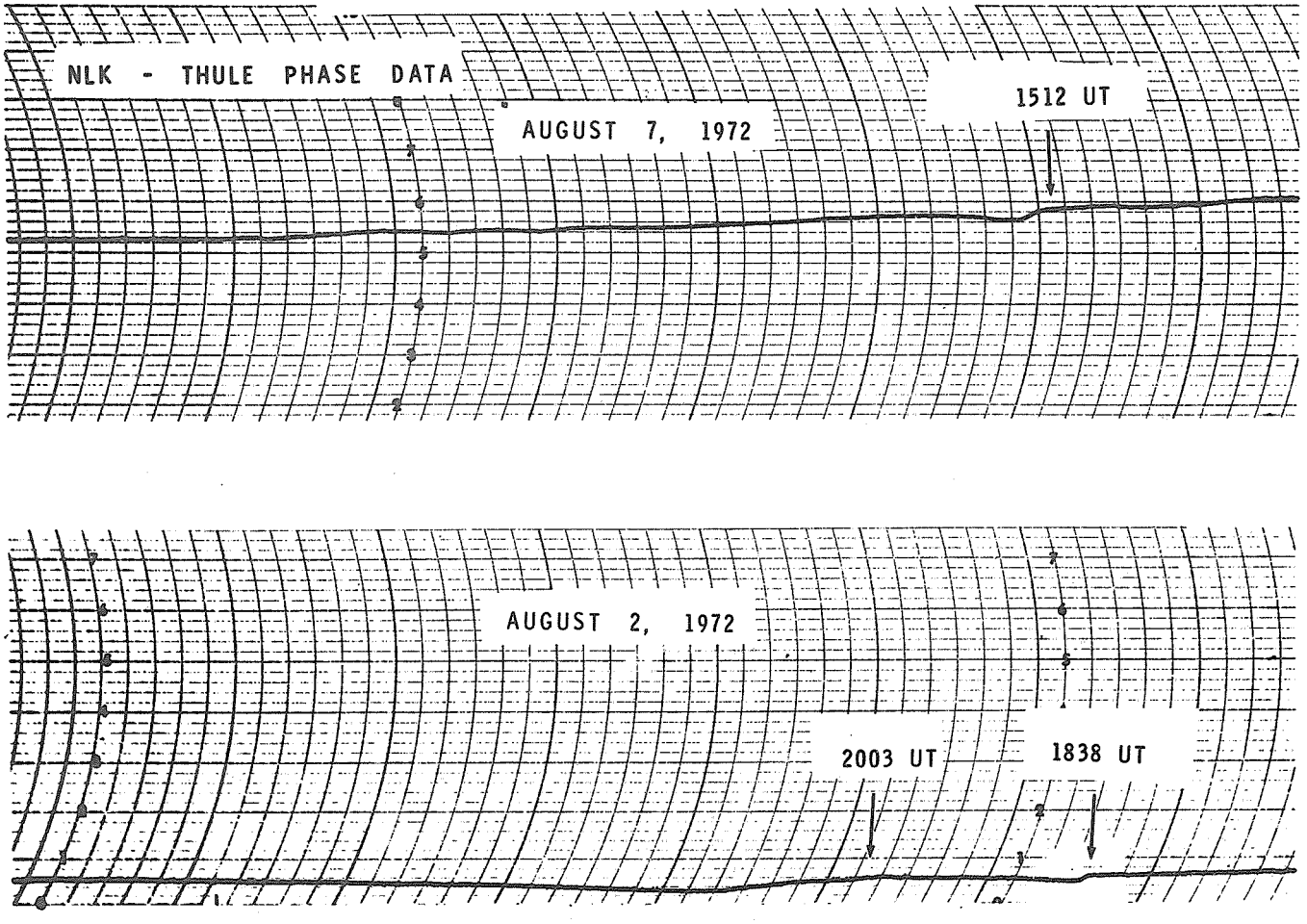

Fig. 6. Sudden ionospheric disturbances on August 2 and 7, 1972.

REFERENCES

CORMIER, R. J.	1973	Polar Riometer Observations during August 1972, this compilation.
POMERANTZ, M. A. and S. P. DUGGAL	1973	Record Breaking Cosmic Ray Storm Stemming from Solar Activity in August 1972, Nature, 241, 331.
	1972	Solar-Geophysical Data, 337 Part I, September 1972, U. S. Department of Commerce, (Boulder, Colorado, U.S.A. 80302).

The Retrospective World Interval July 26 to August 14, 1972 as Observed at the RWC Darmstadt (FTZ)

by

B. Beckmann, R. Eyfrig, P. Suessmann and H. Wegener

Fernmeldetechnisches Zentralamt of the Deutsche Bundespost, D-61 Darmstadt, FRG

The severe radio disturbance of August 1972 became already apparent in the diagrams for the transmission frequency ranges for the North Atlantic transmission path Halifax-Lüchow plotted on page 124 of the Solar-Geophysical Data (Prompt Report) No. 338, Part I (October 1972). There, the field strength was indicated as a function of time for four frequencies. The radio propagation quality indices derived from the field strengths are listed on page 126 of the above report. Further interesting details of this disturbance are dealt with below.

Fig. 1 shows the hourly measured deviations of the field strengths from the values indicated in the FTZ monthly predictions for the radio path Halifax-Lüchow (distance: 5298 km, azimuth 292.4°, frequencies: 22378 kHz, 17084 kHz, 12813 kHz, 8542 kHz) and the Shannon-Lüchow radio path (distance: 1332 km, azimuth: 276.5°, frequency: 5533 kHz) in the solar rotation 1901 (3 parts covering 9 days each). For each of the days records are made for the period from 0000 to 2400 UT. The deviations are plotted in dB versus zero line. If most of the black area enclosed by the curve is in the positive part we speak of positive phases (propagation conditions are more favourable than they are normally), if it is, however, very much in the negative part we speak of drops (disturbances). At the beginning of the rotation, the conditions are almost normal. A slight drop is to be seen between 25 and 28 July. It is the quasi-periodic recurrence of the disturbance which occurred from 26 June to 28 June in the preceding rotation. For the Halifax-Lüchow path the maximum of this disturbance is found to be on 25 July and for the Shannon-Lüchow path on 27 and 28 July. During the period from 29 July to 3 August a positive phase occurs at night mainly on high frequencies, i.e. there is a considerable increase of the MUF and the field strengths reach high values. Before the beginning of the severe disturbance, i.e. in the night from 3 to 4 August, the daytime values for the Halifax-Lüchow path decrease slightly and from 1 to 2 August they decrease particularly for the Shannon-Lüchow path. This drop occurs as a kind of pre-effect, presumably in connection with the increase of the solar activity in McMath region 11976 prior to the disturbance caused by flares in this region near its CMP. The main disturbance occurred on 4/5 August. After a recovery phase on 8 August, this disturbance was followed by a less severe one. After this disturbance, i.e. from August 12, the propagation conditions slowly return to normal.

The radio propagation quality indices Q derived from the daily field strength measurements are plotted in Fig. 2 for the three northern directions of observation i.e. USA-FRG, Canada-FRG and Japan-FRG, and, for comparison, for the southern direction of observation Africa-FRG. These indices are proportional to the mean field strength in the transmission frequency range relative to the running average of this value for the daytime period D and the nighttime period N of the preceding 27 days (one solar rotation). A more detailed description of the calculation is given in the Solar Geophysical Data No. 330 (Supplement), Descriptive Text, February 1972, page 40.

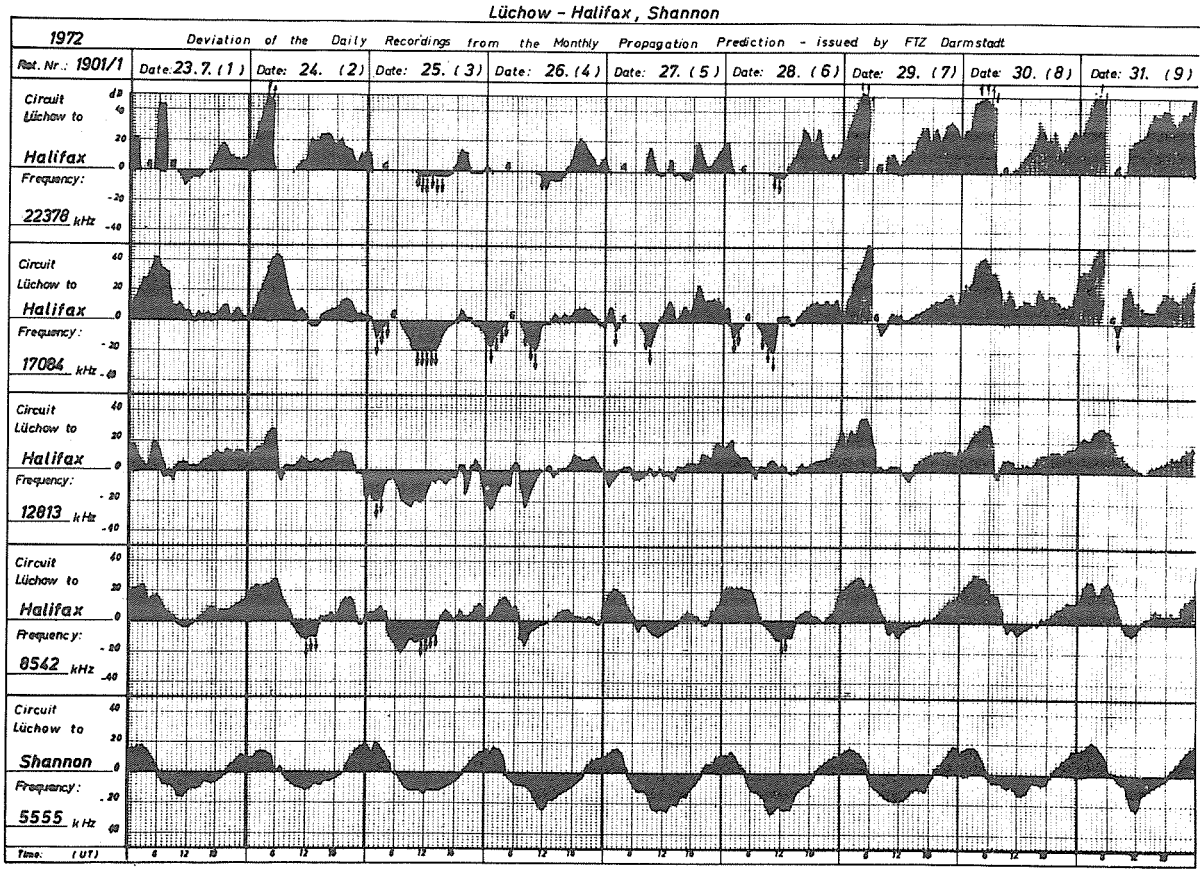

Fig. 1 Field strength deviations of Halifax-Lüchow path, solar rotation 1901/1 and 1901/2

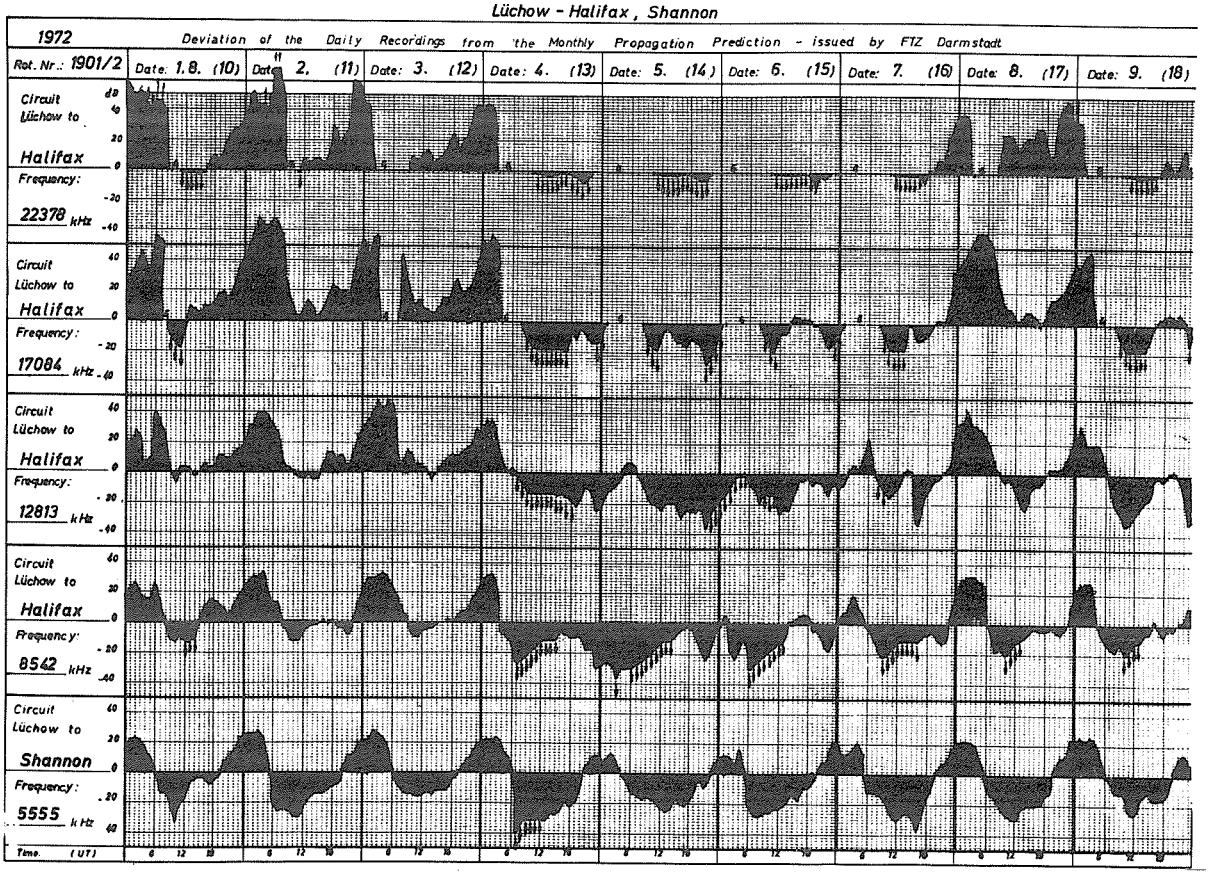

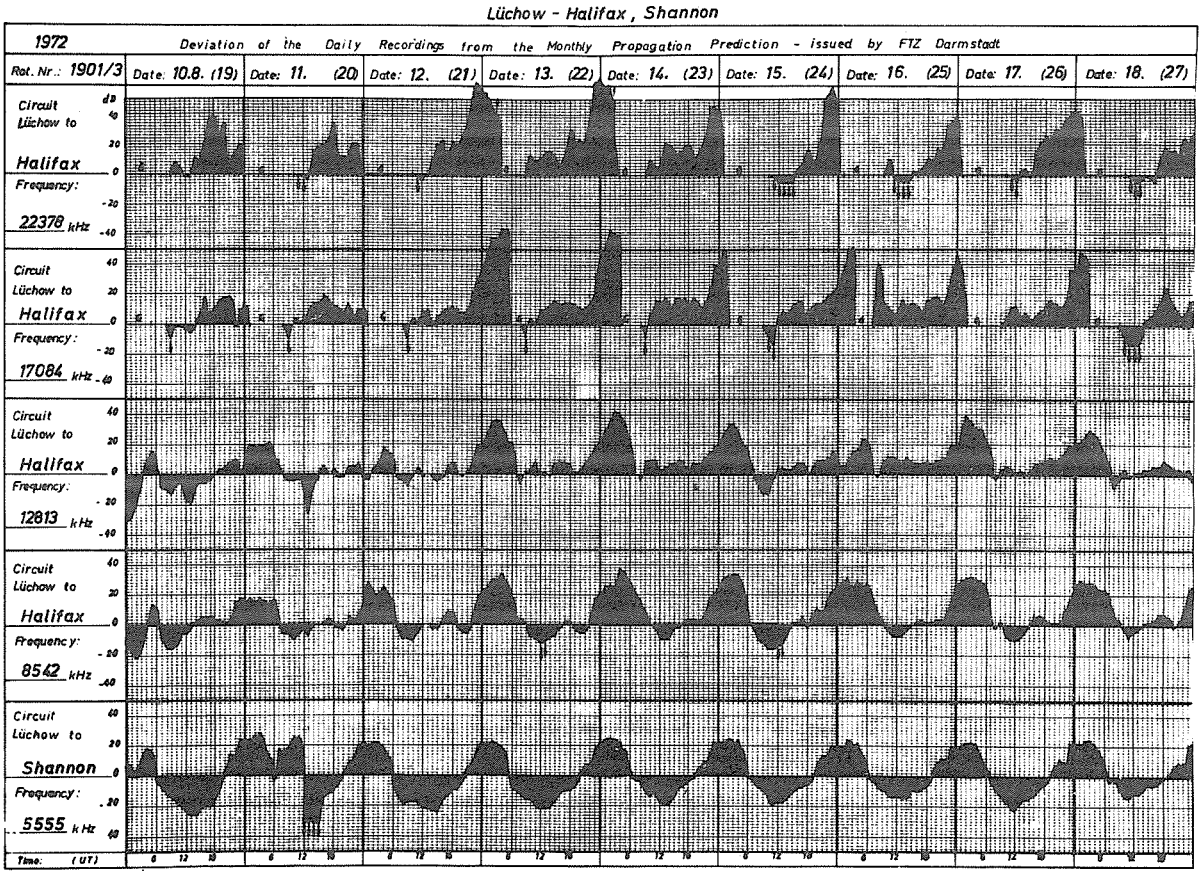

Fig. 1 Field strength deviations of Halifax-Lüchow path, solar rotation 1901/3

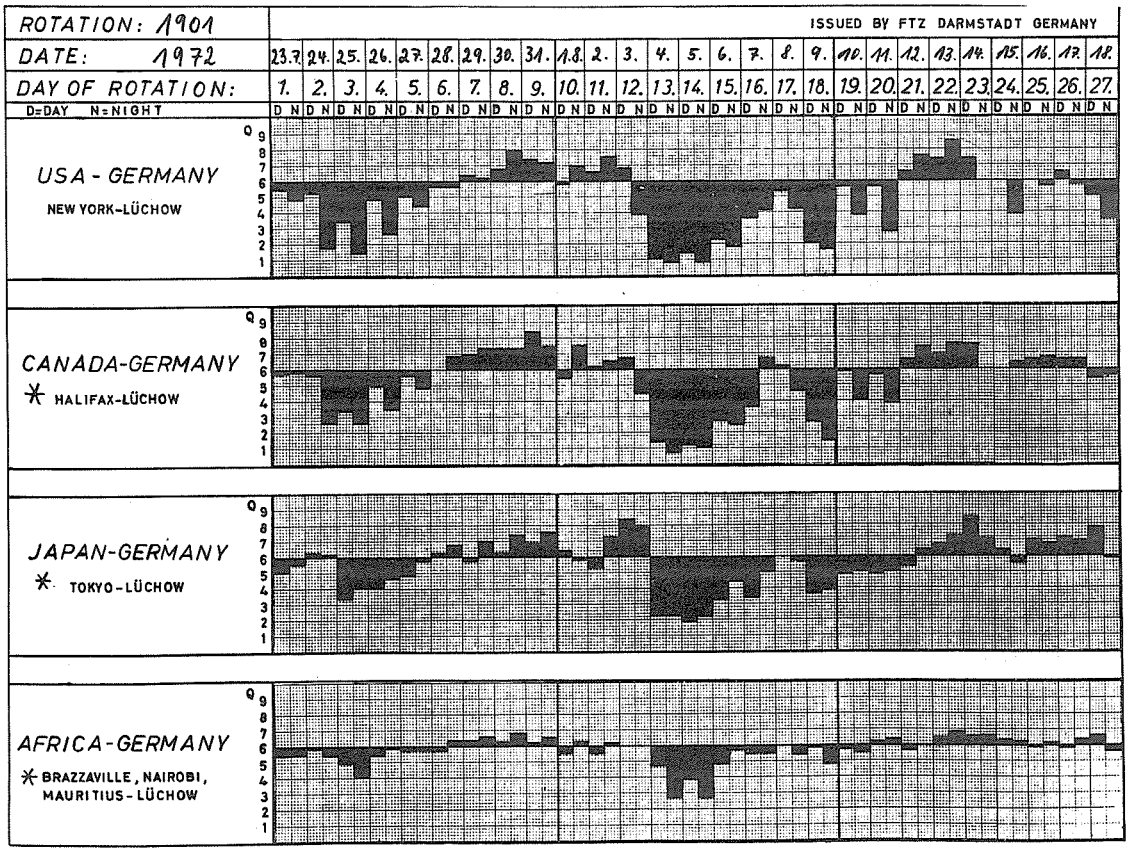

Fig. 2 Radio propagation quality indices Q, solar rotation 1901

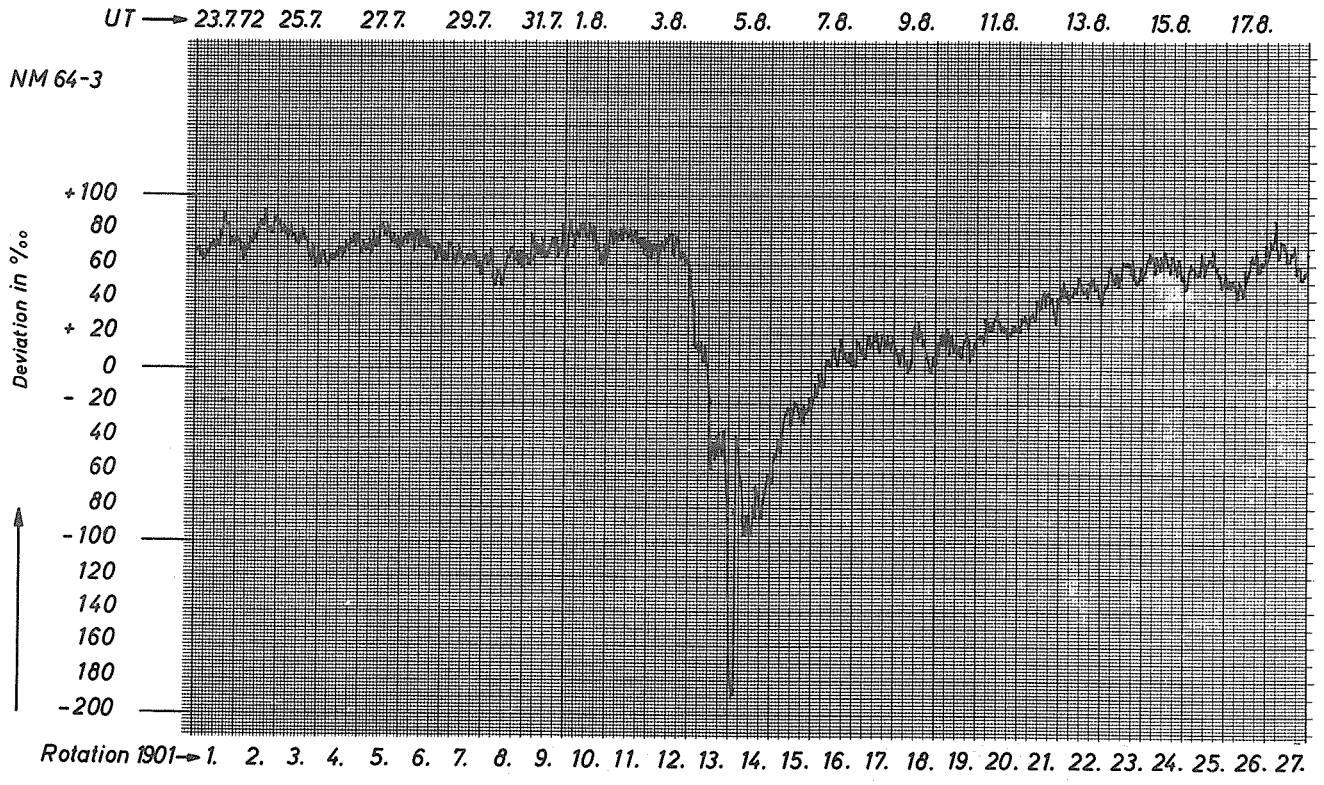

Fig. 3 Neutron component of the cosmic radiation, rotation 1901

Table 1

Cosmic Ray Indices (Super Neutron Monitor) NM 64-3

July - August 1972

	01	02	03	04	05	06	07	08	09	10	11	12	13	14	15	16	17	18	19	20	21	22	23	24
26	3722	3732	3733	3726	3716	3715	3730	3731	3730	3731	3738	3742	3744	3734	3743	3762	3756	3745	3763	3760	3770	3759	3772	3761
27	3742	3752	3751	3744	3747	3759	3742	3774	3750	3759	3758	3785	3789	3788	3777	3778	3789	3767	3760	3769	3756	3752	3756	3751
28	3758	3759	3762	3754	3768	3765	3771	3744	3777	3777	3752	3772	3758	3771	3750	3759	3748	3741	3740	3724	3734	3749	3743	3734
29	3720	3733	3727	3749	3748	3744	3725	3722	3733	3748	3728	3729	3717	3720	3723	3727	3728	3728	3733	3712	3709	3712	3700	3711
30	3724	3730	3717	3724	3737	3688	3671	3688	3700	3695	3676	3682	3706	3734	3729	3738	3745	3726	3727	3730	3718	3734	3713	3731
31	3724	3718	3716	3767	3754	3722	3747	3736	3740	3735	3757	3733	3731	3735	3749	3758	3758	3749	3760	3731	3743	3743	3788	3753
1	3736	3770	3790	3774	3773	3753	3774	3770	3786	3783	3785	3773	3765	3790	3775	3763	3782	3740	3751	3721	3728	3720	3745	3723
2	3745	3773	3772	3756	3773	3765	3771	3776	3766	3783	3776	3778	3768	3780	3765	3771	3772	3760	3757	3755	3762	3742	3754	3734
3	3753	3731	3753	3743	3748	3721	3749	3756	3750	3762	3758	3762	3765	3771	3734	3750	3764	3761	3724	3734	3729	3719	3721	3714
4	3703	3762	3637	3556	3547	3547	3542	3553	3525	3549	3516	3473	3444	3313	3357	3330	3374	3377	3354	3342	3379	3322	3259	3047
5	2892	2854	3220	3373	3364	3321	3278	3208	3177	3209	3188	3210	3179	3227	3212	3270	3254	3230	3217	3244	3257	3278	3296	3292
6	3285	3326	3333	3361	3350	3345	3374	3399	3420	3426	3426	3399	3422	3436	3437	3428	3412	3424	3406	3427	3420	3427	3445	3427
7	3450	3475	3456	3493	3478	3494	3475	3510	3518	3518	3513	3540	3546	3529	3520	3538	3558	3547	3529	3530	3526	3512	3520	3531
8	3513	3551	3554	3542	3542	3545	3516	3552	3569	3556	3555	3573	3566	3574	3550	3544	3569	3572	3557	3570	3557	3549	3555	3568
9	3545	3533	3522	3537	3559	3516	3520	3508	3512	3524	3583	3591	3576	3600	3578	3579	3561	3568	3541	3532	3513	3509	3534	3527
10	3561	3549	3575	3568	3579	3556	3590	3546	3577	3560	3558	3564	3551	3555	3544	3559	3572	3584	3574	3535	3554	3548	3559	3584
11	3579	3574	3573	3568	3608	3589	3599	3588	3587	3599	3611	3627	3615	3596	3595	3593	3591	3580	3586	3584	3601	3599	3600	3599
12	3591	3613	3611	3615	3613	3601	3615	3617	3617	3610	3644	3648	3633	3655	3659	3642	3660	3663	3648	3647	3625	3613	3651	3661
13	3669	3684	3661	3666	3647	3659	3660	3675	3674	3671	3694	3690	3675	3667	3669	3658	3682	3684	3691	3677	3672	3673	3658	3643
14	3673	3676	3676	3708	3714	3705	3690	3685	3698	3678	3693	3712	3717	3720	3720	3719	3701	3724	3695	3681	3684	3689	3708	3696

Pressure corrected

Scaling factor 100

Predigtstuhl 47,70 north; 12,88 east; 1614 meters

Fig. 2 shows these daytime and nighttime values D and N of the radio propagation quality indices for the solar rotation 1901. Here, too, we see the rotation disturbances of 25 till 28 July and the development of positive phases between 29 July and 3 August with the slight drop caused by the pre-disturbance on 1 and 2 August, which is followed by the severe disturbance in the night to 4 August. After a recovery period on 8 August, a second, less severe disturbance follows on 9 August. Moreover, we see the normalization which begins approximately on 12 August. Attention is drawn to the slight effect the disturbance has on the transequatorial path Africa-FRG. The pre-disturbance on 1 and 2 August, which is even more noticeable when averaging the field strength recorded for the three northern directions of propagation, is accompanied by slight geomagnetic activity.

Fig. 3 shows the result of the recording of the neutron component of the cosmic radiation, i.e. the hourly mean values for the solar rotation 1901, taken at the Predigtstuhl measuring station of the FTZ. The Forbush effect is to be seen as two parts, the first of which occurred in the night from 3 to 4 August and the second in the following night. The total drop amounts to 26%, an unusually pronounced effect. The very severe disturbance began after the strong X flares on 2 August in the night from 3 to 4 August. The Forbush effect accompanied by a very strong geomagnetic storm occurred almost simultaneously with the deterioration of the ionospheric transmission quality. During the recovering phase of the cosmic radiation a delay caused by the second disturbance occurring on 9 August is to be seen. It is evident that prior to the occurrence of the Forbush effect on 27 July, i.e. approximately at the date when the region of activity causing the disturbance was on the east limb of the sun, no diurnal variations of the cosmic radiation were observed. Instead of it, modulations are to be seen which amount to a maximum of 30% and are presumably connected with the pre-disturbance in the ionospheric propagation.

Complementary to Fig. 3, Table 1 includes the measured values of the cosmic radiation (hourly values) for rotation 1901.

A more detailed report on a comparison of this disturbance with the mean behaviour of other events is given elsewhere by Beckmann [1973].

REFERENCES

Beckmann, B. 1973 Solar-terrestrische Zusammenhänge im Retrospektiven Weltinterval 26 Juli - 14 August 1972. Kleinheubacher Ber. 16, 275-285.

HF Radio Propagation Disturbances August 1-9, 1972

by

Rikio Maeda
Hiraiso Branch, Radio Research Laboratories
Nakaminato, Ibaraki, Japan

This brief report discusses high frequency radio propagation conditions observed at Hiraiso. In the period August 1-9, 1972, several major sudden ionospheric disturbances and ionospheric storms occurred, which severely disturbed propagation conditions of short waves. Measurement of field strength has been carried out for the 15 MHz standard waves transmitted from WWV and WWVH stations. Particulars of the transmitters and the receiver are summarized in the following tables.

Table 1. Transmission

	WWV	WWVH
Location	Fort Collins, Colorado(40°41'N, 105°02'W)	Kauai, Hawaii(22°00'N, 159°46'W)
Distance from Hiraiso	9150 km	5910 km
Carrier Power	10 kW	10 kW
Modulation	50 %	50 %
Antenna	half wave length, vertical	half wave length, vertical

Table 2. Reception

Location	Hiraiso, Ibaraki(36°22'N, 140°38'E)
Band Width	80 Hz for the upper side band
Calibration	every an hour
Antenna	4.5 m vertical rod

In Figure 1, the solid lines were derived from hourly values of field strength (dB). Moreover, the plots August 4-6 indicate five-minute values. The diurnal variations on August 1, 2, 3, 7, 8 and 9 are typical. The field strength is above 0 dB from about 06-18 UT, and depressed from about 18-06 UT, because of the normal daily variation of LUF. The drop-outs of field strength 03-06 UT on August 2 are short wave fade-outs. The field strength August 4-6, however, changes irregularly. This high frequency radio propagation disturbance is caused by the ionospheric storm which started on August 4 and ended on August 6. The field strengths for WWV and WWVH fell to their noise levels 13-16 UT on August 5, corresponding to the drop-out of MUF.

The effect of geomagnetic disturbances on radio propagation conditions is obvious in Figure 2 where deviations of the field strengths from the monthly medians (on the ordinate upward) and K_p-index (on the ordinate downward) are shown for the period August 1-9. On geomagnetically quiet days, the deviations for WWV and WWVH vary similarly with mean value of zero or more. On the other hand, in a geomagnetically disturbed interval the day-to-day variation of deviation for WWV is not similar to that for WWVH and averages lower. This fact suggests that the geomagnetic disturbance August 4-6 effects are more obvious on the middle latitude circuit than on the low latitude circuit. It should be noted that the diurnal variation of the deviation was not depressed much on August 9 in spite of the moderately severe geomagnetic storm.

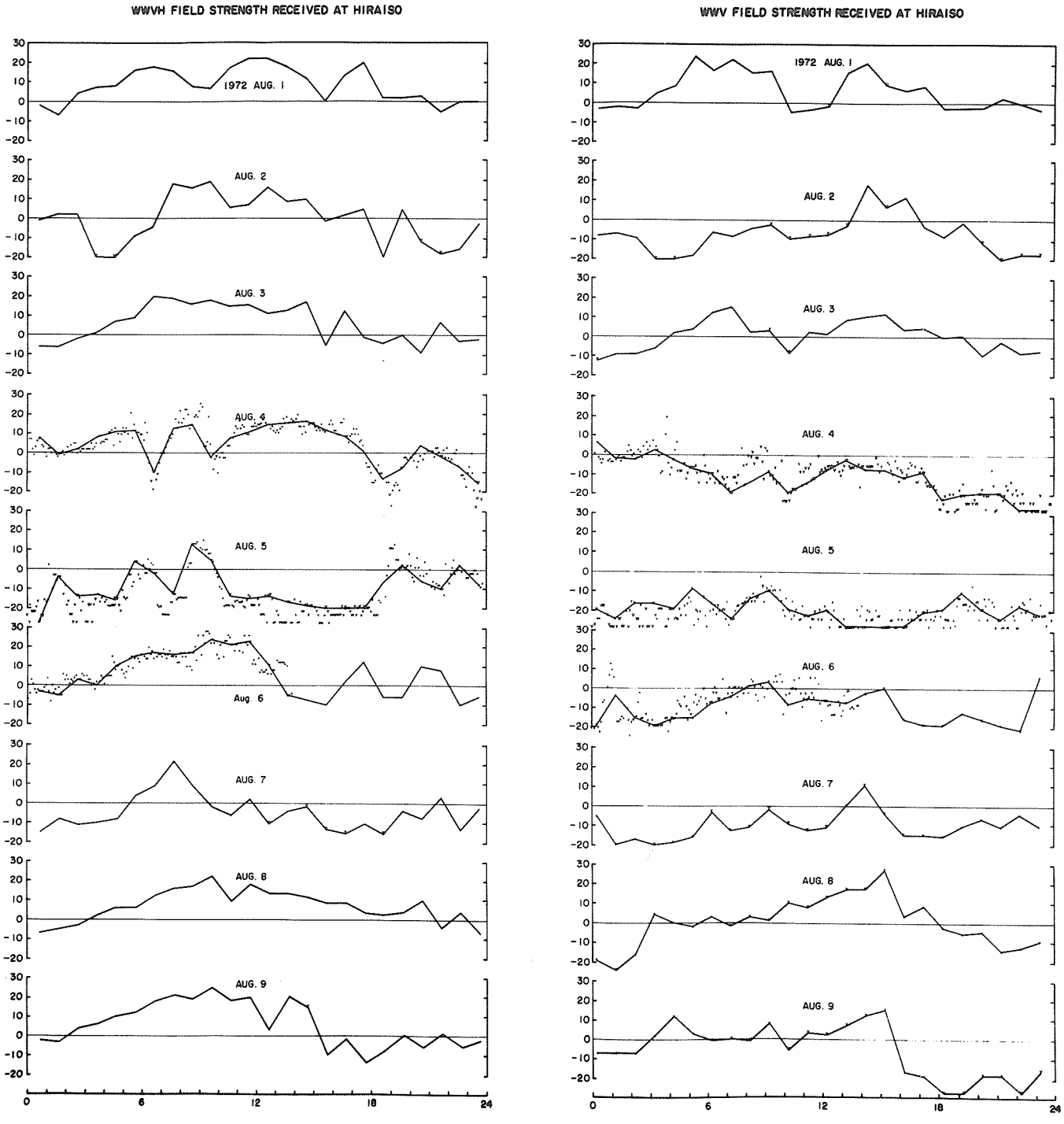

Fig. 1. Field strengths for the 15 MHz standard waves received at Hiraiso.

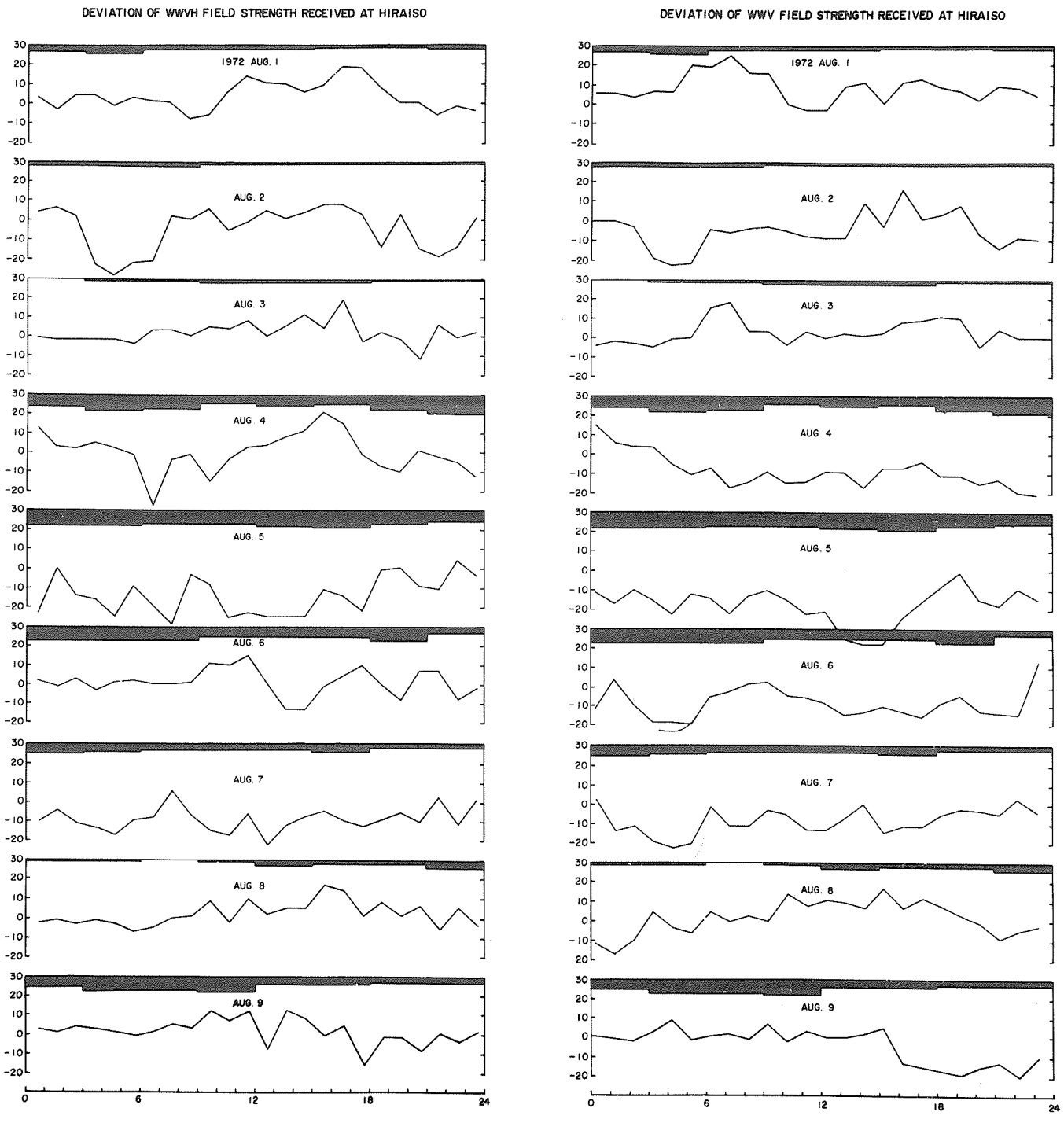

Fig. 2. Deviations of field strengths for the 15 MHz standard waves received at Hiraiso.

14 MHz Fieldstrength Observations on the Transequatorial Path Tsumeb/S.W.Africa - Lindau (Darmstadt)/W.Germany

by

R. Eyfrig
Fernmeldetechnisches Zentralamt der Deutschen Bundespost, D6100 Darmstadt, W.Germany

and

J. Röttger
Max-Planck-Institut für Aeronomie, D3411 Lindau, W.Germany

The fieldstrength variations measured on the transequatorial radio path ZS3MPI (14.000 MHz) in Tsumeb/S.W.Africa to Lindau (Darmstadt)/W.Germany are evaluated for the retrospective world interval. It is evident from these investigations that except for the decrease of fieldstrength during SWFs the diurnal variation on this transequatorial path is just slightly influenced.

The transmitter ZS3MPI in Tsumeb (19°14' S, 17°43' E) runs about 0.4 kW [RÖTTGER, 1973]. The antenna is a 10.6 m high 4-element horizontal Yagi antenna. On the receiving site a similar antenna (14.3 m high) is used in Lindau (51°39' N, 10°07' E) and a log-periodic antenna is used in Darmstadt (49°51' N, 08°24' E). Due to receiver break-down, the fieldstrength data from Lindau and Darmstadt, which is approximately 233 km south-west of Lindau, had to be used for evaluation to get an almost continuous set of data. By comparing synchronous records from both receiving stations, an optimum adjustment of both fieldstrength series provides a statistical deviation of less than 3 dB.

The mean fieldstrength $\overline{P}_M$ during the essentially undisturbed periods 20 July - 3 August 1972 and 15 August - 31 August 1972 is given in the lower diagram of Fig. 1. This plot gives half-hourly mean values which are deduced from receiver output readings taken every fourth minute. Assuming a log-normal fieldstrength distribution, the standard deviation σ is calculated for each half-hour interval (see upper diagram of Fig. 1), taking the entire data of the two undisturbed periods.

The basic values given in Fig. 1 are used for reference to compute the fieldstrength deviations during the disturbed period 4 August - 14 August 1972. The deviations $\Delta P_M = P_M - \overline{P}_M$ are classified by means of the σ limits as shown in the caption of Fig. 2. The heavy circles indicate that the observed deviations are greater than two times the standard deviation. This means that these significant deviations clearly exceed the normal variations during essentially quiet conditions. The bars indicate SWFs observed at 2.61 MHz on the path Norddeich - Lindau (see also paper by SCHWENTEK).

A few characteristic items of transequatorial propagation during disturbed conditions can be deduced from the mean fieldstrength deviations:

(a) SWFs were clearly observed;

(b) The day-time fieldstrength (excluding SWFs) during the period 4 August - 12 August 1972 was somewhat below normal;

(c) The morning peak between 05 UT and 06 UT was not significantly below normal variations;

(d) Except for 10 August 1972, the evening fieldstrength was within the regularly observed variations. On 4 and 5 August 1972 the fieldstrength even exceeded the normal values (positive disturbance);

(e) The night-time fieldstrength (00 - 05 UT) was definitely below normal (except for 7 August 1972). This was because the MUF was lower than the operating frequency 14.0 MHz.

The described observations are consistent with the morphology of ionospheric storm [MATUURA, 1972] which means that except for SWFs and the decrease in night-time fieldstrength the HF propagation in lower latitudes is not strongly influenced even during severe ionospheric disturbances.

References

MATUURA, N. 1972 Theoretical models of ionospheric storms, Space Sci. Rev., 13, 124-189.

RÖTTGER, J. 1973 Langperiodisches Fading von Kurzwellensignalen, Kleinheubacher Berichte, 16, 167-178.

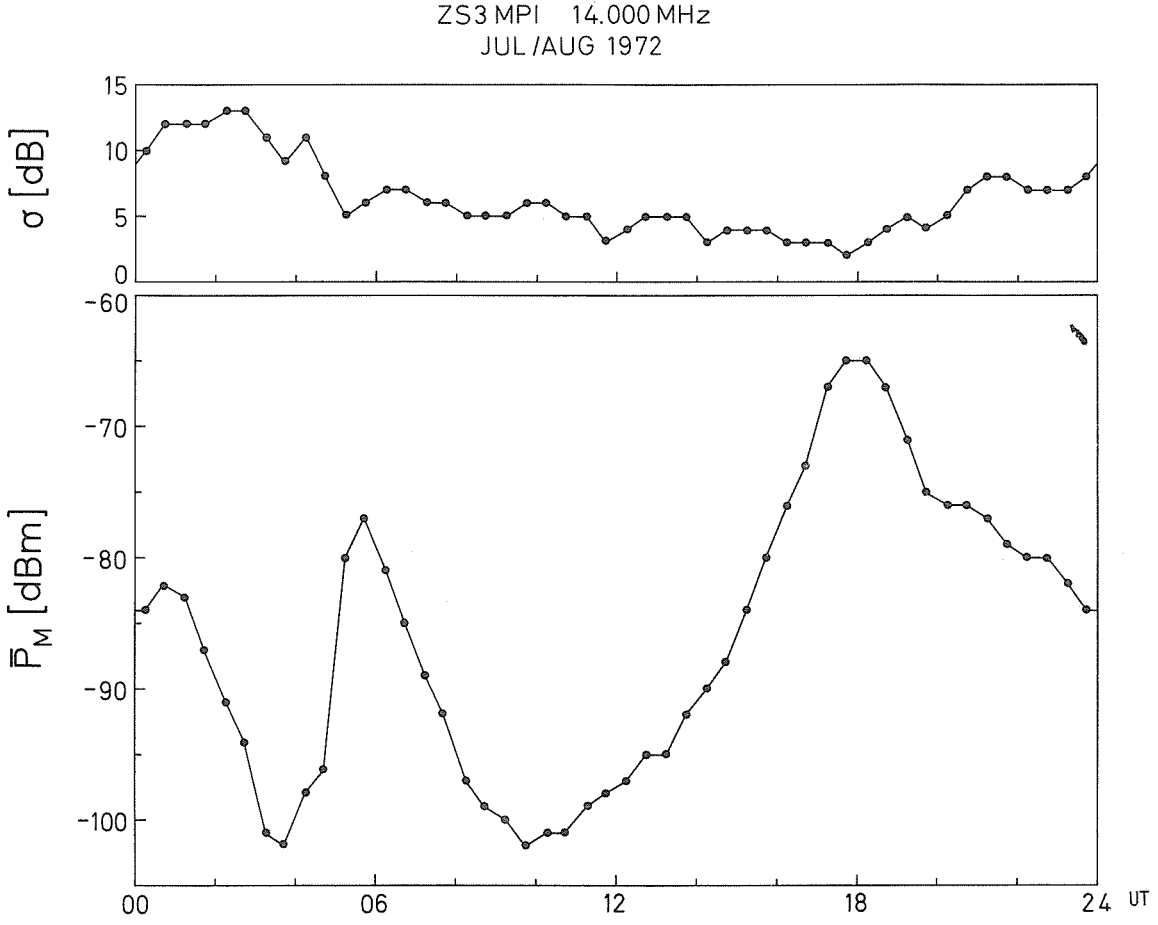
TSUMEB – LINDAU / DARMSTADT
ZS3 MPI 14.000 MHz
JUL / AUG 1972
σ [dB]
15
10
5
0
$\bar{P}_M$ [dBm]
-60
-70
-80
-90
-100
00
06
12
18
24 UT

Fig. 1.

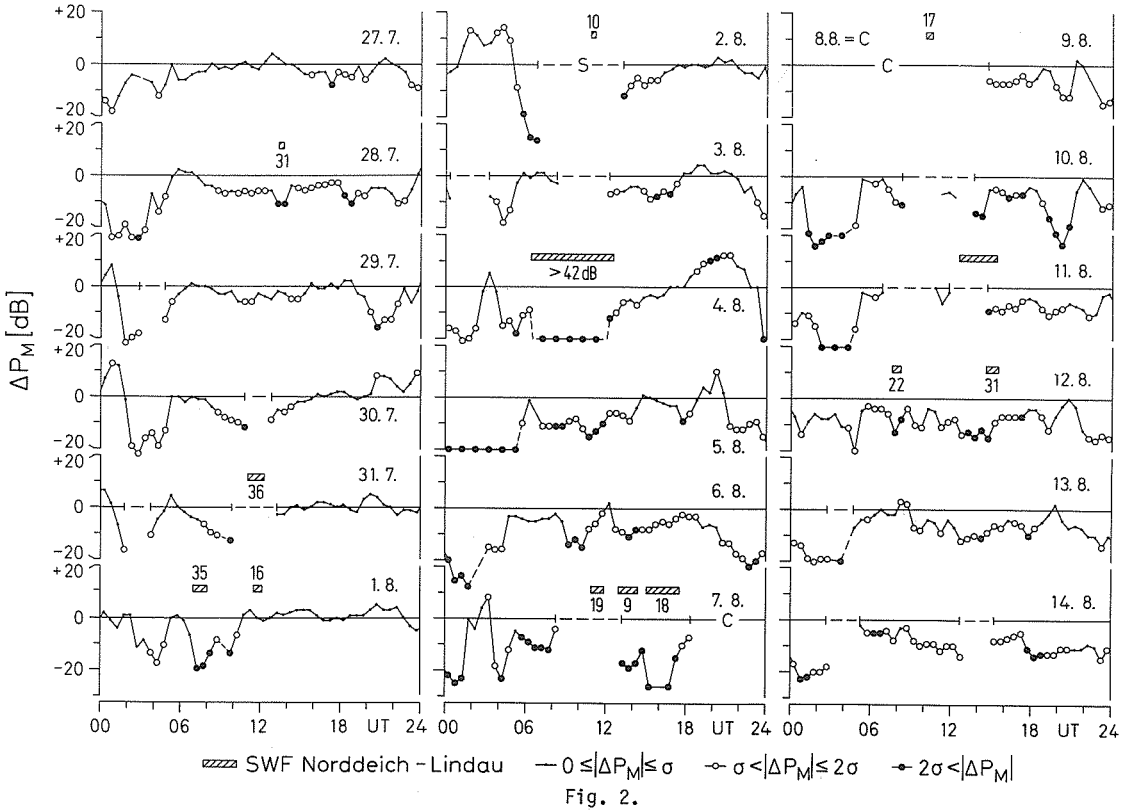
ΔP_M [dB]
+20
0
-20
27. 7.
28. 7.
29. 7.
30. 7.
31. 7.
1. 8.
2. 8.
3. 8.
4. 8.
5. 8.
6. 8.
7. 8.
8. 8. = C
9. 8.
10. 8.
11. 8.
12. 8.
13. 8.
14. 8.
S
C
>42dB
00
06
12
18
UT
24
SWF Norddeich – Lindau
0 ≤ |ΔP_M| ≤ σ
σ < |ΔP_M| ≤ 2σ
2σ < |ΔP_M|

Fig. 2.

EVENTS OF JULY 26 - AUGUST 14, 1972 AS RECORDED BY THE A_3-TYPE ABSORPTION IN THE LOWER IONOSPHERE

Syed Ziauddin, Laurentian University, Sudbury, Ontario

The main feature of this method is that the non-deviative absorption is determined by recording the field strength of a transmitter (CHU-Ottawa) on 3.3 MHz at Sudbury (47°N, 80°W Geographic) over a 340 Km East-West path. The propagation is by the 1E mode and the day-time signal strength reflects generally the effects of changing ionization parameters below 100 Km. The normal diurnal variation of the field strength for the period under discussion follows the dotted line super-imposed on the charts reproduced in this note. The absorption change on a normal day from midnight to midday is close to 60 dB, and in this sense, this method is a more sensitive indicator of changes in ionization parameters below the E-region; and may be considered superior to the riometer technique for some information, where a transmitter is available round the clock and located at an appropriate distance corresponding to 1E propagation mode. This technique to mention only a few, has been extensively used by Lauter [1966] and Schwentek [1966]. The accompanying diagrams show clearly the day-time SID'S prominently, when there was no other super-imposed absorption present, driving the signal strength below the threshold of detection. Due to this latter effect, the signal strength from 6 August to 9 August, was below the threshold level during the day time hours (about 1000 UT - 2300 UT) and the SID'S during this period could not be detected. The corresponding charts have not been reproduced here. Most of the "day-time events" catalogued in the monthly Solar-Geophysical Data reports can be identified on the charts.

The object of this note is only to identify as many of the listed or reported events by the A_3 - Type absorption technique used at Sudbury, and therefore any quantitative evaluation or presentation of theory is not attempted here.

The author is very grateful to Dr. J.S. Belrose for the valuable assitance and useful discussions throughout this work. This work was carried out under CRC contract OGR1-0171.

REFERENCES:

Lauter, E.A., 1966, The Survey of A_3-Absorption Measurements at Low and Medium Frequencies, Annales de Geophysique, 22, 289-299.

Schwentek, H., 1966, The Determination of Absorption in the Ionosphere by Recording the Field Strength of a Distant Transmitter, Annales de Geophysique, 22, 276-288.

FIELD STRENGTH OF CHU TRANSMITTER (3.33 MHz) OTTAWA, RECORDED AT SUDBURY (47° N, 80° W GEOGRAPHIC) AT A DISTANCE OF 430 Km ON AN EAST–WEST PATH.

DOTTED CURVE REPRESENTS NORMAL DAY RECORDINGS FOR THE PERIOD. HOURLY MARKINGS ARE IN UNIVERSAL TIMES. PROMINENT SID'S ARE IDENTIFIED BY ADDITIONAL U.T. MARKINGS.

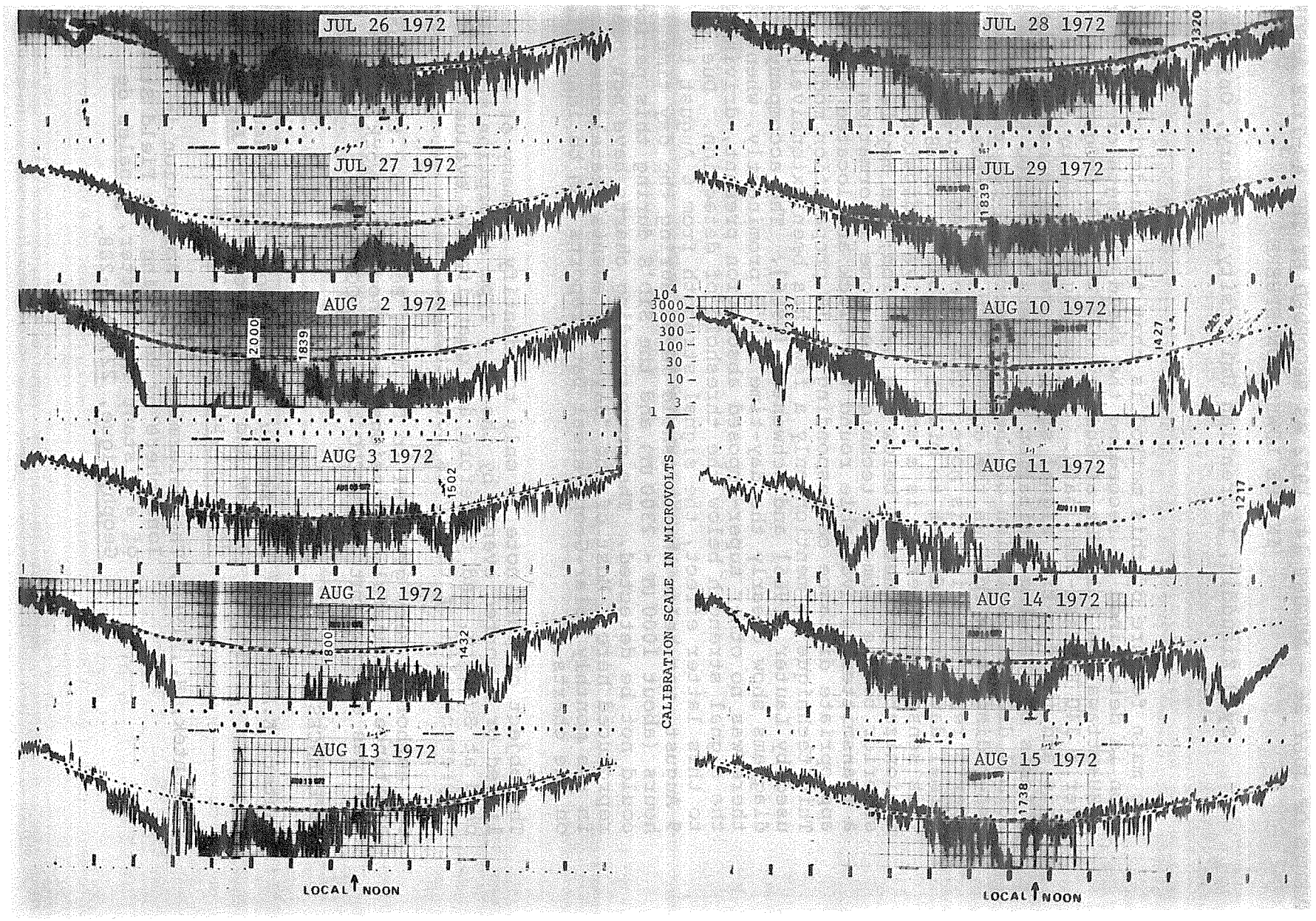

Polar Cap Absorption Event of 3-10 August, 1972 by the Riometer Data

by

V. M. Driatsky and V. A. Ulyev
The Arctic and Antarctic Research Institute
Leningrad, U.S.S.R.

The present study concerns itself with the analysis of the PCA event which occurred on 3-10 August 1972 and was recorded by riometers at the Soviet Arctic and Antarctic stations. Table 1 gives the station list, their positions, invariant latitudes and midnight and noon solar altitudes. The riometer results were compared with solar flare data, proton data, magnetic storm data and preliminary geomagnetic Kp indices ["Solar-Geophysical Data", 1972].

Table 1

LIST OF STATIONS

Station	Geographic Positions		Φ	Solar Altitude August 7, 1972		Remarks
	Latitude	Longitude		noon	midnight	
North Pole-19	88°30' N	350° E	81.6°N	+18°30'	+15°30'	
Heiss Island	80 37	58 03	73.8	+26 23	+7 37	PCA data obtained by radio
Dixon Island	73 30	80 14	67.2	+33 30	+0 30	
Amderma	69 46	61 41	63.9	+37 14	-3 14	
Norilsk	69 26	88 05	63.4	+37 34	-3 34	
Molodezhnaya	67°10'S	45 51	67.6°S	+6 20	-39 20	" " "
Mirny Observ.	66 33	93 01	76.8	+7 00	-40 00	" " "
Vostok Station	78 27	106 52	84.3	-5 00	-28 00	" " "

Notes: Vostok Station riometer operates at 30 MHz; Mirny Observatory - 31.8 MHz; for all other stations the operating frequency is 32 MHz.

At Vostok Station there is a co-phasal two-dipole antenna, directed towards the zenith. Other stations have polar-directed Yagi antennas.

PCA Analysis

The onset of the PCA event was recorded on 3 August between 0000-0400 UT. A noise storm seen in data from the NP-19 drifting station and the Dixon Island Station started on 2 August at 2030 UT. It is known that there is a time difference of several hours between a PCA commencement and a flare [Beiley, 1964]. The analyzed PCA event may be associated with three flares of 1B and 2B intensity, occurring late on 2 August (maximum flare phases are at 2010, 2023, 2058 UT, respectively). The proton counter measuring protons with energies $E_p > 13.9$ Mev on the Pioneer 9 Satellite recorded a four fold increase on 3 August between 0230 and 0600 UT. Thus, the PCA onset by riometer and proton data seems to fall on 0230-0400 UT on 3 August, i.e., 6-8 hours later than the flares which can be held responsible for this PCA event.

During 3 August an enhanced absorption was recorded by all stations. The NP-19 drifting station data show the absorption development more vividly than the others (Figure 7). The PCA caused by the flares started to increase on 2 August. The increase continued up to 0900 UT 3 August, then a slight decrease occurred. AT 1030 UT the NP-19 riometer recorded a new storm which was followed again by an absorption increase which reached its maximum at 1800 UT on 3 August. The noise storm and a new absorption enhancement are likely to be caused by a chromospheric flare. The flare, however, was not shown by the solar activity data. Pioneer 9 Satellite data show increased proton counter rate throughout the whole day of 3 August, but no well-pronounced maximum was found.

Early on 4 August all the stations recorded a sharp absorption increase with a maximum at about 0500 UT. This burst might be related to a magnetic storm with sudden commencement. SSC were recorded at 0118 UT and 0220 UT on 4 August. It is, however, possible that the absorption was caused by a new flare, considering that the North Pole-19 Station riometer recorded the onset of the third noise storm at 2230 UT 3 August and Pioneer 9 Satellite proton counter showed a six fold increase of the proton counter rate between 0400-0800 UT 4 August. The data available on solar flares do not show a suitable flare, which can be taken responsible for the analyzed absorption enhancement on 3 August and early on the next day (4 August).

At 0645 UT 4 August a flare occurred on the Sun with an intensity of 4B showing a sharp increase, then at 0751 UT a flare with 3B intensity was registered. Riometers at North Pole-19 and Dixon Island recorded a new noise storm. The proton counter on the Pioneer 9 Satellite indicated a sharp increase of the proton counter rate during 0800-1200 UT on 4 August. The riometer data do not show an exact time of the PCA onset caused by the 4B flare. It is obscured by both noise storm and earlier absorption effects. It is, however, obvious that this PCA event (by the NP-19 data) started not later than 0900 UT (Figure 1). At 1100 UT at all sun lit stations of the northern hemisphere the absorption reached the limit of the riometer dynamic range (the curves of Figure 1 end at 20 db) and maintained this maximum value for several hours. At the stations of the southern hemisphere the absorption development is distorted by the day/night variation. The absorption maximum at these stations occurred at 2200 UT 4 August. At the same time maximum was recorded by several stations in the northern hemisphere (Amderma, Norilsk). Apparently maximum of the proton flux associated with the 4B and 3B flares occurred at 2200 UT. It is impossible to determine the time of the maximum proton flux from Pioneer 9 Satellite data due to proton counter saturation. It should be noted here that at 2054 UT 4 August an onset of sc storm was recorded that might affect the time and magnitude of the 2200 UT maximum.

During the first hours of the following day the absorption was decreasing, but at 0300-0600 UT all the stations recorded a strong and sudden outburst with the maximum at about 0500 UT. This maximum exceeded the riometer dynamic range at the sun lit stations (NP-19, Heiss Island, Dixon Island, Mirny Observatory); the absorption burst seemed to be associated with a variation of the proton flux. On 5 August the Pioneer 9 Satellite data showed extremely large proton counter rates (counter saturation).

After 0600 UT 5 August the absorption slowly decreased at all the stations. At the auroral zone stations this decrease, however, was obscured by the auroral bays and night/day variation effects.

On 6 August the absorption continued to decrease. At about 0500 UT 6 August Vostok Station, Norilsk and Amderma recorded a new burst of absorption. The proton counter at Pioneer 9 Satellite during 0300-0700 UT recorded an increase in proton counter rates (approximately 2.5 times). This increase poses a certain problem. If it is connected with a variation of the proton flux ejected by the 4B and 3B flares, then we should explain why it was not recorded by other northern hemisphere stations which were sun lit at that time (NP-19, Heiss Island, Dixon Island). Assuming this burst to be of auroral type we should explain its presence at Vostok Station and Thule (the former is sun lit and the latter is not). Both are just in the center of the Polar Cap zone where the auroral absorption occurrence is rather doubtful.

After 0500 UT 6 August the absorption at all stations decreased.

On 7 August the absorption continued to decrease till 1800 UT. The NP-19 riometer indicated a strong absorption increase at about 1800 UT on 7 August. This increase was caused by a new PCA event, caused by a chromospheric flare of 4B, which occurred at 1500 UT 7 August. AT 1520 UT the riometers at NP-19 and Dixon Island recorded a noise storm. At 1609 UT the Pioneer 9 Satellite proton counter marked a beginning of proton counter rate increase. Thus, the commencement of the new PCA event falls on 1520-1609 UT, despite the fact that NP-19 riometer indicated the increase only at 1800 UT. This time delay is attributed to the fact that this new PCA event started against the earlier absorption. The proton flux maximum occurred approximately at 2300 UT 7 August from the Pioneer 9 Satellite data, then the proton counter rate slowly decreased during the next 3 days (August 8, 9, 10). The riometer absorption variation did not follow the proton counter rate change. The riometers at NP-19 and Dixon Island showed absorption maxima at 0000 UT on 9 August. The absorption increase on 8 August which did not correlate with the proton flux variation might be connected with the effects of sc storms (their commencements were recorded at 1342 and 2354 UT 8 August. Assuming this is valid, we still have to interpret the absorption enhancement from 2300 UT 7 August (proton flux maximum occurrence) to 1342 UT 8 August (onset of the first of the two sc storms).

On 9 August the riometers of NP-19 and Dixon Island showed a sharp absorption decrease, then the decrease rate became slower and the absorption disappeared on 10 August. The other riometer stations also showed a somewhat enhanced absorption but the development of a new PCA event was obscured by the effects of the day/night variation and auroral type absorption. At Vostok Station (completely darkened) the maximum occurred at 0300 UT 9 August. This 3-hour shift (comparing to NP-19 and Dixon Island) is attributed to the day/night variation. On 10 August the PCA event slowly disappeared from riometer data at all the stations.

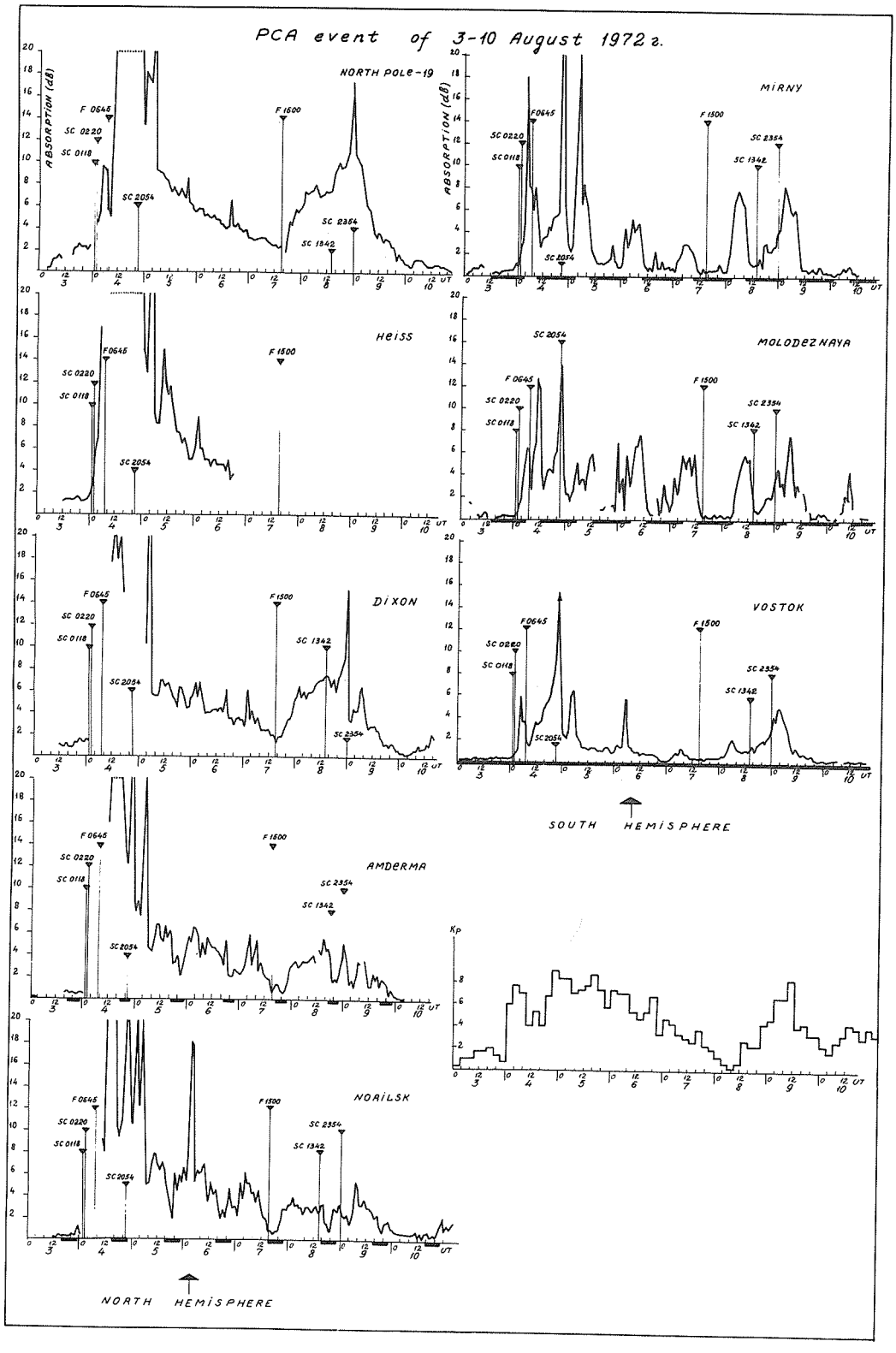

Fig. 1. PCA variations and geomagnetic index Kp changes during 3-10 August, 1972.

Summary

On the basis of riometer, proton flux, solar flare and magnetic storm data we can make the following inferences on the development of the PCA event during 3-10 August, 1972.

1. The analyzed PCA event was caused by several chromospheric flares which followed each other so that the effects of the subsequent flares were superimposed. This resulted in the complex development of the PCA event during 3-10 August.

2. We suggest that there should have been 5 flares. Three of them were indicated by the solar data: 2000-2100 UT 2 August, 0600-0800 UT 4 August, and 1500 UT 7 August. These three flares correlate well with riometer and proton data. The other two, not indicated in the solar data, probably occurred at 1030 UT and 2230 UT, respectively, on 3 August. At this time the riometers recorded the onset of noise storms with the subsequent absorption increase.

3. In general the PCA development (from riometer data of the completely sunlit stations) correlate the variations of the proton counter rate from Pioneer 9 Satellite data. This correlation is only lacking during 8 August and can be partially attributed to the effects of the two sc storms.

4. We cannot explain a strong absorption burst at 0500 UT on 6 August using the available data.

Translated from Russian into English by Anna Minevich.

REFERENCES

BEILEY, D. K. 1964 Planetary Space Science, 12, N 5.

1972 Solar-Geophysical Data, 337, Part I, U.S. Department of Commerce, (Boulder, Colorado, U.S.A. 80302).

Ground Based Ionospheric Observations from the Danish Geophysical Observatories in Greenland during the Period August 1-16, 1972

by

J. Taagholt, P. Stauning and V. Neble Jensen
Ionosphere Laboratory, Danish Meteorological Institute
Technical University of Denmark
DK-2800 Lyngby, Denmark

Acknowledgements

The riometers in Godthåb and Sdr.Strømfjord are installed at communication stations operated by the Greenland Technical Organization (GTO). The Geopole Observatory at Thule AFB is operated by Air Force Cambridge Research Laboratories (AFCRL). The remaining riometers and the vertical sounders are installed at observatories operated by the Danish Meteorological Institute. The computer processing of riometer data was done at the Northern Europe University Computing Center (NEUCC). The support and assistance received from these organizations is gratefully acknowledged.

Introduction

The ionosphere data published below are reduced data based on routine measurements made at the field sites:

Table 1

Location of Observatories

Observatory	Geographic Latitude	Geographic Longitude	Geomagnetic Latitude	Geomagnetic Longitude	100 km L-value	Riometer frequencies MHz	Vertical Sounders type:
Thule, Qanaq	N77.51	W69.33	N89.1	356.42	276		C-4
Geopole, AFCRL	76.55	68.65	88.25	2.67	181.48	20, 30, 50	
Godhavn	69.26	53.51	80.05	30.20	20.41	20, 30	J5W
Sdr.Strømfjord	67.02	50.72	77.60	34.78	14.42	31	
Godthåb	64.19	51.73	74.99	29.93	10.89	30.2	
Narssarssuaq	61.17	45.11	71.35	37.12	7.31	20, 30.2	C3/4 (modified)
Torshavn	62.03	5.76	65.38	85.20	4.47	30	

Some HF propagation data concerning the communication between Godthåb (N64.2, W51.73) are presented to illustrate the problems for HF communications during PCA events.

Observatory Location

The locations of observatories that have supplied material for the present data report are indicated on the map of the north polar region shown in Figure 1. For illustration of the observatory positions relative to the geomagnetic field, contours of constant L at 100 km height are also shown in the map.

Geographic and geomagnetic coordinates and 100 km L-values for observatories, type of ionosonde, and receiving frequencies for the various riometers are shown in Table 1. Further information on observatories and ionospheric measurements in Greenland may be found in Jensen, et al., [1972].

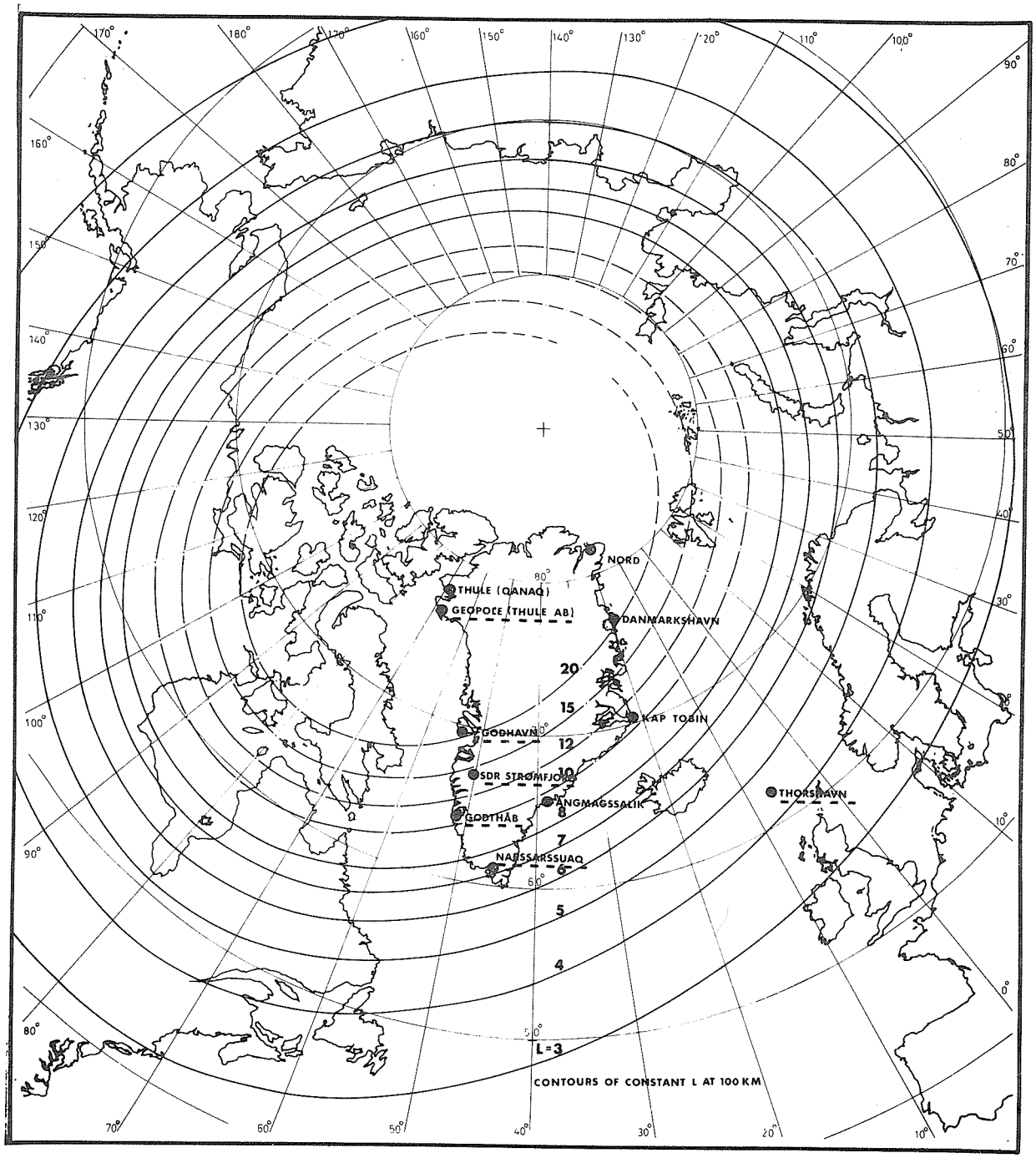

Fig. 1. Observatories in Greenland and at Faroe Islands (the underlined observatories were in operation during the August 1-16, 1972 period)

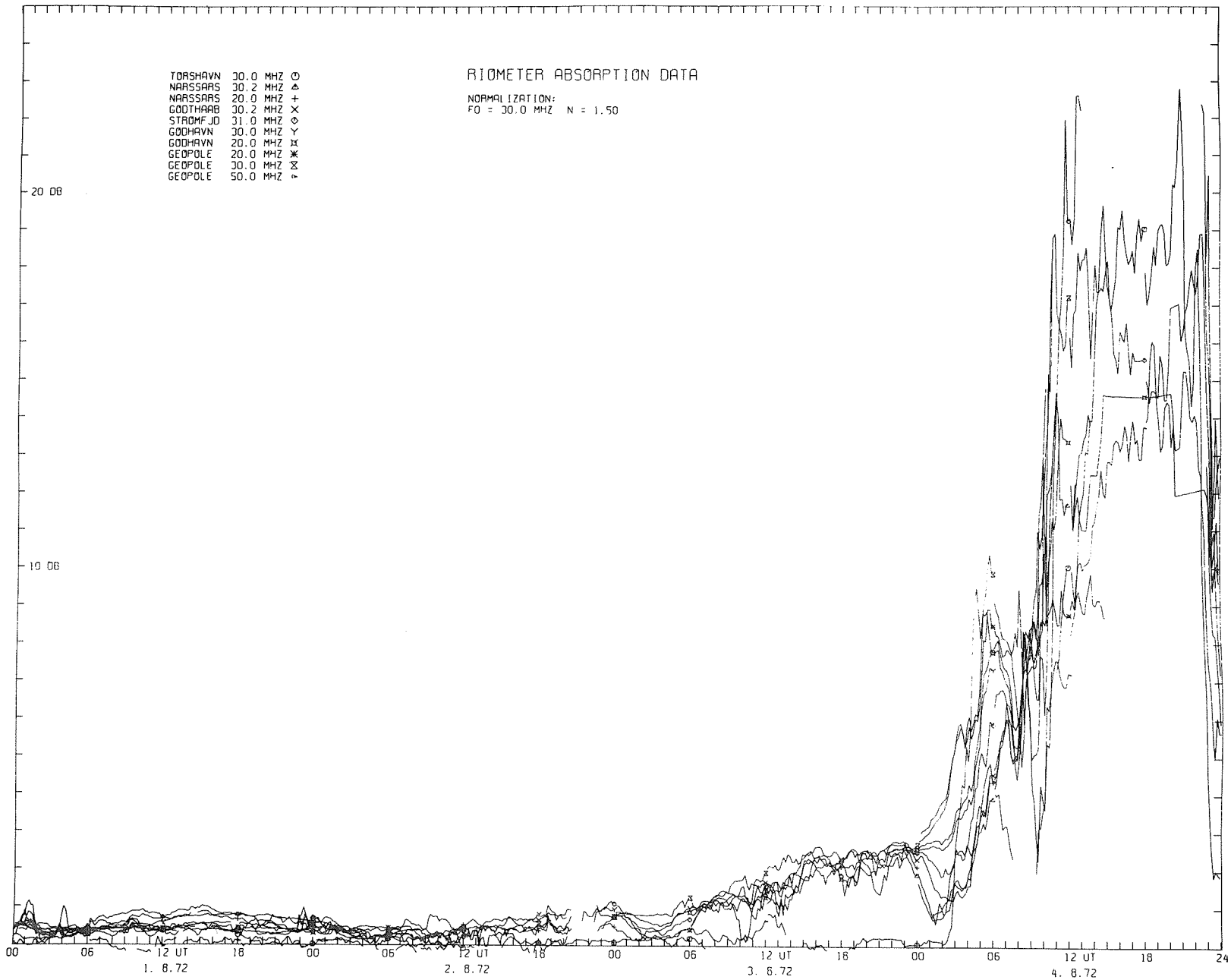

Fig. 2a. Riometer absorption data, 1-4 August 1972.

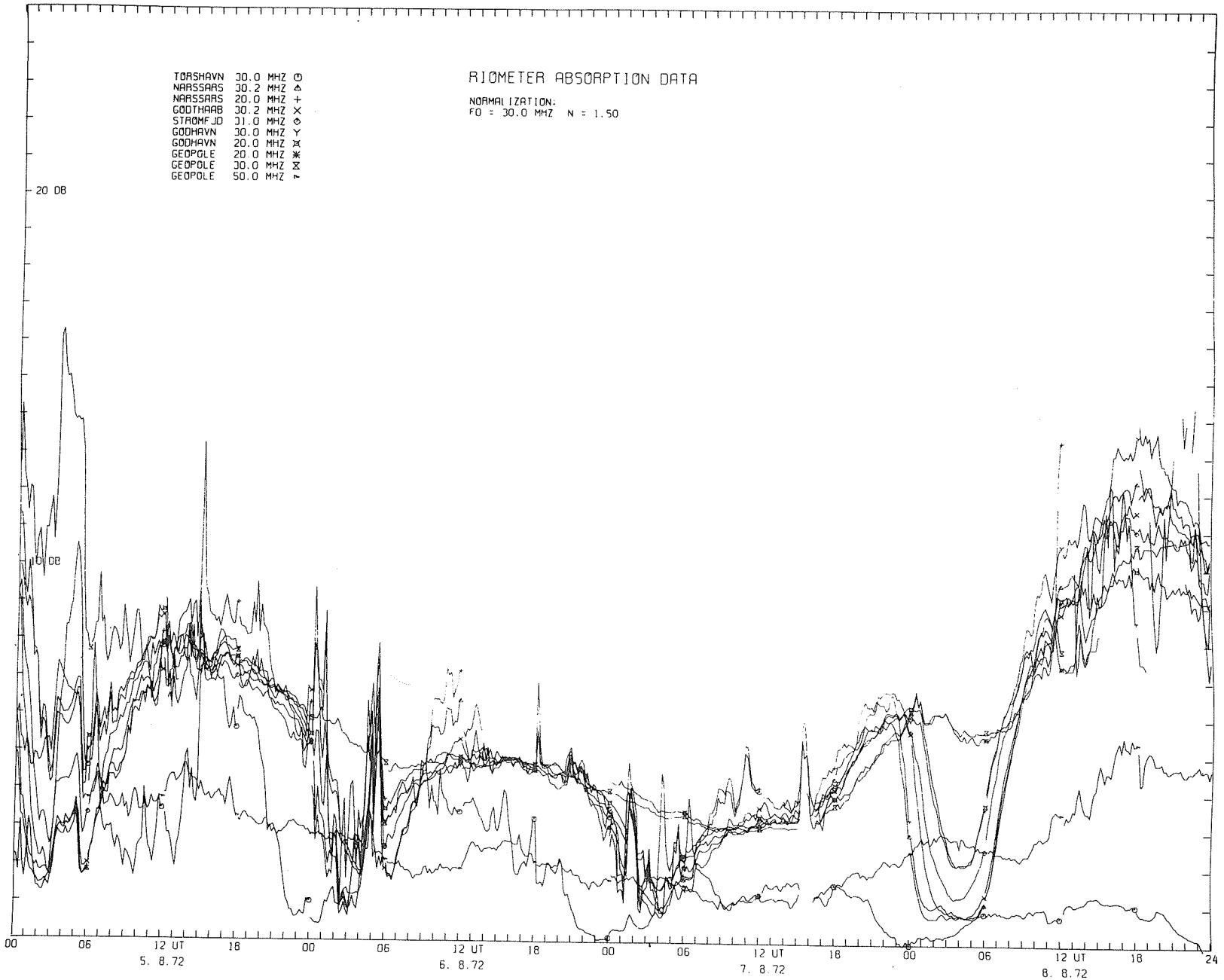

Fig. 2b. Riometer absorption data, 5-8 August 1972.

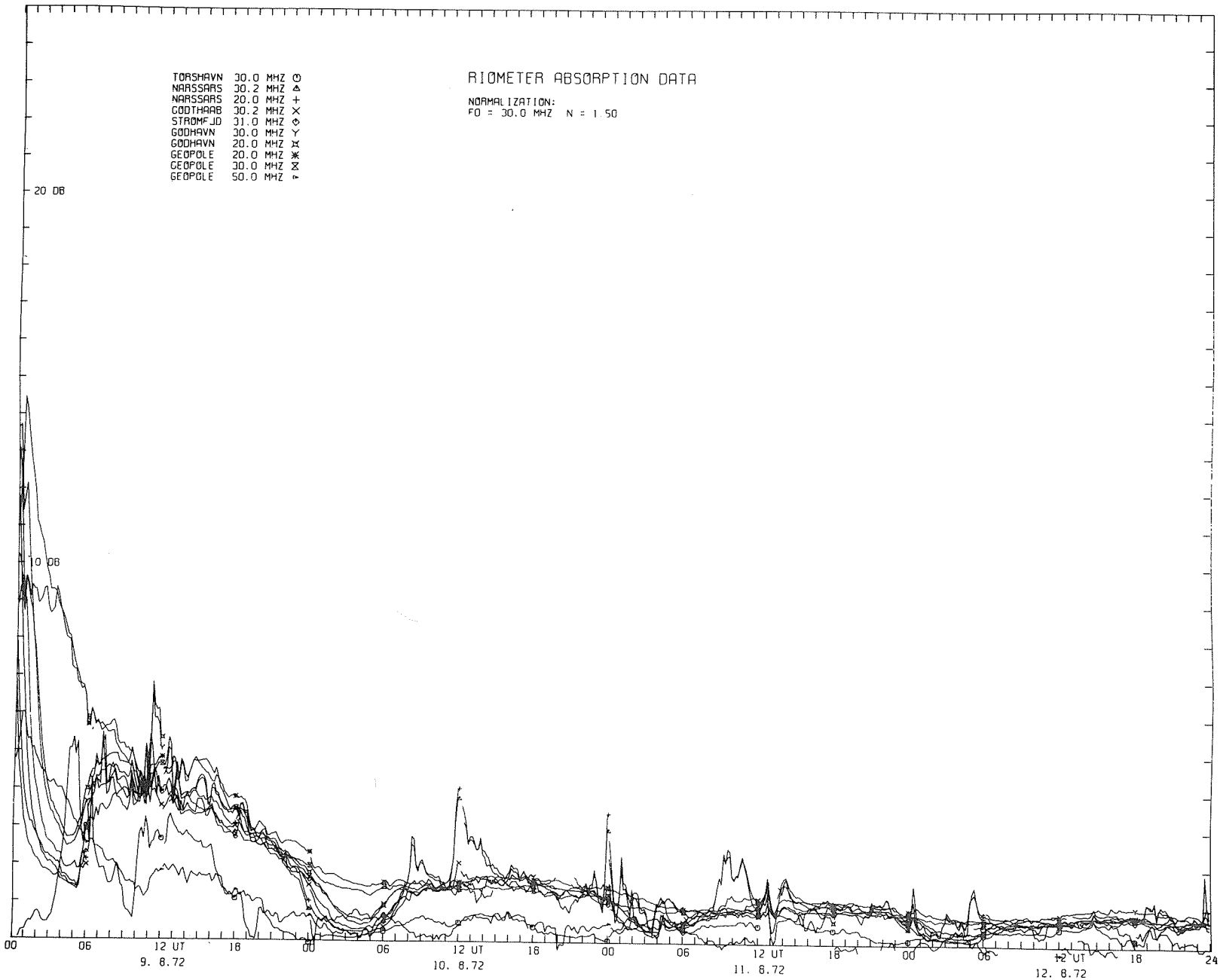

Fig. 2c. Riometer absorption data, 9-12 August 1972.

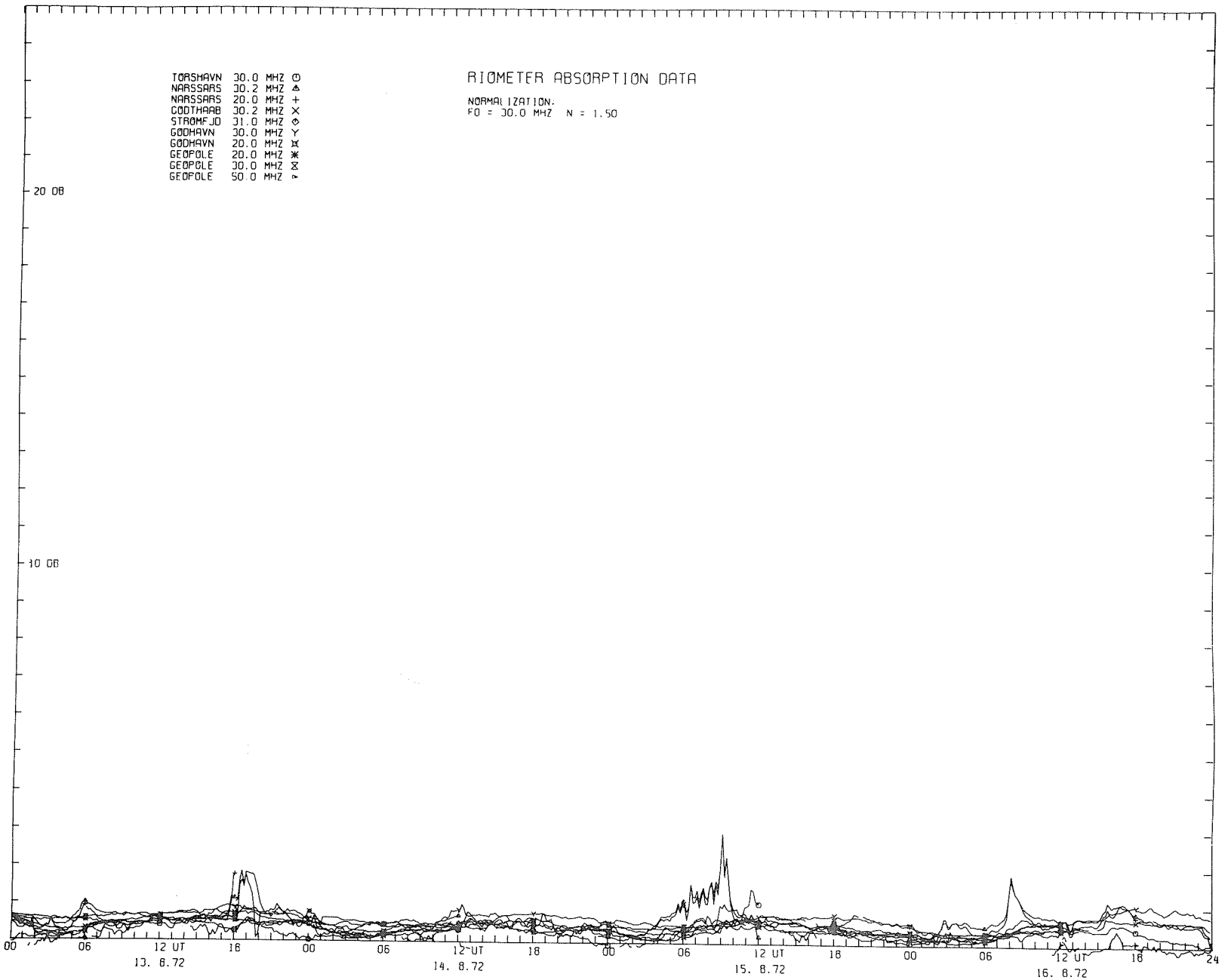

Fig. 2d. Riometer absorption data, 13-16 August 1972.

Equipment

The 30 and 50 MHz riometers at the Geopole Observatory are ARI, Mark II versions, while the remaining 20 and 30 MHz instruments are IONLAB, Model II, riometers constructed and manufactured at the Ionosphere Laboratory. In the standard set-up the riometer data are recorded on Esterline Angus curvilinear recorders. Timing of the charts is accomplished by a crystal controlled digital clock system.

Data

(a) Riometer

Figures 2a-d present plots of all absorption data normalized to a common reference frequency of 30 MHz, from riometers listed in Table 1.

The riometer records (Esterline chart paper) are read off in 0.8 min. samples by means of a semi-automatic curve follower and A/D converter system.

A major problem for the scaling of riometer recordings is the uncertainty introduced when interfering signals - man-made interference or solar noise bursts - are superimposed on the steady cosmic noise level. In cases where the minimum detection circuitry appears capable of producing a consistent lower envelope for the recorded trace, this lower envelope is read off. Otherwise data from periods with interference are excluded from the further data processing.

The reference levels (QD-curve) have been found as the upper envelopes of "mass plots" of riometer data from a number of 14-day periods through approximately one year. These reference levels are believed to be accurate within approximately 0.2 dB.

The timing of the riometer data samples is believed to be accurate within approximately ± 1 minute.

As mentioned above, the absorption values have been "normalized" to a common reference frequency of 30 MHz. According to the simplified theory, the absorption ($A(f_1)$) at a frequency f_1 which is assumed much higher than the gyro and collision frequencies can be written

$$A(f_1) = K \cdot f_1^{-n}$$

where K is a function of the electron density and the collision frequency. The exponent, n, corresponds to the theoretical frequency dependence of the non-deviative absorption at heights where the electron collision frequency is much smaller than the frequency of the received signal. The total height-integrated absorption will have the same form assuming that the above expression is valid at all heights.

Exponents of 1 and 2 represent extreme values for the frequency dependence of the total ionospheric absorption of cosmic noise signals. The actual value of the exponent reflects to some degree the steepness of the energy spectrum for the high energy solar flare protons. During auroral absorption events, the frequency exponent for absorption values measured at auroral latitudes may change due to the superimposed fluxes of auroral particles.

Figures 2a-d show good correlation for n = 1.5 between recordings on all stations and frequencies except for Torshavn, which is obviously at the border of the area significantly affected by the PCA event, and the Geopole 50 MHz. The reason for the discrepancy of the latter is probably that the 50 MHz riometer was not operating correctly so that these data are doubtful.

The "night and day" effect of solar illumination is clearly seen in most diagrams, especially August 8 at 0400 UT (local midnight) where the absorption on the Geopole riometers stays high because the sun is above the horizon, while the absorption at lower latitudes reaches a deep minimum at local midnight. During the night of August 7-8 the recordings were remarkably free of auroral disturbances.

For further information about data recorded by riometers in Greenland and at Faeroe Islands during the event period refer to Stauning [1973].

(b) Vertical Sounder

Some f-plots covering the period for the three stations Narssarssuaq, Godhavn and Thule are shown in Figures 3a-e.

The amount of information gathered from the vertical soundings is limited during such a big event, since no reflections are recorded during most of the period. The f-min stays above normal until August 14.

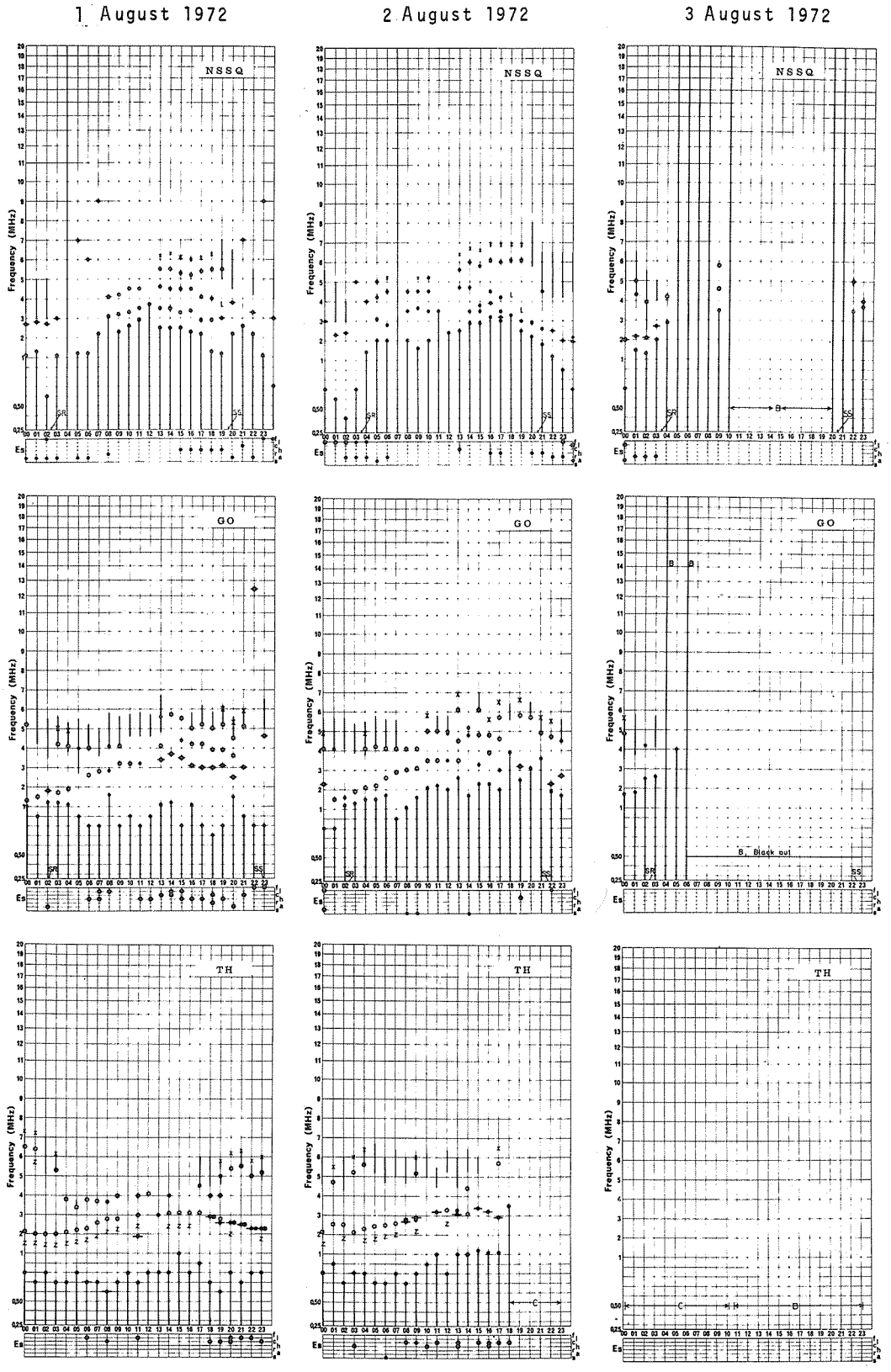

Fig.3a. f-plot of ionospheric data for Narssarssuaq (NSSQ), Godhavn (GO) and Thule (TH). All stations: Time zone 45 W.

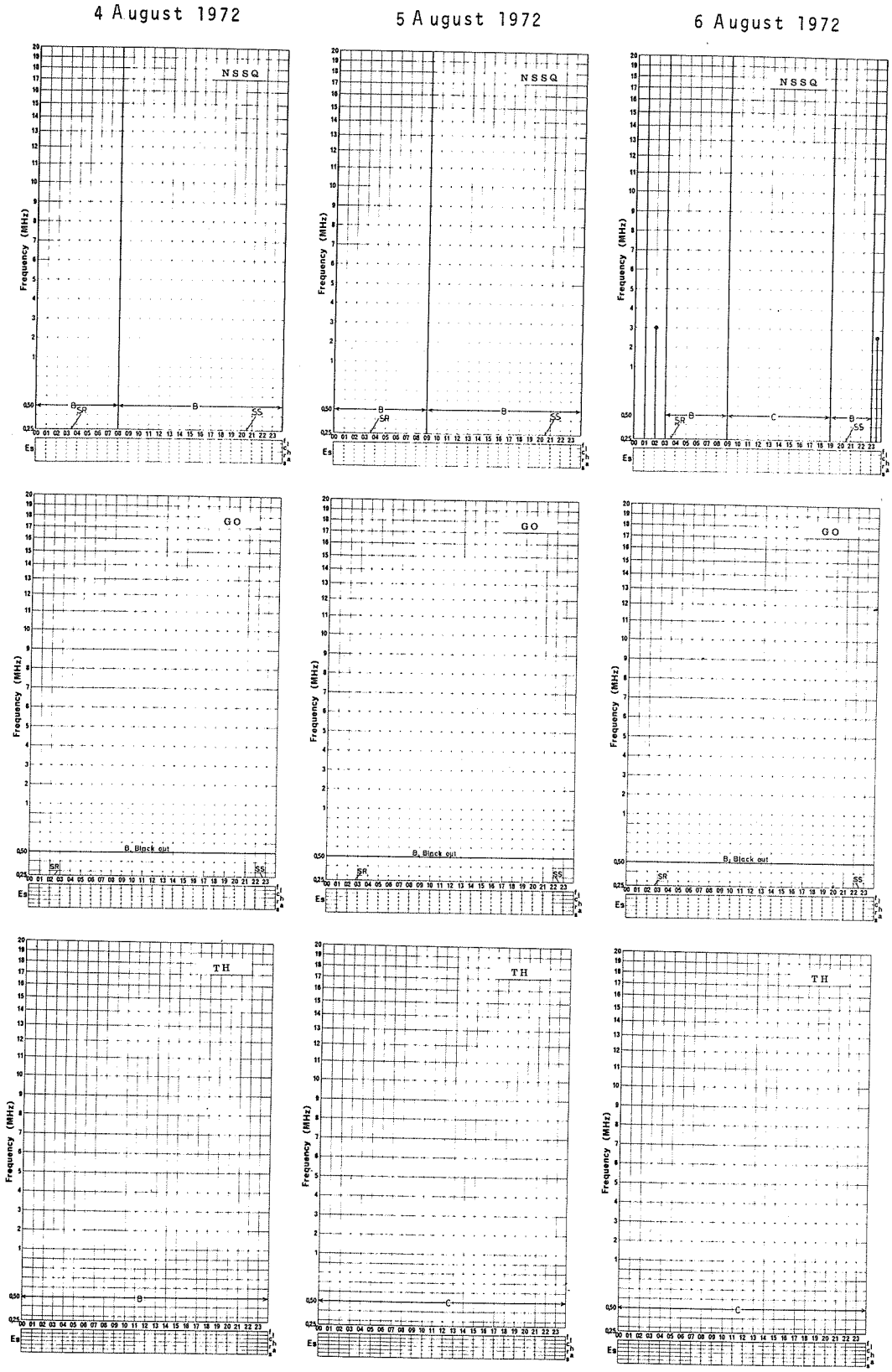

Fig.3b. f-plot of ionospheric data for Narssarssuaq (NSSQ), Godhavn (GO) and Thule (TH). All stations: Time zone 45 W.

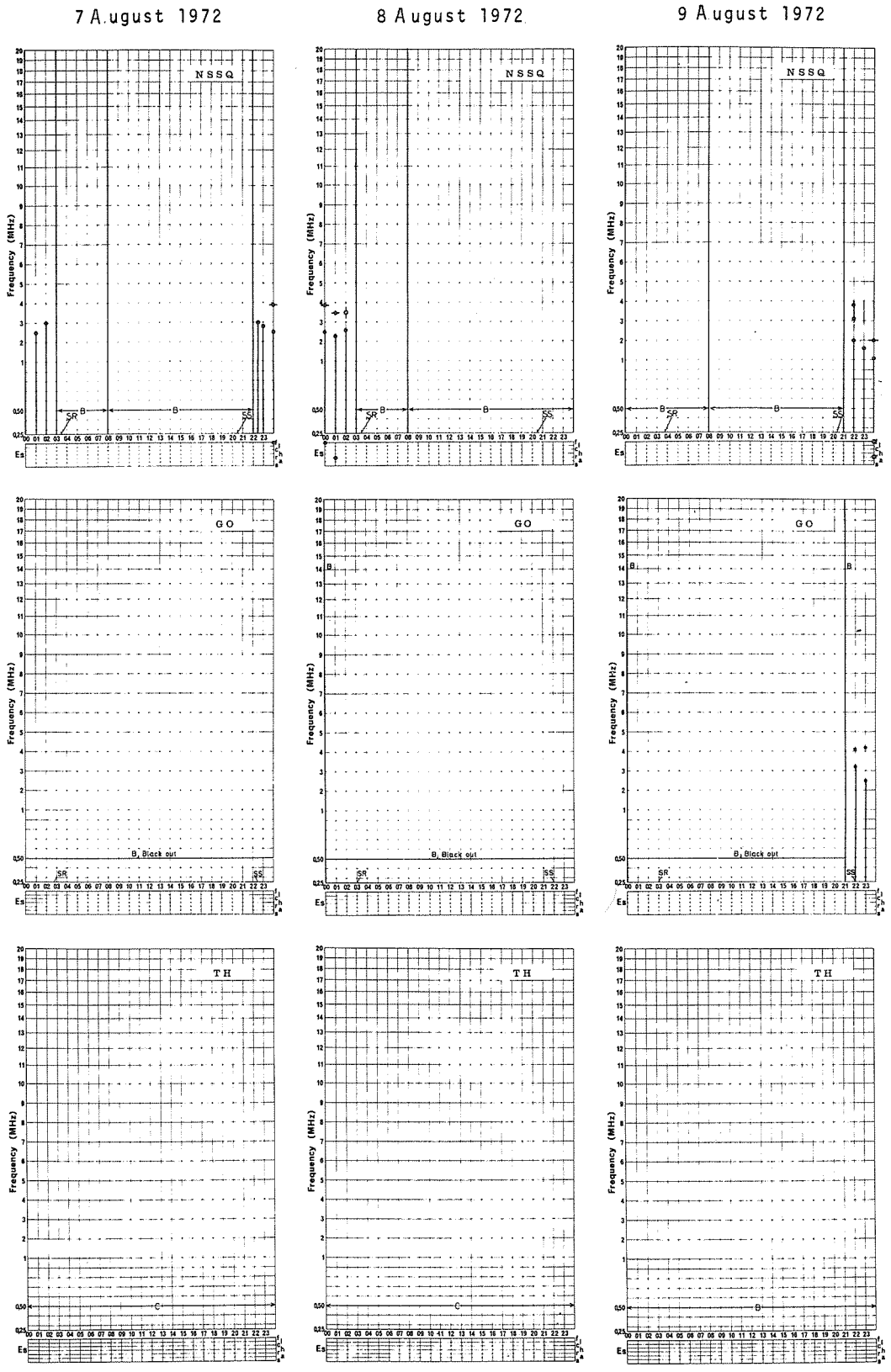

Fig.3c. f-plot of ionospheric data for Narssarssuaq (NSSQ), Godhavn (GO) and Thule (TH). All stations: Time zone 45 W.

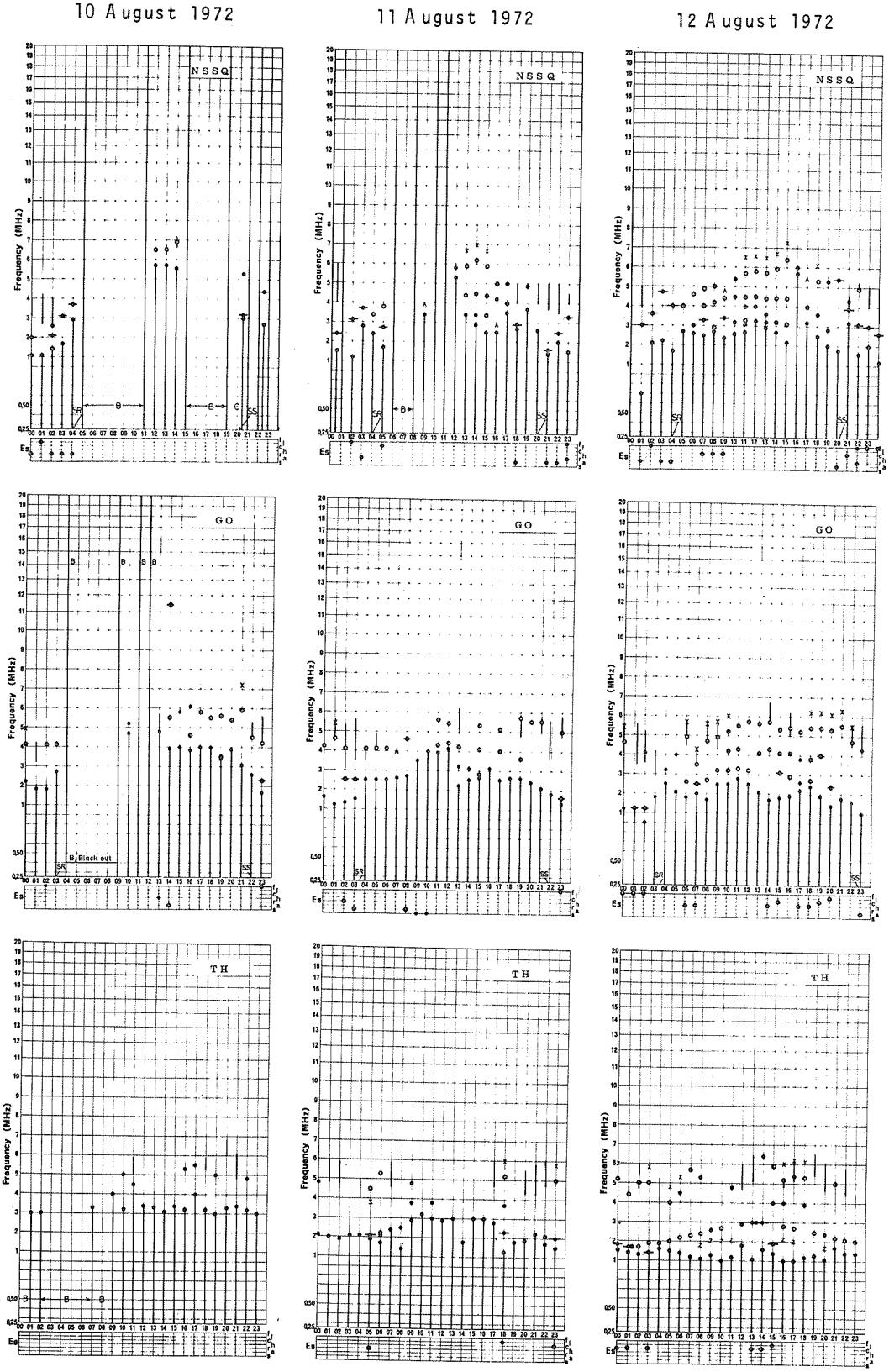

Fig.3d. f-plot of ionospheric data for Narssarssuaq (NSSQ), Godhavn (GO) and Thule (TH). All stations: Time zone 45 W.

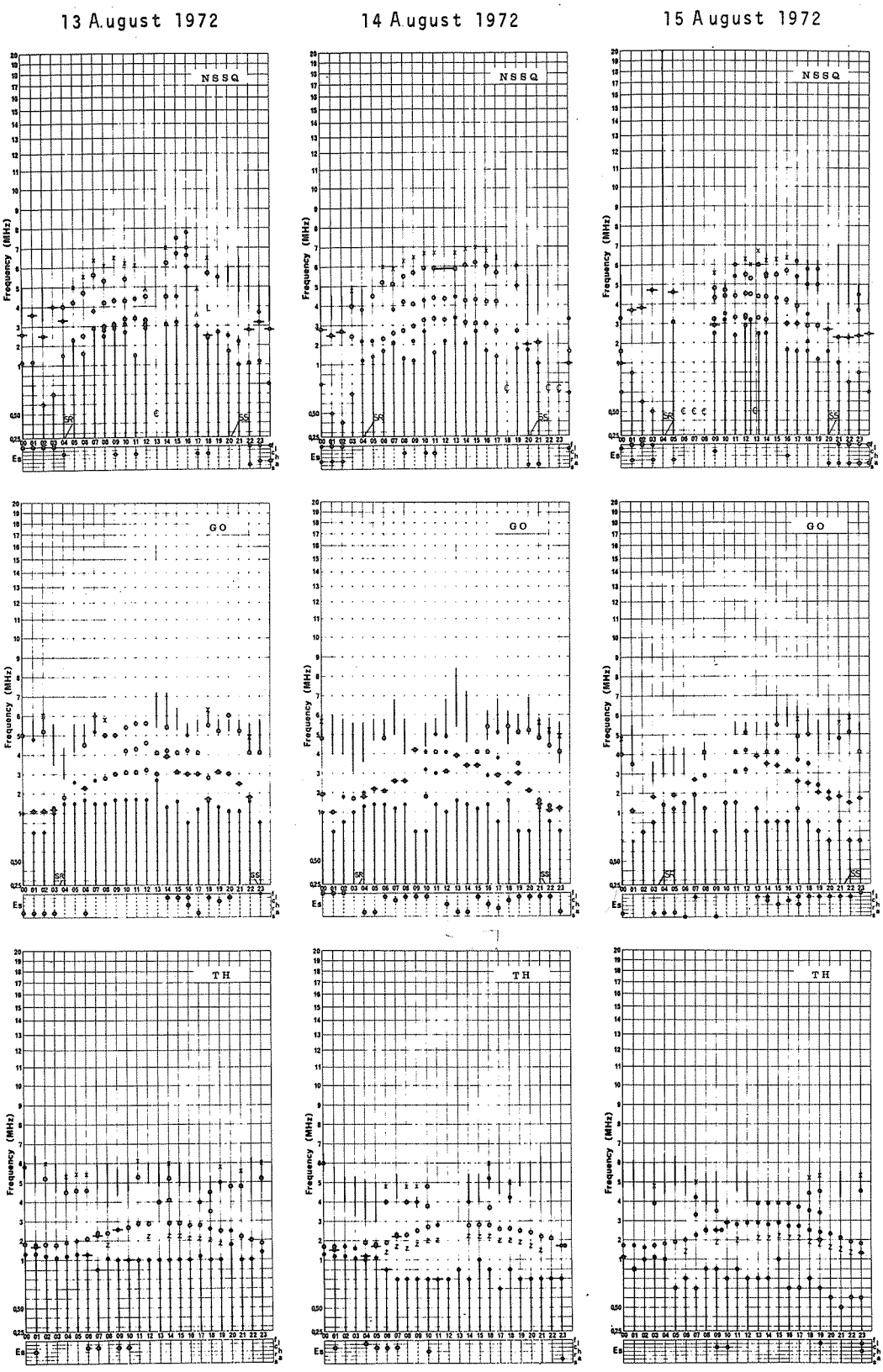

Fig.3e. f-plot of ionospheric data for Narssarssuaq (NSSQ), Godhavn (GO) and Thule (TH). All stations: Time zone 45 W.

(c) HF-communication

Some HF-propagation data from the commercial network between Denmark (Reersø, N55.1; E11.0 near Copenhagen) and Greenland (Godthåb, N64.2, E308.2) are presented in Figures 4a-b together with riometer data from Godthåb, Greenland, and Torshavn on the Faeroe Islands.

The full line in the communication data represents periods with good conditions, the thin line represents fair conditions, and no line, with a "B", represents no communication, i.e., "black out".

REFERENCES

JENSEN, V. N. and J. TAAGHOLT 1972 IONLAB Report B55.

STAUNING, P. 1973 Riometer Data August 1-16, 1972, IONLAB Report IR89, February 1973.

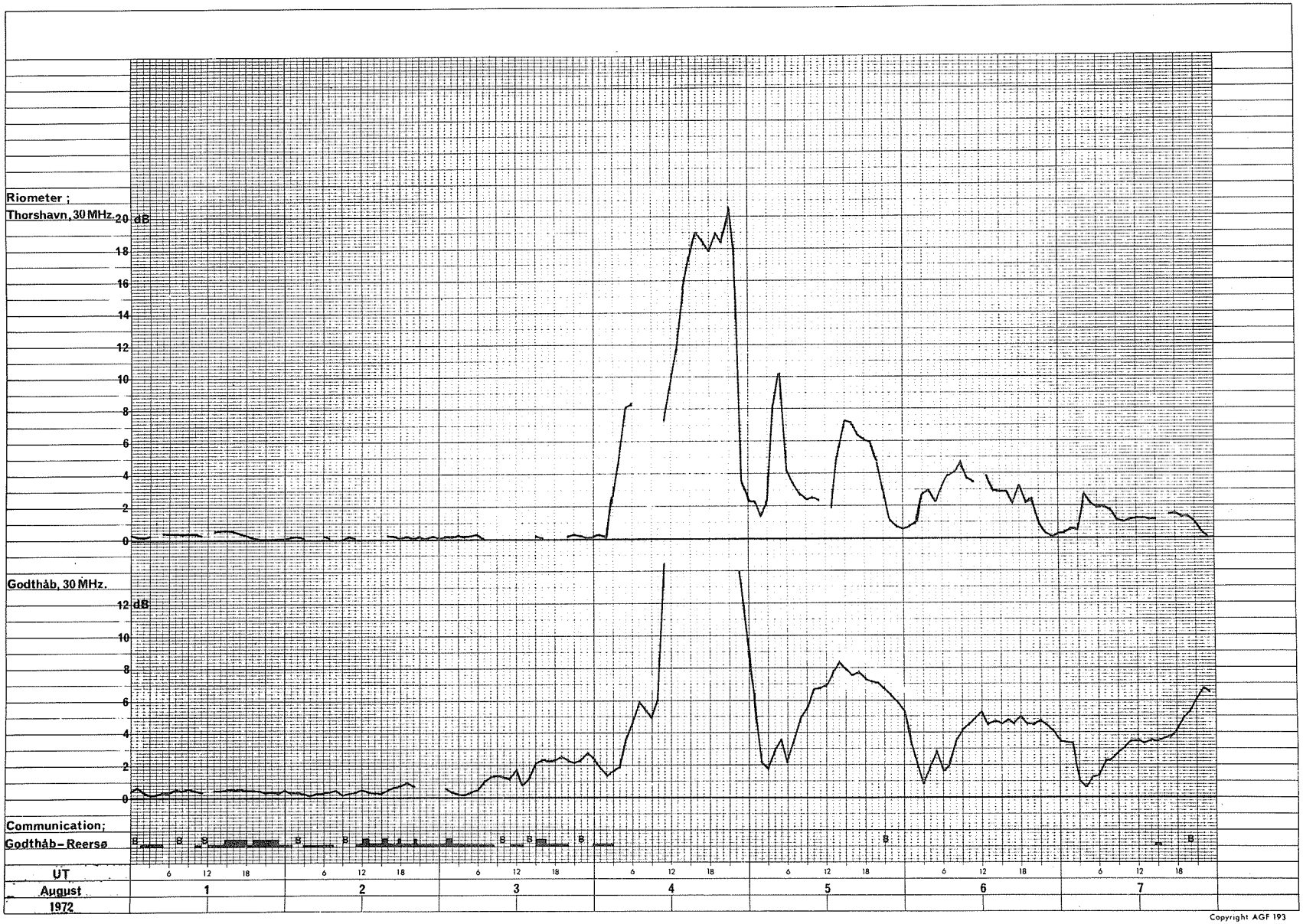

Fig.4a. HF-propagation data, Godthåb-Reersø. 1-7 August 1972.

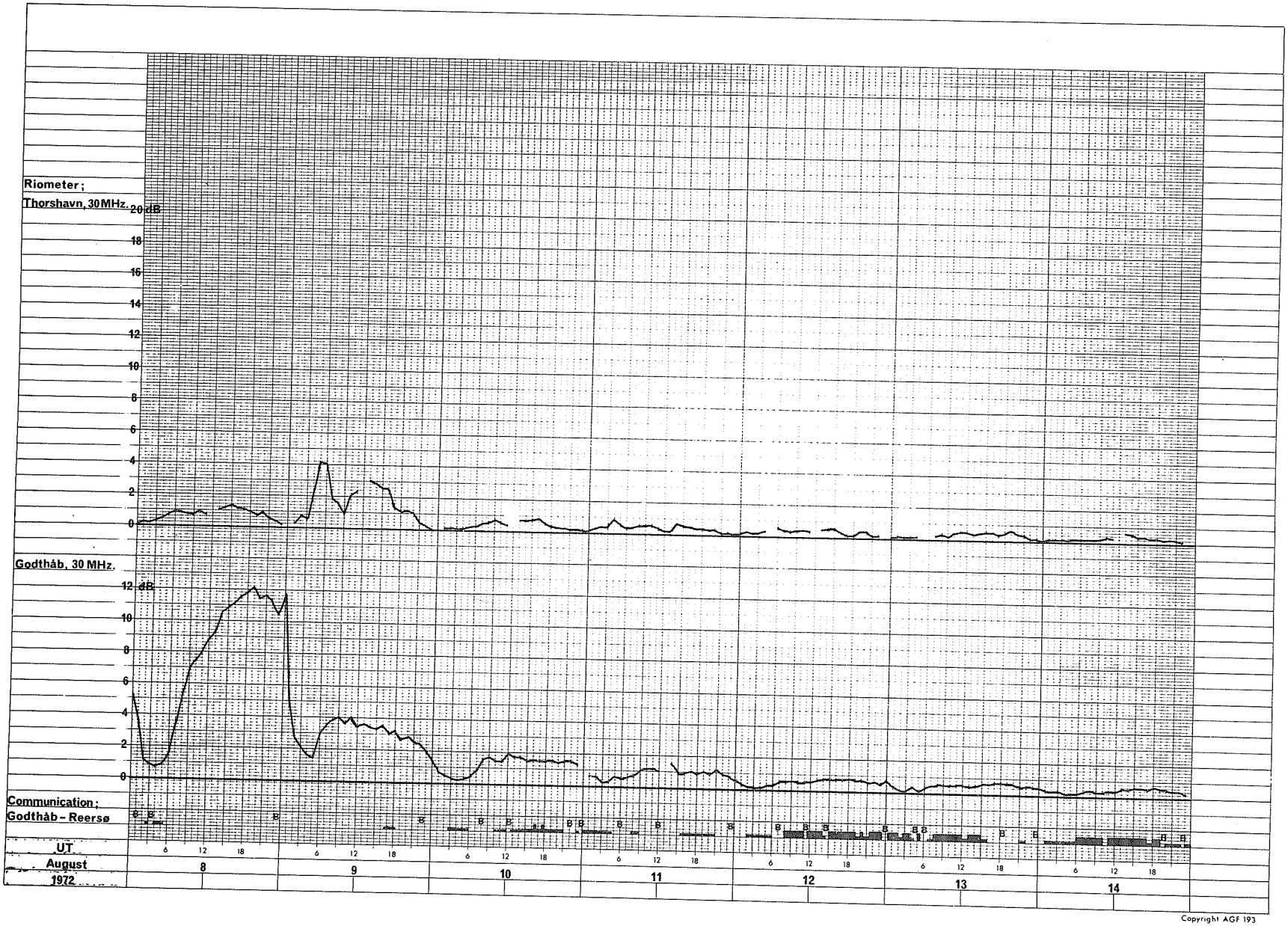

Fig.4b. HF-propagation data, Godthåb-Reersø. 8-14 August 1972.

Polar Riometer Observations during August 1972

by

Raymond J. Cormier
Air Force Cambridge Research Laboratories
L. G. Hanscom Field
Bedford, Massachusetts 01730

During the events of August 1972, riometer data were collected on a routine basis at Thule and Godhavn, Greenland, and Goose Bay, Labrador, Canada. The site coordinates are given in Table 1. All the riometer receivers used are ARI, 100 types, the antennas are all zenith pointing. Thule and Godhavn sites utilize a two element YAGI antenna over a ground screen; Goose Bay uses a duo-dipole separated by approximately 1/2 wavelength, at a height of 1/4 wavelength over a ground screen.

Absorption values were obtained by referencing the daily riometer event readings to a provisional "quiet-day" curve modified by the daily values taken three days prior to the disturbed period. The absorption data are presented as plots of dB absorption values versus universal time; however, the reduced data are available in five-minute increments. The plots are placed on one figure to facilitate the intercomparison of data from the three sites. Also, plotted on the figure for easy reference are the values of the square root of the proton flux of energies > 10 Mev as reported in the Solar-Geophysical Data reports.

The plots are self-explanatory. I would like to comment on a few "no-data" periods. For example, the riometer receiver at Thule was saturated during the times on August 4 from 1200 - 2200 hours UT and on August 8 at 1900 hours UT. The Godhavn riometer was saturated on August 4 from 1400 to 2300 hours UT and on August 8 between 1400 and 1600 hours UT.

Acknowledgements

I wish to thank Dr. S. Silverman and personnel at AFCRL for the operation and maintenance of the riometer equipment at the AFCRL geopole station at Thule, Greenland, and the technicians responsible for the Godhavn, Greenland, and Goose Bay, Labrador, riometer data.

REFERENCE

1973 Solar-Geophysical Data, 342, Part II, February 1973, U.S. Department of Commerce, (Boulder, Colorado U.S.A. 80302), 90.

TABLE I

Station	Geographic Coordinates	Corr. Geomagnetic Coordinates
Thule Greenland	76°31'N 68°50'W	86.0°N 38.1°E
Godhavn Greenland	69°15'N 53°20'W	77.7°N 41.7°E
Goose Bay Labrador	53°18'N 60°30'W	64.5°N 20.4°E

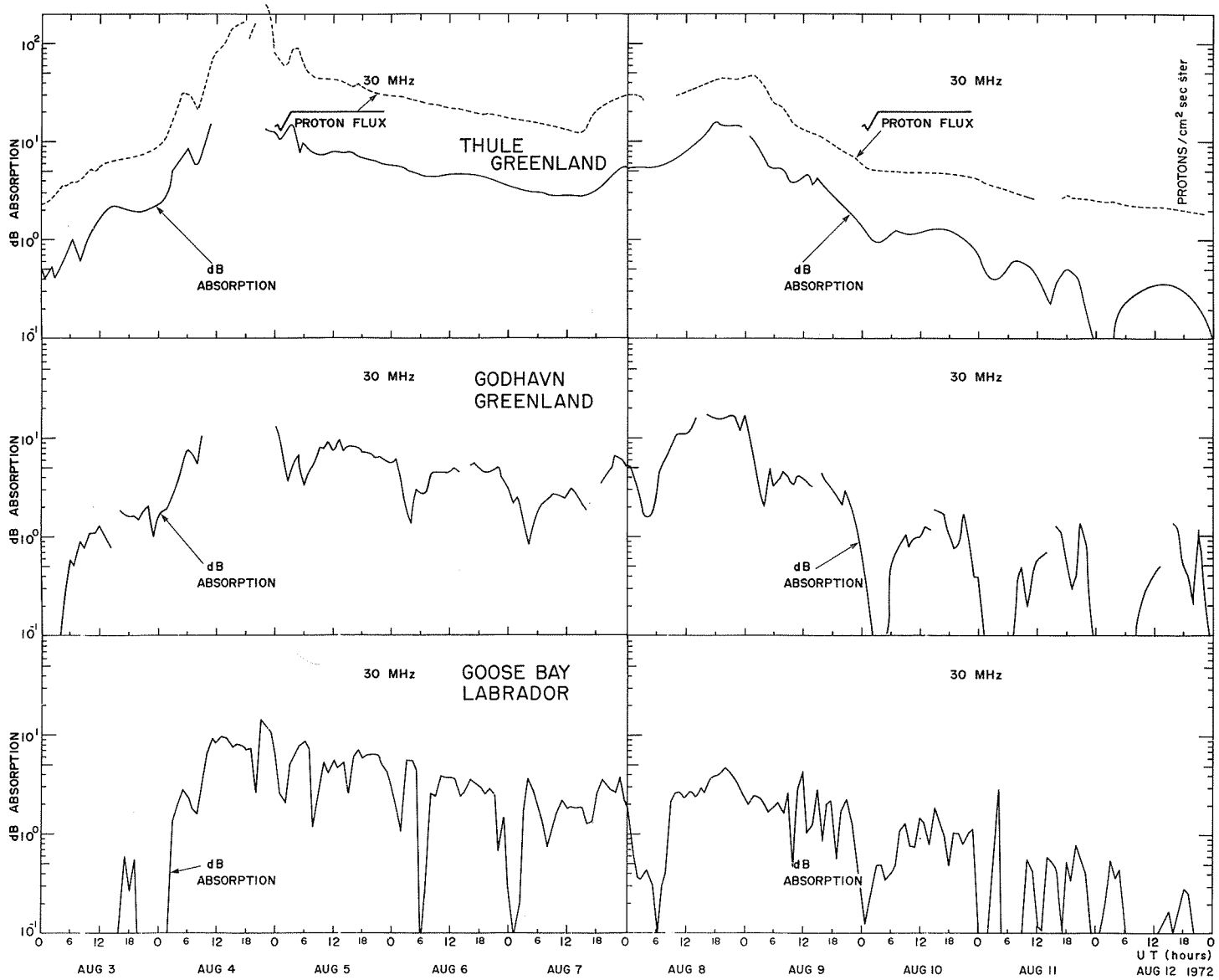

RIOMETER OBSERVATIONS AUGUST 1972

Polar Cap Disturbances of August 1972 Observed on Transpolar VLF Phase Measurements

by

Y. Hakura, T. Ishii, T. Asakura, and Y. Terajima
Radio Research Laboratories
Japan

Phase measurements of VLF waves propagated over great distances have been made at Inubo Radio Wave Observatory, RRL (N35.7, E140.85). It was shown elsewhere [Ishii et al., 1973] that the measurement of transpolar waves with a cesium frequency standard provided a very sensitive method for detection of polar cap disturbances (PCD) caused by solar protons with energies of 10 - 100 Mev. This report gives the time history of proton-flare-associated PCD's and their modifications due to geomagnetic disturbances that occurred during the first part of August 1972, by analyzing the phase measurement data for waves received from NAA-17.8 kHz, GBR-16.0 kHz, and NPG-18.6 kHz. The propagation paths for these VLF waves pass through the polar cap, the auroral zone, and the sub-auroral zone, in the northern hemisphere.

McMath plage region 11976 produced a series of major flares during its presence on the visible disk of the sun in the first part of August 1972. Among them, four flares, F-1 through F-4 given in Table 1, are selected here because of their radio, optical, and X-ray characteristics. The Kakioka Magnetic Observatory reported four major geomagnetic storms with sudden commencements (ssc's), M-1 through M-4 in Table 1 . The onset times and the maximum Kp-indices during each of the four storms are given in columns 15 and 16 of this Table.

Table 1

Summary of SPA's and PCPA's Associated with Four Major Solar Flares and Geomagnetic Storms in August 1972

Event No.	FLARE	NAA-17.8 kHz				GBR-16.0 kHz				NPG-18.6 kHz				GEOMAGNETIC SSC	
		SPA	PCPA			SPA	PCPA			SPA	PCPA				
	onset	$\Delta\varphi$	onset	max. time	$\Delta\varphi$	$\Delta\varphi$	onset	max. time	$\Delta\varphi$	$\Delta\varphi$	onset	max. time	$\Delta\varphi$	onset	max. Kp
F-1	2/0310	64°	2/1400	3/05	48°	53°	U	U	U	90°	-	-	-		
F-2	2/1959	58	3/0810	3/23	106	-	3/0815	3/16	70°	119	-	-	-		
M-1			4/02	4/06	173		4/02	4/06	90		4/0353	4/12	120°	4/0119 0220	8+
F-3	4/0619	83	4/0754	4/13	346	153	4/0738	4/15	340	112	-	-	-		
M-2			4/1938	4/21 *5/01 5/04	417 -235 +100		4/2027	4/23	240		U	U	U	4/2054	9
M-3			5/10	5/16	165		5/13	5/16	210		-	-	-	5/1400	9
F-4	7/1505	-	7/1612	7/23	202	35	U	U	U	-	-	-	-		
M-4			8/10	8/14	150		8/1011	8/13	190		-	-	-	8/2354 9/0037	8+
1	2	3	4	5	6	7	8	9	10	11	12	13	14	15	16

Δ : Phase advance

-: No event

* Initial phase recovery followed by redevelopment

U: Uncertain

Figure 1 shows diurnal phase variations of the three signals for July 31 through August 13, 1972. The onset times of the selected flares and the geomagnetic storms are indicated at the top and the bottom of the Figure. Regular quiet-day diurnal variations seen on July 31 and August 1 were increased violently by the solar and magnetospheric disturbances after 0300 UT on August 2. Figure 2 shows the deviations of the phase of the NAA signal from its average diurnal phase variation on magnetically quiet days (July 31, August 1, 15, and 17). The effects of solar and magnetospheric disturbances are seen more clearly in this graph than in Figure 1. Concurrently with the four flares designated F1 through F4 VLF waves traversing the sunlit hemisphere underwent sudden phase anomalies denoted S(F1) through S(F4) in Figure 2. The maximum phase advances attributed to solar X-ray bursts are given in columns 3, 7, and 11 in Table 1.

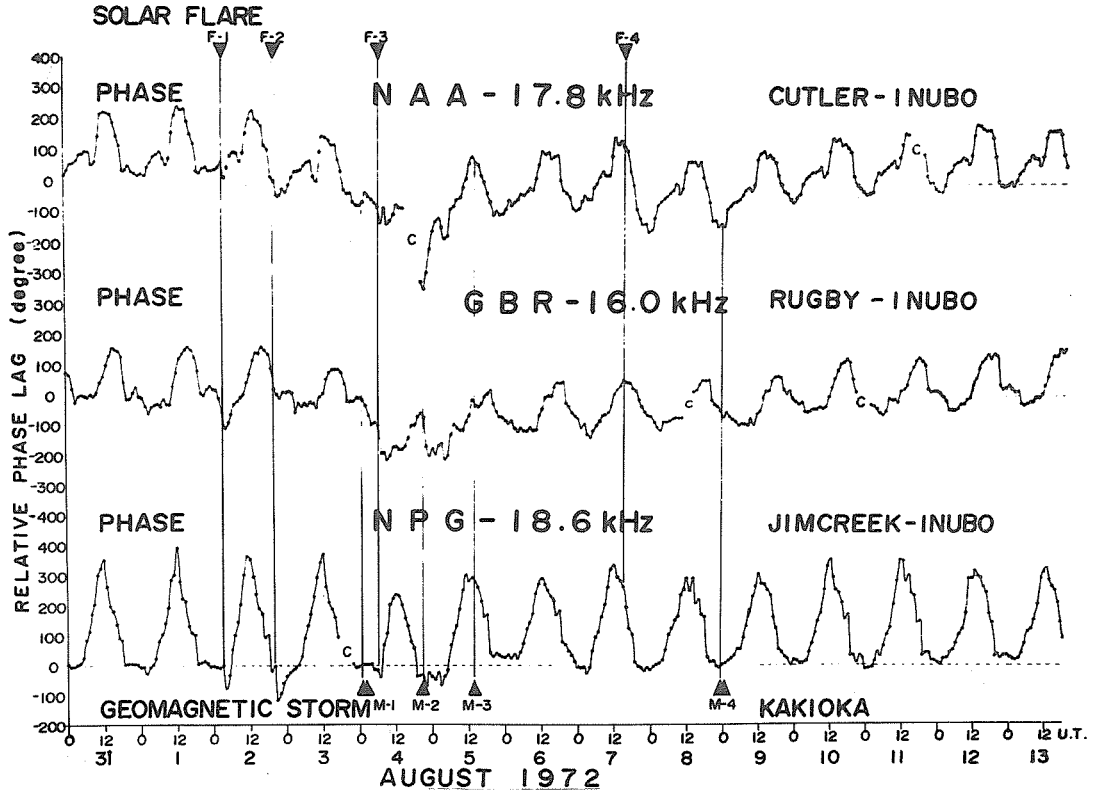

Fig. 1. Diurnal phase variations of VLF waves over three transpolar paths for July 31 through August 13, 1972.

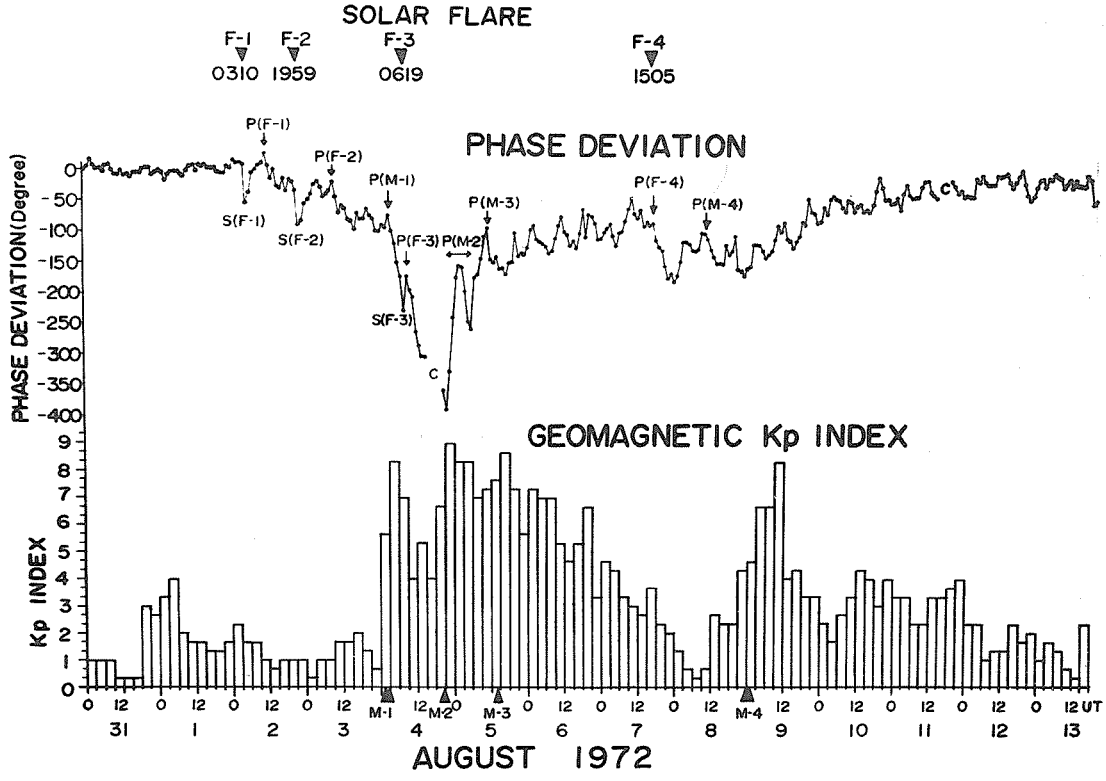

Fig. 2. Phase deviation of NAA-17.8 kHz signal from average quiet-time diurnal variation and geomagnetic Kp indices for July 31 through August 13, 1972.

From considerations of their radio, optical and X-ray characteristics, these flares are supposed to have emitted energetic protons into the interplanetary space. Actually, phase variations in the NAA signal marked four PCD's successively, about 11, 12, 1.6, and 1.1 hours after each of the solar flares. The onset times, the times of maximum phase anomaly, and the maximum phase advances in degrees are shown in columns 4-6 of Table 1. The mark P(F-i) in Figure 2 shows the onset of a PCPA (polar cap phase anomaly) due to the i-th flare. During the first PCD, the GBR signal showed little phase anomaly, indicating that the event was on a minor scale and the region of PCD was restricted to the polar cap. On the other hand, effects of the next three PCD's appeared in the trans-auroral zone phase measurement, characteristic parameters of which are given in columns 8-10 of Table 1. Phase anomalies of the NAA and GBR signals were also observed in connection with geomagnetic storms. They are denoted P(M-i)'s in Figure 2. During the first two geomagnetic storms, the region of PCD shifted into the sub-auroral zone, as seen in phase anomalies of the NPG signal on August 4 and 5 shown in Figure 1.

Figure 3 shows time variations of the solar proton flux in two energy ranges, Ep > 10 Mev and > 60 Mev, observed by IMP 5 and 6 [Bostrom, et al., 1972]. It also shows the smoothed phase deviation of the NAA signal, the geomagnetic equatorial Dst value [Sugiura and Poros, 1972], and the galactic cosmic ray intensity observed at Mt. Norikura [Wada, et al., 1972] on August 2 through 10, 1972. It may be seen that the slow-onset type PCPA's, P(F-1) and P(F-2), and the ssc-associated PCPA's, P(M-1), P(M-2), and P(M-4), are correlated with 10 Mev proton flux enhancements, while the time variation of the fast-onset-type PCPA's, P(F-3) and P(F-4), during their early stages is similar to that of 60 Mev proton flux. A recovery followed by a redevelopment of the phase anomaly occurred on the NAA signal during the eight hours following 2100 UT on August 4, in the course of the second geomagnetic storm, M-2. According to a McMurdo report of 30 MHz riometer absorption [Axford and Chivers, 1972], the considerable oscillation of PCD seen in the northern hemisphere was also observed at an Antarctic station. It is interesting to note that the similar oscillations appeared not only in the satellite observation of 10-60 Mev solar protons near the earth, but also in the ground-based observation of 10 Gev cosmic rays as seen in Figure 3.

Based on the present study of VLF phase anomalies, the August 1972 event is considered to be the most severe disturbance thus far in the present sunspot cycle and to be of a scale comparable with the famous February 11, 1958 event [Hakura and Nagai, 1964]. Synoptic analysis of PCA using riometers and fmin records all over the world should be made in the future in order to obtain a more detailed picture of this very interesting solar-terrestrial disturbance.

REFERENCES

AXFORD, W. I. and H. J. A. CHIVERS	1972	World Data Center A for Solar-Terrestrial Physics, Report UAG-21, 110.
BOSTROM, C. O., et al.	1972	The solar proton flux - August 2-12, 1972, preprint, Applied Physics Lab., Johns Hopkins Univ.
HAKURA, Y. and M. NAGAI	1964	Synthetic study of severe solar-terrestrial disturbances on Feb. 9-12, 1968, JRRL, 11, 197-250.
ISHII, T., Y. HAKURA, T. ASAKURA, and Y. TERAJIMA	1973	Polar disturbances of VLF waves observed at Inubo, Quart. Rev. RRL, in press.
	1973	Solar-Geophysical Data, 342, Part II, U.S. Department of Commerce, (Boulder, Colorado U.S.A. 80302).
SUGIURA, M. and D. M. POROS	1972	World Data Center A for Solar-Terrestrial Physics, Report UAG-21, 126-127.
WADA, M., et al.	1972	Cosmic ray intensity variance during August 1-10, 1972, RISRJ, 26, 298-305.

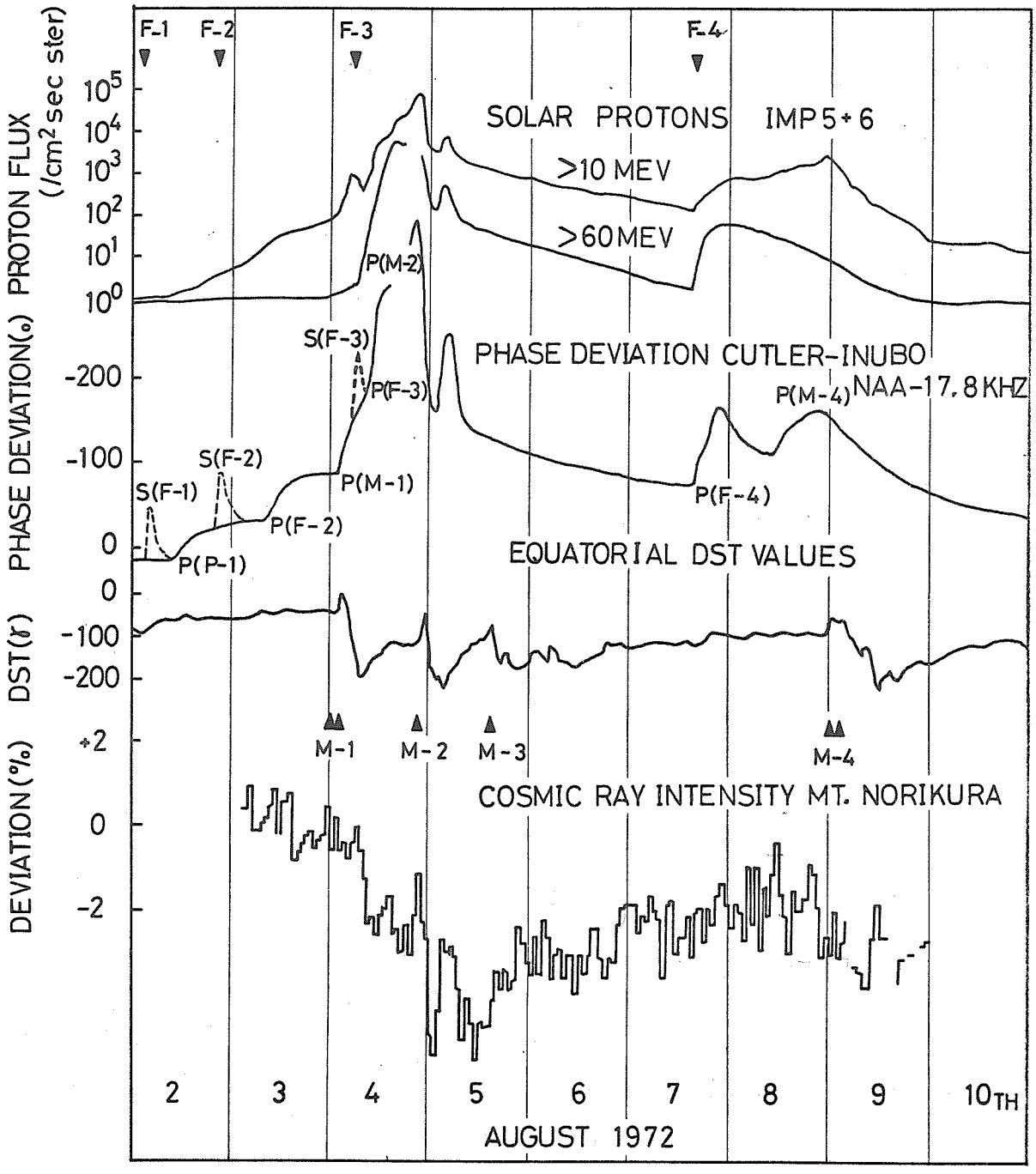

Fig. 3. Variation in smoothed phase deviation of NAA signal, in comparison with those in solar proton flux, geomagnetic equatorial Dst value, and galactic cosmic ray intensity, for August 2 through 10, 1972.

Polar Observations During the August 1972 Solar Cosmic Ray Events

by

A. J. Masley and M. B. Baker
Space Sciences Department
McDonnell Douglas Astronautics Co.-West
Huntington Beach, California 92647

Introduction

The McDonnell Douglas Antarctic Geophysical Observatory is located at McMurdo Sound (77°51'S, 166°43'E). The magnetically conjugate Arctic observatory is located at Shepherd Bay, N.W.T. (68°49'N, 93°26'W). These stations, at a geomagnetic latitude of 80° are located inside the polar cap regions, removed poleward from the auroral zones to minimize auroral interference and geomagnetic cutoff effects.

Radio techniques are used which allow effects taking place at altitudes from 30 to 90 kilometers to be observed with ground-based equipment. Riometers are operated which measure the signal strength of galactic radio noise at 30 and 50 MHz. The ionization produced by the interaction of the charged particles with the atmosphere increases the electron density so that radio waves passing through the ionosphere are significantly absorbed. The absorption of the radio waves at a given frequency is proportional to the square root of the intensity of charged particles for a fixed energy spectrum. This technique is sensitive to protons from about 5 to 100 MeV. Other equipment operating at the stations includes magnetometers and photometers at 3914Å and 5577Å.

Discussion of Observations

The 2 August and 7 August 1972 Solar Cosmic ray events were the largest observed since the McDonnell Douglas Polar Station Program began operation in February 1962 [Baker, Masley and Satterblom, 1972; Masley and Baker, 1972]. Our analysis of riometer data suggests that the peak intensities for > 10 MeV were comparable to those during the 2 November 1960 event. During this event, McMurdo was experiencing only short periods of daylight as shown by the arrows in Figure 1. The Shepherd Bay station had continuous sunlight down to 30 km, although the earth's shadow reached a higher level each day and was at 23 km on 10 August. A significant diurnal effect can be seen in the data.

Riometer absorption at 30 MHz began to increase at about 0800 UT on 3 August at both polar stations. Significant radio noise was seen on the Shepherd Bay riometers during the period 2000-2400 UT on 2 August. At 0000 UT on 4 August the absorption began to increase rapidly. The Shepherd Bay 30 MHz riometer was saturated from about 1120 to 2330 UT on 4 August. The McMurdo 30 MHz riometer was saturated from 2110 to 2250 UT on 4 August just before McMurdo sunrise at 30 km (see Figure 1).

The absorption decayed until 7 August. At 1600 UT on 7 August, 30 and 50 MHz radio noise was observed at Shepherd Bay. At 1700 UT absorption was increasing, reaching 15 dB for 30 MHz at 0030 UT on 9 August.

Determination of Space Particle Intensity

Using the relationship between riometer absorption and the intensity of greater than 10 MeV protons established by Kane and Masley [1969, 1972] the particle intensity can be determined.

$$\mathrm{ABs(dB)}_{30} = 0.32\ J(>10)\ \mathrm{cm}^{-2}\mathrm{sec}^{-1}\mathrm{ster}^{-1}$$

During the period when the 30 MHz riometer was saturated, the 50 MHz absorption was used (Figure 2). The 30 MHz/50 MHz ratio determined during other parts of the event was used to obtain the effective 30 MHz absorption. We therefore had continuous unsaturated absorption measurements throughout the event. Although this is one of the major reasons

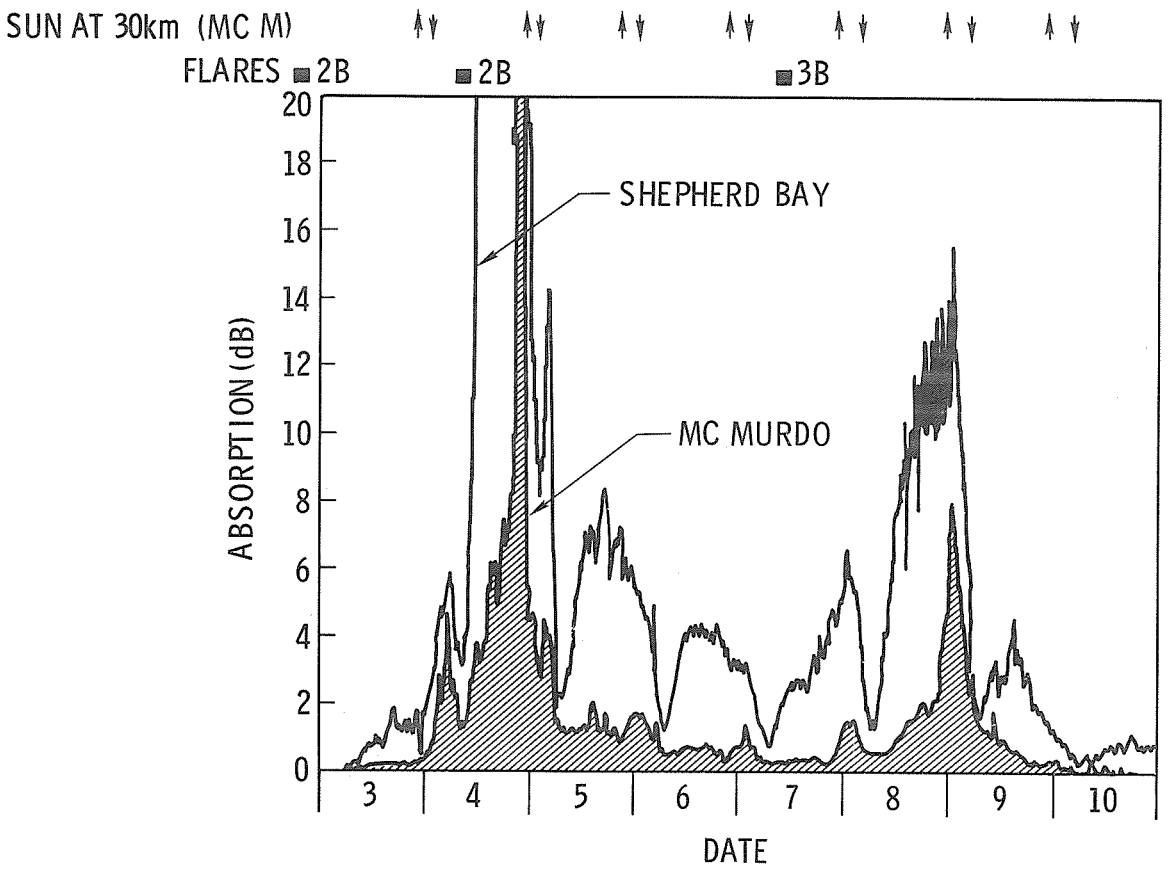

Fig. 1.

for operation of a 50 MHz riometer in addition to 30 MHz, this was the first time it was required during the past 11 years. The peak intensity for greater than 10 MeV protons inferred from the riometer measurements was $\sim 3 \times 10^4$ cm^{-2}sec^{-1}ster^{-1} at 2130 UT on 4 August. Since many satellite experiments were saturated or had undetermined intensities during the peak of this event, this information may be helpful in interpretation of satellite data. This intensity is equivalent to the peak greater than 10 MeV intensity during the 12 November 1960 event, one of the largest observed to date.

Solar Cycle Dependence

Figure 3 shows the integrated greater-than 30-MeV proton intensity for the past two solar cycles based on McDonnell Douglas analyses which have been continuously updated. The August 1972 events provided the highest production of solar particles of any event during this cycle. Due to the August events the 1972 production is near that of 1960, which was due primarily to the November 1960 events. The 1972 production surpassed that of 1969, which was due to the July 1969 events. There is considerable uncertainty in the 1969 number due to the quality of data available for the analysis.

Acknowledgements

This work was supported by the Office of Polar Programs, National Science Foundation under contract NSF-C393 and the McDonnell Douglas Independent Research and Development Program. We are indebted to the Canadian Government for allowing operation at the Shepherd Bay location.

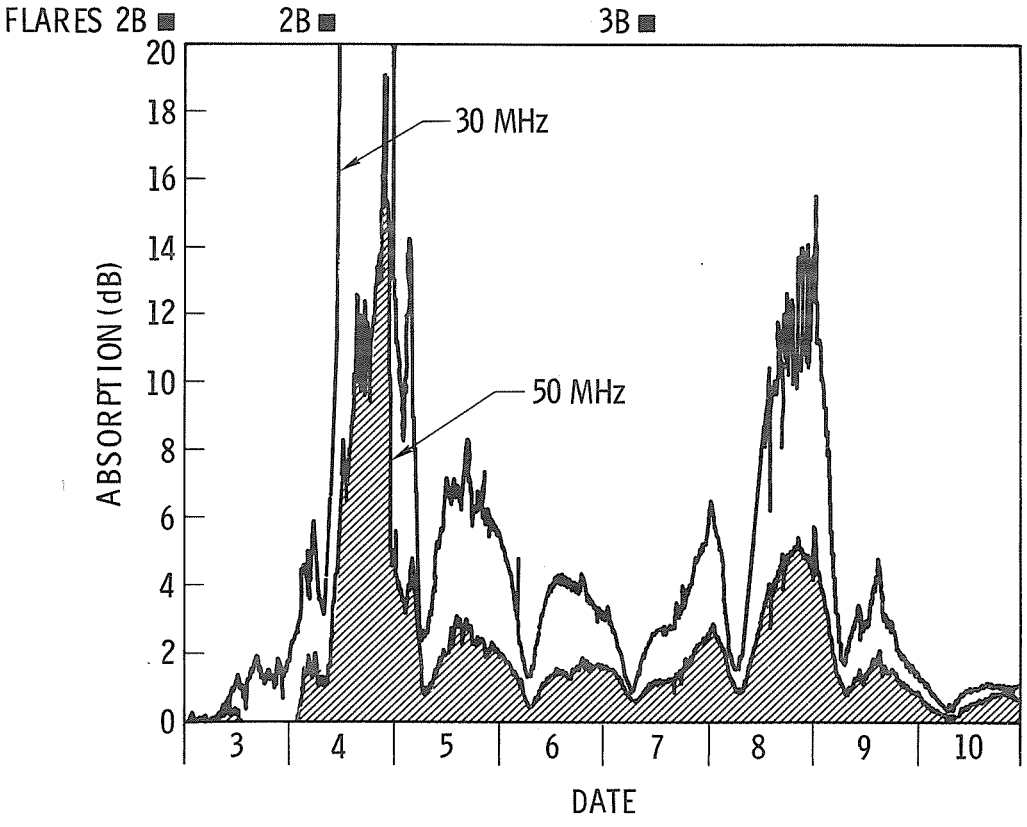

Fig. 2.

REFERENCES

BAKER, M.-B., A. J. MASLEY and P. R. SATTERBLOM 1972 Polar Riometer Observations of the August 1972 Solar Proton Events, EOS Trans. AGU, 53, 1056.

KANE, S.-R. and A. J. MASLEY 1969 The Relationship Between Polar Riometer and Solar Cosmic Ray Measurements in Space, EOS Trans. AGU, 50, 463.

KANE, S.-R. and A. J. MASLEY 1973 The Relationship Between Polar Riometer and Space Measurements During Solar Cosmic Ray Events, McDonnell Douglas Astro. Co. Paper WD 1030.

MASLEY, A.-J. and M. B. BAKER 1972 August 1972 Solar Particle Intensities, EOS Trans. AGU, 53, 1056.

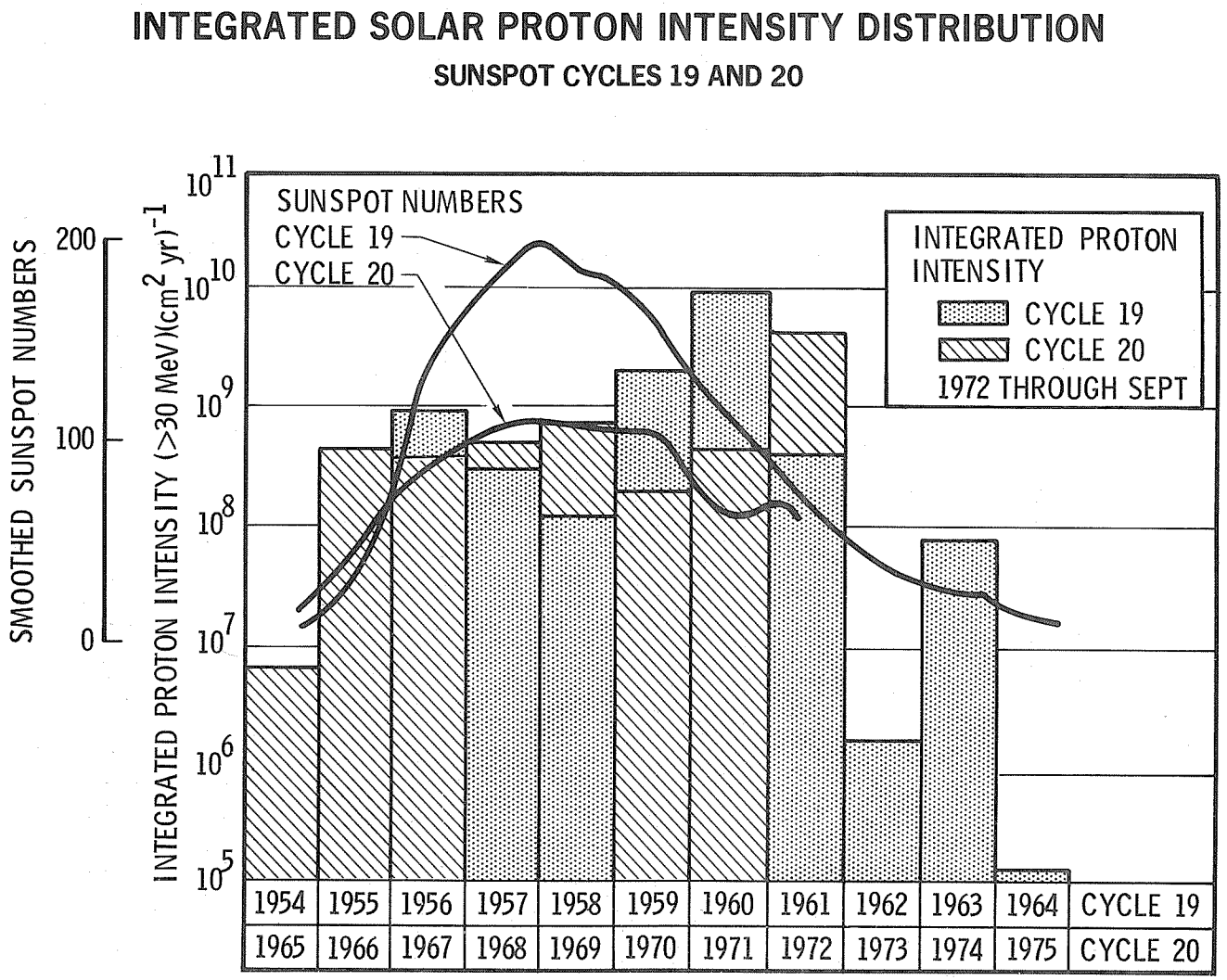
INTEGRATED SOLAR PROTON INTENSITY DISTRIBUTION
SUNSPOT CYCLES 19 AND 20
SMOOTHED SUNSPOT NUMBERS
200
100
0
INTEGRATED PROTON INTENSITY (>30 MeV)(cm^2 yr)$^{-1}$
10^{11}
10^{10}
10^9
10^8
10^7
10^6
10^5
SUNSPOT NUMBERS
CYCLE 19
CYCLE 20
INTEGRATED PROTON INTENSITY
CYCLE 19
CYCLE 20
1972 THROUGH SEPT
1954 1955 1956 1957 1958 1959 1960 1961 1962 1963 1964 CYCLE 19
1965 1966 1967 1968 1969 1970 1971 1972 1973 1974 1975 CYCLE 20

Fig. 3.

Characteristics of the August 1972 Solar Particle Events as Observed Over the Earth's Polar Caps

by

J. B. Reagan, W. L. Imhof, and V. F. Moughan
Lockheed Palo Alto Research Laboratory
Palo Alto, California 94304

Introduction

During the intense solar flares of early August, 1972, the fluxes and spectra of solar protons, electrons and alpha particles were measured over the earth's polar caps at 800 km altitude with the Lockheed experiment aboard the polar orbiting satellite 1971-089A. The experiment contains a comprehensive collection of low and high energy particle detectors as well as an earth-reflection-ionospheric sounder (ERIS) measurement. Data were collected on nearly every polar cap crossing during the period 3-12 August by means of on-board tape recorders.

The data presented in this preliminary report are from the high-energy-proton spectrometer (HEPS) in this experiment. This instrument, which has been described in detail elsewhere [Reagan et al., 1972], is a multi-element silicon detector stack mounted within a plastic scintillator guard counter to form a particle telecope that is oriented at 20° to the zenith to observe precipitating particles. The energy spectra of protons from 1.0-100 MeV, electrons from 0.76-2.1 MeV and alpha particles from 6-400 MeV are measured in four time-shared modes of operation with 256-channel pulse-height resolution. Counting rates from each of the main elements of the telescope and the guard counter corresponding to these modes are measured every 32 ms. Digital samples of individual pulse height data are made at the rate of 1024 samples/sec such that statistically meaningful spectra of all three particle types over the above energy ranges are obtained every several seconds. An identical spectrometer (HEAPS) is oriented at 90° to the zenith to observe mirroring particles.

Differential flux profiles of protons and electrons over the polar caps in several energy intervals have been processed and analyzed to date. In addition, the energy spectra of the protons, electrons and alpha particles have been generated at several different times throughout the events. Peak and integrated proton fluxes have been compared to previous large solar events in the present and previous solar cycle. The present polar cap data for the period 3-7 August clearly indicate that this event was the most intense and energetic observed at the earth in the last two decades.

Flux Profiles

The differential flux of protons in the 1-4.5 MeV energy range throughout the 3-13 August period is shown in Figure 1. The data shown have been taken from approximately 150 north and south polar cap crossings that occur every 50 minutes. The data points correspond to measurements taken near the maximum magnetic latitude of each polar pass and represent either 32 ms or 250 ms time averages. Averaging of the data over longer time intervals, which is in progress, will result in smoother profiles since some variations in the flux are observed on many polar cap crossings. On a few occasions large flux depressions were observed over the high latitude south polar cap [Reagan et al, 1973]. In these cases, the lower latitude flux values have been selected as being more representative of the flux incident on the magnetosphere.

Examination of the spectra of all three particle types indicates that the spectrometer functioned normally throughout the entire period. On a few polar passes at the peak of the event when the combined counting rates in the spectrometer exceeded 10^5 counts/sec, some shifting of the spectrum was observed due to pile-up effects. Corrections for pile-up were applied in these cases. In particular, careful examination of the data has been made to assure that the intense fluxes of energetic electrons present during these events were not contaminating the proton measurements. In no case was this evident. The spectra of the in-flight calibration sources (Am-241) in each detector reveal that no gain shifts of greater than 2 percent have occurred since launch, including the period of these events. Dead-time and chance-coincidence corrections amounting to no greater than 25 percent at the peak have been applied to the data. Cosmic-ray and calibration-source backgrounds have been subtracted.

The flux profile of these lower energy protons reveals several interesting features. First, the flux of these protons over the polar caps was substantial even as early as 0050UT on 3 August, some 24-hours prior to the arrival of the high energy protons associated with the large event of 4 August. These lower energy protons probably resulted from the flare of 2B importance that occurred in McMath Region 11976 at 1958UT on 2 August [Lincoln and Leighton, 1972]. The 1-4.5 MeV protons reached an initial peak flux of 5.7×10^4 protons/cm^2-sec-sr at 0530UT on 4 August. Sudden storm commencements as reported by NOAA [Lincoln and Leighton, 1972], and indicated at the top of Figure 1, occurred at 0119 and 0220UT on 4 August.

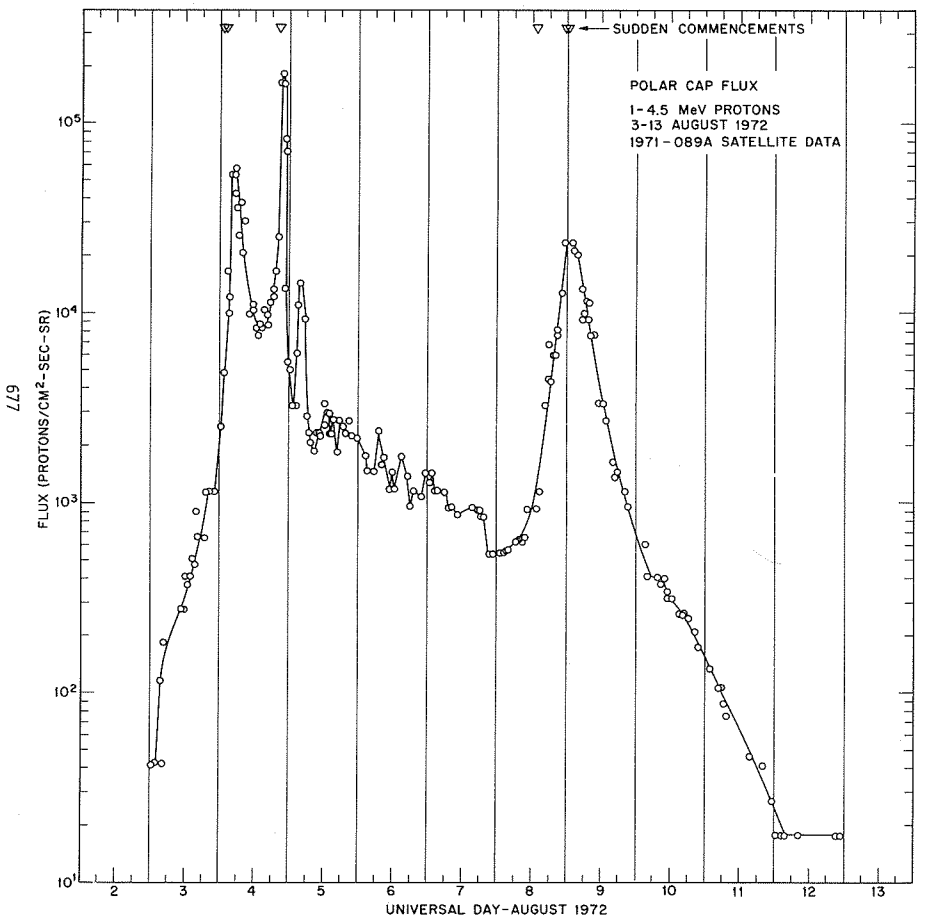

Fig. 1. Differential flux of 1 - 4.5 Mev protons as measured by the Lockheed spectrometer on the 1971-089A satellite during the 3-13 August 1972 solar particle events.

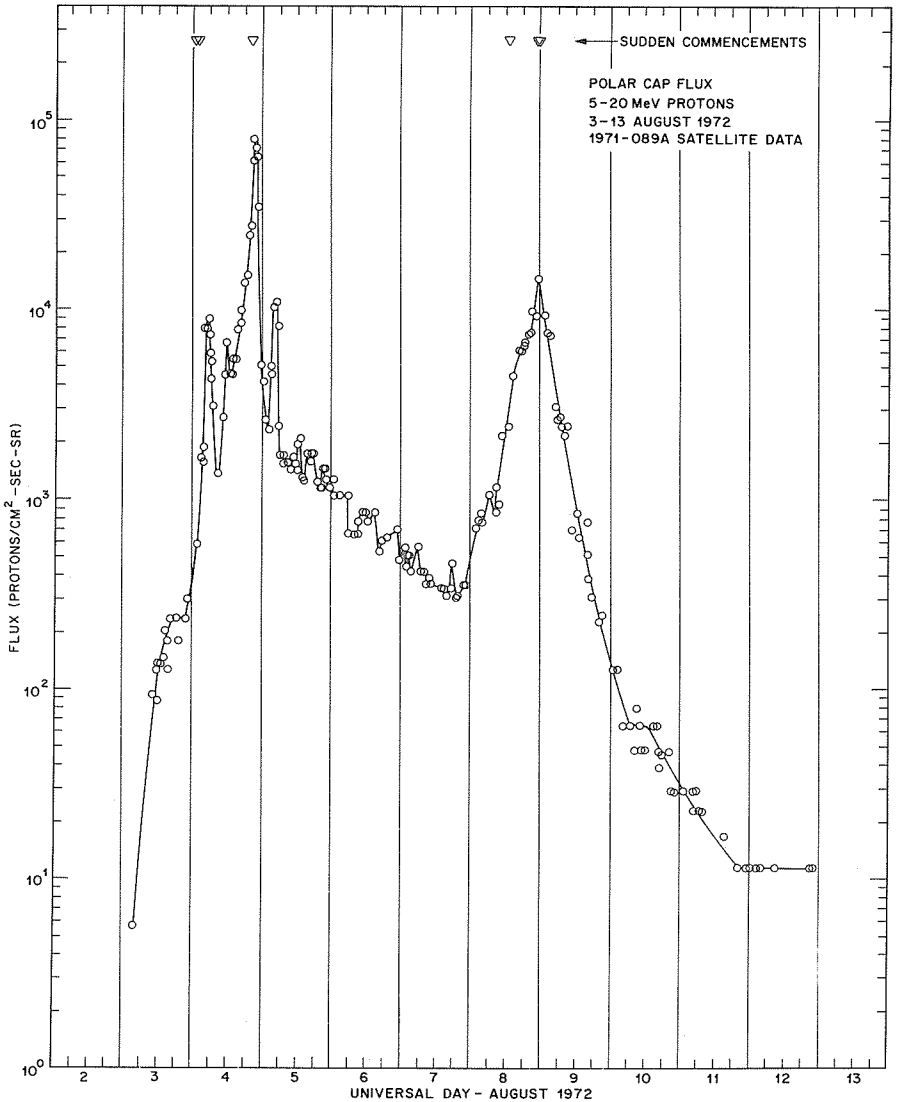

Fig. 2. Differential flux of 5-20 Mev protons as measured by the Lockheed spectrometer on the 1971-089A satellite during the 3-13 August 1972 solar particle events.

The flux decreased exponentially over the next 10 hours but at ~1600UT began to rise sharply to a peak value of 1.85 x 10^5 protons/cm^2-sec-sr at ~ 2200UT on 4 August. Examination of the higher energy proton and electron data show that the peak flux at all energies occurred at approximately this time. A sudden commencement occurred at 2054UT. This intense peak is most probably associated with the flare of 3B importance that occurred at 0530UT on 4 August 1972 in McMath Region 11976 (Lincoln and Leighton, 1972). The rise and fall of the protons near the peak was so rapid that large temporal variations in the flux (~ x 10) were observed over the approximately 15 minute time interval of a polar cap crossing.

At ~ 0300UT on 5 August a peculiar increase in the proton flux occurred. The flux profile between ~ 0300 and ~0530UT has the characteristics of a well-defined square wave as observed over the polar caps. The phenomenon is observed at all energies and particle types measured in the spectrometer. Comparison of the polar-cap temporal profile with interplanetary data indicates that the south polar cap flux decreased some 23 minutes later than the interplanetary flux (Reagan et al., 1973). This phenomenon is currently under study and will be reported at a later time.

Following the above phenomenon, the 1-4.5 MeV proton flux continued to decrease in an exponential manner over the next three days. The structure observed in the data results from observed variations across the polar cap as a result of magnetospheric access, from variations in the interplanetary flux and from the statistical spread associated with the 250 ms averaging. At ~ 1200UT on 8 August the 1-4.5 MeV protons most probably associated with the flare of 3B importance that occurred in McMath region 11976 at 1455UT on 7 August arrived over the polar caps. The flux increased over the next 12 hours to a peak value of 2.4 x 10^4 protons/cm^2-sec-sr at ~ 0030UT on 9 August. Following the peak, the protons decreased in an exponential manner with an e-fold value of 5.5 hours.

The profile of the 5-20 MeV protons shown in Figure 2 is similar to the lower-energy protons. An initial peak of 9 x 10^3 protons/cm^2-sec-sr was observed at 0530UT on 4 August. The main peak which occurred at ~ 2200UT 4 August reached an intensity of 8 x 10^4 protons/cm^2-sec-sr. As mentioned above, the peculiar peak between 0300-0530UT on 5 August is clearly evident in these data also. The peak of the second large event occurred at ~ 0000UT on 9 August at a flux level of 1.4 x 10^4 protons/cm^2-sec-sr.

Figure 3 shows the time profile of the energetic protons between 29-100 MeV. This profile has significant differences when compared with the previous two profiles. First of all, energetic protons were not present over the polar caps prior to ~ 0530UT on 4 August. The solar flares in McMath region 11976 prior to the 3B event at 0530UT on 4 August apparently did not produce energetic protons that reached the earth. The 29-100 MeV protons that arrived shortly after 0530UT increased to a broad peak between 1530 and 2200UT on 4 August at an intensity of 2.4 x 10^4 protons/cm^2-sec-sr. The flux dropped over an order of magnitude in the two-hour period following the major peak and was then beginning to decay exponentially when the peculiar event of 5 August, which is quite pronounced even at these energies, occurred. The flux continued to decay in an exponential manner with an e-fold value of ~18 hours out to ~ 1700UT on 7 August. At this time, the high energy protons and energetic electrons from the flare that occurred at 1455UT on 7 August began to arrive over the polar caps. This particle event was more typical of a classical event in which the higher energy protons with higher transit velocity arrive at the earth followed by the lower energy protons. The major event of 4 August was complicated in this regard by the presence of significant fluxes of lower energy protons from earlier events. The energetic protons peaked at ~ 0500UT on 8 August at a value of 4 x 10^2 protons/cm^2-sec-sr. From comparison of Figures 1, 2, and 3 it is immediately evident that this second major event in the period was characterized by a significantly softer proton spectrum. More details on the spectrum will be given later.

Figure 4 shows the time profile of 0.76-2.1 MeV electrons measured during the period 3-9 August. The temporal characteristics of these relativistic electrons are very similar to the energetic protons. The preliminary peak at ~ 0545UT on 4 August is probably associated with the 3B flare occurrence at 0530UT that produced an outstanding solar radio emission burst at 0540UT, [Lincoln and Leighton, 1972]. The flux increased to a second peak at ~ 1530UT and then to a maximum intensity of 4 x 10^4 e/cm^2-sec-sr at ~ 2200UT on 4 August. Comparisons with other solar electron events [Lin, 1970] clearly indicate that this is the most intense flux of greater than 800 keV electrons ever observed at the earth in the present solar cycle including the large electron events of 13 April 1969 [West and Vampola, 1971; Burrows, 1971], and 2 November 1969 [Reagan et al., 1971]. The effect of these energetic precipitating electrons on ionospheric radiowave absorption is significant and must be considered in addition to the effects of the protons. Also, spacecraft monitors of the solar proton fluxes may be susceptible to these penetrating electrons.

The peculiar event at 0300-0530UT on 5 August is clearly evident in the electron data also. Following this event, the electrons decayed in a near-exponential manner until ~ 1600UT on 7 August. At this time the electrons associated with the second major event began arriving over the polar caps. A peak flux of 4.6 x 10^2 e/cm^2-sec-sr was observed at ~ 2200UT on 7 August. An obvious feature of this second event is the lower peak intensity of the electrons by approximately two orders of magnitude compared to the 4 August event.

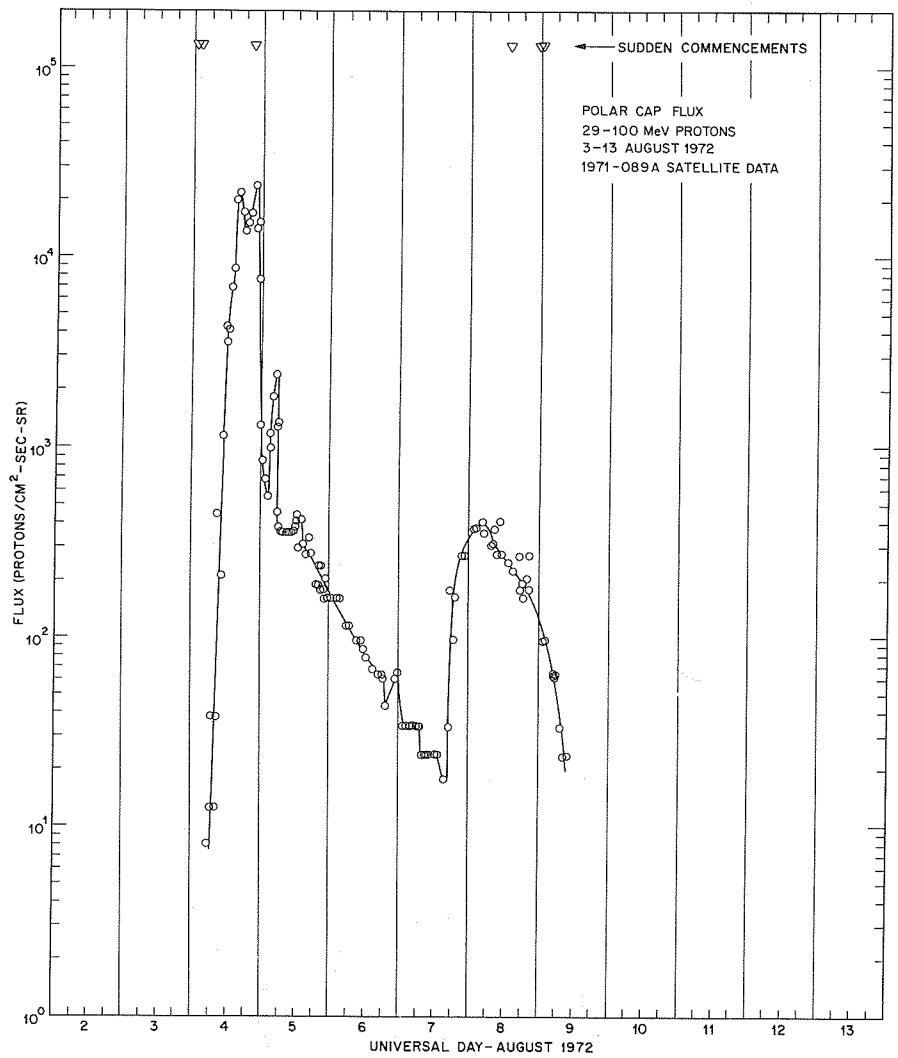

Fig. 3. Differential flux of 29-100 Mev protons as measured by the Lockheed spectrometer on the 1971-089A satellite during the 3-13 August 1972 solar particle events.

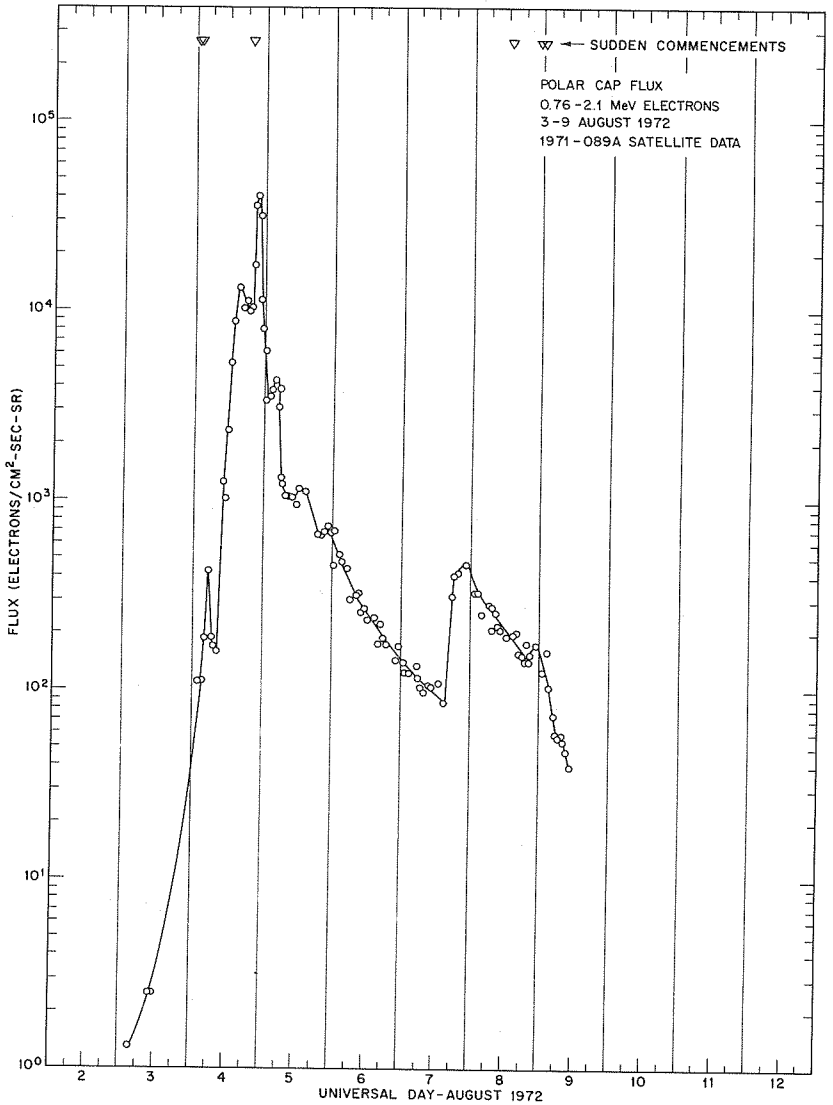

Fig. 4. Differential flux of 0.76 - 2.1 Mev electrons as measured by the Lockheed spectrometer on the 1971-089A satellite during the 3-9 August 1972 solar particle events.

Spectra

Examination of the temporal flux profiles of the protons shown in Figures 1, 2, and 3 immediately indicates that the spectrum is complex and highly time dependent throughout these events. In the main event of 4 August for example, a high intensity of lower energy protons (1 - 4.5 MeV) was present over the polar caps from an earlier flare occurrence. After ~ 0600UT on 4 August, an additional enhancement was observed at all proton energies but especially at the higher energies. The proton spectrum resulting from this combination of time dependent fluxes can therefore be expected to be complex.

In Figure 5 the differential spectra of protons, electrons and alpha particles measured over the south central polar cap in a 250 sec interval at 1102UT on 4 August are shown. The influence of the arriving energetic protons at this time can be clearly seen in the proton spectrum. The spectrum continues to harden, i.e., to have a relatively higher increase in the intensity of the energetic component compared to the lower energy component over the next 10 hours. The overall spectrum between 1 and 100 MeV cannot be fit with a single power law dependence but the protons between 1 and 5 MeV can be described by a dependence of the type $n(E) = n_o E^{-1.53}$.

The electron intensity between 0.76 and 2.1 MeV was very high at this time and unlike the protons exhibited a smooth spectral shape. The electron spectrum as shown in Figure 5 could also be well fit with a power dependence having an exponent -1.53 i.e., the electrons possessed the same spectral shape as the lower energy protons. This is a very energetic electron spectrum and significantly harder than ones typically observed in solar particle events. For example, the electron spectrum in the 13 April 1969 event at these energies could be described by a power-law exponent of -3.3 [West and Vampola, 1971] while the 2 November 1969 spectrum was even softer with an exponent of -3.79 [Reagan et al., 1971]. The resulting effects of these electrons on the lower ionosphere is significant at these times. A 2 MeV electron, for example, can penetrate the atmosphere to an altitude of approximately 49 km. The electrons in addition to the protons must therefore be considered in terms of the effects of solar particles on radio communication attenuation and blackout. It should be emphasized that these spectra were measured some 10 hours prior to the main peak and that the peak flux at ~ 2100UT on 4 August is approximately an order of magnitude higher than at 1102UT.

The alpha particles measured at this time were significantly lower in intensity than either the protons or electrons. The proton to alpha ratio is energy dependent and varies between 17.5 at 7 MeV to 41.5 at 30 MeV. The alpha particles are therefore not as important contributors to ionospheric effects as the protons and electrons.

The spectra of all three particle types over the south central polar cap near the peak of the second major event at 0144UT on 9 August are shown in Figure 6. Once again, the proton spectrum is too complex to fit with a single power law dependence. The proton spectrum at this time is however much softer than that shown in Figure 5 for 4 August and more typical of solar proton events in the present solar cycle as measured by our group. The electron flux at this time is reduced in intensity by approximately an order of magnitude compared to Figure 5, and the spectrum is softer, being described by a power law with exponent -1.75. The proton-to-alpha flux ratio is approximately 30 at 7 MeV, 20 at 10 MeV, 6 at 20 MeV and only 1.8 at 30 MeV.

Comparisons with Previous Data

The period 3-12 August has been divided into two major solar particle events and the flux profiles shown in Figures 1-4 have been integrated over these intervals for comparison with previous solar particle events observed near the earth during the present and previous solar cycles. The first interval was chosen from 0300UT 3 August to 1500UT 7 August. The second interval commences with the arrival of the energetic protons at ~ 1500UT on 7 August out to 2400UT on 12 August. In the case of the energetic protons and the electrons, the flux decreased steeply on 9 August and did not significantly contribute to the integral after these times.

Table 1 shows the peak directional and omnidirectional fluxes observed in the various energy ranges for protons and electrons during each of the above time intervals. The omnidirectional fluxes have been obtained from the measured directional fluxes by assuming an isotropic distribution for the solar protons incident on the earth outside the magnetosphere. The measured integrated directional flux and the derived integrated omnidirectional flux are also shown for these time intervals. A peak omnidirectional flux of 2.33×10^6 protons/cm^2-sec and an integrated omnidirectional flux of 4.08×10^{10} protons/cm^2 for the 1-4.5 MeV protons during the time interval 3-7 August was measured. The 29-100 MeV proton flux measured in this experiment can be compared almost directly with other integral flux measurements of greater than 30 MeV protons made during this event [Bostrom et al., 1972] and during the large solar particle events in solar cycle 19 [Webber, 1963].

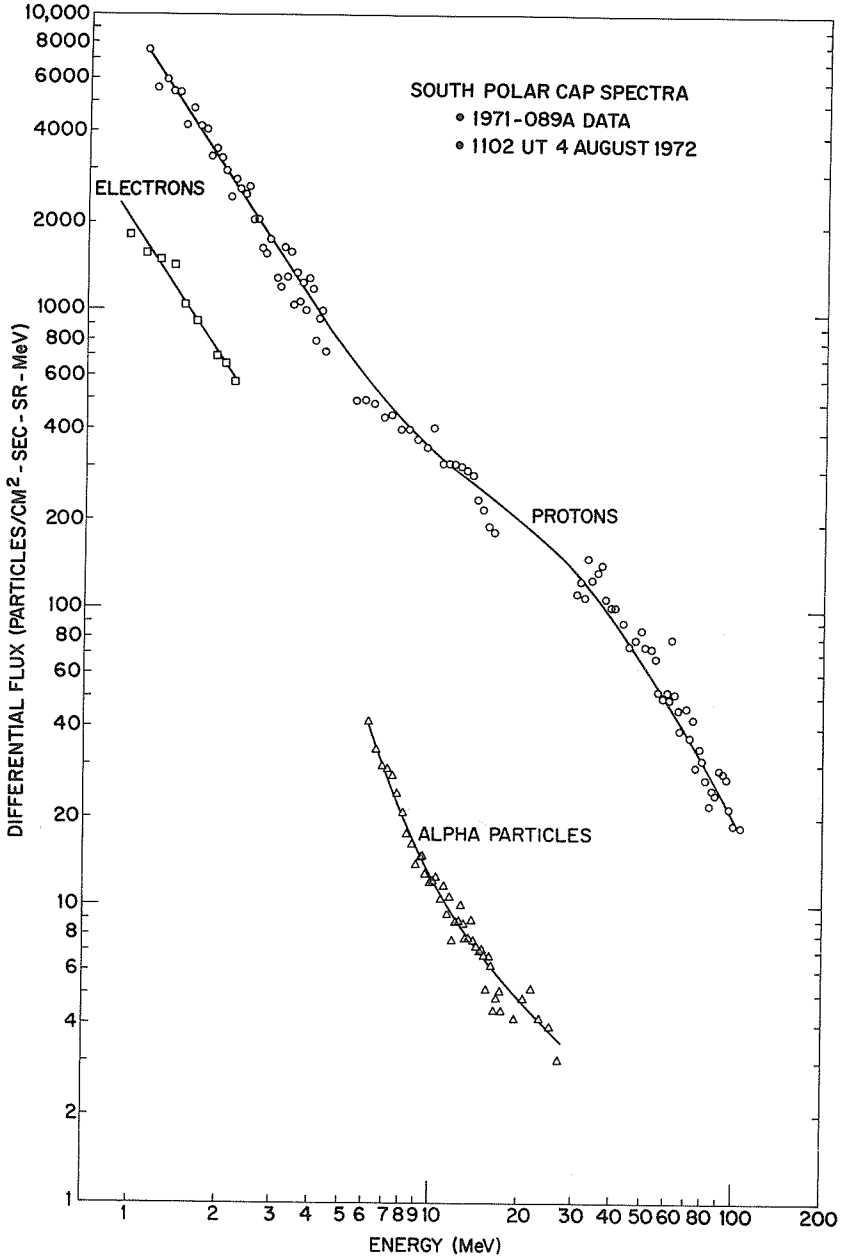

Fig. 5. South Polar Cap Differential Spectra of Protons, Electrons and Alpha Particles measured at 1102 UT on 4 August 1972.

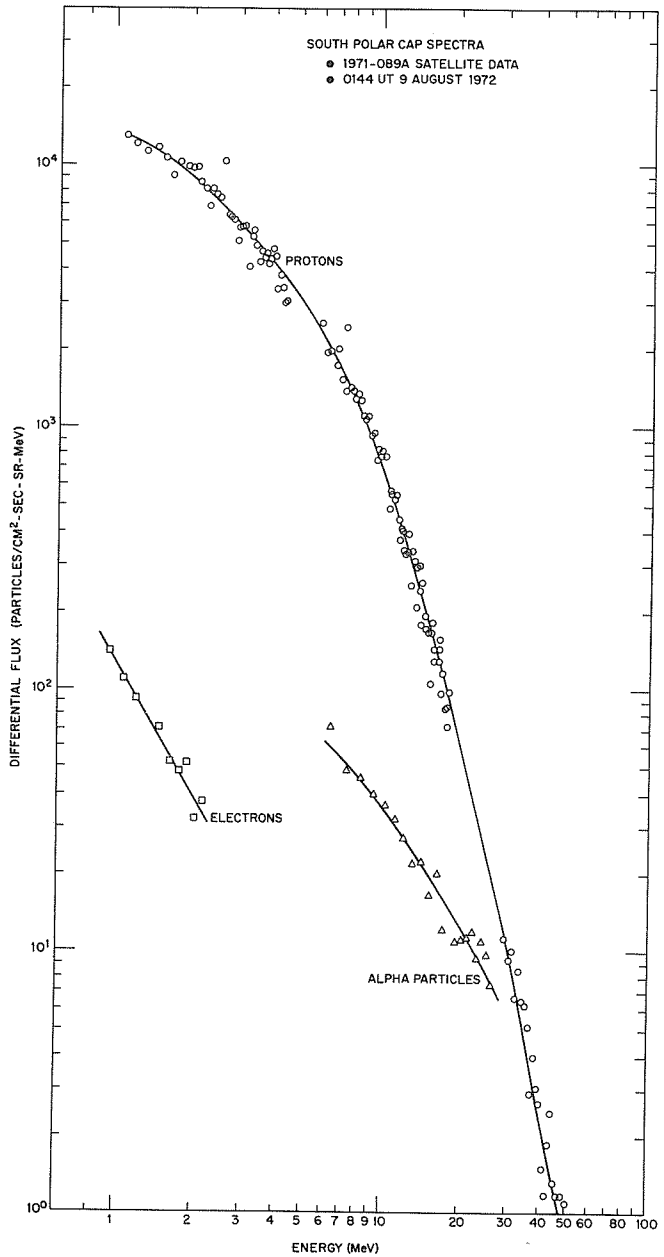

Fig. 6. South Polar Cap Differential Spectra of Protons, Electrons and Alpha Particles measured at 0144 UT on 9 August 1972.

Table 1

Peak and Integrated Fluxes during the August 1972 SPE

Particle Type and Energy	Date	Peak Flux		Integrated Flux		Reference
		Directional (p/cm^2-sec-sr)	Omni (p/cm^2-sec)	Directional (p/cm^2-sr)	Omni (p/cm^2)	
Protons 1-4.5 MeV	3-7 Aug 72	1.85×10^5	2.33×10^6	3.25×10^9	4.08×10^{10}	Present Experiment
	7-12 Aug 72	2.40×10^4	3.02×10^5	1.01×10^9	1.27×10^{10}	
Protons 5-20 MeV	3-7 Aug 72	7.90×10^4	9.93×10^5	1.44×10^9	1.81×10^{10}	Present Experiment
	7-12 Aug 72	1.45×10^4	1.82×10^5	7.02×10^8	8.82×10^9	
Protons 29-100 MeV	3-7 Aug 72	2.36×10^4	2.97×10^5	6.71×10^8	8.43×10^9	Present Experiment
	7-12 Aug 72	4.00×10^2	5.03×10^3	3.06×10^7	3.85×10^8	
Electrons 0.76-2.1 MeV	3-7 Aug 72	4.03×10^4	5.06×10^5	8.69×10^8	1.09×10^{10}	Present Experiment
	7-12 Aug 72	4.65×10^2	5.84×10^3	3.46×10^7	4.35×10^8	
Protons						
> 10 MeV	12 Nov 60				4.0×10^9	Webber (1963)
> 30 MeV	12 Nov 60				1.3×10^9	Webber (1963)
> 60 MeV	12 Nov 60				2.5×10^8	Webber (1963)
> 30 MeV	16 Jul 59		$1.6\text{-}1.8 \times 10^4$			Webber (1963)
> 30 MeV	3-7 Aug 72		2.6×10^5		8×10^9	Bostrom et al. (1972)

The peak omnidirectional flux of 29-100 MeV protons measured during the period 3-7 August was 2.97 x 10^5 protons/cm^2-sec. This value agrees quite favorably with the peak integral flux greater than 30 MeV of 2.6 x 10^5 protons/cm^2-sec as measured by Bostrom et al., [1972] in interplanetary space for the same time period. The integrated omnidirectional flux in this energy and time interval was measured in this experiment to be 8.43 x 10^9 protons/cm^2. Again, this value agrees quite well with the value 8 x 10^9 protons/cm^2 quoted by Bostrom et al., (1972) for protons greater than 30 MeV.

The 4 August 1972 solar particle event is easily the largest event in the present solar cycle. Comparisons of this event with the largest events in the previous solar cycle as reported by Webber [1963] are also shown in Table 1. The largest event in terms of total integrated flux during solar cycle 19 occurred on 12 November 1960. The omnidirectional proton flux of greater than 30 MeV during that event was 1.3 x 10^9 protons/cm^2. This value is a factor of 6.5 times less than the 29-100 MeV flux in the 3-7 August 1972 event. The highest peak omnidirectional flux of greater than 30 MeV in solar cycle 19 was 1.6 - 1.8 x 10^4 proton/cm^2-sec measured during the SPE of 16 July 1959. This peak flux is 17.5 times less than the peak flux of 29-100 MeV protons observed at 2100UT on 4 August. Comparable ratios are observed in Table 1 at the other energies. In every aspect, i.e., in peak and integrated proton flux and in hardness of the spectrum as well as the presence of intense energetic electron fluxes, the 4 August 1972 event appears to be the largest ever observed at the earth in the last two decades.

ACKNOWLEDGMENTS

The authors wish to acknowledge the cooperation and direction of Dr. R. G. Johnson in the performance of this experiment. The valuable contributions of Mr. J. C. Bakke and Dr. J. R. Kilner to the instrumentation design and of Mr. J. D. Matthews and Mrs. S. N. Spencer to the data analysis effort are greatly appreciated. Special acknowledgments are extended to Mr. J. Thielen and Mr. R. Jacobs of the Lockheed Missiles and Space Company and to the members of the U.S.A.F. Satellite Control Facility for their outstanding efforts in acquiring such a large volume of valuable data during this period.

The support of the Office of Naval Research (Contract N00014-69-C-0203) and the Defense Nuclear Agency was essential to performing this work and is greatly appreciated. Partial support of this report was provided by the Lockheed Independent Research Program.

REFERENCES

BOSTROM, C. O., J. W. KOHL, R. W. McENTIRE and D. J. WILLIAMS — 1972 — The Solar Proton Flux - August 2-12, 1972, Johns Hopkins Univ. Report, Nov. 1972.

BURROWS, J. R. — 1971 — A Review of the Magnetospheric Characteristics of Solar Flare Particles, COSPAR Symposium on the November 1969 Solar Particle Event, June 1971 (in press).

LIN, R. P. — 1970 — The Emission and Propagation of ~ 40 keV Solar Flare Electrons, Solar Physics, 12, 266.

LINCOLN, V., AND H. I. LEIGHTON — 1972 — Preliminary Compilation of Data for Retrospective World Interval July 26 - August 14, 1972, World Data Center A for Solar-Terrestrial Physics, Report UAG-21, p. 121, November.

REAGAN, J. B., W. L. IMHOF and E. E. GAINES — 1971 — Satellite Measurements of Energetic Solar Protons, Alpha Particles, Electrons and of Auroral Particles during the 2 November 1969 PCA Event, COSPAR Symposium on the November 1969 Solar Particle Event, June 1971 (in press).

REAGAN, J. B., J. C. BAKKE, J. R. KILNER, J. D. MATTHEWS and W. L. IMHOF — 1972 — A High-Resolution Multiple-Particle Spectrometer for the Measurement of Solar Particle Events, IEEE Trans. Nucl. Sci., NS-19, 1, 554-561.

REAGAN, J. B., W. L. IMHOF, L. J. LANZEROTTI and C. G. MACLENNAN — 1973 — Comparisons of Interplanetary and Polar Cap Fluxes during the 4-11 August Solar Particle Events, Trans. Am. Geophys. U., 54, 419.

WEST, H. I., Jr., and A. L. VAMPOLA — 1971 — Simultaneous Observations of Solar Flare Electron Spectra in Interplanetary Space and within the Earth's Magnetosphere, Phys. Rev. Letters, 26, 458.

VLF Observations at Halley Bay, August 1972

by

W. R. Piggott and T. W. Thomas
Radio and Space Research Station
Ditton Park, Slough, England

A synoptic program of whistler and VLF noise recording is carried out at Halley Bay, Antarctica, S75.51, W26.6, by the British Antarctic Survey working in conjunction with Professor M. G. Morgan, Dartmouth College, U.S.A.

The following note is to indicate what data will be available during the August Retrospective World Interval with some abstracts from the operator's notes. The data have been sent to Dartmouth College, U.S.A., for analysis. The data are reasonably complete for the period of the Retrospective World Interval.

Normal operation involves one minute recordings at 5, 20, 35 and 50 minutes past each hour UT within timing errors of + 0.1 seconds. For the Retrospective World Interval period the data timing is correct to better than 0.05 secs.

Continuous operation was started at 1230 UT on August 3 and maintained until 1620 UT on August 11, when synoptic recording was recommenced with the normal intervals. During the first few days heavy polar blackout reduced signals seriously but many whistler and VLF emissions of all types were heard during the recovery period. The operator's notes draw attention to VLF emissions sounding like barking dogs at 0635 UT August 5, chorus 0735 to 0839 UT August 5, weak chorus 1057-1157 UT and 2043-2212 UT, low frequency warbling 1403-1525 UT, twittering chorus between 0443-0616 UT on August 6, chorus 1143-1452 UT on August 6, strong chorus 1805-1937 UT. Chorus 2243 to 0015 UT was followed by very high activity of all kinds 0150 to 0455 UT on August 7 and 0940 to 1110 UT on August 7. It is probable that the full analysis will show activity at other times since the equipment was usually running unmonitored.

7. GEOMAGNETISM

Summary on page 10.

For basic data and indices for this section and others, see Appendix I for Table of Contents to Report UAG-21.

For data papers presented or published elsewhere which contain additional information on geomagnetic observations and the other categories included in this report, see Appendix II.

For magnetograms specially prepared for the August events held at WDC-A, see Appendix I.

For high-resolution geomagnetic micropulsation records from the United Kingdom for the August 1972 events, see Appendix I.

Auroral Electrojet Indices for August 1972

by

J. H. Allen, C. A. Abston and L. D. Morris
Environmental Data Service
NOAA, Boulder, Colorado 80302

Auroral Electrojet Indices, AU, AL, AE and AO, were derived for each 2½-min of August 1972. The indices are defined in the original paper by Davis and Sugiura [1966] and they have been derived using the same technique described in UAG-22 [Allen, 1972], which similarly covers all months of 1970. Although substantially the same network of stations was used to furnish the data base for the 1970 indices and this special compilation, some substitutions were necessary. Magnetograms were not available from Cape Uelen, Cape Chelyuskin, or Abisko; however, Sodankyla was substituted as a representative Scandinavian station and Sitka records were also used because of the known large variations that were measured there during the active interval of August 4-11. Thus, the present AE (10) indices are generally comparable to those derived for 1970 due to many common stations in the networks used for both derivations.

The station used, their geomagnetic coordinates, and the quiet time H reference level computed for each station are given in Table 1.

Table 1

Observatory		Geographic Coordinates LAT.	Geographic Coordinates LONG.	Geomagnetic Coordinates LAT.	Geomagnetic Coordinates LONG.	HQ_Y
1. Sodankyla	(SO)	N67.4	E26.6	N63.8	E120.0	11941
2. Leirvogur	(LR)	64.2	338.3	70.2	71.0	12235
3. Narssarssuaq	(NAS)	61.2	314.2	71.2	36.8	11816
4. Great Whale River	(GWR)	55.3	282.2	66.6	347.4	10102
5. Fort Churchill	(FC)	58.8	265.9	68.7	322.8	7123
6. Sitka	(SI)	57.1	224.7	60.0	275.3	15854
7. College	(CO)	64.9	212.2	64.6	256.5	13001
8. Barrow	(BW)	71.3	203.2	68.5	241.2	9792
9. Tixie Bay	(TI)	71.6	129.0	60.4	191.4	7911
10. Dixon Island	(DI)	73.6	80.6	63.0	161.6	6444

It is not intended in this data contribution to attempt a detailed analysis of the included indices. However, two features are apparent which have not been noted in studying the graphs of indices for 1970 and for 1968, namely: (1) during many hours of the storms on August 4 - 7 the AO trace (mean of AU and AL) lies above the zero reference line, i.e. the positive deviations from quiet time H exceeded the simultaneous negative deviations by unusual amounts and for relatively long intervals; (2) only the storm on August 9 included a long interval during which all contributing stations were depressed below their average quiet time H-level so that the upper index, AU, was negative for almost one hour.

On the graph for August 4, some of the extreme positive H deviations which provided AU exceeded the plotting range of the microfilm frame. During other disturbed intervals the traces sometimes overlapped or AO was truncated when large negative H deviations occurred. The included tables of hourly average indices were derived from the 2½-min values. These detailed values may be obtained from WDC-A for Solar-Terrestrial Physics on magnetic tape or as computer listings. Microfilm copies of the daily graphs of the indices are also available.

REFERENCES

ALLEN, J. H. 1972 Auroral Electrojet Magnetic Activity Indices (AE) for 1970, World Data Center A for Solar-Terrestrial Physics, Report UAG-22.

DAVIS, T. N. and M. SUGIURA 1966 Auroral Electrojet Activity Index AE and Its Universal Time Variations, JGR, 71, 785-801.

AUGUST 1972 AU INDICES VALUES ARE EXPRESSED IN GAMMAS

	UT	1	2	3	4	5	6	7	8	9	10	11	12	13	14	15	16	17	18	19	20	21	22	23	24	MEAN
	1	144	139	275	160	239	227	281	220	197	220	107	54	102	104	69	61	62	46	45	34	33	66	93	178	132
	2	174	137	104	69	65	111	136	80	49	54	41	47	49	19	28	27	49	58	49	36	78	72	55	36	68
Q	3	30	28	24	33	35	24	21	31	66	70	33	24	34	61	79	46	68	59	51	50	43	38	45	50	43
D	4	34	81	231	694	1009	841	660	323	149	183	127	135	341	361	221	129	101	114	112	216	423	1211	1611	741	419
D	5	537	391	334	357	485	292	214	181	104	181	212	248	185	194	89	-39	219	239	171	58	84	263	193	207	225
D	6	248	350	346	311	209	212	235	273	179	258	238	198	102	191	184	281	295	315	258	198	244	217	149	141	235
	7	119	148	214	257	220	227	124	80	59	58	84	59	61	89	102	163	102	63	46	88	69	80	79	52	110
	8	37	33	30	16	11	8	18	18	22	37	27	16	15	29	77	51	56	111	130	127	61	78	88	134	51
D	9	241	256	153	422	520	637	363	308	214	292	-38	214	144	116	124	146	152	145	146	114	120	141	55	46	210
	10	46	33	20	19	36	70	102	99	61	91	82	178	134	105	147	112	52	72	109	90	105	213	170	97	93
	11	125	109	148	206	98	60	56	40	62	95	138	58	112	43	48	55	126	119	139	147	133	160	148	151	107
	12	87	67	71	102	122	47	70	34	55	48	23	20	15	17	18	30	40	86	78	69	44	47	73	57	55
Q	13	41	45	47	60	98	118	38	37	50	43	25	29	33	14	10	36	81	115	57	34	37	48	28	31	48
	14	52	107	72	60	48	55	38	39	43	54	71	119	120	44	39	44	52	64	95	65	77	80	79	58	66
	15	57	77	70	130	203	294	231	194	258	80	40	62	47	22	27	44	29	26	48	100	94	80	81	124	101
	16	56	94	172	101	65	63	105	106	53	42	31	28	25	65	85	91	53	59	65	75	82	58	68	77	72
	17	63	59	69	56	34	48	51	69	78	60	63	44	43	47	69	28	34	53	43	65	72	50	44	102	56
	18	78	73	57	53	80	122	74	105	92	120	216	138	108	148	106	124	215	245	281	271	244	235	230	177	150
	19	94	89	109	124	110	235	145	106	55	59	38	35	35	115	217	268	223	228	169	91	130	78	57	47	119
	20	93	53	56	52	61	45	60	45	44	56	89	77	54	94	74	93	164	101	194	233	265	178	138	189	105
	21	214	128	54	63	158	201	182	125	98	73	80	67	51	101	75	80	95	110	154	126	83	137	112	102	112
	22	86	60	50	40	30	158	77	55	111	67	52	109	114	80	87	62	51	31	37	61	51	51	44	48	67
Q	23	40	32	36	43	27	36	31	42	48	21	19	21	16	12	18	19	36	33	29	33	40	45	34	29	31
Q	24	26	24	39	40	33	35	27	40	56	39	25	37	26	38	40	41	58	69	37	53	50	41	56	67	42
Q	25	45	54	36	31	35	36	59	87	93	59	72	68	80	102	48	42	44	74	58	53	57	52	40	74	58
	26	85	117	101	190	226	178	328	125	74	79	66	47	32	37	74	71	100	194	86	61	80	93	118	104	111
D	27	67	135	106	158	171	213	195	287	336	431	338	262	158	141	74	100	101	69	64	73	83	71	73	61	157
	28	70	49	41	48	38	37	40	32	46	60	50	34	80	110	86	54	74	138	187	134	137	96	84	78	75
	29	47	53	77	101	69	107	147	166	122	65	36	51	37	70	70	64	50	39	167	236	195	143	85	114	96
	30	130	86	51	39	43	37	38	51	59	45	57	61	43	66	45	32	22	46	63	85	113	64	55	61	58
	31	119	73	82	119	126	130	126	173	127	59	43	42	33	28	36	28	39	52	81	127	64	39	35	54	76
	MEAN	106	103	106	134	152	158	138	115	99	100	80	83	78	86	80	77	92	102	105	103	109	136	136	112	108*
5Q	MEAN	36	37	36	41	46	50	35	47	63	46	35	36	38	45	39	37	57	70	46	46	46	45	41	50	44
5D	MEAN	225	243	234	388	479	439	333	274	196	269	175	211	186	201	138	123	174	176	150	132	191	381	416	239	249

* THIS MEAN (108 GAMMAS) IS BASED ON 31 COMPLETE DAYS

DATE OF PRINTOUT 15 JUN 73

PREPARED BY NATIONAL GEOPHYSICAL AND SOLAR-TERRESTRIAL DATA CENTER

ENVIRONMENTAL DATA SERVICE----------NATIONAL OCEANIC AND ATMOSPHERIC ADMINISTRATION

AUGUST 1972 AL INDICES AL INTENSITY IS -500 PLUS TABULAR VALUES, IN GAMMAS

	UT	1	2	3	4	5	6	7	8	9	10	11	12	13	14	15	16	17	18	19	20	21	22	23	24	MEAN
	1	185	121	197	123	20	157	225	257	333	381	444	482	475	412	391	433	388	468	478	472	487	443	459	336	340
	2	225	307	345	444	458	432	415	387	402	372	441	374	387	481	500	505	491	452	449	483	461	473	471	465	426
Q	3	483	480	479	477	482	445	464	474	434	317	435	479	473	458	365	390	387	416	464	483	477	468	470	469	449
D	4	486	476	287	329	285	137	10	65	143	337	286	303	176	197	396	263	295	430	409	251	130	-272	273	290	249
D	5	61	196	249	207	-113	37	213	296	232	137	-25	20	80	115	-269	-291	214	415	-14	-493	-94	255	359	305	87
D	6	232	218	128	-237	-587	-447	120	215	-2	110	37	257	209	160	236	-27	29	-159	113	268	138	125	304	308	73
	7	126	-60	-28	10	30	8	223	404	396	428	247	394	416	388	287	347	363	408	406	368	417	446	456	455	289
	8	474	473	465	455	473	471	467	461	456	455	454	455	447	437	334	297	379	297	324	318	413	410	407	338	415
D	9	192	300	441	343	339	-59	-275	-145	354	99	-645	39	269	226	338	316	337	317	258	386	413	237	389	423	204
	10	431	407	453	461	446	363	362	207	350	401	367	53	102	151	152	301	353	312	318	461	388	248	130	239	311
	11	202	128	127	112	286	424	464	460	383	246	272	432	258	333	443	377	193	324	202	379	227	110	376	402	298
	12	422	431	392	374	279	354	443	462	457	429	446	454	458	425	479	462	405	266	313	448	473	469	452	379	416
Q	13	456	447	445	439	419	289	432	476	473	469	466	465	470	479	489	461	343	238	449	477	470	466	467	470	440
	14	453	359	418	457	472	476	479	476	468	466	451	346	384	474	453	464	422	423	433	405	445	456	425	461	440
	15	452	445	415	337	268	134	67	159	134	401	442	484	481	487	495	449	495	492	474	453	479	480	457	444	393
	16	446	423	281	346	486	489	463	386	325	457	466	460	461	434	331	383	380	414	422	392	408	461	459	464	418
	17	444	407	388	466	489	486	479	477	462	334	393	482	479	481	369	441	448	472	451	424	446	470	476	436	446
	18	332	434	445	440	324	339	409	441	345	316	199	358	376	266	329	345	347	327	88	209	250	324	253	196	321
	19	354	430	358	184	347	324	379	372	457	482	471	476	474	436	128	81	209	235	305	475	448	451	429	456	365
	20	429	428	467	454	413	442	456	472	465	452	311	324	436	443	321	249	229	328	304	250	258	307	287	123	360
	21	282	339	388	339	87	123	298	417	429	417	311	391	434	421	384	330	303	372	316	281	445	359	291	358	338
	22	318	427	481	472	457	259	271	414	249	404	462	291	329	335	325	305	404	454	398	428	466	480	486	487	392
Q	23	485	481	478	479	388	399	443	437	472	469	458	451	465	477	476	478	459	427	476	480	473	471	477	480	462
Q	24	477	469	467	475	481	475	466	479	465	331	451	466	457	448	455	425	429	384	420	476	472	470	472	473	453
Q	25	465	422	483	487	481	479	459	363	273	330	351	343	349	322	406	422	392	368	472	474	497	493	491	488	421
	26	480	367	27	159	228	202	228	386	450	440	453	456	467	470	413	293	304	308	457	498	466	425	366	442	366
D	27	463	429	235	244	176	164	262	206	174	149	100	104	265	185	261	295	239	469	486	462	462	444	477	443	300
	28	474	470	464	461	472	469	475	470	453	453	409	416	369	251	374	450	426	320	216	329	376	418	444	462	413
	29	443	394	309	351	415	424	431	403	419	447	467	426	450	453	420	396	474	494	355	212	344	420	462	370	407
	30	172	406	467	478	483	479	477	469	464	406	386	404	436	449	446	451	466	492	476	431	392	433	472	479	438
	31	430	281	336	397	404	327	305	278	400	456	460	465	473	475	481	485	479	479	403	431	482	484	481	467	423
	MEAN	367	366	351	341	313	294	336	359	365	367	331	366	381	373	355	341	357	369	359	368	387	378	410	400	360*
5Q	MEAN	473	460	470	471	450	417	453	446	423	383	432	441	443	437	438	435	402	367	456	478	478	474	475	476	445
5D	MEAN	287	324	268	177	20	-34	66	127	180	166	-49	145	200	177	192	111	223	294	250	175	210	158	360	354	183

* THIS MEAN (-140 GAMMAS) IS BASED ON 31 COMPLETE DAYS

DATE OF PRINTOUT 15 JUN 73

PREPARED BY NATIONAL GEOPHYSICAL AND SOLAR-TERRESTRIAL DATA CENTER

ENVIRONMENTAL DATA SERVICE----------NATIONAL OCEANIC AND ATMOSPHERIC ADMINISTRATION

AUGUST 1972 AE INDICES VALUES ARE EXPRESSED IN GAMMAS

	UT	1	2	3	4	5	6	7	8	9	10	11	12	13	14	15	16	17	18	19	20	21	22	23	24	MEAN
	1	459	518	578	537	719	570	556	463	364	339	163	72	126	192	177	128	174	78	67	62	47	123	134	342	291
	2	449	330	259	125	107	179	221	193	148	182	99	173	162	38	28	22	58	106	100	54	118	99	84	72	142
Q	3	48	48	45	55	53	79	57	57	132	253	98	45	61	103	214	156	182	143	87	66	66	69	76	80	95
D	4	48	105	444	865	1224	1204	1149	758	506	346	341	332	665	664	326	366	307	184	203	465	792	1983	1838	950	669
D	5	977	695	585	650	1098	755	501	385	372	544	738	728	605	579	858	751	506	325	685	1051	678	508	334	402	638
D	6	516	632	718	1048	1296	1159	615	558	681	648	701	442	393	530	448	808	766	975	645	430	606	592	345	333	662
	7	492	708	743	747	691	720	401	176	163	130	336	164	145	200	315	317	239	155	140	220	153	134	123	97	321
	8	64	60	65	61	37	37	51	57	67	82	73	61	68	92	243	254	177	314	305	309	148	169	181	296	136
D	9	548	456	212	580	681	1196	1138	954	361	693	1107	675	375	390	286	330	314	328	389	228	206	403	166	122	506
	10	115	126	67	58	90	207	240	392	211	189	215	625	533	454	495	311	200	260	291	129	217	465	540	358	283
	11	423	481	521	594	312	136	92	80	179	349	366	126	354	210	105	178	433	294	437	268	406	551	272	248	309
	12	165	136	180	228	343	193	127	72	98	119	77	66	57	92	39	68	135	320	265	121	71	77	121	178	140
Q	13	86	98	102	121	179	328	105	61	77	74	58	63	63	34	21	75	238	377	108	57	67	81	61	61	108
	14	99	248	154	102	76	79	59	63	75	88	120	273	235	70	86	81	129	140	163	161	132	125	155	97	125
	15	105	133	155	293	435	659	664	535	623	179	98	78	66	35	32	95	35	33	74	146	115	100	124	180	208
	16	110	171	391	255	79	74	142	220	228	84	65	68	64	131	254	208	173	145	144	183	174	97	109	112	153
	17	119	152	181	90	44	62	71	92	115	226	170	61	64	66	200	87	86	81	92	140	126	80	68	166	110
	18	246	139	111	112	256	283	165	164	248	305	517	280	232	382	277	279	368	418	693	562	493	411	476	480	329
	19	240	159	252	440	262	412	266	234	97	76	67	58	61	179	589	687	514	492	364	115	182	127	127	91	254
	20	164	125	89	98	148	103	104	73	78	104	278	253	118	151	253	344	434	273	390	484	507	370	351	566	244
	21	432	290	155	224	582	579	383	207	169	155	269	176	117	180	191	249	292	238	337	345	138	278	321	244	273
	22	268	133	68	67	73	399	306	141	362	163	90	319	284	245	262	258	147	78	139	133	85	71	59	61	175
Q	23	55	51	58	64	139	137	88	105	75	52	61	69	51	34	42	41	77	106	53	52	67	74	57	49	69
Q	24	49	55	72	65	52	60	61	60	91	208	74	71	70	91	86	117	130	185	118	78	79	71	84	94	88
Q	25	80	131	53	44	54	57	100	224	320	229	222	225	230	280	142	120	152	206	86	79	60	59	49	86	137
	26	106	251	573	531	498	476	601	239	124	139	113	91	65	67	161	278	296	386	129	63	114	168	252	162	245
D	27	104	206	371	414	495	549	434	581	662	782	738	658	393	456	313	304	362	100	78	111	120	127	95	118	357
	28	96	79	77	86	66	67	65	62	93	107	142	117	211	359	212	104	147	318	471	305	260	178	139	116	162
	29	103	159	268	250	153	184	217	263	203	118	70	126	86	117	150	168	76	45	311	523	351	223	123	244	189
	30	458	180	85	61	60	57	61	82	95	140	171	157	107	117	98	81	55	54	87	154	221	131	83	82	120
	31	188	292	245	222	222	304	321	395	227	103	83	77	60	54	55	42	60	73	179	196	82	55	54	87	153
	MEAN	239	237	254	293	339	365	302	256	234	232	249	217	197	213	224	236	234	233	246	235	222	258	226	212	248*
5Q	MEAN	64	77	66	70	95	132	82	101	139	163	103	95	95	108	101	102	156	203	90	66	68	71	65	74	99
5D	MEAN	439	419	466	711	959	973	767	647	516	603	725	567	486	524	446	512	451	382	403	457	480	723	556	385	566

* THIS MEAN (248 GAMMAS) IS BASED ON 31 COMPLETE DAYS

DATE OF PRINTOUT 15 JUN 73

PREPARED BY NATIONAL GEOPHYSICAL AND SOLAR-TERRESTRIAL DATA CENTER

ENVIRONMENTAL DATA SERVICE----------NATIONAL OCEANIC AND ATMOSPHERIC ADMINISTRATION

AUGUST 1972 AO INDICES VALUES ARE EXPRESSED IN GAMMAS

	UT	1	2	3	4	5	6	7	8	9	10	11	12	13	14	15	16	17	18	19	20	21	22	23	24	MEAN
	1	-85	-120	-14	-108	-120	-58	3	-12	15	51	25	18	38	8	-20	-3	-25	7	11	3	10	5	25	7	-14
	2	-50	-28	-25	6	12	22	25	-16	-24	-37	-9	-39	-32	0	14	16	20	5	-1	9	19	22	13	1	-3
Q	3	6	4	1	5	8	-15	-7	3	0	-56	-16	1	4	9	-28	-32	-22	-12	8	16	9	3	7	9	-4
D	4	10	28	9	261	397	239	85	-56	-104	10	-43	-31	9	29	58	-54	-52	22	10	-17	26	219	691	265	84
D	5	49	43	42	32	-64	-85	-36	-11	-82	-91	-156	-115	-117	-96	-340	-415	-33	77	-171	-467	-255	9	26	6	-94
D	6	-10	34	-13	-213	-439	-367	-72	-6	-162	-66	-112	-23	-94	-75	-40	-122	-88	-172	-64	-17	-59	-79	-23	-25	-96
	7	-127	-206	-157	-116	-125	-132	-76	-8	-23	-7	-84	-24	-11	-11	-55	5	-17	-14	-24	-22	-7	12	17	4	-50
	8	5	3	-3	-15	-8	-11	-8	-10	-11	-4	-9	-15	-19	-17	-44	-76	-32	-46	-23	-27	-13	-6	-3	-14	-17
D	9	-33	28	47	132	180	39	-206	-168	34	-54	-591	-123	-43	-78	-19	-19	-6	-19	-48	0	16	-61	-27	-15	-43
	10	-12	-29	-13	-10	-9	-33	-18	-97	-45	-4	-26	-134	-132	-122	-100	-44	-47	-58	-37	25	-4	-19	-100	-82	-48
	11	-86	-131	-112	-91	-58	-8	10	0	-27	-79	-45	-5	-65	-62	-4	-34	-90	-28	-79	13	-70	-115	12	26	-47
	12	5	-1	-18	-12	-49	-49	6	-2	6	-12	-15	-13	-13	-28	-2	-4	-27	-74	-55	8	9	8	12	-32	-15
Q	13	-2	-4	-4	0	8	-46	-15	7	11	6	-4	-3	2	-3	0	-2	-38	-73	3	5	3	7	-3	0	-6
	14	3	-17	-5	8	10	15	8	8	5	10	11	-17	2	9	-4	4	-13	-6	14	-14	11	18	2	9	3
	15	4	11	-8	-16	-14	-36	-101	-73	-54	-9	-9	23	14	5	11	-3	12	9	10	25	36	30	19	34	-3
	16	1	8	-24	-27	25	26	34	-4	-61	0	-2	-6	-7	-1	-42	-13	-33	-14	-7	-16	-5	9	13	20	-5
	17	4	-17	-21	11	11	17	15	22	20	-53	-22	13	11	14	-31	-15	-9	12	-3	-6	9	10	10	18	1
	18	-45	3	1	-3	-48	-19	-8	23	-31	-32	-43	-2	-8	-43	-32	-15	31	36	-65	-10	-3	29	-8	-63	-15
	19	-26	10	-16	-96	-22	29	12	-11	6	20	4	5	4	25	-77	-75	-34	-18	-13	33	39	15	-7	1	-8
	20	11	-9	11	3	-13	-6	8	8	4	4	-50	-49	-5	18	-52	-79	-53	-35	-1	-8	12	-7	-38	-94	-18
	21	-2	-16	-29	-48	-122	-88	-10	21	13	-5	-54	-21	-8	11	-20	-45	-50	-9	-15	-46	13	-2	-49	-20	-25
	22	-47	-6	15	6	-5	-41	-76	-15	-70	-14	7	-50	-28	-42	-44	-66	-22	-7	-32	-6	8	16	15	17	-20
Q	23	12	6	7	11	-42	-32	-13	-10	10	-5	-12	-14	-9	-5	-3	-1	-3	-19	2	5	6	8	5	4	-4
Q	24	2	-4	3	8	7	5	-3	9	10	-65	-12	1	-8	-7	-2	-17	-7	-23	-21	14	11	6	14	20	-2
Q	25	5	-12	9	9	8	7	9	-25	-67	-55	-38	-44	-35	-38	-23	-18	-31	-29	15	13	27	22	15	31	-10
	26	32	-8	-186	-75	-23	-60	28	5	12	9	10	2	0	3	-6	-68	-48	1	21	29	23	9	-8	23	-11
D	27	15	32	-79	-49	-77	-61	-21	-4	5	40	-31	-67	-38	-87	-82	-52	-80	19	25	17	22	7	25	2	-22
	28	22	9	2	4	5	3	7	1	-1	6	-20	-25	-25	-69	-20	2	0	-21	-49	-18	6	7	14	20	-6
	29	-5	-26	-57	-24	-8	15	39	34	21	6	2	-11	-7	11	-5	-20	12	16	11	-25	19	31	23	-8	2
	30	-98	-4	9	8	13	8	7	10	11	-24	-28	-17	-10	7	-5	-9	-6	19	19	8	3	-1	14	20	-2
	31	24	-73	-41	8	15	-21	-34	-24	13	7	1	4	3	2	8	6	9	15	-8	29	23	11	8	10	-0
	MEAN	-13	-16	-22	-13	-18	-24	-13	-13	-18	-16	-44	-25	-20	-20	-33	-41	-25	-14	-18	-14	-2	7	23	6	-16*
5Q	MEAN	5	-2	3	7	-2	-16	-6	-3	-7	-35	-16	-12	-9	-9	-11	-14	-20	-31	1	11	11	9	8	13	-5
5D	MEAN	6	33	1	33	-1	-47	-50	-49	-62	-32	-187	-72	-57	-61	-85	-132	-52	-15	-50	-97	-50	19	138	47	-34

* THIS MEAN (-16 GAMMAS) IS BASED ON 31 COMPLETE DAYS

DATE OF PRINTOUT 15 JUN 73

PREPARED BY NATIONAL GEOPHYSICAL AND SOLAR-TERRESTRIAL DATA CENTER

ENVIRONMENTAL DATA SERVICE----------NATIONAL OCEANIC AND ATMOSPHERIC ADMINISTRATION

TABLE OF OBSERVATORIES SUPPLYING HOURLY AU-AL

AUGUST 1972

AU = MAXIMUM DELTA H

UT	01	02	03	04	05	06	07	08	09	10	11	12	13	14	15	16	17	18	19	20	21	22	23	24
1	GWR	GWR	BW	BW	BW	BW	BW	TI	TI	DI	TI	DI	DI	DI	DI	LR	LR	NAS	BW	BW	FC	NAS	FC	FC
2	FC	FC	FC	FC	BW	BW	BW	BW	TI	TI	TI	DI	DI	SI	FC	SI	LR	LR	LR	NAS	NAS	NAS	GWR	DI
3	GWR	GWR	GWR	FC	FC	FC	GWR	BW	BW	CO	CO	FC	DI	DI	DI	DI	NAS	LR	GWR	GWR	GWR	GWR	GWR	FC
4	FC	FC	CO	BW	CO	SI	SI	SI	SI	SI	TI	TI	CI	TI	TI	DI	LR	BW	DI	NAS	NAS	FC	FC	BW
5	BW	DI	DI	SI	SI	SI	SI	SI	GWR	FC	DI	DI	SO	SO	NAS	GWR	LR	NAS	GWR	SO	GWR	SO	SO	SO
6	BW	BW	CO	CO	SI	SI	DI	DI	DI	DI	DI	DI	LR	LR	LR	LR	NAS	NAS	NAS	NAS	GWR	FC	FC	FC
7	BW	BW	BW	CO	CO	CO	DI	CO	LR	DI	DI	DI	DI	DI	LR	LR	LR	NAS	NAS	NAS	FC	FC	FC	FC
8	NAS	FC	FC	FC	BW	BW	BW	BW	BW	BW	BW	BW	DI	DI	DI	DI	LR	NAS	NAS	NAS	NAS	NAS	FC	FC
9	FC	FC	BW	BW	CO	SI	SI	TI	TI	TI	DI	DI	LR	LR	LR	LR	LR	NAS	NAS	NAS	NAS	FC	NAS	NAS
10	FC	FC	BW	BW	BW	BW	BW	BW	BW	BW	DI	DI	DI	SO	LR	LR	NAS	NAS	NAS	NAS	NAS	FC	GWR	GWR
11	BW	BW	BW	BW	BW	FC	BW	BW	TI	DI	DI	TI	DI	DI	DI	LR	LR	NAS	NAS	NAS	NAS	FC	FC	FC
12	GWR	BW	BW	BW	BW	BW	BW	BW	BW	BW	TI	TI	DI	DI	TI	DI	NAS	NAS	NAS	NAS	NAS	FC	NAS	FC
13	FC	FC	BW	BW	BW	BW	BW	BW	BW	BW	BW	BW	BW	BW	BW	NAS	LR	LR	NAS	BW	BW	FC	FC	FC
14	FC	FC	GWR	BW	BW	BW	BW	BW	BW	BW	TI	DI	TI	TI	LR	LR	LR	NAS	NAS	NAS	NAS	NAS	FC	FC
15	FC	FC	BW	BW	BW	BW	CO	TI	TI	TI	TI	FC	FC	FC	BW	LR	CO	BW	NAS	NAS	NAS	NAS	FC	FC
16	FC	BW	BW	FC	GWR	BW	BW	BW	CO	BW	BW	TI	TI	DI	LR	LR	NAS	NAS	NAS	NAS	NAS	NAS	NAS	NAS
17	FC	FC	BW	FC	BW	BW	BW	BW	BW	CO	BW	BW	FC	DI	DI	TI	LR	NAS	LR	NAS	NAS	FC	FC	FC
18	FC	FC	FC	BW	BW	BW	BW	BW	BW	DI	DI	DI	DI	DI	DI	LR	LR	NAS	NAS	NAS	NAS	GWR	FC	GWR
19	FC	BW	BW	BW	BW	BW	BW	BW	BW	FC	FC	BW	CO	DI	SO	SO	LR	LR	LR	NAS	NAS	BW	FC	FC
20	FC	FC	FC	BW	BW	BW	BW	BW	BW	BW	DI	DI	TI	DI	SO	SO	LR	NAS	NAS	NAS	GWR	GWR	GWR	FC
21	FC	FC	BW	BW	BW	BW	BW	BW	BW	TI	DI	DI	DI	DI	DI	SO	LR	NAS	NAS	NAS	NAS	NAS	GWR	GWR
22	GWR	DI	BW	BW	SO	BW	BW	BW	TI	TI	TI	DI	DI	DI	DI	SO	LR	LR	FC	NAS	FC	FC	FC	FC
23	FC	FC	FC	FC	BW	BW	BW	BW	BW	CO	TI	FC	TI	FC	SO	SO	NAS	NAS	NAS	FC	FC	FC	FC	FC
24	FC	FC	FC	FC	FC	BW	BW	BW	BW	TI	TI	BW	DI	DI	DI	SO	LR	LR	LR	GWR	GWR	FC	FC	FC
25	FC	FC	FC	FC	FC	FC	BW	BW	BW	DI	DI	DI	DI	DI	DI	LR	LR	NAS	NAS	FC	FC	FC	GWR	FC
26	FC	FC	BW	BW	CO	CO	CO	CO	BW	CO	CO	CO	TI	DI	DI	DI	NAS	NAS	NAS	NAS	FC	FC	FC	FC
27	FC	BW	BW	BW	CO	SI	TI	TI	TI	TI	DI	DI	DI	SO	SO	LR	LR	CO	NAS	NAS	NAS	FC	FC	FC
28	FC	FC	FC	BW	FC	BW	BW	BW	BW	BW	DI	TI	DI	DI	DI	DI	LR	LR	NAS	NAS	NAS	NAS	FC	FC
29	FC	FC	BW	BW	BW	BW	BW	BW	BW	BW	DI	DI	DI	DI	DI	FC	DI	NAS	NAS	NAS	NAS	FC	FC	FC
30	FC	FC	FC	FC	FC	FC	BW	BW	BW	TI	DI	DI	TI	DI	DI	DI	CO	BW	NAS	NAS	NAS	NAS	FC	FC
31	FC	BW	BW	BW	BW	BW	BW	CO	BW	BW	FC	FC	BW	BW	BW	BW	NAS	NAS	NAS	NAS	NAS	BW	BW	GWR

IDENTIFICATION	GEOGRAPHIC LAT	GEOGRAPHIC LONG	GEOMAGNETIC LAT	GEOMAGNETIC LONG
AI = ABISKO	68 21.5	18 49.4	66.0	114.9
BW = BARROW	71 18.2	-156 44.9	68.5	241.1
CC = C CHELYUSKIN	77 43.0	104 17.0	66.2	176.4
CO = COLLEGE	64 51.6	-147 50.2	64.6	256.5
GWR= GREAT WHALE R	55 16.0	-77 47.0	66.5	347.4
DI = DIKSON	73 32.6	80 33.7	63.0	161.5

IDENTIFICATION	GEOGRAPHIC LAT	GEOGRAPHIC LONG	GEOMAGNETIC LAT	GEOMAGNETIC LONG
FC = FT CHURCHILL	58 48.0	-94 06.0	68.7	322.8
LR = LEIRVOGUR	64 11.0	-21 42.0	70.2	71.0
NAS= NASSARSSUAG	61 06.0	-45 12.0	71.0	37.0
TI = TIKSI	71 35.0	129 00.0	60.4	191.4
UE = CAPE UELEN	66 09.8	-169 50.1	56.6	73.4

PREPARED BY NATIONAL GEOPHYSICAL DATA CENTER----------NATIONAL OCEANIC AND ATMOSPHERIC ADMINISTRATION

TABLE OF OBSERVATORIES SUPPLYING HOURLY AU-AL

AUGUST 1972 — AL = MINIMUM DELTA H

UT	01	02	03	04	05	06	07	08	09	10	11	12	13	14	15	16	17	18	19	20	21	22	23	24
1	LR	LR	LR	LR	LR	LR	NAS	NAS	NAS	GWR	SO	SO	GWR	BW	BW	BW	BW	TI	SI	SI	SI	BW	BW	LR
2	LR	LR	LR	LR	NAS	NAS	NAS	GWR	GWR	GWR	GWR	FC	FC	SO	GWR	BW	BW	BW	BW	DI	DI	SI	CO	BW
3	CO	TI	TI	DI	DI	NAS	DI	SO	GWR	FC	FC	SO	NAS	FC	BW	BW	BW	BW	BW	SI	SI	CO	CO	BW
4	CO	NAS	LR	SO	DI	LR	LR	NAS	NAS	NAS	BW	GWR	FC	FC	FC	GWR	GWR	GWR	GWR	TI	TI	CO	GWR	CO
5	FC	FC	FC	FC	FC	BW	BW	BW	BW	BW	CO	CO	CO	CO	CO	CO	CO	DI	CO	CO	BW	DI	LR	LR
6	NAS	NAS	DI	NAS	NAS	NAS	LR	LR	CO	NAS	CO	CO	GWR	CO	CO	CO	BW	BW	TI	BW	SO	SO	SO	DI
7	LR	NAS	LR	LR	LR	NAS	NAS	NAS	CO	GWR	BW	CO	CO	CO	BW	BW	BW	BW	DI	DI	DI	DI	TI	LR
8	TI	TI	LR	NAS	DI	DI	SO	SO	SO	SO	LR	LR	FC	BW	BW	BW	BW	BW	DI	DI	DI	DI	LR	LR
9	LR	LR	LR	LR	LR	LR	NAS	NAS	BW	SI	SI	FC	FC	BW	BW	BW	BW	TI	BW	BW	SO	SO	SO	TI
10	TI	LR	TI	DI	DI	FC	GWR	GWR	GWR	GWR	CO	CO	FC	CO	CO	TI	TI	DI	DI	SI	SO	SO	SO	SO
11	LR	LR	LR	LR	NAS	NAS	SO	SO	GWR	GWR	GWR	CO	CO	CO	BW	TI	TI	BW	DI	TI	DI	DI	DI	SO
12	LR	LR	LR	LR	NAS	NAS	NAS	SO	SO	FC	FC	FC	SO	BW	GWR	FC	BW	DI	DI	DI	SI	SI	DI	LR
13	TI	NAS	NAS	NAS	GWR	GWR	GWR	SO	SO	SO	SO	LR	LR	NAS	NAS	BW	BW	BW	BW	SI	SI	SI	SI	TI
14	LR	LR	LR	LR	NAS	DI	DI	SO	SO	SO	NAS	FC	FC	SO	BW	BW	BW	BW	DI	DI	DI	SI	DI	SI
15	TI	TI	GWR	GWR	NAS	NAS	NAS	NAS	NAS	GWR	FC	SO	NAS	NAS	SO	BW	SO	FC	BW	BW	SI	CO	TI	TI
16	TI	LR	LR	NAS	TI	SO	NAS	GWR	GWR	SO	SO	BW	BW	BW	TI	TI	BW	BW	DI	DI	DI	SI	CO	SI
17	LR	LR	NAS	NAS	DI	DI	DI	DI	GWR	GWR	FC	LR	LR	FC	CO	BW	BW	BW	DI	DI	DI	SI	SI	LR
18	LR	LR	NAS	NAS	GWR	GWR	GWR	GWR	GWR	GWR	CO	FC	FC	CO	CO	CO	CO	DI	BW	BW	DI	DI	SO	SO
19	SO	LR	LR	NAS	GWR	NAS	NAS	GWR	SO	SO	SO	SO	LR	FC	CO	CO	CO	TI	TI	TI	BW	SO	LR	LR
20	LR	LR	LR	LR	NAS	NAS	NAS	DI	SO	LR	CO	FC	FC	FC	CO	CO	TI	TI	TI	TI	TI	DI	SO	LR
21	LR	LR	LR	GWR	GWR	GWR	GWR	NAS	GWR	GWR	GWR	FC	FC	FC	CO	CO	BW	BW	BW	DI	DI	DI	DI	DI
22	LR	LR	TI	NAS	GWR	GWR	GWR	GWR	GWR	GWR	GWR	CO	BW	BW	BW	BW	BW	BW	DI	DI	DI	SI	SI	TI
23	LR	TI	TI	TI	GWR	GWR	GWR	FC	DI	LR	LR	BW	LR	LR	GWR	GWR	BW	BW	BW	SI	SI	SI	CO	BW
24	TI	TI	TI	TI	DI	DI	DI	SO	SO	FC	SO	LR	LR	BW	BW	BW	BW	BW	DI	DI	SI	SI	SI	TI
25	NAS	NAS	TI	TI	DI	DI	GWR	GWR	FC	FC	FC	FC	FC	FC	FC	BW	BW	DI	DI	DI	SI	SI	SI	CO
26	TI	LR	LR	LR	LR	LR	LR	NAS	NAS	GWR	SO	LR	LR	NAS	BW	BW	BW	BW	BW	SI	DI	DI	DI	TI
27	TI	LR	NAS	LR	LR	LR	LR	LR	NAS	NAS	GWR	CO	GWR	CO	CO	CO	TI	TI	DI	DI	DI	DI	LR	LR
28	TI	TI	TI	NAS	DI	DI	DI	SO	SO	SO	GWR	FC	CO	CO	BW	BW	BW	BW	DI	DI	DI	DI	DI	LR
29	LR	LR	NAS	NAS	NAS	NAS	NAS	GWR	GWR	GWR	SO	FC	BW	CO	CO	TI	BW	SO	BW	DI	DI	DI	SO	LR
30	LR	NAS	NAS	TI	TI	DI	DI	SO	SO	BW	FC	FC	FC	FC	CO	BW	BW	SI	SI	DI	DI	DI	SI	TI
31	LR	LR	LR	LR	NAS	NAS	GWR	NAS	GWR	SO	SO	SO	NAS	SO	SO	SO	BW	BW	BW	TI	SI	SI	CO	LR

IDENTIFICATION	GEOGRAPHIC LAT	GEOGRAPHIC LONG	GEOMAGNETIC LAT	GEOMAGNETIC LONG
AI = ABISKO	68 21.5	18 49.4	66.0	114.9
BW = BARROW	71 18.2	-156 44.9	68.5	241.1
CC = C CHELYUSKIN	77 43.0	104 17.0	66.2	176.4
CO = COLLEGE	64 51.6	-147 50.2	64.6	256.5
GWR= GREAT WHALE R	55 16.0	-77 47.0	66.5	347.4
DI = DIKSON	73 32.6	80 33.7	63.0	161.5

IDENTIFICATION	GEOGRAPHIC LAT	GEOGRAPHIC LONG	GEOMAGNETIC LAT	GEOMAGNETIC LONG
FC = FT CHURCHILL	58 48.0	-94 06.0	68.7	322.8
LR = LEIRVOGUR	64 11.0	-21 42.0	70.2	71.0
NAS= NASSARSSUAG	61 06.0	-45 12.0	71.0	37.0
TI = TIKSI	71 35.0	129 00.0	60.4	191.4
UE = CAPE UELEN	66 09.8	-169 50.1	56.6	73.4

PREPARED BY NATIONAL GEOPHYSICAL DATA CENTER----------NATIONAL OCEANIC AND ATMOSPHERIC ADMINISTRATION

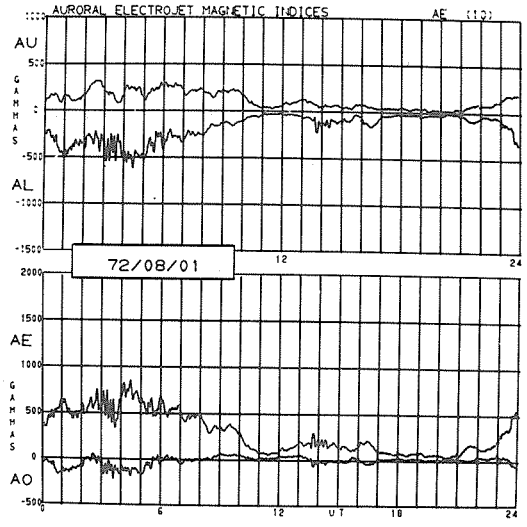
AURORAL ELECTROJET MAGNETIC INDICES
AE (10)
AU
AL
AE
AO
GAMMAS
72/08/01
UT

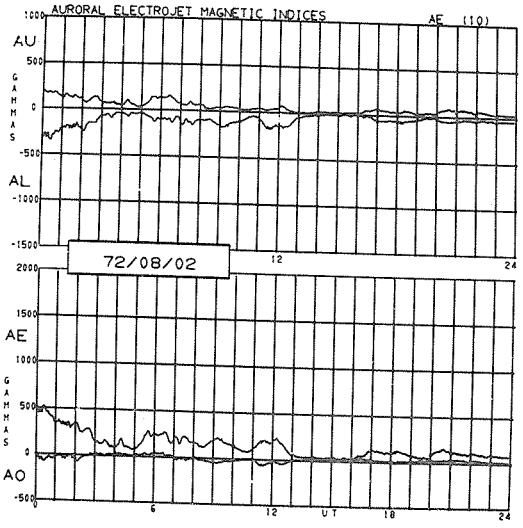
AURORAL ELECTROJET MAGNETIC INDICES
AE (10)
AU
AL
AE
AO
GAMMAS
72/08/02
UT

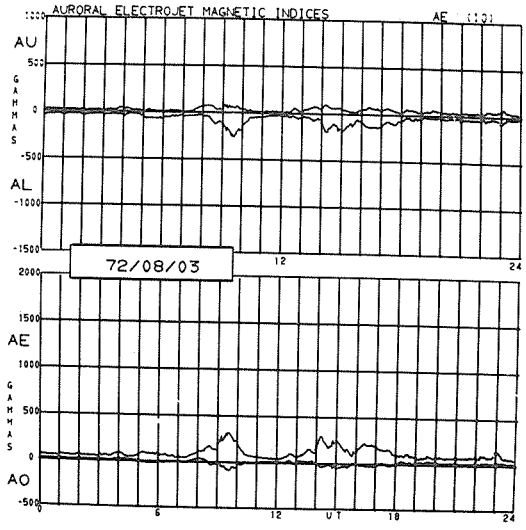
AURORAL ELECTROJET MAGNETIC INDICES
AE (10)
AU
AL
AE
AO
GAMMAS
72/08/03
UT

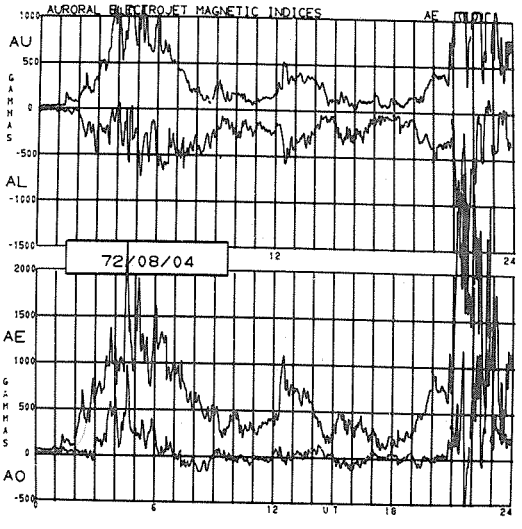
AURORAL ELECTROJET MAGNETIC INDICES
AU
AL
AE
AO
GAMMAS
72/08/04
UT

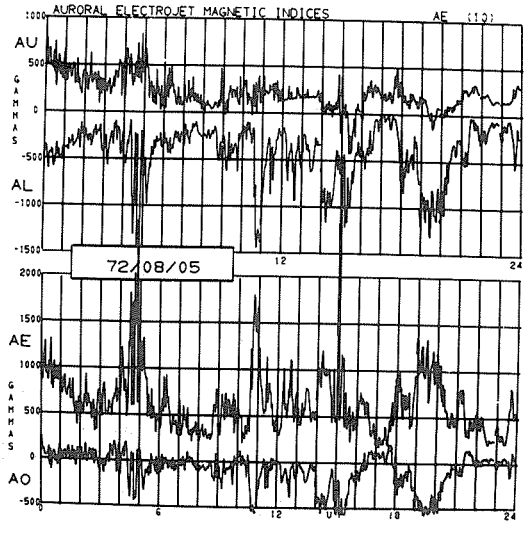
AURORAL ELECTROJET MAGNETIC INDICES
AE (10)
AU
AL
AE
AO
GAMMAS
72/08/05
UT

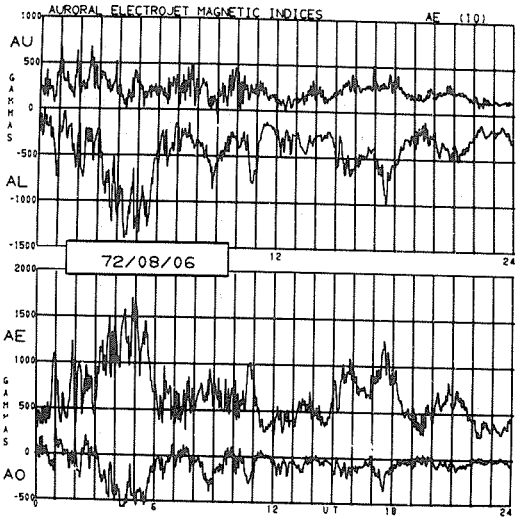
AURORAL ELECTROJET MAGNETIC INDICES
AE (10)
AU
AL
AE
AO
GAMMAS
72/08/06
UT

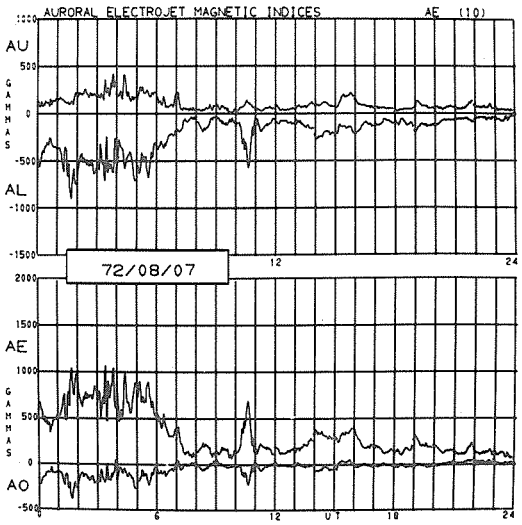
AURORAL ELECTROJET MAGNETIC INDICES
AE (10)
AU
AL
72/08/07
AE
AO
GAMMAS
UT

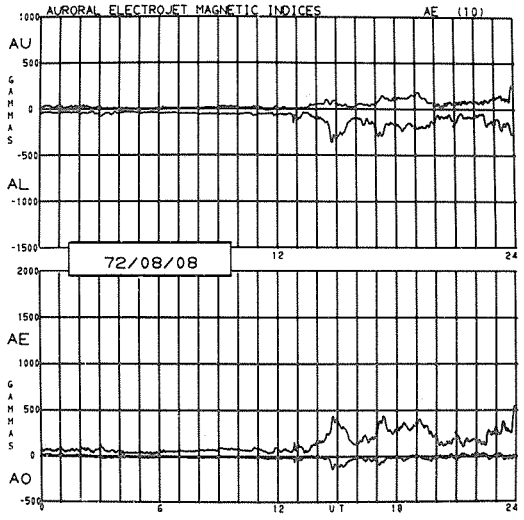
AURORAL ELECTROJET MAGNETIC INDICES
AE (10)
AU
AL
72/08/08
AE
AO
GAMMAS
UT

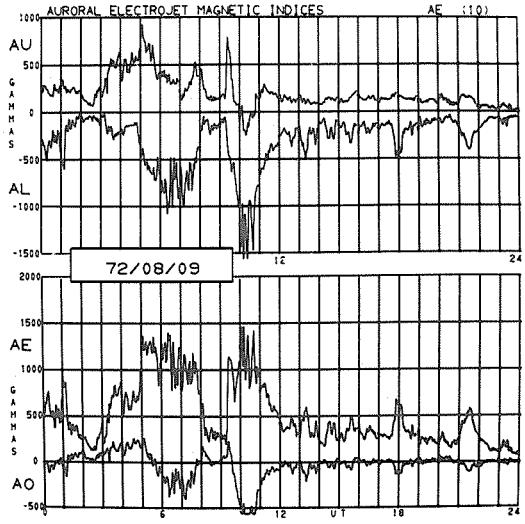
AURORAL ELECTROJET MAGNETIC INDICES
AE (10)
AU
AL
72/08/09
AE
AO
GAMMAS
UT

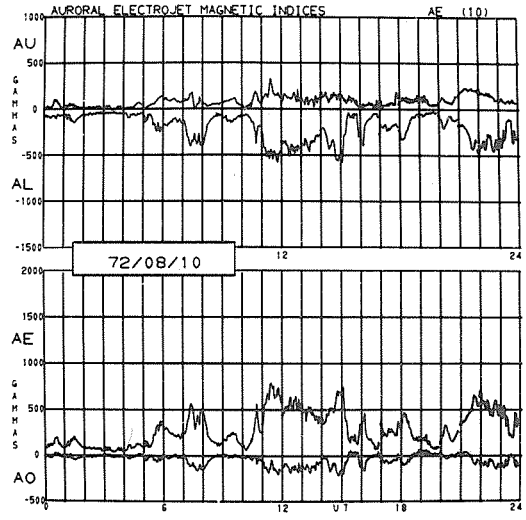
AURORAL ELECTROJET MAGNETIC INDICES
AE (10)
AU
AL
72/08/10
AE
AO
GAMMAS
UT

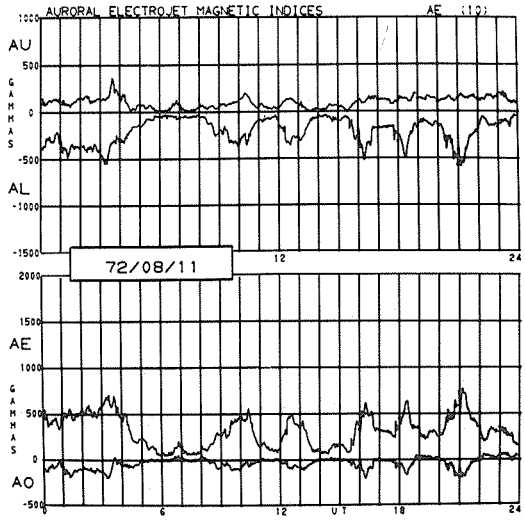
AURORAL ELECTROJET MAGNETIC INDICES
AE (10)
AU
AL
72/08/11
AE
AO
GAMMAS
UT

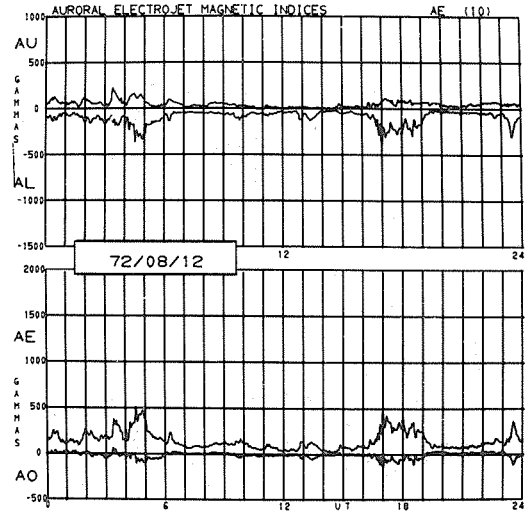
AURORAL ELECTROJET MAGNETIC INDICES
AE (10)
AU
AL
72/08/12
AE
AO
GAMMAS
UT

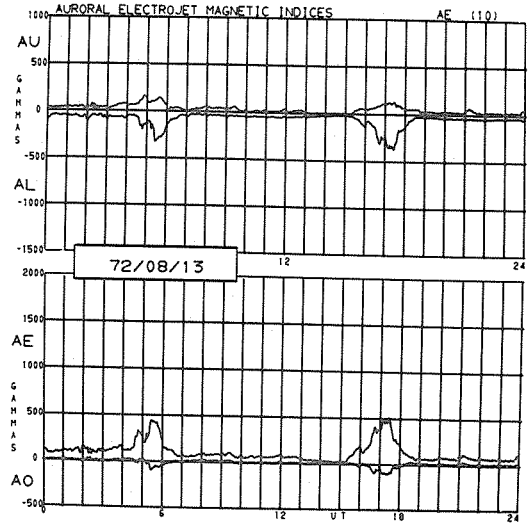
AURORAL ELECTROJET MAGNETIC INDICES
AE (10)
AU
AL
AE
AO
GAMMAS
72/08/13
UT

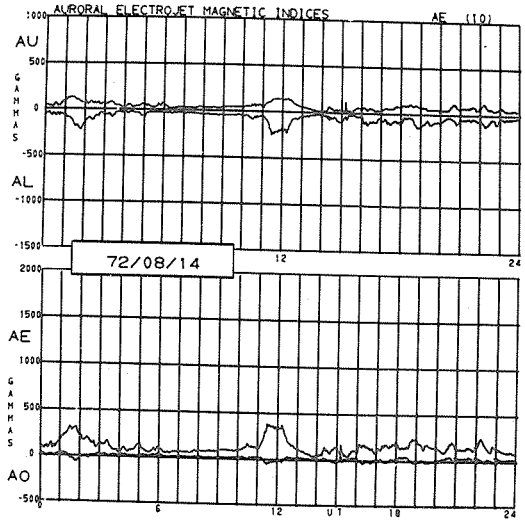
AURORAL ELECTROJET MAGNETIC INDICES
AE (10)
AU
AL
AE
AO
GAMMAS
72/08/14
UT

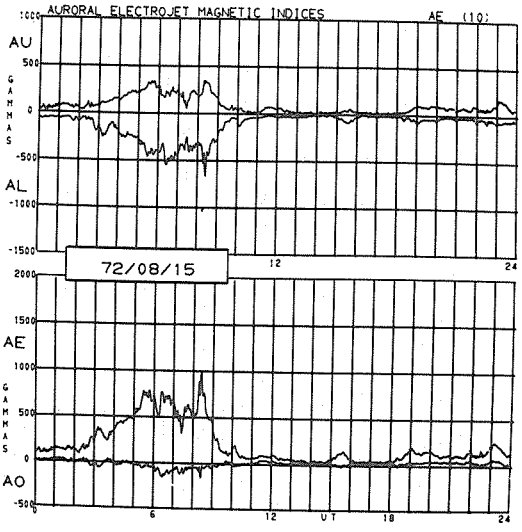
AURORAL ELECTROJET MAGNETIC INDICES
AE (10)
AU
AL
AE
AO
GAMMAS
72/08/15
UT

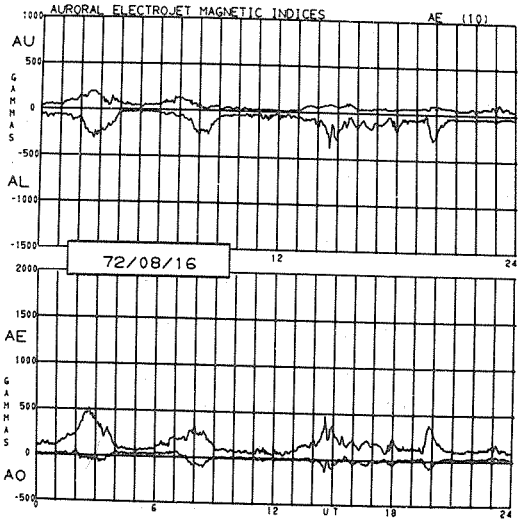
AURORAL ELECTROJET MAGNETIC INDICES
AE (10)
AU
AL
AE
AO
GAMMAS
72/08/16
UT

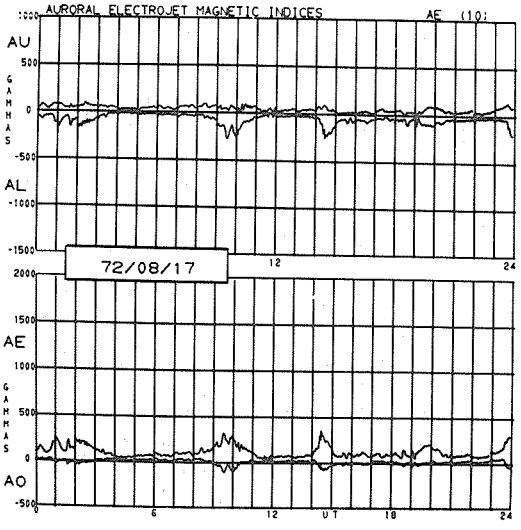
AURORAL ELECTROJET MAGNETIC INDICES
AE (10)
AU
AL
AE
AO
GAMMAS
72/08/17
UT

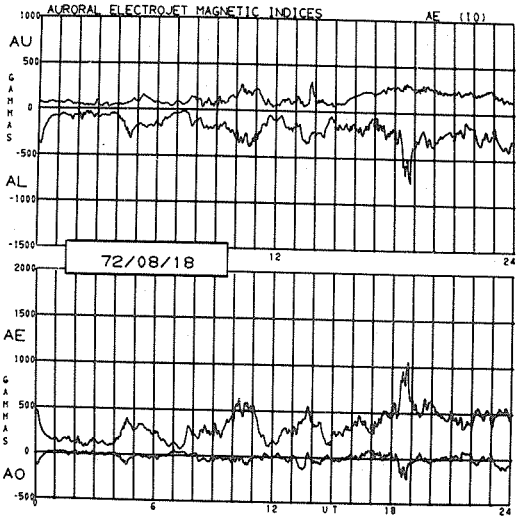
AURORAL ELECTROJET MAGNETIC INDICES
AE (10)
AU
AL
AE
AO
GAMMAS
72/08/18
UT

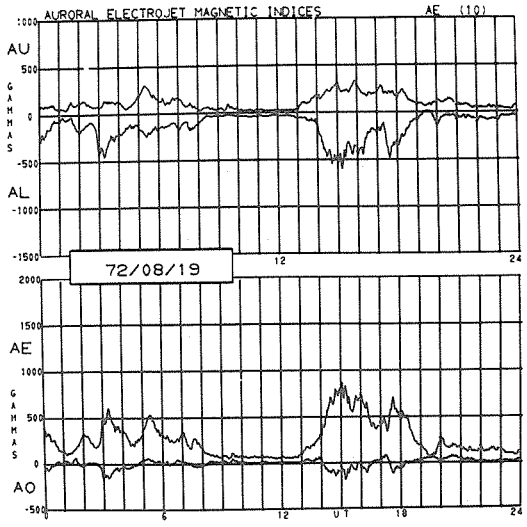
AURORAL ELECTROJET MAGNETIC INDICES
AE (10)
AU
AL
AE
AO
GAMMAS
72/08/19
UT

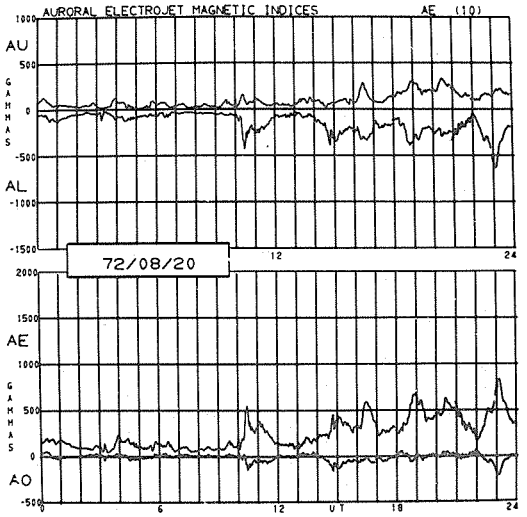
AURORAL ELECTROJET MAGNETIC INDICES
AE (10)
AU
AL
AE
AO
GAMMAS
72/08/20
UT

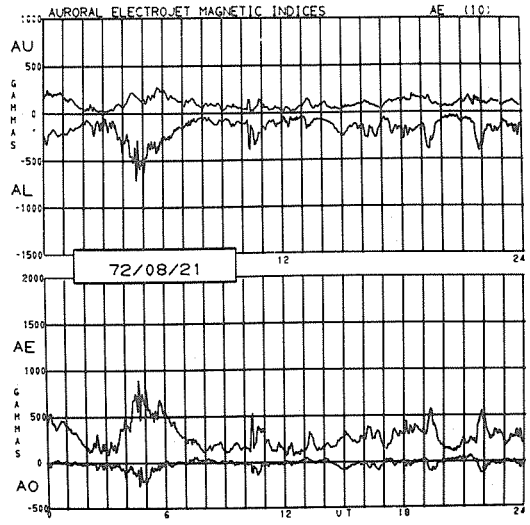
AURORAL ELECTROJET MAGNETIC INDICES
AE (10)
AU
AL
AE
AO
GAMMAS
72/08/21
UT

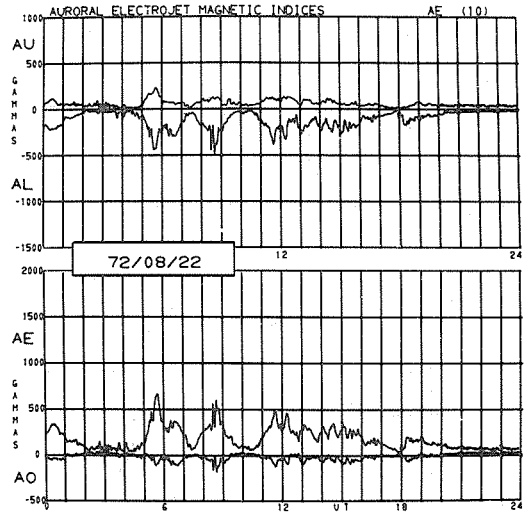
AURORAL ELECTROJET MAGNETIC INDICES
AE (10)
AU
AL
AE
AO
GAMMAS
72/08/22
UT

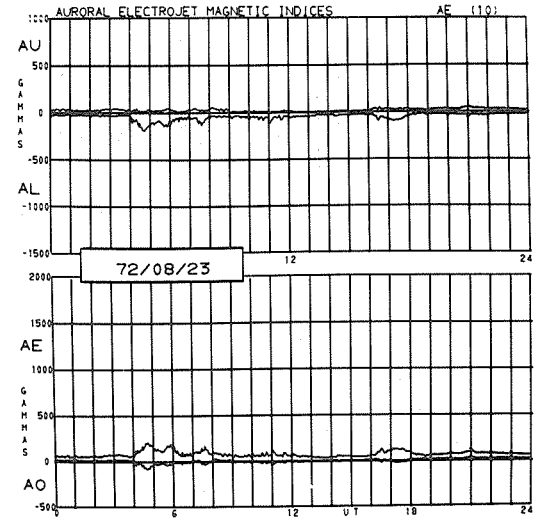
AURORAL ELECTROJET MAGNETIC INDICES
AE (10)
AU
AL
AE
AO
GAMMAS
72/08/23
UT

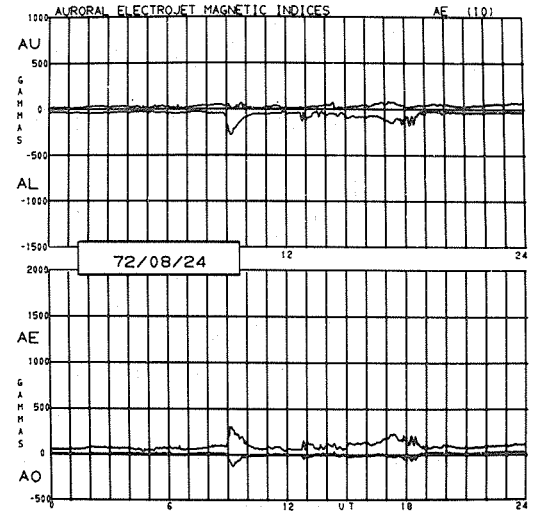
AURORAL ELECTROJET MAGNETIC INDICES
AE (10)
AU
AL
AE
AO
GAMMAS
72/08/24
UT

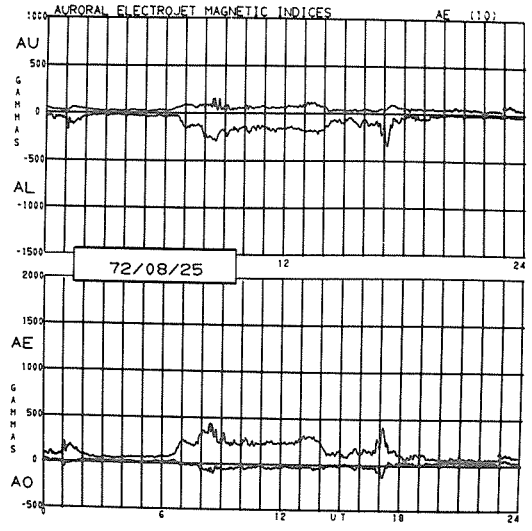
AURORAL ELECTROJET MAGNETIC INDICES
AE (10)
AU
AL
AE
AO
GAMMAS
72/08/25
UT

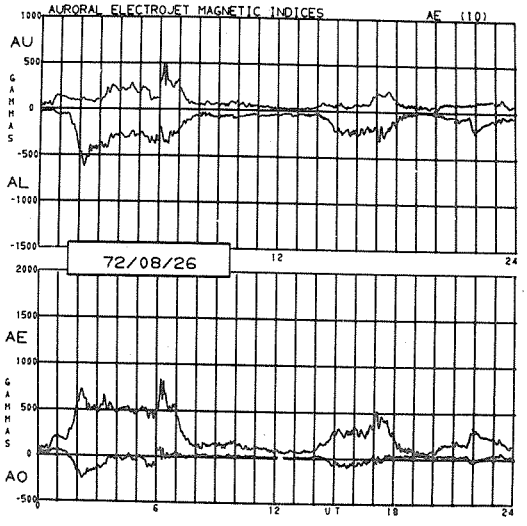
AURORAL ELECTROJET MAGNETIC INDICES
AE (10)
AU
AL
AE
AO
GAMMAS
72/08/26
UT

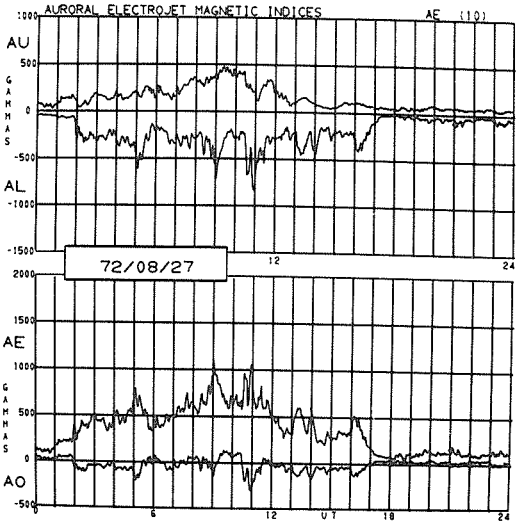
AURORAL ELECTROJET MAGNETIC INDICES
AE (10)
AU
AL
AE
AO
GAMMAS
72/08/27
UT

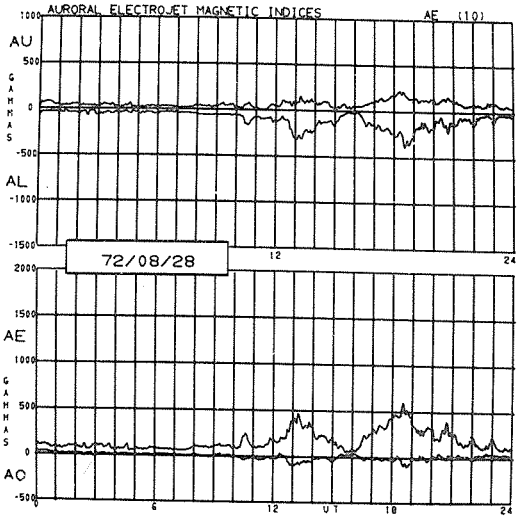
AURORAL ELECTROJET MAGNETIC INDICES
AE (10)
AU
AL
AE
AO
GAMMAS
72/08/28
UT

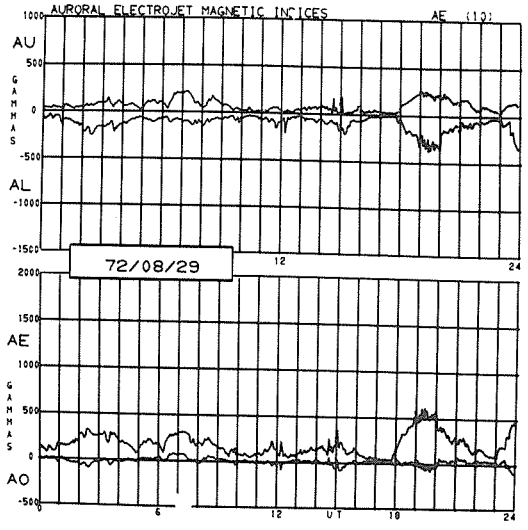
AURORAL ELECTROJET MAGNETIC INDICES
AE (10)
AU
AL
AE
AO
GAMMAS
72/08/29
UT

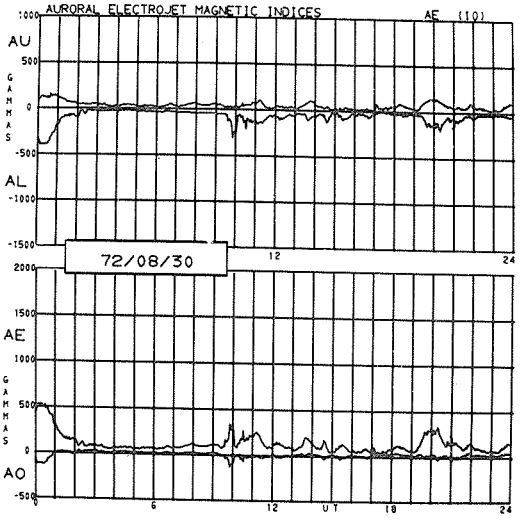
AURORAL ELECTROJET MAGNETIC INDICES
AE (10)
AU
AL
AE
AO
GAMMAS
72/08/30
UT

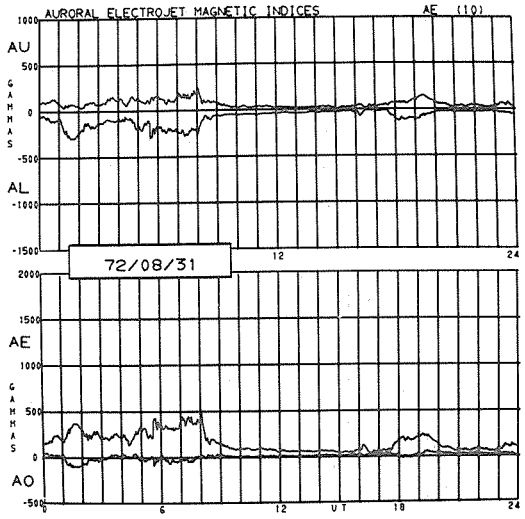
AURORAL ELECTROJET MAGNETIC INDICES
AE (10)
AU
AL
GAMMAS
72/08/31
AE
AO
UT

Hourly Equatorial Dst Values (Provisional)

by

M. Sugiura and D. J. Poros
NASA/GSFC
Greenbelt, MD. 20771

JULY 1972

UNIT=GAMMAS G.M.T.

DAY	1	2	3	4	5	6	7	8	9	10	11	12	13	14	15	16	17	18	19	20	21	22	23	24
1	-20	-19	-16	-14	-10	-8	-8	-12	-13	-10	-8	-1	-2	-5	-5	-4	-7	-8	-7	-4	-2	-2	-4	-4
2	-4	-5	-3	-4	-8	-9	-11	-12	-7	-3	2	3	-2	-3	-2	-2	3	7	9	8	3	7	-1	-9
3	-15	-13	-11	-7	-3	-3	-4	-2	-0	-2	3	7	7	8	4	1	2	0	-7	-7	-3	2	4	2
4	-0	-0	-2	-5	-10	-10	-9	-9	-6	-3	-1	-3	-0	4	6	2	-0	-1	-5	-7	-9	-8	-5	-5
5	-6	-8	-8	-6	-7	-8	-2	-1	-2	-2	-3	-6	-4	-2	1	1	-0	-3	-2	2	3	2	1	-2
6	-7	-8	-5	-2	-0	1	-1	-2	-4	-4	-4	-2	0	0	3	6	9	11	8	6	6	5	9	4
7	-1	-7	-15	-19	-19	-18	-18	-19	-23	-24	-25	-30	-30	-26	-23	-23	-26	-30	-34	-38	-38	-41	-42	-45
8	-48	-45	-40	-42	-48	-49	-42	-36	-36	-32	-30	-29	-26	-23	-24	-21	-17	-12	-6	-5	-2	-2	-9	-15
9	-17	-13	-12	-12	-12	-14	-14	-13	-12	-7	-13	-19	-16	-12	-10	-3	-5	-9	-9	-12	-14	-11	-13	-15
10	-19	-19	-15	-12	-12	-13	-13	-11	-11	-9	-8	-10	-12	-12	-10	-10	-8	-10	-12	-10	-11	-10	-13	-16
11	-15	-13	-9	-4	-3	-6	-11	-13	-13	-11	-9	-7	-3	2	7	9	9	5	-1	-11	-8	-3	-3	-3
12	-3	-2	0	-0	-3	-5	-9	-11	-7	-9	-7	-2	-8	-17	-19	-18	-17	-16	-15	-14	-13	-17	-17	-18
13	-17	-13	-11	-11	-11	-12	-11	-11	-11	-10	-9	-9	-10	-12	-15	-11	-10	-7	-6	-7	-5	-4	-4	-3
14	-4	-3	-0	0	-1	-4	-7	-6	-5	-7	-8	-9	-9	-9	-6	-4	-3	-6	-7	-5	-1	0	0	-3
15	-7	-9	-9	-10	-10	-8	-8	-8	-10	-7	-3	-3	-3	-2	1	2	3	3	-1	-1	3	6	6	3
16	-3	-9	-14	-22	-24	-25	-20	-18	-19	-14	-10	-8	-7	-7	-3	-4	-9	-13	-20	-18	-13	-7	-3	-2
17	-9	-15	-18	-17	-16	-14	-16	-14	-15	-12	-6	-5	-8	-8	-7	-7	-10	-12	-13	-16	-15	-12	-14	-15
18	-17	-16	-13	-16	-15	-16	-11	-11	-9	-3	-3	2	0	-2	-5	-8	-10	-10	-10	-7	-6	-5	-2	-3
19	-4	-6	-10	-15	-13	-9	-8	-3	-4	-9	-17	-10	-3	3	-1	-7	-10	-8	-8	-8	-14	-13	-15	-20
20	-18	-13	-10	-11	-12	-10	-12	-13	-8	-5	-3	-4	-3	-1	-1	-4	-7	-9	-10	-14	-15	-15	-12	-9
21	-7	-7	-9	-11	-13	-10	-8	-7	-6	-4	-2	-3	-4	-4	-4	-5	-4	-5	-6	-9	-11	-5	-0	3
22	3	2	1	1	0	0	1	-0	-0	-2	-3	-3	0	9	19	24	23	23	16	6	-13	-15	-12	-8
23	-9	-9	-6	-9	-4	0	1	-2	-6	-5	-4	-7	-9	-7	-7	-8	-16	-20	-18	-18	-16	-13	-13	-15
24	-17	-15	-13	-10	-8	-7	-9	-11	-13	-13	-14	-23	-21	-17	-19	-25	-25	-21	-20	-17	-21	-36	-42	-57
25	-52	-36	-31	-37	-41	-39	-50	-62	-48	-42	-38	-48	-45	-45	-38	-33	-32	-30	-34	-31	-30	-26	-31	-34
26	-33	-23	-16	-16	-20	-20	-23	-36	-41	-34	-27	-25	-28	-28	-30	-34	-31	-31	-25	-21	-20	-21	-20	-16
27	-16	-16	-16	-20	-22	-29	-31	-26	-22	-20	-19	-23	-23	-19	-15	-14	-15	-15	-14	-16	-21	-23	-24	-25
28	-23	-22	-20	-19	-17	-14	-15	-19	-24	-24	-19	-18	-19	-20	-19	-19	-19	-18	-16	-14	-13	-17	-19	-20
29	-20	-19	-17	-15	-12	-10	-10	-12	-13	-14	-13	-10	-6	-7	-10	-13	-13	-9	-8	-7	-7	-8	-12	-11
30	-12	-14	-14	-11	-5	0	0	-2	-2	-2	4	8	4	4	1	4	6	3	6	3	4	6	7	5
31	0	-4	-7	-7	-2	4	7	6	3	3	5	8	9	11	13	14	16	21	19	16	13	13	12	10

AUGUST 1972

UNIT=GAMMAS

DAY	1	2	3	4	5	6	7	8	9	10	11	12	13	14	15	16	17	18	19	20	21	22	23	G.M.T. 24
1	1	-16	-33	-40	-49	-47	-43	-38	-36	-35	-35	-30	-25	-21	-21	-20	-22	-21	-22	-21	-18	-19	-20	-24
2	-27	-33	-31	-23	-17	-14	-14	-12	-12	-14	-15	-14	-10	-8	-8	-11	-13	-11	-10	-10	-10	-9	-5	-4
3	-7	-7	-9	-8	-5	1	2	1	-4	-6	-5	-2	-1	-1	-2	-3	-4	-5	-3	-0	2	5	6	4
4	-1	6	29	3	-37	-70	-118	-115	-97	-86	-76	-76	-70	-65	-60	-58	-66	-70	-63	-65	-61	-46	-45	-80
5	-97	-96	-115	-125	-111	-94	-93	-76	-77	-65	-65	-50	-51	-51	-16	-65	-95	-81	-91	-92	-100	-102	-102	-94
6	-77	-77	-83	-94	-82	-89	-106	-97	-103	-104	-107	-102	-91	-86	-83	-79	-72	-70	-59	-60	-63	-66	-67	-69
7	-63	-66	-67	-72	-66	-70	-67	-66	-62	-59	-62	-62	-57	-56	-59	-62	-61	-55	-48	-47	-46	-46	-43	-46
8	-51	-55	-55	-54	-48	-44	-42	-44	-44	-45	-46	-44	-43	-40	-39	-44	-47	-46	-45	-46	-49	-50	-48	-43
9	-15	-17	-19	-15	-40	-59	-83	-90	-69	-75	-154	-154	-130	-119	-126	-129	-119	-110	-108	-102	-98	-98	-103	-101
10	-96	-91	-87	-84	-78	-73	-74	-75	-71	-69	-71	-72	-73	-71	-67	-66	-60	-58	-60	-61	-59	-65	-76	-77
11	-69	-70	-71	-70	-63	-53	-48	-49	-51	-54	-58	-56	-51	-52	-53	-57	-56	-53	-49	-49	-55	-58	-59	-64
12	-61	-58	-56	-55	-52	-46	-41	-41	-39	-40	-41	-40	-39	-38	-42	-45	-48	-45	-44	-43	-41	-40	-43	-45
13	-48	-49	-48	-45	-41	-35	-32	-30	-32	-31	-31	-31	-29	-27	-28	-30	-33	-39	-38	-34	-31	-29	-30	-30
14	-31	-37	-39	-36	-27	-18	-17	-16	-15	-15	-16	-21	-24	-21	-19	-22	-26	-26	-28	-26	-27	-32	-37	-40
15	-41	-42	-41	-38	-33	-30	-35	-37	-35	-31	-29	-26	-22	-22	-25	-26	-27	-25	-26	-32	-36	-32	-33	-35
16	-37	-34	-33	-36	-32	-25	-21	-25	-25	-22	-20	-17	-15	-19	-26	-28	-29	-29	-32	-35	-35	-35	-38	-40
17	-40	-37	-32	-27	-19	-11	-9	-8	-10	-16	-21	-19	-14	-14	-18	-24	-23	-22	-23	-26	-29	-30	-31	-30
18	-29	-30	-32	-32	-28	-26	-25	-22	-26	-31	-33	-34	-24	-20	-25	-28	-32	-32	-37	-34	-34	-35	-38	-44
19	-44	-43	-45	-40	-33	-33	-33	-29	-21	-18	-14	-16	-14	-10	-20	-36	-38	-30	-27	-28	-36	-40	-38	-33
20	-35	-35	-32	-31	-28	-22	-20	-15	-12	-11	-14	-13	-12	-12	-19	-25	-25	-22	-21	-28	-34	-44	-40	-37
21	-39	-43	-39	-32	-28	-29	-24	-20	-20	-23	-22	-21	-19	-18	-19	-19	-17	-14	-18	-24	-20	-22	-22	-29
22	-33	-32	-30	-30	-25	-19	-16	-13	-15	-15	-16	-18	-19	-21	-24	-26	-22	-20	-21	-21	-26	-28	-28	-30
23	-27	-25	-24	-22	-19	-14	-11	-10	-13	-14	-15	-15	-17	-16	-15	-13	-12	-14	-15	-18	-20	-23	-25	-26
24	-24	-24	-24	-24	-19	-13	-11	-5	-13	-12	-12	-12	-13	-13	-14	-14	-12	-11	-10	-12	-14	-17	-18	-20
25	-19	-14	-12	-11	-9	-5	-5	-10	-15	-16	-16	-17	-20	-22	-21	-21	-17	-13	-13	-14	-14	-13	-13	-3
26	-3	-10	-25	-26	-29	-34	-31	-31	-26	-29	-29	-24	-17	-13	-17	-19	-19	-19	-15	-11	-22	-27	-28	-22
27	-23	-28	-34	-36	-41	-40	-60	-69	-80	-82	-74	-61	-63	-60	-57	-52	-49	-43	-43	-46	-47	-45	-41	-39
28	-37	-38	-38	-36	-33	-25	-19	-19	-25	-30	-32	-32	-30	-31	-35	-33	-34	-34	-34	-32	-34	-37	-37	-37
29	-36	-34	-31	-31	-29	-22	-18	-21	-24	-26	-25	-24	-27	-29	-33	-30	-24	-20	-21	-30	-33	-31	-28	-28
30	-31	-32	-29	-25	-20	-15	-12	-10	-12	-15	-14	-19	-18	-16	-18	-18	-16	-13	-14	-17	-23	-21	-19	-19
31	-25	-31	-29	-27	-25	-22	-22	-30	-30	-22	-18	-19	-19	-17	-15	-13	-16	-12	-17	-24	-23	-22	-20	-19

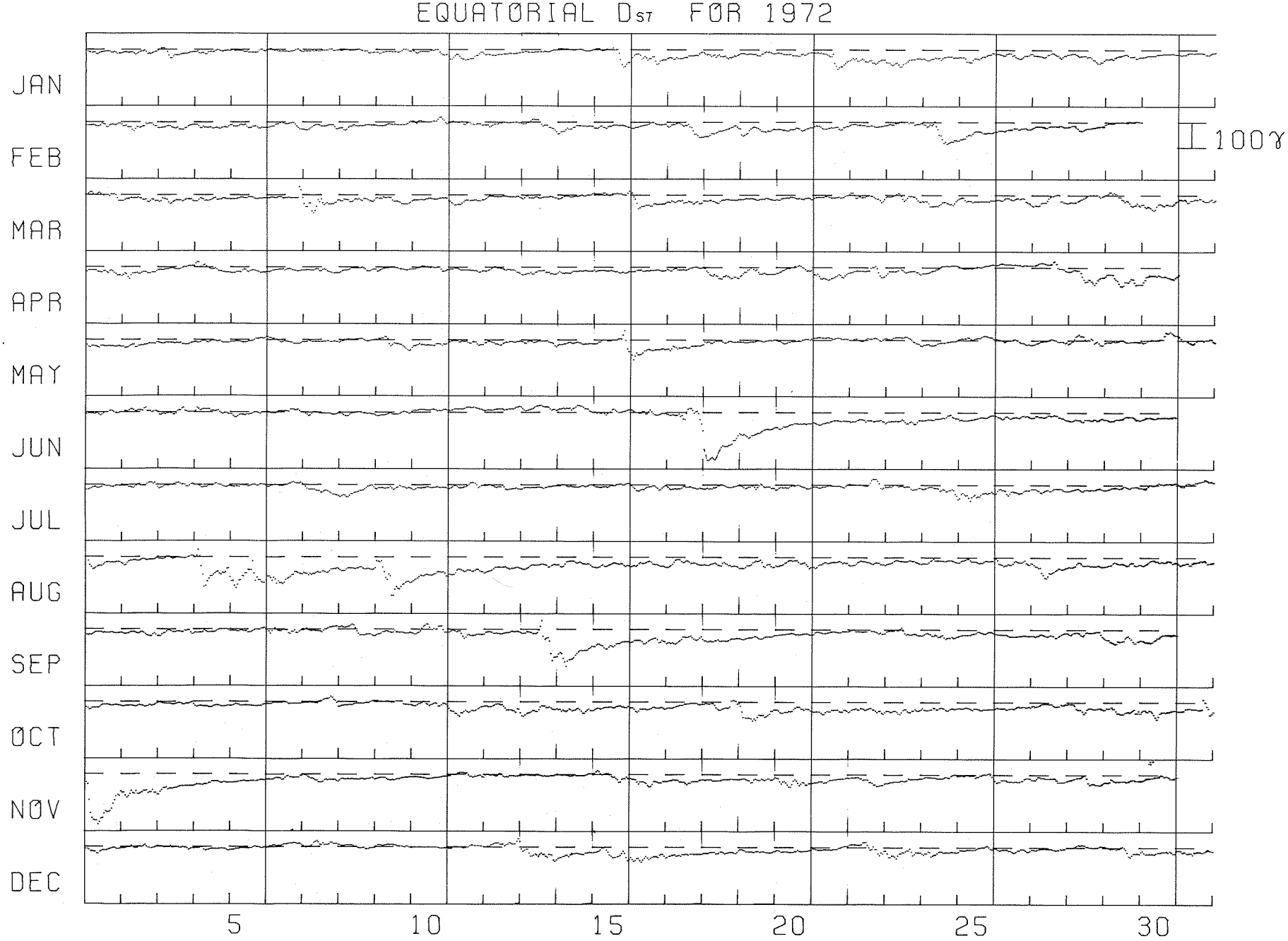
EQUATØRIAL Dst FØR 1972
JAN
FEB
MAR
APR
MAY
JUN
JUL
AUG
SEP
ØCT
NØV
DEC
100γ
5
10
15
20
25
30

Geomagnetic Disturbances of August 4-9, 1972

by

K. Kawasaki*
Cooperative Institute for Research in Environmental Sciences
University of Colorado, Boulder, Colorado

and

Y. Kamide, F. Yasuhara and S.-I. Akasofu
Geophysical Institute
University of Alaska, Fairbanks, Alaska

The geomagnetic disturbances which occurred during the period August 4-9, 1972 were among the most intense ever recorded. In particular, Loomer and van Beek [1972] have reported that the magnitude of the fluctuations at one auroral zone station in the Canadian sector reached some 6,000 gammas. The disturbances were associated with an intense Forbush decrease (∿28%) in cosmic rays in the Canadian sector, large values of the parameters of the interplanetary medium ($|B|$ = 84 gammas and solar wind speeds, U_H+ > 1000 km/sec.), and notable riometer absorption (> 12.6 dB in near totally dark conditions at McMurdo on Antarctica). [Lincoln et al., 1972].

The upper portion of Figure 1 (a, b, and c) shows the maximum and minimum variations of a superposition of the H-component magnetic records of nine high latitude stations (College, Tixie Bay, Dixon Island, Nurmijarvi, Leirvogur, Narssarssuaq, Great Whale River, Meanook. and Sitka), and the lower portion a superposition of the H-component magnetic records of five low latitude stations (Kakioka, Tangerang, Tashkent, San Juan, and Honolulu). For the low latitude records, Sq variations (29 July, 1973) are subtracted. The envelope of the upper traces gives the auroral electrojet indices AU and AL; the distance between the AU and AL indices gives the AE index [Davis and Sugiura, 1966], and the asymmetry (ASY) index is given by the distance between the upper and lower envelopes in the lower part [Kawasaki and Akasofu, 1971].

Individual traces of the records of most of these stations for this period may be found in Lincoln et al., [1972], WDC-A Report UAG-21 and in "Solar-Geophysical Data" [1973].

It is probable that the geomagnetic storms during this period were associated with flares produced by the McMath Plage Region 11976. Five flares of Importance 2F or greater originated in this region located between the meridians E35 and E25 during August 2, 1972. However, McMath Region 11970 on the western limb also produced a significant flare on August 2 (at about 1044 UT), which was reported to be as great as Importance 2B. The transit time from the flare sighting to geomagnetic storm sudden commencement (ssc) is, on the average, 40 hours, but has been inferred to be as short at 19 hours and as long as 72 hours [Akasofu and Yoshida, 1967]; the flares which occurred during August 2, 1972 are all well within this range of transit times to first ssc of August 4, 1972.

The first geomagnetic storm began with a double-structured ssc at 0119 and 0220 UT on August 4; the step function-like changes were of orders 30 and 40 gammas, respectively (see Figure 1). There were only minor enhancements in the AU and AL indices during the sudden commencements.

The initial phase was brief and the main phase decrease began at about 0330 UT. The entire storm was short-lived; by 0700 UT the recovery phase had already begun. Although neither the maximum main phase decrease (∿ 200 gammas) nor the asymmetry indices (∿ 90 gammas) were particularly large, the AU index, the upper envelope of the high latitude records in Figure 1, exhibited an extremely large magnitude during the period 0330-0600 UT on August 4 and was, in general, greater than the AL index. The College record is the main contributor to the AU index. In particular, the largest peak (∿ +1800 gammas) had no significant counterpart in the AL index. The corresponding magnetic record from Great Whale River, then a midnight station, shows negative bays of the maximum intensity of about 500 gammas, while the Ottawa record indicates a negative bay of order 700 gammas during the same period. A more extensive analysis is needed to obtain an accurate current distribution between 0300 and 0600 UT. After 0600 UT, the AU index decreased, while the AL index increased considerably. The AL index reached the maximum intensity at about 0600 UT when the main phase was also near the maximum epoch.

The second storm in this sequence, one of the most complex ever recorded, began with an ssc at 2054 UT before the first storm had fully recovered. It is very likely that this storm was associated with the Importance 3B flare which occurred in McMath Region 11976 (N14, E08) at about 0630 UT on August 4, 1972. This implies a transit time to ssc of order 14 hours which, although of extremely brief duration, may not be too unrealistic considering the large solar wind velocities observed; also, recent work by Yoshida (private communication, 1973) suggests that the transit time for a geomagnetic storm occurring immediately after another is usually much shorter than for an isolated storm.

---

* Guest worker with Environmental Data Services, NOAA.

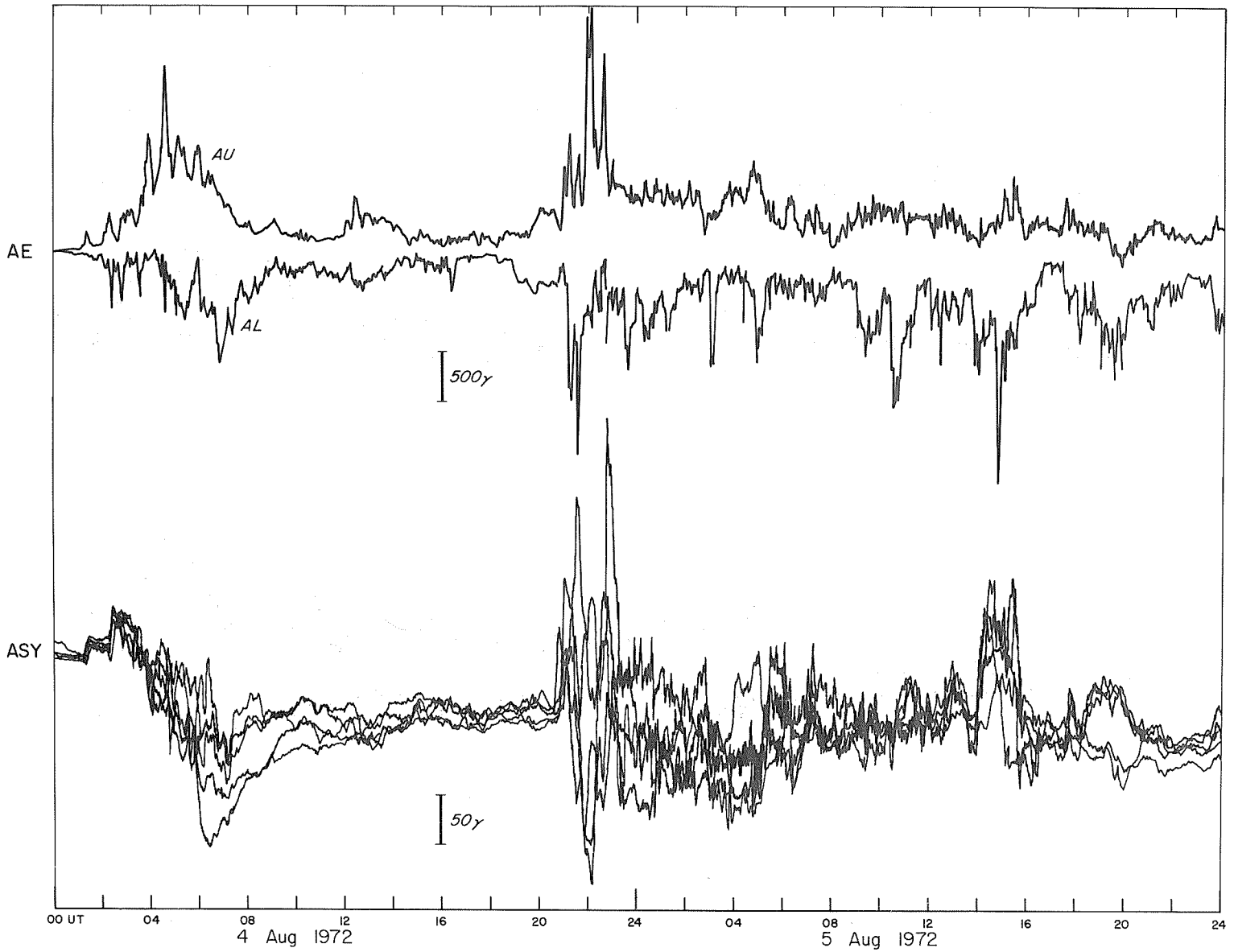

Fig. 1a. The AU, AL, AE and the asymmetry (ASY) indices between 0000 UT on August 4 and 2400 UT on August 9, 1972.

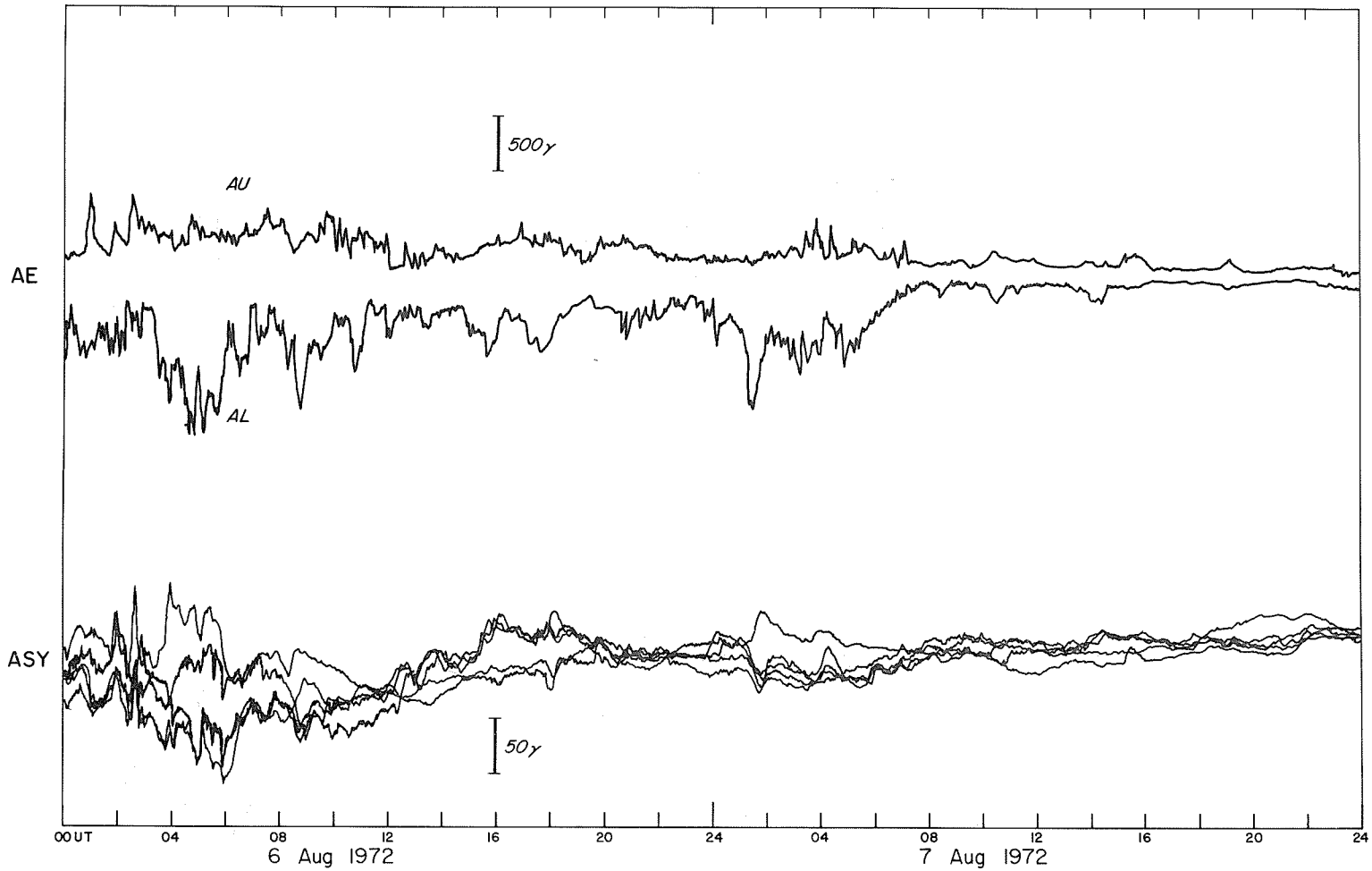

Fig. 1b. The AU, AL, AE and the asymmetry (ASY) indices between 0000 UT on August 4 and 2400 UT on August 9, 1972.

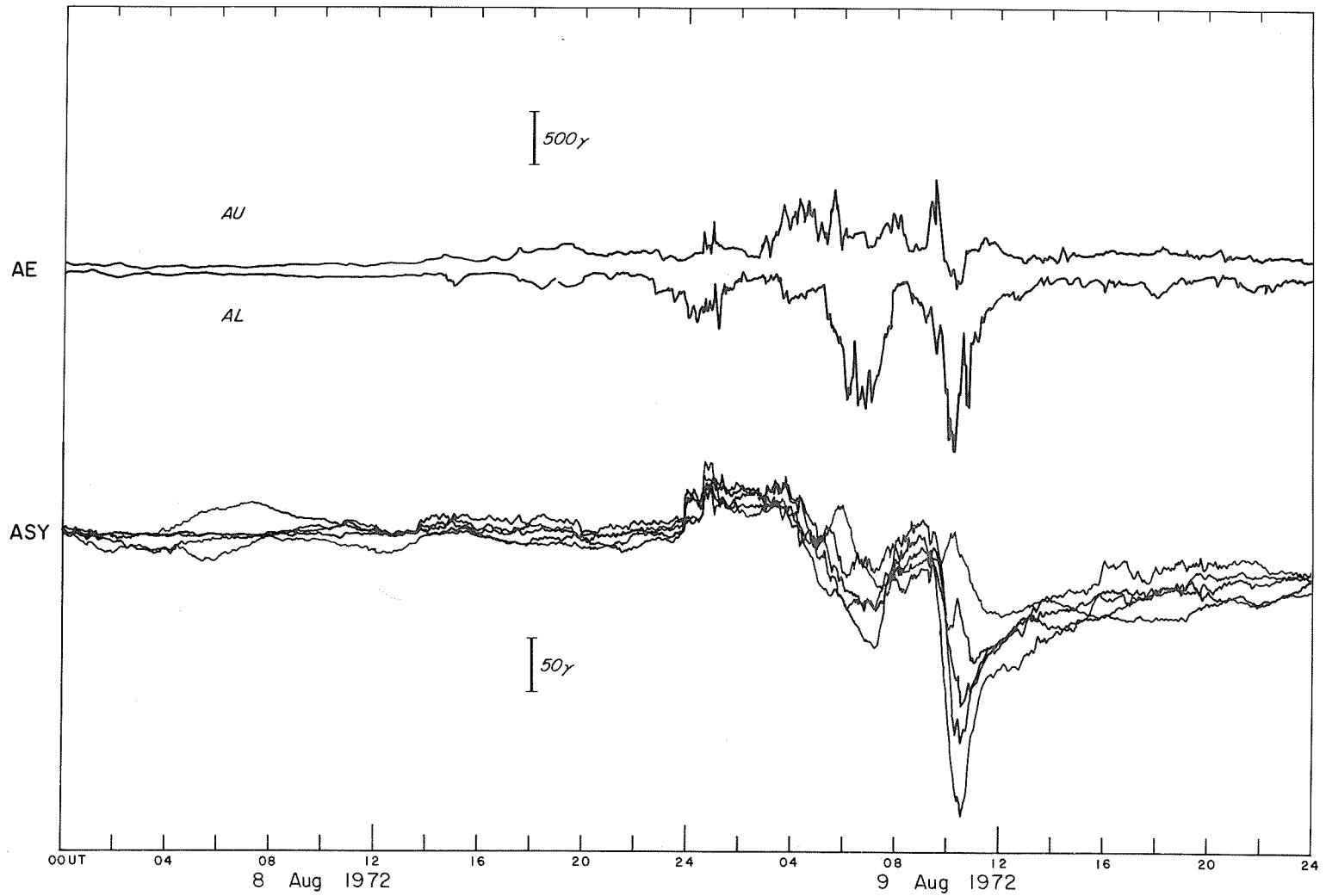

Fig. 1c. The AU, AL, AE and the asymmetry (ASY) indices between 0000 UT on August 4 and 2400 UT on August 9, 1972.

The identification of the 3B flare at 0630 UT as the geomagnetic storm-producing event is further supported by the PCA event observed during the latter half of August 4, 1972 at McMurdo. The event began gradually from a background absorption value of about 1 dB at about 0830 UT, eventually reaching 12.6 dB maximum between 2100 to 2300 UT.

This second storm was remarkable in many respects. First of all, the ssc reached a magnitude of well over 100 gammas at Asian stations, then in the morning sector. Figure 1 shows that immediately following the ssc at 2054 UT on August 4, the ASY index grew to about 250-300 gammas. This was caused by an abrupt decrease of the H component at stations in the late morning sector. A similar unusual feature during great magnetic storms has been reported by Fukushima and Abe [1958] and Akasofu and Chapman [1960].

The most characteristic feature of this storm is the occurrence of violent fluctuations, particularly during the first three hours [Loomer and van Beek, 1972]. There is some resemblance between the storm of July 15, 1959 and the present storm, but the latter was much more violent. At College (see individual magnetograms in Report UAG-21), then near the local noon meridian, a negative pulse of magnitude 2100 gammas was recorded just prior to 2200 UT; the field reversed and by 2200 UT, has reached 2500 gammas in the positive direction. It is probable that the short positive pulse which occurred at about 2240 UT was even larger than that at 2200 UT in the College record, but it could not be scaled even in the storm records because of its rapid rate of change. It may be noted that as with the first storm studied, the AE indices are large because of the occurrence of the large positive variations rather than negative variations as would normally be the case.

Giant pulsations (PC-5) were also extremely prominent during the entire duration of the storm. The pulsations, with periods of order 5 minutes, were observed worldwide; at Sitka, near the noon meridian, the pulsations were as great as 1100 gammas between 0030 and 0100 UT on August 5, 1972, and at low latitude stations, the amplitudes reached well over 100 gammas.

Despite the complexity (some of which may may have been introduced by timing errors) of the superposed low latitude records in Figure 1, it may be recognized that many of the fluctuations appear to be si type activity; see for example the increasing field centered around 2300 UT on August 4 which at some stations began from a large negative value, and later the three prominent structures between 1000 and 1600 UT on August 5. This may also be inferred from the study of Yoshida and Akasofu [1966], who showed that Forbush decreases of large intensity (>8%) were associated with "turbulent" structures of the solar wind as evidenced by si activities during a geomagnetic storm. We note that the Forbush decrease was intense (28% at 0100 UT on August 5, 1972).

Another interesting point to be noted here is that although the Pioneer IX spacecraft was located at a heliocentric distance of about 0.8 AU during these early August events, it appears that the spacecraft did not observe any dramatic changes in the solar wind velocity and interplanetary magnetic field, until after the ssc was observed on the earth. The reason for this may be that Pioneer IX was located too far east in heliographic longitude with respect to the flare location (see Croft [1972; 1973, this issue] for the location of Pioneer IX) to observe the initial enhancement of the interplanetary parameters, which was probably confined to a rather narrow angular region [Haurwitz et al., 1965].

The second storm ended about 1800 UT on August 7; the last two Kp indices were 2+ and 2o. The first half of August 8 was also very quiet (1+, 1-, 0+, 1-); it is interesting that there exists such a quiet period when solar activity is generally high. Minor disturbances began at about 1400 UT on August 8 and continued until the sudden commencement of the third storm.

The third storm during this period, like the first storm, began with double-structured ssc at 2354 UT on August 8 and 0036 UT on August 9 (see Figure 1). The storm was probably caused by the intense 3B flare of August 7, 1972 in McMath 11976, with coordinates N14, W37.

The main phase occurred in two steps; the first decrease began at about 0400 UT, August 9, and ended at about 0700 UT. The storm began to return to the base level between 0800 to 1000 UT, during which time minor si activity was evident.

Onset of a deeper, more intense main phase decrease occurred just prior to 1000 UT. The asymmetry was considerable at about 1030 UT reaching 250 gammas; the high latitude records at about this same time shows the growth of an intense westward current producing a maximum deviation of order -1400 gammas.

Unlike the first two storms during the period studied, the third storm was more or less normal in development. The unusual development of the first two storms, in all likelihood, arose from the exceptionally large magnitudes of the interplanetary magnetic field and solar wind speed.

A few points to be noted here are (i) a relatively larger magnitude of the AU index compared with the AL index near the end of the initial phase, (ii) a very small magnitude of the AU index around

0600 UT and (iii) the total 'lack' of positive bays around 1000 UT. The last feature has often been noted during intense storms.

ACKNOWLEDGEMENTS

One of us (K.K.) would like to thank EDS-NOAA, Boulder, Colorado, where he is a guest worker, for providing its facilities and support in completing this study. We would also like to thank Mr. W. Paulishak WDC A, EDS-NOAA, Boulder for providing the magnetograms used in this study and the support staff of the Geophysical Institute of the University of Alaska for the scaling and digitizing of the magnetograms. This work has been supported in part by the National Science Foundation through its grant GA 28101 to the Geophysical Institute, University of Alaska.

REFERENCES

AKASOFU, S.-I. and S. CHAPMAN 1960 Some features of the magnetic storms of July 1959 and tentative interpretations, IUGG Monographs, 7, 93-108.

AKASOFU, S.-I. and S. YOSHIDA 1967 The structure of solar plasma flow generated by solar flares, Planet. Space Sci., 15, 39-47.

CROFT, T. A. 1972 Traveling regions of high density observed in the solar wind on August 3 and August 9, 1972, Scientific Report No. 7, Center for Radio Astronomy, Radioscience Laboratory, Stanford Electronics Laboratories, Stanford University, November.

CROFT, T. A. 1973 Solar Wind Density Variations Observed on a Long Path during August 1972, elsewhere this compilation.

DAVIS, T. N. and M. SUGIURA 1966 Auroral electrojet activity index AE and its universal time variation, J. Geophys. Res., 71, 785-801.

FUKUSHIMA, N. and S. ABE 1958 The initial phase of the magnetic storm on Feb. 11, 1958, Rep. Ionosphere Res. Japan, 7, 44-49.

HAURWITZ, M. W., S. YOSHIDA and S.-I. AKASOFU 1965 Interplanetary magnetic field asymmetries and their effects on polar cap absorption events and Forbush decreases, J. Geophys. Res., 70, 2977-2988.

KAWASAKI, K. and S.-I. AKASOFU 1971 Low-latitude DS component of geomagnetic storm field, J. Geophys. Res., 76, 2396-2405.

LINCOLN, J. V. and H. I. LEIGHTON 1972 Preliminary Compilation of Data for Retrospective World Interval July 26 - August 14, 1972, World Data Center A for Solar-Terrestrial Physics Report UAG-21, November 1972.

LOOMER, E. I. and G. JANSEN VAN BEEK 1972 Magnetic storm, August 4, 1972, paper presented at Fall Annual Meeting AGU, December 4-7, 1972, (post deadline abstract published in program, page 24).

YOSHIDA, S. and S.-I. AKASOFU 1966 The development of the Forbush decrease and the geomagnetic storm fields, Planet. Space Sci., 14, 979-986.

1973 Solar-Geophysical Data (Comprehensive Reports), 342 Part II, February 1973, U.S. Dept. of Commerce, (Boulder, Colorado, U.S.A. 80302).

On the Geo-Activity of the Solar Flares of 2, 4, 7 and 11 August 1972

by

I. N. Odintsova, L. N. Leshchenko
K. N. Vasiliev and G. V. Givishvili
Academy of Sciences of the USSR
Moscow, USSR

August 1972 is one of the most interesting disturbed periods of late. The intense chromospheric flares of 2, 4, 7 and 11 August produced different disturbances in the ionosphere and the geomagnetic field. A description of the perturbations recorded at the Moscow IZMIRAN station is given below.

The ionospheric disturbances during the above period can be classified into those of wave and corpuscular nature. Consider first, the effects of the X-ray and ultraviolet emission of flares. Solar X-ray flare emission increases the ionization of the low ionosphere and causes the geophysical phenomena of sudden ionospheric disturbances (SIDs). Simultaneously, sudden increases in atmospheric noise level, cosmic ray absorption, short wave absorption and minimum reflection frequencies (fmin) observed by vertical ionosondes take place as well as other phenomena. At the same time as the hard X-rays ($\lambda < 10$ Å), soft X-rays (shorter than 100 Å) are often generated during solar flares, as well as ultraviolet emission (shorter than 1300 Å) which can produce additional ionization in the E- and F2-regions [Odintsova, 1965].

Figures 1 and 2 present data recorded in Moscow, IZMIRAN on 2, 4, 7 and 11 August, 1972: critical frequencies foE, foF1 and foF2, minimum reflection frequencies (fmin), values of ionospheric absorption at 2.2 MHz, and atmospheric noise levels at 35 kHz.

Consider the ionospheric effects of each flare. Flare data are taken from Report UAG-21, Lincoln and Leighton, ed. [1972].

The flare of 2 August 1972 (importance 1B) began at 0016 UT and ended at 0506 UT. Vertical ionospheric sounding data during this flare indicate a slight increase in fmin as well as a 68% increase of electron density in the E-region (see Figure 1). Sporadic-E blanketing prevented a more detailed description of the E-region electron concentration. A slight increase in atmospheric noise level is observed from 0315 UT to 0800 UT. The X-rays were probably absorbed mainly in the E-region and upper D-region. This seems to be supported by a significant absorption effect at 2.2 MHz, measured by the A1 method with the equipment described in [Givishvili et al. 1972]. We can also obtain an estimate of the absorption value at 2.2 MHz using the fmin data. At the beginning of the flare, the absorption is found to be 105±20 dB. By 0700 UT it decreased to 15±10 dB and became imperceptible by 1100 UT.

On 2 August two nighttime flares were observed (1838-1859 UT and 2005-2036 UT). These, of course, did not cause any observable X-ray effect in the ionosphere at the Moscow IZMIRAN station.

The 2B flare of 4 August 1972 occurred from 0621 to 0852 UT. During this flare no ionospheric echoes were observed from 0620 to 0745 UT. After 0745 fmin values returned gradually to their ordinary level by 1030 UT. A considerable increase in atmospheric noise level was observed at 35 kHz from 0620 to 0840 UT. During this flare, X-rays with $\lambda < 10$ Å apparently were generated; these could produce a considerable increase in electron density in the D-region. Owing to the great absorption, ionospheric effects could not be detected in the E- and F2-regions. Comparison of the time variations of the observed effects indicates that the hard X-ray generation began simultaneously with the observed flare emission in Hα.

The 3B flare of 7 August 1972 lasted from 1500 to 2000 UT. This flare is remarkable in having produced an electron density increase in the F2-region (see Figure 2). The electron density at the peak of the F2 layer increased by ∿70%. The effect in the F2-region began earlier than the optical flare in Hα did, suggesting that the generation of active ionizing radiation responsible for the additional ionization in the F2-region began before the observed emission of the flare at Hα. One sees from Figure 2 that during this flare an effect in the D-region is also observed. Also, any effect on the E-region again failed to be observed owing to the great absorption. A great increase of atmospheric noise level occurred beginning at 1500 UT. It should be noted that even though the Sun is near the horizon (elevation h=18°), absorbtion was so great that no vertical incidence echoes could be observed. It is known that an increase of fmin (or total blanketing of ionospheric echoes), observed at stations where the elevation of the Sun is small, is due mainly to hard radiation, the soft component having been absorbed by the overlying layers of the Earth's atmosphere [Dvoryashin et al., 1962]. It seems likely that during this flare hard photons with energies of tens and hundreds of kev were generated. The SOLRAD 10 and Explorer 44 observations [Report UAG-21, Lincoln and Leighton, ed., 1972] during the August 7 flare showed very strong X-ray fluxes in the ranges of 0.5 - 3Å, 1 - 8Å, 8 - 20Å; these exceeded by tens and hundreds of times the quiet solar flux by orders of magnitude.

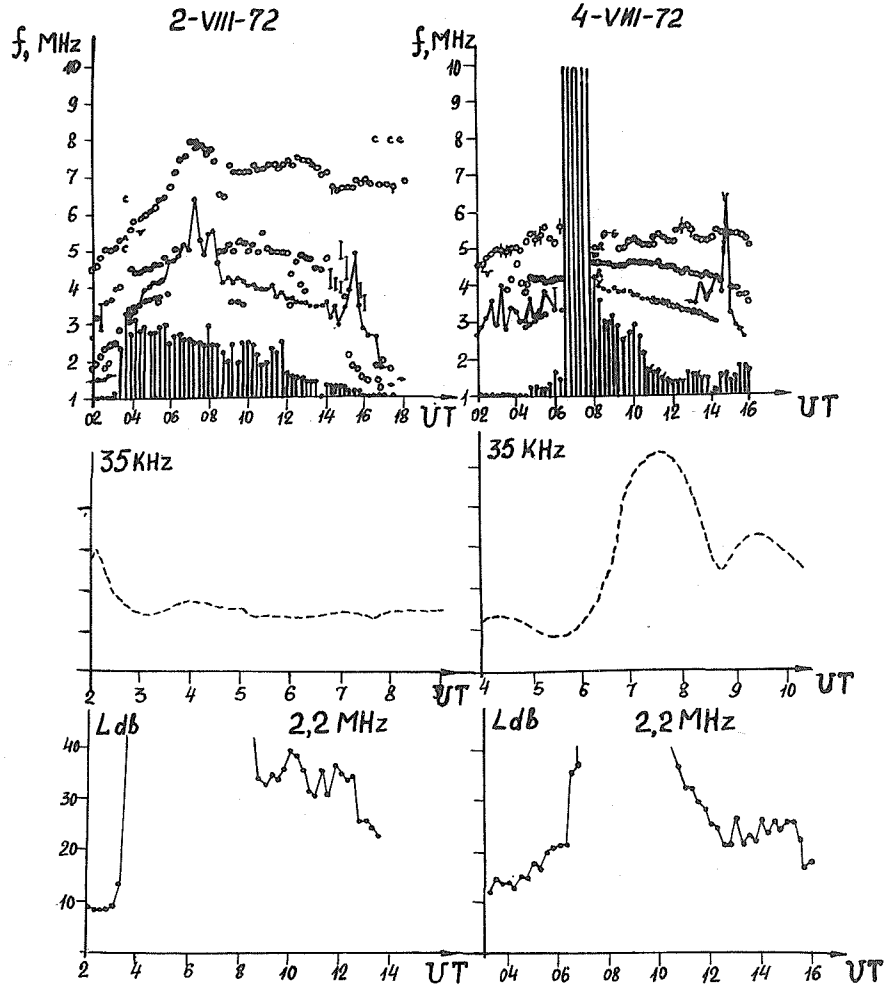

Fig. 1. Critical frequencies foE, foF1 and foF2, minimum reflection frequencies (fmin), values of ionospheric absorption at 2.2 MHz, and atmospheric noise levels at 35 kHz for 2 and 4 August 1972 recorded at IZMIRAN.

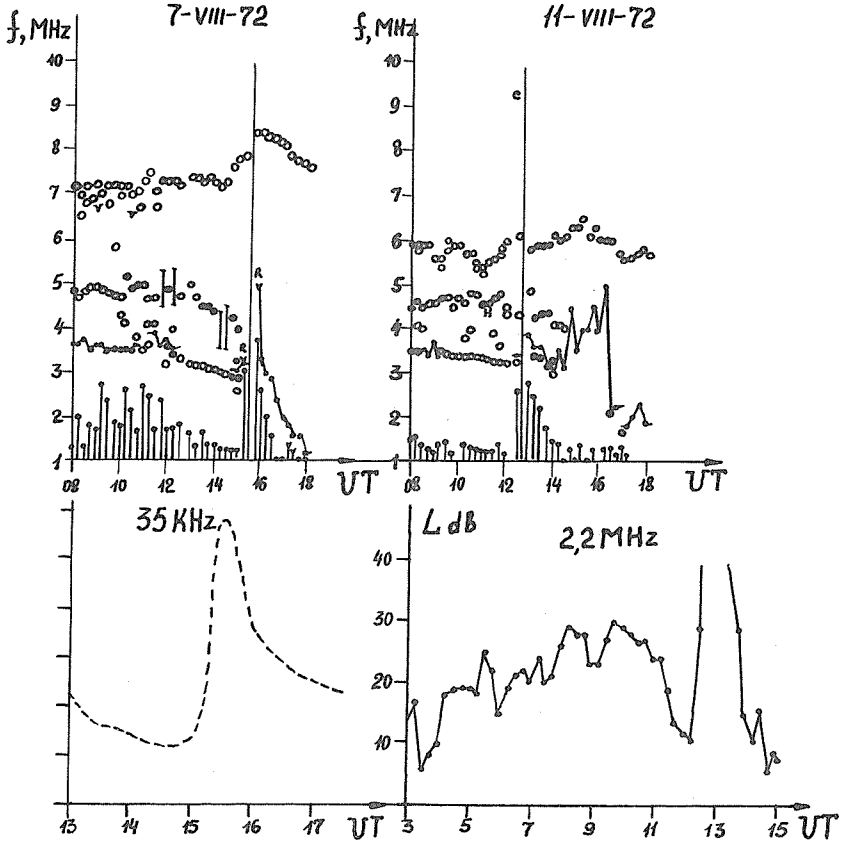

Fig. 2. Critical frequencies foE, foF1 and foF2, minimum reflection frequencies (fmin), values of ionospheric absorption at 2.2 MHz, and atmospheric noise levels at 35 kHz for 7 and 11 August 1972 recorded at IZMIRAN.

On 11 August 1972, from 1200 to 1300 UT, several limb flares were observed. The largest was of importance 2B. During this flare hard X-rays caused an increase in the D-region electron density (a transitory effect of radio wave absorption was observed), and a rise in E-region electron density by ∿20% was detected. The 2.2 MHz absorption data also showed a sharp rise in the absorption, exceeding the equipment sensitivity (by ∿ 60 dB).

Along with the X-rays, the flares also generated corpuscular emission. The investigation of these effects reveals a number of interesting features. On 4 August 1972 at 0120 UT a strong magnetic storm (magnetic indices K=7-8) was detected, which lasted up to 1800 UT 7 August. Simultaneously with the commencement of the magnetic storm an ionospheric disturbance began. The critical frequencies foF2 decreased by up to 80% (see Figure 3). The ionospheric storm lasted for three days and essentially ended on 7 August. Note the simultaneity of the beginning and the end of the ionospheric and magnetic disturbance. The magneto-ionospheric disturbance seems to have been caused by the flares of 2 August and by that of 4 August. It is practically impossible to separate these two disturbances since they are superposed. The day of 5 August is very interesting. In Figure 4 the diurnal variations of the critical frequencies foE, foF1, foF2 for 5 August are shown. The dotted line shows the median values of the critical frequencies for the given month. The critical frequencies foF2 decreased to less than the foF1. At the same time the F2-region minimum heights h'F2 rose sharply to 1.5 - 2 times normal, as seen in Figure 3. It is also interesting to note that during the magnetic storm on the night of 4-5 August, from 2100 30° EMT 4 August to 0030 30° EMT 5 August, an additional ionization was observed in the E-region (the nighttime E).

At middle latitudes the E-region is known to be observed only in the daytime. After sunset, the E-region electron density decreases rapidly, and the E-region is generally not observed in the nighttime. From 2100 30° EMT 4 August to 0000 30° EMT 5 August there is a group delay in the F2-region echoes at the low frequency cut-off of the trace that indicates the existence of the E-region; the foE itself seems to be lower than the low frequency cut-off of the ionosonde (1.0 MHz). However, from 0000 to 0130 30° EMT 5 August a distinct trace of the nighttime E was observed on 1.1 MHz. This is shown in the ionogram of Figure 5, and leads to the conclusion that an additional ionization is present in the E-region, which seems to be caused by a corpuscular flow into the ionosphere.

From 0045 to 0130 30° EMT sporadic-E reflections appear. These E_s reflections are of a diffuse character and are similar to those from the polar E_s shown in Figure 6. At 0145 30° EMT the E_s trace became flat similar to that of f-type E_s, but additional reflections (diffusive ones) appear at heights of 120-130 km. It is known from Dvoryashin, et al. [1960] that similar phenomena are observed most frequently during strong magnetic storms, accompanied by auroras at middle and low latitudes.

On the night of 5-6 August, also, additional diffusive reflections appear in the F2-region at frequencies higher than fxF2 (Figure 7).

On 6 August the ionosphere began gradually to return to its unperturbed state. The F2-region appears and the F1-region shows little change. F2-region heights have increased to 700 km. Many laminations and many new additional formations appear (see Figures 8 and 9).

Following the flare of 7 August, an ionospheric disturbance began on 9 August at 1800 UT. The maximum critical frequencies were depressed by ∿50%. This event was a short perturbation which ended by 0600 UT in the morning of 10 August (see Figure 10). Note that the ionospheric and magnetic disturbances do not begin at the same time. The magnetic disturbance began at 2354 UT 8 August. At 2124 UT 9 August it ended. The ionospheric disturbance started as the magnetic one began to die down and continued while the magnetic field was practically unperturbed. Similar phenomena are described in Hardwick [1953], Mednikova [1957], and Odintsova [1961].

After the flare of 11 August a slight fall in the critical frequencies of the F2-region is also observed. The magnetic field at this time was unperturbed (see Figure 10).

From the above, it appears that the analysis of magneto-ionospheric perturbations indicates that an ionospheric disturbance may be observed at the same time as a magnetic one (4, 5 and 6 August), or at a later time, the ionospheric disturbance being behind the magnetic one (9 and 10 August), or also with an undisturbed magnetic field (12 August). The investigation of analogous phenomena is of great interest for the study of the physical processes taking place in the interaction of the Earth's magnetic field with the electric currents in the F2-region.

The above analysis shows that after a series of flares one observes a sharp growth of a sporadic layer which completely shields the E-region and partly shields the F1- and F2-regions (see Figure 11). Large growth of the sporadic layer is observed up to 17 August. Probably, after a number of magneto-ionospheric disturbances, accompanied by a perturbation of the ionospheric layer structure, the conditions for the formation of a compact shielding layer were created.

Finally, the authors would like to thank Prof. N. P. Benkova for useful discussions, and also the Laboratory assistants of the ionospheric station for helping during the data reduction.

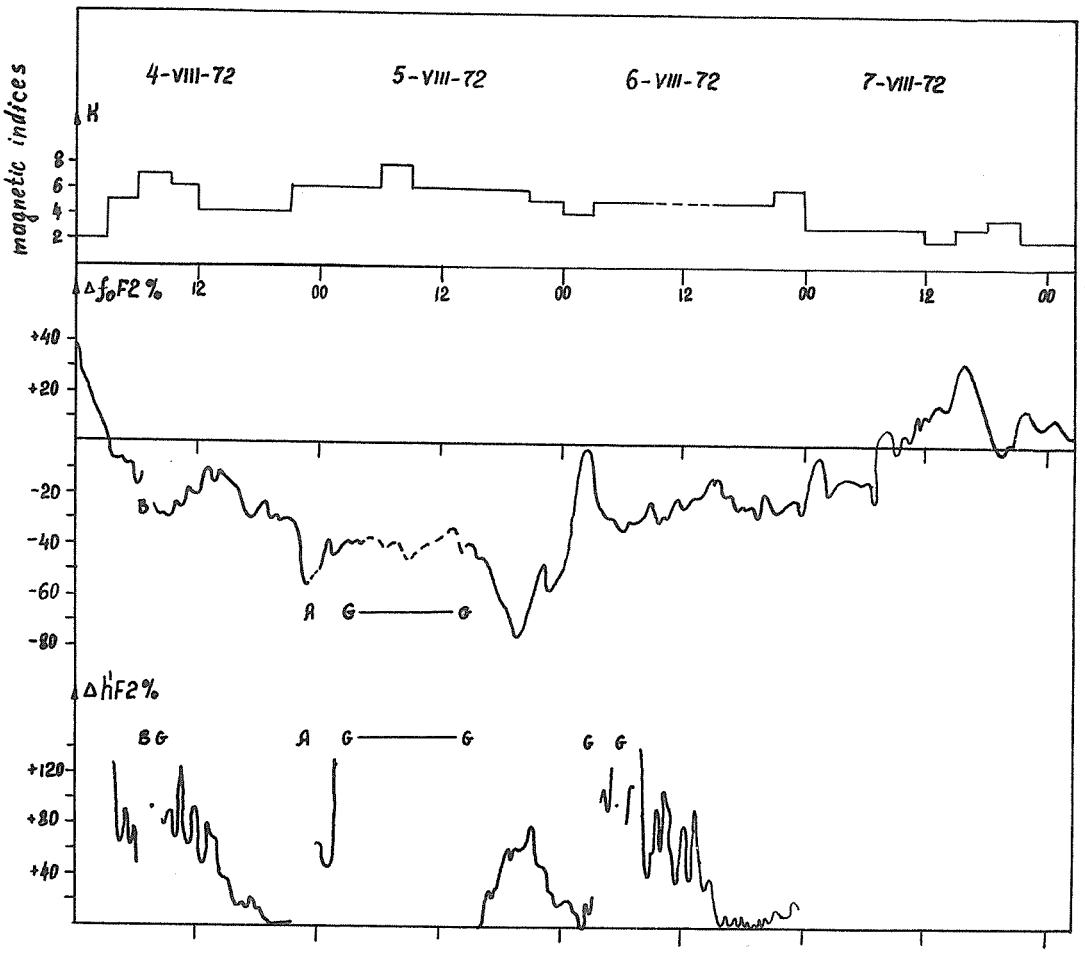

Fig. 3. Magnetic K indices, foF2, and h'F2 variations for the period 4-7 August 1972.

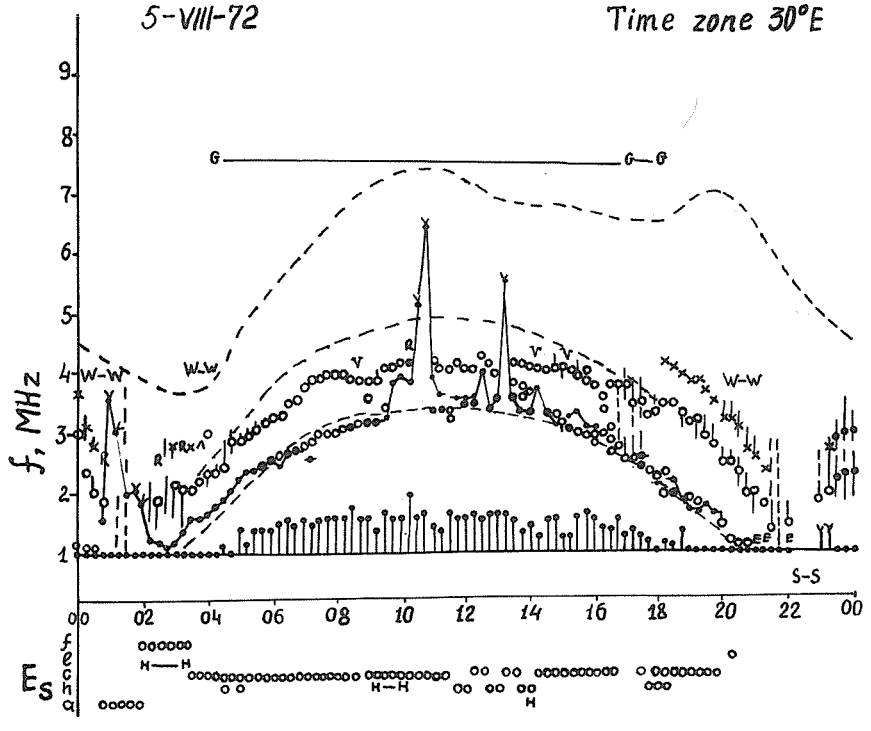

Fig. 4. Diurnal variations of the critical frequencies foE, foF1, and foF2 for 5 August 1972. Dotted line shows median values of the critical frequencies for August.

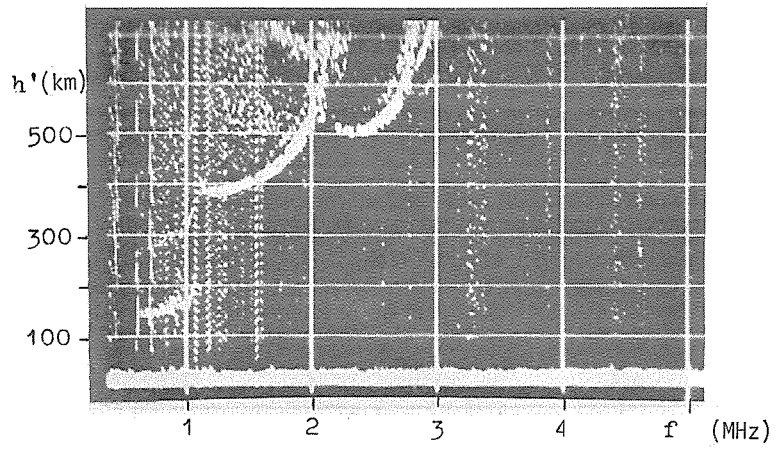

Fig. 5. Ionogram recorded on 5 August 1972 at 0030 30° EMT.

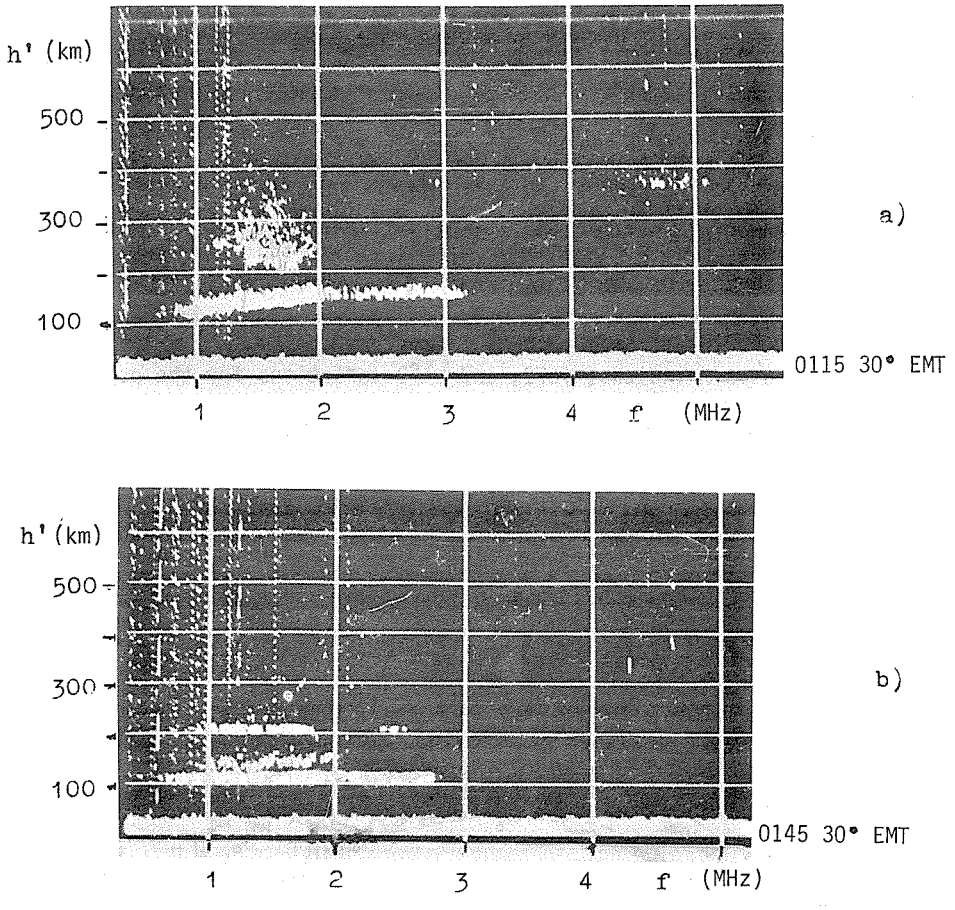

Fig. 6. Ionograms recorded on 5 August 1972 at:
a.) 0115 30° EMT
b.) 0145 30° EMT

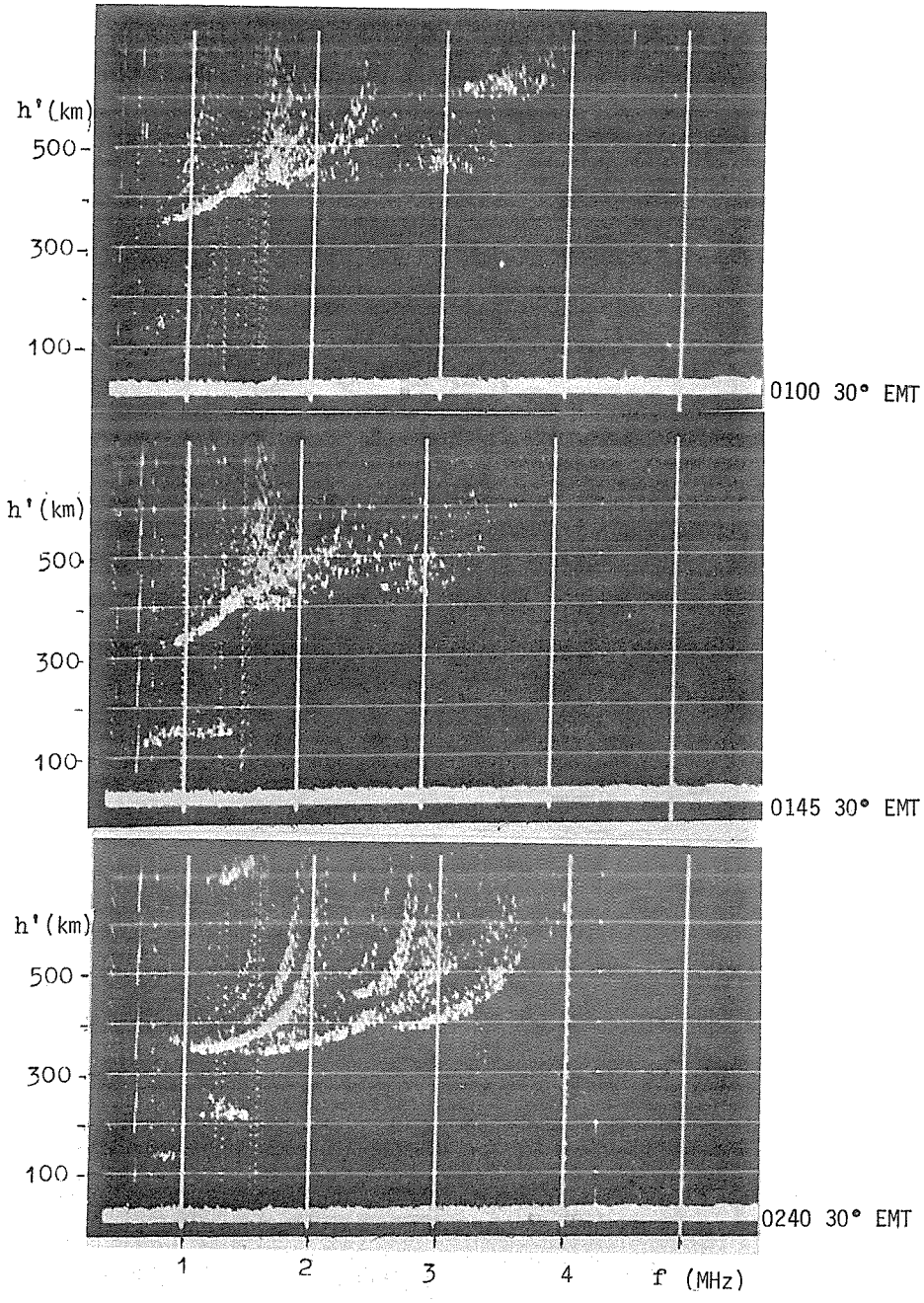

Fig. 7. Ionograms recorded on 6 August 1972 at 0100, 0145 and 0240 30° EMT.

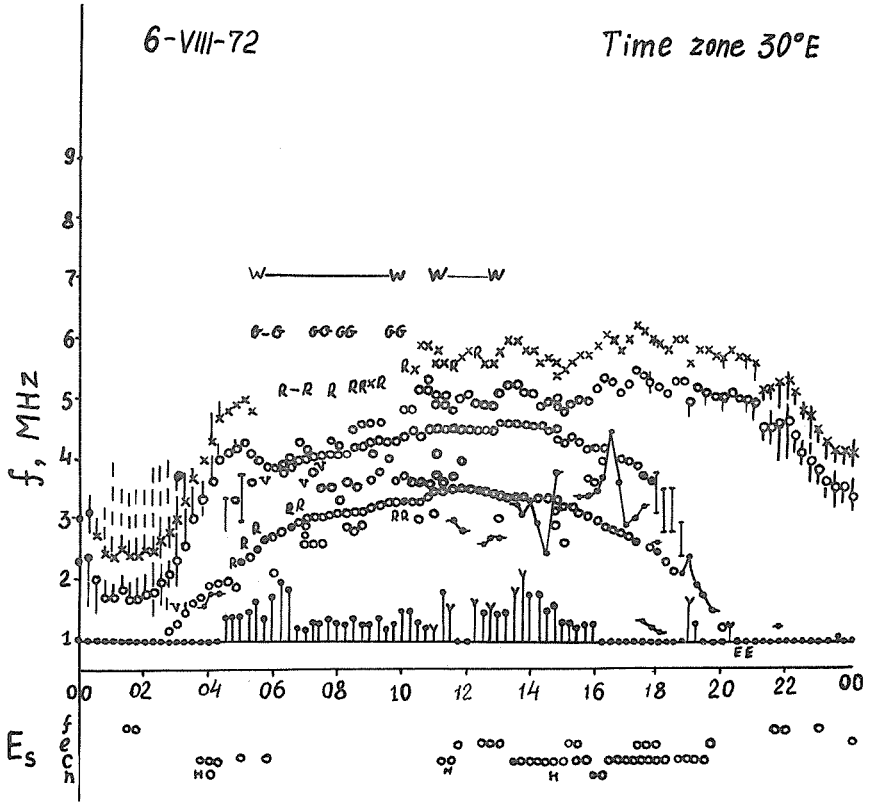

Fig. 8. Diurnal variations of the critical frequencies foE, foF1 and foF2 for 6 August 1972.

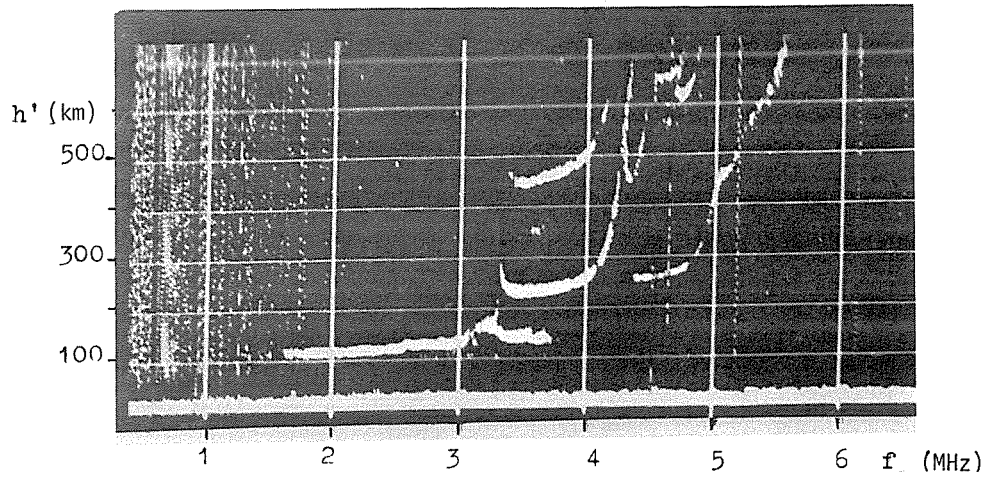

Fig. 9. Ionogram recorded on 6 August 1972 at 1502 30° EMT.

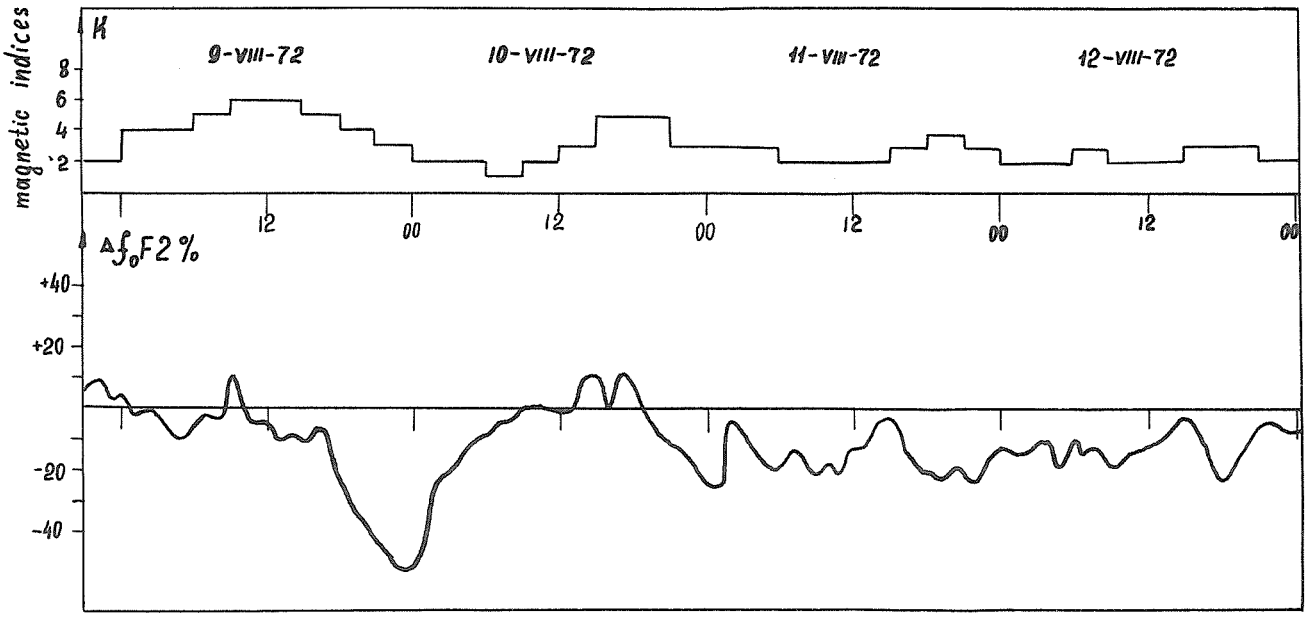

Fig. 10. Magnetic K indices and foF2 variations for the period 9-12 August 1972.

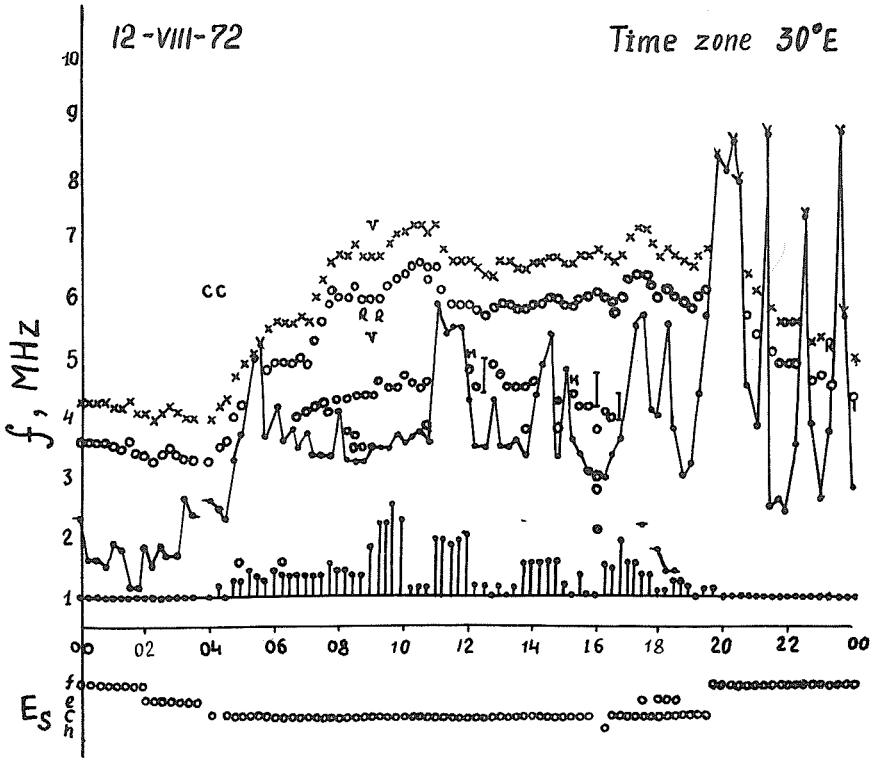

Fig. 11. Diurnal variations of the critical frequencies foE, foF1 and foF2 for 12 August 1972.

REFERENCES

DVORYASHIN, A. S. and I. N. ODINTSOVA	1960	Izvestia of Crimea, Astrophysical Observatory, 23, 113-127
DVORYASHIN, A. S., L. S. LEVITSKY, and A. K. PANKRATOV	1962	Journal of Astronomy, 39, No. 3, 428-438.
GIVISHVILI, G. V., K. N. VASILIEV and V. T. SERIODKIN	1972	Geomagnetism and Aeronomy, 12, No. 1, 139-142.
HARDWICK, B.	1953	J. Atm. Terr. Phys., 3, No. 6, 347.
LINCOLN, J. V. and H. I. LEIGHTON, ed.	1972	Preliminary Compilation of Data for Retrospective World Interval July 26 - August 14, 1972, World Data Center A, Report UAG-21.
MEDNIKOVA, N. V.	1957	The physics of solar-corpuscular fluxes and their effects on the atmosphere of Earth., Academy of Sci., USSR.
ODINTSOVA, I. N.	1961	Izvestia of Crimea, Astrophysical Observatory, 26, 161-170.
ODINTSOVA, I. N.	1965	Dissertation, Moscow State University

Report on the Geomagnetic and Ionospheric Changes Recorded at Ahmedabad during the August 1972 Events

by

S. S. Degaonkar, T. S. G. Sastry and R. G. Rastogi
Physical Research Laboratory
Ahmedabad-9, India

The great solar flare activity which began 2 August 1972 produced a multitude of exceptionally large geophysical events. We describe here the events recorded by the total field magnetometer and the vertical incidence ionospheric recorder at Ahmedabad.

Table 1 gives the time flow of events as recorded on our magnetograms. We missed the data for a few hours from 1730 UT on 3 August to 0500 UT on 4 August 1972 and hence the sudden commencement which started in the early hours on 4 August was not recorded. However, another sudden commencement storm which started at 2047 UT on August 4 has been fully recorded. This storm is unique in many ways. Though the range was not large, very complicated rapidly fluctuating beat-like changes in the magnetic field were recorded. This might have been due to two interfering hydro-magnetic waves of nearly the same frequency. This rapidly fluctuating pattern began at 2300 UT on 4 August and lasted till about 0800 UT on 5 August. The period of oscillations varied between 5 and 10 minutes with amplitude of 70 to 80 γ. Figure 1 shows the magnetograms from 2 to 9 August 1972. As the rapid fluctuations in the magnetic field could not be reproduced in Figure 1, these are shown separately in Figure 2 where every half minute reading has been plotted. There are two sudden depressions centered around 0540 and 0730 UT which may be connected with the rapid enhancement of ring currents in the magnetosphere.

The second storm which began at 2350 UT on 8 August had an initial rise of 32 γ and a total range of 184 γ. This storm lasted for only about 20 hours. The record of this storm is quite smooth and can be seen in Figure 1.

The ionograms concerning the flare period on 2 and 4 August 1972 are shown in Figures 3 and 4. The shortwave fade-outs, partial and/or full, can be seen on the ionograms at 0345 and 0500 UT on 2 August and at 0700 and 0800 UT on 4 August. These are no doubt connected with the solar flares which took place at 0316 UT on 2 August and at 0621 UT on 4 August. There was a similar shortwave fade-out observed during the solar flare at 0906 UT on the same day. It is interesting to note that the riometer did not show an SCNA at 0621 UT on 4 August because of the presence of intense Type IV solar radio noise emission at that time. However the ionogram does show the fade-out due to that solar flare.

Acknowledgement:

This work was supported by the Department of Space, Government of India. Our thanks are due to Mr. M. A. Lateef, Mr. R. Rajagopalan and Miss J. Shah for their help in the reduction of the data.

Table 1

Magnetic Storm Events in Early August 1972 Recorded at Ahmedabad

Date Aug. 1972	Sudden Commencement Time in UT	Initial rise in B from pre-storm level	Range in B in gammas	Remarks
4	2047	80 γ	-	
	2115	144 γ	224 γ	Two sudden commencements or impulses separated by 30 min. Range cannot be estimated accurately as the trace is marked by rapid fluctuations with periods between 6 and 10 minutes, and having amplitudes between 70 and 80 γ. These rapid fluctuations appear from 2300 UT on 4 August to about 0800 UT on 5 August.
5				
8	2350	32 γ	184 γ	Duration of this storm was about 20 hours.

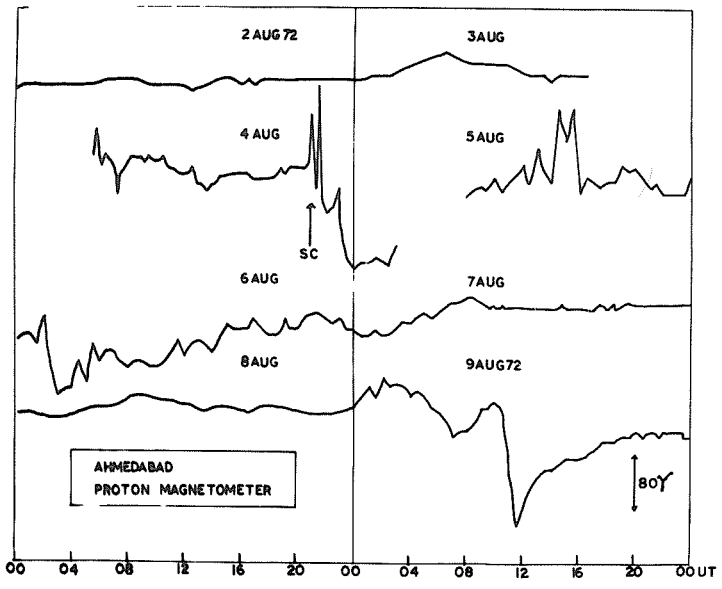

Fig. 1. Proton Magnetometer total field records from 2 August 1972 to 9 August 1972 plotted against UT.

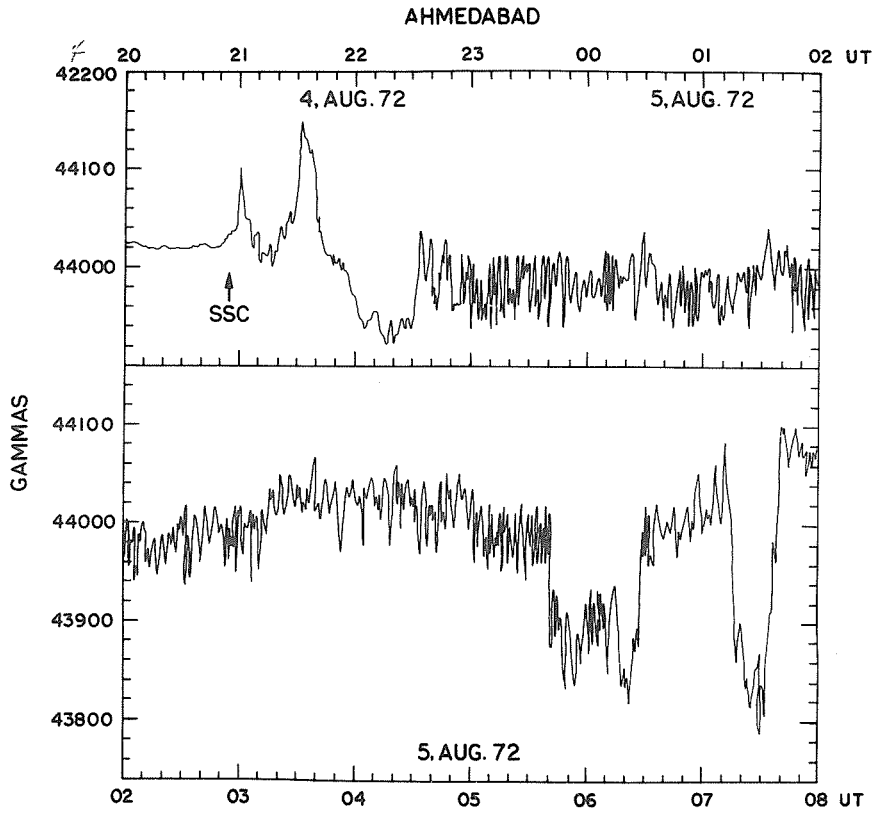

Fig. 2. Proton Magnetometer total field record from 2000 UT on 4 August to 0800 UT on 5 August 1972 showing in detail the storm commencing at 2047 UT on 4 August 1972 and the fluctuations in the magnetic field.

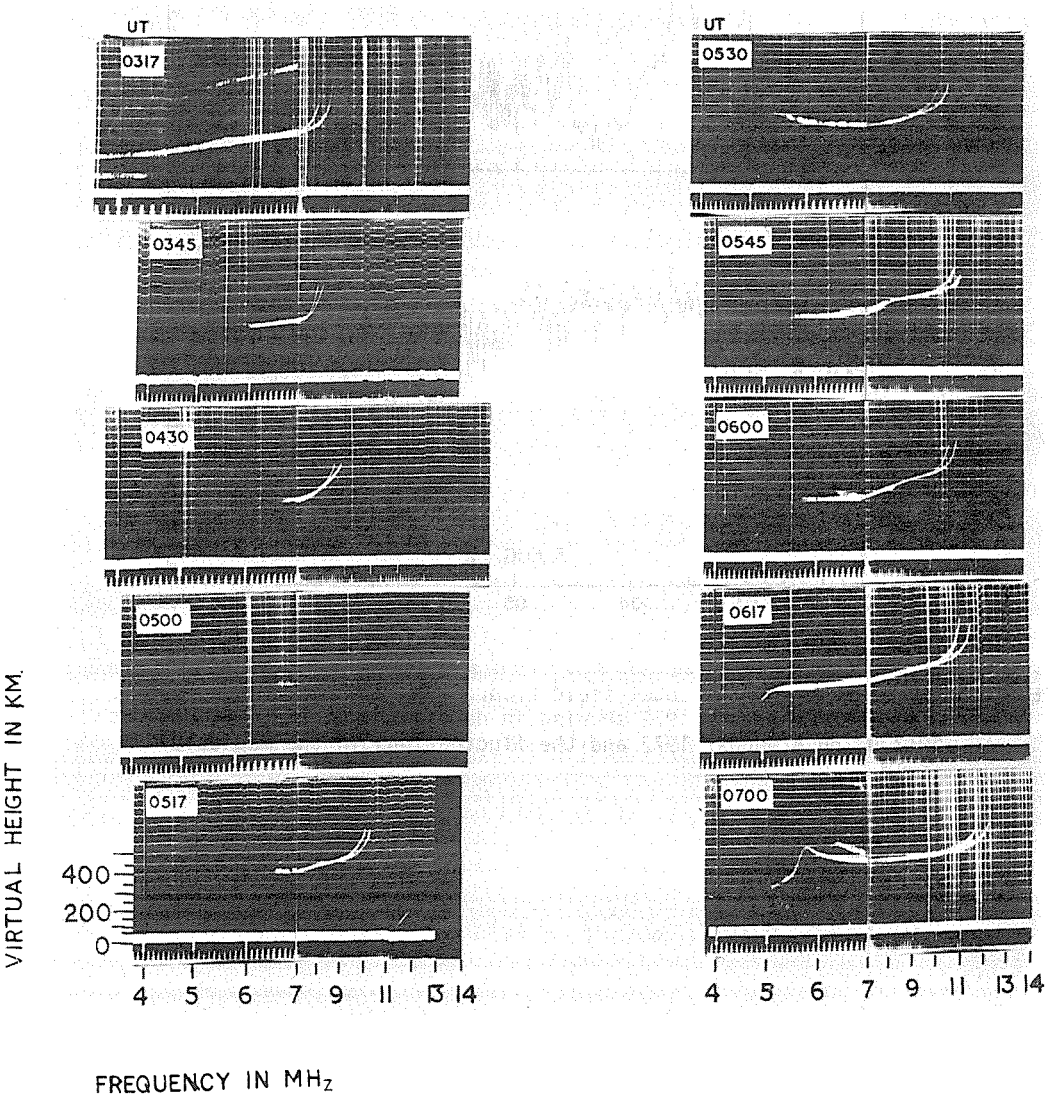

Fig. 3. Ionograms showing the shortwave fade-outs on 2 August 1972.

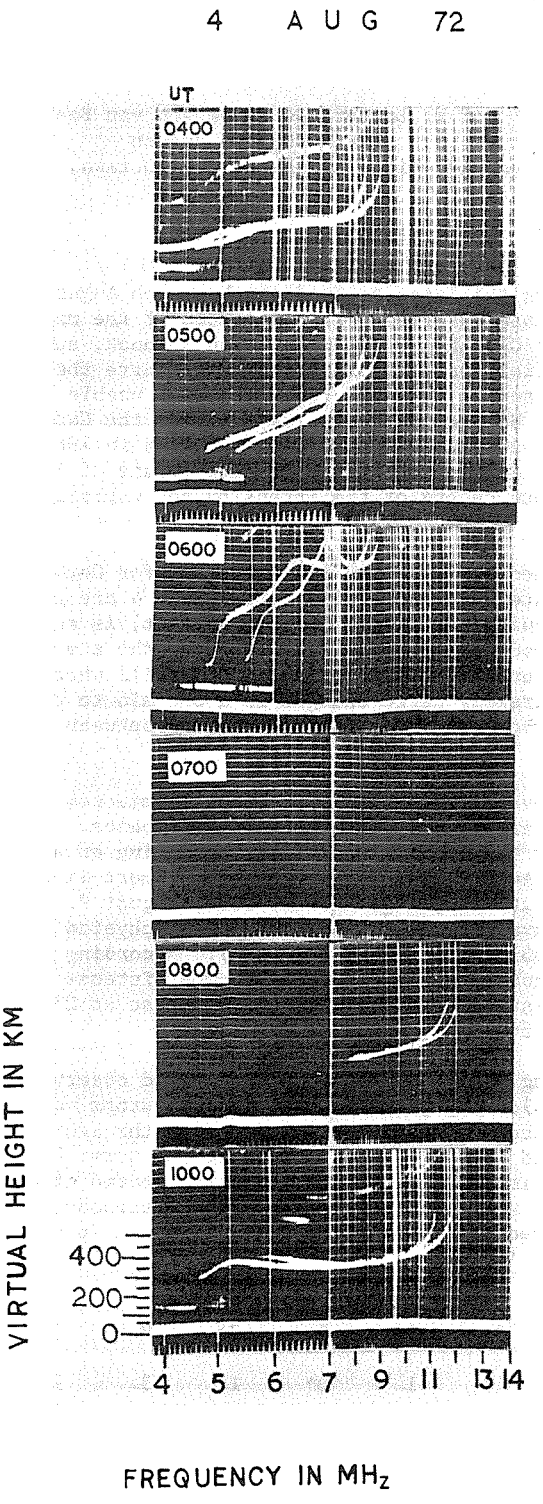

Fig. 4. Ionograms showing the complete short-wave fade-out at 0700 UT on 4 August 1972.

"The Development of Current Vortices in the Polar Cap Preceding the Large Magnetic Storms of August 4-5 and August 9, 1972"

by

E.I. Loomer and G. Jansen van Beek
Earth Physics Branch
Energy, Mines and Resources, Ottawa, Canada

Introduction

Magnetic activity following the large solar disturbance on August 2, 1972, was the largest ever recorded at Canadian magnetic observatories. The amplitude of the magnetic disturbance August 4-5 exceeded 5000 gammas in H(X) at Churchill, Baker Lake and Meanook, and 6000 gammas in Y at Churchill. Maximum rate of change of the field was measured at Meanook where the H component changed by 1800 gammas in a one-minute period. The standard analogue recorders were unable to provide legible records for a disturbance of this magnitude. However at this time seven of the Canadian observatories had been equipped with the new automatic systems designed and developed in 1969 by the laboratory of the Division of Geomagnetism. The automatic digital systems recording values of H, D, Z, F once a minute on digital magnetic tape provided a complete record of the intensity and variations of the magnetic field at all seven stations.

Plots of the magnetic elements drawn from minute values for Cambridge Bay, Baker Lake, Churchill, Meanook and Victoria for the interval 2000 - 2350 U.T. August 4 are given in Figure 1. A plot of the satellite ATS-5 Z component, equivalent to the north component, is shown also for comparison. The midnight level of August 3, a moderately quiet day preceding the storm, is drawn on the plot for each observatory. The greatest disturbance was recorded at Churchill where the range in Y was 6268 gammas between 2136 and 2247 U.T. Extremely large changes in a one-minute period are evident at all locations, and in particular at Meanook, where H changes by 1800 gammas between 2241 and 2242. The corresponding change in D was 1540 gammas.

The sequence of magnetic events began with two sudden commencements at 0119 and 0220 U.T. August 4, followed by 7 or 8 hours of moderate to large magnetic disturbance. A third sudden commencement in the local afternoon of the same day (2055 U.T.) marked the beginning of a period of very intense magnetic disturbance which lasted until August 7. Another large but short-lived storm was recorded on August 9, following sudden commencements at 2354, August 8 and 0036, August 9. August 8 was an international quiet day. The solar flares which gave rise to the outstanding geophysical events of August 1972 originated within the single spot group #331 (McMath region #11976). According to NOAA Technical Memorandum [1972] ERL SEL-22, the ssc at 2055 August 4 which preceded the most intense period of disturbance occurred 49 hours after the second major flare, 1958 U.T. August 2; the ssc at 2354 August 8 occurred about 33 hours after the fourth major flare, 1500 U.T., August 4.

One of the most interesting features of this storm period observed at Canadian stations was the very large magnetic effect in the polar cap preceding the intense storm which began at 2055 August 4. Large magnetic effects were also evident in the polar cap prior to the storm of August 9. Events in the polar cap have been closely identified with the growth phase of substorms [Iijima and Nagata 1972]. This report will concentrate on the intervals prior to the large storms of August 4-5, and August 9, when the high latitude Canadian stations were in the early and late afternoon sectors, respectively. Stations used for this analysis are listed in Table I. Following are the Kp values for these periods:

Aug.	4	6−	8+	7	4	5+	4	7−	9
	5	8+	8+	7	7+	8−	9−	7+	6−
	8	1+	1−	0+	1−	3−	2+	2+	4+
	9	5−	7−	7−	8+	4	4+	3+	3+

The largest negative value of D_{st} during the August 4-5 storm was -224γ which occurred at 2-3 U.T. August 5; the largest value for the August 9 storm was -222γ, at 11-12 U.T.

The interplanetary magnetic field (IMF) was disturbed August 3, and the predominant direction of the field was away from the sun in the interval 0600 August 3 to 0400 August 4. On August 8-9, the IMF was described as quiet. The predominant direction was towards the sun. The count of cosmic ray protons of

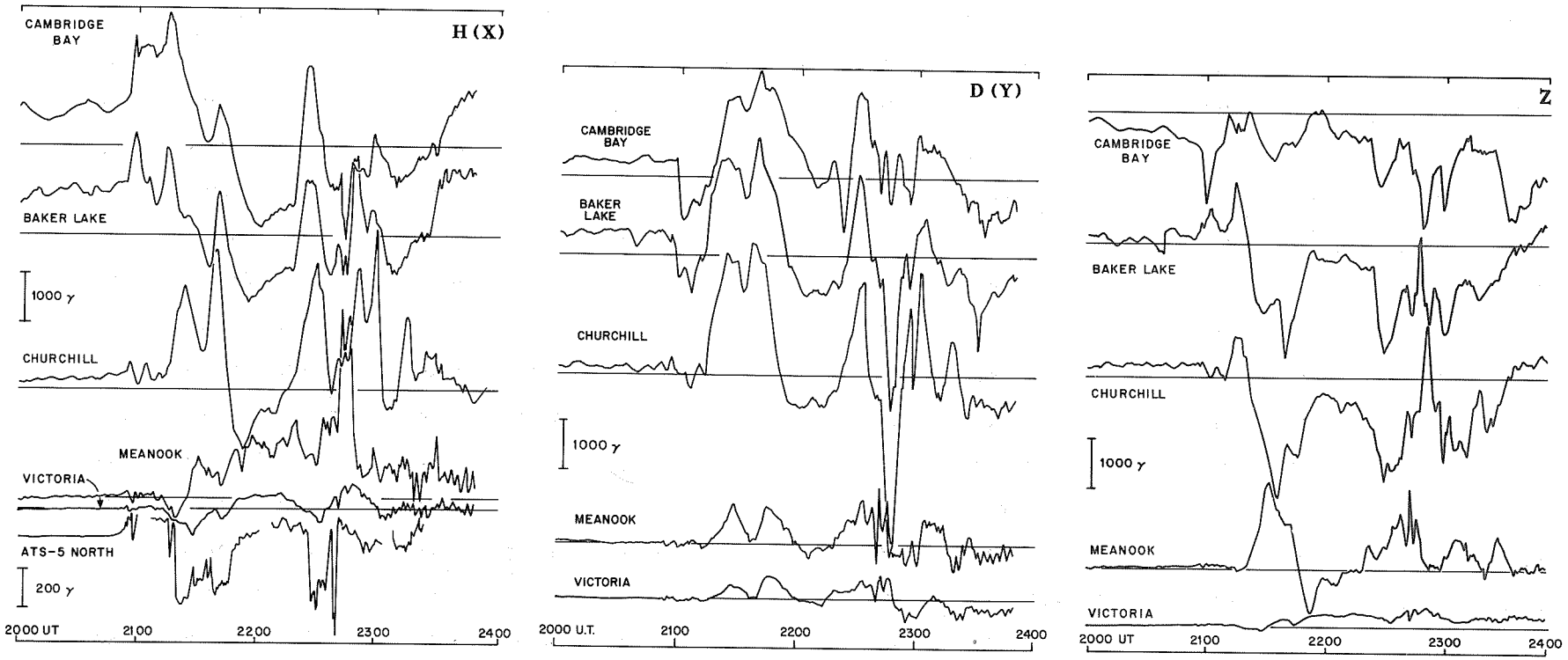

Fig. 1. Plots of the magnetic elements drawn from minute values for Cambridge Bay, Baker Lake, Churchill, Meanook and Victoria for the interval 2000-2350 UT August 4 are shown along with ATS-5 Z-component. The midnight level of August 3 is drawn for each observatory for comparison.

TABLE I

		Geomag. Coords. Lat.N	Long.E	Ψ_E	U.T. of local midnight (hrs)			Geomag. Coords. Lat.N	Long.E	Ψ_E	U.T. of local midnight (hrs)
TH	Thule	89.2	357.4	2.4	04.61	MN	Minsk	51.5	112.0	-18.9	22.14
AT	Alert	85.7	168.7	197.7	04.17	FR	Fredericksburg	49.8	349.8	2.6	05.16
RB	Resolute Bay	83.1	287.7	47.1	06.33	BD	Boulder	49.1	316.3	10.6	07.02
MLB	Mould Bay	79.1	255.4	55.3	07.96	FU	Furstenfeldbruck	48.8	93.6	-17.7	23.25
CB	Cambridge Bay	76.7	294.0	31.3	07.00	SV	Sverdlovsk	48.3	140.8	-13.5	19.93
BL	Baker Lake	73.9	314.8	19.4	06.40	TL	Toledo	43.9	74.9	-14.8	00.27
RY	Leirvogur	70.3	71.6	333.8	01.45	OD	Odessa	43.6	111.3	-16.0	21.94
CHR	Fort Churchill	68.8	322.5	13.8	06.27	DS	Dallas	43.1	327.6	7.4	06.45
PB	Point Barrow	68.4	240.7	33.5	10.45	AE	Almeria	40.7	75.4	-14.2	00.16
GW	Great Whale River	66.8	347.2	4.5	05.18	TU	Tucson	40.6	312.1	10.3	07.39
CO	College	64.6	256.1	27.6	09.86	SF	San Fernando	38.6	84.1	-14.5	23.59
SO	Sodankyla	63.7	120.3	-27.0	22.22	TF	Tbilisi	36.6	122.2	-13.4	21.02
ME	Meanook	61.9	300.7	17.5	07.55	TAS	Tashkent	32.2	144.1	-9.1	19.36
SI	Sitka	60.0	275.0	21.8	09.02	SJ	San Juan	29.8	3.1	-0.7	4.41
NU	Nurmijarvi	57.8	112.9	336.4	22.36	KA	Kakioka	25.8	205.9	6.3	14.65
JO	St. John's	58.7	21.4	353.7	03.51	HO	Honolulu	21.1	266.4	12.6	10.53
OT	Ottawa	57.0	351.5	2.4	05.04	GU	Guam	3.8	212.9	6.5	14.34
LE	Leningrad	56.2	117.6	-21.0	21.95	TAN	Tangerang	-17.8	175.4	-0.9	16.89
NE	Newport	55.0	299.4	15.4	07.83	PM	Port Moresby	-18.8	217.9	7.3	14.19
VI	Victoria	54.3	292.7	16.4	08.23	HR	Hermanus	-33.2	80.4	-14.0	22.72
						TO	Toolangi	-46.8	221.0	9.6	14.30

Note that ΨE, the angle between the geographic and geomagnetic meridians at a station, is measured eastward from the geographic meridian

energy greater than 13.9 mev exceeded 10^4 particles/sec at the satellite Pioneer IX on August 3, 4, and 5. At 2000 U.T. August 4 the count was greater than 16380, compared with a count of 541 at 2300 U.T. August 8 [Lincoln et al., 1972].

Analysis of Data

Perturbations for August 4, 2000-2040 U.T. were measured from the quiet midnight level of August 3; those for August 8-9 were measured from the quiet midnight level of August 8. Perturbations were corrected for the quiet-day variation and were expressed in the geomagnetic coordinate system X', Y', Z. Following the method previously described by Loomer and Jansen van Beek [1971], equivalent ionospheric line currents calculated from the three magnetic perturbation vectors $\Delta X'$, $\Delta Y'$, ΔZ for a height of 112 km were drawn on a polar azimuthal equidistant projection for the period 2000-2040 August 4; 2326, August 8; and 0013, August 9 (Figure 2). Equivalent current vectors are used to provide a concise visual representation of the magnetic disturbance, and are not intended to imply that such disturbance is a result of two-dimensional current flow in the ionosphere at a height of 112 km.

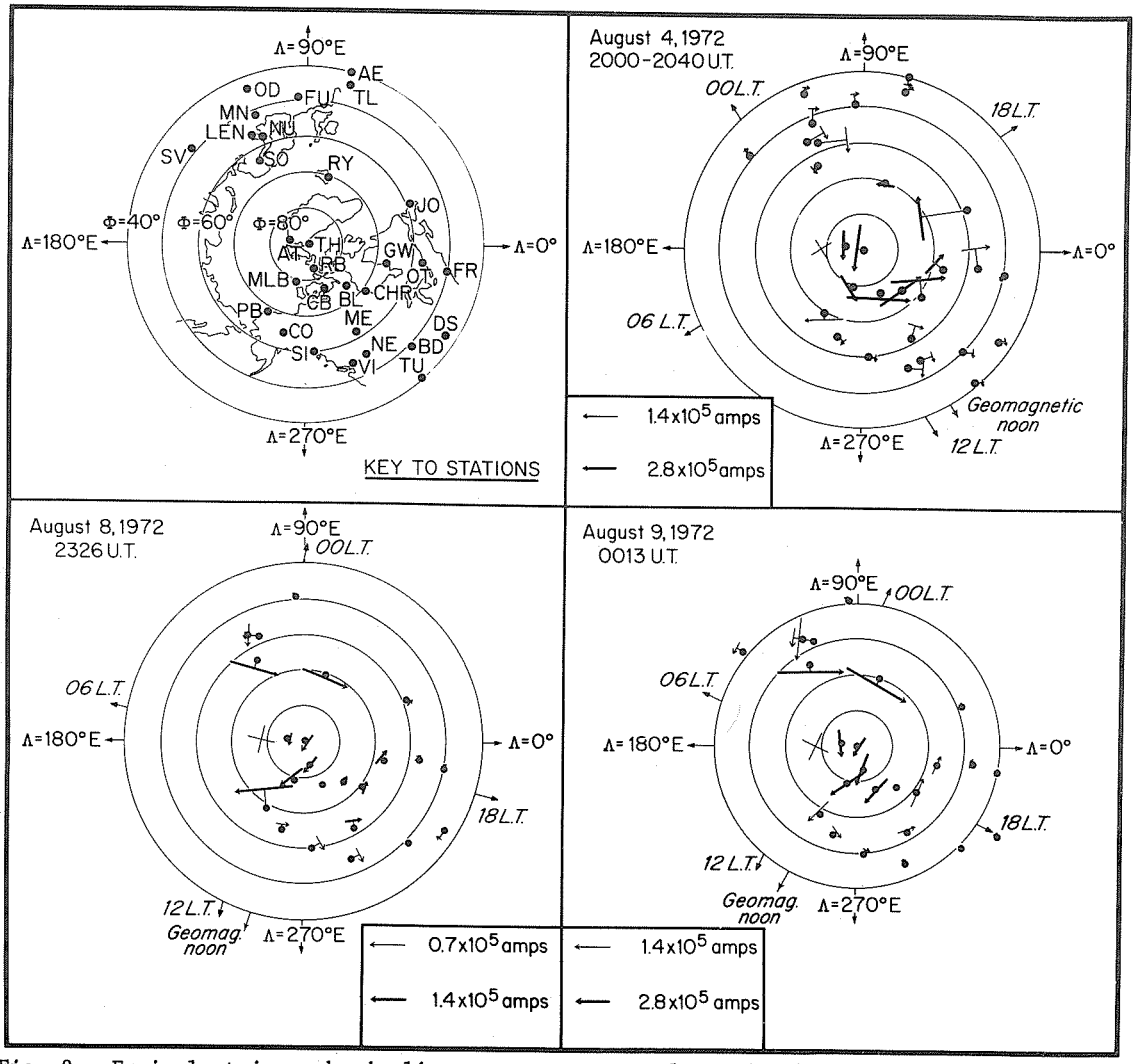

Fig. 2. Equivalent ionospheric line currents on a polar azimuthal equidistant projection for the period 2000-2040 UT August 4, 2326 UT August 8, and 0013 UT August 9 are shown.

In the interval 2000-2040 U.T, August 4, a strong counter-clockwise current circulation exists in the afternoon sector at high latitudes with current vectors across the polar cap directed towards 10 LT. The circulation is contained between the 12 and 22 LT meridians. The center is close to Resolute Bay (geomag. lat. 83°). Eastward current flow in the afternoon sector is along the 75° geomagnetic latitude parallel. Intensity of the current vectors is 3 to 4 x 10^5 amperes. As records were not available for high-latitude stations in the midnight sector, it is not possible to decide if a second current cell existed at this time. Current vectors at low latitude stations located between geomagnetic latitudes +36°, -36° were uniformly westward in all sectors and closely equal in magnitude. The poleward direction of current vectors at middle-latitude stations in the late evening sector and their equatorward direction in the noon sector may indicate the existence of field-aligned currents at these times. However, any interpretation of equivalent current flow at middle latitudes (Φ = 35° to 60° approximately) is necessarily uncertain owing to the lack of data in the geomagnetic longitude sectors 0° to 75° and 140° to 240°.

The main current circulation at 2326 U.T. August 8 and 0013 U.T. August 9 is undoubtedly clockwise and centered between the dawn and midnight meridians. The current vectors are most intense at RY and SO, near 70° geomagnetic latitude in the midnight sector (5×10^5 amperes at 0013 U.T.). As in the previous example the current vectors across the polar cap are directed approximately sunward, and there is the suggestion of field-aligned current flow at middle latitudes in the midnight and noon sectors. The eastward directed currents at auroral zone stations in the afternoon sector at 2326 and 0013 appear as return currents from the much stronger current flow in the polar cap, although it is possible that a second current cell is present in the late afternoon sector, centred near Baker Lake ($\Phi = 74°$). The current pattern at 0013 U.T. is similar to that at 2326 U.T., but with a three-fold increase in intensity. However, between 2253 U.T. (not shown) and 2326 U.T. significant changes were observed in the polar cap, where the current vectors at AT, TH, MLB, PB and RB all rotated to sunward. This rotation was particularly pronounced at MLB and PB where the current vectors almost reversed direction between 2253 and 2326.

Discussion and Conclusions

The unusually large magnetic effects observed at high latitude Canadian stations in the early afternoon sector which followed the storm beginning 2055 U.T. August 4 apparently result from the occurrence of the ssc at a time when local and geomagnetic noon approximately coincide, during a period when the predominant direction of the interplanetary magnetic field was away from the sun. Mayaud [1967] has pointed out that it is at the time when the sun crosses the meridians close to the invariant pole, around 19 U.T., that the lines of force of the field may be expected to offer a particularly weak resistance to the penetration of the solar wind. The time of occurrence may also explain the abnormally large amplitude of the ssc itself, which was approximately 600 gammas at Cambridge Bay and Resolute Bay.

A sunward orientation of current across the pole and the formation of an intense current vortex in the polar cap preceded both the storms of August 4-5 and August 9. Hall current flow along the noon meridian would result from a dawn to dusk electric field across the polar cap. Iijima and Nagata [1972] have concluded that a development of magnetospheric convection with a dawn to dusk electric field is an important characteristic of the growth phase of substorms, which they define as a phase lasting 1 or 2 hours prior to the well-defined breakup and the subsequent expansion phase. They identify two essential signatures for the growth phase: "a gradual development of the polar vortex type current without remarkable current enhancement in the auroral belt, and the asymmetric growth of the low-latitude field-depression in the evening - midnight-early morning sector". Asymmetric growth of the low-latitude field depression was not evident in the data used for the present study. However this study strongly supports their finding that the growth phase of substorms is characterized by large current vortices in the polar cap. In the interval 2000-2040, August 4, when the predominant direction of the interplanetary magnetic field was away from the sun, a counter-clockwise circulation developed in the p.m. sector, with current directed sunward across the pole and eastward at approximately 75° dp latitude. Preceding the storm of August 9, when the IMF was directed towards the sun, a clockwise current vortex developed in the polar cap, with current towards the sun along the noon meridian, and westward along the auroral oval in the midnight sector. A similar correspondence between the sense of the polar cap current circulation and the direction of the IMF has been noted by Friis-Christensen [1971] and Svaalgard [1972].

In conclusion, it would appear that conditions in the polar cap, suitably monitored, may provide some advance indication of the occurrence of polar substorm activity in the midnight sector.

REFERENCES

FRIIS-CHRISTENSEN, E.	1971	The Influence of the Direction of the Interplanetary Magnetic Field on the Morphology of the Geomagnetic Variations at High Magnetic Latitude, Geophysical Papers R-27, Dan. Meteorol. Inst., Copenhagen.
IIJIMA, TAKESI and TAKESI NAGATA	1972	Signatures for Substorm Development of the Growth Phase and Expansion Phase, Planet. Space Sci. 20, 1095-kk12.
LINCOLN, J. V. and H. I. LEIGHTON	1972	Report UAG-21 Preliminary Compilation of Data for Retrospective World Interval July 26-August 14, 1972. World Data Center A for Solar-Terrestrial Physics, Nov. 1972.
LOOMER, E.I. and G. JANSEN VAN BEEK	1971	Magnetic substorms, December 5, 1968, Pub. Earth Phys. Br. 41, no. 10.
MAYAUD, P.N.	1967	Atlas of K indices, pp. 81-87.
SVAALGARD, L.	1972	Polar Cap Variations and Their Relationship with the Interplanetary Magnetic Sector Structure, SU-IPR Report No. 486, Institute for Plasma Research, Stanford University, Stanford, California.
	1972	NOAA Technical Memorandum ERL SEL-22, August 1972, Solar Activity and Related Geophysical Effects, Dec., 1972.

Normal Magnetic Field, Micropulsation and Riometer Observations at Auroral Station Murmansk

by

B. E. Brunelli, G. A. Loginov, G. A. Petrova and L. T. Afanasyeva
Polar Geophysical Institute, Academy of Sciences of USSR
Apatity, Murmansk Region, USSR

The following observations made during the August 4-9, 1972 event were used in the analysis: (1) normal-run magnetograms obtained at Loparskaya, Lovozero and Kem, the scale values of which were equal to 8, 10 and 3 γ /mm, respectively; (2) records of rapid-run magnetometers at Lovozero with chart speeds of 90, 360, 900 and 1000 mm/hour; (3) riometer records at 32 MHz with antenna directed toward the Pole Star and occasionally at 40 MHz with antenna directed toward the zenith.

The period analyzed contained three distinct magnetic storms (see Figures 1-2). An intense chromospheric burst followed by PCA occurred during the first storm. The PCA event continued for four days. Its intensity gradually decreased; the maximum value of the 32 MHz absorption varied from day to day in the following manner: it exceeded 20 dB on the first day (August 4) and was equal to 7, 5 and 3 dB on the second, third and fourth days, respectively. The magnetic storm was characterized by unusually high pulsation activity associated with the PCA event. Another PCA event and a third magnetic storm were associated with a second chromospheric burst which occurred before the end of the second magnetic storm. A detailed description of the phenomena is given below.

The first magnetic storm began at 0118 UT on August 4 with two sudden impulses (Figure 3) which were accompanied by micropulsations with periods increasing from 1.7 to 2.5 sec after the first si and from 1.0 to 1.5 sec after the second. The first si was associated with the small increase of absorption (0.5 dB above the background which was fairly stable during the 12 hours prior to the event). The subsequent absorption increase was more rapid, the maximum observed value was equal to 11 dB. Intense pulsations of Pi-1 type both with normal (7-15 sec) and unusually long periods (80-110 sec) were observed during the storm. The amplitudes of these were equal to 11γ and 200γ, respectively. The first storm continued for approximately 7 hours up to 0800 UT August 4.

An increase of absorption began at 0800 UT. The absorption exceeded the upper limit of measurement at 1115 UT and remained above this limit until 2000 UT, when it began to decrease in accordance with the variation of the ionospheric D-region illumination. The magnetic field was rather quiet during this time, although pulsations of the pc-5 type were observed.

The second storm began at 2052 UT. Simultaneously, absorption increased abruptly to the upper limit of measurement. The storm was preceded by a small two-peak bay accompanied by Pi-2 micropulsations. The magnetic storm was unusual in the behavior of the horizontal component gradually decreasing during the 4 hours preceding and including the onset of the storm at 2052 UT and recovering sharply to the undisturbed level at 2300 UT. The storm continued during the night of August 4-5. A period of positve bays (abnormal for morning hours) was observed after the rather sudden end of the period of negative bays (2200 UT). Another negative bay again with a rather abrupt termination began at about 0320 UT. The absorption decreased to 7 dB during positve bay and exceeded the upper limit of measurement during the negative ones. The abrupt decrease of absorption coincided with the sharp termination of the negative magnetic bay. Intense Pi-1 pulsations were observed during the storm. The Pc-5 pulsations following the end of the bay at 0500 UT had unusually large amplitudes (~500γ) with periods increasing from 260 sec at 0900 UT to 360 sec at 1200 UT.

A new period of magnetic activity started at 1400 UT August 5 with a positve bay which turned abruptly into the negative one with a total range in amplitude of about 1430 γ. A sequence of negative bays followed the first negative bay. Pronounced changes of absorption were connected only with the positive and the first of the negative bays. Then the absorption gradually fell and passed through a minimum between 2300 UT August 5 and 0100 UT August 6. Increasing absorption began at the time of sunrise at Loparskaya. The absorption variations were associated with magnetic disturbances at this time. Intense absorption pulsations were observed during the first half of August 6; large magnetic pulsations continued even longer (up to 1400 UT)

The absorption was relatively constant after 1015 UT until 1748 UT August 6 when there occurred an abrupt spike with a magnitude of 18 dB, that coincided with a steep decrease of the H-component by as much as 620γ. Three more substorms were observed, each of them was accompanied by an increase of absorption superimposed on the smooth rise of the diurnal variation of PCA. However, there is also an increase of absorption in the morning (0600-0700 UT) up to 11 dB while the magnetic field was relatively quiet.

A small absorption bay distorted by increases of the noise intensity at all frequencies probably due to a radio emission burst began at 1508 UT August 7. A smooth absorption rise probably associated with a new chromospheric burst, which was observed at 1449-1500 UT August 7, began at 1600 UT. The new PCA event following this burst lasted two days.

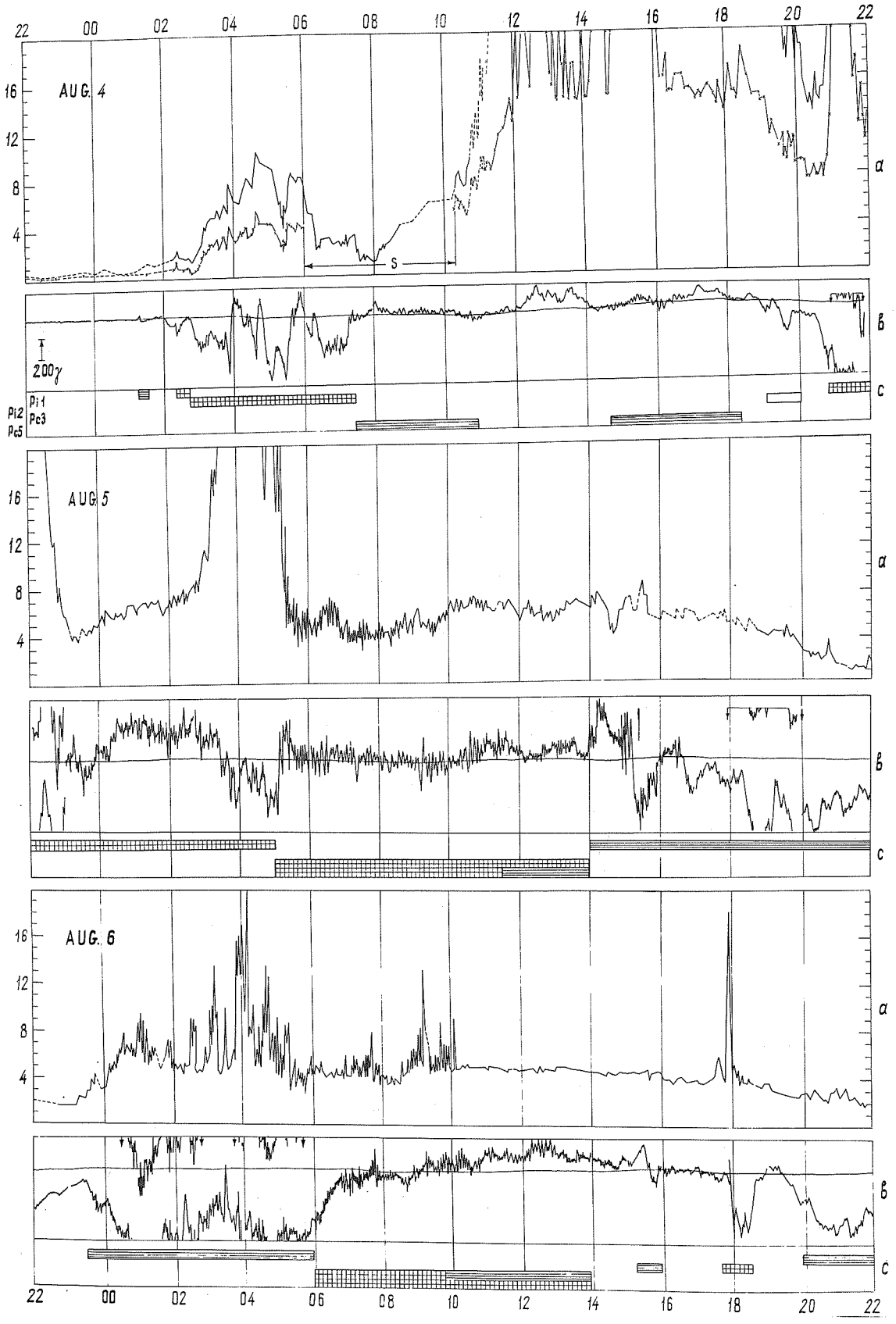

Fig. 1. Development of the event August 4-6, 1972 according to: a) riometer (Loparskaya), b) Magnetogram (storm magnetometer, Loparskaya), c) summary diagram of micropulsation activity (▦ - very intense pulsations, ▤ - moderate intensity pulsations, □ - pulsation traces).

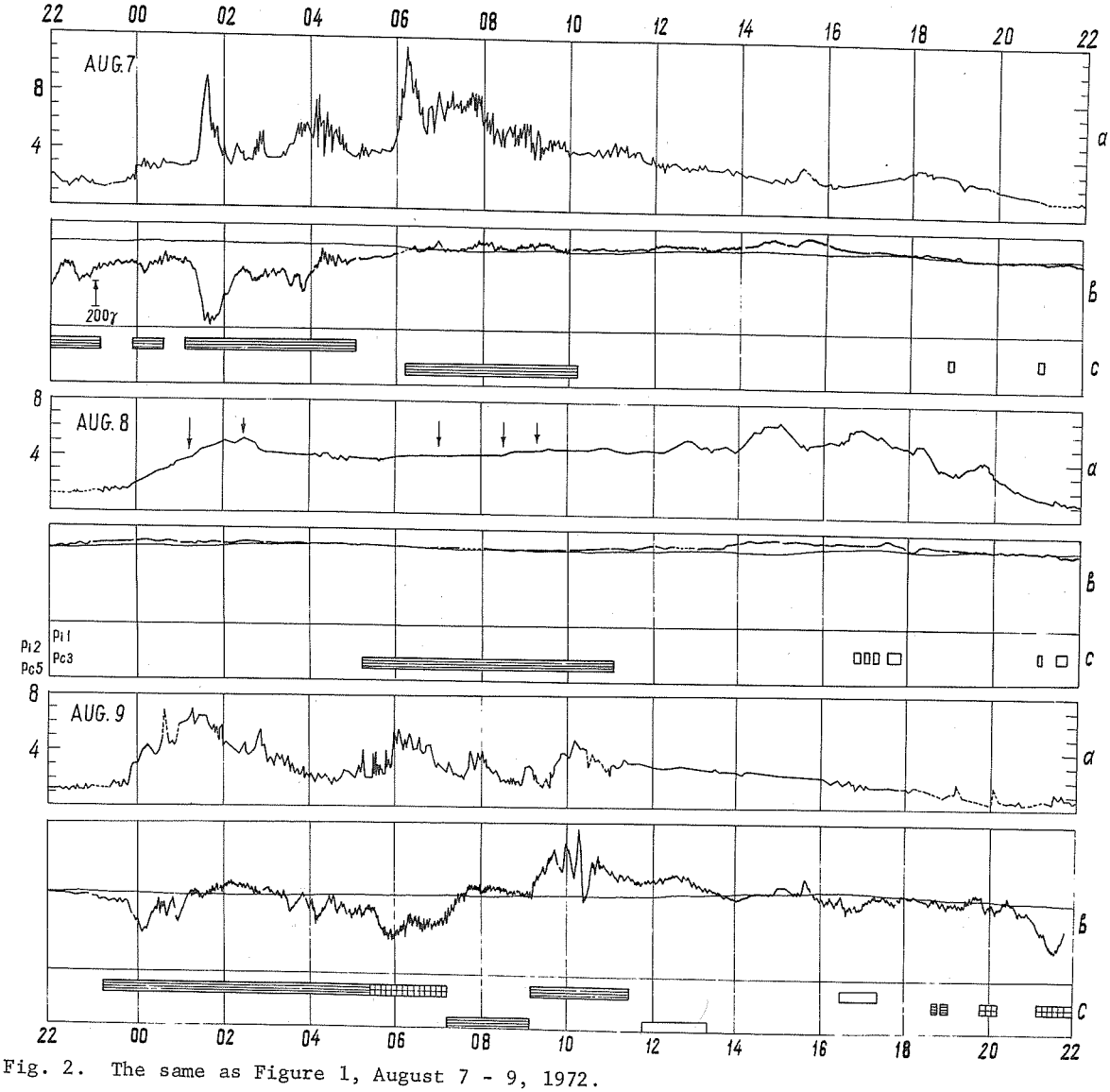

Fig. 2. The same as Figure 1, August 7 - 9, 1972.

Associated with this PCA event a magnetic storm of moderate intensity began at 2350 UT August 8 which consisted of a sequence of negative bays followed by a rather intense positive bay on which unusually large fluctuations were superimposed. This bay also was accompanied by intense irregular pulsations typical of night-time disturbances.

Using the absorption frequency dependence, the electron profiles were derived at the times indicated on August 8 by the arrows in Figure 2. The derived values of the electron concentration lie in the range from 1 x 10^2 to 5 x 10^2 cm^{-3} at 40 km and from 2.5 x 10^3 to 9 x 10^3 cm^{-3} at 60 km.

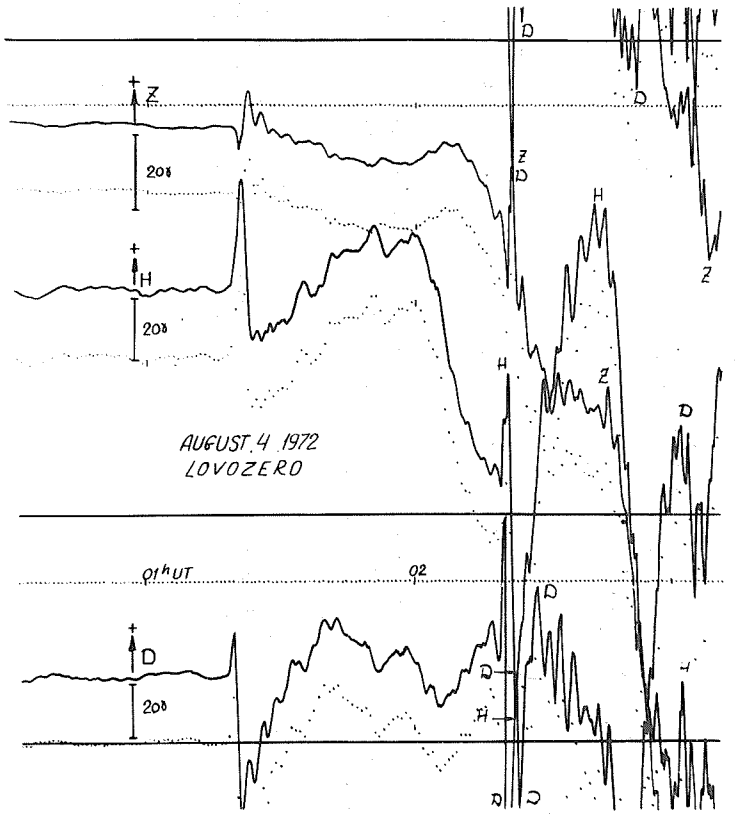

Fig. 3. H, D and Z components of Lovozero during the initial phases of the first storm considered.

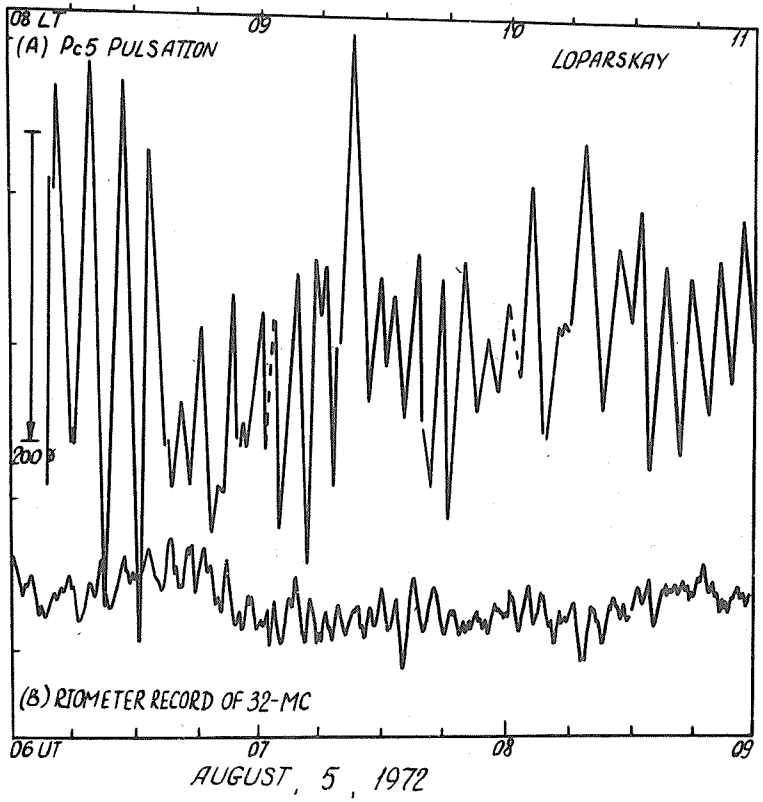

Fig. 4. Pc-5 pulsations of geomagnetic field (top) and absorption (bottom).

Morphological Classification of a Geomagnetically Disturbed Period in the Retrospective World Interval 26 July - 14 August 1972 Carried Out Using the Standard Magnetograms of the Budkov Observatory

by

Jaroslav Halenka
Geophysical Institute, Czechoslovak Academy of Science
Prague, Czechoslovakia

The investigated period consisted of two main disturbed intervals. The first one was permanently and continuously disturbed and it is very atypical from the point of view of the usual division of magnetic storms into recognized phases. Apparently the disturbances were geomagnetic consequences of a sequence of causal events which followed one another in close succession, possibly even overlapping. Because of the complexity of the geomagnetic disturbances and the requirement for further detailed comparison with solar causes, an attempt was made at classifying the disturbed period by individual sections which differ in morphology and level of the geomagnetic field intensity, as reflected on the standard magnetograms of the Budkov Observatory (geographic coordinates N49.06, E14.01, geomagnetic latitude N49.1). Attention was concentrated on the horizontal component of the geomagnetic field.

Duration of the Disturbed Period

The first interval was the most intense and most complex. It began at 0119 UT on 4 August with a very clear ssc on all curves (D, H, Z). The disturbance is continuous until 7 August about 1500 UT, or possibly even 8 August about 0300 UT; in the latter interval the H-curve is only slightly disturbed, just as in some undisturbed intervals, but not as in extremely quiet times with Kp = 0. The end of the disturbance, as usual, is not well defined; however, one may safely say that there are no reasons for assuming the end to have occurred earlier than given.

The second disturbed interval, with a substantially shorter and weaker period of activity, began with an ssc at 1341 UT on 8 August. The activity is continuous until 0300 UT on 10 August (end of the main activity), and after a short calm period in H at about 0400 UT, it carries on with gradual abatement of the activity through the whole of 10, 11 and 12 August until 0500 UT. The end is again very indistinct. The diurnal variation of H comes roughly up to the level of the comparative curve of 29 July only on 14-15 August.

Division of the Disturbed Period

The most active part of the first storm lasted from the first ssc at 0119 UT on 4 August until 0730 UT and it included two ssc's, an exceptional negative bay with an abrupt beginning at 0439 UT and ending at 0600 UT, with a subsequent interval of rapid irregular oscillations. This is followed at about 0730 UT by an interval of oscillations with a smaller amplitude and a temporary decrease in H (the minimum occurred at 1251 UT) with a gradual recovery to the original level, the curve gradually becoming less complex with minor bays, until the beginning of the next storm.

The second storm of this first part of the disturbed period is at first characterized by a strongly abnormal level of H in the interval between the exceptionally large amplitude ssc at 2054 UT on 4 August and about 2300 UT. A period with large rapid oscillations and a gradual decrease of H (minimum around 0300 UT on 5 August) follows, with the subsequent return to normal level being relatively fast. The curve does not change its nature and remains at this level until about 1300 UT. In the interval 1300 - 1800 UT there are a number of negative and positive bays. At the beginning and particularly during the main positive bay at about 1500 UT, these bays are strongly modulated by short-period irregular oscillations which gradually grow weaker after 1600 UT. At 2333 UT there is a sharp onset of a bay-like positive interval with a renewal of the modulating oscillations and a sharp peak at 0154 UT on 6 August. At about 0200 UT the pattern began to change: around the minimum of the negative bay there is an onset of faster oscillations from 0300 UT with a temporary slow decrease of H (minimum at about 0900 UT on 6 August) and a gradual recovery until 1536 UT, when H increased abruptly to a higher level and the curve simplified, terminating in a positive bay (maximum at 1805 UT). The minor oscillations of the curve decayed at about 1600 UT on 7 August so that only slight unrest of the curve could be observed at about 0300 UT on 8 August. From then the curve was smooth until the first ssc in the second part of the disturbed period.

At its beginning the second interval of disturbance has a simple pattern with slight unrest beginning with the ssc at 1341 UT on 8 August and carrying on until the double commencement of the next storm.

The final storm began with a distinct ssc at 2353 UT on 8 August and at 0036 UT on 9 August with subsequent minor modulating oscillations increasing in amplitude over a period of 3 1/2 hours prior to the sharp decrease to the main phase, which began about 0930 UT (minimum of H at 1018 UT). During the recovery, until the end of the main active interval (2200 UT), the modulating oscillations are weak. One then observes minor unrest of the curve from about 0300 UT on 10 August: attenuation between 0300

and 0700 UT, an increase of activity around noon and in the afternoon, and then poorly defined small amplitude bays continuing into the morning of 11 August. The record is slightly disturbed during subsequent days, but the unrest after 0700 UT on 10 August is apparently not directly related to the storm.

Comparison with the Undisturbed Pattern

The H-curve of 29 July is the best compromise for the closest geomagnetically calm day and was adopted as the comparative curve. Sections of the disturbed period were chosen when the H-curve reached at least the normal value of the undisturbed day.

From 0119 UT to 0439 UT on 4 August the H-Curve was above normal, and was strongly abnormal between 0220 (second ssc) and 0336 UT. It was then normal to slightly above normal from 0615 to 1000 UT, exceptionally abnormal from 2054 (ssc interval) to about 2300 UT, then still strongly above normal with two decreases up to about 2330 UT. After 0000 UT on 5 August and around 0100 UT it was twice normal to slightly above normal. Oscillations from the normal to a slightly abnormal level could be observed between 0700 and 1000 UT, then again until 1300 UT individually in the oscillations. Between 1430 and 1600 UT it was strongly above normal in the oscillations, and at about 1745 UT a shorter increase occurred to a slightly abnormal level. Between 0100 and 0200 UT on 6 August an increase occurred to normal level with a strongly abnormal peak at 0154 UT. A further increase to slightly above normal level occurred at about 0500 UT. In the interval from about 1545 to 1830 UT the normal level was approached (slightly exceeded at about 1615 and strongly exceeded by the sharp bay with a maximum at 1806 UT). The H-pattern then roughly follows the normal curve at a generally decreased level through 7 August until 0900 UT on 8 August (beginning of a giant magnetic crochet at 1515 UT on 7 August).

In the second part of the disturbed period, normal level was reached roughly between 1130 and 1500 UT on 8 August (an ssc occurred at 1341 UT), the level of the curve was then still above normal from the ssc at 2353 UT until about 0100 UT on 9 August and then roughly normal until 0400 UT. From 1600 UT the H-curve began to follow roughly the normal curve at a generally decreased level. The curves came closer after 2300 UT. The pattern was similar on 10 and 11 August. After the abrupt change just after 1330 UT on 10 August, the distance between the H-curve and the comparative curve decreased. The levels of the two curves became approximately identical on 14 - 15 August.

On the Magnetospheric Storm of August 1972

by

M. Bossolasco, A. Elena and A. Caneva
Istituto Geofisico e Geodetico, Universita di Genova
Genoa, Italy

Summary

The behavior of the magnetospheric disturbance of August 4, 1972, as recorded at Roburent and Genoa,, Mt. Capellino, Italy, is investigated. The control of the occurrence of pc2, 3, 4 and 5 by the geomagnetic DR-phase is emphasized; moreover, the induced gravity waves in the F2-region are also pointed out.

Introduction

An unusual center of solar activity, sunspot group 331, was the source of a very strong magnetospheric disturbance, early in August 1972 [Lincoln and Leighton, 1972]. The solar flux on 2800 MHz, as recorded at Ottawa reached maximum (156.3) on August 1; and it remained higher on the following days than it was on the last days of July. A solar flare effect occurred on August 2 from 1838 to 1852 UT. The solar wind velocity became abnormally high (585 km/sec) abruptly at 1500 UT on August 3; it reached an absolute maximum (1130 km/sec) at 0000 UT August 5 after which it decreased very slowly, being greater than normal up to August 8.

In this paper, we consider some characteristics of the magnetospheric disturbance of August 4 as recorded at Roburent and Genoa-Mt. Capellino, Italy (see Figure 1).

The Geomagnetic Storm of August 4 as Recorded at Roburent

At Roburent, North Italy (Dipole Lat. +45.8°) the geomagnetic storm began at 0119 UT August 4 with an sc of amplitude -20γ in d, +20γ in H and +8γ in Z; followed by a small DCF-phase of +23γ in H. Another sc at 0220 UT with amplitude -40γ in D, +45γ in H and +23γ in Z, gave rise to a greater DCF-phase of amplitude of +55γ in H and also to DP-fluctuation and to the DR-phase. The sc of 0220 UT behaved as a sudden enhancement of the DCF-phase which, however, almost disappeared at about 0300 UT August 4. The DR-phase was maximum (165γ in H) at about 1500 UT August 4; during this day the DR was prevailing over DP. At 2354 UT August 4 a sudden impulse led to a strong increase of geomagnetic activity: the DR-phase reached amplitude of about 250 γ in H while large DP-variations were also superposed.

The sc's of 0119 and 0220 UT as well as the si of 2354 UT August 4 were roughly coincident with maxima of solar wind velocity as recorded by Pioneer IX.

The behavior of magnetic micropulsations pc2, 3, 4 and 5 at Roburent was investigated with reference to the occurrence frequency given by the hourly ratio of the number of observed 10-min occurences to the corresponding number of analyzed 10-min intervals expressed in percent.

The pc2 frequency increased abruptly from 0300 to 0500 UT August 4, i.e. immediately after the two sc's. During the late morning and early afternoon the occurrence rate was smaller. It suddenly peaked between 2100 and 2300 UT August 4, and it remained very high till 0300 UT August 5. Another maximum of pc2 occurrence was observed in the afternoon of August 5. It decreased during the night from August 5 to 6, and another enhancement of the pc2 frequency was observed at about 0300 UT August 6. At 0700 UT it returned to the pre-storm level.

The pc3 frequency increased suddenly at 0500 UT August 4, i.e. with a delay of about 2 hours with respect to the pc2. It was somewhat reduced from 0800 to 1600 UT and afterwards, it died down until 2100 UT. The pc3 frequency increased abruptly at about 2300 UT August 4 and it remained very high till about 2000 UT August 5 followed by a slight minimum which lasted until 2300 UT. Near sunrise of August 6 the pc3 occurrence frequency increased and then it gradually decreased at evening, reaching very low values at midnight.

The pc4 frequency increased abruptly at 2100 UT August 4 and it remained very high till 1800 UT August 5. After a slight decrease before 1200 UT a very strong maximum occurred from 1200 to 1600 UT August 5; afterward, the pc4 frequency decreased and from 2200 UT August 5 until 0600 August 6 it was practically zero. At 0900 UT August 6, it achieved a very strong maximum which lasted until 1600 UT after which it quickly decreased.

The pc5 occurrence frequency showed a weak maximum from 2200 UT August 4 till 0000 UT August 5; another maximum occurred from 0200 to 0400 UT August 5. The absolute maximum of pc5 activity occurred from 0900 to 1200 UT August 5.

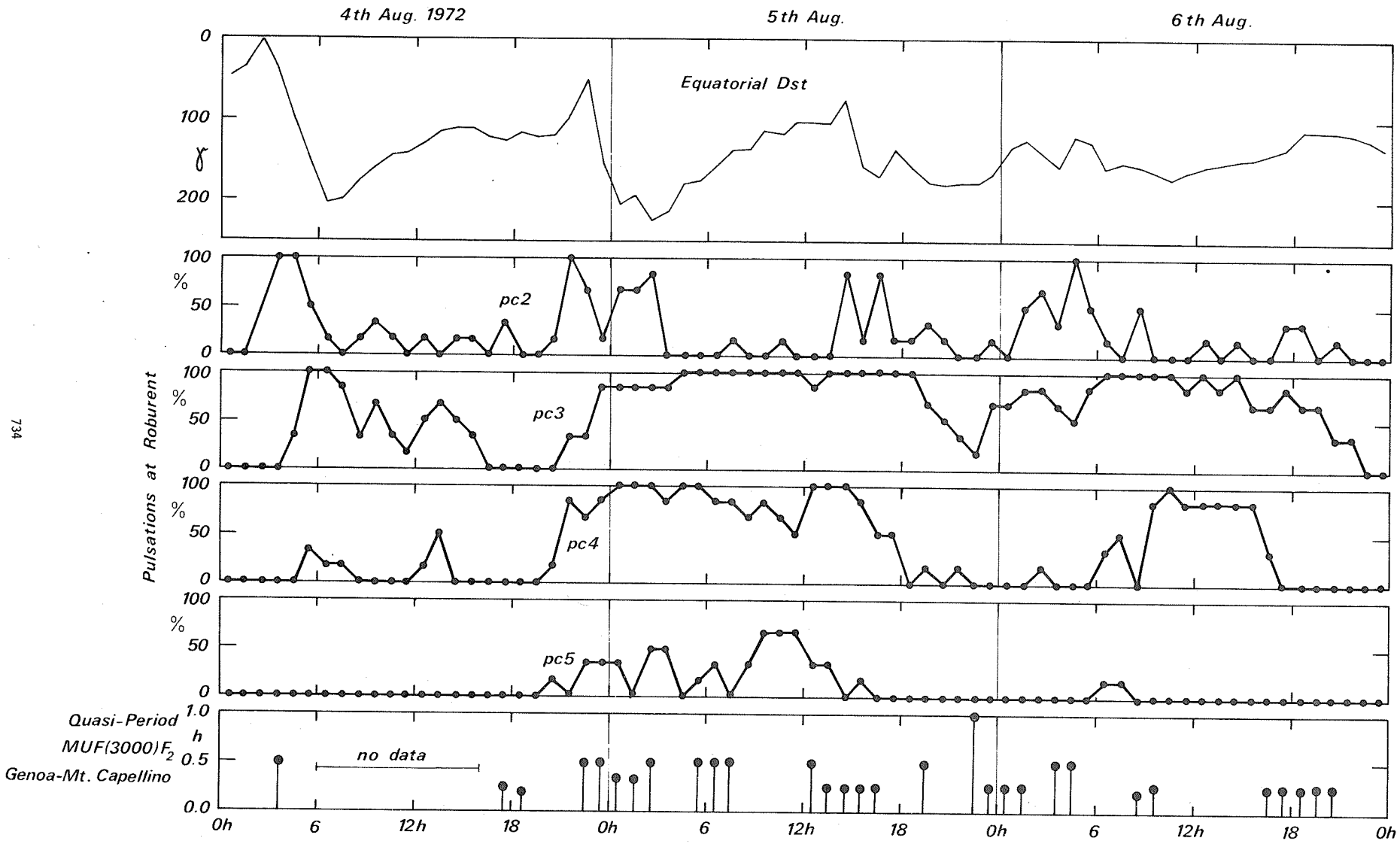

Fig. 1. Equatorial Dst, pulsations recorded at Roburent, and quasi-period MUF (3000) F2 data from Genoa-Mt. Capellino for the period August 4-6, 1972 are shown.

The Ionospheric Disturbance as Recorded at Genoa-Mt. Capellino

At Genoa-Mt. Capellino (Dipole Lat. +45.8°) foF2 at the beginning of the geomagnetic storm was about 33% greater than the monthly median; by 0600 UT August 4 it had decreased about 40%; in the afternoon foF2 recovered somewhat but was generally below normal (34%) in the late evening of August 4, and 60% at 0100 UT August 5. foF2 recovered again in the late afternoon of August 5 but decreased sharply (44%) at 1900 UT and was low all night (54% at 2300 UT, 52% at 0000 UT August 6 and 57% at 0200 UT). The values of foF2 returned to about normal on August 7.

On the morning of August 3 the MUF (3000) F2 reached its daily minimum at 0430 UT. There were baylike oscillations with a quasi-period of about 3/4 hour to 2000 UT August 3. After 0230 UT on August 4, i.e. immediately after the beginning of the geomagnetic disturbance, there was a sharp decrease of MUF which became a minimum (3.2 MHz) at 1000 UT August 5. It reached a secondary maximum (7.3 MHz) at 0245 UT and another minimum (5.5 MHz) at 0340 UT. Irregular fluctuations with a quasi-period of 1-2 hours occurred in the afternoon and evening of August 5; the MUF was a minimum (5.6 MHz) at 0330 UT August 6 and was normal thereafter.

The irregular fluctuations of MUF (3000) F2 happened mainly during the night of August 4 - 5. In the afternoon of August 5 the quasi-period of the baylike oscillations diminished, becoming greater in the evening. On August 6 the fluctuations were more frequent in the afternoon.

Discussion

The geomagnetic disturbance began with an sc roughly at the time of maximum solar wind velocity as due to an intensification of the solar particle stream.

The two recorded sc's at 0119 and 0220 UT August 4 appear as sudden enhancements of DCF, when an intensified solar wind just arrives at the magnetospheric boundary. The DCF was of small amplitude, in comparison with DR, i.e. the development of DR does not seem to be related to the magnitude of the enhanced plasma pressure responsible for DCF [Kawasaki, et al., 1971].

The DR-phase which began at about 2100 UT August 4 was more pronounced than the preceding one, being roughly in the same ratio as the corresponding values of the solar wind velocity. The DP was very strong mainly during August 5. It appears that the DR and DP-fields developed simultaneously; the DP and DR may have the same origin or the one disturbance field may be excited by the other [Grafe, 1972].

The pc2, 3 and 4 occurrence became maximum at about the time of the maximum DR-field as previously found [Bossolasco et al., 1968]. Moreover, there is a parallelism between the pc2 occurrence and the Kp. The pc3 and 4 are also in close agreement with the geomagnetic activity, although there can be an aftereffect [Stening and Gupta, 1972; Vero, 1972].

The pc5 activity was maximum near the maximum of the DR-phase on August 5 in agreement with the finding of Barfield and McPherron [1972].

The global pc activity vanished about 12 hours after the first maximum of the DR-field, and about 20 hours after the second maximum. The reduction of the pc occurrence during the recovery phase of a geomagnetic storm is a feature already found by us [Bossolasco, et al., 1968]. It was noted during the storm of March 13, 1966, when with a DR-field at Roburent of about 120 γ that the delay between the maximum of DR-phase and the minimum of pc activity was about 18 hours, whereas for the storm of May 25, 1967 the delay was of 15 hours after a Dr-maximum of about 270 γ at Roburent.

As far as the effect of the geomagnetic disturbance on the F2-region is concerned we remember that thermal, chemical and electrodynamical processes can be responsible for the same perturbations.

The bay-like variations as observed in the records of MUF (3000) F2 are a normal feature of winter days, also with quiet geomagnetic conditions. Conversely in summer they occur only seldom by geomagnetically disturbed conditions [Bossolasco and Elena, 1973]. Moreover, bay-like oscillations of MUF occur generally during daytime and evening only, the first hours after midnight being almost always free. On the contrary, during the geomagnetic storm of August 4 bay-like disturbances of the MUF occurred almost continuously during the night from August 4 to 5 and from August 5 to 6. These effects of a magnetospheric storm appear as gravity waves, and they were observed also by Alcayde et al. [1972]. Likely, they are generated at higher latitudes by solar corpulcular streams.

REFERENCES

ALCAYDE, D., J. TESTUD, G. VASSEUR and P. WALDTEUFEL (1972) L'Orage Magnetique du 11 fevrier 1969: Etude par Diffusion Incoherente, J. Atmos. Terr. Phys., 34, 1037-1052.

BARFIELD, J. N. and R. L. MCPHERRON (1972) Investigation of Interaction between Pc1 and 2 and Pc5 Micropulsations at the Synchronous Orbit during Magnetic Storms, J. Geophys. Res., 77, 4707 -4733.

BOSSOLASCO, M., A. CANEVA, A. ELENA and C. PALAU (1968) On some Properties of Geomagnetic Stroms, Geofis. Meteor., XVII, 7-12.

BOSSOLASCO, M. and A. ELENA (1973) Midlatitude Ionospheric Irregulatities, Communication at the Symposium on "Structure and Dynamics of the Upper Atmosphere", Erice, Italy, 13-27 June 1971, in press.

GRAFE, A (1972) About the Connection between Equatorial Ring Current and Polar Electrojet, Planet. Space Sci., 20, 183-204.

KAWASAKI, K., S.-I. AKASOFU, F. YASUHARA and C. -I. MENG (1971) Storm Sudden Commencements and Polar Magnetic Substorms, J. Geophys. Res., 76, 6781-6789.

LINCOLN, J. V. and H. I. LEIGHTON (1972) Preliminary Compilation of Data for Retrospective World Interval July 26 - August 14, 1972, World Data Center A for Solar-Terrestrial Physics, Report UAG-21.

STENING, R. J. and J. C. GUPTA (1972) Diurnal Variation of the Correlation of Pc3 and Pc4 Micropulsation Characteristics with Magnetic Activity, J. Geophys. Res., 77, 5590-5596.

" VERO (1972) Experimental Results with the Characterization of Geomagnetic Micropulsations, III, Acta. Geodaet. Geophys. et Montanist. Acad. Sci. Hung., 7, 177-190.

SUBSTORM COMPONENTS
OF THE GEOMAGNETIC STORMS 4 - 9 AUGUST 1972

by

E. SELZER and J. ROQUET

Institut de Physique du Globe de Paris

Université "Paris VI"

A general description of the geomagnetic events to be discussed will not be given here, except in the abstract form of the TABLE 1 . In this TABLE, CHAMBON (short for "CHAMBON-LA-FORÊT) and GARCHY (in France) are representative of middle-latitude stations, and ADDIS ABABA of an equatorial one. (TAHITI, subequatorial station, is also quoted incidentally) .

Our purpose is to question the exact nature of these events and to examine their function in the course of the World-wide storm ("Mother storm") to which they belong. In this respect, the following problems can be approached :

-- Independence, or dependence, of the successive so-called "SSC" (or "SI"), such as at 04/0119 and 04/0221 , for the first group ;
-- 08/1342 , 08/2354 and 09/0037 , for the second group

(Time here is approximate: more precise values are given in the TABLE) .

-- Distinctions to be made between sharp sudden onsets of "Microstructure Substorms" as components of a World-wide storm, with the more classical SSC and SI to be found in this Mother storm, on one side, and with sudden onsets of isolated Substorms, on the other side .

The period of time 03 to 07 August is the one that is the best fitted for such a study, but the following one, 07 to 09 August, has been included also with interest .

Independence - or dependence - of the successive SSC

The double couple of SSC 04/0119 -- 04/0221 on one side
and 08/2354 -- 09/0037 on the other side ,
are quite similar and will be discussed in parallel .

(The case of SSC 08/1342 is different. It is a small, "C" quality SSC , even though it cannot be questioned on this identity : for example, we could not take it as a simple SI , remarking that the geomagnetic perturbed conditions are distinctively different before and after its appearance. For this reason, there might be some implication of this event on a complete interpretation of the following SSC at 08/2354 ... but we will neglect it, so far, in our present discussion) .

In the case of the two pairs quoted above, the following remarks can be made :

1st - In both cases, a single solar flare could be attributed to the corresponding pair : flare 02/0316 for the first one ; flare 07/1509 for the second one. Possible explanations for this pecularity can be summarized as follows :

a) The solar flares involved presented a double structure (supposing that such kind of phenomenon could escape astronomical solar observations) ;

b) The double structure has taken place inside the plasma flux, in the course of its travelling from Sun to Earth, this, for example, resulting in a "split" in the radial structure of the solar wind ;

c) The second magnetic "break" is a magnetospheric "replique" of the first one : this last suggestion cannot be ruled out altogether in the present condition of our knowledge, but we consider, just the same, that it is highly improbable .

As far as a) and b) are concerned, we have no way, so far, to decide, but we can remark that from the standpoint of any magnetospheric secondary effect it seems that there should be very little differences in the two cases, as in "a)" as well as in "b)" , the magnetopause would receive two successive shock waves.

TABLE 1

SOLAR FLARES (°) Start (U.T.)	SSC - U.T. given to the nearest second, having given accuracy (°°)	SUBSTORMS Start (U.T.)	End	ΔH (+) en γ	AURORA (°) Start -- End
02/0316				(CHAMBON)	(Observed in various places)
02/1828					
02/1958					
	04/0118/40 ± 6 (CHAMBON, GARCHY)			22	04/0400--/0430
	04/0118/55 ± 10 (TAHITI)				04/0530--/0600
					04/0800--/1000
	04/0220/37 ± 1 (CHAMBON)	general substorm (microstructure) activity follows closely the 04/0221 SSC, but cannot easily be separated into individual substorms, contrarily to the ones below		55	
04/0621					
	04/2054/06 ± 2 (CHAMBON, GARCHY)	04/2054		86	04/2100--05/0430
	04/2054/11 ± 5 (ADDIS ABABA)	instead SSC ?			04/2307
		05/1402	05/1615	85	04/2310--/2325
		05/1743	05/1840 (°°°)	75	04/2350--05/0010
		05/2332	06/0315	36	05/0200--/0500
		06/0353	06/0402	30	05/0300
		06/0420	into Pc3 (°°°°)	10	05/0355
		06/1751	06/1810	106	06/2130
07/1509					
	08/1341/40 ± 10 (CHAMBON, GARCHY)				
	08/2352/02 ± 10 (ADDIS ABABA, gradual onset)				
	08/2353/40 ± 10 (CHAMBON, gradual onset)				
	08/2354/15 ± 1 (CHAMBON, GARCHY) } sudden				
	08/2354/15 ± 5 (ADDIS ABABA) } onset				
	09/0036/33 ± 5 (CHAMBON, GARCHY)	general substorm (microstructure) activity starts just after 09/0037 , and lasts about 12 hours, but cannot easily be separated into individual substorms			
	09/0036/45 ± 10 (ADDIS ABABA)				

(°) Given only as a general reference
(°°) U.T. includes day/hour,minute/second ± the approximation (in seconds)
(°°°) or : 05/2200 , but much less intense after 05/1840
(°°°°) around 06/1000 ; these Pc3 (mixed later with Pc4) are intense till 06/1620

(for graphical display see Figure 1 for substorm beginning 20h54m06s August 4, and Figures 2-4 for substorm between 1751 to 1810 UT August 6, 1972).

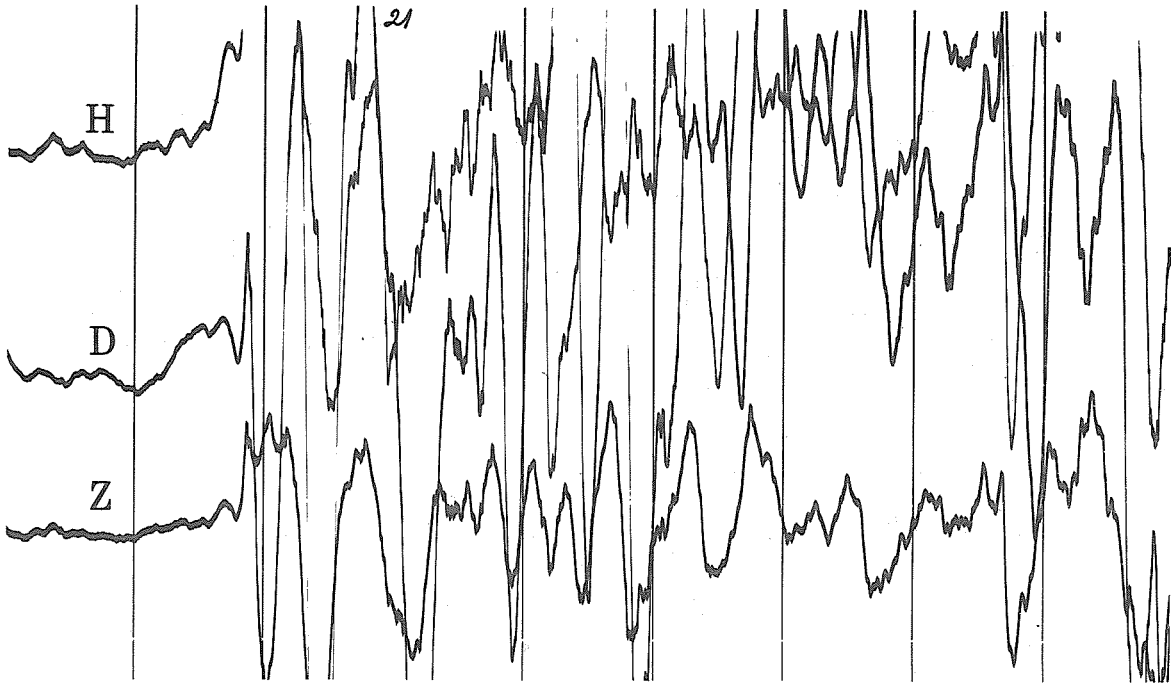

Fig. 1 - GARCHY, August 4 . Sudden onset at $20^h\ 54^m\ 06^s \pm 2s$.

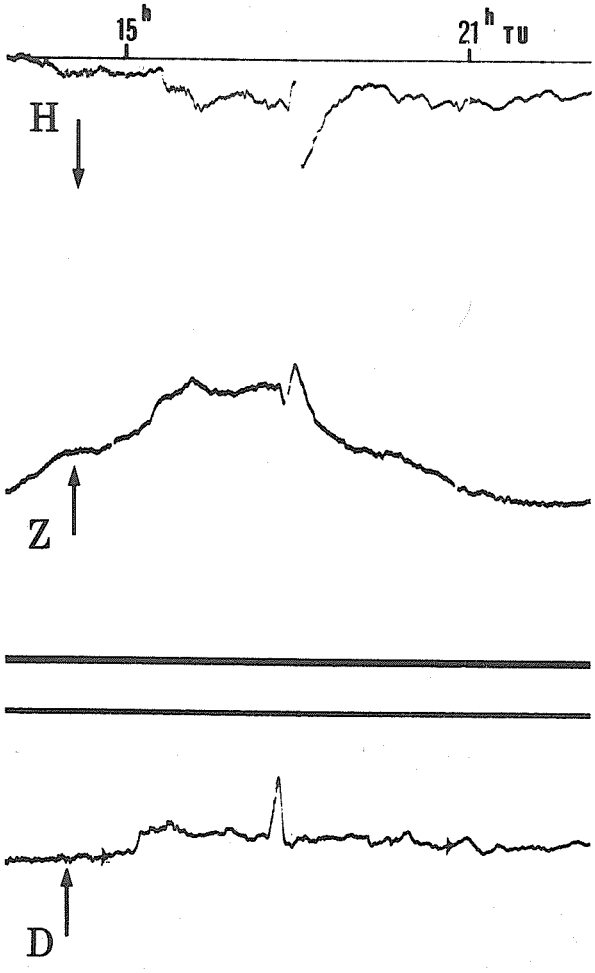

Fig. 2 - CHAMBON-LA-FORET, August 6 . Substorm between $17^h\ 51^m$ and $18^h\ 10^m$, having the shape of a SI on a classical (normal speed) magnetogram.

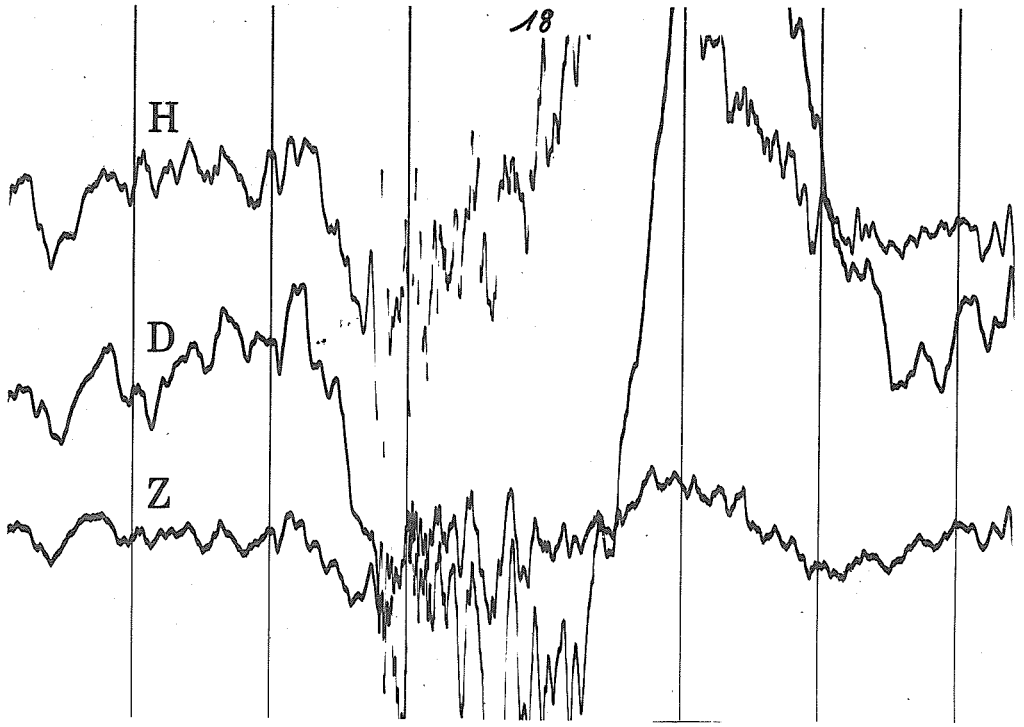

Fig. 3 - GARCHY, August 6 . Same event as the one given in Fig. 2 , but as given on rapid (about 5 mm/min) magnetograms. (Same type of registration has been also obtained in CHAMBON-LA-FORÊT).

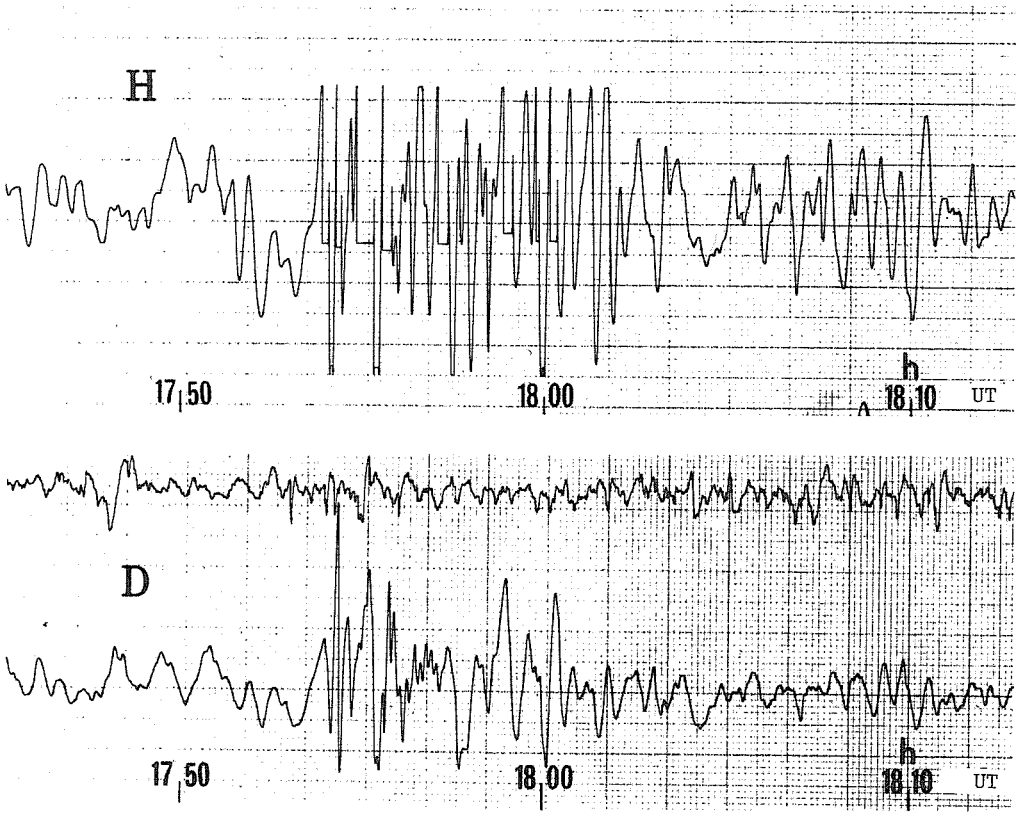

Fig. 4 - ADDIS ABABA, August 6. Same event as the one given in Figs. 2 and 3 , obtained on rapid (about 6 mm/min) magnetograms. One should note that the equipment which was used has strongly attenuated the slower component (in bay-like shape) visible on the other illustrations of this event.

2nd - Even if the two shock waves constituing a pair exert their action in a like manner on the outer boundary of the magnetosphere, they cannot produce the same effects inside this boundary as long as the second shock will find magnetospheric conditions already perturbed - or, at least, transformed - by the first one. As a consequence, we cannot simply add linearly the D field components ("D" is taken here in its general implication) relative to each one of the theoretical storms that might be caused by the two shocks. For instance, the duration of the "first phase" that might have presented the "second storm" (if it could have happened alone) can be expected to be reduced in accordance with the magnetospheric changes operated by the first one. This is particularly well evidenced for the two cases we are considering :

- Very soon after the second sudden onset 04/0221, changes in H reverse (positive to negative), and general intense microstructure activity (although it is not dissociable into separate substorms before the next day) takes place. Very nearly the same can be said about the second case, after 09/0037.

3rd - Concerning the first SSC of this last pair, at around 08/2354 , a remark of another kind (and independent, probably, of the existence of a pair) can be made : the more-than-one-minute discrepancy between the times observed for the gradual onsets at the equatorial station of ADDIS ABABA and at the middle-latitude station of CHAMBON (ADDIS ABABA being in advance, the ultra-rapid magnetograms showing that it is not a question of a poor definition of these onsets but a real phenomenon), specially when compared with the absolute exact synchronism of the sudden onsets that follow (see TABLE 1).

Substorm components of World-wide storms, compared to isolated substorms

The disturbed period under study provides the opportunity to investigate these two species of substorms and to examine how far they should be considered as a single type of phenomenon (that just happens to arrive in different general geomagnetic situations), or two different types. The nomenclature has been rather confusing on this subject : Birkeland's "polar elementary storms", "magnetic bay disturbances", refer, generally, to isolated events ; Akasofu and Chapman have applied, indifferently, the symbol "DP" to both types, and the same can be said about Troitskaya's "IPDP" [AKASOFU S.-I. and S. CHAPMAN, 1961 ; AKASOFU S.-I. , 1968 ; TROITSKAYA V.A. and M.V. MELNIKOVA, 1959 and 1961 ; SELZER E. , 1959 and 1968].

From microstructure registrations for the August 1972 events, obtained in CHAMBON-LA-FORÊT, GARCHY and ADDIS ABABA, we were able to determine the successive substorms components listed in TABLE 1, and to make the following remarks :

- 1 - All substorm components coincide - within the limits of the experimental accuracy - at the three stations.

- 2 - The dominant periods (or "pseudo-periods") of the magnetic pulsations forming the microstructure of these substorm components, are of the same order of value at these stations. (Only detailed spectral analysis - now, under way - of the magnetic-tape registration permanently made at CHAMBON, will be able to determine the full range of these periods, but they are as small as 0.5 s - at CHAMBON - in many cases ; at ADDIS ABABA it is difficult to ascertain precise values).

- 3 - Intensity, spectral density ("nervousness"), of the microstructure components, were at a higher level than what is observed in CHAMBON, from time to time, during the development of a regular bay with pulsations (including "IPDP"-like, components), synchronous with an auroral (isolated) polar substorm. This, of course, was to be expected, and illustrates - by the means of microstructure activity - the general tendancy of auroral and magnetic substorms to expand towards lower latitudes during the main phase of a World-wide storm.

Conclusion

A full interpretation of the exact nature of the substorm components of a World-wide magnetic storm is out of the scope of this contribution paper. For this reason, we will limit our remarks on a single, but important, characteristic of substorms : the sudden onset, or "break", which is not, necessarily, the absolute "beginning" of the substorm (and the same can be said about SSC), but is generally the sign of a sudden happening in the magnetospheric, and ionospheric, conditions around us. In formulating this statement - and in spite of the comparison we have just made, on a definite point, with the SSC, we anticipate on an idealistic distinction that could be made between these SSC (of World-wide storms) and "SC" (or sudden onsets) of substorms. In both cases, the discontinuity exists,

or is created, at a time which can be taken (with a proper convention) as the one marking the beginning of the event, but this discontinuity has to be assigned to the interplanetary space in the first one, and to the magnetosphere (plasmasheet, neutralsheet, cusp, tail, etc.) in the other one. For this reason, it looks as if the substorm components of a World-wide storm have much closer analogy with isolated substorms than with their Mother-storm, although some doubt can still subsist on the possible "outside" (interplanetary space, solar wind, etc.) direct origin of a certain kind of magnetic "noise" constituting one of the numerous components of the substorms.

Our last question is, then, to try to determine the line between SC of substorm components (of a World-wide storm) and SC of isolated substorms. For this, we have to turn to the so-called "preliminary phase" (prior to the SC relative to the "expansion phase"), also called : "the growth phase" [McPHERRON, 1972]. If the substorm is part of a Mother-storm, the general conditions necessary to ensure the growth phase are permanently secured as soon as the first (compression) phase of the Mother-storm is replaced by the main phase. The coincidence between the SC onsets of each substorm component, and the sudden ΔH recoveries of the general H depression, statistically maintained during this main phase, in connection with the ring current (see TABLE 1), is one of the convincing facts which support this view. This has as a consequence that it is in a much larger magnetospheric domain - compared to where the growth phase of an isolated substorm takes place - that these build-up conditions can be simultaneously fulfilled, and maintained for many hours. This, in turn, augments considerably the number of field lines (and of plasma flux) affected together, at the same moment, by the expansion (or "reconnection") phase of each substorm, and explains the World-wide extent - together with that of the Mother-storm - of the substorm components themselves. In this sense, the extension, towards lower latitudes, of magnetic substorm events, when World-wide storm conditions prevail, appears to be a much more magnetospheric affair than an ionospheric one.

REFERENCES

AKASOFU S.-I. and S. CHAPMAN	1961	The ring current, geomagnetic disturbances, and the van Allen radiation belts, J. Geophys. Res., 66 (5), 1321-1350.
AKASOFU S.-I.	1968	Polar and magnetic substorms, D. Reidel Publishing co., Dordrecht - Holland.
McPHERRON R.L.	1972	Substorm related changes in the geomagnetic tail : The growth phase, Planet. Space Sci. 20 (9), 1521-1539.
ROQUET J. and P. GOUIN	1972	Equatorial microstructure of the magnetic storm on January 13-14 1967, Journ. Atm. Terr. Phys., 34, 465-474.
SELZER E.	1959	Résultats d'ensemble des stations françaises, Symposium IAGA d'Utrecht, Urania, 250, et Bulletin IAGA, 16c, 1961, 63-70.
SELZER E.	1968	Les sous-orages magnétiques mondiaux (World-wide substorms), Ann. Géophys., 24 (2), 233-242.
TROITSKAYA V.A. and M.V. MELNIKOVA	1959	On characteristic intervals of pulsations diminishing in period and their connection with phenomena in the high atmosphere, Dokl. Akad. Nauk. SSSR, 128.
TROITSKAYA V.A. and M.V. MELNIKOVA	1961	On characteristic intervals of pulsations diminishing by periods (IPDP) and their connection with phenomena in the high atmosphere, IAGA Bull., 16c, 135.

Low Latitude Observations of the Geomagnetic Field for the Retrospective World Interval July 26 - August 14, 1972

by

B. N. Bhargava
Indian Institute of Geomagnetism
Bombay, India

Three major geomagnetic disturbances were observed in the low latitude magnetograms in India during the Retrospective World Interval and these were presumably associated with the major solar events of 1958 UT August 2, 0530 UT August 4, and 1458 UT of August 7.

A magnetic storm with a small main phase began on August 4, 1972 with two sudden commencements in succession, the first at 0118 UT and the second at 0220 UT with amplitudes in H of 10 and 25 gammas respectively at Alibag. The second sudden commencement was followed by a much larger positive phase than the first sudden commencement and was also marked by the beginning of moderately severe agitation of the field. The agitation was greatly enhanced at the equatorial stations, Trivandrum and Annamalainagar.

While the recovery phase of this storm was still in progress a sudden commencement of large amplitude (85 gammas at Alibag) was registered at 2052 UT on August 4, 1972 and was followed by a large positive phase. However, an event of greater significance following the sudden commencement was a very large SI at 2238 UT. The SI followed the sudden commencemnt after 106 minutes. The amplitude of the SI was 301 gammas at Alibag and 386 and 464 gammas at Annamalainagar and Trivandrum respectively.

The SI observed at 2238 UT on August 4, 1972 marked the beginning of an intense agitation of the equatorial field during the main phase. Agitation was so severe that excursions on the charts were lost on several occasions in the records of the two equatorial electrojet stations. The agitation lasted about 18 hours at the equatorial electrojet stations. The agitation again appeared on the following day after sunrise and lasted for about 7 hours.

The third storm during the Retrospective Interval began on August 8, 1972 with a sudden comcencement of amplitude 21 gammas at Alibag at 2351 UT. Moderately severe agitation of the field followed the sudden commencement and the greatest main phase of the storm occurred at 1042 UT on August 9.

Magnetic records of the equatorial electrojet stations, Trivandrum and Annamalainagar and of the low latitude station, Alibag, which is outside the effect of the electrojet suggest a considerable enhancement of the day-time agitation of the field at the equatorial stations. These magnetograms are available through the WDC-A for Solar-Terrestrial Physics, Boulder, Colorado 80302.

Total Magnetic Field Variation at Thumba during 3 - 10 August 1972

by

P. D. Agarwal
Space Physics Division
Vikram Sarabhai Space Centre
Trivandrum 695022, India

The geomagnetic total field variations during the period 3-10 August 1972 at Thumba (dip -0.9, geographic latitude N 8.6, geographic longitude E 76.9) recorded on the Proton Precession Magnetometer are presented in Figure 1. Total field values averaged over a 12 minute period are plotted.

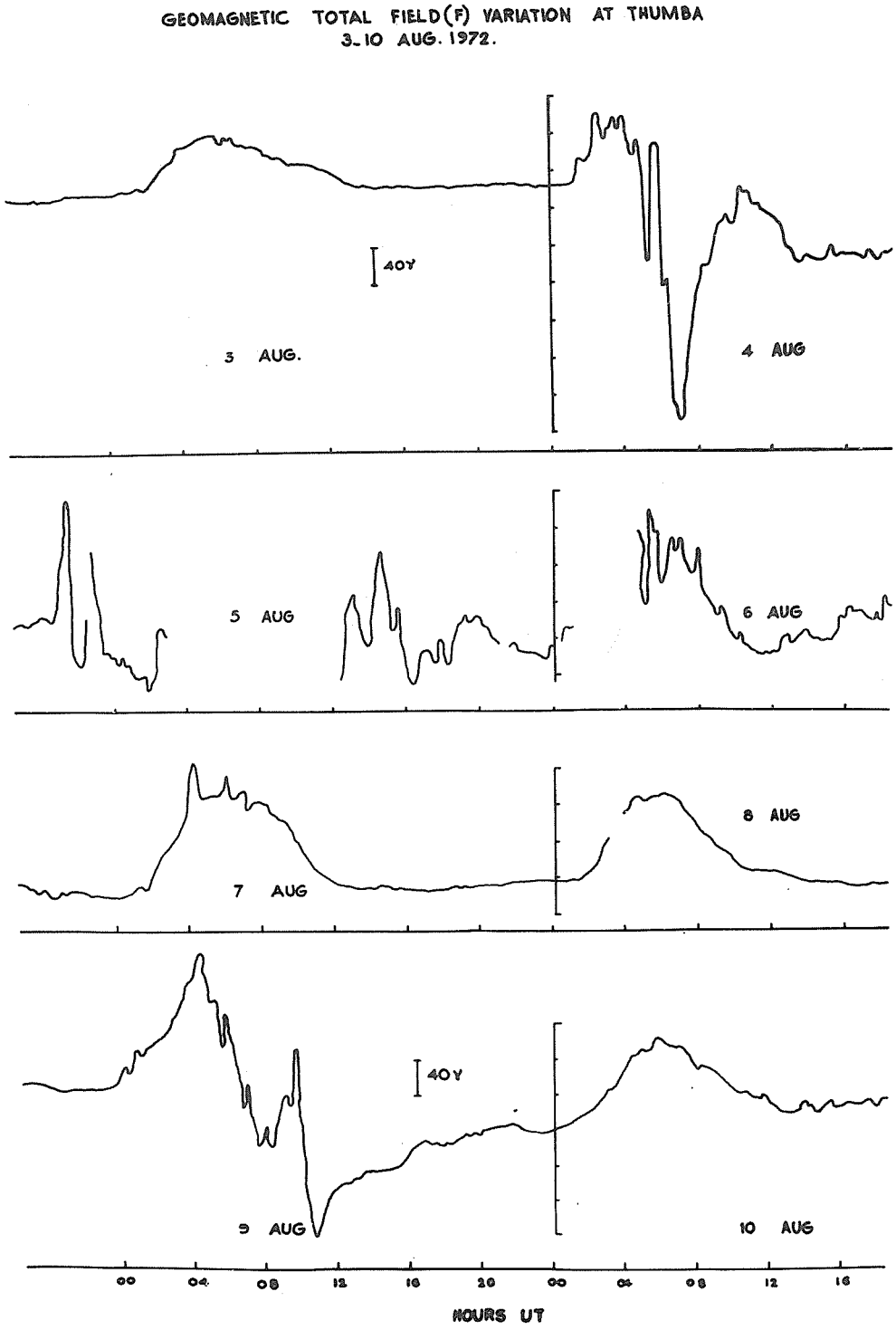

The Behavior of the Geomagnetic Pulsations during Two Magnetic Storms of August 1-10, 1972

by

O. V. Bolshakova, A. L. Kalisher,
E. T. Matveyeva and R. V. Shchepetnov
Academy of Sciences of the USSR
The Borok Geophysical Observatory, USSR

The behavior of the different types of geomagnetic micropulsations during the storm August 4-8, 1972 is shown in Table 1. In this analysis the records of micropulsations of the Borok Observatory were used.

The main characteristics of all types of pulsations such as the period, intensity, duration, etc. are presented in Table 1.

Table 1

Storm 4-10 August 1972

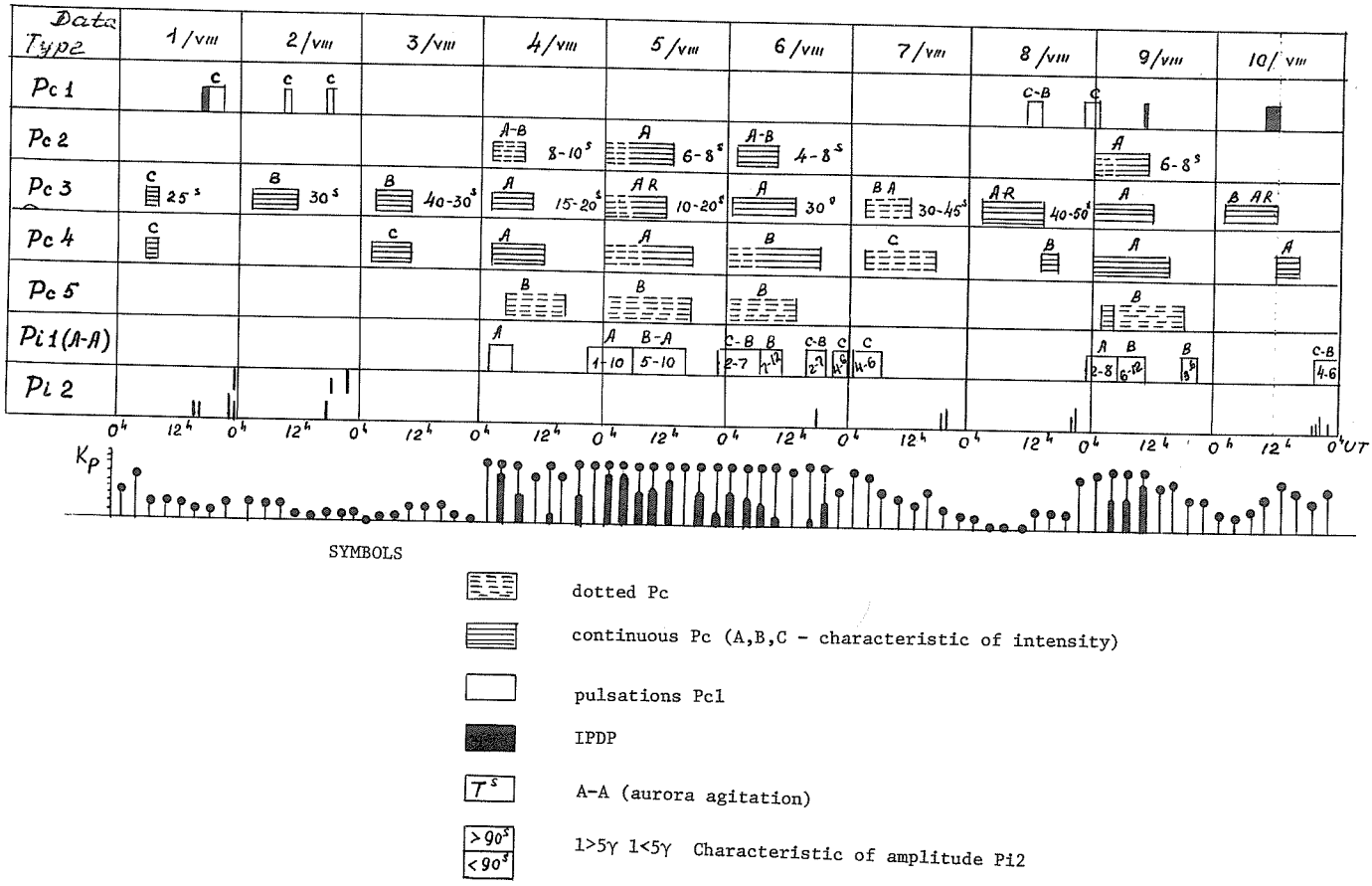

SYMBOLS

dotted Pc

continuous Pc (A,B,C - characteristic of intensity)

pulsations Pc1

IPDP

A-A (aurora agitation)

$>90^s$ / $<90^s$ 1>5γ 1<5γ Characteristic of amplitude Pi2

A rather calm interval preceded the first storm: the mean Kp did not exceed 1 during three days. The storm of August 4, 1972 had two SSC's (0119 and 2053 UT) and it was very intensive (Kp about 9 during some hours). This storm lasted three days. The second storm began on August 8 after the ending of the first storm and it was like an echo but less intensive and shorter. It had very small SSC's at 1342 UT and 2352 UT August 8. Let us consider a qualitative picture of the generation of different types of pulsations in the course of these storms.

Pc1 pulsations were observed before and after the storm of August 4. They appeared after the IPDP of August 1 in which the pulsation periods in the IPDP interval decreased from 3.3 sec to 2.0 sec. Pearls also were observed on August 2. Then the Pc1 were also observed after the large storm of August 8. The first series of pearls finished an hour before the first sc and another series began 13 minutes afterwards. It is interesting to note that the period of the pulsations after the sc is shorter than for those before.

The second sudden commencement at 2352 UT August 8 appeared against a background of a series of pearls which was observed from 2228 UT August 8 to 0030 UT August 9. The period of the pulsations after the sc decreased by a jump from 1.0 sec to 0.7 sec. After the storm of August 8 pearls were observed during some days beginning from 10 August. The periods of these pulsations $T \leq 1.0$ sec are shorter than ones observed before the storm. The decrease of Pc1 period after the storm probably indicates the penetration of resonant particles on smaller L-shells [Troitskaya, et al., 1969]. A series of IPDP pulsations was observed on August 10.

Table 1 shows increasing intensity of all Pc2-5 with increasing Kp. Amplitude of Pc3 reached approximately 4-5 γ August 4. This value is well above the average level of amplitudes of Pc3. The period of Pc3 decreases during the storm with Kp growth. The appearance of intensive and continuous Pc2 during August 4, 5, 6 and 9 seems to be connected with increase of the solar wind pressure and of its stability [Bolshakova, 1966]. The long period Pc5 pulsations which were observed during the same time confirm this suggestion.

It is necessary to note that the regular continuous pulsations with period 40-50 sec appeared August 8 and 13 (at the "tails" of storms). As a rule these pulsations arise as an interaction of the Earth and the fluxes of low intensity ions [Gringauz et al, 1971].

From the table it is seen that the irregular pulsations of the type AA (aurora agitation) were not observed during August 1-3, 1972. These pulsations appeared on August 4 (about 0200 UT) after the beginning of the disturbance and continued during the storm (till 0600 UT August 7). The same picture was observed in the second storm: AA pulsations appeared at 2300 UT August 8 and finished about 1100 UT August 9. Pulsations AA connected with substorm were observed August 9 and 10 during night hours.

The Pi2 pulsations given in the table are divided into two types ($T > 90^s$ and $T < 90^s$) and they are shown located on different levels. The Pi2 intensity is given in the vertical scale. Regular Pi2 with periods >100 sec, without following bays, were observed during August 1-2. There were no Pi2 before the storm on August 3-4. It is very difficult to separate the individual series of Pi2 on August 5-6 but one can note that the irregular pulsations in the Pi2 range had a low intensity in spite of a general high level of disturbance. The Pi2 pulsations with period $T \leq 60$ sec were observed at night hours in the local time of August 6-10, either they preceded the bays or they accompanied the bays with sharp commencement.

In conclusion we should note that excitation of the pulsations during these storms seems not to differ from the usual picture which is observed during any great storm. On the other hand it is necessary to note that during the main phase of this magnetic storm the pulsations of the type IPDP were not observed.

REFERENCES

BOLSHAKOVA, O. V. 1966 The continuous geomagnetic micropulsations and solar corpuscular flux, Geoma. and aeron. IV, No. 6, 1080-1093.

GRINGAUZ, K. I., V. A. TROITSKAYA, E. K. SOLOMATINA and R. V. SHCHEPETNOV 1971 J. Geophys. Res., 76, N 4, 1065.

TROITSKAYA, V. A., and E. T. MATVEYEVA 1969 The excitation of the rapid micropulsations of geomagnetic field during the proton flares, Solar-Terrestrial Physics, 1, 41-43.

Spectral Structure of Storm-Associated Geomagnetic Pulsations Observed at Onagawa during the Period of August 4-11, 1972

by

Takao Saito, Tohru Sakurai, Minoru Kondo,
Tadayoshi Tamura and Masaei Abe
Onagawa Magnetic Observatory
Tohoku University, Sendai, Japan

The present report outlines the dynamic spectral characteristics of geomagnetic pulsations recorded at the Onagawa Magnetic Observatory (Φ=28:3, λ=206:8), Japan during the magnetic storms of August 4-11, 1972. During the storm period magnetic disturbances were recorded at Onagawa by the following five sets of magnetometers.

(1) Low-sensitivity normal-run magnetometers
(2) High-sensitivity (La Cour-type) normal-run magnetometer
(3) High-sensitivity (La Cour-type) rapid-run magnetometer
(4) Helicoidal pen-recording induction magnetometer
(5) FM-tape recording induction magnetometer

The magnetograms obtained by the magnetometers (1), (2) and (4) are shown for the August 9 storm period as an example event in Figure 1 together with the dynamic spectrum of geomagnetic pulsations recorded by the magnetometer (5). The dynamic spectrum was obtained using the high-speed dynamic power spectrum analyzer (P-hissa), by which one-day's data of geomagnetic pulsations can be transformed within 24 seconds to one sheet of dynamic spectrum covering almost all the period range from Pc1 through Pc5 bands [Saito, 1973] as shown in Figure 1. The block diagram of the P-hissa is shown in Figure 2.

The hissagrams for the period of August 4-9, 1972 are shown in Figure 3. The portion of the hissagrams indicated by DM is the one which is not yet analyzed because of an improper recording. The ssc's during the period are given by triangles below the hissagrams.

Dynamic spectral feature of Pc2, 3

At low-latitude stations like Onagawa, Pc3 and Pi2 are most predominant among the seven types of geomagnetic pulsations, Pc1-5 and Pi1-2. The characteristics of these pulsations have been reported to change during storm-time conforming to the following general laws.

1. Statistically, amplitudes of both Pc3 and Pi2 are enhanced with ssc and decrease approximately exponentially with the progress of storm time t.

2. Period of both Pc3 [Kato and Watanabe, 1957] and Pi2 [Yanagihara, 1960] are shortened with increasing Kp.

3. The local time of the shortest Pc3 period advances gradually from about 12h for Kp=1 to 7h for Kp=6 [Nagata and Fukunishi, 1968] as shown in Figure 4a.

From the above Law 1 we can derive the following two main types of low-latitude storm from the viewpoint of geomagnetic pulsations [Saito, 1962].

Pc3-type storm--When the ssc takes place in the daytime (about 0400-1600 LT) it follows very enhanced Pc3-like disturbances for about half a day and slightly enhanced Pi2-like fluctuations for the successive half a day.

Pi2-type storms--When the ssc takes place in the nighttime (1600-0400 LT) it follows very enhanced Pi2-like disturbances for about half a day and slightly enhanced Pc3-like disturbances for the successive half a day.

This general tendency is also seen in the storm events in the present report: the storms belong to the Pc3-type as a rule, since all the five ssc's took place during the morning hours from 0500 to 1200 LT. This is in contrast with the Pi2-type of the last severe storm of March 8, 1970 in which the ssc took place during the night (2300 LT) [Saito, 1971]. In the initial part (0800-1200 LT) of the August 9 storm event, the dynamic spectral pattern exhibited two sets of vertical patterns followed by the elongating period trends (Figure 1). The two vertical patterns are due to the Psc's associated with successive ssc's (see the solid triangles) and the two elongating period trends are explained by the fragments of the Pc2, 3 diurnal variations (Law 3, above) and the sudden shortening of the Pc2, 3 periods at the time of the second ssc (Law 2).

From the hissagrams in Figure 3, the time variations in the Pc2, 3 periods are extracted and superposed on a same LT-period diagram in Figure 4a, where the Kp for each Pc2, 3 is distinguished

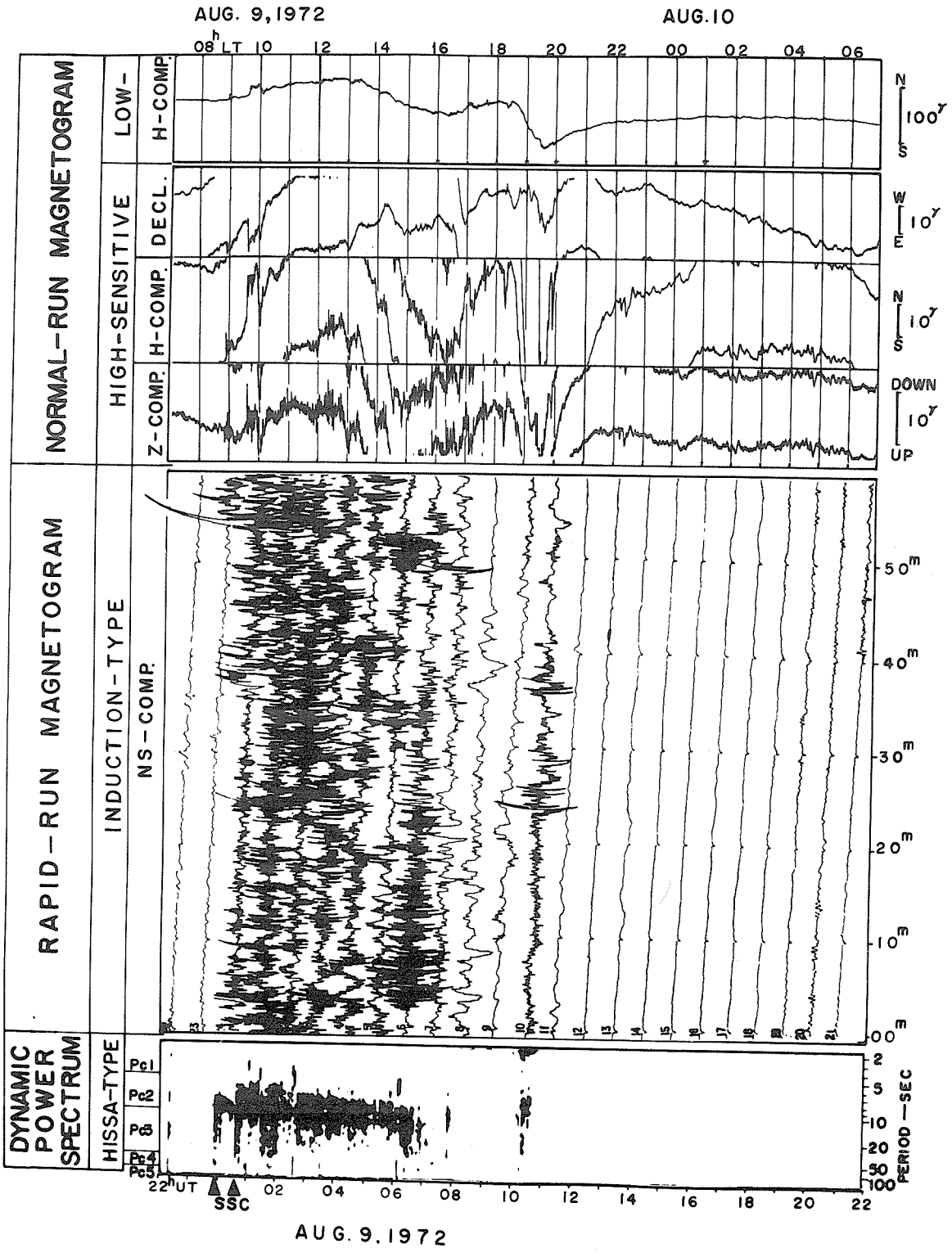

Fig. 1. Magnetic records for the August 8-9 storm event obtained at the Onagawa Magnetic Observatory. Top: Normal-run low- and high- sensitivity magnetograms. Middle: Rapid-run induction magnetogram obtained by the helicoidal pen-recorder. Bottom: Wide-range dynamic power spectrum of geomagnetic pulsations. ULF signals registered on a magnetic tape were analyzed by a newly-designed high speed power spectrum analyzer (P-Hissa).

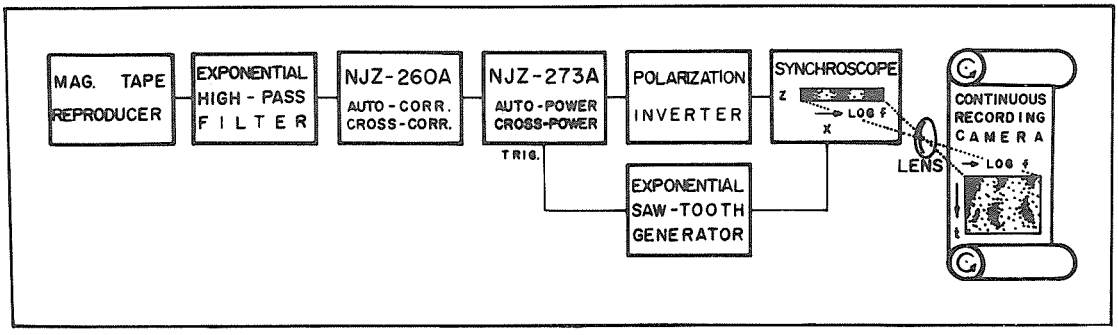

Fig. 2. Block diagram of P-Hissa [Saito, 1973].

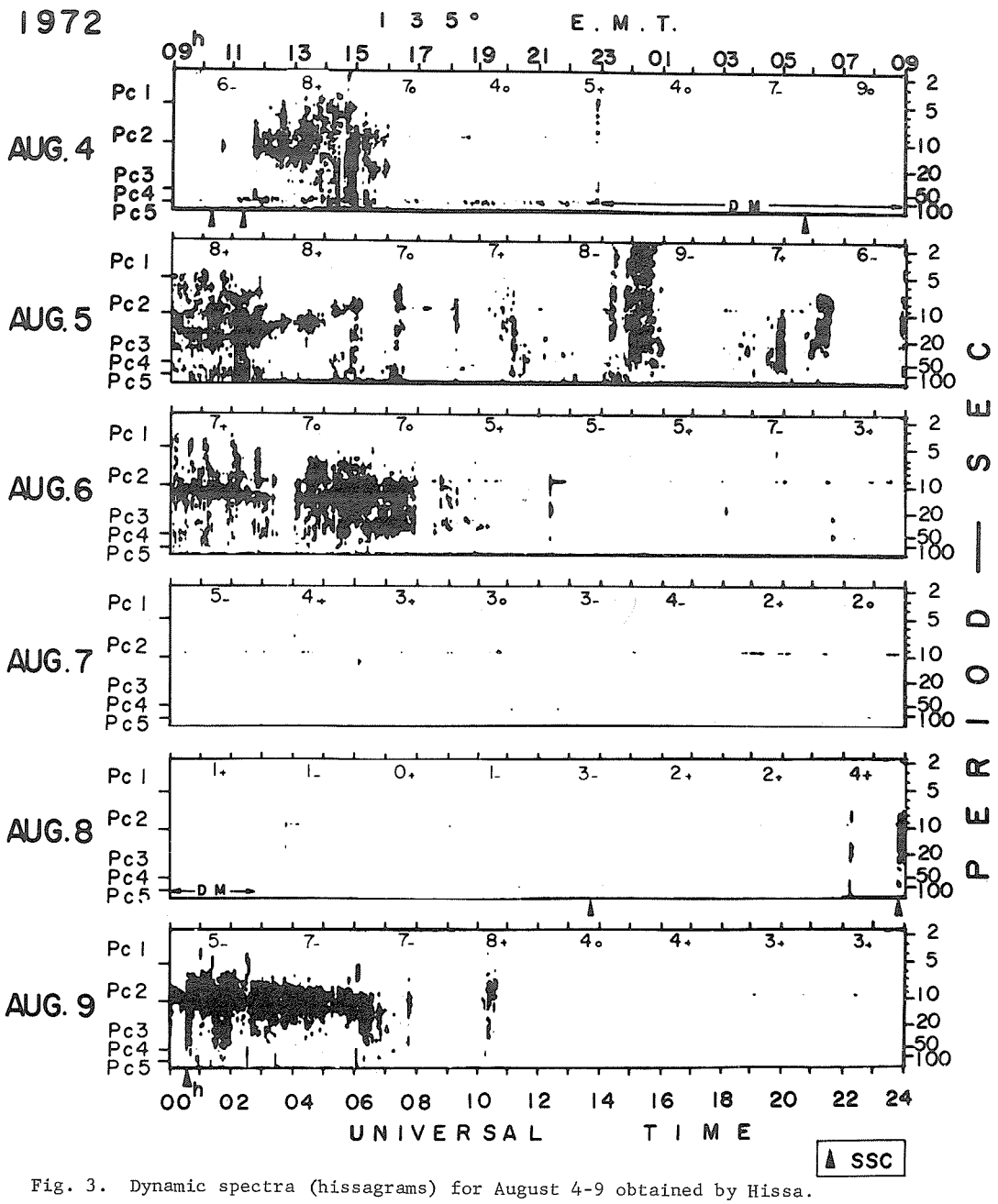

Fig. 3. Dynamic spectra (hissagrams) for August 4-9 obtained by Hissa.

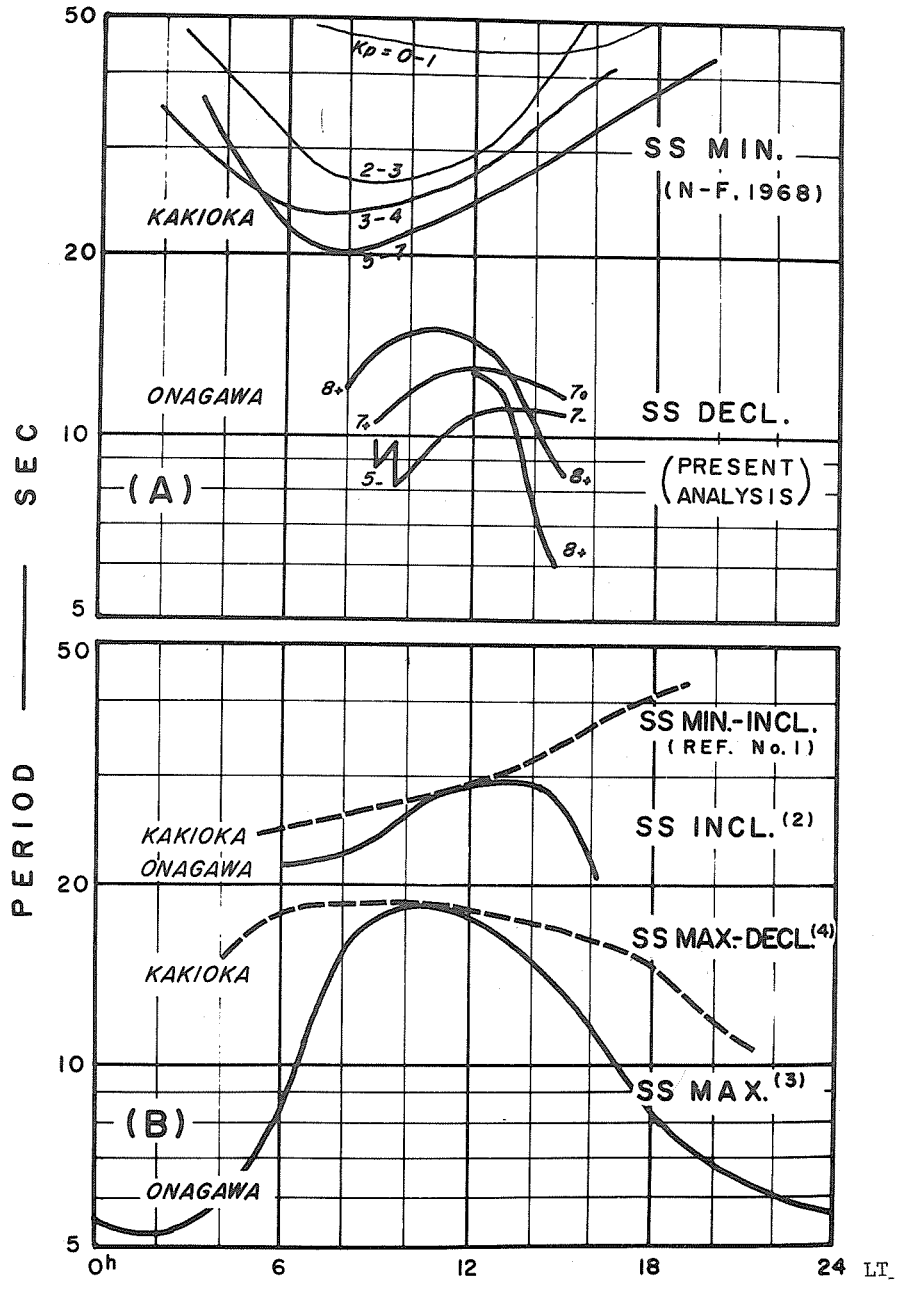

Fig. 4. Diurnal variation in the Pc2, 3 period (A) Present result compared with the result by Nagata and Fukunishi [1968]. (B) Various results based on the data for various phases of the solar cycle obtained by (1) Hirasawa and Nagata [1966]; (2) Kato and Morioka [1970]; (3) Kato and Saito [1959]; (4) Kawamura [1969]. See also the discussion given by Sakurai et al. [1969].

by the thickness of the trend curves. The statistical trends for Kp=0-7 obtained by Nagata and Fukunishi [1968] are also superposed on the same diagram. The Figure seems to show that the trends change from the U-type period diurnal variation during the quiet time to the inverted-U-type in very disturbed conditions like the present storm events. (The reader should take care that the U- and the inverted-U-type variations are named when the increase of the period is expressed to the upward direction of a diagram). It is interesting that the Pc2, 3 period trend in the severest storm of August 5 shows a clear inverted-U-type variation as was so during IGY. (Note also that the sunspot number during IGY when the remarkable inverted-U-type variations were frequently observed was still about three times larger than that during August 1972). This change of the trends from Kp=0 to Kp=8 may support our idea on the effects of both solar and geomagnetic activities on the type of the Pc2, 3 period diurnal variation [Saito, 1969: Sakurai, et al., 1969].

Other types of geomagnetic pulsations

When severe magnetic storm takes place, many types of geomagnetic pulsations characterized at higher latitudes, for example, Pc4, Pc5, PiC, etc., are generally observable even in low latitudes [Saito, et al., 1971]. The remarkable Pc5 variations during the severest August 4-5 storm event may be due to this nature of the low-latitude magnetic storm.

Pearl-type Pc1 pulsations occurred during the period from 1300 to 1800 UT on August 11 about 3 days after the ssc of the August 9 storm. (The hissagrams of August 10 and 11 are not presented in Figure 3 since they are quite transparent as is the hissagram for August 7). The occurrence of the PP seems to follow the general law that PP tends to occur on 3-7 days after a storm [Campbell, 1965; Tepley, 1966; McPherron and Ward, 1967].

REFERENCES

CAMPBELL, W. H. 1965 A review of seven studies of geomagnetic pulsations associated with auroral zone disturbance phenomena, Radio Sci. J. Res. Natl. Bur. Std/USCN-USRI 69D, 1187.

HIRASAWA, T. and T. NAGATA 1966 Spectral analysis of geomagnetic pulsations from 0.5 to 100 sec in period for the quiet sun condition, Pure Appl. Phys. 65, 102-124.

KAWAMURA, M. 1969 On the diurnal variation in the Pc3 period at Kakioka, paper presented to National ELF and ULF symp. held at Toyokawa, Japan on Jan. 26.

KATO, Y. and T. WATANABE 1957 A survey of observational knowledge of the geomagnetic pulsations, Sci. Rep. Tohoku Univ., Ser. 5, Geophysics 8, 157-185.

KATO, Y. and T. SAITO 1959 Preliminary studies on the daily behavior of rapid pulsations, J. Geomag. Geoele. 10, 221-225.

KATO, Y. and A. MORIOKA 1970 Study of the origin of geomagnetic pulsations in equatorial, low and middle latitudes, Rep. Ionos. Space Res. Japan, 24, 192-206.

MCPHERRON, R. L. and S. H. WARD 1967 Correlation between occurrence of pearl pulsations and interplanetary magnetic field sector boundaries, J. Geophys. Res. , 72, 393-398.

NAGATA, T. and H. FUKUNISHI 1968 Dependence on geomagnetic activity of magnetic pulsation frequency of Pc3 and Pc4 range, Geophys. J. Roy. Astron. Soc. 15, 69-78.

SAITO, T. 1962 Statistical studies on three types of geomagnetic continuous pulsation, Part 1, Type Ipc (5-40 sec), Sci. Rep. Tohoku Univ., Ser. 5, Geophys. 14, 81-106.

SAITO, T. 1969 Geomagnetic pulsations, Space Science Reviews 10, 319-412.

SAITO, T., T. SAKURAI and A. MORIOKA 1971 Spectral structure of geomagnetic pulsations during the severe magnetic storm on March 8, 1970, Rep. Ionos. Space Res. Japan 25, 70-73.

SAITO, T. 1971 Magnetic storm of March 8, 1970 at Onagawa Magnetic Observatory, Tohoku Univ., Report UAG-12. III, 386-387.

SAITO, T. 1973 Geomagnetic pulsations as a possible cause of cosmic ray microvariations, Cosmic Ray Research (Uchûsen Kenkyû) in press.

SAKURAI, T., A. MORIOKA and T. SAITO 1969 The structure in the period of Pc2, 3 geomagnetic pulsations, Proc. 2nd IASY Symp. 76-85, Publ. by Inst. Space Aeronaut. Sci. Univ. Tokyo.

TEPLEY, L. 1966 Recent investigations of hydromagnetic emissions. Partl. Experimental observations, J. Geomag. Geoelectr. 18, 227-256.

YANAGIHARA, K. 1960 Geomagnetic pulsations in middle latitudes, Morphology and its interpretation, Mem. Kakioka Mag. Obs. 9, 15-74.

Storms between August 4 and 11, 1972

by

Bohumila Bednářová-Nováková
Geophysical Institute, Czechoslovak Academy of Sciences
Prague, Czechoslovakia

The special case of a series of storms between August 4 and 11, 1972 is an example of the interaction of solar fields following one another, as if they were interconnected, so that they act as a whole, although they in fact represent a long series, or a large area. Similar cases were also observed earlier when a series of active centers, following one another, was involved. It is interesting that a series of this kind usually acts on the geomagnetic field in the same way: if a storm follows the CMP of the first group, a storm follows the CMP of the other centers, associated with this system.

In the case of the storm of August 1972 there was a series of unstable solar fields, following one another and dependent on one another. This can be seen,e.g., on the photographs in the Photographic Journal of the Sun Nos. 62 and 63 of August 1 -9, 1972. Figure 1 illustrates this schematically. Using the observations, made at the Geophysical Institute of the Czechoslovak Academy of Sciences on July 28, a storm was forecast for August 4 and 5 according to the chromospheric structure and the occurrence of prominences. Unfortunately observations could not be made over the whole critical period because of unfavorable weather and for technical reasons. We then observed the sun on August 7, after some of the systems of fields had already disappeared.

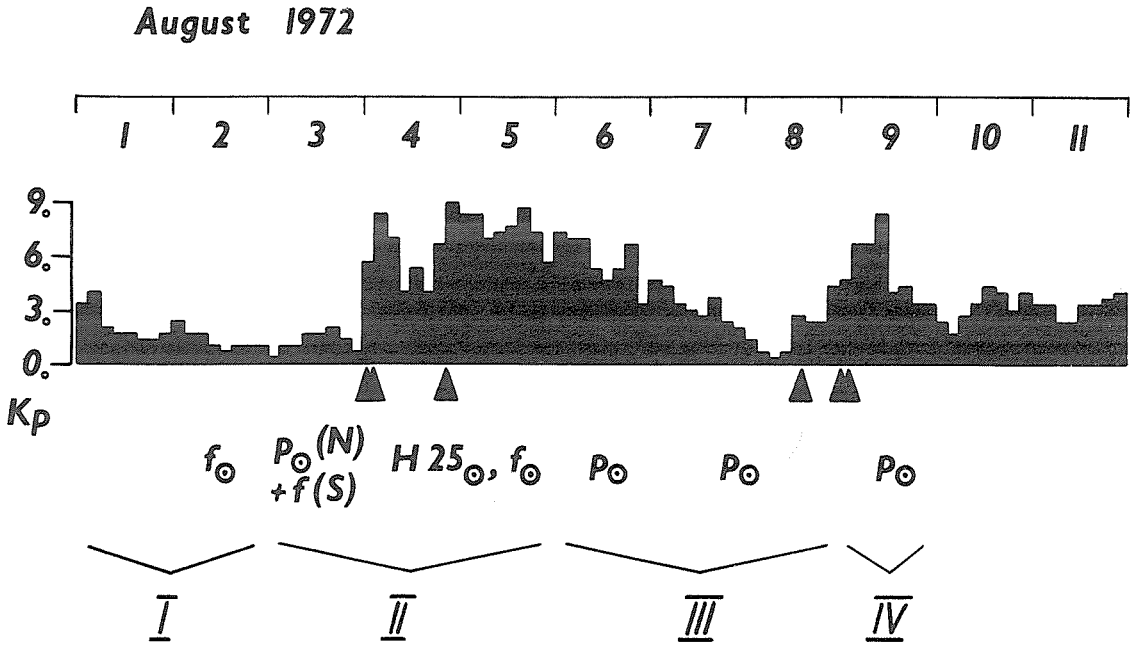

Fig. 1. At the top is shown the character of the geomagnetic activity in terms of the Kp-index for the interval August 1 - 11, 1972. The symbols indicate the times of ssc's. The solar situation preceding the geomagnetic storms is indicated by the symbols: f⊙-filament at the center of the disk; and P⊙ - plage at the center of the disk. At the bottom are shown the approximate time periods for the passages of the four principal systems of solar fields before the geomagnetic storms.

The solar situation preceding the geomagnetic storms of August 4 - 11, 1972 can be divided into 4 principal parts:

1) The first part is characterized by a central filament and an H-alpha plage at the center of the solar disk and by the occurrence of a prominence on July 27 and 28 at the east limb. After its CMP a geomagnetic storm began with two ssc's on August 4 at 0119 and 0220 UT.

2) The second part was under the influence of a very strong local, very variable field H 25 directly in the center of the solar disk (it overlapped the H-alpha plage). It was characterized by a prominence on July 29 at the east limb and on the west on August 11. The geomagnetic storm began at 2054 UT on August 4 with an ssc and continued until August 7.

3) H-alpha plages passed through the center of the solar disk on August 7 and 8. Two ssc's followed at 1342 and 2354 UT on August 8 and at 0036 UT on August 9.

4) Further H-alpha plages passed through the center of the sun on August 9. The prominence at the west limb on August 14 and 15 was associated with them. A weaker storm followed on August 10 and 11.

Since all four systems of solar fields were very close to one another, they could act on one another very easily. Changes in one system could easily be reflected in the neighboring system. Because all these variable systems reached out into the center of the disk, they resulted in the generation of geomagnetic storms, since conditions had been created for the existence, or additional generation, of coronal formations which were positioned radially above the center of the solar disk. This situation is described in the model which was developed at the Geophysical Institute of the CSAS. [Bednarova-Novakova, 1966]. These systems, following one another, can also be seen on the Mt. Wilson magnetograms of August 6, 7 and 8, and August 12 and 13 and on the solar H-alpha maps from Boulder [Lincoln et al, 1972].

REFERENCES

BEDNAROVA-NOVAKOVA, B 1966 The Solar Causes of the Occurrence of Selected Geomagnetic Storms and Geomagnetic Quiet, Studia geoph. et geod., 10, 437-445.

LINCOLN, J. V. and H. I. LEIGHTON 1972 Preliminary Compilation of Data for Retrospective World Interval July 26 - August 14, 1972, World Data Center A for Solar Terrestrial Physics , Report UAG-21, November 1972.

Discussion of the Geomagnetic Data Recorded at Hyderabad, India during July 26 - August 14, 1972

by

B. J. Srivastava
National Geophysical Research Institute, Hyderabad, India

ABSTRACT

The geomagnetic data recorded at Hyderabad (a low-latitude station outside the electrojet region in India) during July 26 - August 14, 1972 are presented and discussed. Unusual and unexpected magnetic activity was observed at Hyderabad on August 4, 5, 6 and 9 in the form of three sc storms in association with solar flares. The second storm of August 4, 1972 is compared with the great magnetic storm of July 17, 1959 as recorded at Alibag. The average estimated speeds of the solar wind causing the August 1972 events are compared with the speeds as measured by Pioneer 9 instruments.

Introduction

Established toward the end of 1964, the NGRI magnetic observatory at Hyderabad is located just outside the influence of the equatorial electrojet and is well inland so as not to be affected by the oceanic induced electric currents. It is an important low-latitude station. The coordinates of the station are: Geographic Latitude N17.41, Longitude E78.55; Geomagnetic Latitude N7.6, Longitude 148.9.

The observatory is equipped with a set of La Cour variometers fully compensated for temperature changes, for continuous photographic recording of the three magnetic elements H, D and Z at a normal paper speed of 15 mm/hour, in a semi-underground room where the daily range of temperature is less than $1/2^{o}$C. Two sets of QHMs and BMZs are used for calibrating the magnetograms. The scale values of the variometers are:

H	4.6γ/mm
D	0.3'/mm(3.5γ/mm)
Z	3.8γ/mm

The purpose of this paper is to discuss the geomagnetic data recorded at Hyderabad during the Retrospective World Interval, July 26-August 14, 1972 which was characterized by unusual solar and geomagnetic disturbances.

The Data

The mean hourly values of D, H, and Z recorded at Hyderabad for the period July 26 - August 14, 1972 are given in Tables 1, 2 and 3 respectively. The data on principal magnetic storms observed at Hyderabad are given in Table 4 and the K and C indices of geomagnetic activity in Table 5. Table 6 gives the details of the solar flares responsible for the magnetic storms, the average enhanced solar wind speeds as calculated from the sun-earth distance 1.495×10^{8} km and the delay time between the flare and the associated sc, and the solar wind speeds as measured by Pioneer 9 at a distance of 1.1618×10^{8} km from the sun within the earth orbit, the earth-sun probe angle being 45^{o} for Pioneer 9.

Discussion

An inspection of the Hyderabad magnetograms for the period July 26 - August 14, 1972 shows that the magnetic conditions were fairly calm from July 26 to August 3. Following intense solar flare activity, a sudden increase in the geomagnetic activity occurred from August 4 to August 6. During the next two days, August 7 and 8, calm conditions existed. But again towards the end of August 8, the geomagnetic activity increased which continued on August 9. This sudden increase in geomagnetic activity was rather unusual and unexpected in 1972. From August 10 to August 14, once again fairly quiet magnetic conditions prevailed. Thus during the Retrospective World Interval, three days (August 4, 5 and 9) were extremely disturbed. August 6 was moderately disturbed.

Pioneer 9 recorded solar wind velocity >1000 km/sec on August 5 at 0030 UT, which happens to be the highest velocity ever recorded on the Pioneer series of spacecrafts, the speed ordinarily observed being 300-400 km/sec [Solar-Geophysical Data, 1972].

We now discuss the magnetic storms given in Table 4. The first storm of moderate intensity began with a sudden commencement on August 4 at 0119 UT, followed by another sc after an hour at 0220 UT, and showed a range of 149γ in H at Hyderabad. The storm ended the same day around 1800 UT without a well-developed main phase. Very rapid oscillations (pulsations) of the geomagnetic field over seconds and minutes were observed during the storm. Following a 3B flare, the second storm of severe intensity commenced suddenly on August 4 at 2054 UT. The sc amplitude in H was 99γ which is the highest on record at the Hyderabad Observatory during the past eight years of its existence. It is significant that this large sc-amplitude was recorded at Hyderabad during night time. Shirgaokar

Table 1

Hourly values of Declination (West), D (July 26-August 14, 1972
(Averages for sixty minutes centered at half hours of Universal Time) D
1°W plus tabulated values in tenths of minute of arc (W)

Hyderabad

Date 1972	HOURS UT 00-01	01-02	02-03	03-04	04-05	05-06	06-07	07-08	08-09	09-10	10-11	11-12	12-13	13-14	14-15	15-16	16-17	17-18	18-19	19-20	20-21	21-22	22-23	23-24	Daily Mean	Maximum Time	Maximum Mag.	Minimum Time	Minimum Mag.	Range†
July 26D	382	373	373	384	389	391	398	400	396	390	386	384	380	385	390	389	389	387	385	384	384	384	385	381	386	0203	370	0724	400	27
27	374	363	365	370	378	389	403	407	407	408	407	398	394	395	396	395	393	392	390	390	389	389	390	389	390	0140	362	0902	408	45
28	385	373	368	371	380	393	408	414	419	419	413	404	396	393	392	394	394	394	394	394	394	394	395	395	392	0224	365	0828	421	51
29Q	383	372	370	373	388	402	415	419	415	406	394	391	389	393	397	396	398	398	396	397	397	396	394	392	394	0224	365	0828	421	51
30	387	373	365	370	385	401	416	428	433	429	421	409	400	397	400	400	400	398	398	397	395	394	395	395	399	0240	363	0826	433	68
31	392	381	373	372	373	380	394	409	418	419	417	410	403	399	402	402	401	399	398	395	393	395	395	397	397	0304	371	0900	419	47
August 01	391	379	370	370	375	391	409	413	413	411	396	389	386	392	395	394	390	389	388	389	390	392	393	391	391	0258	366	0800	414	44
02	382	370	367	367	374	387	397	406	413	414	410	405	396	393	395	395	395	396	396	395	396	394	393	392	393	0351	364	0900	417	47
03Q	384	375	376	384	393	403	411	421	421	412	402	394	391	394	397	398	397	397	397	396	394	394	393	391	396	0200	374	0756	423	46
04D	385	381	382	381	394	397	400	404	407	406	409	411	406	400	401	400	397	393	395	395	393	389	354	342	393	2308	310	0526	416	69
05D	353	338	338	361	375	395	403	414	415	414	406	402	397	394	404	389	379	387	387	397	388	381	377	374	386	0201	324	0713	424	78
06D	358	352	349	361	370	375	388	399	402	399	392	389	386	383	387	385	385	386	391	387	388	385	383	379	382	0238	335	0746	406	53
07	368	355	357	364	377	391	399	399	401	404	400	390	385	386	385	384	385	386	386	386	386	386	386	386	385	0157	353	0927	405	48
08	379	371	370	379	395	407	413	410	403	395	387	386	390	391	391	391	391	389	389	386	385	384	383	380	389	0204	369	0610	413	43
09D	369	358	361	374	388	396	397	403	394	392	368	373	384	387	392	390	388	385	382	378	375	374	375	370	381	0140	356	0709	407	45
10	363	359	365	376	396	409	415	411	403	389	379	373	375	380	385	388	395	392	392	389	388	386	381	380	386	0117	358	0610	415	56
11	366	352	353	365	385	403	411	409	406	405	403	394	389	389	398	392	388	389	389	388	385	386	384	380	388	0143	349	0630	412	59
12	369	350	345	356	381	397	412	415	413	408	399	389	386	388	390	391	391	391	391	390	389	387	386	383	387	0202	343	0720	416	70
13Q	376	367	368	377	393	405	413	421	420	410	403	397	391	392	395	394	391	390	390	390	390	389	388	386	393	0207	364	0756	421	53
14	379	363	359	371	386	400	408	422	424	413	402	389	385	392	396	395	392	393	392	391	390	388	386	382	392	0220	358	0800	426	65

† Range is the difference between maximum and minimum hourly values for the day.

Table 2

Hourly Values of Horizontal Intensity H (July 26-August 14, 1972)
(Averages for sixty minutes centered at the half hours of Universal Time)
39,500 γ plus tabulated values in gammas (γ)

H

Hyderabad

Date 1972	HOURS UT 00-01	01-02	02-03	03-04	04-05	05-06	06-07	07-08	08-09	09-10	10-11	11-12	12-13	13-14	14-15	15-16	16-17	17-18	18-19	19-20	20-21	21-22	22-23	23-24	Daily Mean	Maximum Time	Maximum Mag.	Minimum Time	Minimum Mag.	Range†
July 26D	425	425	433	446	457	459	457	426	418	416	413	408	401	401	397	385	401	398	402	404	406	408	412	412	417	0610	470	1524	379	74
27	413	412	416	419	418	426	426	439	441	434	423	406	404	410	413	414	412	419	417	416	414	414	416	415	418	0820	442	1209	401	36
28	417	417	422	432	450	463	471	467	452	444	433	424	417	416	413	411	413	415	417	419	420	420	419	420	429	0636	472	1546	411	60
29Q	420	422	429	447	468	483	490	484	468	451	436	428	426	424	424	421	421	424	422	423	424	424	422	425	438	0632	492	0052	420	70
30	426	431	439	455	476	489	494	490	477	465	455	448	439	436	438	436	438	435	438	437	436	437	440	439	456	0644	495	0000	425	68
31	440	439	437	442	451	462	472	476	472	464	458	451	450	453	454	455	455	457	455	451	448	449	445	447	453	0750	477	0240	436	39
August 01	438	435	426	425	439	444	454	458	449	437	424	409	399	398	402	406	406	410	413	417	418	418	416	413	423	0728	461	1236	396	59
02	413	409	413	427	444	460	470	476	469	452	439	426	423	427	428	426	426	425	426	424	424	425	429	429	434	0728	477	0128	408	66
03Q	431	439	449	469	488	499	498	491	474	460	457	448	437	430	429	431	430	430	430	432	432	434	434	434	449	0544	503	1440	427	70
04D	435	446	474	460	436	410	412	384	406	405	400	380	367	351	356	361	359	354	362	369	378	444	409	348	396	2244	591	2353	291	126
05D	327	315	307	294	298	379	366	378	351	359	359	373	372	364	424	362	319	337	348	377	355	342	331	337	349	1436	476	0204	228	129
06D	350	344	328	314	346	364	350	350	333	331	329	328	342	349	347	362	380	372	387	373	367	371	367	367	352	1808	399	0346	304	73
07	369	369	381	382	399	402	406	405	407	407	391	384	379	377	382	381	378	378	381	381	381	384	389	389	387	0700	415	0141	364	38
08	388	388	390	400	418	424	424	422	414	406	401	399	397	395	396	394	391	392	393	390	385	387	388	396	399	0556	425	2000	382	39
09D	422	428	436	453	445	420	386	377	386	357	193	244	271	285	295	305	326	324	328	333	337	340	333	334	348	0348	464	1032	164	259
10	340	349	366	381	397	407	403	389	388	377	364	355	342	353	353	361	363	365	369	367	371	373	363	360	369	0532	408	0000	333	67
11	358	355	365	376	389	403	405	401	390	377	369	372	371	375	377	372	382	377	388	377	378	386	378	378	379	0708	406	0119	352	50
12	380	386	399	417	428	436	437	432	419	401	392	385	387	389	389	387	385	394	393	390	388	389	389	389	399	0618	439	0009	378	58
13Q	392	393	403	419	432	436	435	432	421	413	409	408	409	407	406	407	397	395	394	399	400	401	403	404	409	0500	439	0000	390	45
14	408	406	412	424	439	446	448	451	452	444	429	408	398	405	407	404	399	400	404	407	405	402	404	401	417	0812	454	1232	395	54

† Range is the difference between the maximum and minumum hourly values for the day.

Table 3

Hourly Values of Vertical Intensity Z (July 26-August 14, 1972)
(Averages for sixty minutes centered at half hours of Universal Time)
14,500γ plus tabulated values in gammas (γ)

Hyderabad

Date 1972	HOURS UT 00–01	01–02	02–03	03–04	04–05	05–06	06–07	07–08	08–09	09–10	10–11	11–12	12–13	13–14	14–15	15–16	16–17	17–18	18–19	19–20	20–21	21–22	22–23	23–24	Daily Mean	Maximum Time	Maximum Mag.	Minimum Time	Minimum Mag.	Range†
July 26D	396	402	401	398	400	399	395	388	395	402	400	399	395	392	393	393	394	395	395	395	395	395	396	396	396	0156	405	0732	386	14
27	399	395	389	379	370	365	362	367	369	371	375	376	380	383	387	389	390	392	391	392	392	392	392	393	383	0030	400	0602	360	36
28	396	398	392	386	378	376	377	377	378	382	385	386	386	385	387	388	390	391	392	392	392	392	392	393	387	0148	398	0546	375	23
29Q	394	391	385	378	374	372	372	375	377	379	379	381	383	384	385	387	388	389	389	389	390	390	390	391	384	0032	395	0556	370	22
30	393	396	393	388	381	374	369	370	371	373	374	377	380	381	384	386	387	388	389	389	389	389	389	389	383	0120	396	0700	368	27
31	392	397	396	391	386	374	363	360	361	365	372	376	381	382	384	385	386	388	388	389	388	389	389	389	382	0152	398	0752	360	36
August 01	391	392	388	384	383	372	363	371	381	386	389	389	388	385	386	389	390	391	389	389	389	388	389	389	385	0153	392	0644	362	29
02	392	391	387	381	367	358	353	356	355	357	364	374	380	380	381	384	385	385	387	386	387	387	387	387	377	0036	392	0644	351	38
03Q	391	391	391	389	384	382	386	386	384	382	386	386	384	383	384	385	386	387	387	388	388	388	389	389	386	0120	392	0502	381	9
04D	389	387	381	374	369	365	386	392	386	374	371	373	378	384	385	389	389	390	391	391	392	404	402	406	385	2257	423	0550	354	40
05D	394	400	386	379	380	381	381	378	387	393	389	386	389	391	396	394	388	391	393	397	393	392	390	392	389	0058	410	0715	369	22
06D	397	391	378	362	363	369	368	371	380	386	389	390	392	391	392	393	394	393	393	392	391	391	391	392	385	0011	400	0358	358	35
07	395	391	382	372	361	365	365	366	370	379	384	387	387	385	385	387	387	388	389	387	389	389	389	390	382	0026	396	0426	359	35
08	392	390	389	374	369	365	368	372	378	386	386	384	382	384	385	387	387	388	389	390	389	389	389	391	384	0033	393	0546	365	27
09D	396	395	386	374	362	364	367	379	389	386	369	395	383	386	391	392	394	395	394	394	394	393	392	393	386	0107	398	0424	358	34
10	395	394	392	387	382	384	383	383	392	395	392	387	385	385	387	388	388	389	389	391	392	392	392	392	389	0858	396	0444	381	14
11	396	393	383	374	368	370	375	383	384	383	381	381	382	384	385	388	388	389	390	390	390	391	390	392	385	0048	397	0414	367	28
12	395	395	386	372	362	366	370	378	382	385	384	381	381	383	385	385	386	388	389	389	389	389	389	389	383	0044	397	0420	362	33
13Q	392	392	387	381	377	379	379	377	377	381	383	384	385	385	385	384	385	386	387	387	388	388	388	389	384	0040	393	0424	376	16
14	393	394	387	378	376	373	370	367	377	386	390	392	386	384	385	386	387	388	388	388	388	388	388	388	384	0112	395	0714	365	28

† Range is the difference between the maximum and minimum hourly values for the day.

TABLE 4

Magnetic Storms Recorded at Hyderabad during July 26 to August 14, 1972

Date	Storm Time UT Start	Storm Time UT End	Type	Sudden Commencement Amplitudes D(')	Sudden Commencement Amplitudes H(γ)	Sudden Commencement Amplitudes Z(γ)	C-figure activity	Maximal activity on K-scale (0-9) d	Maximal activity on K-scale (0-9) 3-hr. period.	Maximal activity on K-scale (0-9) K-index	Ranges D(')	Ranges H(γ)	Ranges Z(γ)
1972 August													
04	0119	0418	SC	-0.2	+12	-2	MS	04	2	7	5	149	42
04	0220	--	SC	-0.2	+34	-3	-	-	-	-	-	-	-
04	2054	0711	SC	-1.1	+99	-5	S	04	8	9	11	363	63
05	2344	-	SI	-0.3	+22	-2	-	-				-	
08	1340	-	SC	-0.2	+8	-1	-	-				-	
08	2353	0922	SC	-0.2	+24	-1	S	09	4	8	5	301	40
09	0036	-	SC	-0.1	+18	-1			-			-	

*S = Severe
MS = Moderately Severe

TABLE 5

HYDERABAD, INDIA

K AND C INDICES OF GEOMAGNETIC ACTIVITY, JULY 26–AUGUST 14, 1972

Scale values of variometers: (La Cour)
Lower limit for K 9 = 300 γ H 4.6 γ/mm
D 3.5 γ/mm (0.3'/mm)
Z 3.8 γ/mm

Recording speed 15 mm/hr.

DAY UT	JULY 1972 K-Indices	Sum	C	DAY UT	AUGUST 1972 K-Indices	Sum	C
26	2342 2313	20	1	1	3221 1111	12	0
27	1332 1211	14	1	2	1111 1111	8	0
28	1111 1100	6	0	3	2221 2111	12	0
29	0101 1111	6	0	4	5764 4479	46	2
30	0012 2212	10	0	5	7876 7754	51	2
31	1111 1133	12	1	6	6653 4442	34	1
				7	2332 2221	17	1
				8	1111 2224	14	1
				9	4668 6433	40	2
				10	2232 4323	21	1
				11	3222 2333	20	1
				12	2212 1311	13	0
				13	1211 1321	12	0
				14	2123 3232	18	1

TABLE 6

Comparison of Computed Solar Wind Velocity with those observed by Pioneer 9

Observed solar flare (importance) UT	SSC (UT)	Time interval between flare and SSC in hours (approx)	Computed average solar wind velocity (approx. km/sec)	Observed solar wind velocity at Pioneer 9 (average for the flare-SC interval) (Km/sec)
1972 August d h m/ h m	d h m			
02 18 38/18 52 (also sfe)(Sb)	04 01 19	31	1,340	516
02 20 06/01 11 (Ib)	04 02 20	31	1,340	516
04 06 45/10 00 (3b)	04 20 54	14	2,966	776
07 03 48/04 50 (also sfe)(1b)	08 13 40	35	1,187	515
07 15 13/1615 (also sfe)(3b)	08 23 53	33	1,258	479

and Srivastava [1963] pointed out while discussing the July 1959 events that large sc's of 100γ and above in H had a tendency to occur during night-time at Alibag. Again Srivastava [1966] demonstrated the occurrence of large sc amplitudes around local midnight in low and middle latitudes. The second storm was also characterized by numerous large-amplitude rapid oscillations (micropulsations over seconds and minutes) throughout. A range of 363γ in H was observed during the storm and the highest K-index was 9. The storm was fairly long-drawn-out and ended around 1100 UT on August 7. An SI was also observed at 2344 UT on August 5.

This storm resembles the great magnetic storm of July 17, 1959 in several respects. In Figure 1 are reproduced the Alibag and Hyderabad magnetograms of the storms. Both the storms were associated with solar flares. The storm of July 17, 1959 started with an sc at 1638 UT (night-time at Alibag) of amplitude 148γ in H at Alibag and showed a range of 305γ with one K-index of 8 [Shirgaokar and Srivastava, 1963]. Very rapid large-amplitude pulsations similar to the present ones were also recorded during that storm. The sc, pulsatory character and severity of the second storm of August 1972 thus compare with those of the July 17, 1959 storm which occurred near the sunspot maximum , indicating an abrupt increase in the magnetic activity in the first week of August 1972 when the activity should have been on the decline following the sunspot cycle.

The third storm began with an sc on August 8, 1972 at 2353 UT. A small sc was also observed much earlier at 1340 UT. Another sc was noticed at 0036 UT on August 9. The storm ended around 2200 UT on August 9. It was of severe intensity with a range of 301γ in H and one K-index of 8 at Hyderabad. This storm was different in character from the first two storms in that the large-amplitude rapid oscillations were not very prominent in this storm although some pulsations were still there in its initial phase and the early part of its main phase.

We now turn to Table 6. The average speed of the solar wind responsible for the first and the third storms works out as 1,300 km/sec, while for the second storm it is of the order of 3,000 km/sec, which agrees with the solar wind speeds of 1,000 - 3,000 km/sec generally estimated for storm-generating solar winds or corpuscular streams [Chapman and Bartels, 1940]. But the average solar wind speed as measured by Pioneer 9 was about 500 km/sec for the first and the third storms, and 800 km/sec for the second storm, at a distance of about 5,000 earth radii from the earth on its sunward side. This apparent discrepancy in the solar wind speed will have to be fully understood.

Let us now examine Table 5, which gives the K and C indices observed at Hyderabad during the Restrospective World Interval. July 26 was slightly disturbed with one K-index of 4. From July 27 to August 3 calm magnetic conditions with individual K-indices of 3 or less than 3 were observed. August 4, 5 and 9 were heavily disturbed with K-indices of 8 and 9. August 6 was moderately disturbed. August 7, 8, 10, 11 and 14 were only slightly perturbed. August 12 and 13 were again quiet days.

Acknowledgments

I am grateful to Dr. Hari Narain, Director, National Geophysical Research Institute, Hyderabad, India, for his kind permission to publish this paper. I am also indebted to my colleagues at the Hyderabad Geomagnetic Observatory for the excellent records and the routine magnetic data discussed above.

REFERENCES

CHAPMAN, S. and J. BARTELS 1940 Geomagnetism (Clarendon Press, Oxford), II, 852.

SHIRGAOKAR, A. J. and B. J. SRIVASTAVA 1963 Geomagnetic storms in July 1959, Proc. IGY Symp., February 13-16, 1961, New Delhi, II, 74-77.

SRIVASTAVA, B. J. 1966 On the occurrence of large SSC amplitudes in the horizontal intensity of geomagnetic field in middle latitudes around local midnight, J. Geomag. Geoelec (Japan), 18, 437-442.

1972 Solar-Geophysical Data, 337, Part I, 8-10, 29-30. U.S. Dept. of Commerce (Boulder, Colorado, USA, 80302).

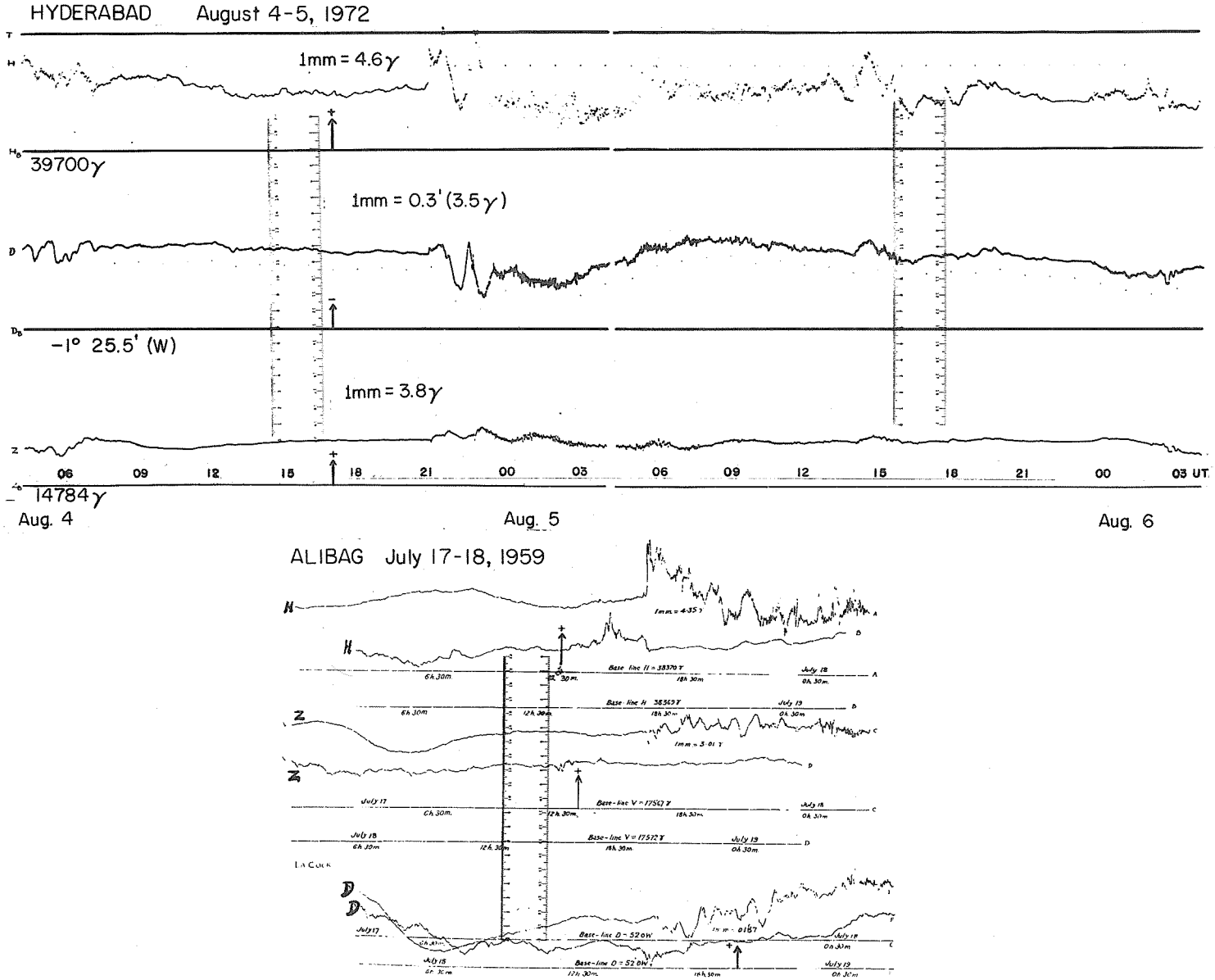

Fig. 1. Reproductions of the Hyderabad magnetogram of the August 4, 1972 storm and the Alibag magnetogram of the July 17, 1959 storm, showing the pulsatory character of the two severe storms.

On the Giant Pulsations of the 04-06 August 1972 Geomagnetic Storm Observed at Manila

by

J. E. Salcedo, Manila Observatory

The first shock front of the series of solar activities on August 2, 1972, McMath region 11976, commenced as a seemingly mild storm, producing an SSC of 32 gammas on the geomagnetic X-component at 0119 to 0123 UT on 04 August. About an hour later at 0221 to 0224 UT another SI of 45 gammas was felt while going through a typical regression. A bigger magnetic storm with fluctuations followed until about 0730 UT.

At 2054 UT a third shock was felt from the compression of the X-component of 85 gammas in a period of only one minute. Fluctuations similar to the initial phase followed until about 2130 UT when it underwent a great 250-gamma magnetic bay. Before its recovery from the bay, quasi sinusoidal variations were observed with a period of about one minute on the average. At 2242 UT an intense SI of 160 gammas, with only about a minute duration, was felt. The accompanying figure shows a reproduction of the geomagnetic storm on the X-component.

The giant pulsation storm activity can be grouped into the following: pulsations with a period of 1 minute or less, from 2238 to 2330 UT; pulsations with a period of about 3 minutes, from 2330 to about 0300 UT on the 5th; and pulsations with a period of about 5 minutes, from 0300 to about 0510 UT. At 0510 UT activity reverted to the 3-minute period pulsations until about 0740 UT when damped to a typical mag-storm variation. Peak-to-peak amplitude variations of 200 gammas were reached on at least two occasions. Average amplitude variation for the 3-minute period pulsations was about 100 gammas, while for the 5-minute period pulsations it was about 40 gammas.

It is interesting to note that the giant pulsations were observed during the local daytime of 05 August while the damped activity can be traced to past midnight. The pronounced pulsations coincided with the optimizing of the ionosphere by solar illumination. This suggests that the ionosphere on the daytime of the 5th provided a favorable medium for the transmission of hydro-magnetic waves excited by the gusty structure of the solar wind impinging on the magnetosphere.

Prior to the great geomagnetic storm on 04 August, there were three groups of reported brilliant flares from McM 11976 which are tabulated below:

Grp	Day/Start-Max (UT)	Imp	Loc.	Associated Event	Day/Start-Max (UT)	Int (γ)
1	02/0316-0355	*1B	N14E35	SSC	04/0119-0123	32
1	02/0505-0515	*2B	N13E35	SI	04/0221-0224	45
2	02/1839-1844	1B	N14E26	SSC	04/2054-2055	85
2	02/1958-2058	2B	N13E28	SI	04/2242-2243	160
2	02/2248-2248	*1B	N12E25			
3	04/0617-0640	3B	N14E08			
3	04/0740-0751	*2B	N13E08			
3	04/0858-1008	*1B	N15E06			

The third group was the most energetic but least in the contribution to the geomagnetic storm. The second group, based on solar wind speeds reported by Pioneer satellites, was most likely the origin of the great pulsation storm. The initial phase of the storm can be associated with the first group of activities on 02 August.

We thank AFCRL for supporting this work and V. L. Badillo and J. J. Hennessey for their encouragement.

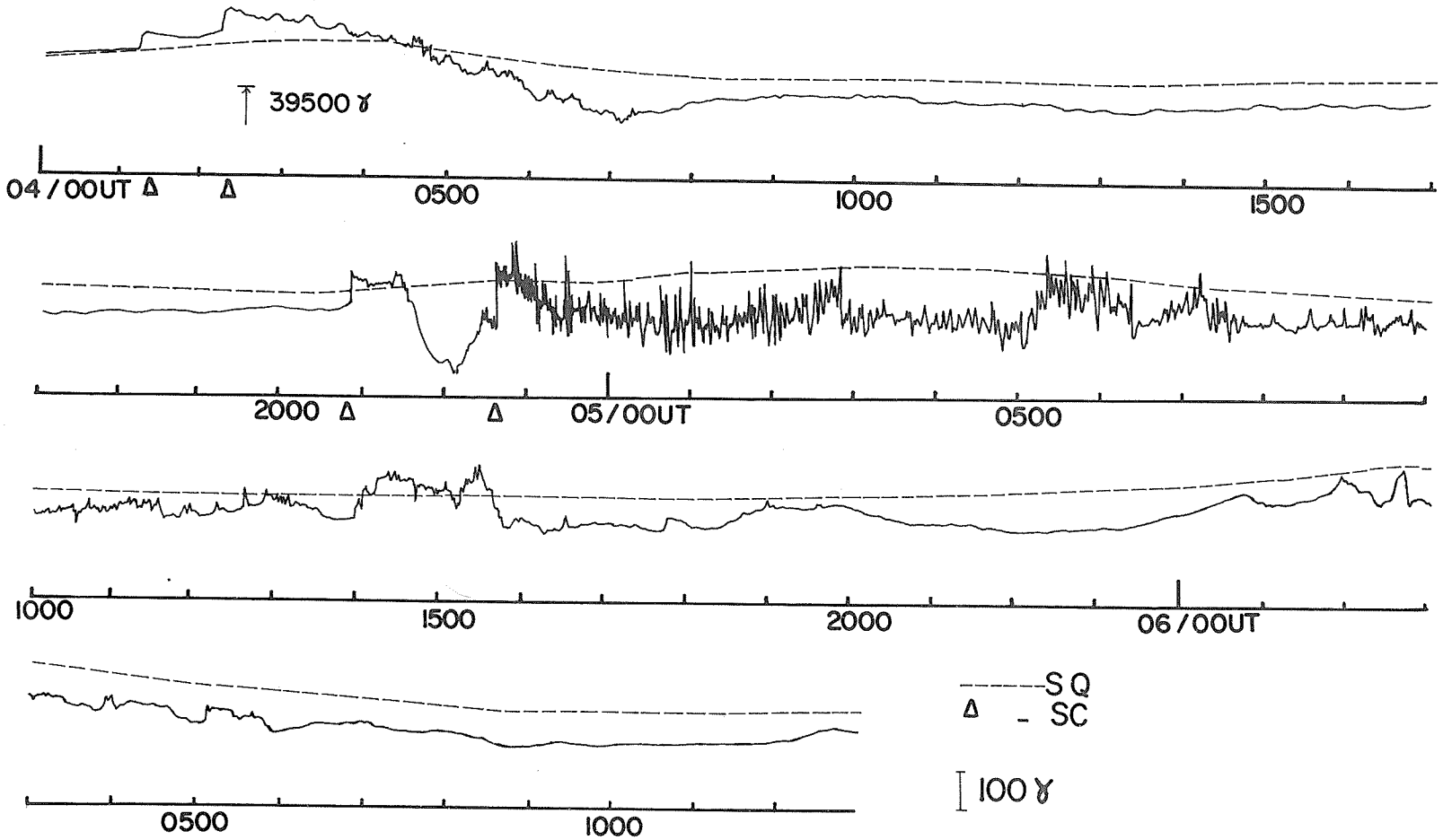

MAGNETOGRAM (X-COMPONENT OF THE FIELD) OF THE GEOMAGNETIC STORM RECORDED AT MANILA OBSERVATORY ON AUG. 4-6, 1972.

Observations of Storm-Associated Pc5 Magnetic Oscillations at the Geosynchronous Orbit: August 9, 1972

by

Joseph N. Barfield
Environmental Data Service
National Oceanic and Atmospheric Administration
Boulder, Colorado 80302

Large amplitude magnetic field oscillations are regularly observed at the geosynchronous satellite ($L \sim 6.6$) during magnetic storms [Barfield and Coleman, 1972; Barfield et al, 1972; Barfield and McPherron, 1972 a,b]. To briefly review, the storm-time magnetic oscillations are quasi-sinusoidal, display periods in the Pc5 range, and have amplitudes up to 20 γ. The oscillations are highly eliptical, and the major axis of polarization lies close to the meridional plane. The oscillations are typically associated with the main phase or early recovery phase of geomagnetic storms and are usually confined to the afternoon sector. The observed events have been closely associated with magnetospheric substorms. [For a detailed discussion of the storm-time oscillations, see Barfield and McPherron, 1972b.]

Barfield and McPherron [1972b] suggested that the storm-time Pc5 oscillations are generated by an instability of the enhanced storm-time ring current and its associated hot ($\beta \geq 1$) plasma. In addition, they showed that the oscillations were statistically associated with the peak in the partial ring current, i.e., that region with the greatest ring-current proton population. Thus, they concluded that the storm-time oscillations observed at ATS-1 are a regular feature of the geomagnetic storm and provide an effective monitor of the substorm injection process.

On August 9, 1972, during the late recovery phase of a geomagnetic storm, a storm-time Pc5 event was observed at ATS-1. The event began at $\sim$ 1830 UT (0830 LT) and was still in progress at $\sim$ 2100 UT (1100 LT) when data acquisition was interrupted.

At that time, the data acquisition procedure on ATS-1 was such that the data could not be corrected for spacecraft offsets. Therefore, only the relative magnetic field was available. In addition, the sun sensor had previously failed, so that the direction of transverse component could not be unambiguously determined. However, the data was available in the form $B_{||}$ (northward component) and $B_{\perp}$ (total component in the equatorial plane.)

The somewhat crude form in which the data was available for the August 9 event precluded rigorous analysis. However, it is possible to discuss the properties of the waves in light of previous observations.

The ATS-1 magnetic-field data for the period of interest are shown in Figure 1. The oscillations began at $\sim$1830 UT and lasted at least until a data gap occurred at $\sim$2100 UT. The waves displayed a period of $\sim$350 sec and peak-to-peak amplitude of 14 γ. The waves were first observed at 0830 local time, which is the farthest toward the dawn meridian that they have been observed to date. Thus, based on earlier observations which have been reviewed here, the partial ring current was quite far into the morning hours at that time. Due to the data gap which began at $\sim$2100 UT, it is not possible to determine the duskward extent of the region of instability.

As is typical of the storm-time Pc5 oscillations, there was evidence of two distinct frequency shifts during the wave event, at $\sim$1925 UT and $\sim$2015 UT. Such distinct frequency shifts are suggestive of magnetospheric eigenmodes of oscillation as suggested earlier. [Barfield et al, 1972].

In summary, the storm-time Pc5 oscillations observed at ATS-1 on August 9, 1972 suggest that at that time the state of the partial ring current was such that the region of instability for the waves extended into the morning sector to $\sim$ 0830 LT. Such an extension of the Pc5 region is compatible with an intense local injection (or acceleration) of ring current protons on the dayside, or, alternatively, the dayside extension of an unusually intense ring current. Since the main phase minimum occurred at $\sim$ 1000 UT, on August 9, when ATS-1 was at local midnight, it is possible that the oscillations began, long before they were observed on ATS-1, which would occur only when the satellite entered the region of instability.

ACKNOWLEDGEMENT

I wish to thank P. J. Coleman, Jr., for the use of the UCLA ATS-1 magnetometer data.

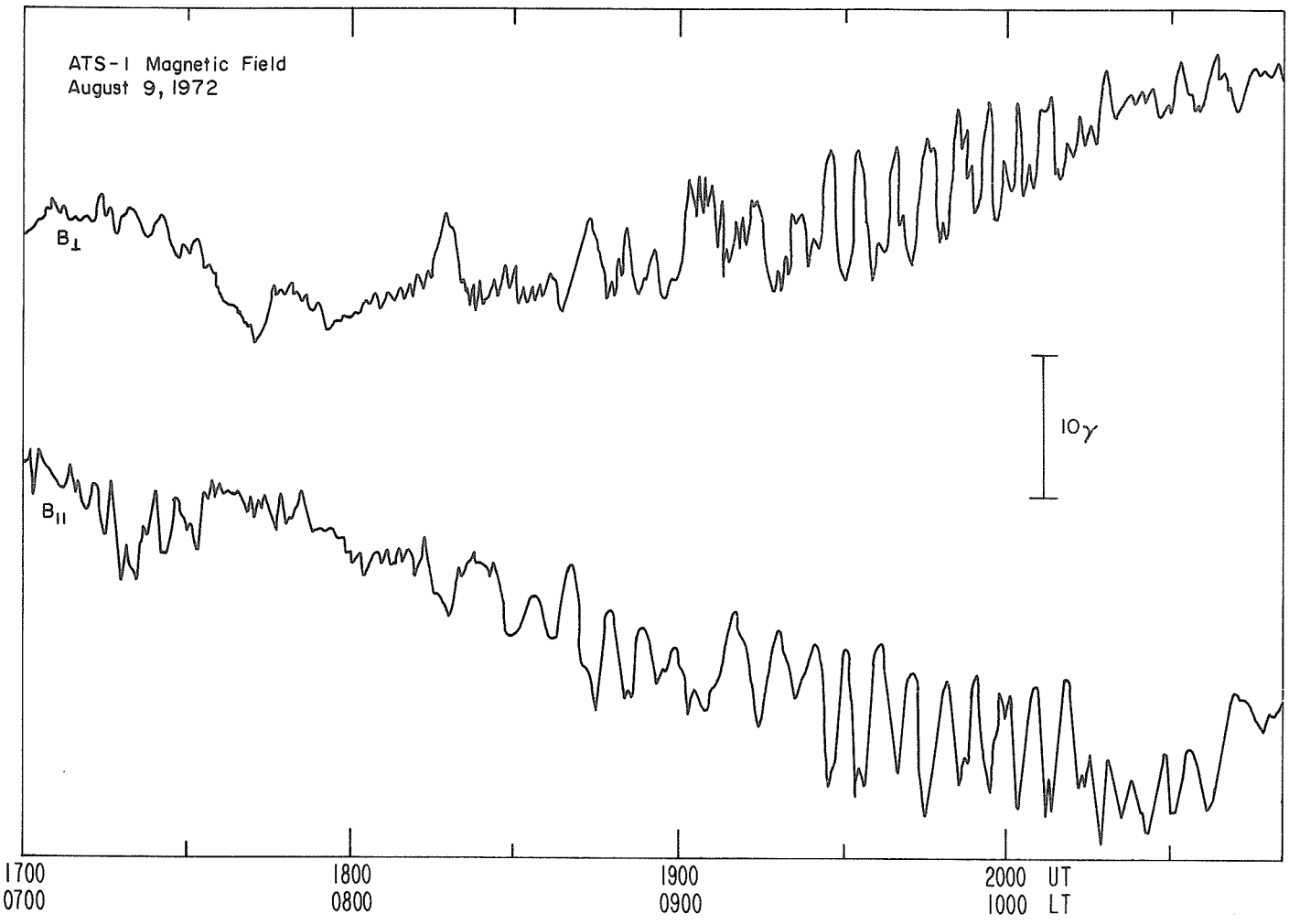

Fig. 1. ATS-1 magnetic-field data: 1700-2050 UT August 9, 1972.

REFERENCES

BARFIELD, J. N. and P. J. COLEMAN, JR. 1970 Storm-related wave phenomena observed at the synchronous equatorial orbit, J. Geophys. Res., 75, 1943.

BARFIELD, J. N. and R. L. MCPHERRON 1972a Statistical characteristics of storm-associated Pc5 micropulsations observed at the synchronous equatorial orbit, J. Geophys. Res., 77, 4720.

BARFIELD, J. N. and R. L. MCPHERRON 1972b Investigation of Interaction between Pc1 and 2 and Pc5 Micropulsations at the Synchronous Orbit during Magnetic Storms, J. Geophys. Res., 77, 4707.

BARFIELD, J. N., R. L. MCPHERRON, P. J. COLEMAN, JR., and D. J. SOUTHWOOD 1972 Storm-associated Pc5 micropulsation events observed at the synchronous equatorial orbit, J. Geophys. Res., 77, 143.

Southern Polar Region Micropulsation Activity Associated with the 11976 Event

by
H. Robert Willard and Ward J. Helms
University of Washington
Department of Electrical Engineering
Seattle, Washington

and

Harold B. Liemohn
Battelle Northwest
Richland, Washington

A geomagnetic micropulsation system has been operated as part of an Unmanned Geophysical Observatory (UGO) near McMurdo Station, Antarctica. Digital data from the experimental packages installed in the observatory is sent via Intelsat IV to the continental U.S. to provide experimenters access to polar region data with minimal time delay. Spectral characteristics of micropulsation activity covering frequencies ranging from 0.002 to 0.3 Hz are presented for times of disturbances associated with the McMath Region 11976 event. As a basis for comparison, similar data for more normal activity at a time prior to the disturbance is also included.

Analog signals from a micropulsation pickup coil are amplified and filtered prior to connection to the UGO multiplexer. The digitized data from the micropulsation signals as well as that from other experiments is transmitted via communication satellite Intelsat IV to the Comsat terminal at Jamesburg, California and then relayed by telephone data line to a tape logging facility operated by Stanford University. Individual experiment data is subsequently transferred from the master tapes to user tapes and mailed to the appropriate experimenters. Operating in this mode, data from the polar region can reach an investigator for analysis with a few days delay rather than waiting for return shipment in the January or February Antarctic summer.

Micropulsation spectral power data for the period 2 August through 6 August 1972 (days 215 through 219) recorded by the North-South oriented pickup which is part of the Unmanned Geophysical Observatory at McMurdo Station, Antarctic (S78° Lat., E167° Long. geographic coordinates or S78° geomagnetic) is presented in Figures 1 through 5. The increased magnetic activity associated with the August 4 geomagnetic storm is indicated by activity in the 0.005 through 0.140 Hz power plots (Figures 3 and 4).

The Figures display micropulsation power received in 21 contiguous spectral bands centered at 0.005 through 0.322 Hz. The year and day number are shown for time measured from the asterisk near the horizontal axis. An attenuation factor ranging from unity through 2048 (4 through 2048 for these Figures) indicates relative power scaling factors applied to the plots.

Figures 1 and 2 are typical of "normal" polar micropulsation activity as recorded at McMurdo. Little power appears above about 0.033 Hz and low frequency activity frequently reaches a maximum in the 1700 to 2200 UT period. Figure 3 shows the 4 August storm onset near 2100 UT, with strong activity at low frequencies.

Figure 4 displays the storm period for 4 and 5 August. Note the large amplitude (indicated by a 2048 attenuation factor) and the existence of higher frequency activity.

Missing data are due to system overloading (2230 on 4 August) and to communication channel errors (presumed to be the telephone lines between Jamesburg and Palo Alto, California).

A general 6 dB per octave high frequency boost is applied to the entire spectral display. In addition, low pass filtering rejects high frequencies much above 0.3 Hz, so that system sensitivity is down 6 dB below the boosted response at 0.3 hz.

Acknowledgment

The University of Washington micropulsation experiment is supported by a grant from the National Science Foundation Office of Polar Programs. Stanford University operation of the UGO system is supported by contract with the same office.

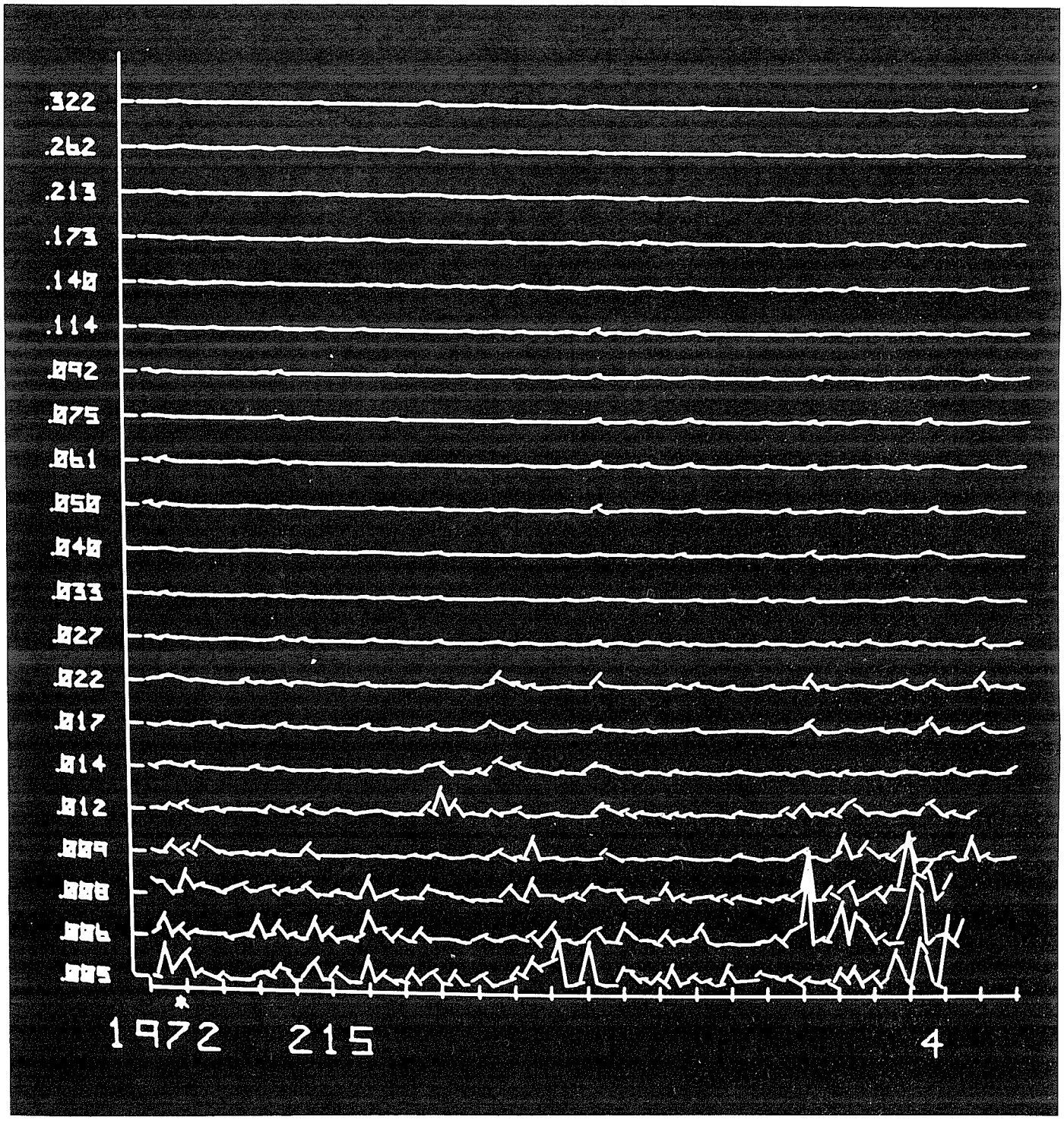

Fig. 1. Relative micropulsation power as a function of time (hours) on 2 August 1972 (day 215). An arbitrary graph scaling factor of 1/4 has been used. This plot is typical of "normal" polar micropulsation activity.

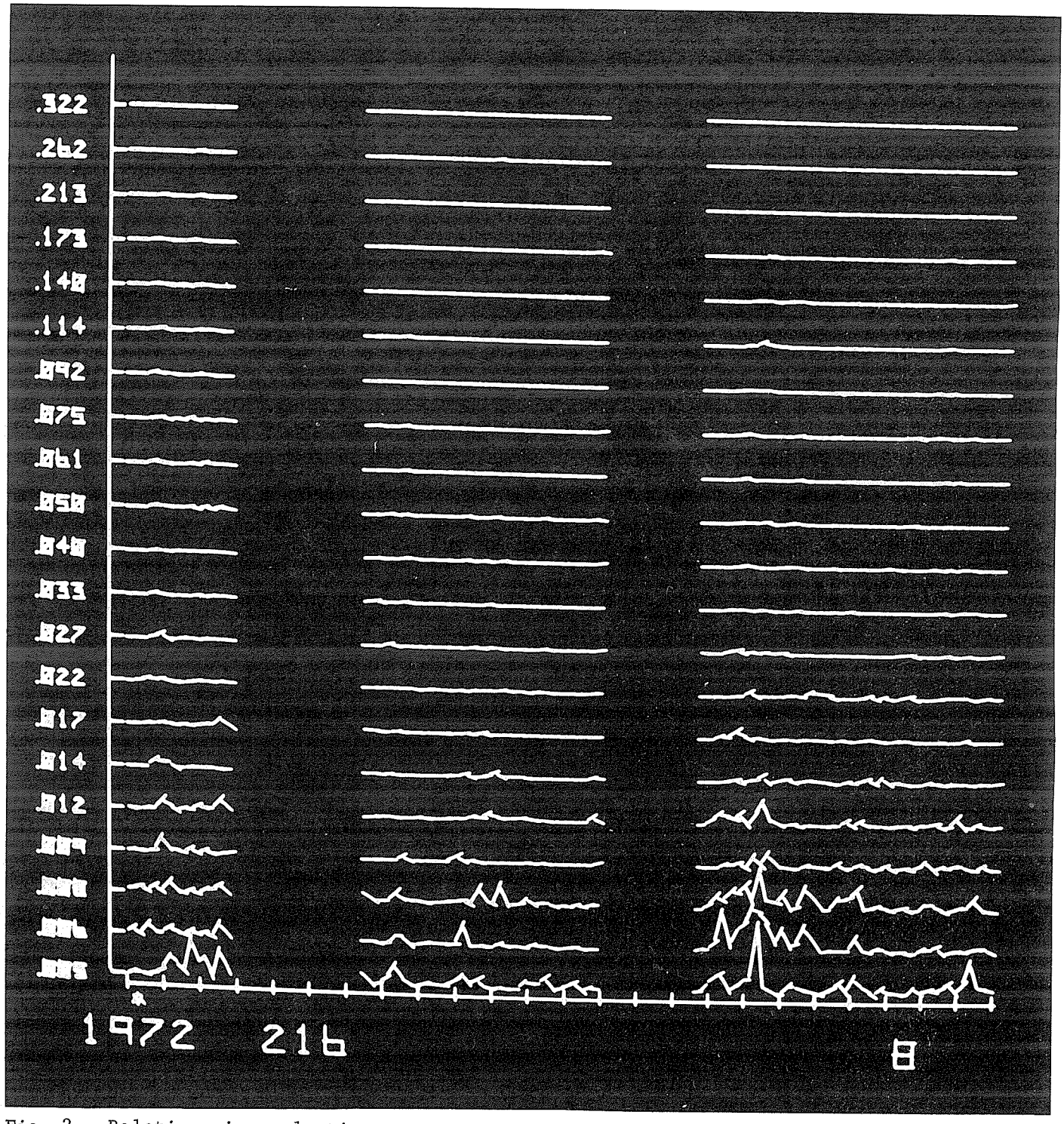

Fig. 2. Relative micropulsation power vs. time for 3 August 1972 (day 216). The arbitrary scaling factor is 1/8.

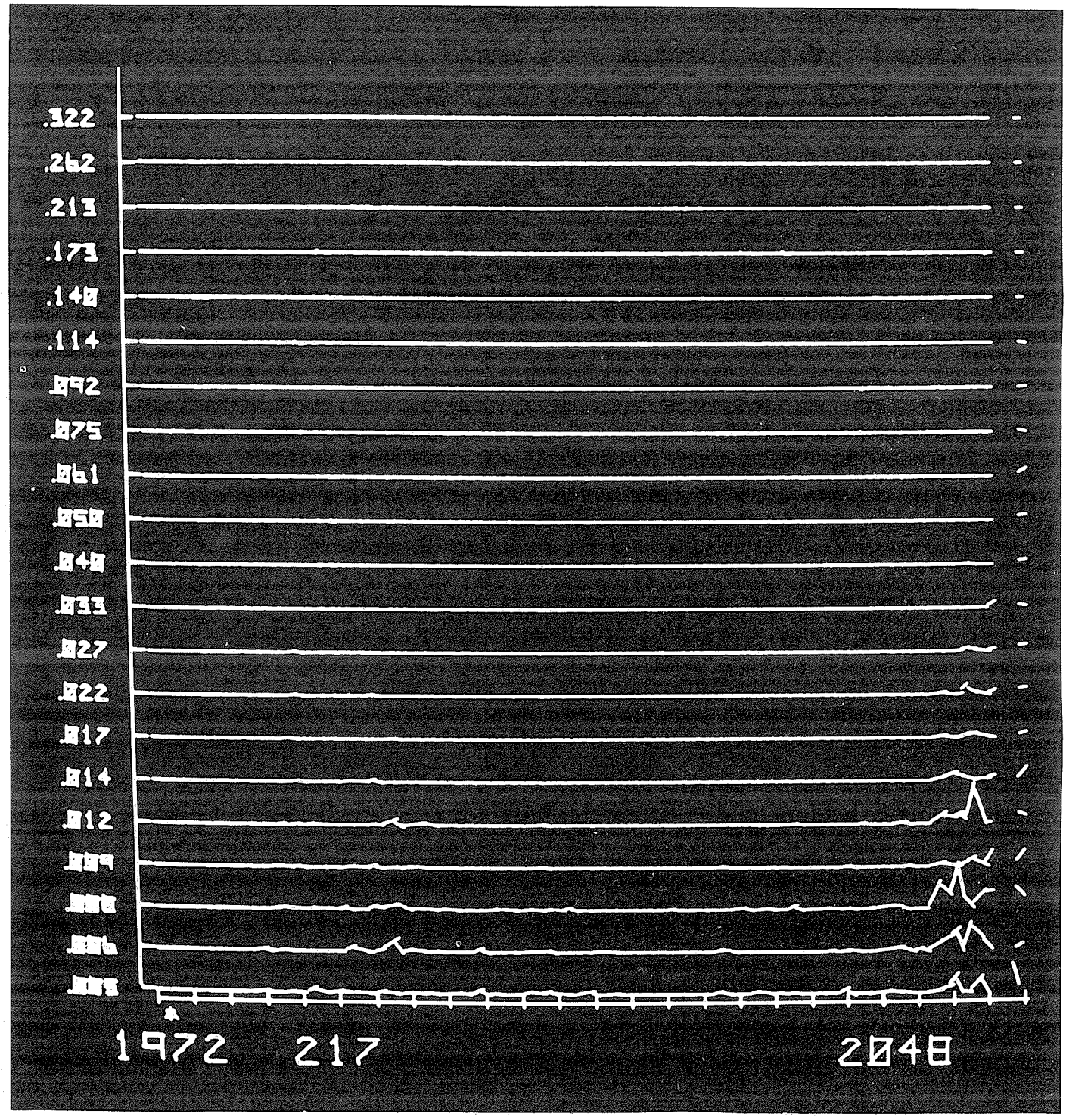

Fig. 3. Relative micropulsation power vs. time for 4 August 1972 (day 217). The strong magnetic activity requires a scaling factor of 1/2048.

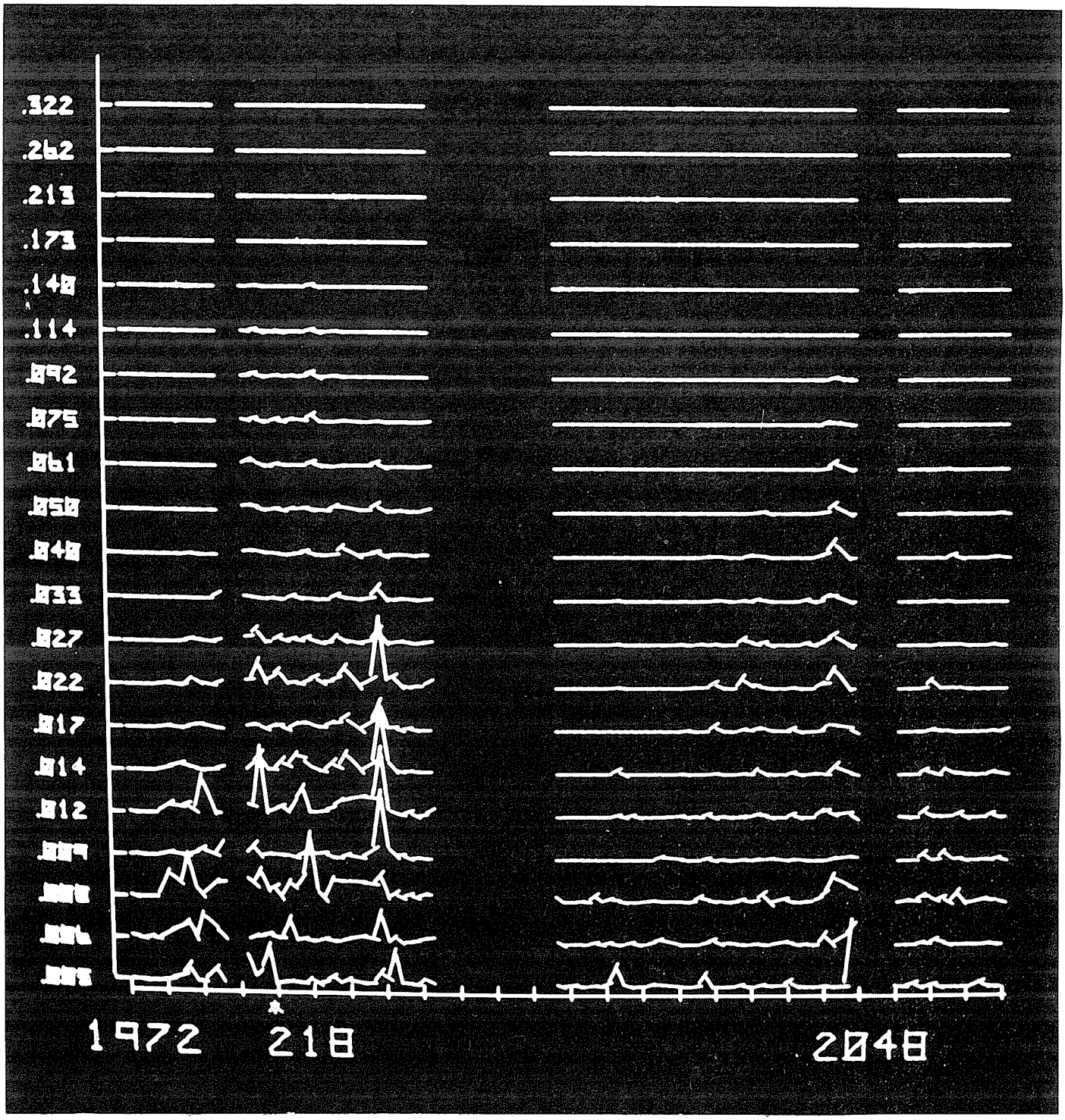

Fig. 4. Relative micropulsation power vs. time for 4 and 5 August, 1972. Scaling factor is 1/2048.

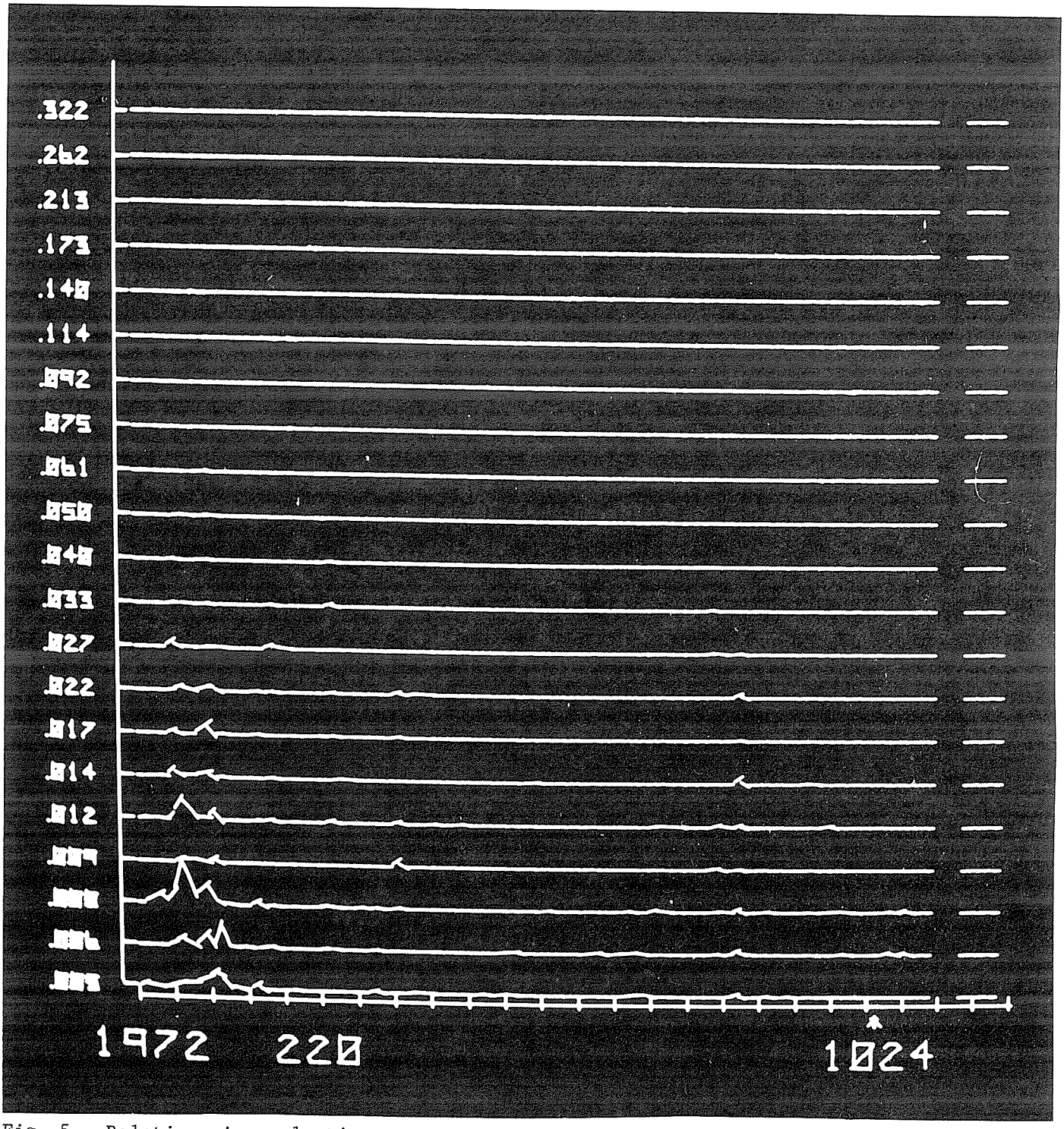

Fig. 5. Relative micropulsation power vs. time for 6 August 1972 (day 219). Scale factor is 1/1024.

Magnetic Micropulsations Observed at Several Ground Stations
August 3 - 14, 1972

by

R. R. Heacock and V. P. Hessler
Geophysical Institute
University of Alaska
Fairbanks, Alaska

J. S. Reid
Antarctic Division
Department of Science
Melbourne, Australia

M. Kivinen
Finnish Meteorological Institute
Helsinki, Finland

J. K. Olesen
Ionosphere Laboratory
Technical University of Denmark
Lyngby, Denmark

The sites involved in this study are listed in Table 1 with coordinates and L-values as given in WDC-A Catalogue UAG-20. Induction magnetometers were operated at each site, and data in the frequency range 0.005 to 10 Hz were recorded on magnetic tape with timing accuracy 1 second or better.

Table 1

Micropulsation Recording Sites

Site	Geomagnetic Latitude	Geomagnetic Longitude	L-Values
Nurmijärvi	57.9°	112.5°	3.4
Sodankyla	63.8	120.0	5.1
Thule	89.0	358.0	264.0
College	64.6	256.5	5.4
Macquarie	-61.1	243.1	5.3

Micropulsation Activity During the Stormy Interval August 3-11, 1972

It is seen, from Figure 1, that the activity generally took the form of broadband Type Pi 1 micropulsations during the stormier intervals, in agreement with previous studies [e.g. Hessler et al., 1972]. Amplitudes larger than 10 milligammas appear as black areas on the spectral displays. In case of Type Pi 1 activity, this minimum amplitude is seen at the high frequency fringe with amplitudes increasing towards the lower frequencies, sometimes reaching tens of gammas between 0.1 and 0.01 Hz.

Amplitude histograms are shown for the Thule and College sites; these were derived from scaling of broadband waveform traces. Amplitude scales for two frequencies, 0.1 and 0.01 Hz, are shown.

During weak-to-moderate storms, Type Pi 1 activity is generally observed only at sites located on the night-morning side [Hessler et al., 1972]. However, during this intense storm, Pi 1 activity was seen on the day side and in the polar cap as well as on the night side. Still, the largest Pi 1 amplitudes are observed at auroral oval sites located on the night-morning side.

Pc 1-2 Micropulsations Associated with Storm Sudden Commencements

There are two classes of Pc 1-2 micropulsations associated with ssc's. One consists of the higher frequency [>0.1 Hz] portion of the ssc impulse, and when present the onset of this signal defines the ssc time to a greater accuracy than can be obtained from the lower frequency component or from the ssc as seen on normal magnetograms [Benioff, 1960; Troitskaya, 1961; Heacock, 1969]. The second class of Pc 1-2 activity consists of events seen during the hour following the ssc, usually beginning within several minutes after the ssc [Heacock and Hessler, 1965; Oguti and Kokubun, 1969].

There were five magnetic storm sudden commencements during the interval of interest here, three on August 4, one late in August 8, and one early in August 9. Table 2 gives the ssc times for the five ssc's as observed at our micropulsation sites, i.e. the onset times for the higher frequency portion of the ssc impulses. Although timing accuracy was 1 second or better, the form of the initial ssc micropulsation excursion was often such as to introduce a subjective uncertainty of up to several seconds, particularly where the ssc excursion was superimposed on micropulsations in progress.

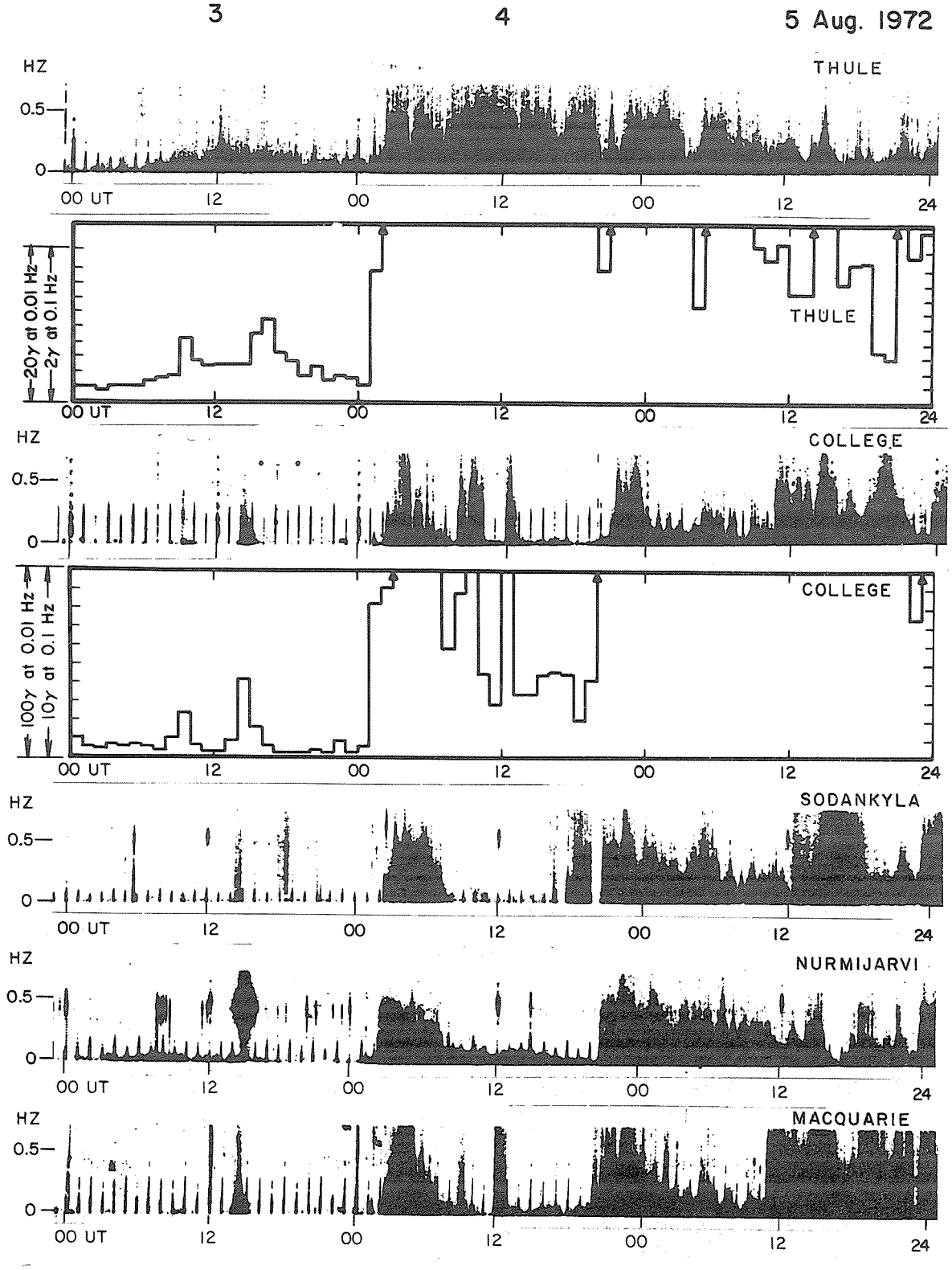

Figure 1a. Micropulsation activity observed at the sites listed in Table 1, August 3-5, 1972.

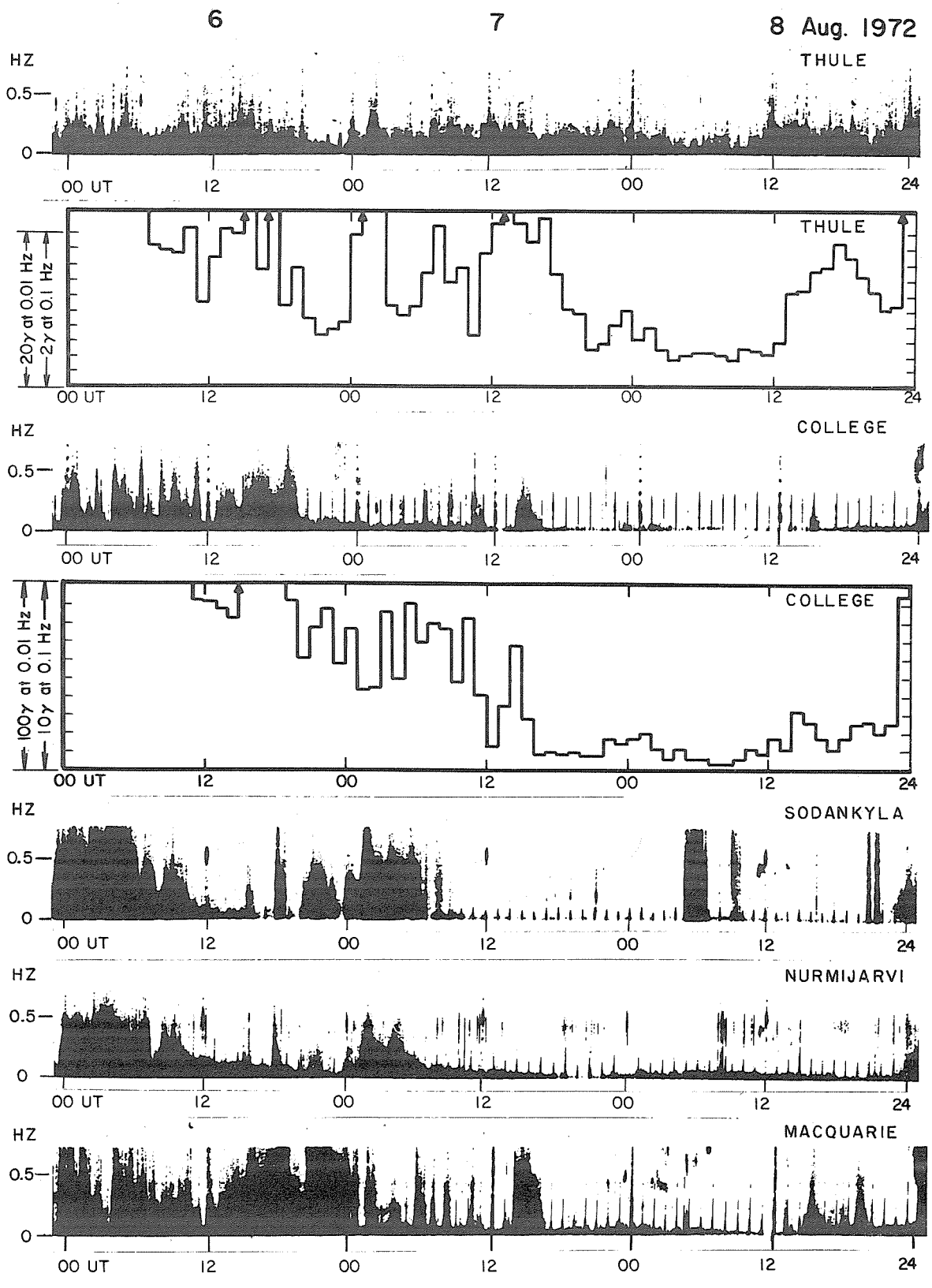

Figure 1b. Micropulsation activity, August 6-8, 1972.

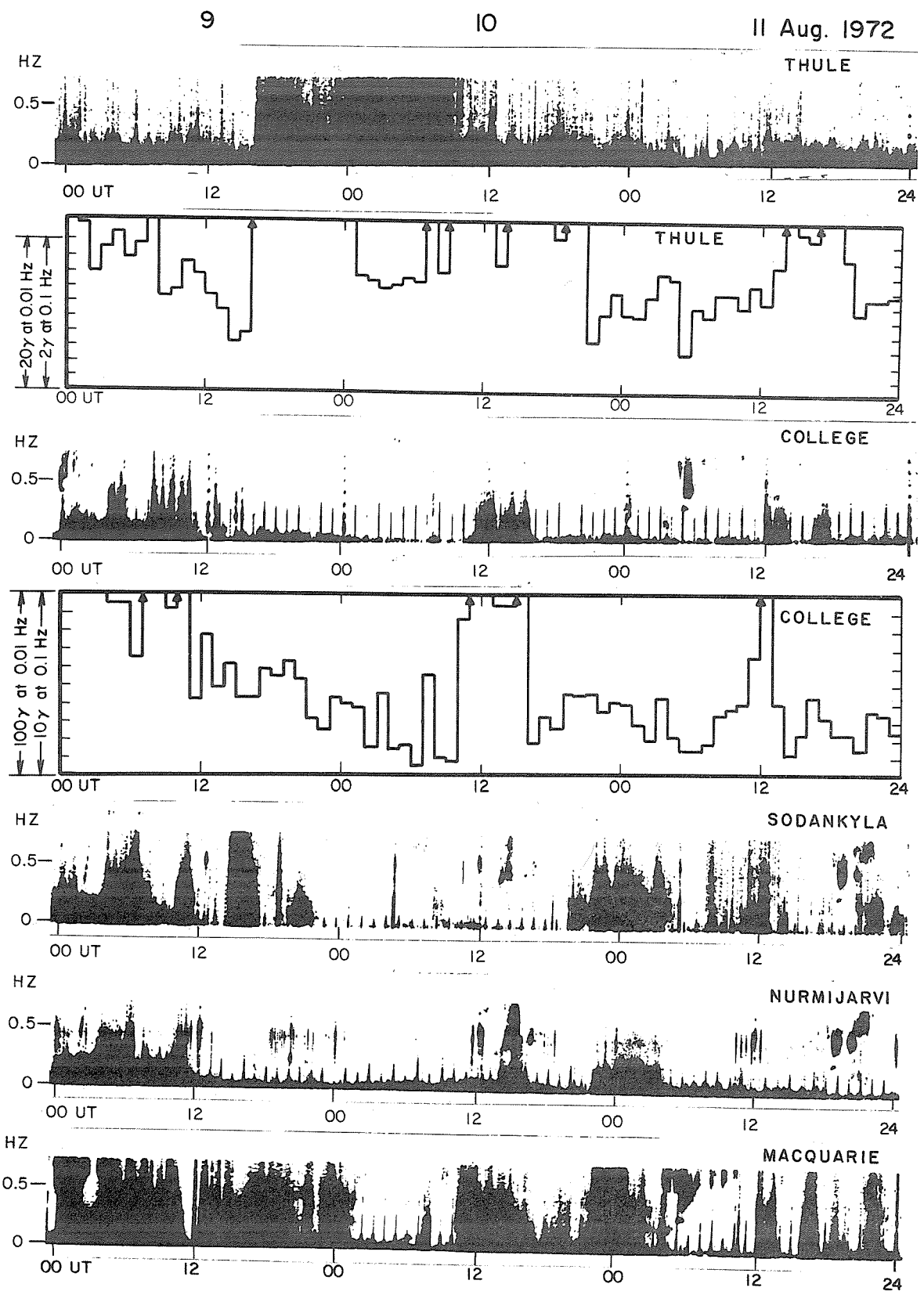

Figure 1c. Micropulsation activity, August 9-11, 1972

Table 2

Micropulsation SSC's Observed in Early August 1972

SSC No. / Date	1 Aug. 4	2 Aug. 4	3 Aug. 4	4 Aug. 8	5 Aug. 9
Nurmijärvi	0118:35	0220:52	2054:30	2343:11	-------
Sodankyla	0118:32	0220:53	2054:28	-------	-------
Thule	0118:40	0220:55	-------	-------	-------
College	0118:41	0220:34	2054:28	2354:01	0036:18
Macquarie	0118:51	0220:32	2054:34	-------	-------

Except for the Macquarie case, where the faster tape transport was inoperative on August 8 and 9, omissions in Table 2 mean that micropulsation activity in progress prevented the determination of ssc times to an acceptable accuracy.

There are some interesting differences between ssc's 1 and 2. Ssc 1 was received significantly later in Finland. The pole site Thule tends to line up with College and Macquarie in the case of ssc 1, but with the Finland sites for ssc 2. These two ssc's occurred only about 1 hour apart, hence it seems that local time effects cannot explain the differences. These observations suggest that an acceptable theoretical model should take into account such features as the orientation of the plasma shock front with respect to the magnetosphere, orientation of the interplanetary field, and the configuration of hydromagnetic waveguide ducts within the magnetosphere. Also, it is possible that convection processes occurring within the magnetosphere between one ssc and the next will significantly alter the pattern of hydromagnetic wave ray paths and hence the pattern of ssc times as received on the ground.

For these ssc's, the maximum spread between sites is approximately 20 seconds (for ssc 2). Troitskaya [1961] reported spreads of a few seconds for two IGY ssc's as observed at eight USSR micropulsation sites.

Figure 2 shows ssc Pc 1-2 micropulsation effects as observed at the four auroral oval sites. Effects were observed at Thule also, but only at frequencies below Pc 2 or of Pi 1 form. Pc 1-2 events during the hour following the ssc are more likely to be observed at sites located on the day side, and such events are more likely for ssc's that are preceded by quiet field conditions, i.e. low values of Kp [Heacock and Hessler, 1965; Oguti and Kokubun, 1969]. In the cases of the August 1972 ssc's, the western hemisphere sites were more nearly located on the day side, and we observe that ssc Pc 1 effects were indeed more prominent at College and Macquarie than at the Finland sites. Ssc 3 was not preceded by quiet field conditions and Pc 1 effects were not observed.

It now seems that quiet field conditions generally mean that the plasma-pause is relatively far out [Chappell et al., 1970], a condition favorable for Pc 1 production [Mullen and Heacock, 1972].

Curious Pc 1 effects are seen on the Macquarie records at times preceding ssc's 1, 4, and 5, and at College for 4 and 5. In each case, two Pc 1 events occurred in succession, each with a falling frequency characteristic.

Some ssc's seem to trigger substorms [Burch, 1972, and references therein]. Pi 1 micropulsation activity is highly correlated with substorm activity [Hessler et al., 1972] hence ssc's that trigger substorms can generally be identified by the Pi 1 storms that immediately follow the ssc. It is interesting to note that ssc 2 triggered a substorm whereas ssc 1 did not. Substorm activity commenced with ssc 3 at the Finland sites and was enhanced at College and Macquarie. A substorm was already in progress at Sodankyla in the cases of ssc's 4 and 5. Substorms are known to be correlated with a southward interplanetary field [e.g. Foster et al., 1971], hence future studies might look for relations between differences in ssc onset time patterns as observed on the ground, ssc triggering effects on substorms, and orientations of interplanetary field.

Structured Pc 1 Activity on the Ring Current Recovery Phase

Periodically structured Pc 1 events tend to occur on storm recovery phases [Wentworth, 1964; Heacock and Kivinen, 1972; Heacock and Akasofu, 1973]. Presumably the protons in the high energy tail of the ring current spectrum are responsible through the electromagnetic cyclotron instability, and are brought to their stable trapping limit by the increasing cold plasma density of the filling plasmasphere. The August 1972 storms produced an unusual amount of structured Pc 1 activity. Some examples are shown in Figure 3 for the Macquarie site. Nearly all of the events shown are of the periodically structured variety though the structures are not resolved in the figure. Prominent structured Pc 1 activity was observed in the quiet interval between storms August 7 - 8 and for about a week following the second storm interval, i.e. August 10-16.

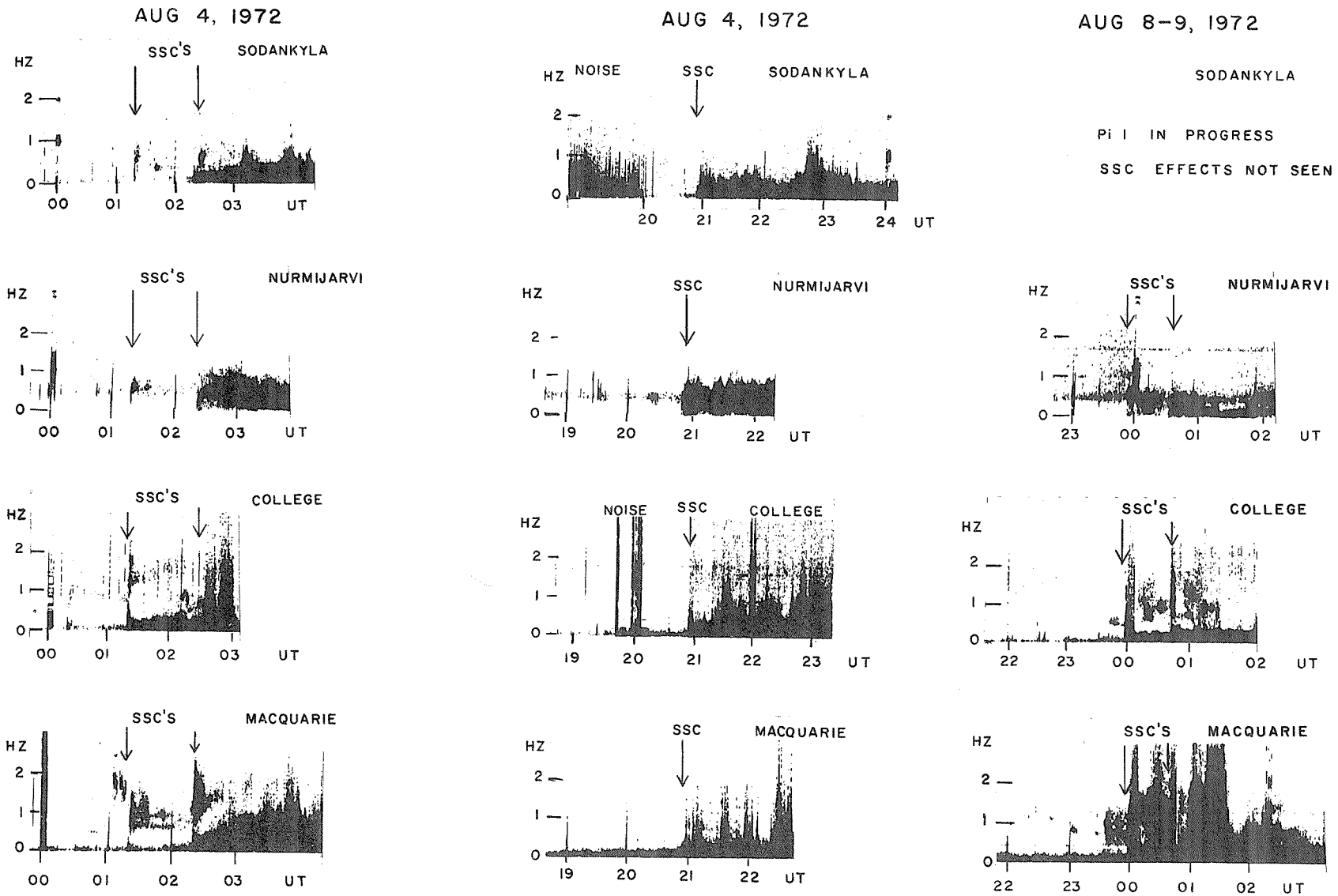

Figure 2. Micropulsation activity associated with the five magnetic storm sudden commencements listed in Table 2.

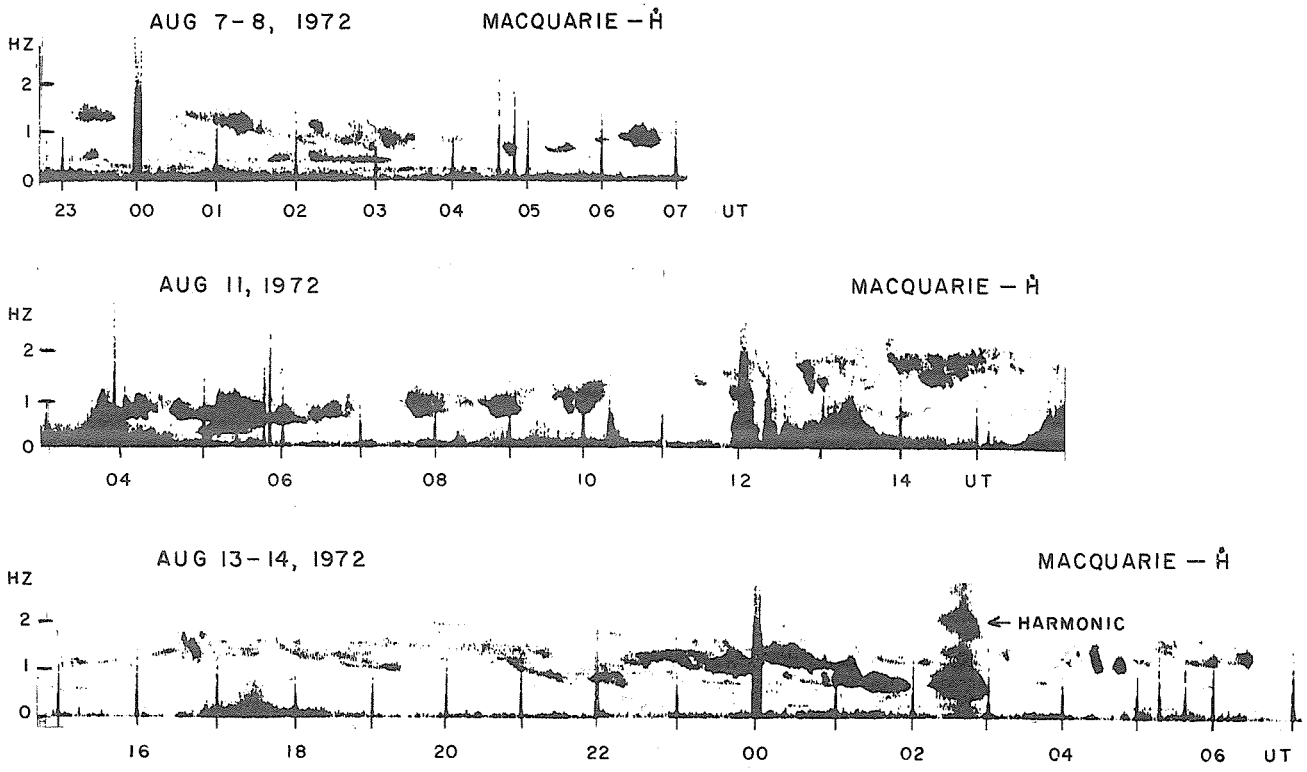

Figure 3. Examples of Pc 1 micropulsation activity observed at Macquarie during the ring current recovery phases.

Acknowledgement

This work was supported by the National Science Foundation, Atmospheric Sciences Section and Office of Polar Programs, under Grant Nos. GA-32390, GA-34280, and GV-32925.

REFERENCES

BURCH, J. L. 1972 Preconditions for the triggering of polar magnetic substorms by storm sudden commencements, J. Geophys. Res., 77, 5629-5632.

BENIOFF, H. 1960 Observations of geomagnetic fluctuations in the period range 0.3 to 120 seconds, J. Geophys. Res., 65, 1413-1422.

CHAPPELL, C. R., K. K. HARRIS, and G. W. SHARP 1970 A study of the influence of magnetic activity on the location of the plasmapause as measured by OGO-V, J. Geophys. Res., 75, 50-56.

FOSTER, J. C. D. H. FAIRFIELD, K. W. OGILVIE, and T. J. ROSENBERG 1971 Relationship of interplanetary parameters and occurrence of magnetospheric substorms, J. Geophys. Res., 76, 6971.

HEACOCK, R. R., and V. P. HESSLER 1965 Pearl-type micropulsations associated with magnetic storm sudden commencements, J. Geophys. Res., 70, 1103-1111.

HEACOCK, R. R. 1969 Some observations of ssc micropulsation wavepackets, Planet. Space Sci., 17, 767-768.

HEACOCK, R. R., and M. KIVINEN 1972 Relation of Pc 1 micropulsations to the ring current and and geomagnetic storms, J. Geophys. Res., 77, 6746-6760.

HEACOCK, R. R., and S.-I. AKASOFU 1973 Periodically structured Pc 1 micropulsations during the recovery phase of intense magnetic storms, J. Geophys. Res., in press.

HESSLER, V. P., R. R. HEACOCK J. OLESEN, C. SUCKSDROFF, and J. KANGAS 1972 Micropulsations associated with polar magnetic substorms, paper in "Polar Micropulsations", edited by V. P. Hessler and V. A. Troitskaya, Geophysical Institute Scientific Report No. UAG R-220, University of Alaska, Fairbanks.

MULLEN, A. J., and R. R. HEACOCK 1972 Correlation of ground-based measurements of structured Pc 1 micropulsations with OGO-V plasma pause observations, Ann. Geophys., 28, 519-525.

OGUTI, T., and S. KOKUBUN 1969 Hydromagnetic emissions in high latitudes associated with storm sudden commencements-II, Rep. Ionos. Space Res. Japan, 23, 162-174.

TROITSKAYA, V. A. 1961 Pulsation of the earth's electromagnetic field with periods of 1 to 15 seconds and their connection with phenomena in the high atmosphere, J. Geophys. Res., 66, 5-18.

WENTWORTH, R. C. 1964 Enhancement of hydromagnetic emissions after geomagnetic storms, J. Geophys. Res., 69, 2291-2298.

Observations of Geomagnetic Micropulsations at a Midlatitude Station

by

J. W. Münch
Max-Planck-Institut für Aeronomie, Institut für Stratosphärenphysik
Lindau, Germany

Micropulsations of the H- and D-components of the geomagnetic field with periods between 3 and 200 seconds were recorded at Lindau in August 1972. A description of the instrumentation is given by Wilhelm [1966]. The geographical coordinates of the station are: N51.55, E9.96.

The data from August 3 to 7, 1972, which are presented here were recorded on strip charts. The amplitudes of the pulsations, particularly in the H-component, were sometimes so large that the pen reached both sides of the recording paper. As these distorted amplitudes could not be measured properly, only the micropulsation periods are utilized here.

The occurrence frequency of periods of the sinusoidal pulsations with amplitudes greater than 0.06 γ were determined. Table 1 gives the numbers of single pulsations which occurred within a given band of periods during a two hour interval. During geomagnetic storms, pulsations of different periods frequently occur simultaneously. When superposition did occur, the base period was analyzed for only the periods of those superposed pulsations which had an amplitude of at least one third of that of the base period. The black bars in Table 1 indicate the times when analysis of the pulsations was not possible due to instrumental problems.

On August 3, 1972, quiet-time Pc's with periods between 30 and 35 seconds prevail [e.g., compare Voelker, 1963]. During the main phase of the storm, shorter period pulsations occur during daytime. Such pulsations are only observed at this latitude at times of high Kp values, e.g., see Münch [1965].

REFERENCES

MÜNCH, J. W. 1965 Das Auftreten von Pulsationen des erdmagnetischen Feldes in Abhängigkeit von der erdmagnetischen Aktivität, Z. Geophy., 31, 192-199.

VOELKER, H. 1963 Zur Breitenabhängigkeit erdmagnetischer Pulsationen, Mitt. MPI Aeronomie, 21.

WILHELM, K. 1966 Registrierung und Analyse erdmagnetischer Pulsationen der Polarlichtzone, sowie ein Vergleich mit Bremsstrahlungsmessungen, Mitt. MPI Aeronomie, 27.

TABLE

	August 3, 1972													August 4, 1972										
UT	00 02	02 04	04 06	06 08	08 10	10 12	12 14	14 16	16 18	18 20	20 22	22 24		00 02	02 04	04 06	06 08	08 10	10 12	12 14	14 16	16 18	18 20	20 22	22 24
Periodrange (sec)	H - Component																								
5-9																									
10-14																	1	3		1					
15-19																3	6	7	7	2					
20-24					1			1								1	1	7	5	1					
25-29					1			3								3	2	4		1					
30-34				17	33	4		13	1							4	2	5	3	5					
35-39				13	9	1		7	5							2	2	8	6	3	2				
40-44				5	1												1	3	2	3					
45-49				2	3	1			1							2	7	12	6		2				
50-54				1	1											2		3	13		1				
55-59						1										1	2	3	2						
60-64					1			1								2	3	6	6						
65-69				1												1	1	9	3						
70-74																	1	3			1				
75-79								1									4	5	6	2	1		•		
80-84																2		2	1	1	1				
85-89																		3	2						
90-99																		8	6	5	4				
100-119								1									2	7	6	4	1				
120-149																1	1	4	5	2	6				
150-180																1	1	6	2	7	2				
> 180																1		2	7	2	4				

TABLE (cont.)

	August 3, 1972													August 4, 1972										
UT	00 02	02 04	04 06	06 08	08 10	10 12	12 14	14 16	16 18	18 20	20 22	22 24		00 02	02 04	04 06	06 08	08 10	10 12	12 14	14 16	16 18	18 20	20 22	22 24
Periodrange (sec)	D - Component																								
5-9																	1								4
10-14																			1					1	5
15-19																6	5	6	2	2				2	15
20-24					5											3	2	5	3	1				2	3
25-29				2	4										1	3	1	3	1	2	1				2
30-34				10	25											8	5	13	11	16	1			2	3
35-39				6	5											4	3	10	4	12	1			1	4
40-44				1	1											1	2	7	7	1					
45-49				2	1										1	1	3	16	6	10	2				6
50-54					1												7	13	11	4				6	1
55-59																1		9	6	4	1			2	2
60-64					1										1		1	12	10	7	1			4	3
65-69				1											1	1	2	5	5	4				2	6
70-74															1		1	4	2	2				2	2
75-79															2	2	1	5	8	4	1			2	5
80-84															2	4		3	1	3	2			3	1
85-89																		1		3				3	
90-99				1											4	4	1	7	8	9	2			6	
100-119															2	2	1	6	5	5	2			8	2
120-149															2	4	1	2	2	4	1			3	
150-180																	1	1		1	2			2	
> 180															2	3	1				6				

TABLE (CONT.)

	August 5, 1972													August 6, 1972											
UT	00 02	02 04	04 06	06 08	08 10	10 12	12 14	14 16	16 18	18 20	20 22	22 24		00 02	02 04	04 06	06 08	08 10	10 12	12 14	14 16	16 18	18 20	20 22	22 24
Periodrange (sec)	D - Component																								
5-9	4	1	11	5	29	22		14							24	35		4				1	14		
10-14	5	4	9	6	18	19	3	20		2		1			15	25	3	11	1			4	28		
15-19	10	8	28	5	20	34	10	19	3	7	1	1		5	35	46	18	25	27	4	2	6	8		
20-24	15		19	5	19	9	14	25	2	9	7	3		10	22	30	15	19	13	5	6	4	7	1	
25-29	6		7	7	8	8	8	18	2	7	3	1		7	11	27	27	34	15	9	10	6	9	1	
30-34	8	12	21	24	29	15	14	16	5	7	9	6		10	21	38	36	46	28	21	12	12	18	4	
35-39	6	4	15	20	27	21	14	16	3	10	8	3		8	17	28	26	35	15	21	23	11	8	3	
40-44	4	2	10	4	13	11	2	9	5	4	3	1		6	2	9	24	18	8	11	7	7	4	3	
45-49	8		8	14	17	11	11	10	5	8	13	5		3	7	7	12	14	11	14	15	12	7	18	
50-54	4	3	16	5	4	6	6	9	6	9	4	4		4	5	7	13	7	12	14	9	4	4	12	
55-59	3	2	2	3	3	5	8	2	5	3	2	6		3	3	1	4	6	5	6	3	5		2	
60-64	3	2	9	2	6	11	11	3	4	6	4	4		5	6	5	4	7	8	11	14	1	3	7	
65-69	4	2	7	6	4	9	11	5	3	6	5	1		3	6	3	3	2	2	6	6	5	2	2	
70-74	1	1	4	2		4	5	2	4	5	4			1	2	3	1			4	2	2			
75-79	3	4	5	3	4	8	6	5	6	5	4	4		3	4	1	4	1	4	5	4	1		1	
80-84	5	1	2	3	4		3	1	4	3	1			1	4	1			5	3	2		1	1	
85-89	1	1	1	3		3	4	5	1	1	1			1					2	1	3			1	
90-99	6	2	2	2	2	2	6	4	3	3	3	2		7	4	1	1		4	2	5	1			
100-119	6	9	3	5	4	1	5	2	6	4	2	5		8	5	1			3	4	1	1			
120-149	6	2	4	6	3	2	4	2	1	5	2	1		8	4		2		3	2	5		1		
150-180	3	1	1	3			1	1	3	1	2			8	4						1				
> 180		1		4		1		1	3					2							1			1	

TABLE (CONT.)

	August 7, 1972											
UT	00 02	02 04	04 06	06 08	08 10	10 12	12 14	14 16	16 18	18 20	20 22	22 24
Periodrange (sec)	D - Component											
5-9			7									
10-14		2	11									
15-19	6	7	38	1	3							
20-24	12	12	16	1	9	6						
25-29	5	3	15	2	1	16						
30-34	21	8	28	18	9	12						
35-39	6	4	13	16	11	3						
40-44	2	3	7	10	6	1						
45-49	6	3	21	11	10	5						
50-54	1		10	7	1	1						
55-59			5	4	4	1						
60-64	5		10		4	2						
65-69	2	1	4	6	5							
70-74	1			1	1							
75-79			1	1	3							
80-84	1				3							
85-89			1									
90-99	2		2		3	1						
100-119					5							
120-149					2	1						
150-180					1							
> 180					1							

8. AERONOMY AND MISCELLANEOUS

For basic data and indices for this section and others, see Appendix I for Table of Contents to Report UAG-21.

For data papers presented or published elsewhere which contain additional information on aeronomy and miscellaneous observations and the other categories included in this report, see Appendix II.

ATMOSPHERIC DENSITIES AT HEIGHTS BETWEEN 300 AND 900 KM OBTAINED FROM THE DRAG OF FIVE SATELLITES DURING THE INTERVAL 22 JULY TO 16 AUGUST 1972

L. G. Jacchia and J. W. Slowey

Smithsonian Astrophysical Observatory, Cambridge, Massachusetts 02138

Atmospheric densities were derived from the drag of five satellites for the interval from 22 July to 16 August 1972, which includes the exceptionally intense magnetic storm of 4–6 August. Table 1 gives the identification of the five satellites with some pertinent orbital data.

Table 1

Satellite	Perigee height (km)	Apogee height (km)	Inclination	$\bar{z}$ (km)
1966 44A (Explorer 32)	278	2230	64°.6	300
1966 70A (OV3-3)	358	4200	81.5	390
1960 ξ1 (Explorer 8)	415	2090	49.9	450
1959 α1 (Vanguard 2)	565	3242	32.9	600
1968 66A (Explorer 39)	748	2215	80.7	900

The last column in Table 1 gives the standard height $\bar{z}$ to which the densities were reduced; this height is an approximate mean of the effective height. The effective height is the average of the actual height around the satellite's orbit weighted by the local atmospheric drag. The local drag was estimated for this purpose by using an atmospheric model. For a description of the method followed in deriving densities from the observed drag, see Jacchia and Slowey [1962, 1972].

Table 2 gives, for each satellite as a function of the Modified Julian Day (MJD = JD - 2,400,000.5) in the first column, a tabulation of the observed rate of change $\dot{P}$ (the orbital acceleration) of the orbital period P; the acceleration due to direct solar radiation pressure $\dot{P}_r$, computed under the assumption of specular reflection from a spherical satellite with the area-to-mass ratio of the satellite; the atmospheric component $\dot{P}_a$ of the acceleration ($\dot{P}_a = \dot{P} - \dot{P}_r$); the density at perigee height ρ_π and the density ρ_s reduced to the standard height appropriate for the satellite; the perigee height z_p above the geoid in kilometers; and, in the last two columns, the differences in right ascension and declination between the satellite perigee (α_π, δ_π) and the sun ($\alpha_\odot$, $\delta_\odot$). The temperature T_∞ in the seventh column is the exospheric temperature obtained from ρ_s when introduced in a static model (Jacchia's model 39H, unpublished). Such a temperature, of course, has only a reference value, because static models are not expected to give reliable temperatures during rapid density variations.

In Table 3, we have assembled, for all satellites, the residuals $\Delta \log_{10} \rho$ from Jacchia's static model 39H when all the known variations, except for the geomagnetic effect, have been suppressed. If the model, the area-to-mass ratios of the satellite, and the assumptions made in the reduction of the data were 100% correct, the quantity $\Delta \log_{10} \rho$ would represent the increase of density at any given time above the density corresponding to $K_p = 0$. Apart from noise in the original data (satellite positions), the tabulated densities are affected by a smoothing factor, different from satellite to satellite, caused by the limited resolution of the drag method.

The data of Table 3 are plotted in Figure 1a; the 3-hour geomagnetic planetary indexes a_p and K_p are shown in the lower part of the diagram. For comparison, Figure 1b shows values of $\Delta \log_{10} \rho$ derived from six satellites during the geomagnetically perturbed period in May–June 1967, which included the great storm of 25–26 May. The 1967 data had a better resolution than did those of 1972 because they were derived from accurately reduced photographs taken with the Baker-Nunn cameras, which yield a precision of 3 to 4 arcsec in position. The 1972 data, on the other hand, were derived from radar positions and field-reduced Baker-Nunn photographs. To this date, the accurate reduction of the photographs has not been done, and in view of the reduced number of Baker-Nunn stations in operation, it is doubtful whether any better results could be obtained from them.

REFERENCES

JACCHIA, L. G. and J. W. SLOWEY, 1962. Accurate drag determinations for eight artificial satellites; atmospheric densities and temperatures, Smithsonian Astrophys. Obs. Spec. Rep. No. 100, 99 pp.; also Smithsonian Contr. Astrophys., 8, no. 1, 1-99, 1963.

JACCHIA, L. G. and J. W. SLOWEY, 1972. A supplemental catalog of atmospheric densities from satellite-drag analysis, Smithsonian Astrophys. Obs. Spec. Rep. No. 348, 323 pp.

Table 2.

MJD	$-10^7 \dot{P}$	$10^7 \dot{P}_r$	$-10^7 \dot{P}_a$	$\log \rho_\pi$	$\log \rho_s$	T_∞ (K)	z (km)	$\alpha_\pi - \alpha_\odot$ (deg)	$\delta_\pi - \delta_\odot$ (deg)
				1959 α1					
41524.00	0.03	0.18	0.21	-16.41	-16.67	792	563.1	257.2	-42.9
26.00	0.04	0.19	0.23	.39	.63	803	564.6	259.1	-46.4
28.00	0.07	0.20	0.27	.32	.56	823	565.9	261.8	-48.9
30.00	0.12	0.22	0.34	.21	.44	856	566.7	265.1	-50.3
41532.00	0.12	0.22	0.34	-16.21	-16.44	857	567.0	268.7	-50.4
33.00	0.57	0.23	0.80	-15.82	.05	977	566.9	270.6	-50.0
34.00	1.17	0.23	1.40	.56	-15.78	1076	566.7	272.4	-49.3
35.00	0.71	0.23	0.94	.73	.95	1014	566.4	274.1	-48.2
36.00	0.03	0.23	0.26	-16.29	-16.52	832	566.0	275.7	-46.9
37.00	0.10	0.23	0.33	.20	.44	855	565.4	277.2	-45.2
38.00	0.40	0.23	0.63	-15.92	.16	939	564.8	278.5	-43.3
39.00	0.55	0.23	0.78	.82	.07	969	564.1	279.6	-41.2
40.00	-0.06	0.23	0.17	-16.49	.75	769	563.3	280.5	-38.9
41542.00	-0.04	0.23	0.19	-16.45	-16.72	777	561.7	281.9	-33.6
44.00	-0.07	0.23	0.16	.53	.81	753	560.2	282.6	-27.9
				1960 ξ1					
41524.00	5.01	0.04	5.05	-14.62	-14.88	1031	415.4	343.5	-22.1
24.50	4.80	0.04	4.84	.63	.90	1021	415.2	342.2	-20.9
25.00	3.88	0.04	3.92	.72	.99	975	415.0	340.9	-19.7
25.50	3.66	0.04	3.70	.75	-15.02	963	414.9	339.6	-18.4
26.00	3.69	0.04	3.73	.74	.02	964	414.8	338.3	-17.2
26.50	3.71	0.04	3.75	.74	.02	964	414.7	337.0	-16.0
27.00	3.73	0.04	3.77	.74	.02	965	414.6	335.7	-14.7
27.50	3.99	0.04	4.03	.71	-14.99	977	414.5	334.4	-13.5
28.00	4.25	0.04	4.29	.68	.96	990	414.5	333.1	-12.3
28.50	4.51	0.04	4.55	.66	.94	1002	414.4	331.8	-11.1
29.00	4.54	0.04	4.58	.65	.94	1003	414.4	330.5	-9.8
29.50	4.57	0.04	4.61	.65	.93	1004	414.4	329.2	-8.6
30.00	4.59	0.04	4.63	.65	.93	1005	414.4	328.0	-7.4
30.50	4.38	0.04	4.42	.68	.95	995	414.4	326.7	-6.1
31.00	5.12	0.04	5.16	.61	.88	1029	414.5	325.4	-4.9
31.50	5.15	0.04	5.19	.61	.88	1030	414.5	324.2	-3.7
32.00	5.41	0.04	5.45	.58	.86	1040	414.6	323.0	-2.5
32.50	5.44	0.04	5.48	.58	.86	1041	414.6	321.7	-1.3
41533.00	4.77	0.04	4.81	-14.64	-14.92	1012	414.7	320.5	-0.1
33.20	6.25	0.04	6.29	.53	.80	1075	414.8	320.0	0.4
33.40	4.79	0.04	4.83	.66	.91	1015	414.8	319.5	0.9
33.60	7.75	0.04	7.79	.45	.70	1131	414.9	319.1	1.4
33.80	7.76	0.04	7.80	.44	.70	1131	414.9	318.6	1.9
34.00	12.19	0.04	12.23	.25	.50	1269	415.0	318.1	2.4
34.20	16.62	0.04	16.66	.14	.37	1385	415.0	317.6	2.8
34.40	12.21	0.04	12.25	.28	.50	1270	415.1	317.2	3.3
34.60	7.81	0.04	7.85	.46	.70	1134	415.1	316.7	3.8
34.80	9.30	0.04	9.34	.39	.62	1183	415.2	316.2	4.3
35.00	6.36	0.04	6.40	.55	.78	1081	415.2	315.8	4.7

Table 2 (Cont.)

MJD	$-10^7\dot{P}$	$10^7\dot{P}_r$	$-10^7\dot{P}_a$	$\log \rho_\pi$	$\log \rho_s$	T_∞ (K)	z (km)	$\alpha_\pi-\alpha_\odot$ (deg)	$\delta_\pi-\delta_\odot$ (deg)
				1960 ξ1 (Cont.)					
41535.50	4.93	0.04	4.97	-14.65	-14.89	1021	415.4	314.6	5.9
36.00	4.77	0.04	4.81	.66	.91	1013	415.5	313.5	7.1
36.50	4.52	0.04	4.56	.67	.93	1001	415.7	312.4	8.3
37.00	4.50	0.04	4.54	.67	.94	999	415.8	311.3	9.4
37.50	3.78	0.04	3.82	.74	-15.01	963	416.0	310.2	10.6
38.00	3.53	0.04	3.57	.77	.04	951	416.2	309.2	11.7
38.50	5.87	0.04	5.91	.56	-14.82	1059	416.4	308.2	12.9
39.00	5.15	0.04	5.19	.62	.87	1029	416.6	307.2	14.0
39.50	3.72	0.04	3.76	.75	-15.01	961	416.8	306.2	15.1
40.00	3.23	0.04	3.27	.81	.07	935	417.0	305.2	16.2
40.50	2.75	0.05	2.80	.88	.14	907	417.2	304.3	17.3
41.00	2.50	0.05	2.55	.92	.18	891	417.5	303.4	18.4
41.50	2.24	0.05	2.29	.96	.23	873	417.7	302.5	19.5
42.00	2.23	0.05	2.28	.96	.23	871	417.9	301.7	20.5
42.50	2.21	0.05	2.26	.96	.24	870	418.1	300.9	21.6
43.00	2.20	0.05	2.25	.96	.24	869	418.3	300.1	22.6

MJD	$-10^6\dot{P}$		$-10^6\dot{P}_a$	$\log \rho_\pi$	$\log \rho_s$	T_∞ (K)	z (km)	$\alpha_\pi-\alpha_\odot$ (deg)	$\delta_\pi-\delta_\odot$ (deg)
				1966 44A					
41524.00	1.33		1.33	-13.58	-13.81	884	277.8	113.9	-84.1
24.50	1.22		1.22	.62	.85	863	277.8	112.0	-84.0
25.00	1.22		1.22	.62	.85	864	277.8	110.0	-83.8
25.50	1.21		1.21	.62	.85	867	277.8	108.1	-83.7
26.00	1.23		1.23	.61	.85	878	277.8	106.2	-83.6
26.50	1.24		1.24	.61	.84	885	277.8	104.2	-83.5
27.00	1.19		1.19	.63	.86	875	277.8	102.3	-83.4
27.50	1.21		1.21	.62	.85	882	277.8	100.3	-83.2
28.00	1.21		1.21	.62	.85	882	277.8	98.4	-83.1
28.50	1.20		1.20	.63	.85	879	277.8	96.4	-83.0
29.00	1.22		1.22	.62	.85	881	277.8	94.5	-82.8
29.50	1.25		1.25	.61	.84	890	277.8	92.6	-82.7
30.00	1.24		1.24	.62	.84	881	277.8	90.6	-82.6
30.50	1.31		1.31	.60	.82	892	277.8	88.7	-82.4
31.00	1.34		1.34	.59	.81	904	277.8	86.7	-82.3
31.50	1.38		1.38	.57	.79	917	277.8	84.8	-82.2
32.00	1.45		1.45	.55	.77	937	277.8	82.9	-82.0
32.50	1.46		1.46	.55	.77	937	277.8	80.9	-81.9
33.00	1.51		1.51	.54	.76	935	277.7	79.0	-81.7
41533.20	1.52		1.52	-13.54	-13.75	937	277.7	78.2	-81.7
33.40	1.53		1.53	.54	.75	908	277.7	77.5	-81.6
33.60	1.54		1.54	.54	.75	904	277.7	76.7	-81.5
33.80	1.99		1.99	.43	.64	1008	277.7	75.9	-81.5
34.00	2.29		2.29	.37	.58	1052	277.7	75.1	-81.4
34.20	3.18		3.18	.24	.44	1156	277.7	74.4	-81.4
34.40	3.19		3.19	.24	.44	1130	277.7	73.6	-81.3
34.60	3.05		3.05	.25	.46	1139	277.7	72.8	-81.2
34.80	2.19		2.19	.40	.60	995	277.7	72.0	-81.2
35.00	1.61		1.61	.53	.73	895	277.7	71.3	-81.1

Table 2 (Cont.)

MJD	$-10^6 \dot{P}$	$-10^6 \dot{P}_a$	log ρ_π	log ρ_s	T_∞ (K)	z (km)	$\alpha_\pi - \alpha_\odot$ (deg)	$\delta_\pi - \delta_\odot$ (deg)
			1966 44A (Cont.)					
41535.50	1.52	1.52	-13.55	-13.76	899	277.7	69.3	-81.0
36.00	1.53	1.53	.54	.75	913	277.7	67.4	-80.8
36.50	1.35	1.35	.59	.80	886	277.7	65.5	-80.7
37.00	1.33	1.33	.59	.81	894	277.7	63.6	-80.5
37.50	1.32	1.32	.59	.81	900	277.7	61.6	-80.3
38.00	1.34	1.34	.59	.81	892	277.6	59.7	-80.2
38.50	1.71	1.71	.49	.70	948	277.6	57.8	-80.0
39.00	1.77	1.77	.47	.69	967	277.6	55.9	-79.8
39.50	1.61	1.61	.51	.73	947	277.6	53.9	-79.7
40.00	1.44	1.44	.55	.78	908	277.6	52.0	-79.5
40.50	1.23	1.23	.62	.84	864	277.6	50.1	-79.3
41.00	1.24	1.24	.62	.84	867	277.7	48.2	-79.2
41.50	1.25	1.25	.61	.83	875	277.7	46.3	-79.0
42.00	1.26	1.26	.60	.83	884	277.7	44.4	-78.8
42.50	1.26	1.26	.60	.83	885	277.7	42.4	-78.6
43.00	1.27	1.27	.60	.82	887	277.7	40.5	-78.5
			1966 70A					
41524.00	0.75	0.75	-14.32	-14.58	940	357.5	117.8	-9.5
24.50	0.73	0.73	.33	.59	933	357.5	116.9	-8.6
25.00	0.78	0.78	.30	.57	949	357.5	116.0	-7.6
25.50	0.76	0.76	.31	.58	943	357.5	115.1	-6.7
26.00	0.74	0.74	.32	.59	936	357.6	114.2	-5.7
26.50	0.69	0.69	.34	.62	920	357.6	113.3	-4.8
27.00	0.67	0.67	.36	.63	914	357.7	112.4	-3.8
27.50	0.72	0.72	.32	.60	930	357.7	111.5	-2.9
28.00	0.70	0.70	.34	.61	924	357.8	110.6	-1.9
28.50	0.79	0.79	.29	.56	952	357.9	109.7	-1.0
29.00	0.81	0.81	.28	.55	959	358.0	108.8	0.0
29.50	0.79	0.79	.29	.56	953	358.0	107.9	0.9
30.00	0.91	0.91	.24	.49	988	358.1	107.0	1.9
30.50	0.90	0.90	.25	.50	986	358.3	106.0	2.8
31.00	0.95	0.95	.22	.47	1000	358.4	105.1	3.8
31.50	1.01	1.01	.19	.45	1017	358.5	104.2	4.7
32.00	1.03	1.03	.18	.44	1022	358.6	103.3	5.7
32.50	1.08	1.08	.16	.42	1036	358.8	102.4	6.7
33.00	1.07	1.07	.17	.42	1034	358.9	101.5	7.6
41533.20	1.23	1.23	-14.11	-14.36	1075	359.0	101.1	8.0
33.40	1.45	1.45	.06	.28	1126	359.0	100.8	8.4
33.60	1.24	1.24	.13	.35	1077	359.1	100.4	8.8
33.80	2.11	2.11	-13.89	.12	1266	359.2	100.0	9.2
34.00	2.34	2.34	.85	.07	1310	359.2	99.7	9.6
34.20	2.35	2.35	.86	.07	1307	359.3	99.3	9.9
34.40	1.71	1.71	-14.01	.22	1180	359.4	98.9	10.3
34.60	1.29	1.29	.12	.33	1089	359.4	98.6	10.7
34.80	1.30	1.30	.12	.33	1091	359.5	98.2	11.1
35.00	1.53	1.53	.05	.26	1143	359.6	97.8	11.5
35.20	1.11	1.11	.18	.40	1046	359.6	97.5	11.9
35.40	1.12	1.12	.18	.39	1049	359.7	97.1	12.3
35.60	0.91	0.91	.27	.48	994	359.8	96.7	12.7
35.80	0.95	0.95	.24	.46	1004	359.6	96.3	13.1
36.00	1.37	1.37	.08	.30	1109	359.7	96.0	13.4

Table 2 (Cont.)

MJD	$-10^6 \dot{P}$	$10^6 \dot{P}_r$	$-10^6 \dot{P}_a$	log ρ_π	log ρ_s	T_∞ (K)	z (km)	$\alpha_\pi - \alpha_\odot$ (deg)	$\delta_\pi - \delta_\odot$ (deg)
				1966 70A (Cont.)					
41536.50	0.93		0.93	-14.24	-14.47	999	359.9	95.1	14.4
37.00	0.88		0.88	.26	.49	985	360.0	94.1	15.4
37.50	0.93		0.93	.23	.47	999	360.2	93.2	16.3
38.00	1.06		1.06	.18	.41	1035	360.4	92.3	17.3
38.50	1.19		1.19	.14	.36	1068	360.6	91.3	18.3
39.00	1.01		1.01	.21	.43	1023	360.8	90.4	19.3
39.50	1.00		1.00	.21	.43	1021	361.0	89.4	20.2
40.00	1.00		1.00	.21	.43	1021	361.2	88.5	21.2
40.50	0.97		0.97	.22	.44	1013	361.4	87.5	22.2
41.00	0.83		0.83	.28	.51	974	361.6	86.6	23.2
41.50	0.76		0.76	.32	.54	953	361.8	85.6	24.1
42.00	0.73		0.73	.33	.56	944	362.0	84.7	25.1
42.50	0.67		0.67	.37	.60	926	362.3	83.7	26.1
43.00	0.67		0.67	.37	.59	926	362.5	82.7	27.1
				1968 66A					
41524.00	-0.26	0.51	0.25	-17.32	-17.86	862	748.0	172.3	21.2
24.50	-0.32	0.50	0.18	.47	-18.00	778	747.9	171.1	20.2
25.00	-0.31	0.49	0.18	.47	.00	777	747.9	170.0	19.3
25.50	-0.32	0.48	0.16	.53	.05	739	747.9	168.8	18.4
26.00	-0.28	0.48	0.19	.47	-17.97	796	747.9	167.7	17.4
26.50	-0.29	0.46	0.17	.53	-18.01	763	747.8	166.5	16.5
27.00	-0.28	0.45	0.17	.53	.01	762	747.8	165.4	15.6
27.50	-0.34	0.44	0.10	.76	.24	683	747.8	164.2	14.6
28.00	-0.36	0.43	0.07	.92	.40	682	747.8	163.1	13.7
28.50	-0.29	0.42	0.13	.64	.13	682	747.8	162.0	12.8
29.00	-0.31	0.41	0.10	.75	.25	683	747.7	160.9	11.8
29.50	-0.25	0.40	0.15	.57	.07	681	747.7	159.8	10.9
30.00	-0.18	0.39	0.20	.43	-17.95	788	747.7	158.7	10.0
30.50	-0.15	0.37	0.23	.35	.90	818	747.7	157.6	9.1
31.00	-0.13	0.36	0.23	.36	.89	818	747.7	156.5	8.1
31.50	-0.17	0.35	0.18	.47	-18.00	749	747.7	155.4	7.2
32.00	-0.14	0.34	0.20	.43	-17.95	781	747.7	154.3	6.3
32.50	-0.05	0.33	0.28	.29	.80	865	747.8	153.2	5.4
41533.00	-0.01	0.32	0.31	-17.24	-17.76	886	747.8	152.2	4.4
33.20	0.31	0.32	0.63	-16.91	.46	1025	747.8	151.7	4.1
33.40	0.80	0.31	1.11	.59	.23	1112	747.8	151.3	3.7
33.60	0.80	0.31	1.11	.58	.23	1111	747.8	150.9	3.3
33.80	0.97	0.30	1.27	.56	.17	1136	747.8	150.4	2.9
34.00	1.13	0.30	1.43	.49	.12	1153	747.8	150.0	2.6
34.20	1.30	0.29	1.59	.39	.07	1175	747.8	149.6	2.2
34.40	1.14	0.29	1.43	.42	.10	1165	747.9	149.2	1.8
34.60	0.99	0.28	1.27	.49	.17	1137	747.9	148.7	1.5
34.80	0.51	0.28	0.79	.69	.37	1061	747.9	148.3	1.1
35.00	0.35	0.28	0.63	.79	.47	1022	747.9	147.9	0.7

Table 2 (Cont.)

MJD	$-10^6 \dot{P}$	$10^6 \dot{P}_r$	$-10^6 \dot{P}_a$	$\log \rho_\pi$	$\log \rho_s$	T_∞ (K)	z (km)	$a_\pi - a_\odot$ (deg)	$\delta_\pi - \delta_\odot$ (deg)
				1968 66A (Cont.)					
41535.50	0.22	0.27	0.48	-16.95	-17.59	963	748.0	146.8	-0.2
36.00	0.02	0.25	0.28	-17.21	.82	846	748.0	145.8	-1.1
36.50	-0.07	0.24	0.17	.45	-18.03	701	748.1	144.7	-2.0
37.00	-0.06	0.23	0.17	.48	.01	699	748.2	143.7	-3.0
37.50	-0.02	0.22	0.20	.43	-17.93	764	748.3	142.6	-3.9
38.00	0.17	0.21	0.38	.13	.66	915	748.4	141.6	-4.8
38.50	0.26	0.20	0.45	.02	.60	944	748.5	140.5	-5.7
39.00	0.19	0.18	0.37	.12	.67	903	748.6	139.5	-6.6
39.50	0.02	0.17	0.19	.44	.95	738	748.7	138.4	-7.5
40.00	-0.02	0.16	0.14	.57	-18.08	689	748.8	137.4	-8.5
40.50	0.02	0.15	0.17	.49	-17.99	690	748.9	136.3	-9.4
41.00	0.08	0.14	0.22	.38	.87	779	749.1	135.3	-10.3
41.50	0.07	0.13	0.19	.46	.93	739	749.2	134.3	-11.2
42.00	0.10	0.11	0.22	.42	.85	784	749.4	133.2	-12.1
42.50	0.09	0.10	0.19	.48	.91	743	749.6	132.2	-13.0
43.00	0.08	0.09	0.17	.53	.96	701	749.8	131.1	-13.9

Table 3. Density residuals.

1963 53A		1968 66A		1959 α1		1960 ξ1		1966 70A		1966 44A	
MJD	Δlog ρ	MJD	Δlog ρ	MJD	Δlog ρ	MJD	Δlog ρ	MJD	Δlog ρ	MJD	Δlog ρ
41524.00	.370	41524.00	.120	41524.00	.179	41524.00	.297	41524.00	.217	41524.00	.157
41524.50	.293	41524.50	-.024	41526.00	.151	41524.50	.274	41524.50	.193	41524.50	.112
41525.00	.256	41525.00	-.032	41528.00	.141	41525.00	.171	41525.00	.204	41525.00	.101
41525.50	.237	41525.50	-.092	41530.00	.181	41525.50	.128	41525.50	.169	41525.50	.082
41526.00	.305	41526.00	-.025	41532.00	.144	41526.00	.114	41526.00	.134	41526.00	.074
41526.50	.289	41526.50	-.083	41533.00	.523	41526.50	.103	41526.50	.084	41526.50	.065
41527.00	.303	41527.00	-.093	41534.00	.803	41527.00	.093	41527.00	.053	41527.00	.035
41527.50	.360	41527.50	-.334	41535.00	.637	41527.50	.112	41527.50	.067	41527.50	.031
41528.00	.388	41528.00	-.501	41536.00	.057	41528.00	.130	41528.00	.039	41528.00	.020
41528.50	.325	41528.50	-.245	41537.00	.146	41528.50	.148	41528.50	.078	41528.50	.006
41529.00	.188	41529.00	-.373	41538.00	.462	41529.00	.147	41529.00	.077	41529.00	.005
41529.50	.150	41529.50	-.201	41539.00	.601	41529.50	.149	41529.50	.058	41529.50	.010
41530.00	.041	41530.00	-.096	41540.00	-.048	41530.00	.147	41530.00	.108	41530.00	-.002
41530.50	-.023	41530.50	-.058	41542.00	.041	41530.50	.116	41530.50	.088	41530.50	.009
41531.00	.088	41531.00	-.068	41544.00	.018	41531.00	.173	41531.00	.095	41531.00	.008
41531.50	.392	41531.50	-.184	41546.00	.078	41531.50	.169	41531.50	.108	41531.50	.012
41532.00	.441	41532.00	-.139	41548.00	.339	41532.00	.193	41532.00	.111	41532.00	.030
41532.50	.462	41532.50	.010	41550.00	.414	41532.50	.208	41532.50	.135	41532.50	.035
41533.00	.477	41533.00	.056			41533.00	.166	41533.00	.137	41533.00	.052
41533.50	.513	41533.20	.356			41533.20	.289	41533.20	.199	41533.20	.056
41534.00	.536	41533.40	.599			41533.40	.183	41533.40	.273	41533.40	.058
41534.50	.562	41533.60	.605			41533.60	.397	41533.60	.207	41533.60	.062
41535.00	.331	41533.80	.654			41533.80	.399	41533.80	.437	41533.80	.173
41535.50	.254	41534.00	.709			41534.00	.600	41534.00	.483	41534.00	.234
41536.00	.215	41534.20	.800			41534.20	.742	41534.20	.485	41534.20	.378
41536.50	.207	41534.40	.786			41534.40	.614	41534.40	.346	41534.40	.381
41537.00	.245	41534.60	.695			41534.60	.420	41534.60	.223	41534.60	.359
41537.50	.309	41534.80	.494			41534.80	.499	41534.80	.226	41534.80	.215
41538.00	.334	41535.00	.391			41535.00	.337	41535.00	.296	41535.00	.080
41538.50	.318	41535.50	.232			41535.50	.227	41535.20	.155	41535.50	.051
41539.00	.171	41536.00	-.013			41536.00	.217	41535.40	.157	41536.00	.053
41539.50	.138	41536.50	-.230			41536.50	.202	41535.60	.065	41536.50	-.000
41540.00	.141	41537.00	-.219			41537.00	.210	41535.80	.080	41537.00	-.004
41540.50	.116	41537.50	-.137			41537.50	.147	41536.00	.239	41537.50	-.003
41541.00	.124	41538.00	.141			41538.00	.142	41536.50	.073	41538.00	.010
41541.50	.214	41538.50	.222			41538.50	.399	41537.00	.051	41538.50	.130
41542.00	.266	41539.00	.150			41539.00	.368	41537.50	.079	41539.00	.156
41542.50	.274	41539.50	-.130			41539.50	.237	41538.00	.149	41539.50	.119
41543.00	.177	41540.00	-.264			41540.00	.189	41538.50	.222	41540.00	.073
		41540.50	-.173			41540.50	.137	41539.00	.166	41540.50	.011
		41541.00	-.055			41541.00	.114	41539.50	.165	41541.00	.021
		41541.50	-.107			41541.50	.085	41540.00	.169	41541.50	.033
		41542.00	-.031			41542.00	.101	41540.50	.164	41542.00	.045
		41542.50	-.087			41542.50	.117	41541.00	.106	41542.50	.054
		41543.00	-.129			41543.00	.136	41541.50	.077	41543.00	.066
								41542.00	.071		
								41542.50	.046		
								41543.00	.059		

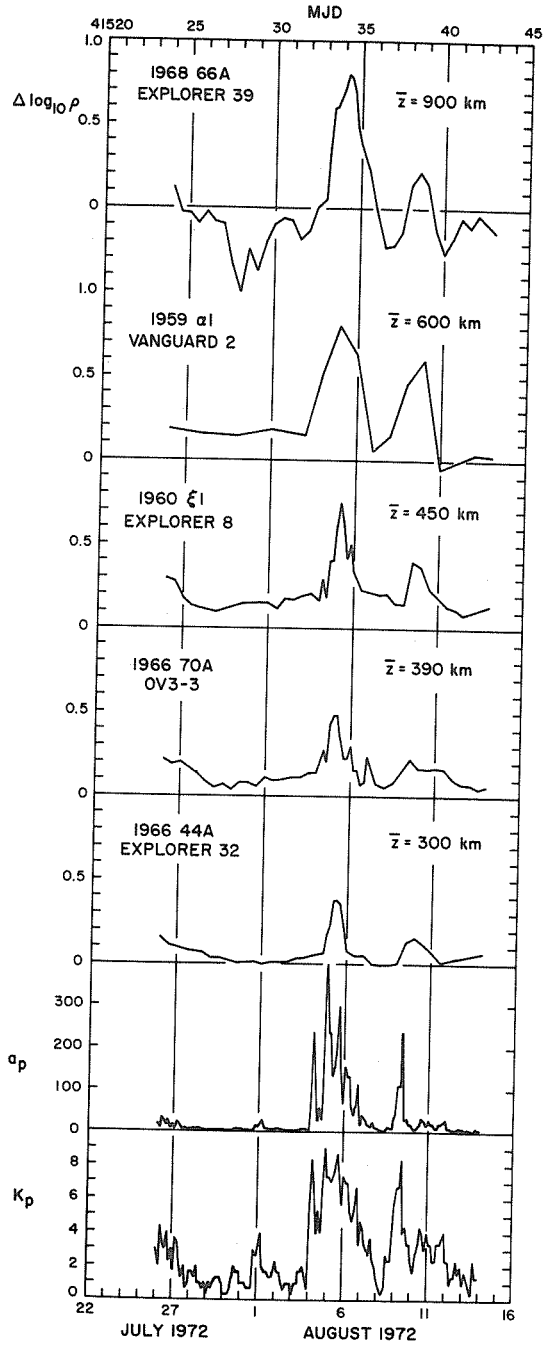

a: July–August 1972

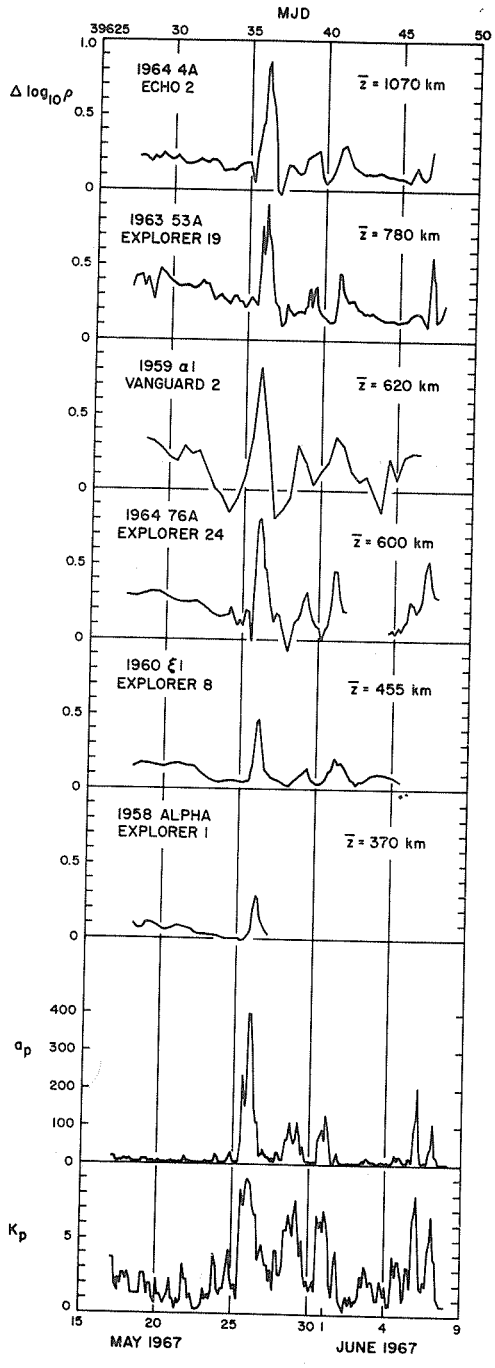

b: May–June 1967

Figure 1.–Residuals in atmospheric density, $\Delta \log_{10} \rho$, when all the known variations except for the geomagnetic effect are subtracted from the observed densities by using an atmospheric model. The 3-hour geomagnetic planetary indexes a_p and K_p are shown in the lower part for comparison.

Discontinuous Change in the Terrestrial Length of Day After Great Solar Flare of August, 1972

by

S. H. Plagemann
NASA GSFC, Institute for Space Studies, New York 10025

and

J. Gribbin
Nature, London, W.C. 2, U.K.

It is well known that with the development of accurate methods of timekeeping by atomic clocks, changes in the average level of solar activity can be correlated with changes in the spin rate of the earth [Challinor, 1971]. There is also considerable interest in direct solar-terrestrial relationships, since any sharp change in the length of the day must produce tides within the solid earth which then may act to trigger seismic activity [Gribbin, 1971]. However, the question of a one-to-one relationship between specific events on the sun and sudden changes in the length of day has remained open, chiefly because of the lack of data.

This has now been rectified by observations made before and after the great solar flare of August 2, 1972 (events associated with this flare are discussed in Pomerantz and Duggal [1973], Chupp et al. [1973], and Mathews and Lanzerotti [1973]). Only once before in four decades of routine monitoring has an event of comparable magnitude been observed. After the great flare of July 1959, there was considerable controversy over the reality of Danjon's [Danjon, 1962a, 1962b, 1962c] reports of changes in the length of day (LOD). The amplitude of the discontinuity in the LOD in Danjon's study depended on a method of reducing temporal data involving the subtraction of seasonal variations. Thus some observers [Yeh and Shaw, 1960] have confirmed Danjon's result, while others [Ijima and Okazaki, 1961] have disagreed with it. A comprehensive discussion of this controversy in the early 1960's on the nature of an interaction of large flares with the LOD is given by Schatzman [1966].

Aside from questions about seasonal corrections to data on LOD and the reality of the effect claimed by Danjon, much controversy has centered on finding a mechanism for the solar-terrestrial interaction. We shall not discuss that difficulty here, except to point out that we believe Schatzman's conclusion [Schatzman, 1966] that solar phenomena probably influence the large scale circulation of the Earth's atmosphere and the subsequent changes in angular momentum introduce certain irregularities in the LOD. However, there still exists a need for a detailed mechanism linking solar activity and the lower atmosphere phenomena [London, 1957].

The very large flare of August 1972 provides an ideal opportunity to check Danjon's data. For example, its remarkable strength allowed observations for the first time of relativistic particles which left the Sun only five minutes before the second phase of the flare maximum [Mathews and Lanzerotti, 1973]. We simply present the data, provided by the United States Naval Observatory, for the irregularities in the rate of spin of the Earth as measured by the difference between atomic time and celestial time (At-UT2). In Figure 1 we illustrate this time data modified by the removal of the seasonal terms some one month before and after the great solar flare of August 2, 1972. We also include the AT-UT2 data for a six month period, roughly three months before and after the flare of August 1972 (Figure 2) and point out that the LOD jump after this solar flare was the biggest of any irregular fluctuation during that time interval. The entire August event was followed by the southern station of the United States Naval Observatory; nightly observations on 25-35 stars showed a standard deviation of about 0.015 seconds.

Finally, it is widely accepted that one possible link with solar activity with the Earth's atmospheric tides and movement of low pressure systems at high latitudes [Macdonald and Roberts, 1960]. Statistical studies are consistent with a model that shows that small tidal influences can influence the timing of events like the initiation of precipitation [Brier, 1965]. Thus it is not unreasonable to allow several days to elapse before weather systems develop sufficiently to change the LOD through angular momentum transfer. This could well be why the effect on the LOD is seen a few days after the August solar flare, although we do not suggest this as the only possible link.

While the evidence we present is not conclusive in itself, yet taken together with Danjon's work, it essentially predicts that large solar flares will be associated with measurable changes in the LOD. In addition, exchanges of angular momentum (due to changes in the LOD of a few milliseconds) on the order of 10^{32}gm cm^2/sec, taken over a few days, require dissipation of torques of more than 10^{26} dyne cm. Thus rapid changes in tidal stress after the great solar flare of August 1972 comparable in magnitude to slow changes generated by changes in the LOD over periods of 10^3 days may have contributed significantly to triggering tectonic processes [Challinor, 1971; Schatzman, 1966; Shlien, 1972; and Shaw et al., 1971].

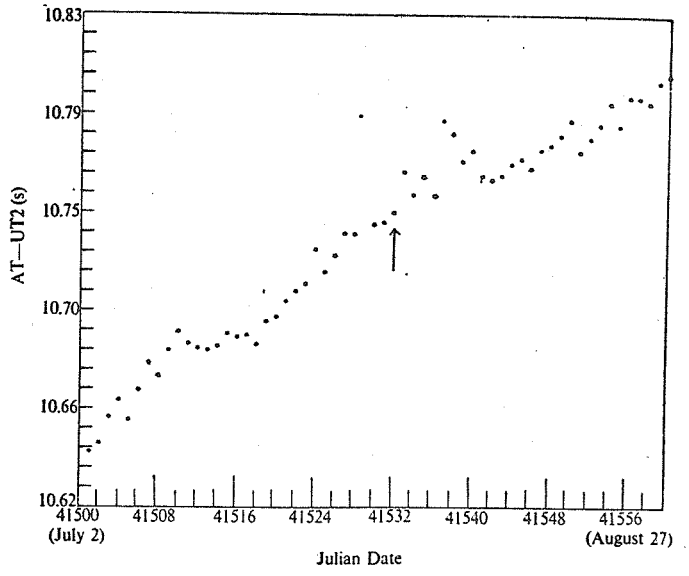

Fig. 1. United States Naval Observatory time service measure of the length of day (LOD) with seasonal terms subtracted. At-UT2 is shown as one measurement per day over the interval J.D. 41500 and J.D. 41565 (2 July 1972 to 5 September 1972). The arrow points to the day of the solar flare on August 2, 1972.

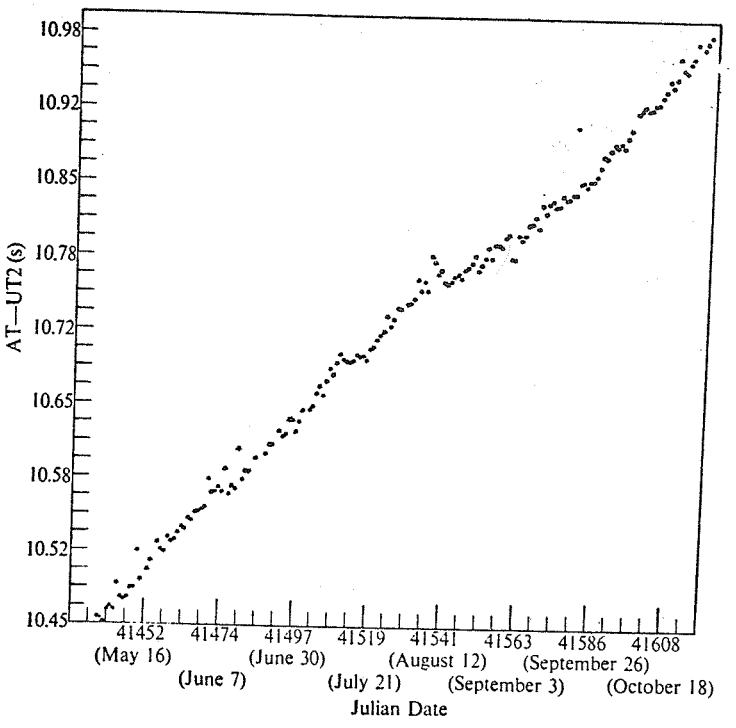

Fig. 2. United States Naval Observatory time service data on At-UT2 over three months before and after the great solar flare (1 May 1972 to 31 October 1972).

Acknowledgement

We thank the United States Naval Observatory for supplying the raw data used in the preparation of Figures 1 and 2.

REFERENCES

BRIER, G. W. 1965 Mon. Weath. Rev., 93, 93.

CHALLINOR, R. A. 1971 Science, 172, 1022.

CHUPP. E. L., D. J. FORREST P. R. HIGBIE A. N. SURI C. TSAI and P. O. DUNPHY 1973 Nature, 241, 333.

DANJON, A. 1962a Compt. Rend., 254, 2479.

DANJON, A. 1962b Compt. Rend., 254, 3058.

DANJON, A. 1962c Notes et Informations de l'Observatoire de Paris, 8, No.7.

GRIBBIN, J. 1971 Science, 173, 558.

GRIBBIN, J. and S. PLAGEMANN 1973 Nature, 243, 26-27.

IJIMA, S. and S. OKAZAKI 1961 Publ. Astron. Soc. Japan, 13, 125

LONDON, J. 1957 Trans. N. Y. Acad. Sci., 19, 138.

MACDONALD, N. J. and W. O. ROBERTS 1960 J. Geophys. Res., 65, 529.

MATHEWS, T. and L. J. LANZEROTTI 1973 Nature, 241, 337.

POMERANTZ, M. A. and S. P. DUGGAL 1973 Nature, 241, 331.

SCHATZMAN, E. 1966 The Earth-Moon System (ed. by A. G. W. Cameron and B. G. Marsden) page 12 (Plenum, New York).

SHAW, H. R. R. W. KISTLER and J. F. EVERNDEN 1971 Bull. Am. Geol. Soc., 82, 869.

SHLIEN, S. 1972 Geophys. J. R. Astr. Soc., 28, 27.

TAMRAZYAN, G. P. 1968 J. Geophys. Res. 73, 6013.

YEH, S. H. and B. T. SHAW 1960 Acta. Astron. Sinica, 8, 68.

Photometric Observations of Mid-Latitude Aurora during the August 1972 Solar-Geophysical Event

by

E. G. Mullen and D. J. Davis, Jr.
AFCRL (LKA)
L. G. Hanscom Field
Bedford, MA 01730

The great solar flares of August 1972 were responsible for large scale ionospheric disturbances, especially in polar cap areas where intense PCA effects were recorded. At Hanscom Field, Bedford, Massachusetts an interference-filter photometer was coupled to a digital readout system being tested for use at Thule, Greenland, and measurements of the green line at 5577 angstroms were recorded at 2 second intervals for the nighttime periods from 4 to 10 August. The photometer was pointed at the zenith sky and had a 5° field of view.

Quantitative measurements of the auroral light are presented in Figure 1 which contains computer produced logarithmic graphs of 2 second interval 5577 A intensities vs. time. The data gap on the morning of August 8 was due to a severe lightning storm. Although the equipment was not turned on until the night of August 4, auroral effects were then quite evident, and at approximately 2150 EST an intense bright auroral form with spectral intensities in excess of 10 kilorayleighs passed overhead. By the morning of August 8 the intensities had returned to the normal airglow level of 100-200 rayleighs. The flare of August 7 produced increased activity on the night of August 8, but by the following night normal intensity levels had again returned.

The geomagnetic latitude of the observing station is N53.5, and the longitude is E357.8.

These data were previously published in Sky and Telescope, 45, No. 2, February 1973.

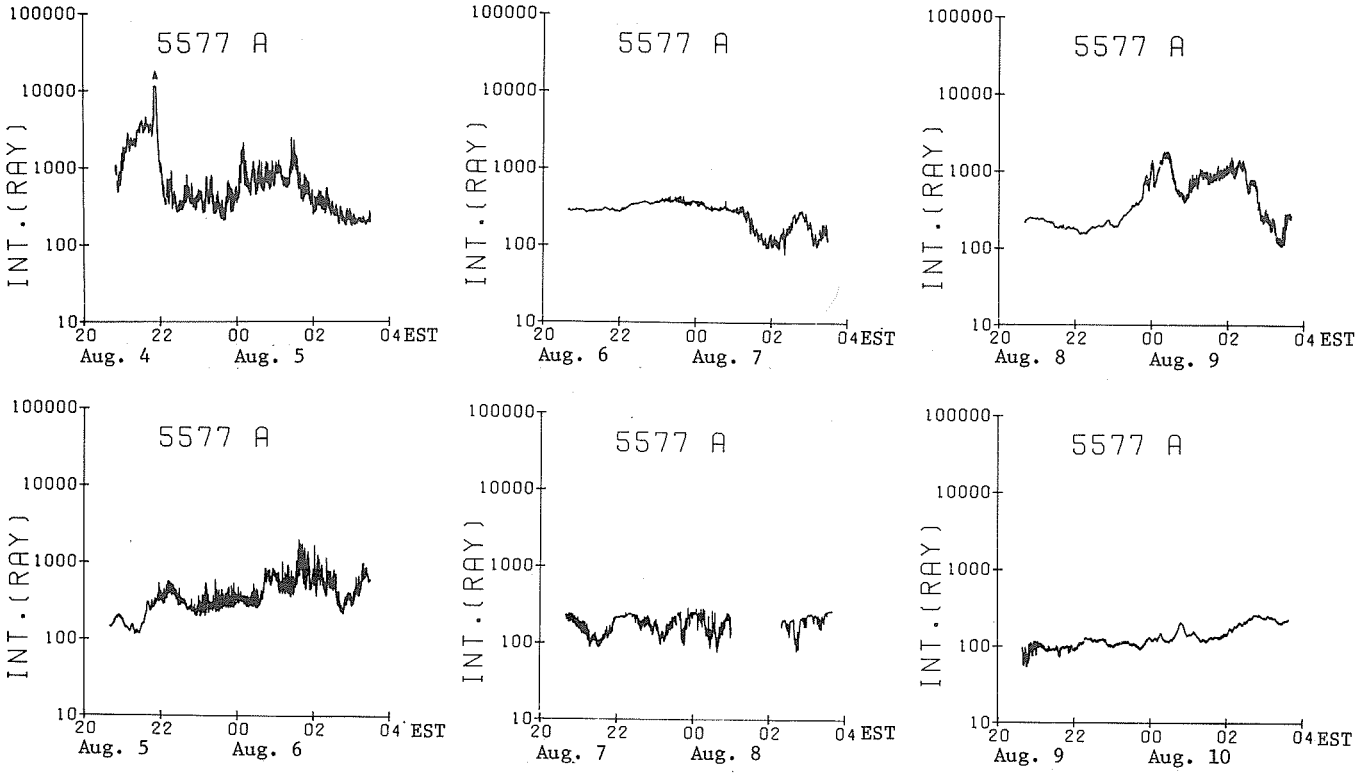

Fig. 1. Intensity of the green line at 5577 angstroms as recorded with a filter photometer at Bedford, Massachusetts, August 4-10, 1972.

Aurora Backscatter Observations from August 3 to August 10, 1972

by

P. Czechowsky
Max-Planck-Institut fur Aeronomie
3411 Lindau/Harz
Federal Republic of Germany

Since 1969 the Max-Planck-Institut at Lindau/Harz has carried out VHF aurora backscatter observations in Scandinavia. The geographical locations of the transmitter at Borlange (SK4MPI) and the receiver station at Lycksele, the corresponding antenna directions (arrows), and the backscatter curves indicate the region in the E-layer (height = 110 km) with optimum conditions for the scattering processes of VHF radio waves, which are fulfilled, if the sum of the angles between the normals of the incident and the scattered radio waves and the direction of the earth magnetic field is $\Sigma = 180°$.

The frequency of the transmitter is 145.96 MHz with a power output of about 150 Watts. The radiated cw-signal is interrupted once a minute by the call sign SK4MPI, which causes a characteristic structure on the backscatter recordings. The 4 x 6-element Yagi antenna system is directed toward geographic north and has a half-power beam width of 60° and a gain of 12 dB. At Lycksele the amplitude and the frequency shift of the scattered signals were observed from different directions with two separate receiving antennas. The antennas, with a half-power beam width of 30° and a front to back ratio of about 21 dB, point to 30° West and to 60° East.

The first backscatter echoes of this period were observed on August 4, 1972 from 0310 to 0830 LT (Local Time = 15° East Meridian Time) and from 2200 to 0700 LT on August 4/5. The field strength and the Doppler shift Δf of the scattered radio waves received from both directions at Lycksele are shown in Figures 2 and 3. From the amplitude variation measured by the east antenna (second diagram from the top in Figure 2) two different types of signals can be distinguished: a) backscatter echoes characterized by the call sign structure, and b) an extremely high increase of the noise level starting with sunrise from about 0300 to 0600 LT and from 0710 to 1100 LT, caused by solar radio emission in this frequency range. The same types of signals, with lower intensity, however, were received by the backward lobe of the westward-directed antenna (upper diagram in Fig. 2) from about 0720 LT on August 4. Strong auroral backscatter echoes were superimposed on these noise signals until 0835 LT.

From 0300 to 1100 LT on August 4 and from 2200 to 0600 LT on August 4/5 the Doppler shift Δf of the signals received from the two different directions had the same sign. This can be interpreted by a northward (August 4) and by a southward (August 4/5) movement of the scattering structures. An analysis and exact calculation of the velocity of these scattering centers are not possible without measurements of the earth magnetic disturbance vectors, since the excitation and the propagation of the scattering structures depend on the direction, strength, and extent of the polar electrojet [Czechowsky, 1973]. Normally the Doppler shifts observed from both antennas have different signs as is shown in Figure 4 for November 2/3, 1972, which indicates that the scattering centers are moving close to an east-west direction.

Figure 5 presents the variations of the field strength of the auroral backscatter echoes received from both directions from August 3 to August 10, 1972. The amplitudes of the signals were analyzed every 15 minutes in steps of 2 dB. The main phases of auroral activity occur from August 4 to August 6 and on August 9; these are well correlated with the periods of maximum magnetic disturbance (cf. planetary magnetic indices).

REFERENCE

CZECHOWSKY, P. 1973 Movement Processes of Auroral Structures (in preparation for publication in J. Atmosph. Terr. Phys.).

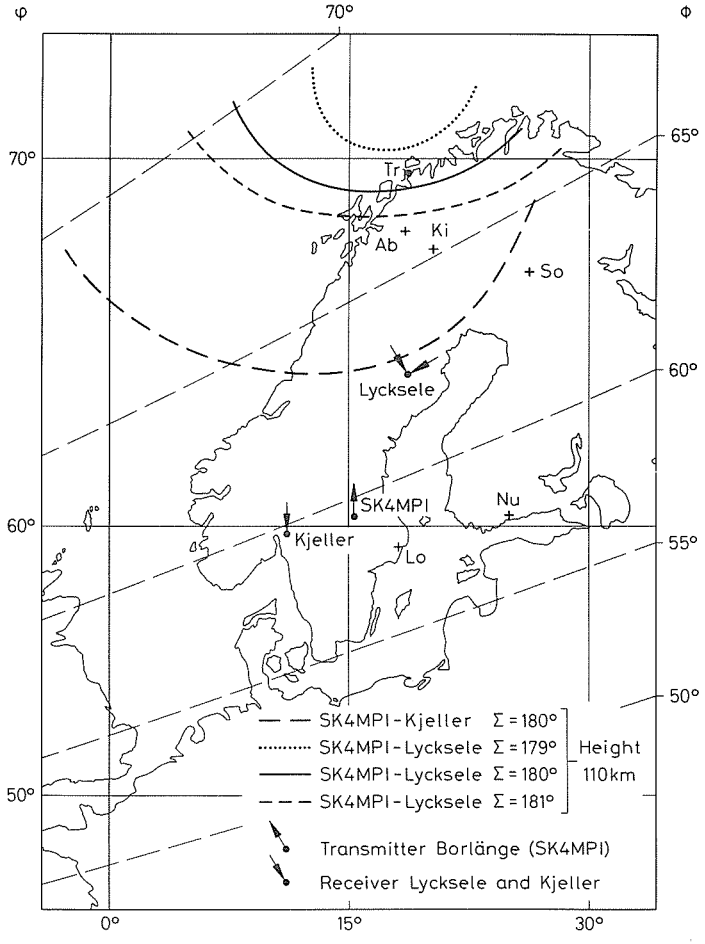

Fig. 1. Location of transmitting and receiving stations with corresponding antenna directions (arrows) and backscatter curves.

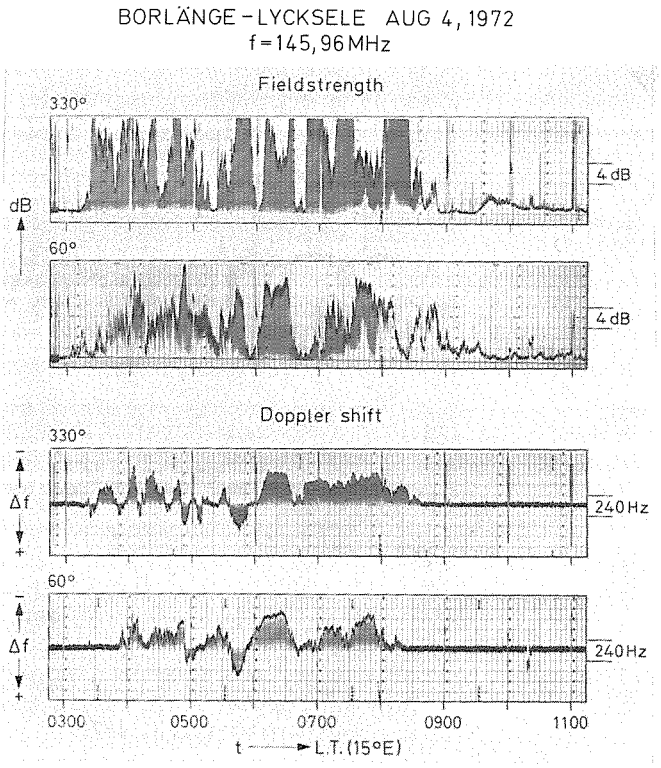

Fig. 2. Field strength and Doppler shift of the backscattered signals received on August 4, 1972. (Concerning the enhanced solar noise level compare with the contribution of H. Schwentek in this issue.)

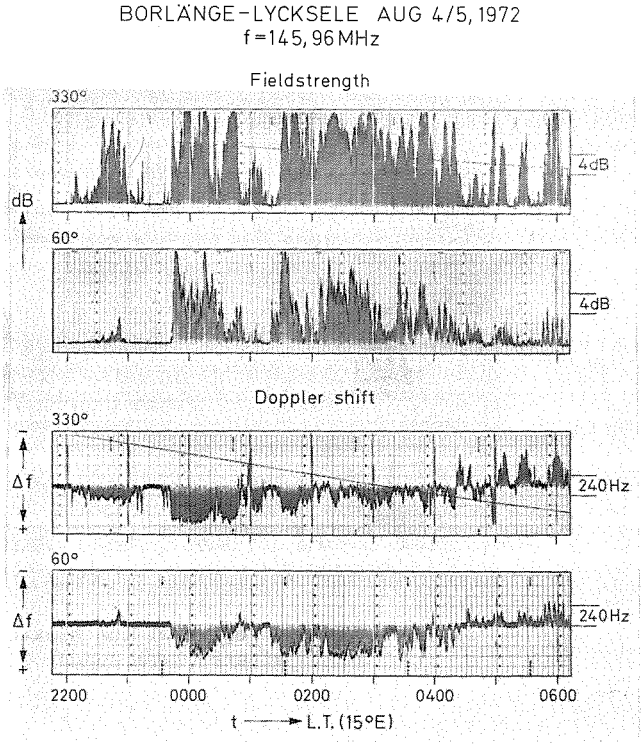

Fig. 3. Field strength and Doppler shift of the backscattered signals received on August 4/5, 1972.

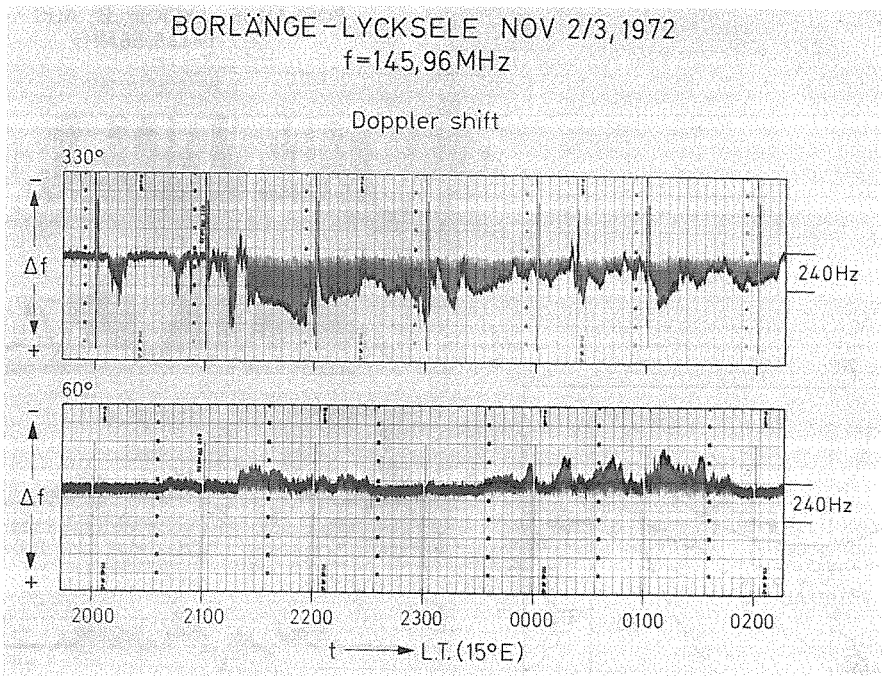

Fig. 4. Doppler shift of the backscattered signals received on November 2/3, 1972.

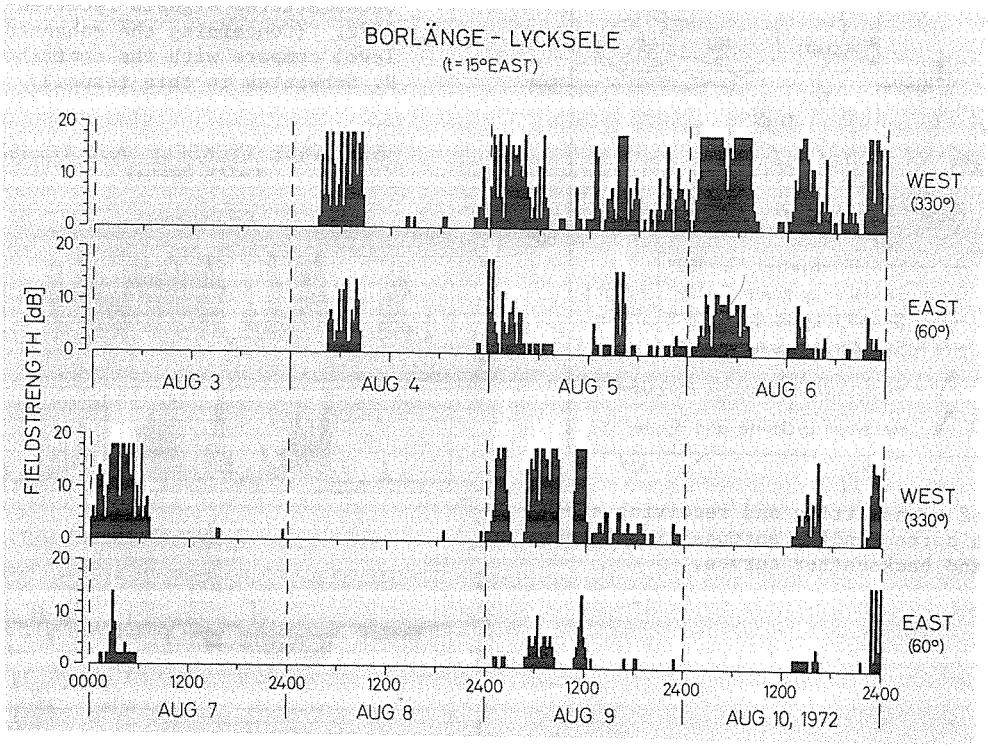

Fig. 5. Field strength of the backscattered signals received in intervals of 15 minutes from August 3 to August 10, 1972.

Simultaneous Pulsations in Radio Aurora, Magnetic Field, and Absorption Observed during the August 1972 Storms

by

J. G. Keys
Physics and Engineering Laboratory Auroral Station
D.S.I.R.
Omakau, New Zealand

Abstract

A sequence of pulsating radio aurora is compared with absorption and magnetic data. The degree of phase coherence between corresponding pulsations on the different records suggest a common controlling mechanism. It is proposed that the radar echo and absorption production may each be influenced by hydromagnetic wave activity.

Introduction

During the large magnetic storm of August 1972 several periods of pulsation activity were recorded on the records of the Slope Point, New Zealand, auroral radar. Details of this equipment are given by Keys [1970].

Although periodically-varying echoes in the radio aurora have been observed previously [Kaneda, et al., 1964; Brook , 1967; McDiarmid, et al., 1972], and a change in the character of the magnetic record at Macquarie Island has been observed when pulsating echoes were recorded on the Bluff auroral radar [Keys, 1965], the present data are unusual in that simultaneously with the radar pulsations, prominent pulsations in the ground fluxgate magnetometer, earth-current and 30 MHz riometer records were observed at Campbell Island ($L \simeq 4$), which lies under the radar beam.

Periodic variations in absorption are considered to be a consequence of a modulation in the precipitating electron flux, and while long period (Pc 5) magnetic pulsations sometimes accompany those in absorption, there is no peak-to-peak correlation between them [Brown, 1966].

It is of interest, then, that the present data not only show the simultaneous occurrence of periodically varying radio aurora and absorption, not previously observed, but also demonstrate a near-constant phase relationship between the corresponding pulsations recorded on different equipment. A comparison of the radar and riometer data shows a tendency for two radar echoes to be produced for each absorption cycle.

Data

The slant range from the radar to the 100 km level above Campbell Island is approximately 650 km. The riometer is a conventional instrument operating at 30 MHz using a ground plane antenna with a beamwidth of 60° to the half power points. Magnetic data reproduced here is from a single component fluxgate magnetometer recording the D component, as the records from standard 3-component variographs at Campbell Island were so disturbed as to be unusable. The earth-current data shown is that from the north/south component.

Figure 1 shows a section of radar record with pulsations present, beneath which are reproduced the magnetometer, earth-current and riometer records on the same time scale. A long period intensity modulation (2-4 minutes) is evident in each set of data.

The riometer data has been processed in a computer lowpass filter to remove noise, and a section of the resultant output is shown in Figure 2. The solid sections of the trace indicate the times when the radar echoes can be distinguished above the system noise at a range of 650 km, which corresponds to the radar slant range to the center of the riometer beam at a height of 100 km above Campbell Island. For clarity, the radar record is again reproduced, with echoes at the range of interest being intensified.

Discussion

Figure 1 illustrates the degree of phase coherence that exists between the pulsations in each set of data.

From about 0705 UT the radar echoes become visible at 650 km. It is noticeable that the pulsations tend to appear alternately strong and weak, and that after about 0730 UT the weak echo appears to fall in amplitude below the detection level. The amplitude of the weak echo does not appear to be

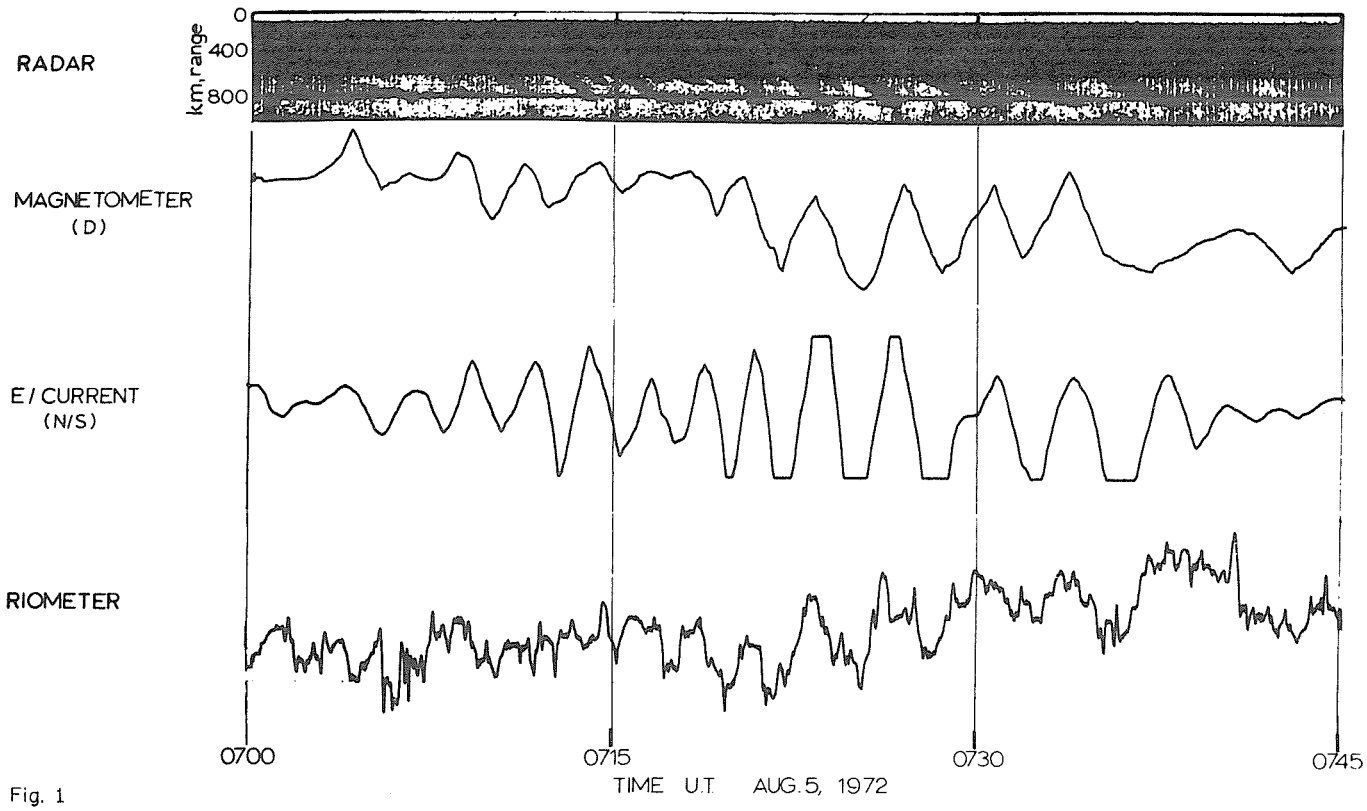
RADAR
km, range
0
400
800
MAGNETOMETER
(D)
E/CURRENT
(N/S)
RIOMETER
0700
0715
0730
0745
TIME U.T. AUG.5, 1972

Fig. 1

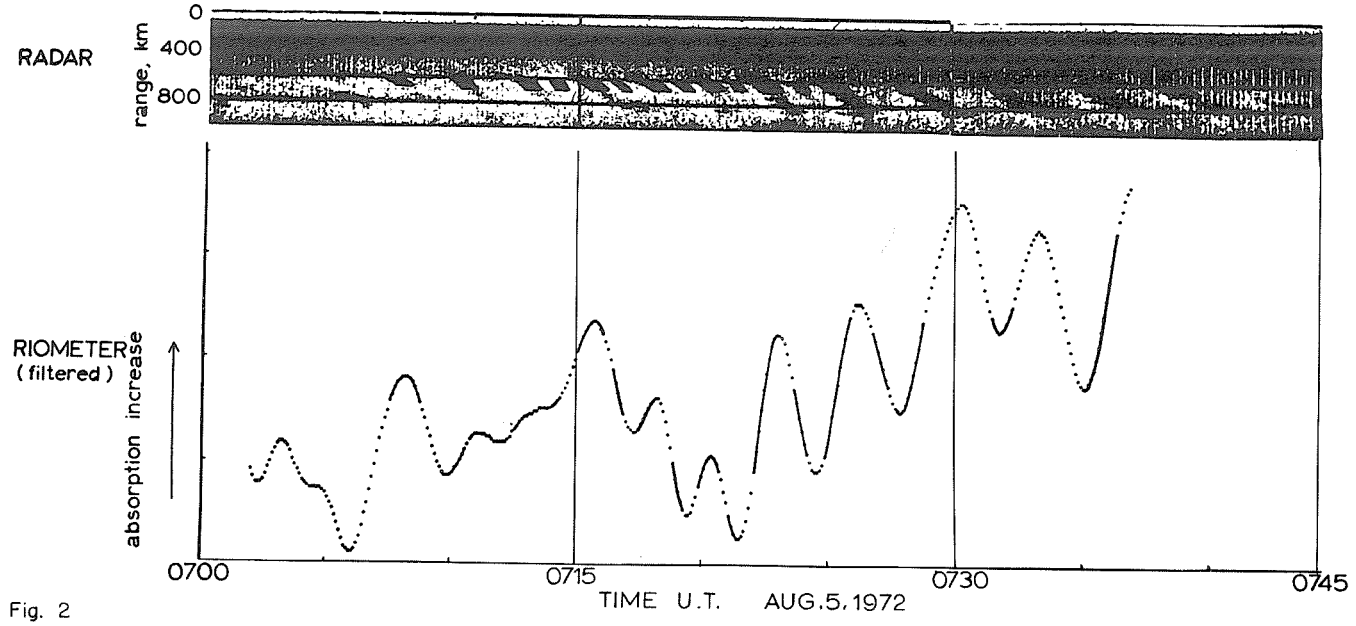
RADAR
range, km
0
400
800
RIOMETER
(filtered)
absorption increase
0700
0715
0730
0745
TIME U.T. AUG.5, 1972

Fig. 2

related to that of its stronger counterpart. In Figure 2 it can be seen that from 0715 UT to 0727 UT two radar echoes are present during each absorption cycle, and that beyond this time the absorption retains its modulated form, but that only one echo per cycle is distinguishable.

Because the magnetic data shown in Figure 1 is that from a single component, it is not possible to trace the position of the magnetic vector with time. The appearance of the record suggests, however, that we may be observing a rotating magnetic vector of the sort often ascribed to hydromagnetic wave activity [e.g. Wilson and Sugiura, 1961]. As in the absorption data it can be seen that a radar echo tends to occur on each half cycle of the pulsations.

The inference drawn from the data is that the radar pulsations are not a direct consequence of the precipitation observed by the riometer, but are closely related to the mechanism producing it. The apparent association between pulsating echoes and Pc 5 magnetic pulsations has been ascribed by Unwin and Knox [1971] to the ion-acoustic instability process operating as a consequence of an oscillating electric current at ionospheric heights. Thus an echo is produced each time the current exceeds the threshold value for the instability - i.e., either once or twice per rotation of the magnetic vector, depending on the amplitude of the current.

The present data is in agreement with this hypothesis, although without complete magnetic information a full analysis of the results is not possible. In addition, well resolved Doppler spectra from the radar are required to categorically define the instability mechanism, as pointed out by McDiarmid and McNamara [1972].

The riometer pulsations, with periods twice that observed in the radar data, are attributed to a process such as that suggested by Singh [1964], where the loss cone of precipitating electrons is subjected to a periodically varying modification by the hydromagnetic wave.

REFERENCES

BROOKS, D.	1967	J. Atmos. Terr. Phys. 29, 589.
BROWN, R. R.	1966	Space Sci. Rev. 5, 311.
KANEDA, E., S. KOKUBUN, T. OGUTI, and T. NAGATA	1964	Rept. Ionos. Space Res. Japan, 18, 165.
KEYS, J. G.	1965	J. Atmos. Terr. Phys. 27, 385.
KEYS, J. G.	1970	J. Atmos. Terr. Phys. 32, 1975.
McDIARMID, D. R. and A. G. McNAMARA	1972	Ann. Geophys. 28, 433.
SINGH, R. N.	1964	Nature, 203, 69.
UNWIN, R. S. and F. B. KNOX	1971	Radio Science, 6, 1061.
WILSON, C. R. and M. SUGIURA	1961	J. Geophys. Res., 66, 4097.

Acknowledgements

The author is indebted to Mr. P. J. Gill for the loan of the Campbell Island earth current record, and to Mr. L. Tomlinson for his assistance in computer processing the riometer data.

Ground-Based Measurements of the 6300A OI Airglow Intensity and Temperature during Period 4-14 August 1972

by

R. E. Smith and G. R. Swenson
Aero-Astrodynamics Laboratory
NASA, Marshall Space Flight Center
Huntsville, Alabama

A 15-cm aperture Fabry-Perot Interferometer, similar to the one at the University of Michigan, is routinely used to make measurements of the 6300A OI intensities and Doppler temperatures at the Marshall Space Flight Center, Alabama. It has a pressure scanning system which uses dry nitrogen gas with a photoelectric detector system. During the Retrospective World Interval, 26 July-14 August 1972, observations were made on the nights of 4, 5, 6, 8, 13, and 14 August 1972, although the weather was somewhat marginal and restricted the observation time to a few hours each night. The observations reported here are those made where clouds did not interfere.

Figure 1 is a computer plot of two 6300A emission line profiles observed vertically over Huntsville, Alabama on August 4, 1972. These are typical of the line profiles observed on each of the six nights of the storm period. A computerized version of the technique described by Hays and Roble [1971] was used to derive temperatures from the Doppler broadening of the profiles.

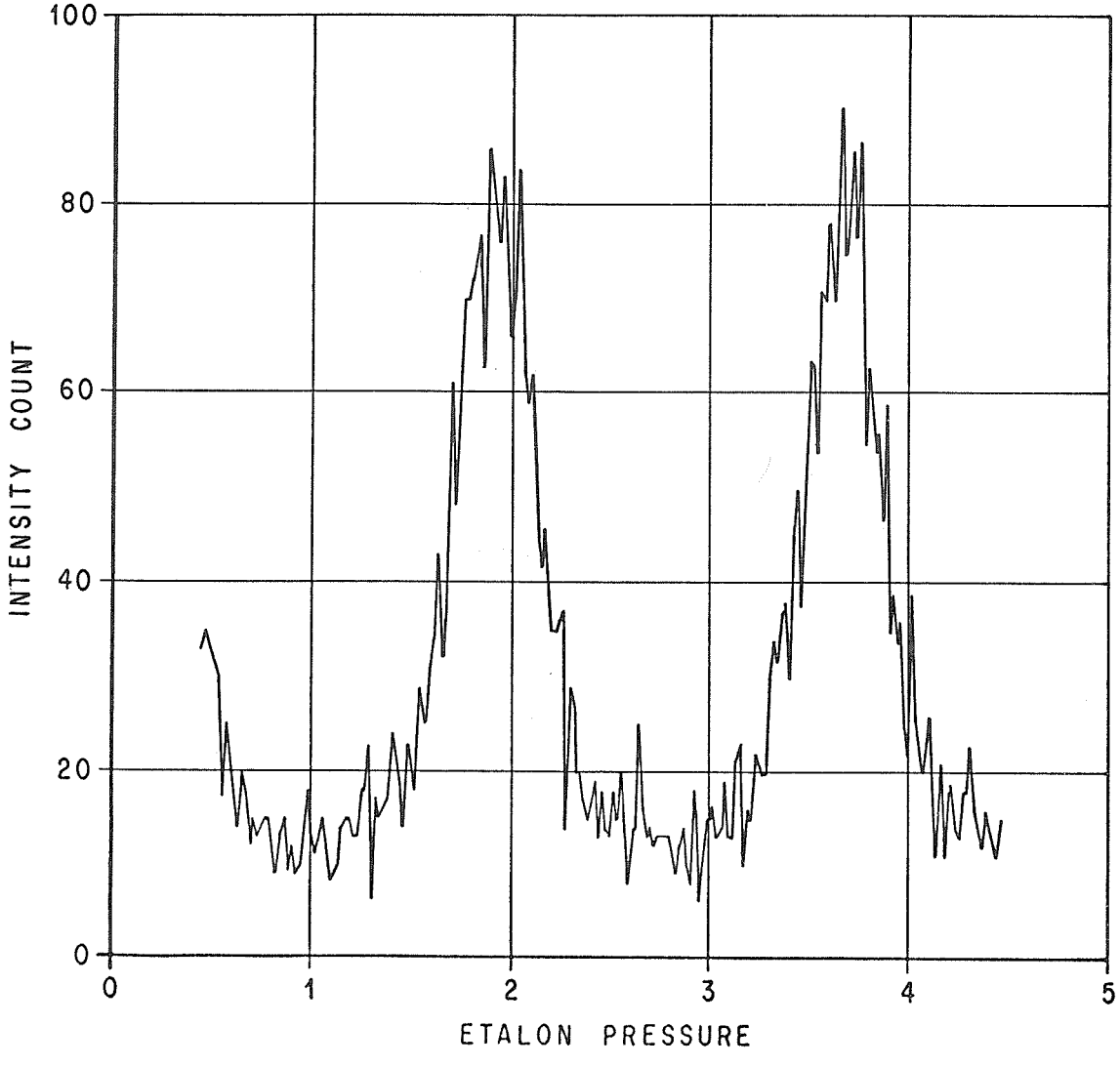

Fig. 1 6300A OI fringe: Computer plot of two 6300A emission line profiles, 4 August 1972.

The temperatures derived in this manner are shown as a function of Local Daylight Time (LDT) in Figure 2. Large fluctuations in very short time periods are seen in the observed temperatures with three or four extremely cold temperatures being derived for the night of 8 August 1972. Other than the fact that they are extremely low, there is no additional evidence for discounting these temperatures. All the criteria set up in the computer program for judging whether or not the derived line profile fits the data and, therefore, that the derived temperature is acceptable, were met by these low temperatures equally as well as the 'more reasonable' temperatures. They are, therefore, included herein in order to provide as much observational data as possible even though no feasible physical explanation is available at this time.

Figure 2 also shows that in general the temperatures on the night of 4 August 1972 were substantially higher than those on the following nights. They also appear to be far more stable with none of the large fluctuations seen on the other nights.

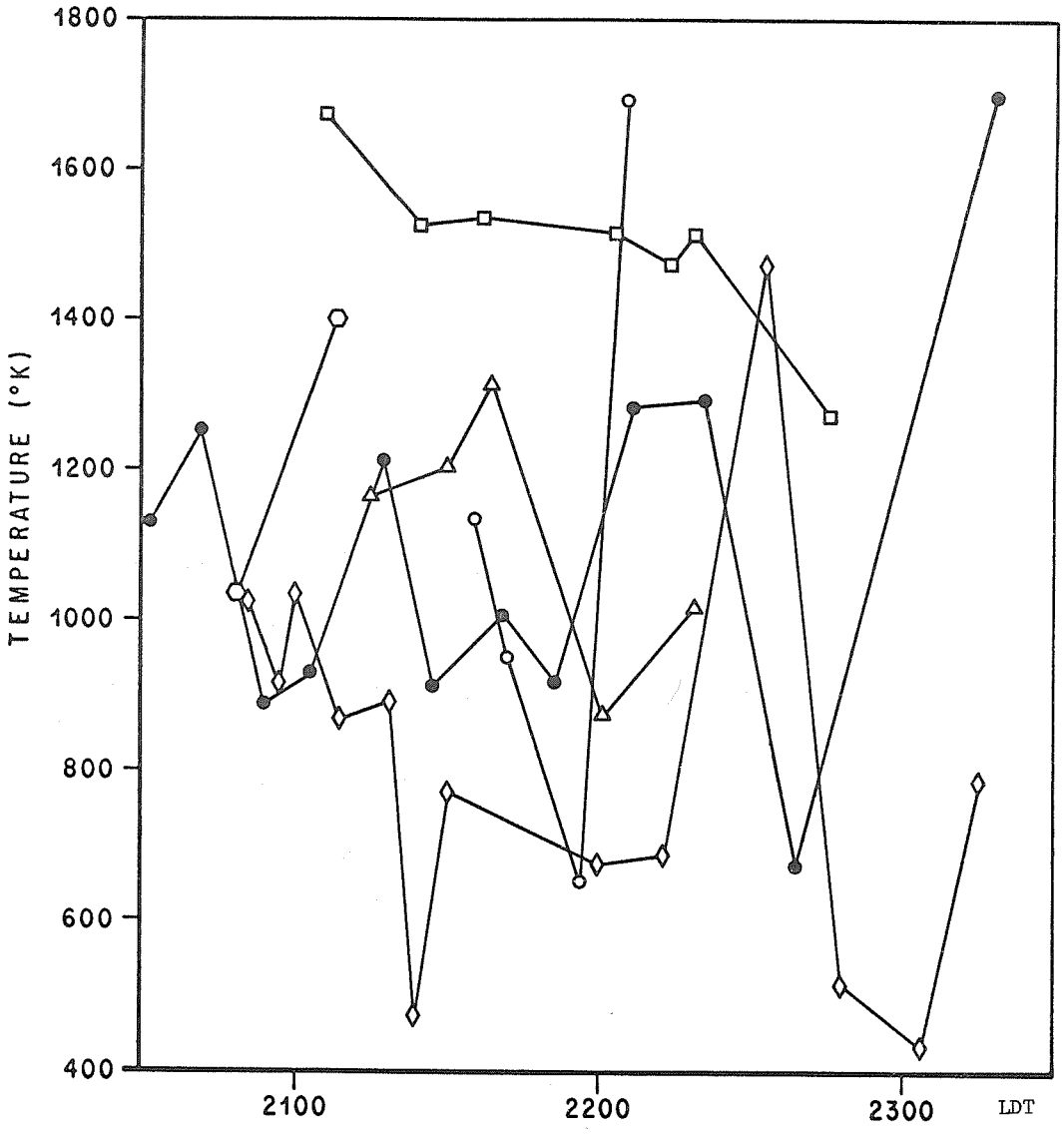

Fig. 2 6300A OI Doppler Temperatures for the Local Daylight Time 2100-2300 LDT, 4, 5, 6, 8, 13 and 14 August 1972.

□ AUG. 4, 1972
○ AUG. 5, 1972
△ AUG. 6, 1972
◇ AUG. 8, 1972
⬡ AUG. 13, 1972
● AUG. 14, 1972

The intensity of the 6300A emission was obtained by integrating the area under the emission line profiles. Figure 3 shows the intensity as a function of time for the same six nights. The intensity on the night of 4 August is substantially greater than the other five nights. The fluctuations in the intensity are far greater on this night than the other nights in contrast to the greater stability in the temperature.

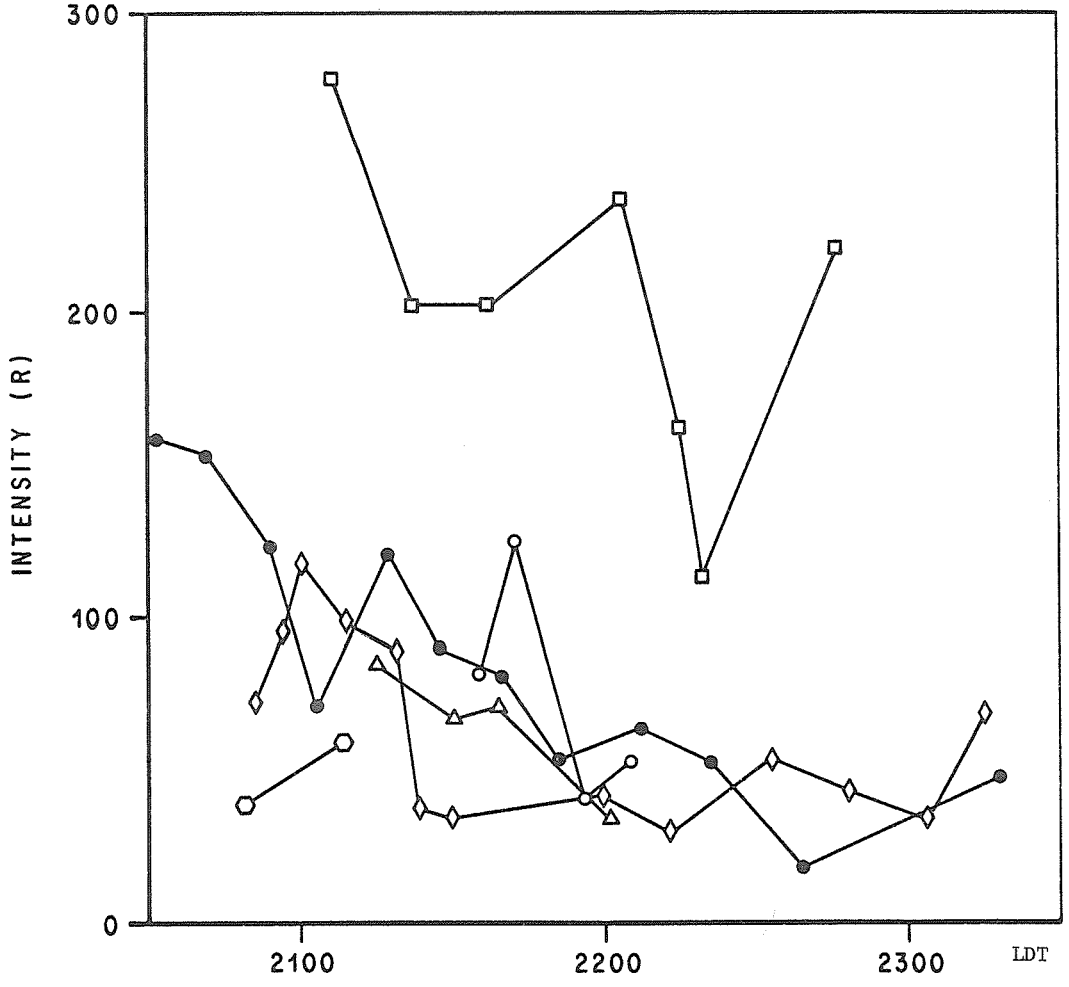

Fig. 3 6300A OI Intensity for the Local Daylight Time 2100-2300 LDT, 4, 5, 6, 8, 13 and 14 August 1972.

□ AUG. 4, 1972
○ AUG. 5, 1972
△ AUG. 6, 1972
◇ AUG. 8, 1972
⬡ AUG. 13, 1972
● AUG. 14, 1972

On each of these nights scans were made with a turret-type photometer to see if there was a red arc; however, there were clouds on the horizon which prevented observation of the normal van Rhijn effect on 4 August 1972. Although red arcs were not detected, it is possible that an arc was directly overhead on 4 August. This would account for the greater intensity on this night.

REFERENCES

HAYS, P. B. and R. G. ROBLE — 1971 — A Technique for Recovering Doppler Line Profiles from Fabry-Perot Interferometer Fringes of Very Low Intensity, Appl. Optics, 10, 193.

Airglow Observations from Southern Africa during the Interval 4 August - 7 August 1972

by

E. H. Carman and M. P. Heeran
University of Botswana, Lesotho and Swaziland
Roma, Lesotho, Africa

A program of ground based airglow observations employing intercalibrated photometers [Carman et al., 1969] is proceeding at the following stations: Olorgesailie (1.5°S, 36.5°E geographic), Ewanrigg (17.5°S, 31.0°E) and Roma (29.7°S, 27.7°E). In the present paper 6300 Å behaviour which is definitely related to the magnetic activity of the Retrospective World Interval July 26 - August 14, 1972 is presented. The data features observation of a stable auroral red arc (SARARC) from Roma. Detailed results of the SARARC will be published elsewhere but a summary of the results is discussed in the present paper.

For eighteen months of airglow data at Roma involving fifty one separate nights and including twenty two occasions when $K_p > 4$ there was no systematic variation of 6300 Å with K_p index. However, there is still the possibility that a systematic decrease in 6300 Å is characteristic of nights following a severe disturbance when the field is depressed by more than 150 γ. On the 17/18 December 1971 a 200 γ storm produced a 0.7 kR arc and on 4/5 August 1972 a 300 γ storm produced a 0.9 kR arc south of Roma. Table 1 gives values of the red line averaged throughout the respective nights in a part of the sky away from the arcs.

TABLE 1

1971			1972		
17/18 Dec.	19/20 Dec.	20/21 Dec.	4/5 Aug.	5/6 Aug.	6/7 Aug.
51 R	42 R	28 R	30 R	6 R	10 R

The tabulated decreases in 6300 Å emission are consistent with observed mid-latitude behaviour of the F2 region accompanying a geomagnetic disturbance [Taylor, 1961; Lawrence et al., 1963]. A substantial reduction in peak electron density and general decrease in electron content is to be expected. Hence a decrease in 6300 Å emission resulting from dissociative recombination process will result.

Figs. 1, 2 and 3 illustrate the SARARC of the 4/5 August 1972. Fig. 1 shows that this event was first observed as an enhancement superimposed (perhaps at a different altitude) on dissociative recombination emission of the 6300 Å line at 2300 UT. The enhanced contours form straight lines tending to align with invariant latitude excepting near dawn when the effects of sunrise in the ionosphere caused an anticlockwise skewing. Typical structure for the arc is illustrated in Fig. 2 which represents the cross-section of the arc in the azimuthal direction of the 0.9 kR photometric maximum.

There are important differences in the relative geomagnetic activities associated with the SARARCS of December 1971 and August 1972. Comparison is interesting because the observation of an arc from Roma with a low L value (1.8) is rare and the reported events are the only two so far observed in Southern Africa. The A_p index shows that the latter event corresponded to three times the magnetic activity of the former. It was also accompanied by a depression of the neutron count rate six times as great and X-ray flux increases of more than an order of magnitude greater. This high level of activity is also evident in Fig. 3 which was obtained from the Hermanus magnetogram; the figure shows that the arc began during the onset of the main phase of the 2024 UT SC storm of 4 August 1972.

To interpret SARARC development one must consider the processes following injection of storm particles from the magnetospheric tail into the ring current. This results in movement of the plasmapause and for sufficiently disturbed conditions leading to a main phase SARARC ring current energy is transferred to the plasmasphere when the ring current penetrates into the plasmapause. Transfer of this energy to the ionosphere will be mentioned in the next paragraph. Experimental satellite observations lead to the relationship between the position of the plasmapause and magnetic activity as measured by K_p index. Chappell et al.'s [1970] OGO 5 ion concentration measurements as a function of L and local time indicate a decrease in plasmapause radius as K_p increases. A linear extrapolation of Fig. 3 of their data to the minimum L value of the present arc (L = 1.8) shows that this position of the plasmapause should occur when K_p is about 8 in agreement with the actual main phase value (K_p = 8) for the present storm.

Nagy et al. [1970] have recently reviewed several SARARC theoretical models including the soft electron flux theory of Walker and Rees [1968] and the thermal conduction model of Cole [1965]. The latter has been investigated in detail by Cornwall et al. [1971] and Chandra et al. [1972] and is the most appropriate model to interpret the observed features of the present SARARC. In the thermal conduction hypothesis ring current energy transfer to plasmaspheric particles occurs with subsequent thermal conduction to the ionosphere via the electron ion gas in the magnetic tubes of force. The heated electrons then excite the SARARC by collisions with ionospheric oxygen atoms.

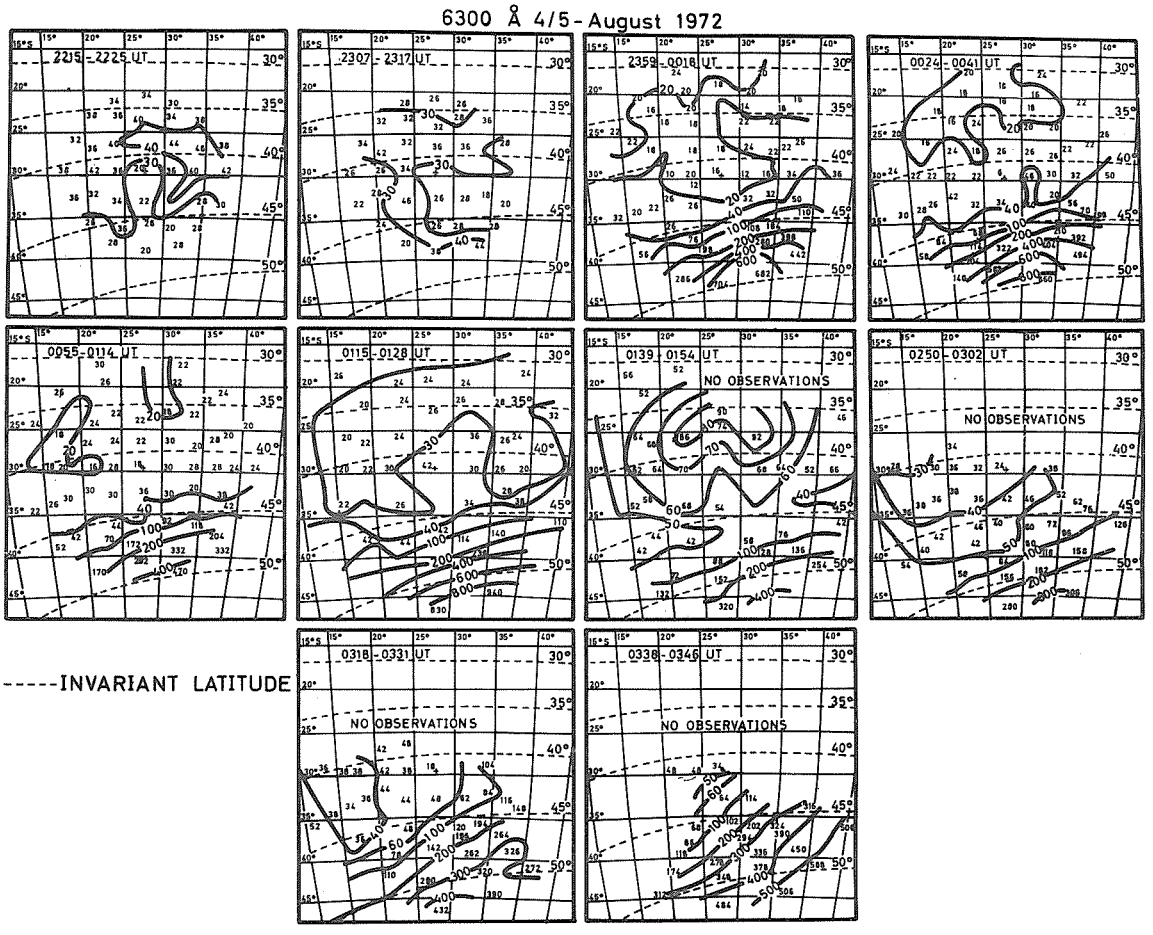

Fig. 1 Isophote sky maps of 6300 Å emission showing the development of a SARARC over several hours

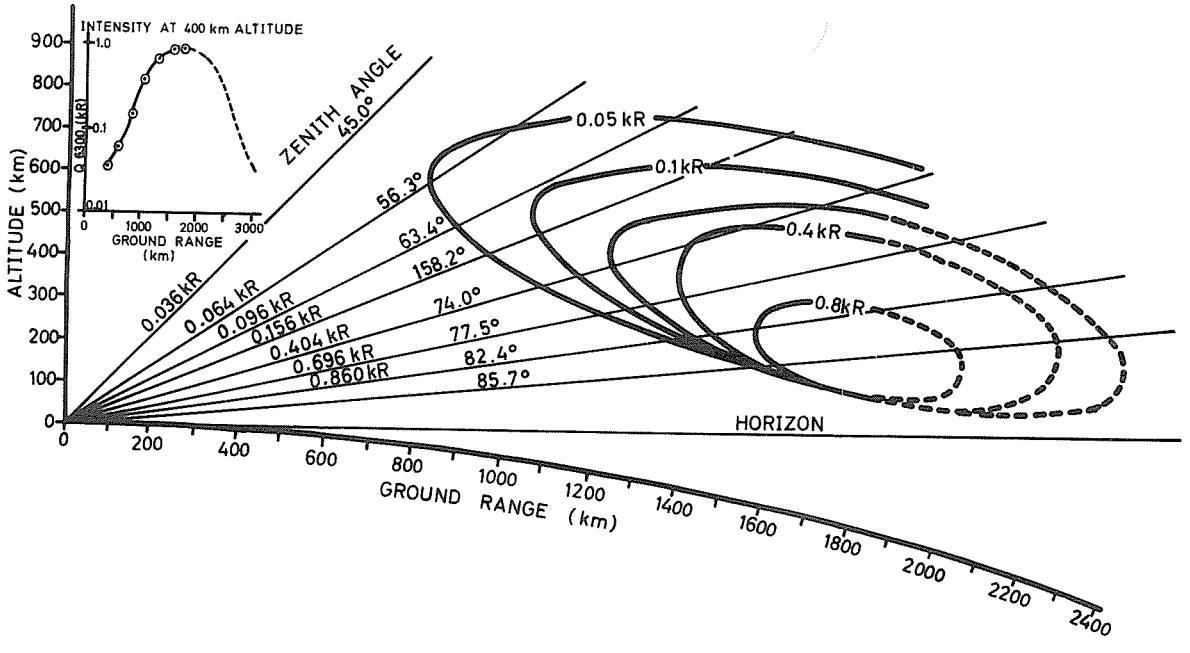

Fig. 2 Cross-sectional representation of the SARARC shown in plan in Fig. 1 for the time interval 0024-0041 UT.

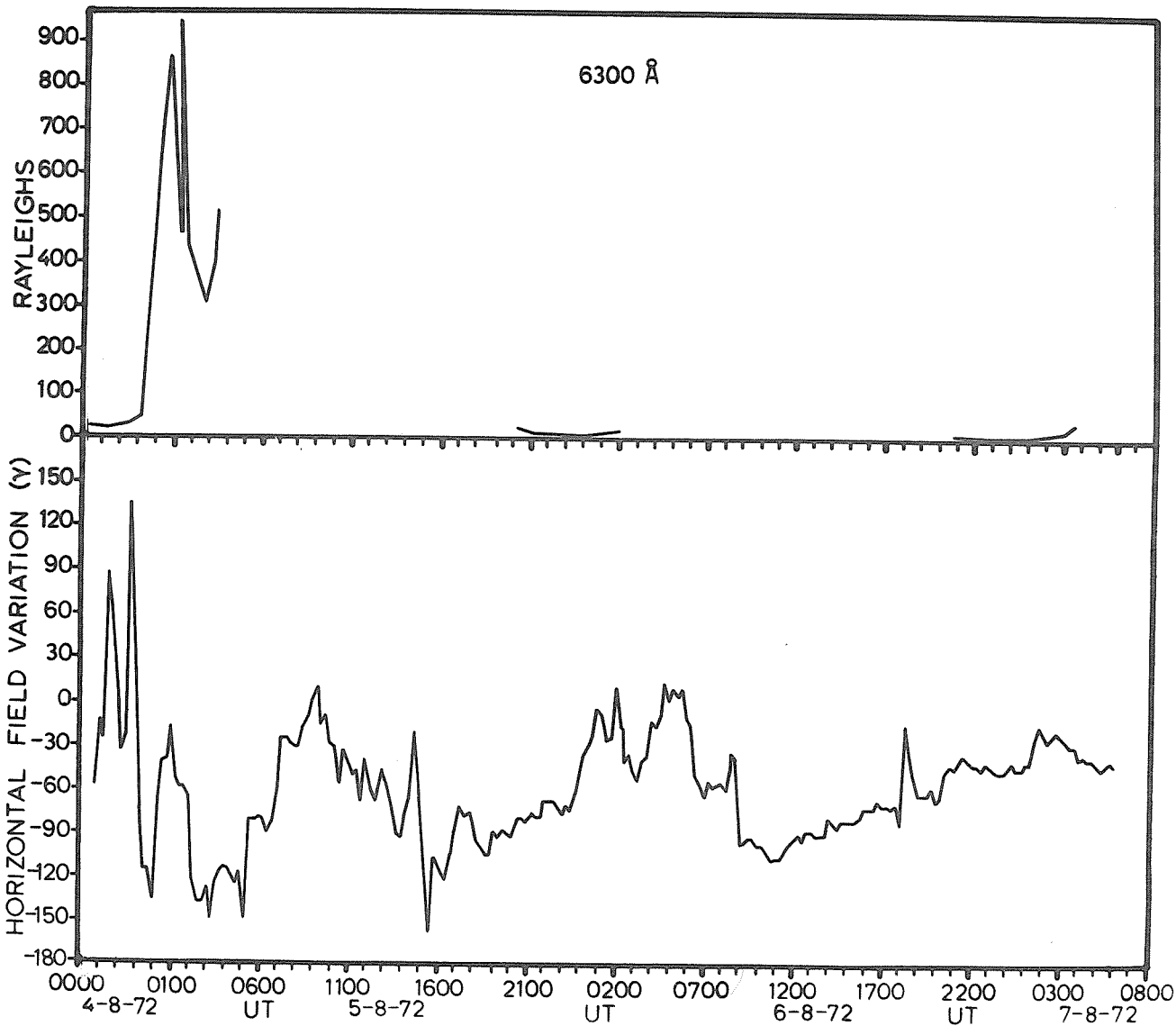

Fig. 3 Maximum observed intensity in the direction of the SARARC photometric centre. Observed 6300 Å emissions in the same direction for the nights of 5/6 and 6/7 August 1972, together with magnetic field variations, are also plotted.

Arc characteristics and storm details are summarised in Table 2. D_{st} range and storm duration were obtained from the Hermanus magnetogram. The storm duration is taken to be the time from the sudden commencement to the time when the field has returned to about 10 γ corresponding to the end of the rapid recovery phase [Cornwall et al., 1970]. This is fairly clearly defined when the recovery phase is smooth but the present storm is very complex, the recovery phase being interrupted by repeated substorms and finally terminated by the onset of a further major storm. Proton energy densities are based on the assumption that the proton energy spectrum [Frank and Owens, 1970] is independent of D_{st} which itself is proportional to proton number density [Cornwall et al., 1971]. These values were used to calculate the total proton energy in a tube based on 1 cm^2 in the ionosphere near the photometric centre of the arc. Total heat fluxes were obtained by averaging values taken from Walker and Rees' [1968] and Roble's [1969] heat flux - volume emission rate curves. This leads to a used storm energy fraction of 7% which is considerably less than a theoretical estimate of 25% [Cornwall et al., 1971]. This suggests that for low L values (<2) the necessary plasmapause contraction to produce a SARARC can only occur with very severe storms with low efficiency for arc production.

TABLE 2

Magnetic Storm					
D_{st}(H) range (γ)	Storm duration (s)	Proton no. density (cm^{-3})	Proton energy density (eV cm^{-3})	Total proton energy (eV cm^{-2})	Energy loss rate (eV cm^{-2} s^{-1})
310	0.9×10^5	65.7	10.5×10^5	52.5×10^{15}	58×10^{10}

SARARC		
Maximum intensity (kR)	Total heat flux (eV cm^{-2} s^{-1})	Fraction of storm energy used
0.9	4.3×10^{10}	0.07

REFERENCES

CARMAN, E.H., M.P. HEERAN and V. WILTSHIRE 1969 A simple airglow photometer with improved red sensitivity, Planet. Space Sci. 17, 1073-1074.

CHANDRA, S., E.J. MAIER and P. STUBBE 1972 The upper atmosphere as a regulator of subauroral red arcs, Planet. Space Sci., 20, 461-472.

CHAPPELL, C.R., K.K. HARRIS and G.W. SHARP 1970 A study of the influence of magnetic activity on the location of the plasmapause as measured by OGO 5, J. Geophys. Res., 75, 50-56.

COLE, K.D. 1965 Stable auroral red arcs, sinks for energy of D_{st} main phase, J. Geophys. Res., 70, 1689-1706.

CORNWALL, J.M., F.V. CORONITI and R.M. THORNE 1970 Turbulent loss of ring current protons, J. Geophys. Res., 75, 4699-4709.

CORNWALL, J.M., F.V. CORONITI and R.M. THORNE 1971 Unified theory of SAR Arc formation at the plasmapause, J. Geophys. Res., 76, 4428-4445.

FRANK, L.A. and H.D. OWENS 1970 Omnidirectional intensity contours of low energy protons (0.5<E<50 keV) in the earth's outer radiation zone at the magnetic equator, J. Geophys. Res. 75, 1269-1278.

LAWRENCE, R.S., D.J. POSAKONY, O.K. GARRIOTT and S.C. HALL 1963 The total electron content of the ionosphere at middle latitudes near the peak of the sunspot cycle, J. Geophys. Res., 68, 1889-1898.

NAGY, A.F., R.G. ROBLE and B.P. HAYS 1970 Stable mid latitude red arcs: observations and theory, Space Sci. Rev., 11, 709-727.

ROBLE, R.G. 1969 A theoretical and experimental study of the stable mid-latitude red arc (SAR-arc), Ph.D. Thesis, University of Michigan, Ann Arbor.

TAYLOR, G.N. 1961 The total electron content of the ionosphere during the magnetic disturbance of November 12-13, 1960, Nature, 189, 740-741.

WALKER, J.C.G. and M.H. REES 1968 Excitation of stable auroral red arcs at sub-auroral latitudes, Planet. Space Sci., 16, 915-928.

Atmospheric Electric Data during August 4th - 12th, 1972

by

R. Muhleisen
Astronomisches Institut der Universitat Tubingen
Aussenstelle Weissenau/Fed. Rep. of Germany

and

R. Reiter
Institut fur Atmospharische Umweltforschung der Fraunhofer Gesellschaft
Garmisch-Partenkirchen/Fed. Rep. of Germany

For some years deviations of the air electric parameter from normal behavior have been found when a solar event occurred 1 to 4 days previously [Reiter, 1960, 1964, 1969, 1971; Muhleisen et al., 1971].

This phenomenon was also studied during August 1972. The electric voltage between the ionosphere and the earth (V_I) was determined for 6 consecutive days from 2 to 10 August 1972 at Weissenau (Figure 1). The electric potential gradient (E) and the vertical current density (i) were measured continuously at the Zugspitze station (3000 m NN). The product E x i, corresponding to the electric power in the global electric circuit, is also plotted in Figure 1.

The interesting feature is the similar behavior of V_I and E x i with maxima 2 days after type IV radio bursts and a short time later than solar proton flux maximum. This is in good agreement with earlier findings.

REFERENCES

MUHLEISEN, R., H.-J FISCHER and H. HOFFMAN (1971) Horizontal electric fields in the ionosphere derived from air-electric measurements. ZS, Geoph. 37, 1055-1059.

REITER, R. (1960) Relationship between atmospheric electric phenomena and simultaneous meteorological conditions, Final Report Contract AF 61 (052)-55.

REITER, R. (1964) Felder, Strome and Aerosole in der unteren Troposphare. Nach Untersuchungen im Hochgebirge bis 3000 m NN, Dr. D. Steinkopff Verlag, Darmstadt.

REITER, R. (1969) Solar-Flares and their Impact on Potential Gradient and Air-Earth Current Characteristics at High Mountain Stations. Pure and Applied Geophysics, PAGEOPH, 72, 259-267.

REITER, R. (1971) Further Evidence for Impact of Solar Flares on Potential Gradient and Air-Earth Current Characteristics at High Mountain Station, Pure and Applied Geophysics, PAGEOPH, 86, 142-158.

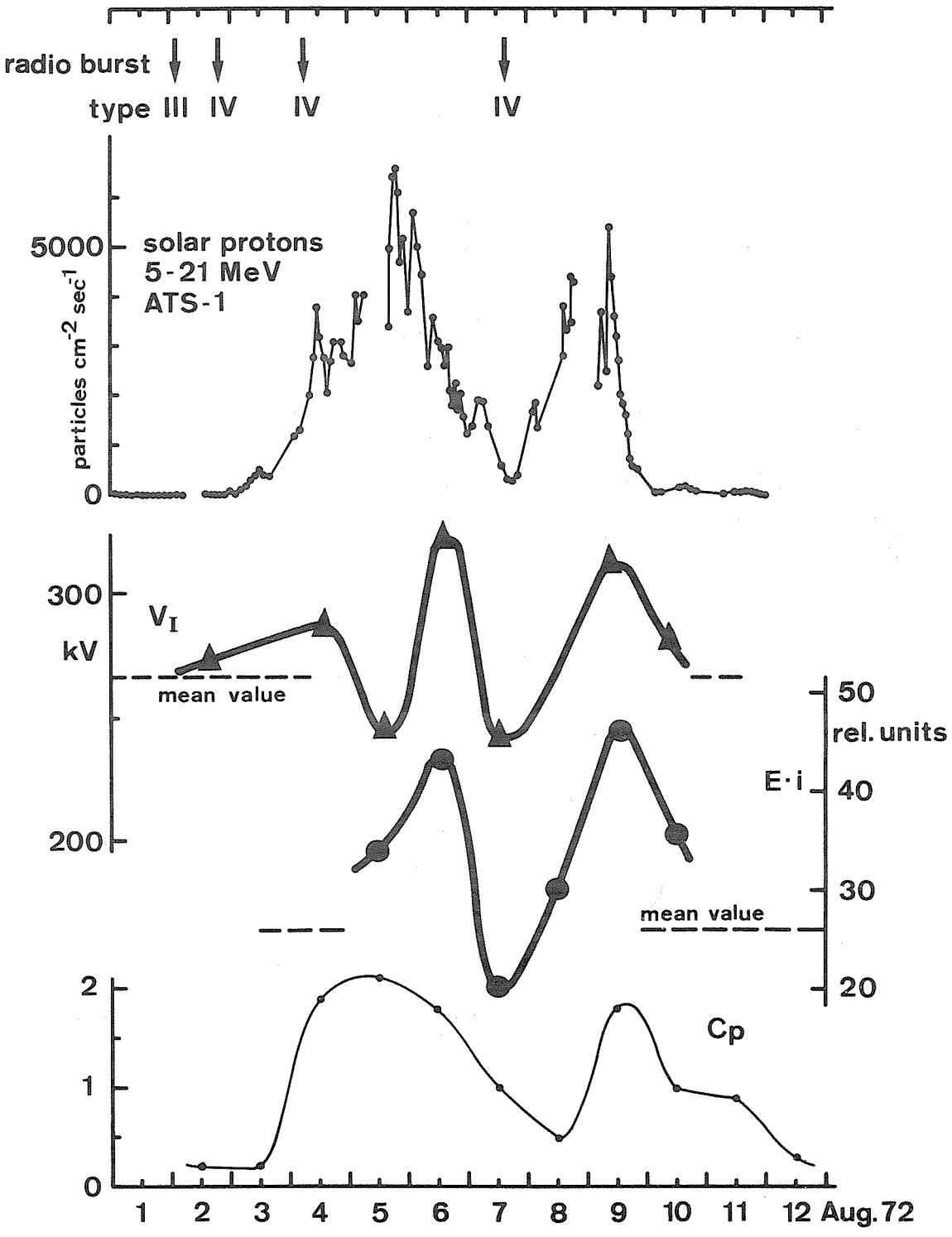

Fig. 1: AIR ELECTRIC, SOLAR AND GEOMAGNETIC DATA, AUGUST 1 - 12, 1972.

▲ Values of the electric voltage V_I between ionosphere and earth determined by single radiosonde ascents.

● Daily means of the product of electric field E and vertical current density i, both measured at a mountain station, 3000 m above sea level.

Recurrence of the Solar Corpuscular Events

by

Maria Torelli
Rome Astronomical Observatory
Via del Parco Mellini, 84 - Rome

The recurrence in the McMath 11976 center, as in most regions of the same kind, of corpuscular flares in the same location and with analogous characteristics supports the hypothesis that the peculiar magnetic structure of these centers is relatively stable and not substantially modified by the occurrence of the events.

Assuming that the interval between a proton flare and the subsequent one is the time necessary for restoring the released energy, we see from Figure 1 and the histogram in Figure 2 that the most frequent spanning time of two consecutive events is 40 - 60 hours.

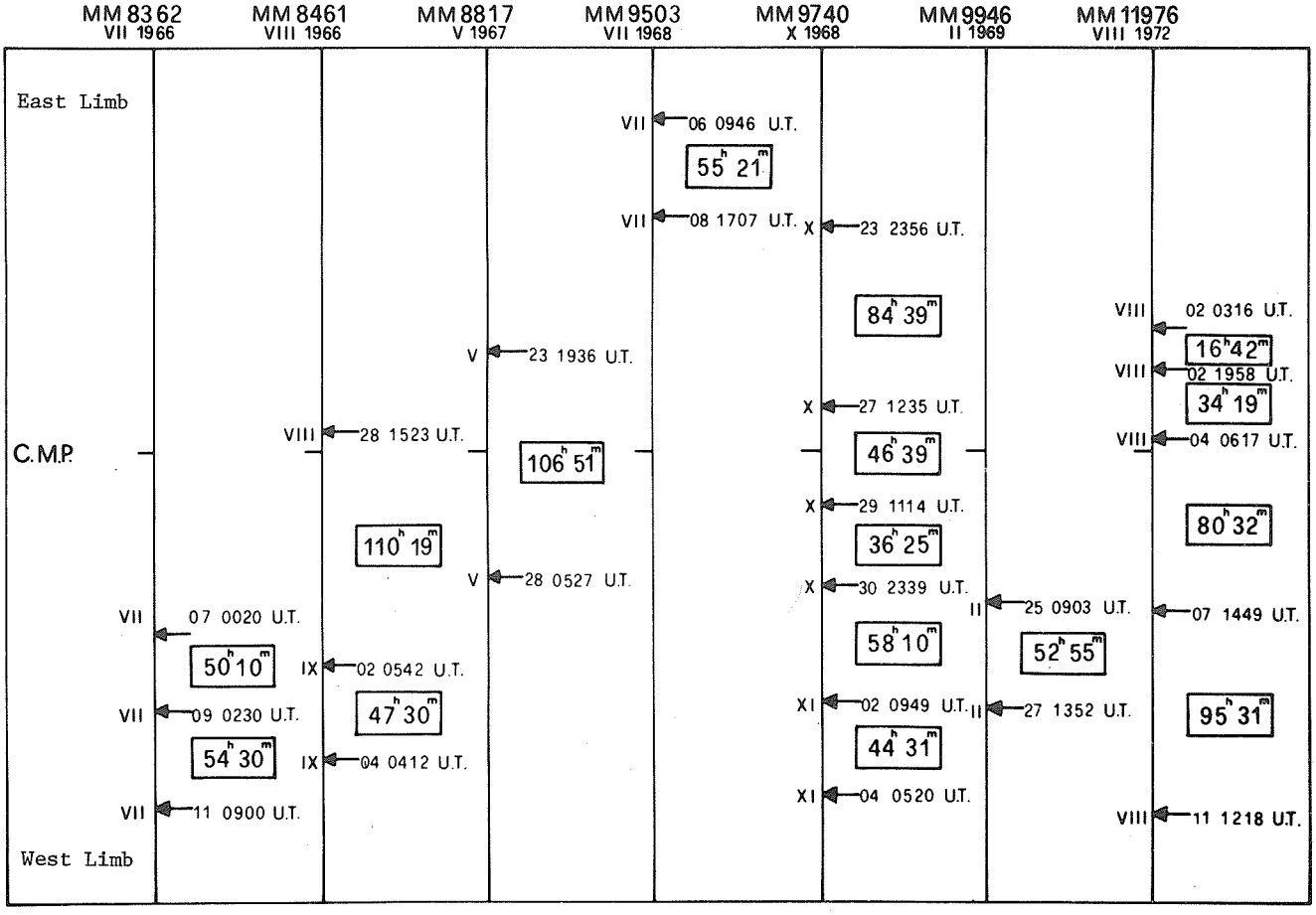

Fig. 1. Time distribution of recurrent proton flares. The numbers in the frames are the intervals between two consecutive events.

This value is consistent with the time which we obtain with the more recent views on the mechanisms of the solar flares.

If, for example, the flare is due [Pneuman, 1967] to the impediment (by closed magnetic lines) of the normal energy flux, supported by the spicules, passing from the subphotospheric convective layers to the corona, an expedite calculation of the time gives:

$$t = E_t/F_s x A_s = E_t/7 x F_c x 0.5 A_p = 1.7 \times 10^5 \text{sec} \simeq 47 \text{ hours}$$

where: E_t(total energy released during a proton flare) = 10^{33} ergs.
A_s(area covered by the spicules in the plage) = $0.5A_p$ [de Jager et al., 1970].
A_p(plage area) = $3x10^{20}cm^2$ for McMath 11976 on August 5, 1972 (CMP).
F_s(energy flux through the magnetic elements or spicules) = $7x5.6x10^6$ ergs/cm^2sec [de Jager et al., 1970; Athay, 1966].

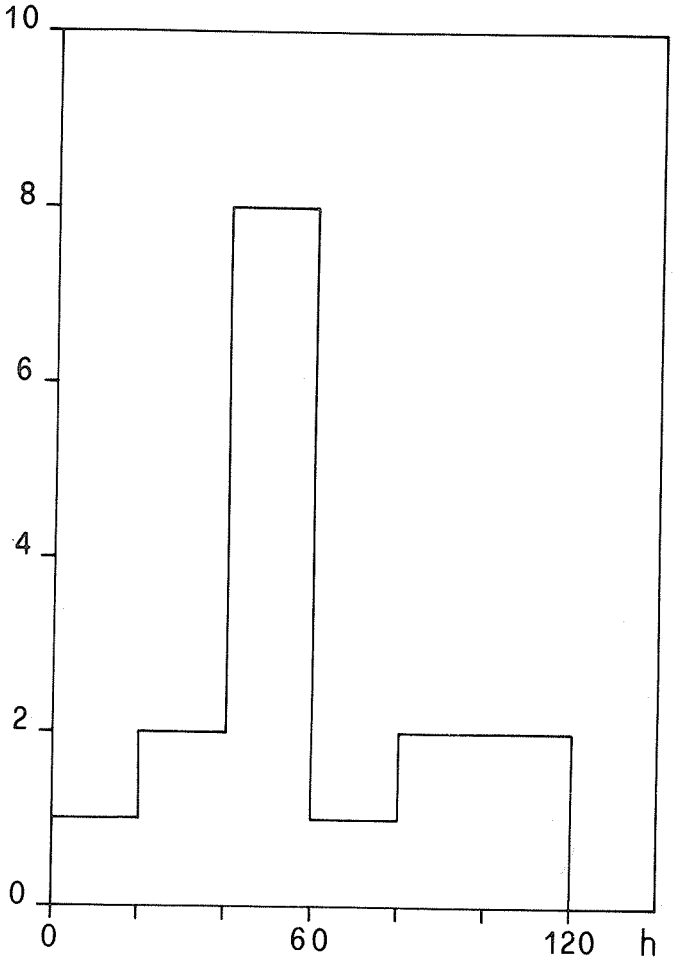

Fig. 2. Frequency of intervals (in hours) between two consecutive corpuscular events in the same active center.

REFERENCES

ATHAY, R. G. 1966 Radiative energy loss from the solar chromosphere and corona, Ap. J., 146, 223-240.

DE JAGER, C., and C. DE LOORE 1970 On the ratio between the mechanical fluxes in and outside the solar chromospheric mottles, Solar Phys., 13, 126-130.

PNEUMAN, G. W. 1967 Solar flares as resulting from the temporary interruption of energy flow to the corona, Solar Phys., 2, 462-483.

APPENDIX I: Miscellaneous Data and Information from WDC-A

1. Reprint of Table of Contents and Introduction for UAG-21 ("Preliminary Compilation of Data for Retrospective World Interval July 26 - August 14, 1972", compiled by J. Virginia Lincoln and Hope I. Leighton, WDC-A for Solar-Terrestrial Physics, November 1972).

TABLE OF CONTENTS

	Page
FOREWORD	i
INTRODUCTION	1
SOLAR AND INTERPLANETARY DATA	
Solar Indices (July 26 - August 14, 1972)	3
Rz	
R_A'	
2800 MHz Solar Flux	
Solar Flux adjusted to 1 AU	
15400 MHz 2800 MHz 606 MHz	
8800 2695 410	
4995 1415 245	
Maps (July 26 - August 14, 1972)	4
X-rays (OSO-5, University of Leicester)	
8.6 mm (Prospect Hill)	
Magnetograms (Mt. Wilson)	
9.1 cm (Stanford)	
21 cm (Fleurs)	
Calcium Plages (McMath-Hulbert and Catania)	
Hα (Boulder and Ramey AFB)	
Sunspots (Boulder)	
Coronal λ 5303 (Kislovodsk, Norikura, Pic-du-Midi, Lomnicky Stit)	
White-light Corona (OSO-7, NRL)	
FeXV, 284A (OSO-7, NASA, GSFC)	
Calcium Plage and Sunspot Data for McMath Region 11976, July 28 - August 11, 1972	44
Coronal Emission λ 5303 West Limb Passage of McMath Region 11976, August 5-14, 1972	45
Radio Interferometric Observations (Nançay)	46
169 MHz (July 25 - August 20, 1972)	
Radio East-West Scans	
10.7 cm (Algonquin) July 25 - August 16, 1972	47
21 cm (Fleurs) July 25 - August 16, 1972	48
43 cm (Fleurs) July 25 - August 16, 1972	49
Pioneer VI July 26 - August 14, 1972	50
Solar Wind	
Cosmic Ray Protons	
Pioneer IX July 26 - August 14, 1972	51
Solar Wind	
Interplanetary Electric Field	
Interplanetary Magnetic Field	
Cosmic Ray Protons	
SOLAR FLARE ASSOCIATED EVENTS	
Hα Spectroheliogram of Flare at Boulder 1526 UT, August 7, 1972	53
Flare Data (July 26 - August 14, 1972)	54
Surges and Active Prominence Regions (July 26 - August 14, 1972)	64
Radio Events (Fixed Frequency) (July 26 - August 14, 1972)	65
Selected Bursts August 2, 4 and 7, 1972	80
Radio Spectral Events (July 26 - August 14, 1972)	83
X-rays (SOLRAD 9 - Explorer 37) July 26-31, 1972	
(SOLRAD 10 - Explorer 44) August 1-31, 1972	
1-8A Hourly Averages	94
8-20A Hourly Averages	96
Outstanding Events	98
Sudden Ionospheric Disturbances (July 26-August 14, 1972)	100
Protons	
Near Earth	
Hourly values (ATS-1) 5-21 MeV	101
21-70 MeV	102
RIOMETER DATA	
Alaskan Stations July 27 - August 14, 1972	103
(Ft. Yukon, College, Paxon, Sheep Mt., Anchorage)	
McMurdo August 4-10, 1972	110

TABLE OF CONTENTS (CONT'D)

		Page
IONOSPHERIC DATA		
f-plots July 26 - August 14, 1972		111
Thule, Godhavn, Narssarssuaq, Churchill, St. John's, Wallops Island, Mexico City, Maui		
COSMIC RAYS		
Indices July and August 1972		114
Graphs of Hourly Totals July and August 1972		116
GEOMAGNETIC ACTIVITY		
Kp, Ci, Cp, Ap	July 26 - August 14, 1972	118
Principal Magnetic Storms	July 26 - August 14, 1972	120
Sudden Storm Commencements	July 26 - August 14, 1972	121
Reduced Magnetograms	August 4-10, 1972	122
Leirvogur, College, San Juan, Honolulu		
Dst		126
AURORAL ACTIVITY		
Visual Observations August 4-6, 1972		128

INTRODUCTION

by

J. Virginia Lincoln and Hope I. Leighton
World Data Center A for Solar-Terrestrial Physics
Environmental Data Service
National Oceanic and Atmospheric Administration
Boulder, Colorado 80302

In this report are presented the solar-terrestrial physics data available in early October 1972 for the period of unusual solar activity July 26 - August 14, 1972, associated with the transit of McMath Plage Region 11976. Much of the data has appeared or will appear in the monthly "Solar-Geophysical Data" reports. Because of the promptness of this report some of the data will be more complete at the time of the Comprehensive Reports, January through March 1973 issues, of "Solar-Geophysical Data".

The advantage of this report is that the data are collected in one place rather than distributed through several issues. In addition, data not routinely published are included. The data come from worldwide sources and are part of the archives of World Data Center A for Solar-Terrestrial Physics.

Since this period is of such interest containing the greatest geomagnetic storm to date of the current solar cycle, together with many associated terrestrial effects, we plan to issue at a later date a special catalog of all the data for this period submitted to the World Data Center. We also plan to request contributions for a more complete data compilation from the worldwide community including interpretations of their data. This too will be a UAG-Report in this series and will be planned for distribution before the September 1973 Kyoto meeting of IAGA.

This data compilation is ordered roughly as is "Solar-Geophysical Data". Most of the data are self-explanatory, but for more details as to interpretation, instrumentation used, etc., reference should be made to the "Solar-Geophysical Data" Descriptive Text, No. 330 (Supplement), issued February 1972.

The daily solar maps are as indicated in the Descriptive Text with the FeXV maps described in "Solar-Geophysical Data" No. 335, Part I, Prompt Reports, July 1972. They are from the Goddard EUV Spectroheliograph on OSO-7 recording radiation from a small element of the solar disk at extreme ultraviolet wavelengths between 120A and 400A.

A table presents the λ 5303 green coronal line intensities associated with the west limb passage of McMath Region 11976. There were insufficient data to prepare a similar table of east limb data.

Though all of the solar flare data which will eventually be received are not available at this time, it was considered worthwhile to prepare a preliminary listing of confirmed grouped flare reports. In the margin the flares of importance 2B or greater are highlighted. They occurred at 1958 UT August 2, at 0530 UT August 4, at 1455 UT August 7 and at 1227 UT August 11, 1972.

From the archives of the World Data Center a table of the outstanding surge and prominence reports was prepared from the data available.

The most outstanding solar radio emission bursts for fixed frequency have been highlighted in the margin in a manner similar to the flares. These are at 0305 UT August 2, at 1946 UT August 2, at 0540 UT August 4, at 1425 UT August 7, and at 1208 UT August 11, 1972. As with the flares, there will be further reports available later. The graphs of several selected bursts on August 2, 4 and 7, 1972 are presented.

The ATS-1 proton data are the only satellite data reduced in time for this publication. They are believed to be subject to large error for two reasons: 1) sensor degradation and 2) an overflow of registers used to display the fluxes in the Boulder Warning Center.

The proton events and geomagnetic disturbances are evident in the riometer records reproduced from the Alaskan chain of riometers. Caution should be exercised in their interpretation since the equipment was not operating in such a manner as to make it possible to prepare a reliable quiet day curve against which the raw riometer data could be compared.

The McMurdo riometer data are thanks to W. I. Axford and H.J.A. Chivers of the University of California, San Diego. The McMurdo instrument transmits the data via satellite to California where they are reduced in the usual way by comparing the observed intensities with the derived quiet day curve. The graphs indicate, as Axford and Chivers state, major activity beginning about 0000 UT August 3, 1972, reaching maxima at 2200 UT August 4 and 0100 UT August 9, 1972, of greater than 12.6 dB and $\sim$5.6 dB, respectively. These peaks are close to local noon for McMurdo although the station was not sunlit at all during the events.

S. M. Ostrow prepared the ionospheric f-plots presented on pages 112-113. The two graphs are preceded by a description of the data and their significance.

In the "Geomagnetic Activity" section the reduced magnetograms are thanks to K. Kawasaki, CIRES Fellow and Guest Worker with the National Geophysical and Solar-Terrestrial Data Center of the Environmental Data Service in Boulder, and S. -I. Akasofu, Geophysical Institute, College, Alaska. Only a few magnetograms were available for prompt reduction. The four selected cover latitudes from the auroral zone to near the equator. Leirvogur and College are reduced to the same 500 γ range. San Juan and Honolulu are reduced to the same 50 γ range. Dr. M. Sugiura and D. M. Poros of NASA, Goddard Space Flight Center, submitted the provisional equatorial Dst calculations.

Unfortunately the Alert and Deep River Charts for August have not been received in time for this publication. Calgary and Sulphur Mountain indicate the Forbush decreases at the time of the geomagnetic storms.

The final table lists auroral reports received from visual observers at the times of the geomagnetic activity.

It is to be hoped that this data collection will assist the many research workers in their detailed analysis of their observations during this most exciting period of solar-terrestrial activity.

2. Supplementary Information on Solar Data

Hα flare patrol film from Culgoora held at WDC-A.

WDC-A holds Hα flare patrol film from Culgoora covering the period July 23 to August 18, 1972. The patrol was generally at the rate of one photograph per minute though at times it is speeded up to 6 photographs per minute. The patrol times are as follows:

1972 July	23	0015-0200 UT	1972 August	6/7	2240-2253
	25/26	2215-0555			2359-0347
	26/27	2218-0553			0412
	27/28	2241-2340			0414
		0055-0555			0426-0450
	28/29	2235-2355			0450-0600
		0004-0527		7/8	2235-2240
		0631			2242-0520
	29/30	2231-2259		8/9	2230-2240
		2315-0558			2300
	30/31	2225-2243		10/11	2215-2240
		2249-0519			2345-0114
	31	2222-2433		11/12	2234-2314
August	1	0100-0407			2321-0604
	2/3	0228-0600		12/13	2349-2352
	3/4	2217-2239			0000-0603
		2243-0648		13/14	2230-2254
		0650-0700			2303-0116
	4/5	2225-2323			0125-0558
		2334-0612		16/17	2200-2312
	5/6	0137-0625			2322-0515
				17/18	2234-0112

Detailed charts of flare patrols and observations for August 1, 2, 4, 7 and 11, 1972

We present here graphical representations of the flare patrol data covering the principal solar flares in August 1972 from data of thirty-three solar observatories reporting to WDC-A for STP.

There is a separate chart for each of the days August 1, 2, 4, 7 and 11, and a separate line for each observatory. The observatories are in order of longitude with a numerical code to key to the observatories listed in the Table below.

In the charts, observation times are indicated by an open box, where C, V and P indicate patrol is cinematographic, visual or visual with some photographs, respectively. Lines with arrows indicate nighttime at each of the stations. Sunrise and sunset are only approximate, depending on where in the 15° time zone the station lies.

Reported flares are shown by a cross-hatched area below the open boxes. Flares with importance ≥ 1F are marked with the importance rating. Any second flare reported at the same time is shown with reversed cross-hatched areas. Due to lack of space, if there were three flares whose durations overlap, the overlapping period of the second and third is simply blackened in.

The very top line gives the same information for the flare patrol network as a whole. The flare data are the "Grouped Flare Reports" from Solar-Geophysical Data.

Table of Observatories

01	Herstmonceux	N50 E00	18	Abastumani	N41 E42
02	Haute Provence	N44 E05	19	Tehran	N35 E51
03	Locarno	N46 E08	20	Tashkent	N41 E69
04	Zürich	N47 E08	21	Kodaikanal	N10 E77
05	Arcetri	N34 E11	22	Siberie	N52 E104
06	Monte Mario	N41 E12	23	Carnarvon	S25 E114
07	Wendelstein	N47 E12	24	Manila	N14 E121
08	Capri-F	N40 E14	25	Voroshilov	N43 E132
09	Capri-S	N40 E14	26	Mitaka	N35 E139
10	Ondrejov	N49 E14	27	Culgoora	S30 E147
11	Catania	N37 E15	28	Palehua	N21 E204
12	Upice	N50 E16	29	Boulder	N40 E255
13	Athens 1,2	N37 E23	30	McMath	N42 E277
14	Bucharest	N44 E26	31	Huancayo	S12 E285
15	Istanbul	N41 E28	32	Ramey	N18 E292
16	Kiev	N50 E30	33	Gran Canaria	N28 E345
17	Kharkov	N50 E36			

SOLAR FLARE OBSERVATIONS FOR AUGUST 1, 1972

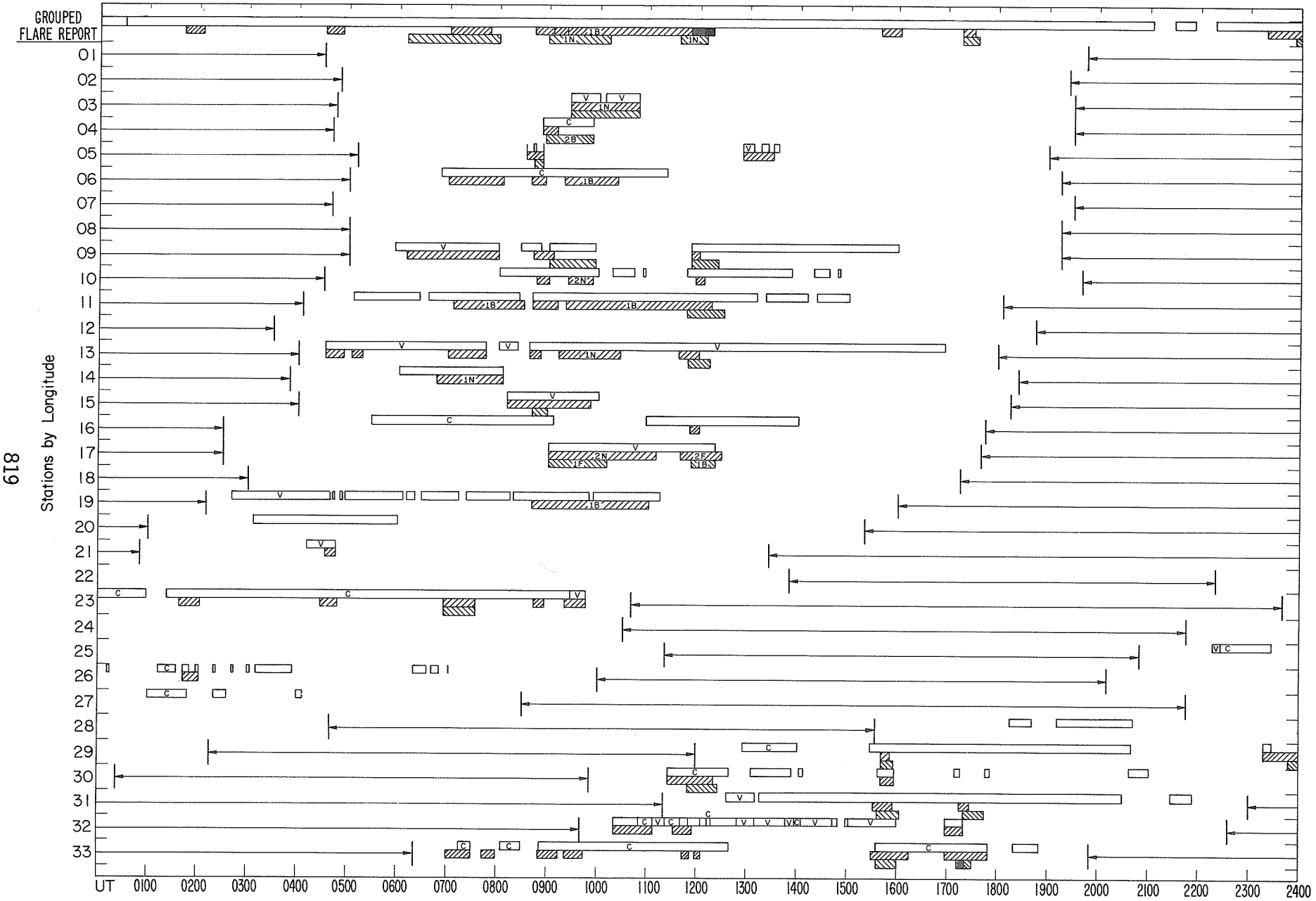

SOLAR FLARE OBSERVATIONS FOR AUGUST 2, 1972

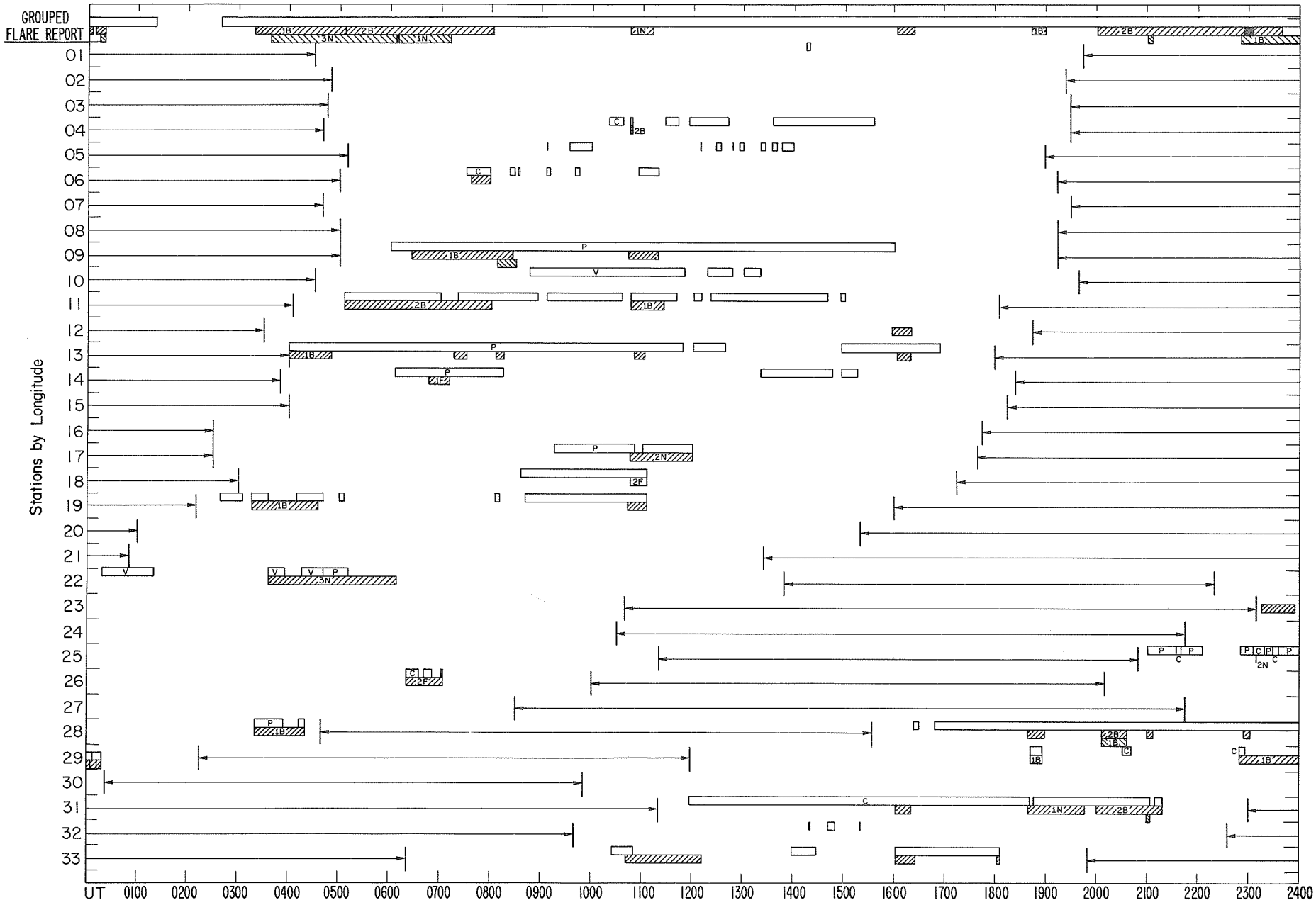

SOLAR FLARE OBSERVATIONS FOR AUGUST 4, 1972

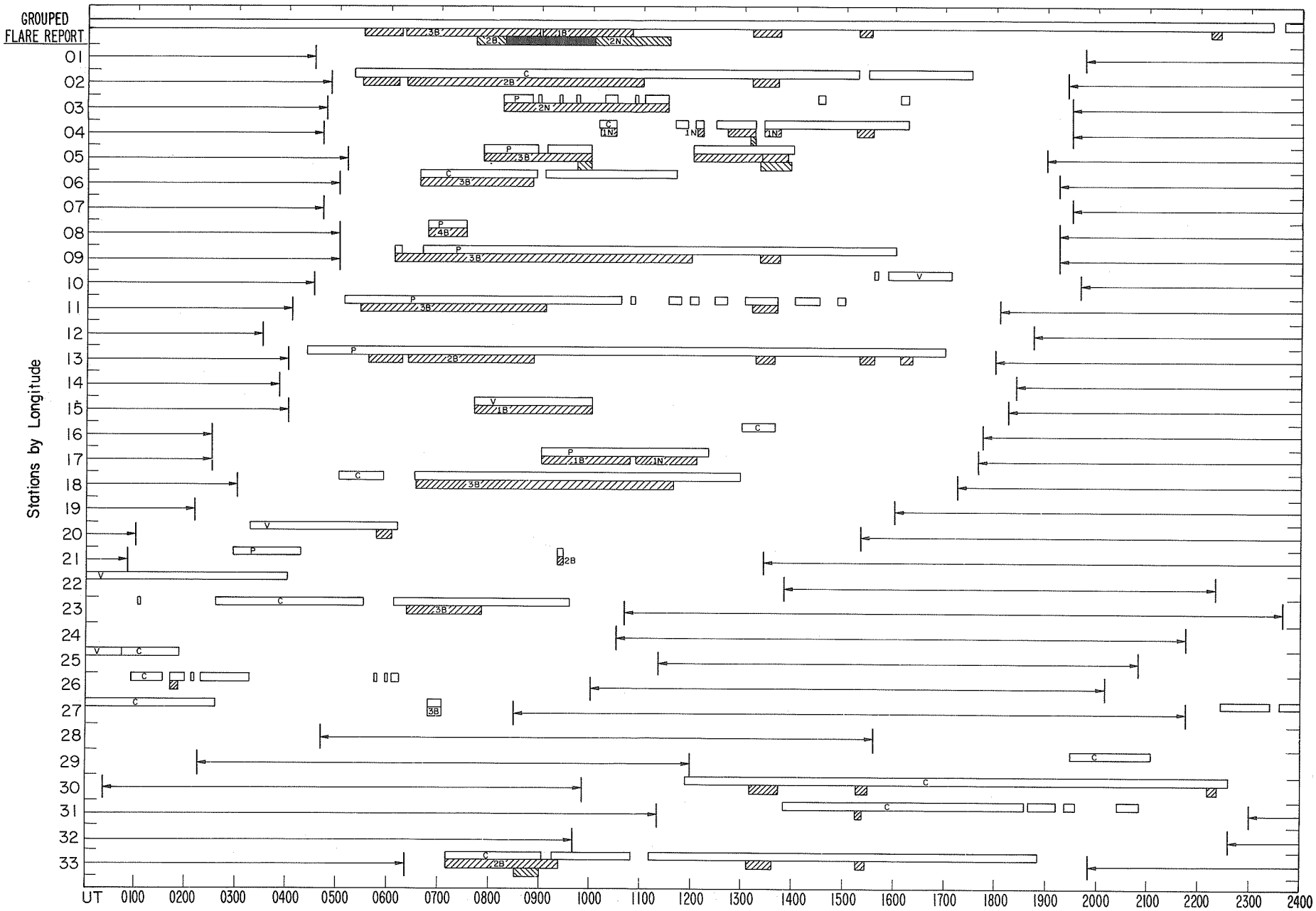

SOLAR FLARE OBSERVATIONS FOR AUGUST 7, 1972

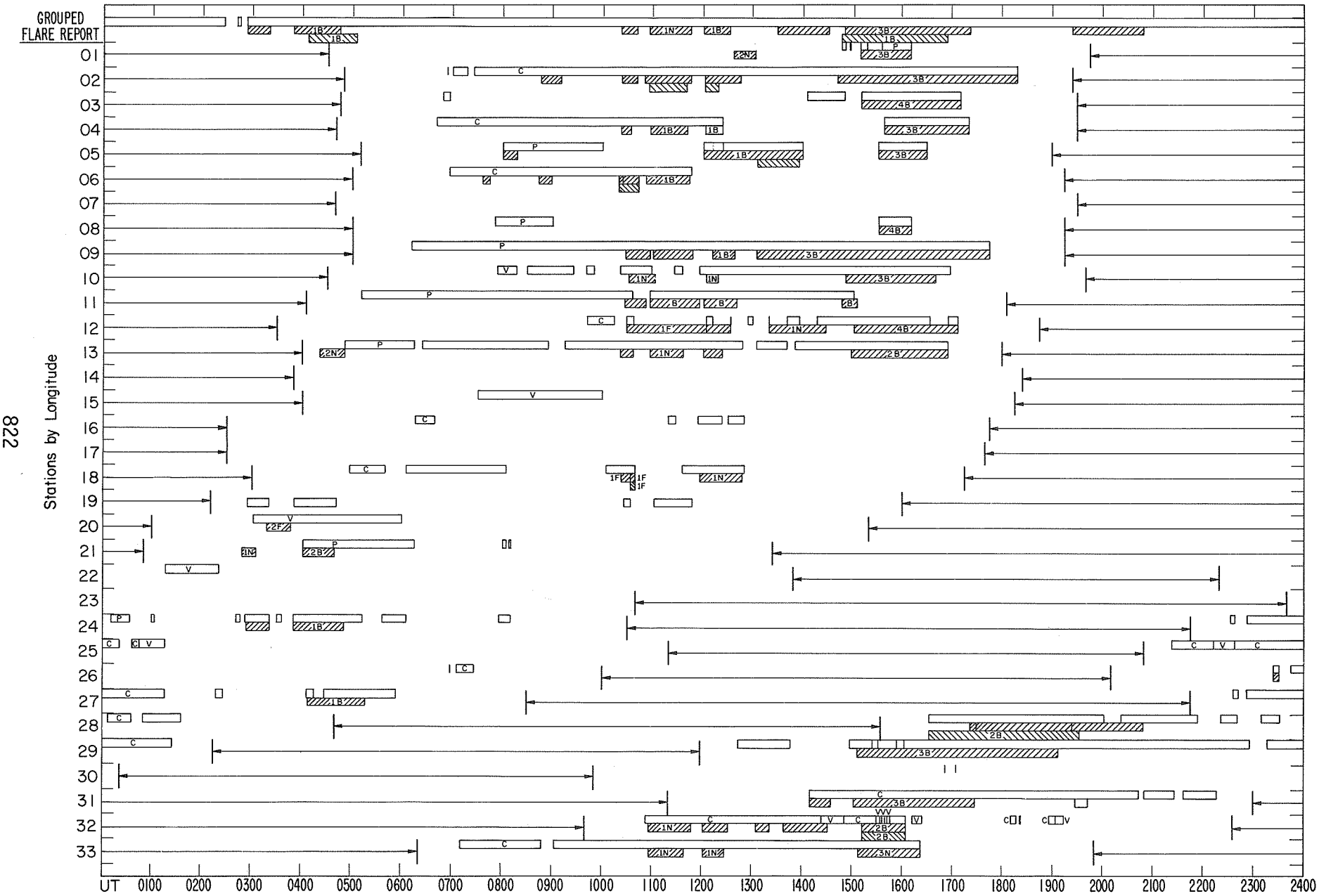

SOLAR FLARE OBSERVATIONS FOR AUGUST 11, 1972

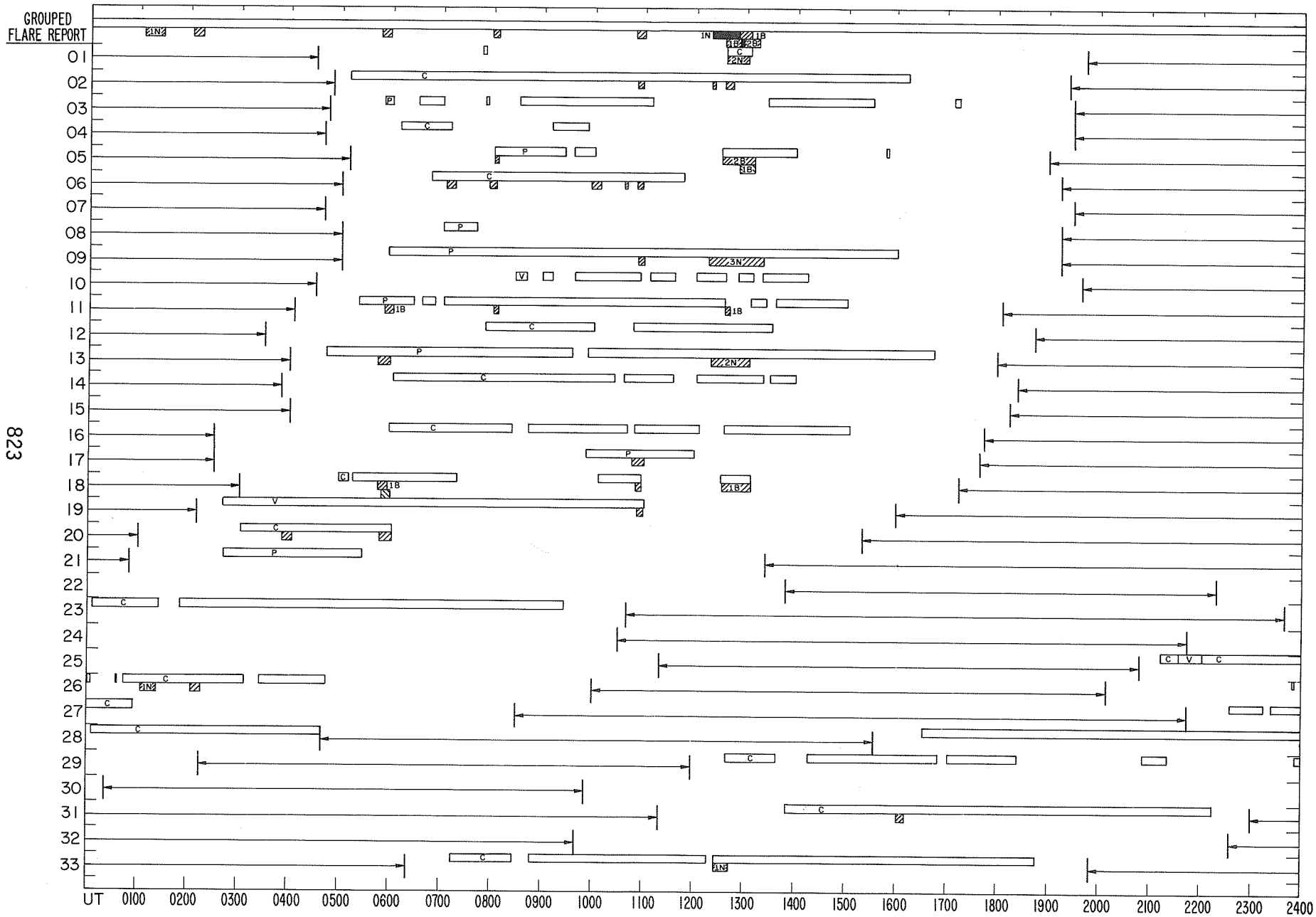

3. Analog Recordings of Selected Solar Noise Bursts (Toyokawa)

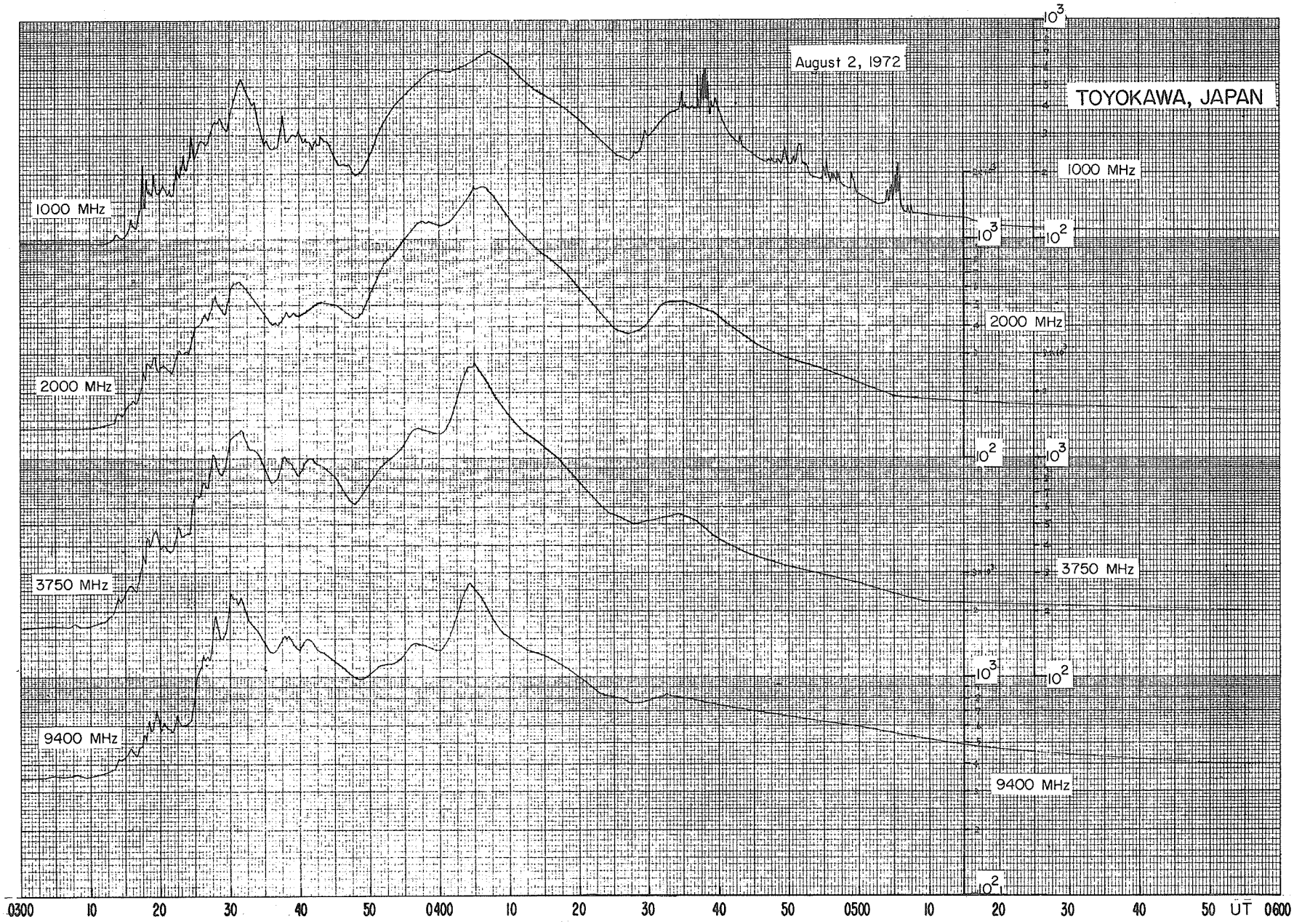

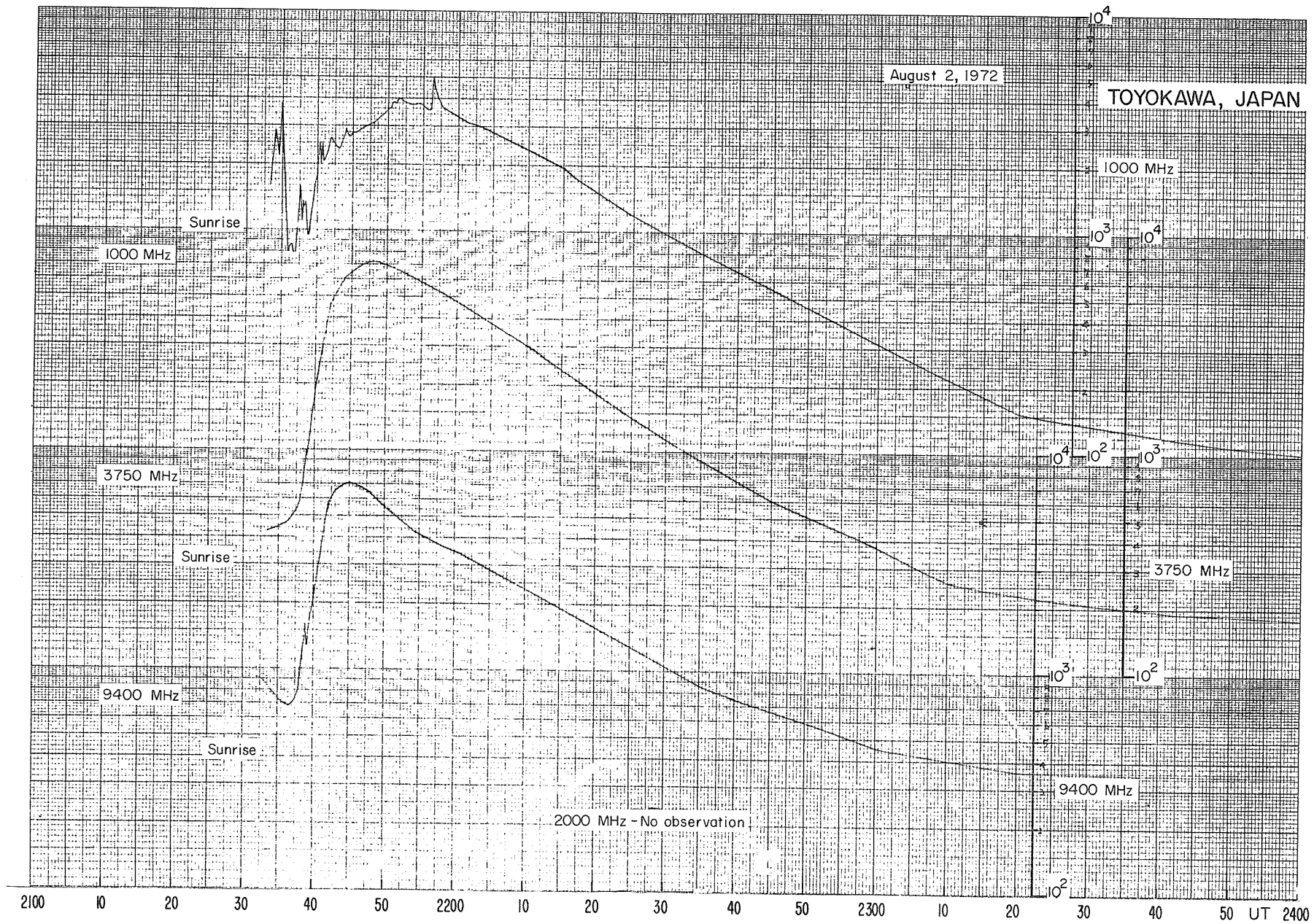
August 2, 1972
TOYOKAWA, JAPAN
1000 MHz
Sunrise
1000 MHz
3750 MHz
Sunrise
9400 MHz
Sunrise
2000 MHz - No observation
3750 MHz
9400 MHz
10^4
10^3
10^2
2100
10
20
30
40
50
2200
10
20
30
40
50
2300
10
20
30
40
50
UT 2400

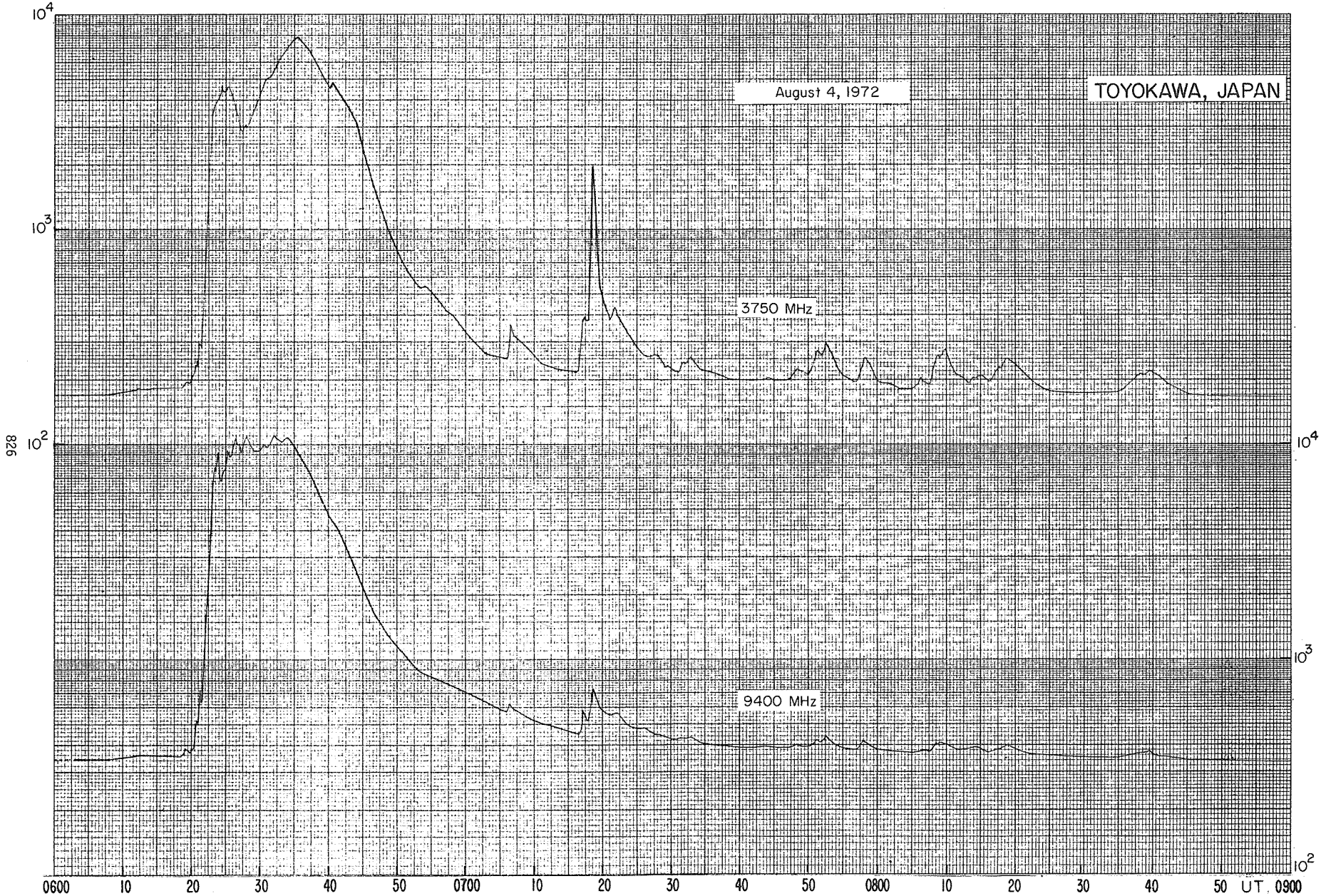
August 4, 1972
TOYOKAWA, JAPAN
3750 MHz
9400 MHz
10^4
10^3
10^2
826
0600
10
20
30
40
50
0700
10
20
30
40
50
0800
10
20
30
40
50
UT. 0900

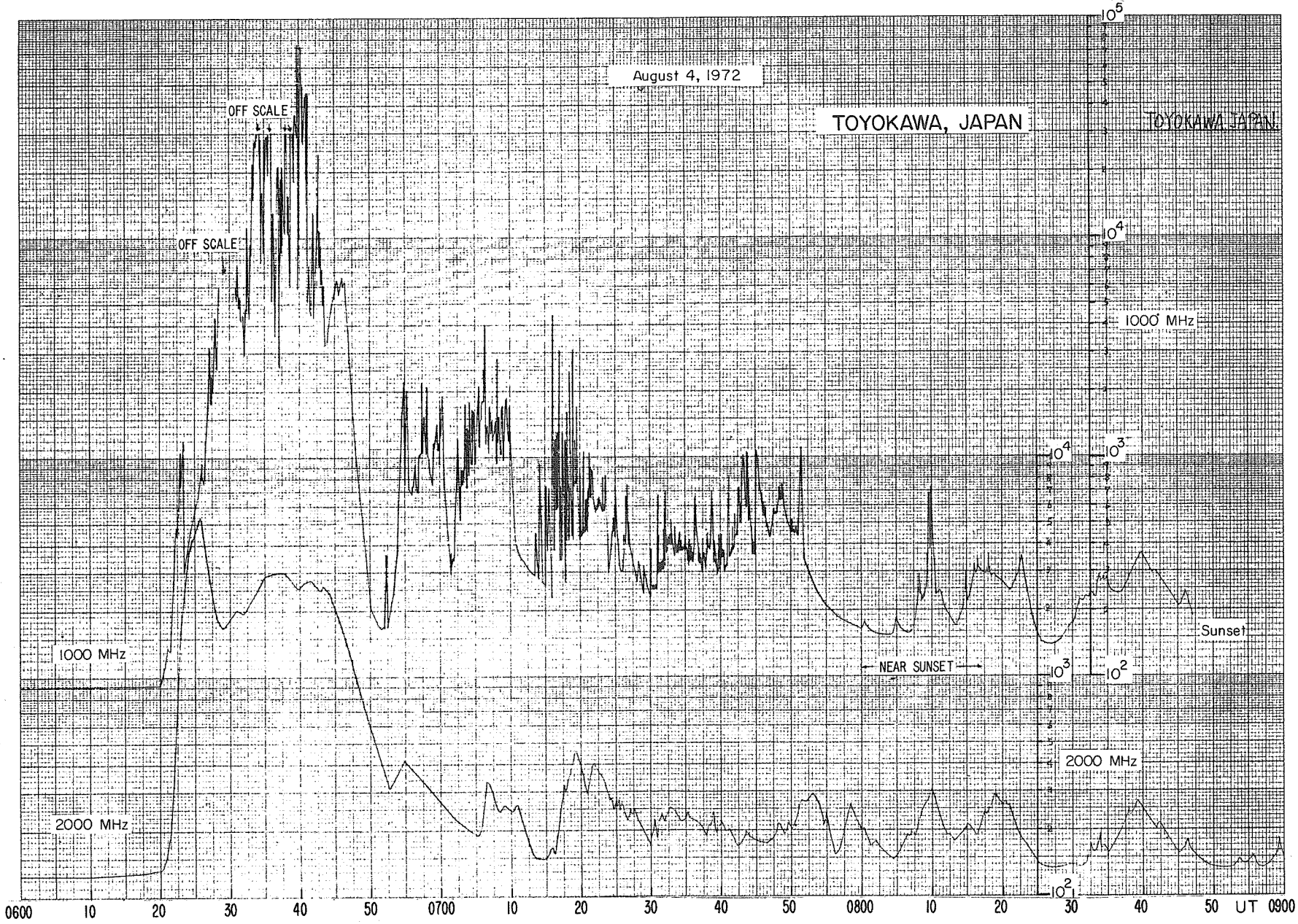
August 4, 1972
TOYOKAWA, JAPAN
TOYOKAWA, JAPAN
OFF SCALE
OFF SCALE
1000 MHz
2000 MHz
NEAR SUNSET
Sunset
1000 MHz
2000 MHz
10^5
10^4
10^3
10^2
10^4
10^3
10^2
0600
10
20
30
40
50
0700
10
20
30
40
50
0800
10
20
30
40
50
UT 0900

4. Supplementary Information on Cosmic Ray Data

[There are much detailed data in the World Data Centers from ground-based Cosmic Ray monitoring which cannot as a practical matter be included in this data report, though some data tables with discussion of results do appear. The following is an inventory of unpublished data on deposit in WDC-A. Hourly data are available for all, and 5-, 10- or 15-minute data as indicated. Most data are in the form of tables; some are or will shortly be on magnetic tape. Ed.]

A. Neutron Monitors

Syowa Station S69.0 E39.6 Cut-off 0.42 GV 12-NM-64
Pressure corrected data for the period August 1-10.
Hourly values

Tixie Bay N71.6 E129 Cut-off 0.53 GV 16-NM-64
Pressure corrected data for the period August 1-15.
Hourly values except 1100, 1800 UT August 8
0200, 0700 UT " 9
1300-2400 UT " 10
2100 UT " 11
5-minute values except 1005-1045 UT August 8

Apatity N67.55 E33.3 Cut-off 0.65 GV IQSY-NM-64
Pressure corrected data.
Hourly values 1100-2400 UT August 5
0100-2400 UT " 6
0100-1500 UT " 7
15-minute values 0800-1400 UT " 1
2200-2400 UT " 3
0015-2400 UT " 4
0015-1045 UT " 5
1515-2045 UT " 7 except 1730 UT
Graph: July, August, September.

General Belgrano S77.97 E321.20 Cut-off 0.77 GV 6-NM-64
Pressure corrected data.
Hourly values August 2-11 (graphs)
5-minute values 1200-2400 UT August 4
1200-2400 UT " 7

Sanae S70.46 E357.51 Cut-off 1.06 GV 3-NM-64
10-minute values August 4, 5
August 7, 9

Ottawa N45.4 E284.4 Cut-off 1.08 GV IGY-NM
Pressure corrected data.
Hourly values July 26 - August 14

Yakutsk N62.0 E129.7 Cut-off 01.7 GV 6-NM-64
Pressure corrected data.
Hourly values July 27 except 0100-0200 UT
July 28 - August 14
15-minute values August 3 except 0000-1700 UT
August 4, 5
August 7 except 0000-0800 UT
August 8 except 0300-2300 UT

Oktyomtsy N61.5 E129.7 12-NM-64
Pressure corrected data.
Hourly values July 28 except 0300 UT
July 29-31
August 1 except 1300-1400 UT
August 2
August 3 except 1400-1900 UT
August 4, 5
August 6 except 0200 UT
August 7 except 0100-0700 UT
August 8-10
August 11 except 0300 UT
August 12 except 0200-0400; 1400-2400 UT
August 13 except 0100-2200 UT
August 14

Oktyomtsy (continued)
15-minute values — August 3 except 0000-1700 UT; August 4; August 5 except 1560-1630 UT; August 7 " 0000-0800 UT; August 8 " 0300-2300 UT

Kiel N54.3 E10.1 — Cut-off 2.29 GV — 18-NM-64
Pressure corrected data.
5-minute values — 0000-2400 UT August 4; 0000-1100 UT August 5; 1200-2300 UT August 7

Moscow N55.47 E37.30 — Cut-off 2.46 GV — 12-NM-64
Pressure corrected data.
5-minute values — 1300 UT August 3 - 1000 UT August 6

Hafelekar N47.3 E11.4 — Cut-off 4.37 GV — 3-NM-64
Pressure corrected data.
Hourly values — July 26 - August 14 (graph) except 0800-0900 UT August 13
10-minute values — July 25 - August 14

Hermanus S34.42 E19.20 — Cut-off 4.9 GV — 9-NM-64
Pressure corrected data.
10-minute values — August 4, 5

Potchefstroom S26.70 E27.10 — Cut-off 7.30 GV — IGY-15
Pressure corrected data.
10-minute values — August 4, 5

Mexico City N19.33 E260.8 — Cut-off 9.53 GV — IQSY-NM-64
Pressure corrected data.
Hourly values — July 26 - August 14 except 2100-2400 UT August 5

Morioka N39.7 E141.13 — Cut-off 10.13 GV — IGY-6
Pressure corrected data.
Hourly values — July 26 - August 14 except 1500-1900 UT August 2; 0200, 0500-0600 UT August 6; 0600-0800 UT August 8; 1900-2400 UT August 13; 0100-0400 UT August 14

Buenos Aires S34.58 E301.50 — Cut-off 10.63 GV — 18-NM-64
Pressure corrected data.
Hourly values — August 2-11 (graph)

Mt. Norikura N36.12 E137.55 — Cut-off 11.39 GV — 4-NM-64
Pressure corrected data.
Hourly values — August 1-10

Tokyo-Itabashi N35.75 E139.72 — Cut-off 11.61 GV — 18-NM-64
Pressure corrected data.
Hourly values — August 1-10

Gulmarg N34.07 E74.4 — Cut-off 11.91 GV — IGY-NM
Pressure corrected data.
Hourly values — July 1 - August 31

B. Ionization Chambers

Hafelekar N47.3 E11.4 — Cut-off 4.37 GV
Pressure corrected data.
Hourly values — July 26 - August 14 except 1300-1600 UT August 1; 1100-1200 UT August 2; 1100-1400 UT August 3; 1200 UT August 4; 0100-0200 UT August 5; 0500 UT August 6
(graph)

B. Ionization Chambers (continued)

Sapporo N43.03 E141.35 Cut-off 8.22 GV
Pressure corrected data.
Hourly values
August 1-10

Mt. Norikura N36.12 E137.55 Cut-off 11.39 GV
Pressure corrected data.
Hourly values
August 1-10 except
0100 UT August 1
1400 UT August 1
2300-2400 UT August 2
0100-0300 UT August 3
0600 UT August 9
1500-1600 UT August 9
1900 UT August 9
2100-2200 UT August 9
0100-0300 UT August 10

Koenji N35.7 E139.63 Cut-off 11.58 GV
Pressure corrected data.
Hourly values
July 26 - August 14 except 2000-2300 UT August 3
1900-2300 UT August 7
0600-0700 UT August 14

Tokyo-Itabashi N35.75 E139.72 Cut-off 11.61 GV
Pressure corrected data.
Hourly values
August 1-10 except
2200 UT August 2
1500 UT August 4
1100-2400 UT August 7
0100 UT August 8
1000 UT August 9
1700 UT August 10

Hong Kong N22.42 E114.20 Cut-off 16.23 GV
Pressure corrected data.
Hourly values
August 1-10 except
1900 UT August 1
0200 UT August 8
0500 UT August 8
1900 UT August 8
0700 UT August 9
0800 UT August 10
1200 UT August 10

C. Muon and Meson Telescopes

Yakutsk N62.02 E129.72 Cut-off 1.70 GV Semicubical Telescope
Pressure corrected data.
Hourly values
July 25
July 26 except 1800-2400 UT
July 27 - August 1
August 2 except 1200-1400 UT
August 3 - August 5
August 6 except 2000 UT
August 7, 8
August 9 except 1000 and 1200 UT
August 10 - August 14

Semicubical Telescope
vertical at 7 m.w.e. underground
Hourly values
July 25
July 26 except 1800-2400 UT
July 27 - August 5
August 6 except 1800-1900 UT
August 7, 8
August 9 except 1000 and 1200 UT
August 10-14

C. Muon and Meson Telescope (continued)

Yakutsk (continued)			Semicubical Telescope Vertical at 20 m.w.e. underground
Hourly values		hourly same as vertical at 7 m.w.e. underground	
			Semicubical Telescope Vertical at 60 m.w.e. underground
Pressure corrected data. Hourly values		July 25 July 26 except 1900-2400 UT July 27 - August 5 August 6 except 1700-1900 UT August 7, 8 August 9 except 1000 and 1200 UT August 10-14	
Utrecht	N52.08 E05.13	Cut-off 2.76 GV	Meson Monitor
Not pressure corrected, pressure values also given. Hourly values		July 26 - August 14	
Hafelekar	N47.3 E11.4	Cut-off 4.37 GV	Muon Telescope
Pressure corrected data. Hourly values		July 26 - August 14 (graphs)	
Takeyama	N35.22 E139.62	Cut-off 11.89 GV	Meson Telescope, vertical
Not pressure corrected Hourly values		August 1-10 except 0200-0400 August 3	

STATIONS REPORTING HOURLY foF2 AUGUST 1-11, 1972

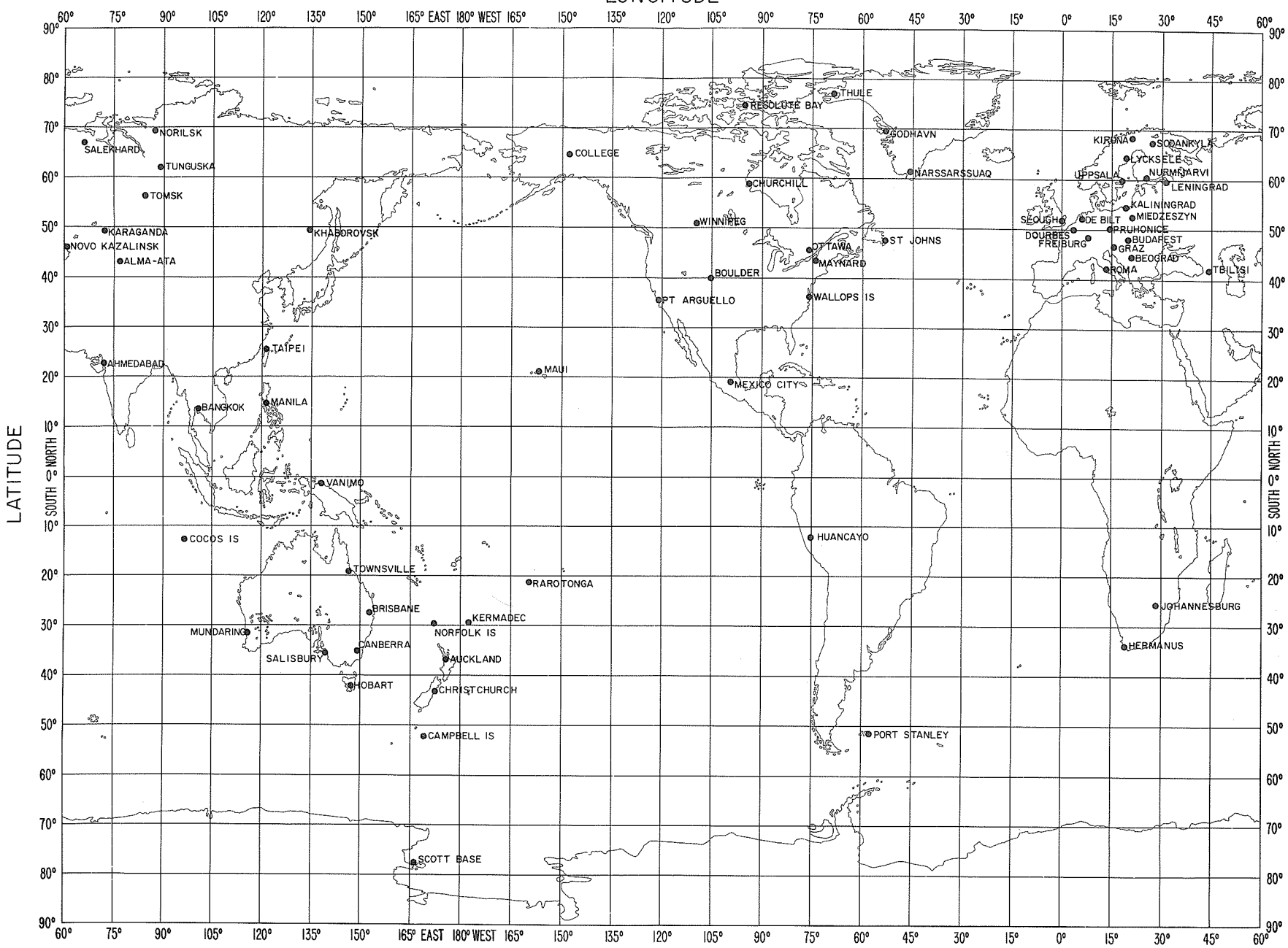

Hourly foF2 August 1-11, 1972, with median and count
Stations in order of latitude north to south
LONGITUDE 30.0E---120.0E

Station Latitude Longitude		LOCAL TIME																								
		00	01	02	03	04	05	06	07	08	09	10	11	12	13	14	15	16	17	18	19	20	21	22	23	
	1	F 060	059	053	057 F	058	060	063 U R	B	B	064	068	069	070	070	065	061	063	065	063	061	G56	051	047	045	1
NORILSK,USSR	2	048	049	043	043 F	046 F	048	052	055	057	062	065	067	068	069	070	071	072	073	073	069	069	070	064 F	060	2
69.4N	3	057	053	052	051	053	056	056	058	059	062 F	063 I B	065 B	069	070 B	071 B	070 B	070 B	070 B	068 B	068 B	068 B	068 B	062 B	055 B	3
88.1E	4	051 B	053 B	057 B	057 B	056 B	055 B	057 B	060 B	062 B	058 B	054 B	8	059 B	B	B	B	B	B	B	B	B	B	B	B	4
Geomag. Lat.	5	B	B	B	B	B	B	B	B	B	B	B	B	B	B	B	B	B	B	B	B	B	B	B	B	5
58.5N	6	B	B	B	B	B	B	B	B	B	B	B	B	B	B	B	B	B	B	B	B	B	B	B	B	6
90.0E LMT	7	B	B	B	B	B	B	B	B	B	B	B	B	B	B	B	B	B	B	B	B	B	B	B	F	7
	8	053	046 F	B	B	B	B	B	B	B	B	B	B	B	B	U R 063	B	B	070	B	069	066 B	054 B	054 B	054 U F 052	8
	9	058 C	059 B	B	B	B	B	B		057 G	057	062	I B 063 U R	067		B	B	B	B	B	B	B	B	C	B	9
	10	F	F	F	B	B	B		042	044	045	047	049	050	051	052	055	054	056 F	054	042	042	051 F	045 F	047 F	10
	11	046	050	046				050	052	053	052	053	053	055 U	055	054	054	054	057	061	060	047	050	047	040	11
	MED	049	049	046	048	045	048	050	052	054	057	060	062	060	062	063	062	062	062	061	061	059	054	051	049	MED
	CNT	021	022	020	019	019	021	022	023	026	027	026	024	024	024	025	024	025	026	025	026	025	024	023	022	CNT
	1	057 F	055 F	054 F	058	060	060	061	063	070	073	071	F 071	074	068	062	061	057	060	061	064	060	049	044 F	042	1
SALEKHARD,USSR	2		035	037	044	048	049	051	055	062	068	070	072	073	074	073	075	071 R	070	069	069	064	063	063	062	2
66.5N	3	058	057	052	052	054	055	061	064	066 B	070 A	073 B	076 B	073 B	074 B	072 B	073 B	070 B	068 B	069 B	070 B	075 B	064 B	058 B	056 B	3
66.5E	4	055 B	053 B	051 B	049 B	050 B	059 B	064 B	061 B	B	B	B	B	B	B	B	B	B	B	B	B	6	B	B	B	4
Geomag Lat.	5	B	B	B	B	B	B	B	B	B	B	B	B	B	B	B	B	B	B	B	B	6	B	B	B	5
57.3N	6		B			B		B	B	B	B	B	B	B	B	B	B	B	D R	050			044		039	6
60.0E LMT	7	041		040	045		043												068	066	066	068	061	056	049	7
	8	046 F	049 F	049 F	049 U F	050 F	051	055	054	058	057	061	064 R	065 B	060 B	059 B	060 B	061 B	061 B	060 B	059 B	059 B	060 B	060 A	051 A	8
	9	A	A	B	050 U R	054	056	056	059	060	060	065	067									F			U F	9
	10				032	035	039	042	045	048	052	058	056	061	061	062	063	059	061	049	049	046	046	043 F	046 U F	10
	11	046	044	045	044	048	050	053	053	055	054	055	056	053	055	053	051	052	058	055	056	054	043	042	043	11
	MED	044	043	038	037	042	047	052	056	058	061	063	064	067	064	062	062	065	062	061	060	059	055	052	046	MED
	CNT	020	022	022	025	027	029	028	028	027	027	027	027	026	026	026	025	024	027	027	026	025	024	022	023	CNT
	1	060 U F	058 R	U R 052	049	050	J R 051	064	063	067	065	069 C	073	072	071	073	073	068	071	063	060	066	069	067 F	059 F	1
TUNGUSKA,USSR	2	053	U S	039 S	038 U S	040	043 C	050	059	065	067	C	076	073	072	071	073	071	071	071 C	071 C	070 C	071 R	070 R	065	2
61.6N	3	060	057	R	055	058 I R	R	065 R	065 R	069 R	069 R	C	069 C	069 R	072 C	072 C	070 C	070	071	U R	C	C	C	A	060 F	3
90.0E	4	053 U F	049 U F	048	048 U R	049 C	C	054 C	C	C	C	C	C	C	C	C	C	048 C	050 C	051 C	C	C	C	C	036 C	4
Geomag. Lat.	5	030 C	026 C	024 C	025 C	C	C	C	C	C	C	C	C	C	C	C	C	C	C	C	C	C	C	C	C	5
50.6N	6	C	C	C	C	C	C	C	C	C	C	C	C	C	C	C	C	C	C	C	C	C	C	C	C	6
90.0E LMT	7	C	C	C	C	C	C	C	C	C	C	C	C	C	C	C	C	C	C	C	C	C	C	C	C	7
	8	C	C	C	C	C	C	C	C	C	C	C	C	C	C	C	C	C	C	C	C	C	C	C	C	8
	9	C	C	C	C	C	C	C	C	C	C	C		C	C	C						S	S	F	F	9
	10	F	F	F	F	F	F						054				059	062	063	060	064					10
	11							047	049	053	050	055	059	059	058	058	057	057	055	055	059	060	061	059	049	11
	MED	042	039	036	031	035	043	049	055	058	062	067	068	067	068	068	068	067	064	063	064	067	062	058	050	MED
	CNT	023	021	020	022	021	020	023	021	023	022	019	023	024	023	021	024	025	026	024	022	021	022	021	024	CNT
		00	01	02	03	04	05	06	07	08	09	10	11	12	13	14	15	16	17	18	19	20	21	22	23	

Hourly foF2 August 1-11, 1972, with median and count
Stations in order of latitude north to south
LONGITUDE 30.0E---120.0E

Station Latitude Longitude		LOCAL TIME																							
		00	01	02	03	04	05	06	07	08	09	10	11	12	13	14	15	16	17	18	19	20	21	22	23	
	1	C	C	C	C	C	C	C	C				F		F	F							F	F	U F	
		F	F	F	F	F				068	069	076	074	073	066	062	061	060	058	056	056	055	051	049	046	1
LENINGRAD,USSR	2	041	036	034	036	041	046	049	053	064	068	071	070	070	072	072	071	068	066	065	065	U F	F	D C	D C	
				F	F	F					J R	U R	U R							F		065	067	070	069	2
60.0N	3	063	055	055		048	056	066	072	082	091	084	084	078	077	076	069	070	073	078	070		U C	D C		
		U F	U F	F	F	F	F	F	E G	E G	B	E G	E G		E G		B		B	B	B	068	070	070	068	3
30.7E	4	061	056	051		045	046	042	037	039		043	043	049	043	044		046						F	F	
		B	B	B	B	A	B	B	E G	E G	E G	E G	E G	E G	E G	E G	E G	A	E G	E G	F	043	037	033	029	4
Geomag. Lat.	5								035	039	039	040		041	040	040	040		038	036	031	U F	F	F	F	
56.2N		F	U F	U F	U F	U F	E G	E G	E G	E G	E G	E G		E G		E G				F	F	032				5
30.0E LMT	6	027	025	031	035	034	033	035	039	040	041	042	044	044	047	044	046	049	052	051	050	F	F	F	U F	
		U F	U F	F	U F	F														I C		040	038		025	6
	7	029	030		032	033	037	041	046	047	052	055	058	063	063	070	067	069	073	075	071	070	064	054	053	
			F	F	F								F										U F	U F	F	7
	8	049	043	040	037	041	047	052	056	059	062	063	060	058	063	060	065	063	064	065	070	072	065	059	053	
		U F	F	F	U F	U F	F	F					F			F	F				F	F	F	F	U F	8
	9	050	043	041	034	038	046	047	049	054	055	060	059	060	063	054	055	056	055	057	048	042	029		025	
		U F	F	U F	U F																		U R	U F	U F	9
	10	024		024	025	039	035	041	045	053	060	064	069	069	066	062	066	067	059	068	065	067	063	053	041	
		U F	F	U F	C	C	C	C	C						V			I C					F	F	F	10
	11	029		023						052	056	053	055	055	055	056	059	058	058	056	056	053	050	050	040	
		F	F	F	F	F																		F	F	11
	MED	042	036	033	032	033	042	048	054	058	065	065	070	067	066	066	066	064	062	064	064	063	063	054	047	MED
	CNT	027	024	026	024	027	027	027	028	031	030	030	029	031	031	031	030	030	030	030	030	030	029	025	026	CNT
	1	060	056	051	050	050	052	062	061	066	064	072	074	074	075	080	076	070	072	071	U S 064	060	062	067	065	1
																								I C		
TOMSK,USSR	2	058	052	044	040	039	044	052	062	070	070	078	078	078	078	074	074	075	073	073	072	072	073	071	065	2
																								U S		
56.5N	3	061	056	055	054	054	058	066	069	074	074	080	079	075	076	077	073	074	072	072	075	082	076	076	065	3
								F							I B						I A				F	
84.9E	4	059	052	052	050	048	051	062	071	067	072	065	074	082	085	084	064	059	056	053	054	055	061	056	045	4
			F			F	U R	F	E G	F	E G	E G	E G	E G	A	E G	E G	E G	E G	E G	E G		F	I B	F	
Geomag. Lat.	5	041	036	033	031	028	027		033	037	039	040	042	043		040	040	039	036	034	031	034	030	022		5
45.9N		U F		F	U F						E G		F													
90.0E LMT	6	020	021		024	036	036	040	045	044	042	049	053	053	055	058	060	059	059	059	057	056	061	059	053	
		F	F	F		F																		U F		6
	7	046	033	030	028	029	036	042	052	056	062	065	073	080	083	085	080	073	074	075	075	079	080	074	069	
						U S						H	I C													7
	8	060	050	042	040	038	045	048	054	058	059	066	066	063	067	066	069	064	061	063	068	069	069	062	061	
				F		F																	F	F	F	8
	9	055	050	046	040	036	041	047	050	053	062	065	067	075	080	075	076	069	070	071	060	062	052	047	035	
		F				F																				9
	10	026	022	019	018	023	033	043	048	049	057	059	062	064	071	068	065	072	068	067	070	075	074	060	049	
													F													10
	11	042	034	030	028	029	039	045	049	053	053	058	060	062	062	062	059	058	058	056	061	065	069	066	056	
	MED	048	043	042	036	036	040	048	055	058	063	066	070	073	073	073	070	069	068	067	068	069	066	062	053	MED
	CNT	031	031	030	031	031	031	029	030	030	030	031	031	031	030	031	031	031	031	031	031	031	031	031	030	CNT
	1	S	S	J S	I S	N	U S	I S	I R												S	S	J S	S	J S	
				053	050	048	053	059	063	070	081	077	082	090	090	090	082	075	077	072			073		073	1
		S	U S	U S			U S		J S		J R										U S		S	J S	A	
KARAGANDA,USSR	2		062	056	050	050	052	057	068	070	073	083	087	086	084	080	077	075	075	075	075	070		073		2
					U S	U S	I S	U S			J R								J R				J S	J S	I S	
49.8N	3	060	060	059	055	054	065	073	080	083	087	089	090	090	083	080	074	077	083	079	080	080	080	081	066	3
			I S		U S	U S		I S	J S					I C			I R	J R	J R			I A	I S	I S	S	
73.1E	4	060	058	054	054	053	057	066	073	077	070	083	097	101	101	087	070	067	067	070	060	060	057	053		4
		S	S	A	S		I A	I R		I R	I A					A	C	C	C	C	C	C	C	C	C	
Geomag. Lat.	5					020	025	028	033	042	044	042	045	044	043											5
40.2N		C	C	C	C	C	C	C	C	C	C	C	C	C	C	C	C	C	C	C		S	S		I S	
75.0E LMT	6																				060			060	052	6
		U S		J S		U S				I R					U R									J S	S	
	7	047	046	043	043	036	040	050	057	065	069	077	083	093	093	089	077	074	080	080	084	090	083	073		7
		I S					U S				I R	J R						I R	J R	J R	I S	U S	U S	S	S	
	8	057	050	050	048	045	045	053	057	060	065	068	074	075	077	075	073	070	067	069	074	078	077			8
		S																		U S		U S	S	S	S	
	9		050	045	042	038	042	047	054	060	073	080	084	083	084	090	084	077	080	055	079	077				9
		S	J S		I S		J S	I S	I R	J R		U R											J S	C	C	
	10		033	030	028	026	037	046	055	067	073	076	076	083	075	078	084	079	070	070	080	080	075			10
		C	C	C	C	C	I S			I C		J R	R	C	R			I S	A	S	S	S	A	A	A	
	11						051	057	057	058	060	063				064	059	064								11
	MED	052	050	046	044	042	043	053	059	067	074	080	081	082	083	080	075	074	073	071	075	075	073	059	055	MED
	CNT	016	020	026	026	029	030	029	029	029	028	028	028	028	029	029	029	028	027	025	023	020	013	013	015	CNT
		00	01	02	03	04	05	06	07	08	09	10	11	12	13	14	15	16	17	18	19	20	21	22	23	

Hourly foF2 August 1-11, 1972, with median and count
Stations in order of latitude north to south

LONGITUDE 30.0E---120.0E

Station Latitude Longitude		LOCAL TIME																						
		00	01	02	03	04	05	06	07	08	09	10	11	12	13	14	15	16	17	18	19	20	21	22	23	
	1	C	C	C	C	C	C	C	C	082	I C 080	085	091	094	090	087	080	076	070	068	075	073	075	069	071	1
NOVO KAZALINSK,USSR	2	068	060	C	C	055	055	065	070	I C 080	088	I C 088	090	090	085	083	078	078	078	U S 075	075	073	073	070	068	2
45.8N	3	065 J R	060 J R	058 J R	058 J R	055 J R	063	078 C	085 C	088	090	095	088 C	080 C	088 C	080	083	083 I A	083	078	080	085	083	070	065	3
62.1E	4	061	060	058	057	053	058 I A	I A		070 E G	078	098 A	A	A	A	073	075	078	085 N	073	088	070	066	058 I A	053	4
Geomag. Lat.	5	050 I A	050	043	031 N	022	026	030	034	040 I A	046					049 I C	048	045		040	037	037 I C	035	033	030	5
37.6N	6	025	023	025	024	025	038	044	049	060 C	068	077 C	075 C	078 C	085	084	077	069	069	067	068	068	071	066	062	6
60.0E LMT	7	058	055	049	044	040	043	052	058						093	083	085	090	085	078 U S	098	093	073	065	063	7
	8	058	055	055	050	048	053 I C	055	063	068	075	085	080	083	078	078 I C	078 C	070 C	073 C	078 C	088 C	085 C	070 C	065 C	058 C	8
	9	055 C	055 C	053 C	045 C	040 C	043 C	053 C	060 C	068 C	075 C	078 C	085 C	095 C	100 C	095 C		C	C	C	C	C	C	I A	9
	10		I A					C	C	C	C	C	C				088					A	A	068 A	061	10
	11	058	052	048	043	038	045							069	070	063	068	070	070	073	073			043		11
	MED	055	052	048	045	045	045	055	066	076	078	084	084	083	085	080	078	074	072	072	073	068	068	060	056	MED
	CNT	027	028	028	028	029	029	027	026	027	028	026	025	027	027	029	028	027	026	028	028	025	027	030	028	CNT
	1	U S 063	S	N	U S 052	F	049	056	U S 064	079	082	085	089	I C U R 099	103	R	092	082	080	078	076	U S U S U S 075	074	072	071	1
ALMA-ATA,USSR	2	U S U S U S 064	059	056	051	049 U S	056	064 U S	079	083	080	084	087 U S	093	094	090	C	C	C	078	U S 078	I S U S U S U S 069	069	072	070	2
43.2N	3	064 S	060 S	059 U S	U S	055 S	059	073	080	083	081	088	093	089 I R	082	083	081	079	087	089	088 U S	080 U S	078 U S	074 U S	066 U S	3
76.9E	4			057 U F	055		054 I R	067	076 A	075 A	076 A	079 R	096 A	106 A	115 R	099 I A	073 U R	075	073	079	073 A	075	082	052	045	4
Geomag. Lat.	5	043	042 U R	043	034	025	025	029	U S	J R					U R	058	055	050		U S		037	037 U S	032 I S	033 I S	5
33.4N	6	033	026 U S	023	024	026 U S	036	050	065	072	069	078	084	082	082 U R	092	090	084	078	073	072 U S	069	072	061 U S	054 U S	6
75.0E LMT	7	048	047 U S U S	048	040	038	043 U S	057	073	079	086	098 U R	089	100	104	098	088	078	080	088	091 C	091	080 C	072 C	062 C	7
	8	059 C	054 C	055 C	053 C	049 C	055 C	060 C	060 C	068 C	075 C	082 C	088 C	080 C	082 C	083 C	079 C	C	C	C	C	C	C	C	C	8
	9	C	C	C	C	C	C	C	C	C	C	C	C	C	C	C	C	C	C	C	C	C	C	C	C	9
	10	C	C	C	C	C	C	C	C	C	C	C	C	C	C	C	C	C	C	C	C	C	C	C	C	10
	11		U S U S U S			U S							U S							U S U S			U S U S U S		11
	MED	057	052	050	048	046	048	060	068	073	079	082	086	090	087	088	082	077	078	075	076	069	064	060	058	MED
	CNT	017	018	020	021	022	022	025	020	019	019	019	019	018	016	021	020	020	023	019	016	014	016	020	016	CNT
	1	C	C	C	C	C	C	070	C	C	C	I C 089	093	I C 098	096	090	088	J X 081	J X 080	C	U C 084	C	C	C	C	1
TBILISI,USSR	2	C	C	C	C	S	S	066	C	C	C	C	C	C	I C 081	080	I R 078	C	R	R	R	R	I A 068	R	R	2
41.7N	3	U C 060	062	059	055	U R 053	058	065	U R 070	080	080	080	090	094	089	081	088	U R 080	U C 085	C	080	C	U C 075	U C 065	U C 062	3
44.8E	4	066	065	067	050	U C 047	044	C	J X 056	A	A	C	100	095	C	075	A	J X 084	A	A	A	J X 082	J X 059	C	C	4
Geomag. Lat.	5	055	053	045	048	C	C	C	R	R	C	R	C	C					063	070	070	068	058	053	056	5
36.2N	6	030	024	029	C	R	R	C	C	C	R	C	C	C	R	C	C	C	C	I C 065	U C 070	050 C	050 C	048 C	043 C	6
45.0E LMT	7	C	C	C	C	C	C	C	I C 061	065	Y X 076	089	091	U C 100	093	096	C	C	C	C	072 C	C	C	C	C	7
	8	U C 065	U C 060	C	U C 050	042	I C 048	065	C	085	090	090	I C 085	095	U C 090	085	U C 080	U C 085	U C 083	U C 085	C	070	C	C	C	8
	9	C	C	R	047	040	R	C	C	C	C	C	C	C	C	I C 094	085	S	S	090	S	S	A	A	C	9
	10	C	038	045	040	043	045	045	050	058	063	068	I C 075	080	083	088	090	080	073	080	078	070	063	062	058	10
	11	U R 060	056	054	050	045	040	U R 050	U C 055	060	065	070	071	I R 072	070	I C 072	U C 073	R	U C 075	U C 074	C	C	C	C	C	11
	MED	058	055	052	050	046	044	060	061	071	075	081	084	084	081	081	080	078	073	070	072	070	063	062	058	MED
	CNT	019	023	023	023	020	017	021	022	021	023	022	022	023	025	026	023	019	024	018	013	013	014	012	009	CNT
		00	01	02	03	04	05	06	07	08	09	10	11	12	13	14	15	16	17	18	19	20	21	22	23	

Hourly foF2 August 1-11, 1972, with median and count
Stations in order of latitude north to south

LONGITUDE 30.0E---120.0E

Station Latitude Longitude		LOCAL TIME																						
		00	01	02	03	04	05	06	07	08	09	10	11	12	13	14	15	16	17	18	19	20	21	22	23	
	1	U S 070 F	C C	065 C	C C	C C	064 C	071 C	070 C	070 C	078	093 B	111	125	138	134	135	127 C	120	119	117	C	075	C	C	1
AHMEDABAD,INDIA	2										086		106	118	134	145	146		137	148	137	130	112	091	078 U F	2
23.0N	3	080 U F	079 U F	067 F	057	053	055 U F	063 U F	077	085	088	096	094	090 B	098	106	108	114	121	123	120	103 U S	090 U S	084 U S	088 U F	3
72.6E	4	092 U S	080 U S	U S	072	067	067	084	091	078	083	082	084		116	118	112	107	099	103	106 D S	078 D S	079 U S	079 U S	084 U S	4
Geomag. Lat.	5	077	074	064	067 U F	044 F	022 U F	030 A	051 A	047	097	121	090	113	082	117	128	120	124	130	070	070	080	073	065	5
13.8N	6	057 U S	053 U S	037	028	U F	026			070	085	105	106	122	146	155	140 C	128	132 D	144 U	124 U	096	083	070	074 A	6
75.0E LMT	7	075 U F	074 U F	070 U F	058 U F	056 U F	055 U F	066 U F	080	084	104	110	145	143	140	142		145 D	150	139 C	144	139	101	099		7
	8	099	087	095	088	078	082	080	081	094	089	088	096	118	134	132	138	140 A	168		129	122	122 D S	122 D S	100 U S	8
	9	098 S	098 U S	080 U S	065 U S	049	042	052	073	087	088	101	112	121	137	145	152	A	110	118	133	090	070	070	062	9
	10		073	060	062 U F	066 U F	047 U F	057 U F	067	068	078	080	102	114	127	129	140		164	142	112	091	076	068	073 C	10
	11	073	062	067	057	047	046	062	074	067	077	102	113	132	138	147	157	160	133	114	111	084	074	064		11
	MED	067	062	059	055	047	042	057	080	084	085	095	106	120	136	141	145	142	137	135	122	091	080	068	069	MED
	CNT	028	027	029	027	027	029	027	027	029	029	030	030	029	031	030	030	028	031	029	029	028	028	027	026	CNT
	1	F	F	F	F	F	F	F	080	080	085	D R 087	080	078	080	093	102	102	100	104	D R 084	U R 085	092	080	083	1
						F							C	C	C	C	C	C								
BANGKOK,THAILAND	2	084	078	073	065		042	044	078	090	092	096							083	083	083	085 F	085 F	082 F	090 F	2
13.7N	3	080 F	084 F	080 U R	065 F	056 D R	056	060 N	076	084	086	098	102	100	102	105 B	110	120	130	114	112	U R				3
100.6E	4			062		075	062	060	075	085	091	077	071	073	080		112	114	106	104	103	100	104	102	076	4
Geomag. Lat.	5	072	070	065	056	050	031 A	034	057	104	063	066	100	095	095	093	120	120	075	090	085 U R	090	095	095	082	5
2.3N	6	090	095	056	035	023		039	071	093	100	085	082	086	090	100	104	108	103	100	092 D R	085	095	105	103	6
105.0E LMT	7	096	090	075	057	054	048	054	080	100	106	104 C	079	080	085	090	095	103	110	114	110	110	092	091 F	090 F	7
	8	088 F	082 U R	076	060	061	052	045	077	090	095 J R	J R	095	092	097	095	095	104	102 U R	102 U R	093	085	083 U R	U R		8
	9		093	080	052 V	043	031	046	076	082	080 C	081	084	080	090	100	116	128	122	120	105 D R	104 U R	092	065 F	077 F	9
	10	060 F	057 D R	054 D R	051	052	040	043	069	081		080	086	086	088	100	106	107	112	115	095	080	073			10
	11		070	065	068	070	045	039	063	070	070	070	066	074	077	080	083	093	100	098	090	082	080	077	070	11
	MED	092	092	070	058	048	039	042	075	089	088	081	083	085	087	093	100	105	106	106	105	099	094	092	090	MED
	CNT	27	29	30	28	28	29	29	31	30	27	28	29	28	29	26	29	30	31	31	31	29	27	24	25	CNT
	1	U F 046 F	035	029	027	028	U S 024	047	064	077	093	094 D R	077 D R	085	104 U R	105 U R	099 U R	089 D R	088 A	079 U R	J S 053 U S	042 D S	U F 035	U F 037	F	1
COCOS I Indian Ocean	2	F	035 F	033 U F	027 U F	024 U F	026	048	067	088	098	090	090	110	112	123	125	113		102 J S	092 J S	056	032	034		2
12.2S	3	F		024	025	027 U F	026	049	070	084	090	089	086	085 U R	080 B	085	088 U R	086	079 U R	073	077 U S	061	039 U S	032	030	3
96.8E	4		029	027 U F	028 F	029 U F	030 A	053	075	096	089	084	085 J R	102		110	122 U R	104 U R	093	105	093	058	052 U R	058	055	4
Geomag. Lat.	5	036 R	026 U R	025 A	A	027 D R	U R	031	084	084	076	104 U R	104 U R	110 U R	085 U R	053 U R	124 D R	124 U R	066 U R	043 U R	038	030	026 U S	029	030 U S	5
23.3S	6	U S	038 U R		J R	019 B	021	055	070	087 J R	099 U R	115 U R	125 U R	128 U R	129 U R	150	150 U R	151 U R	120 J R	104 A	090	066 J R	051 F	055 U S	059 U F	6
90.0E LMT	7	037	037	033	020		019	046	086 U S	104 U R	118 U C	110 C	118 C	135 C	124 C	110 C	115 C	110 U R	104		065	052	A	044	027	7
	8	029 A	026	021	024	026	027	051	087	112 U R	114							092	084 U S	070 C	070 C	044 C	C	044 C	037 C	8
	9	C	027 C	022 C	023 C	024 C	023 C	050 C	080 C	092 C	098 C	097 C	113 C	100 C	099 C	100 C	101 C	110 C	094 C	C	C	C	C	C	C	9
	10	C	C	C	C	C	C	C	C	C	C	C	C	C	C	C	C	C	C	C	C	C	C	C	C	10
	11																									11
	MED	036	035	026	024	026	026	050	078	090	098	105	112	110	113	110	116	110	094	089	078	052	044	048	046	MED
	CNT	012	015	015	014	017	015	018	018	017	018	018	018	019	018	020	020	021	020	018	018	018	013	016	016	CNT
		00	01	02	03	04	05	06	07	08	09	10	11	12	13	14	15	16	17	18	19	20	21	22	23	

Hourly foF2 August 1-11, 1972, with median and count
Stations in order of latitude north to south
LONGITUDE 30.0E---120.0E

Station Latitude Longitude		LOCAL TIME																						
		00	01	02	03	04	05	06	07	08	09	10	11	12	13	14	15	16	17	18	19	20	21	22	23	
	1	038	035	039	041	042	029	032	042	060	066	070	079	085 B	084 B	092 B	100	092	076	062	051	042	038	042 F	040 F	1
MUNDARING, Australia	2	042 F	040	041	041 F	044 F	042 F	037	047	066	070	079	079				080 V	065	076	073	056	036	036	039	038	2
32.0S	3	036 F	038 F	039 F	040	040 F	037 F	036 F	046	063	076	078	072	080	080		069 B	072	070	068	058	052	040	036	036	3
116.2E	4	037 F	036 F	039 F	040 F	042 F	038 F	030 F	046 F	067	069	076	088	072	083	090		117	097 A	084	070 F	045 A	046 F	050 F	046	4
Geomag. Lat.	5	047 A	047 A	047 F	029	024	025 R	021 A	037 F	030 F	034	038	039	039	039	039	034	033		029	020		019	020	020	5
43.4S	6			017	017	015			028 F	045	064	078	072	089	090	092	092	094	088	090	069	038	035	036 F	030 F	6
120.0E LMT	7	033 F	030 A	027 A	027 F	027 F	028 F	021 F	042	066	075	080	081	090	085	092	088	086	071	060	049 F	039 F	032 F	029 F	026 F	7
	8	025 F	F	F	028 F	025 F	023 F	022 F	043 F	066	079	086	088	075	082	079	088	070	070 U S	059	038 U S	031 F	033	027	022	8
	9	024	025	027	028	029	026	022	039	062	073	080	085	090	083	088	088	102	100	078	066	036	042	047	037	9
	10	036 F	031 F	022 F	027 F	029 F	027 F	028 F	048	068	077	092	090	091	080	082	084	082	069	056	045	044	041	038 F	036	10
	11	033	028	030	032 F	034 F	030	025	047	070	083	083	088	085	083	092	090	076	070	062	045	043	042	038	038	11
	MED	036	036	036	037	036	033	030	048	067	075	080	085	086	084	089	086	078	075	066	056	044	041	039	037	MED
	CNT	030	029	030	030	029	028	028	028	028	027	028	029	028	028	028	029	031	030	031	031	030	031	031	031	CNT
		00	01	02	03	04	05	06	07	08	09	10	11	12	13	14	15	16	17	18	19	20	21	22	23	

Hourly foF2 August 1-11, 1972, with median and count
Stations in order of latitude north to south
LONGITUDE 120.0E--210.0E

Station Latitude Longitude		LOCAL TIME																						
		00	01	02	03	04	05	06	07	08	09	10	11	12	13	14	15	16	17	18	19	20	21	22	23	
	1	R 076	063	062	060	060	064	065	068	065	F 067	071	077	079	081	081	083	082	079	070	069	073	I C 080	C	J R 076	1
KHABOROVSK,USSR	2	070	069	063 J R	063	062 I C	067 U R	080 R	090 C	085	079 C	071	073 U R	080	080 U C	079 U C	077 A	073 A	070 C	075 A	085 A	089 I C	081 I R	079 I A	071 C	2
48.5N	3	066 C	064 C	063 C	062 A	060	060		C	075 A	A	055 C	062 J C	060	063 U C	063 C		I C	J C	C		082 U C	075	075 C	C	3
135.1E	4					057	058						071	082	067		092	099	090		060	060	061			4
Geomag. Lat.	5	060	051	043	041	039	040	043	E G 042	E G E G E G 042	041	043	A	C	C	C	C	A		038	037	033	033	032	030	5
37.8N	6	027	023	021	025	024	I C 035	039	044	050	R	I C 057	053	I C 061	U C 065	078	A	U S 070	C	C	C	C	U R 060	C	C	6
135.0E LMT	7	A U C	U C 046	I C 047	U R 043 I C	041	045	C	U C 060 A	A C	U C 054	060	058	054 I C	C	U R 062	U C 063 C	C	C	C	C	C	C	C U C 065	7
	8	060	056	056	051 J R	047	049	054			072	082	073	070	068	071					072	074	075	070	066 C	8
	9	064 J R	061	056	053	051	051	052	061	070	072	073 C	067	072	076	080 C	083 C	088	095 C	090 C	096 C	096	090 J R	080		9
	10	073	066	050	043	041	037	046 I C	049	049 I C	050		051	054	055			055				070	070	065 J R	059	10
	11	055	051	050	045	044	057	068	070	063	069	067	069	071	072	072	068	063	059	063	064	073	072	068	065	11
	MED	060	052	051	050	049	050	056	066	067	066	066	068	070	070	070	070	070	070	070	072	076	072	068	060	MED
	CNT	024	025	025	026	027	026	024	024	025	026	027	028	027	026	027	023	026	025	025	026	026	027	024	022	CNT
	1	061	072 A	093	101	100 B	100 B	106 B	113 B	109	105 A	104	100	082 N	078 A	076 A	070	070 S	068 F	073	071 S	070 F	072	060	066	1
TAIPEI,CHINA	2	075		082	093			108	120	109		076	071	100			075	070		070			064	068	070	2
25.0N	3	072	064 A	067	080	082	096 S	099	101 B	106	106	105	100	078	080	081 A	082 A	073	071	076	068	067	062 N	077	075	3
121.2E	4	063	S	073 A	084 A	085		107		145 A	113	087	060	063	065			065 F	066	058	051	050 B		083	085	4
Geomag. Lat.	5	065				101	086 R	096	094		121	072	102	055	050	048	048		041	043	041		049	050	075	5
13.6N	6	073	070	050	042	042 B	R	042	052	148	146	140	115	097	094	100	101	094	096	086 F	082 F	062 F	069 F	060	064	6
120.0E LMT	7	077	082	099	113 S	S	S	129 S	116 S	092 S	073 S	078 S	072 S	059	064	073	070 S	062	053					065	068 A	7
	8	070	088	106	126	138	126	144	148	146	137 S	123	121	105 A	091 A	087 A	083 A	090	086	076	074	050	048	062	A	8
	9	072 A	072	085	085	082	100 R	112 R	105	121	120	083 S	088 S					060	052 S	048 S	048 S	052	053	080		9
	10		077 S	091 S	097 R	125 R	140 R	142 R	130	123 S	131 S	130	091	071	071	091	095	100	090	088	106 F	086 F	070 S	075	092	10
	11	080	093	116					137	146 S	133 S	122	120	110	081	074	075	076	075	066			051	073	072	11
	MED	072	082	091	101	118	124	125	129	138	135	130	105	089	083	083	077	080	079	076	068	060	051	065	075	MED
	CNT	28	27	29	28	24	25	30	28	27	28	30	31	30	29	26	23	28	28	28	25	24	26	30	27	CNT
	1	090 V	095	092	078	065	057	053	070	069 H	U A 063	I A 056	059 B	064 U R	069	074	081	094	097	084	076 J S	071	072	063 J S	060 U S	1
MAUI, U.S.A. HI	2	060 U S	056 U S	053	048	049 J G	048	055	068	060	062	064		086	100	105	118	121	116	113	103 U S	093 J S	092 D R	106 J S	102	2
20.8N	3	090	090	086	092	090	077	045	059	060	074 U F	070	074	087 V	094 D W	105 E G	118 E G	123	117	114	110	138	170 V	151 U N	112	3
156.5W	4	095	096 V	093	084	080	075	066	068	081	084	079	072	077 U W	068	046	044	073	044	049	051	066 J S	051 U R	045 U S	063 U S	4
Geomag. Lat.	5	043 U S	031 J S	029	032	039	038	045	060	067	071	059 V	066	069 V	104 J S	088	089	082	088	089	097	130	124	097	090	5
20.8N	6	107	082	075	065	054	040	039	069	068	064 V	070	088	084	088	106 J S	116	098	087	075	077	076	081	070	062	6
150.0W LMT	7	061	059 U F	054 U F	047 U F	047 U F	047 V	050	056	058	062	064	070 U W	075	080	089	098	098	076	068	064	066 J S	060 F	057 F	055 U S	7
	8	053 U S	057 U S	054 U F	052 U F	047	040 F	041 U F	058	062	061	063	072 V	084 V	098 U F	111	123	129	116	118	115	105			097 V	8
	9	095 V	083 U F	058	059 U F			039	058	079	081	081	094	108	102	100	100	098	093 J S	098	090 U S	077	077	068	058	9
	10	055 F	049 U F	044 U F	042 U F	040 U F	039 U F	047	065	063 V	063	067	082	094	104	111	118	127	119	120	080	061	060	056	051	10
	11	048	045 U N	040 S	045	044	042	047	059	052	057	065	077	085	083	095	106	101	100	101	102	090	079	065	058	11
	MED	069	066	058	055	046	040	045	065	068	072	079	088	094	103	107	118	127	130	120	105	090	080	072	071	MED
	CNT	31	31	31	31	30	30	31	31	31	31	31	30	31	31	31	31	31	31	31	31	31	29	29	29	CNT
		00	01	02	03	04	05	06	07	08	09	10	11	12	13	14	15	16	17	18	19	20	21	22	23	

Hourly foF2 August 1-11, 1972, with median and count
Stations in order of latitude north to south
LONGITUDE 120.0E--210.0E

Station Latitude Longitude		LOCAL TIME																						
		00	01	02	03	04	05	06	07	08	09	10	11	12	13	14	15	16	17	18	19	20	21	22	23	
	1	J X 073	N 062	060	F	D F 055	D F 042	064	066	076	C	C	D R 087	D S 085 B D R	090	102	109	112	U S D S 113	112	111	115	D S 085	083	079	1
MANILA, Philippine Is.	2	074 U S	072	068	071	072	031	054 U S	074	088	094	100	104		106	126	134 D S	130	U S 117	110	110	D S 102	U S 096	100	D S 107	2
14.7N	3	091 D S	078 D S	084	077 D S	066 J S	059 F	075	079	085	085	093	100 H	107 U R	107	108	110 I B	110	113	113	095 J S	090			100	3
121.1E	4	100	090	085	090	078		060	071	078	085	089 G	089 J W	090	085	090	107	110	098 U R	101 U R	099 U S	092 U S	083	083	079	4
Geomag. Lat.	5	064 J S	056 J S	050	046	042	042 D S	055	074	066	121	064	075	097	094	102	098	146 U S	133 D S	095 D S	096 D S	085 D R	082 D S	084 U S	070 U R	5
3.3N	6	065 U S	072	075	072	037	022	052	083	087	085	091	095 U R	095 D R	100	113	114	115	120	116 U R	108	104	116	117	087	6
120.0E LMT	7	094 D S	090	091 J S	073 U N	058 N	049 N	060 V	075 J S	088	097	102 U S	102	090	097	108 C	114 C	114	125	112	110 D S	107 D S	105 F	078 D S	062 D S	7
	8	048 D F	048	045	040	041	037	056	072	085	088	087	086	090	100	I C		108	112	113	108 C	096 C	J S	085 D S	090	8
	9	090	106	064 A	046	037 N	037	058	067	076	086	096	097 D R	102 C	110 C	122 D S	131 U S	133 D S	130 D S	125 C	C		101 F	064 F	051 D S	9
	10	054 F	034 U F	F	033 F	035	025	057	077	088	098 U S	100	099 C	C		115	123	127	132	C	C	094		090	10	
	11		070			064	068	078	079	084	083	076			079	085	092	107	124			081	068	063	061	11	
	MED	090	082	076	066	054	043	060	076	087	094	094	097	098	102	108	110	114	114	110	108	103	099	093	090	MED
	CNT	029	029	028	029	031	027	031	031	030	027	026	026	022	026	028	030	028	031	028	018	017	021	021	028	CNT
	1	075	072	063	053 F	051	051	043	058	071	083	103	J R 111	130 J R	119	138 B	137 J R	123 J R	115	105	S 107	U S 093	S 090	067	066	1
VANIMO, NEW GUINEA	2	053	033	031 F	029 F	035 U F	038 F	033 F	059	083	095	094	100	111	099		115	111	094	091	090	087	080	059 U S	049 R	2
2.7S	3	043	037	030	027	033	029	030	064	085	103	098	094	087	095 R	095 D R	112 D R	123 U R	131 U R	130	139	138 R	132 U R	123 U S		3
141.3E	4	054 U F	037 U F	031	033 F	033 F	028	023	061	093 R	117	120	124	128		110	112	123	123	118	119	108	090 U S	088	050	4
Geomag. Lat.	5	050 J S	059 R	052 R	R	R	056 R	057 F	080 F	097	103	073	077	096	094	123 U R	108 U R	134	080	048	140	080	064	086 S	087 U S	5
12.6S	6	103 U S							053	123	145	137 J R	106	123	134	135	139	141	148	139	124 S	125 D R	128 D R	094 S	096 S	6
150.0E	7	100	072	050	046 F	044 F	039 F	034	073	083	105	113	118	133 U R	135 R	132 U R	140 R	140 U R	128 U R	118	111	115 U S	115 R	085 U R	066 D R	7
	8	062 R	058 R	034 F	026 F	028 U F	025	019	056	092 R	120 C	128	118 J R	123	126	128	123	123	117	122	124	128 R	131 D R	125 D R	140 R	8
	9	123 R	A	A	U F	032 A	029 F	021 F	055 F	091	C	119	114	119	133	125	118	119	122 R	133 R	126		125	075	R D R	9
	10	U R	U R		039	F	F	C	065 C	094 C	C	111 R	125 U R	139 D R	133 D R	133 U R	126	122	115	109	117 S	130	127 S	126	110	10
	11	109	097	068	045	030	026						118	120	120	128	135	126	123	124	119	110		085 U	075	11	
	MED	094	078	060	050	042	038	033	062	092	114	120	118	126	124	127	125	126	124	124	125	128	132	123	104	MED
	CNT	025	024	026	025	026	026	025	028	025	028	030	031	030	030	030	031	030	030	029	029	029	029	028	028	CNT
	1	U F 038 F	039 U F	037 F	038 F	038 F	034	030 J S	054	080	087	084 J R	075	075 R	090	091 R	078 J R	082	089 J R	074	057	041	042	F	037 F	1
TOWNSVILLE, Australia	2	J R	045		U F	F	036 F	033 F	057	074	092	104	081		087		084	077	072 J R	068	060	050 J R	052 F	F	049 F	2
19.3S	3	038 F	042 F	041 F	037 F	F	037 F	038 F	068 J S	088	091	074 U R	081	084	085	084	087	074	079 U R	062 J R	050 D R	049 J R	F	F	F	3
146.7E	4	F	F	F	F	A	A	A	060	080	094	103 R	089 J R	084 J R	091	087	084 J R	096 H	108 H	090	070	052		053		4
Geomag. Lat.	5		054 J S						057 J S	082	073 R		072	073	062	060	071	060 C	042	043	045	036 J R	028 J S	024	027	5
28.4S	6	026	030	027 A	024 U R	026 J A		021 J S	062	075	103 H	088 D R	075 J R	076	079	087	105		096	086 J R	084	041	032 F	033	034	6
150.0E LMT	7	034	038 F	F	027 F	031 F	031 F	034	071	081	085	080	084	085	078	083	089	097	088 J R	069	065	047 F	038 U F	032 J S	034 J S	7
	8	034 J R	037	J R	037	029	027	030	058	072 J S	089	099	099	090	084 J R	076	078	080	078	063	047 D R	J S	045 F	046	033 F	8
	9	032 F	032 J S	034 D R	034	031	032 F	032	055	074	092	093	088	075	072	075 J R	076 J R	084	088 J R	090	065	062	A	F		9
	10	F	097	020	026	030	030	037	075	088 J S	087	091 D R	099 D R	080	075	083	078 C	075	071	063 J R	056	045 J R	F	F	044 F	10
	11	047 F	038 F	039 F	029 F	027 F	027 F	030	054	078	093	103	113	097	077	070		093	090	072	047	042		F	F	11	
	MED	044	040	040	037	033	034	035	062	080	089	095	094	084	080	083	081	080	080	072	061	052	049	049	050	MED
	CNT	018	023	020	020	020	025	027	031	031	031	030	030	028	029	027	030	029	030	031	031	029	023	016	019	CNT
		00	01	02	03	04	05	06	07	08	09	10	11	12	13	14	15	16	17	18	19	20	21	22	23	

Hourly foF2 August 1-11, 1972, with median and count
Stations in order of latitude north to south

LONGITUDE 120.0E--210.0E

Station Latitude Longitude		LOCAL TIME																						
		00	01	02	03	04	05	06	07	08	09	10	11	12	13	14	15	16	17	18	19	20	21	22	23	
					F	N	N					N	H												
	1	056	055	053	038	034	035	048	078	081	088	080	072	085	084	083	076	082	091	092	058	053	052	045	042	1
										H			B						S	J S		H				
RAROTONGA, Cook I.	2	044	042	039	036	027	025	038	066	080	092	095		093	099	091	089	090		110	097	068	057	059	052	2
		F		N	N	F											H				J S	S		S		
21.2S	3	047	056	070	062	030	024	038	074	081	083	092	081	086	104	094	082	084	090	085	136		127		077	3
					F	S	F	F		H									J S							
159.8W	4	083	075	058				046	072	084	082	084	089	103	079	094	108	080	104	074	073	059	062	094	073	4
			H				N						J R						J R	R	R	R	R	R	R	
Geomag. Lat.	5	024	034	036	056	045	040	044	092	082	067	081	118	122	104	080	094	102	109							5
		S		F	F	N	F																			
20.9S	6		084	057	043	032	031	047	085	105	092	090	083	078	082	083	085	087	070	054	061	070	067	044	039	6
																									F	
165.0W LMT	7	040	034	030	028	029	023	042	073	096	095	084	086	087	087	076	070	074	078	068	058	052	052	047		7
		F	F	F	F	F	F	F									J S					F	F	F	F	
	8		032	033	027	030	026	036	067	085	093	085	077	095	106	101	103	095	090	090	094					8
		F	F	F	F	F	F																		U F	
	9						042	034	080	112	119	099	097	108	080	071	079	079	087	064	056	050	047	044	043	9
				F			F											J R					N	F	N	
	10	045	045	043	042	037	032	044	069	073	092	099	105	098	101	110	113	103	076	053	052	040	038	036	038	10
		F	F	F	U F								J R						J S			H				
	11	035	034	037	028	029	029	036	077	085	097	090	071	071	082	080	083	090	098	090	069	058	048	045	043	11
	MED	047	044	044	037	033	031	044	080	091	093	095	090	094	092	090	091	090	090	087	069	058	057	052	050	MED
	CNT	025	026	027	027	028	027	030	031	029	031	030	029	030	031	030	030	028	026	027	023	020	024	023	022	CNT
		U F	U F	F	U F	U F	F	F		F				H						S	U F	U F	U F	U F	U F	
	1	044	045	044	051	049	040	041	065	089	080	066	093	072	074	086	086	092	080	069	052	045	046	047	045	1
		F	F	F	U F	F	F	F						H						F	F	F	F	U F	U F	
BRISBANE, Australia	2	048	050	050	049	045	043	039	065	079	070	077	079	079	089	085	079	075	072	063	054	051	052	048	053	2
		U F	U F	F	F	F	F	F			V		H									F	U F	F	U F	
27.5S	3	048	046	049	049	047	047	048	066	075	078	077	079	083	078	081	076	078	068	052	044	046	044	045	048	3
		F	F	F	F	F	F	F									H		S	S		S		F	F	
152.9E	4	049	050	051		047	034	036	064	069	078	083	078	082	083	084	080	092	116	086	063	053	053	050	055	4
		U F	F	U F	F	F	F	F		F		E G	D W	H	E G	E G	H	E G	A					U F	A	
Geomag. Lat.	5	061		064	062	024	025	034	065	067	090	044	046	043	041	038	040	033		035	033	037	027	020		5
			I A	A	U F	I B	F		H															F		
35.7S	6	022	024		022	016	020	031	048	073	072	084	074	066	081	075	077	083	075	070	069	046	039	036	036	6
			F	F	F	U F	F	F	S		V	V	F			F					S	F	F	U F	U F	
150.0E LMT	7	039	036	033	030	037	024	032	061	080	088	083	076	075	077	089	078	072	072	063	052	038	036	037	040	7
		U F	U F		F	F	F	U F	S					V		H					F	F	F	F	F	
	8	031	038	032	028	023	022	028	058	073	085	083	082	074	075	079	073	065	066	054	039	042	038	036	036	8
		F	U F	U F	F	F	U F	U F														U F	F	F	F	
	9	036	038	035	036	032	027	029	056	069	083	081	082	070	081	080	082	080	079	069	063	057		048	046	9
		F	F	F	F	F	F	F			V					S							S		F	
	10	055	055	031	031	032	032	035	071	078	075	088	074	071	073	068	066	068	060	049	041	038	039	037	040	10
		F	U S	F	F	U F	F	F														F	F	U F	U F	
	11	040	041	042	038	029	026	033	056	066	076	089	090	075	080	080	077	076	068	061	047	041	038	041	039	11
		F	F	F	F	F	F	F															F	F	F	
	MED	048	044	044	044	040	036	040	065	073	078	083	085	077	081	082	076	075	072	063	057	052	051	048	048	MED
	CNT	028	028	028	026	029	028	030	031	030	030	030	031	031	031	031	031	031	030	031	031	030	028	030	028	CNT
		U F	F	F	F	F	F	F	F			C	C							U S			F	S	F	
	1	050					052	045	050	067	070			077	081	067	067	069	083	082	065	053	050		050	1
		F	F	F	F	F	F	F	F																	
NORFOLK I. S. Pacific	2	053	048			046	044	042	035	058	070	078	081	073	089	087	074	075	086	077	065	053	047	048	050	2
		U R	F					F																	F	
29.0S	3	050	053	051	050	047	044	032	033	061	076	075	076	079	080	078	078	076	078	078	065	042	042	039		3
		U F	F	F		F	F	F	F												R		A		F	
168.0E	4	042	044	043	046	049	040	034	032	055	070	076	087	080	078	086	081	069	073	081		075		058	053	4
		U R	U R		U R									R									F	F	A	
Geomag. Lat.	5	053	053	058	050	047	045	033	032	063	078	079	084		060	052	049	044	048	035	032	041	050	048		5
		A					F	F																		
34.7S	6		020	020	024	023	018	020	031	058	059	066	076	081	079	067	076	081	090	082	069	060	060	056	051	6
					F												A									
180.0E LMT	7	046	050	046	042	040	036	029	021	067	070	071	079	073	074	077		068	072	073	053	047	040	028	028	7
		F	F	F		A	A																	F	F	
	8	028	029	029	032			023	030	060	075	066	079	077	079	083	073	069	073	061	058	047	042	033	038	8
		F	F	F	F	F	F																	U S	U S	
	9	038	036	038	036	037	036	027	028	060	068	074	077	080	081	075	078	076	073	070	063	053	053	052	053	9
			U S		U S		C	C	C	C																
	10	048	043	050	055	031					078	079	075	073	070	072	066	069	069	065	054	041	041	038	040	10
				F	F	F	F								U S								F	U F	U F	
	11	038	040	038	038	041	030	027	032	056	063	077	081	074	081	082	081	079	071	066	058	044	040	040	038	11
			F				F																			
	MED	048	046	045	045	043	040	035	038	064	074	076	080	080	079	083	079	073	071	071	063	053	050	050	050	MED
	CNT	030	030	029	029	029	028	029	030	030	031	030	030	030	031	031	030	031	031	031	030	031	029	030	029	CNT
		00	01	02	03	04	05	06	07	08	09	10	11	12	13	14	15	16	17	18	19	20	21	22	23	

Hourly foF2 August 1-11, 1972, with median and count
Stations in order of latitude north to south

LONGITUDE 120.0E--210.0E

Station Latitude Longitude		LOCAL TIME																							
		00	01	02	03	04	05	06	07	08	09	10	11	12	13	14	15	16	17	18	19	20	21	22	23
KERMADEC I, S. Pacific	1	S	F 039	S	S	S	S	S	S	061	062	055	071	069	061	059	053	060	062	S	048	S	039	038	S
	2	S	S	S	S	S	S	029 S	S	049 C	C	C	C	C	C	C	C	C	C	S	S	S	S	S	S
29.2S	3	S	S	S	S	S	S	S	S	C	C	C	C	C	C	C	C	C	C	C	C	C	029	S	S
177.9W	4	028	A	S	S	S	022	023	048	060	062	070	077	076	068	060	071	061	S	A	060	S	042	045	S
Geomag. Lat.	5	040	S	042	S	S	S	S	S	057	080	S	A	A	S	A	A	A	S	A	A	S	A	S	C
32.3S	6	S	S	S	S	S	S	S	S	S	060	070	071	081	S	060	062	080	092	070	057	050	S	S	S
180.0W LMT	7	S	S	S	S	S	S	C	C	C	C	070	071	A	077	060	063	058	068	055	S	049	S	S	S
	8	F 028	F 028	029	029	021	020	020	S	059	080	070	C	C	C	C	050	060	060	048	041	039	S	S	S
	9	S	S	S	S	S	C	C	S	S	050	065	068	070	080	065	060	S	070	045	S	048	S	S	S
	10	034	S	S	S	S	018	017	041	058	069	062	C	C	C	C	C	C	C	C	C	C	C	032	032
	11	030	032	033	A	029	A	A	040	051	058	075	C	C	077	075	C	C	C	C	032	029	030	A	026
	MED	034	040		030		020	028	048	060	072	070	070	070	077	072	064	060	062	055	043	040	039	038	
	CNT	007	006	004	006	004	005	009	005	021	024	021	022	022	023	025	022	018	019	018	017	017	007	005	003
SALISBURY, Australia	1	F 030 U F	030	030	033	F 036 F	F 029 F	F 030 F	S 055 J S	070	074	F 079	083	085	H R	R U R 091 R	096 R	090	075	F 056	F 047	F 043	F 040	F 040	F 040
	2	043	049	051	050	048	041	039	062	070	080	077	089	088		078	087	078	070	058	057	045	042	039	037
34.7S	3	F 037	F 036	F 038	F 038	F 037	S 035	F 038	R 061	070	071	080	V 080	093	078	082	S 078	J C 074	063	056	048	F 040	F 038	F 041	F 040
138.6E	4	F 039	F 039	F 040	F 041	S 043	F 031	F 030	056	065	070	078	088	084	074	092	086	R	R	084	R	F 041	F 040	F 042	F 044
Geomag. Lat.	5	F	041 A	042 A	040 F	F	U F B	F	V	F 053	035	038	040	040	038	U R 040	R	030	029	F 026	S 029	J B 019	J B 018	A	A
44.6S	6	019	F	F	024	F 023	F	020	038	F 054	064	075	F 070	077	085	088	084	082	076	F 062	049	F 037	F 033	F 030	F 024
135.0E LMT	7	F 023	F 023	F 021	F 020	F	F 022	F 031	059	H 069	075	080	081	080	080	075	084	084	081	060	047	F 038	F 031	F	F
	8	F 028	F 026	F 023	F 022	F 020	F 019	F 021	055	075	074	F 075	F 076	083	082	082	F 070	U F 068	068	F 046	F 044	F 040	F 028	F 025	F 026
	9	F 027	F 027	F 027	F 029	F 029	F 020	F 024	F 052	F 061	H 070	F 072	072	086	089	082	086	090	080	074	F 059	S 061	F 050	F U F 050	051
	10	F 038	F 036	F 025	F 022	F 024	F 020	F 025	F 047	F 056	F 058	070	075	070	078	072	068	066	057	F 048	F 041	F 040	F 039	F 037	F 032
	11	F 031	F 033	F 034	F 031	F 026	F 022	F U F 024	052	F 068	F 070	082	083	081	089	079	084	070	S 065	U S 054	051	043	040	F 036	F 036
	MED	F 036	F 036	F 038	F 038	F 038	F 032	F 031	057	069	072	076	080	081	081	080	082	076	070	058	050	F 047	F 043	F 040	F 039
	CNT	029	029	030	031	030	028	031	030	031	030	030	030	031	029	031	030	030	030	031	029	031	031	029	029
CANBERRA, AUSTRALIA	1	F 042 F	F 036 F	F 037 F	F 038 F	F 037	F 031	F 031 F	F 047	062	070	075 S U R	089	088	080 C	078 C	098	090	080	061	049	042	040	039	040
	2	040	040	042	041	040	039	035	055	075	062	080	086	078			083	079	076	065	061	053	047	044	045
35.3S	3	044	042	045	046	050	044	043	054	070	072	074	081	074	085	084	076	073	072	055	054	039	038	F 039	F 041
149.0E	4	043	043	044	045	046	032	024	044	063 R	074	077 E G	074 E G	091 E G	091 E G	072 E G	087 E G	084 A	106	089	070	057	040	047 A	054 A
Geomag. Lat.	5	039	045	042	044 B	035	027 J S	025 B	049	055	068	035	038	039	038	037	036		031	029	029	031 F	027 F	F	
43.9S	6	020	020 F	019		015	015 F	F	035 F	045	057	063	066	070	065	070	073 C	071	070	072	052	040 A	036	030 A	031 F
150.0 E LMT	7	028	027	027 F	022 F	018 U F	018 F	F U F	045	070	065	075	073	078	079	078		073	069	065	053		030		026
	8	029	030	030	029	025	020	020	044	065	072	076	076	081	078	080	070	065	067	055	048	039	032	030	027
	9	028	029 F	029 F	030	029	022	020 F	044	061	064	069	070	074	082	090	084	081	076	066	065	055	053	044 F	041 F
	10	042 A	040 F	032 F	030 F	024	021	021 F	038	048	054	056	060	059	065	060	060	056	054	045	037	032	031	030	031
	11		034	030	035	030	024	022	045	057	073	070	069	075	081	086	074	067	063	057	050	048	039	039	036
	MED	040	040	038	039	037	035	034	050	063	068	073	076	078	081	080	078	074	070	062	054	051	045	042	041
	CNT	030	031	029	029	031	029	028	030	031	031	029	030	030	027	026	029	030	031	031	031	030	031	028	029
		00	01	02	03	04	05	06	07	08	09	10	11	12	13	14	15	16	17	18	19	20	21	22	23

Hourly foF2 August 1-11, 1972, with median and count
Stations in order of latitude north to south

LONGITUDE 120.0E--210.0E

Station Latitude Longitude		LOCAL TIME																						
		00	01	02	03	04	05	06	07	08	09	10	11	12	13	14	15	16	17	18	19	20	21	22	23	
	1	F	F	F 040	F	F F	F	F	F	062	063 H	R	071	082	R	J N 068	N 068	080	071	068	056	055 F	052 F	N 052	049	1
AUCKLAND, New Zealand	2	044	043	047	046	046	043	039	035	057	072	071	073	082	083	073	073	077	075	067	053	049	042	042	043	2
37.0S	3	044	044	F	F 044	038	F 025	024	055	065	C	073	080	079	080	076	078	073	068	059	052	045	042	J S 038	039	3
175.0E	4	040	040	F 041	F 040	041	034	F 028	037	060	066	072	075	083	082	081	073	072	067	068	080	062	054	052	042	4
Geomag. Lat.	5	040	039	038	033	031	027	A	034	N 053	063	065	090	E G 043	043	A	A	C	C	C	C	C	C	C	C	5
41.2S	6	C	C	C	C	C	C	C	C	C	C	C	C	C	C	C	C	C	C	C	C	C	C	C	C	6
180.0E LMT	7	C	C	C	C	C	C	C	C	C	C	F 060	066	074	074	071	064	071	067	054	042 F	041 F	038	031 F	029 F	7
	8	030 F	030 F	N 030 F	F 032 F	F U F 027 F	021 F	F F	F 034 F	056	062	072	072	077	070 R	075 H	072	070	064	062	049	048	044	037 U N	038	8
	9	037	036		038 N	037			037	058	063	072	073	079		079	075	078	070	060	052	053	052	050	039 N	9
	10	036 F	035 F	039 F	036	025	021	020	031	050	054	058	058	062	064	064	068	064	059	051	044	042	038	036 A	036	10
	11	037	034	036	034	033	030	024	035	054	062	069	070	075	071	074	071	070	067	060	042	042	040		034	11
	MED	042	042	042	043	041	034	032	044	061	064	069	072	075	077	076	073	071	068	060	053	052	050	050	042	MED
	CNT	019	022	022	023	024	024	020	025	027	026	027	029	028	026	027	028	028	028	028	027	027	024	024	024	CNT
		U F	U F	U F	U F	U F	U F	U F	U F	U F	U C	U C	U C					U C				U F	U F	U F	U F	
	1	025 U F	023 U F	021 U F	020 U F	022 U F	021 U F	019 U F	028 U F	055 U F	065	075	082	077	078	088	090 F	090 F	082 F	067 U F	052 U F	042	038	040	038 U F	1
HOBART, TASMANIA	2	040 U F	038 U F	035 U F	035 U F	034	033 U F	028 U F	033	053	063	080	080	083	085	082	080	080	070	063	060	052 U F	047	039	035 U F	2
42.9S	3	031 U F	032 U F	033 U F	033 U F	034 U F	033 U F	033 U F	039 U F	056	065	074	074	082	078	080	072	077	064 U F	060 U F	053 U F	038 U F	034 U F	033 U F	031 F	3
147.2E	4	030 U F	025 U F	025 U F	024 U F	026 U S	027 A	022 B	029 U F	057 B	064 U F	073 U F	072 U F	082 U F	083 U F	076	081	078 F	085 U F	070 U F	030 B	023 B	025 U F	025 A	F	4
Geomag. Lat.	5	022 U F	016 U F	015 F	015 A	014 U F	U F	U F	022 U F		032	034	036	037	035	036	033		024 U F	020 U F	U F	U F	028 U F	U F	U F	5
51.7S	6	016 F	018 F	F	016 U F	019 U F	025 U F	017 U F	025 U F	034 U F	040	046 U F	054	051	057	060	067	072	069	057 U F	031 U F	025 U F	027 U F	028 U F	020 U F	6
150.0E LMT	7	F	F	U F	022 U F	020 U F	021 U F	020	031 U F	055	065	068	070	071	080	077	075	071	067	061	047	031	026	020	017	7
	8		014 U F	014 U F	014 U F	014 U F	014 U F	015 U S	029 U F	055	060	067	067	073	084	077	074	074	066	053	053 U F	038 U F	028 U F	024 U F	022 U F	8
	9	021 U F	021 U F	018 U F	019 U F	019 U F	017 U F	016 U F	030 U F	054	060	069	069	077	093	090	081	083	072	067 U F	055 U F	040 U F	033 U F	031 U F	038 U F	9
	10	040 U F	033 U F	030 U F	024 U F	020 U F	018 U F	017 A	027 U F	041 U F	043	047 U F	046	051	052	052	052	054	050	042	036	031 U F	027 U F	022 U F	018 U F	10
	11	017 U F	015 U F	015 U F	025 U F	016 U F	015 U F	U F	030 U F	052	060	064	074	082	083	079	076	074	073	059	052	040 U F	035 U F	029 U F	028 U F	11
	MED	028	026	025	022	022	022	022	034	055	060	067	072	075	078	077	076	074	070	062	054	047	038	033	030	MED
	CNT	029	028	028	030	031	030	029	030	030	031	030	031	031	031	031	031	030	031	031	030	030	030	030	028	CNT
	1	F	F	F	F	F	U F	F	F F	052	063	070	075	076	070	068	083	078	071	061	057	056 F	052 F	F 048 F	F 046 F	1
CHRISTCHURCH, New Zealand	2	N 042	041	041	041	039	038	032	F 027	045	058	068	081	074	075	073	080	080	069	067	054	049	046	039	036	2
43.6S	3	035 F	036 U F	F 036 U F	F 040 U F	040 F	F 030 U F	F U F 019 F	U F 021 F	F 047 F	062	064	080	U N 076	076	074	077 N	074	061	058	050 N	U F 046 N	U F 039 N	F 038 A	U F 038 N	3
172.8E	4		039	039	039	037	031	023 J R	H	048	062	066 N	080 H	081 E G	083 E G	081 E G	078 E G	068	062	053	073 U N	U F	U F	F	026 F	4
Geomag. Lat.	5	024 A	027 A	024 A	022 J S	019 A	017 F	016 U F	023 U F	042 F	053	056	071	036	036	034	033	036	037	034 N	032 N	033 U F	026 U F	U F	F	5
48.0S	6	U F	F	F	017 F	F	J S	018 B	018 F	033 F	043	051	059	067	065 H	071	072	077	069	055 U F	059 F	056 F	052 F	040 F	F	6
180.0E LMT	7	031	F	F	018 F	017 F	015 F	F	F U F	036 F	043	047	053 N	064	063 N	062	069	073	060	046	030		030	025 F	023 U F	7
	8	023 F	U F	F	F	F	F	F	U F	047	055	069	069 H	072	069 H	067 H	072	069	063	060	052	049 N	040 N	034 F	033 F	8
	9	032 F	033 F	031 F	031 F	F	021 U F	021 U F	029 U F	051	063	067	069	074	071	079	088	080	063	061	056	049	048 F	032 F	F	9
	10	F	F U F		F	F	021 F	018 F	022 F	039 N	051	053	052	056	057	059 H	061	059	052	047	043	037	031	030	026 F	10
	11	025 F	023 F	021 F	017 F	017 F	F	F	024 F	047	056	063	063	071	070	070	068	069	063	052	053	044	035 F	033 F	032 F	11
	MED	037	036	036	035	036	030	027	029	050	061	063	066	072	071	073	072	072	063	058	055	049	043	040	039	MED
	CNT	019	016	018	020	018	018	018	022	027	027	027	027	028	027	028	027	027	027	027	026	022	025	020	017	CNT
		00	01	02	03	04	05	06	07	08	09	10	11	12	13	14	15	16	17	18	19	20	21	22	23	

Hourly foF2 August 1-11, 1972, with median and count
Stations in order of latitude north to south

LONGITUDE 120.0E--210.0E

CAMPBELL I.

New Zealand
52.5S
169.2E
Geomag. Lat.
57.2S
165.0E LMT

	00	01	02	03	04	05	06	07	08	09	10	11	12	13	14	15	16	17	18	19	20	21	22	23	
	U F	U F	U F	U F	U F	U F	U F	U F	U F	U S	U S	U S	U F	U S	U F	U S	U S	U S	U S	S	U F	U F	S	U S	
1	029	028	025	024	024	023	022	019	032	056	070	070	072	072	070	082	083	066	054		052	048		048	1
	U S	U S	U F	U F	U F	U R	U S	U S	U F	U F			U F				U S	U F	U F	U F	U F	U F	U F	U F	
2	047	043	037	036	034	017	016	017	028	044	058	068	064	076	076	068	072	067	062	053	049	042	035	031	2
	U F	U F	U F	U F	U F	U F	U F	U F	U F	U S	U F	U F	U F		U F	U R	U F	U F	U F	U F	U F	U F	U F	U F	
3	024	022	020	019	019	018	017	017	031	052	058	066	072	074	076	072	066	066	056	052	042	038	035	033	3
	U F	U F	U F	U F	U F	U F	U F	U F	U F	U F	U F	U F	U F				U F	B	B	B	B	B	B	B	
4	030	026	023	022	022	020	018	018	032	053	062	066	070	076	076	075	054								4
	B	B	B	B	B	B	B	B	B	B	B	B	B	B	B	B	B	B	B	B	B	B	B	B	
5																									5
	B	B	B	B	B	B	B	B	B	U R	B	U R		U R	U R	B	B	B	B	B	B	B	B	A	
6										037		049	054	058	076										6
	A	B	B	B	B	B	B	B		U R	U R	U R	U R	U R	U R	U F	U F	U F	U F	U F	F	U F	U F	U F	
7									026	037	042	047	048	050	055	064	048	038	023	026		033	031	023	7
	U F	U F	U F	U F	U F	U R	U F	U R	U F				U R	U R	U R							U S	U F	U F	
8	028	023	024	024	023	021	020	017	031	047	052	058	063	065	064	065	066	068	054	054	045	041	036	031	8
	U F		U F		U F	U F	U F	U R	U F	U F					U F	U F	U R	B	B	B	B	B	B	B	
9	027	025	023	021	019	020	021	020	036	049	057	064	068	072	084	080	070								9
	B	B	B	F	B	B	B	B	U F	U F	U F	U F	U R	U F	U F			U F	U F	U F	U F	U F	U F	U F	
10									030	048	051	052	052	053	054	054	054	052	046	041	029	026	019	031	10
	U R	F	A	B	U F	U F	U F	U F	U F		U R		U R	U F	U F	U F	U F	U S	S	U F	U F	U F	U F	U F	
11	030				025	025	021	019	034	048	053	062	062	064	070	064	064	060		047	036	020	031	030	11
	U F	U F	U F	U F	U F	U F	U F	U F	U F	U	U	U F	U	U	U	U	U S	U S	U F	U F	U F	U F	U F	U F	
MED	030	028	025	023	024	023	021	020	036	050	058	064	066	068	070	069	070	066	060	054	047	040	036	032	MED
CNT	022	021	021	022	023	021	024	023	027	029	028	028	028	028	028	027	027	023	022	022	022	022	021	022	CNT

SCOTT BASE, Antarctica

77.9S
166.8E
Geomag. Lat.
79.0S
165.0E LMT

	00	01	02	03	04	05	06	07	08	09	10	11	12	13	14	15	16	17	18	19	20	21	22	23	
	U F		F	F	F	F	U F	U F	F	F	U F	F	U F	U F	R	U F	U F	A	F	F	F	F	B	A	
1	045						060	050			050		072	060		090	098								1
	U F	R	A	F	F	F	A	F	C	C	F	U F	F	U F	U F	U F	F	U F	U F	U F	F	U F	U F	F	
2	025											059		056	052	060		062	065	060		050	036		2
	B	F	F	U F	F	F	F	F	C	F	F	R	U F	F	U F	F	U F	U F	F	U F	U F	U F	F	F	
3				040									048		060		070	066		072	063	052			3
	F	F	B	B	B	F	R	F	R	R	R	F	F	F	B	B	B	B	B	B	B	B	B	B	
4																									4
	B	B	B	B	B	B	B	B	B	B	B	B	B	B	B	B	B	B	B	B	B	B	B	B	
5																									5
	B	B	B	B	B	B	B	B	B	B	B	B	B	B	B	B	B	B	B	B	B	B	B	B	
6																									6
	B	B	B	B	B	B	B	B	R	R	B	B	B	B	B	F	R	R	F	F	F	B	B	B	
7																									7
	B	B	B	B	B	B	A	A	B	B	B	C	C	B	B	B	B	B	B	B	B	F	C	B	
8																									8
	B	B	B	B	B	B	B	B	B	B	B	B	B	B	B	B	B	B	B	B	B	B	B	B	
9																									9
	B	B	B	B	B	B	B	F	F	F	B	R	R	U F	R	F	R	F	U F	R	A	F	B	B	
10														055					061						10
	A	A	R	U F	F	F	F	B	C	U F	U F	C	C	C	C	C	C	C	C	C	C	C	C	C	
11				035						054	060														11
	U F	U F		U F				U F	U F	U F	U F	U F	U F	F	U	U F	U F	U F	U F	U F	U F	U F	U F	U F	
MED	042	033		030				054	060	066	062	060	070	064	063	066	070	066	065	072	070	052	053	050	MED
CNT	006	005	003	005	002	004	003	006	007	006	011	008	013	015	015	012	015	016	012	011	010	008	009	006	CNT

	00	01	02	03	04	05	06	07	08	09	10	11	12	13	14	15	16	17	18	19	20	21	22	23	

Hourly foF2 August 1-11, 1972, with median and count
Stations in order of latitude north to south

LONGITUDE 210.E--300.0E

Station Latitude Longitude		LOCAL TIME 00	01	02	03	04	05	06	07	08	09	10	11	12	13	14	15	16	17	18	19	20	21	22	23	
THULE, GREENLAND 77.5N 69.2W Geomag. Lat. 89.0N 75.0W LMT	1	065	064	F	053	F	F	F	F	F	F	R	F	F	R	R	R	R	F	F U F	050	054	055	050	052	1
	2	F	047	F	052	056	F	F	F	F	052	F	F	F	F	F	F	C	057	A	C	C	C	C	C	2
	3	C	C	C	C	C	C	C	C	C	C	C	B	B	B	B	B	B	B	B	B	B	B	B	B	3
	4	B	B	B	B	B	B	B	B	B	B	B	B	B	B	B	B	B	B	B	B	B	B	B	B	4
	5	B	B	B	B	B	B	B	B	B	B	B	B	B	B	B	B	B	B	B	B	B	B	B	B	5
	6	B	B	B	B	B	B	B	B	B	B	B	B	B	B	B	B	B	B	B	B	B	B	B	B	6
	7	B	B	B	B	B	B	B	B	B	B	B	B	B	B	B	B	B	B	B	B	B	B	B	B	7
	8	B	B	B	B	B	B	B	B	B	B	B	B	B	B	B	B	B	B	B	B	B	B	B	B	8
	9	B	B	B	B	B	B	B	B	B	B	B	B	B	B	B	B	B	B	B	B	B	B	B	B	9
	10	B	R	R	B	B	B	B	R	B	R	U R 050	F	R	R	R	R	U R 053	U R 055	F	U R 050	F	F	U R 048	F	10
	11	U R 048	F	F	R	F	045	053	F	R U R 049		R	R	R	R	R	R	R	F	052	R	F	F	F	050	11
	MED	055	052	F 050	051	054	049	047	052	050	052	U V 053	053	053	057	055	054	052	056	052	053	053	053	052	052	MED
	CNT	12	7	7	8	7	6	7	10	8	8	9	8	6	6	9	12	14	14	13	13	11	13	11	14	CNT
RESOLUTE BAY, Canada 74.7N 94.9W Geomag. Lat. 82.9N 90.0W LMT	1	068	048	F C	047	037	G 039	G 039	042	F	046	048	F	R	R	F 047	F 049	F 051	058	058	059	058	054	F 050	F	1
	2	F 056	F 052	F 057	F 057	F 052	058	F 059	060	050	051	050	F 056	057	058	061	062	061	F 058	F 062	059	061	061	059	058	2
	3	C	F 057	C	F 062	063	060	B	B	B	B	B	B	B	B	B	B	B	B	B	B	B	B	B	B	3
	4	B	B	B	B	B	B	B	B	B	B	B	B	B	B	B	B	B	B	B	B	B	B	B	B	4
	5	B	B D R 023	D R 021		B	D R 022	B	B	B	B D R 022	C		C	C	C	C	C	C	C	C	C	C	C	C	5
	6	C	C	C	C	C	C	C	C	C	C	C	C	C	C	C	C	C	C	C	C	C	C	C	C	6
	7	C	C	C	C	C	C	C	C	C	C	C	C	C	C	C	C	C	C	C	C	C	C	C	C	7
	8	C	C	C	C	C	C	C	C	C	C	C	C	C	C	C	C	C	B	B	B	B	B	B	B	8
	9	B	B	B	B	B	B	B	B	B	B	B	B	B	B	B	B	B	B	B	B	C	F	F		9
	10	044	047	041	040	043	F 050	044	054	D R 048	F 047	C	F 054		062	056	050	055	058	056	C	C	050	062	048	10
	11	049	D C 054	044	048	052	052	F 045	F 047	048	F 050	048	049	F	F	054	R	R	056	F 064	060	048	050	048	051	11
	MED	056	056	U 051	053	052	U 054	U 048	053	052	055	U 056	055	058	060	061	057	054	056	058	059	057	055	053	054	MED
	CNT	022	018	017	021	021	021	020	021	021	020	021	019	018	019	016	020	020	019	022	020	020	024	024	021	CNT
COLLEGE, U.S.A. AL 64.9N 147.8W Geomag. Lat. 64.6N 150.0W LMT	1		040 U S							054				055 B	056							052				1
	2		046 F							056 F						057						059 8				2
	3		045 B							055 B				061 B		061 B										3
	4		B							B				B		B						8				4
	5		B							B				B		B						8				5
	6		B							B				B		B						8				6
	7		045							B				B		B						8				7
	8		042 R							B				B		B						B				8
	9		B							B				B		B						044				9
	10		B							U R 048				B		B						045 B				10
	11									047				B		054										11
	MED		040							054				055		056						049				MED
	CNT		019							021				019		020						021				CNT
		00	01	02	03	04	05	06	07	08	09	10	11	12	13	14	15	16	17	18	19	20	21	22	23	

Hourly foF2 August 1-11, 1972, with median and count
Stations in order of latitude north to south

LONGITUDE 210.E--300.0E

Station Latitude Longitude		LOCAL TIME																							
		00	01	02	03	04	05	06	07	08	09	10	11	12	13	14	15	16	17	18	19	20	21	22	23	
		F	F	F	F	F	F	F	F	F	F	F	F	F					V	F	F	F	F	F	A	
	1	055	056		030	040	038	045	048	048	052	051	051	052	053	054	055	055	056	049	045	054	041	037		1
		F	F	F	U F	F	F	F	F				F											F	F	
CHURCHILL,CANADA	2	054	049	050	044	045	051	048	048	054	062	062	060	066	063	063	068	068	064	064	063	063	060	051	045	2
		F	F	F	F	A	F						F	F	F	F	F	F	F	F	F	B	B	A	C	
58.8N	3	043	053	045	049		045	051	052	055	059	059	061	057	062	062	063	068	066	066	070					3
		B	B	A	B	B	B	B	B	C	C	C	C	B	B	B	B	B	B	B	B	B	B	B	B	
94.2W	4																									4
Geomag. Lat.		B	B	A	A	B	B	B	B	B	B	B	B	B	B	B	B	B	B	B	B	B	A	B	A	
	5																									5
68.6N		F	F	A			B	B	B	B	B	B	B	B	B	B	B	B	B	B	B	B	B		F	
90.0W LMT	6	040	043		040	030																		049	053	6
		N	F	F	U F	F	B	B	B	B	B	B	B	B	B	B	B	B	B	C	B	B	S	F	F	
	7		046	054	035	042																	052	051	046	7
		F	F	F	F	B	B	B	B	B	B	B	B	B	B	B	B	B	B	B	B	B	B	B	F	
	8	044	036	035	032																				051	8
		B	B	F	F	S	B	B	B	B	B	B	B	B			F	F				F	F	F	F	
	9			043	035	038									054	057	049	045	043	043	041	040	038	044	042	9
		A	F	A	F	F		F	B	A	B	I B	I B	F	F		F	F	F	F	F	I A	F	F	F	
	10		043		039	030	035	036				050	054	055	059	061	068	060	058	060	058	055	052	050	048	10
		F	F	F	F	F	F	F	F	I B	F	F		F	F	F	F	F		F	F	I A	F	F	F	
	11	044	040	038	046	049	038	048	048	050	051	051	053	055	061	063	066	069	060	062	052	051	050	049	044	11
		F	F	F	F	F	F	F	F								F	F	F	F	F	F	F	F	F	
	MED	044	044	043	039	040	040	045	048	052	054	056	058	060	061	062	065	063	064	062	057	052	048	048	046	MED
	CNT	024	026	024	027	027	024	021	020	021	022	024	024	024	025	025	025	025	026	026	026	025	025	025	026	CNT
		A	A	S	D S	S	S	S	C				D R	C	C	C			S	S	D S	S	S	S	S	
	1			046	038	040	040	042		054	051	060	057				059	059	060	069	057	068	066			1
		S	S	C	S	S			C	C	C	C				C		C	C	C	S	D S	S	D S	C	
WINNIPEG,CANADA	2	033			033	029	038	046					057	066	069		069				067	068		058		2
		S	C	S	S	C		C		S	C	C		C	C	C	C	C	C	C	C	C	C	C	C	
49.8N	3				033		035		053	058			071													3
		C	C	C	B	B	B	B	B	B	B	B	B	B	B	B	B	B	B	B	B	B	B	B	B	
94.4W	4																									4
Geomag. Lat.		B	B	B	B	B	B	B	B	B	B	B	B	B	B	B	B	B	B	B	B	B	B	C	A	
59.8N	5																									5
		C	C	C	C	C	C	C	C	B	B	B	B	B	B	B	B	B	B	C	C	C	C	C	C	
90.0W LMT	6																									6
		C	C	C	C	C	B	B	C			B		C	B	B	B	B			C	C	C	C	C	
	7									048	053		056						055	056						7
			C	C				C			B				C		C	C	C	V		B	C	B	B	
	8	036			024	022	031		049	056		064	066	068		066				064	071					8
		B	B	B	B	B	B	B	B	B	B	B	B	B	B	B	C	C	C	C	C	C	C	S	C	
	9																							039		9
		C		C	C	C	C	B	B	C	B	B	C	C	C	C	C	C	C	C	C	C	C	C	C	
	10		024																							10
		C	C	C	C	S	C	C	C	C		C		C						D R	S	D S	S	S	S	
	11					033					047		053		055	055	053	060	066	070		057	058			11
		S	S	S	S	S						U	U								U S	U S	S	U S	S	
	MED	032	026	025	027	026	030	039	046	050	054	058	060	062	060	064	064	063	063	065	066	062	057	046	038	MED
	CNT	012	012	013	014	016	015	019	018	022	020	019	022	022	022	020	022	019	021	022	020	015	017	014	011	CNT
		S	D S	D S	S	S				D R											S	D S	S	D R	S	
	1		037	038	049	045	038	047	050	053	056	056	060	057	058	057	057	058	060	061	060	058	058	056		1
		S	S	S	S	S												B			D S	S	S	D S	S	
OTTAWA,CANADA	2	046	040	029	029	031	037	043	051	058	058	064	063	066	066	067	067		071	074	058	068	065	056	058	2
		D S	S		S	F	S				D R	D R										S	D S	S	B	
45.4N	3	047	051	047	042	039	043	056	059	065	051	053	066	067	065	065	066	064	067	064	067	068	057	053		3
		B	B	B	B	B	B	B	B	B	B	B	B	B	B	B	B	B	B	B	B	B	B	A	B	
75.9W	4																									4
Geomag. Lat.		B	B	A	A	B	B	B	B	B	B	B	B	B	B	B	B				S	S		A	A	
56.8N	5																	061	051	054	045	039	032			5
		A	A	B	B	B	B	B	B	B	B	B	B	B	B	B	B	C			S	D S	S	D S	S	
75.0W LMT	6																		064	059	058	037	037	030	038	6
		S	S	S		S		G	C				B	B	B	A	D R				S	S		S		
	7	042	040	043	037	038	040	044		048	052	053					051	054	058	058	059	062	057	048	046	7
					F																	D S	S	S	S	
	8	040	036	032	029	026	035	047	051	057	061	066	067	069	072	070	069	069	066	067	072	067	058	058	046	8
		B	S	B	B	S	B	B	B	G	G	D R	D R	D R	D R	D S			S	S	S	S	S	A	D S	
	9		037			048				038	039	048	050	049	049	042	051	056	058	056	054	044	041		029	9
			S	S	S	S				G			F							S	S	D S	S			
	10	028	025		027	018	029	040	044	044	052	056	056	059	058	058	063	062	070	078		057	058	045	036	10
		D S	D S		F	F			V											S	S	D S	D S	F	F	
	11	030	031	033	032	028	028	039	045	048	051	056	058	057	066	061	062	063	069	076	077	066	051	037	028	11
		S	S		S	U						U	U	U	U	U	U			S	S	U S	S	U S	U S	
	MED	039	037	034	032	030	032	043	047	055	056	057	062	062	064	063	066	063	067	066	066	066	057	050	046	MED
	CNT	023	024	026	022	021	025	027	025	027	028	025	024	025	024	023	026	027	029	029	023	023	025	021	023	CNT
		00	01	02	03	04	05	06	07	08	09	10	11	12	13	14	15	16	17	18	19	20	21	22	23	

Hourly foF2 August 1-11, 1972, with median and count
Stations in order of latitude north to south

LONGITUDE 210.E--300.0E

Station Latitude Longitude		LOCAL TIME 00	01	02	03	04	05	06	07	08	09	10	11	12	13	14	15	16	17	18	19	20	21	22	23	
	1	U R					U R		U G	U G J R	U G U R			U G U G		A	A	A U A U A								
		057	051	055	047	044	041	058	055	058	057	056	058	058	056			082	062	058		063	060	059	053	1
MAYNARD, U.S.A. MA	2						U R	U R	U G			U G		U G												
		046	043	039	032	032	049	050	055	058	061	062	065	063	066	068	068	066	072	075	073	069	066	062	059	2
42.7N				U R			U R			U F		U G U G						D F U R					U R	A	
	3	054	052	051	045	041	047	057	063	063	075	070	074	072	072	071	072	071	074	076	078	073	067	051		3
71.8W		A	B	B	B	D F		B	G	B	B	B	B	B	B	B	B	B	B	B	B	B	B	B	B	
	4					027	029																			4
Geomag. Lat.		B	B	B	B	U F	B		B	G	G	G	U G	G	G	G	U G		U G	D F			U F	D F	D F	
	5					021		033					047				055	065	057	060	045	036	039	027	025	5
53.9N		A	G	G	U F	G		G	G	G	G	U G	U G	U G	U G	U G	U G	U G				D F	D F	D F	D F	
	6				023		030					048	052	054	051	058	056	056	063	067	064	064	055	037	021	6
75.0W LMT		D F	D F	D F	D F	D F		G	U G	U G	U G	U G	B	B	U G	U G	U G						D F	D F	D F	
	7	026	031	033	033	031	036		048	048	047	053			056	056	055	057	057	059	061	062	053	047	042	7
		D F	D F	U F	U F	D F															H			U F		
	8	040	035	033	029	024	040	049	057	058	061	067	071	074	072	070	071	075	069	070	075	068	063	061	057	8
		D F	D F	D F	D F	D F	B	U R		H	G	G	G	G	G	U G	U G	U G		D F	U D	U D	U D	U D	U D	
	9	031	037	033	038	037		037	036	040						051	055	057	062	048	052	047	041	038	033	9
		U D	U D	U D		U D			D F	U D	U D	U D	U D	U D	U D	U D			U F	U F		U R	U F	U F	U F	
	10	028	025	021	020	018	032	046	048	051	055	057	060	062	061	062	067	067	071	081	085	070	061	051	045	10
		U F	U F	U F	U F	U F	U F		U G	U R	U R	U G	D F			D F				H		U F	U F	U F	U F	
	11	043	043	033	027	026	033	043	047	051	057	059	059	063	068	065	064	067	071	079	075	068	060	058	036	11
			U	U	U	U			U	U	U	U										U				
	MED	046	044	037	037	035	036	048	054	058	061	062	066	063	066	066	067	067	069	073	073	068	062	054	050	MED
	CNT	027	027	027	028	028	027	026	026	025	025	025	025	024	026	027	027	028	029	029	029	029	029	029	028	CNT
	1	061	058	057	049	043	040	050	058	066	072	069	070	071	071	074	076	072	068	067	065	065	057	050	058	1
		F	F	F						U S		U S	J S			B	U R	U S		F		U F	U F	U F	F	
BOULDER, U.S.A. CO	2	049	047	041	033	033	035	046	056	052	075	068	082	088	089		073	076	075	073	071	068	060	049	055	2
		F	F	F	F	F					J S								F	U F	F	F	U F		C	
40.0N	3	055	048	040	038	037	038	052	064	077	074	082	089	088	090	084	081	074	069	069	071	070	056	050		3
		J F	F	F	F	F	F	E G	E G	E G U F			U F	U F	E G	U F	E G	F	E G	U F		F	F	U F	A	
105.3W	4	032	030	029	026	019	027	031	039	040	048	055	049	051	047	050	043		038	049	046	053	041	019		4
Geomag. Lat.		A	A	E S	E S	E S	F	F	F	F	E G	E G	E G		F	F	E G	F	F			F	F	F	U F	
	5			017	017	017	033	045	052	052	042	045	045	052	056	055	044	053	048	054	054	051	046		037	5
48.8N		F	U F	U F	U F	U F	F	U F		E G	E G		U R	U R		E G						F	F	F	F	
105.0W LMT	6	038	027	019	020	024	030	042	044	042	044	050	049	052	050	047	053	054	051	054	053	052	055	048	041	6
		F	U F	F	F	F	F	J F	F		B							F					F	U S	U F	
	7	040	040	039	037	033	031	038	049	050		058	059	060	060	059	059	057	057	059	056	053	050	046	041	7
			A	F							F	F														
	8	037		030	029	029	034	049	054	057	064	067	070	071	072	074	073	073	072	069	070	075	060	051	049	8
			F		U F	J F	F	F		F		E G	E G	E G												
	9	041	037	042	036	033	031	040	041	049	048	044	044	045	050	051	052	051	053	054	052	053	043	035	035	9
		F	F	F	F	U F	C	C	C	C	C	C		J C									J C	U C	U C	
	10	030	028	025	025	022							050	050	054	054	055	060	062	060	056	052	047	042	042	10
		J C	U C	U C	U C	U C																		U C	F	
	11	043	036	035	035	027	030	040	048	050	060	057	055	057	061	057	060	064	061	065	056	050	040	042	035	11
						F			F		F	F	N				H			F			F			
	MED	041	039	038	036	033	033	047	052	056	064	067	066	067	071	070	072	070	068	067	067	062	056	048	044	MED
	CNT	27	25	24	25	25	27	27	29	29	27	27	29	29	28	28	29	28	29	29	29	29	29	27	25	CNT
	1	J S												A						A		J S	J S		U R	
		063	057	058	057	052	044	054	061	068	064	060	066		062	062	062	062	064		063	064	063	066	059	1
													U N													
WALLOPS, U.S.A. VA	2	057	048	042	040	035	035	048	056	062	065	067	067	068	068	067	069	070	073	076	076	071	064	063	060	2
						U S	U S																		J R	
37.8N	3	058	057	055	049	044	043	055	063	071	072	073	073	076	074	072	073	070	072	074	074	069	065	059	052	3
		U F	J F	F	F	U F	F	F	G	G	A	G							D W		U W	F	U F	U F	F	
75.5W	4	030	035			025			037	041		046	050	051	053	052	052	054	040	059	042		042	032		4
Geomag. Lat.		B	B	F	F	F	G	G	G	G	G	G	G		D W	D W						U S	S	U S	U F	
49.3N	5						027	031	038	041	043	045	045	051	050	047	054	058	050	059	055	064		050	042	5
		F	F	F	F	F	F	G	U G	G										A						
75.0W LMT	6							038	041	042	050	050	056	058	057	063	061	057	059		063	061	059	058	054	6
				F	F	F	F	G					B	U R							U S			A	U F	
	7	054	048					041	050	051	054	057		060	059	057	057	058	058	060	061	064	053		046	7
		U F	U F	U F								U R												U R	U R	
	8	048	047	042	036	035	035	047	058	059	064	067	072	079	079	075	076	076	071	072	076	069	066	060	058	8
			F	F	F	F	F	F	G	G	G			R	G												
	9	048							037	041	042	052	050		041	055	056	060	066	058	057	056	053	050	044	9
		U F	U S		F	U F	U F								U S			U S				U S		U R	
	10	046	033			022	019	030	048	048	054	058	064	064	065	069	065	070	072	068	080	080	071	065	066	060	10
					U F	U F	U F	U F					U R		U R								U S	U S	U F	U S	
	11	056	055	052	043	036	036	043	050	057	061	061	068	065	069	070	068	068	068	080	070	069	059	055	049	11
			S		F	F	F					R	N									S	S			
	MED	049	048	047	043	038	037	047	051	057	061	061	067	068	068	068	068	068	069	072	070	069	061	057	052	MED
	CNT	25	25	22	23	23	23	29	30	30	29	29	29	28	30	30	31	31	30	29	29	24	26	29	26	CNT
		00	01	02	03	04	05	06	07	08	09	10	11	12	13	14	15	16	17	18	19	20	21	22	23	

Hourly foF2 August 1-11, 1972, with median and count
Stations in order of latitude north to south

LONGITUDE 210.E--300.0E

Station Latitude Longitude		LOCAL TIME																						
		00	01	02	03	04	05	06	07	08	09	10	11	12	13	14	15	16	17	18	19	20	21	22	23	
	1	066 F	063 F	060 J F	056 J F	052 F	044 F	052	056	C	C	072 J R	076	086	083	084	084	079	075	072	076	070 J R	066	U F 060	U F 059	1
POINT ARGUELLO, U.S.A. CA	2	059	056 F	051	049	047	041	046	053	059	058	081	092	095	094	091	091	089	080	076	076	077	067	059	057	2
35.6N	3	050 J R	045	044	045	045	045	054	067	080 U C	094	098	095	102 E G	100	099	094	085 E G	081	078	074	069	070	068 I A	053	3
120.6W	4	060	054	039	035 A	030 A	027 U A	041 A	042	045	058 U F	054	053	048	058	061	065	040	047	044	046	030	037	024	020	4
Geomag. Lat.	5	025	033	031			031		064	049	072	072	087	089	072	070	074	074	073	073	062	057	057	051	049	5
42.1N																										
120.0W	6	048	047	042 F	036 F	030 F	030 F	043	048	051 B	053 B	056 J R	058 J R	062	067	063	063	065	065 I A	069 I A	062	061 F	057 F	051 F	045 F	6
	7	045 U F	046 F	043 F	040 U A	039 F	038 F	039	047			060	059	058	053	053 C	054 C	057	057	057	054	052	050	042	042	7
	8	042	039	036	033 F	032	033	047	053	055 U G	069	072	079	087	091			102	094	083	082	075	070	058	053	8
	9	055 U F	057	055	031	028	029 U A	032 F	045	042	047 U G	048 U G	055 G	053 U G	055	056	053 A	054 A	056	057 I A	057	047	041	038 J A	035	9
	10	032	033 U F	034 U F	035 U F	034 J F	035 U F	039	045	046 U A	045 A	044 A	045 J A	048	053	054			056	055 I A	053	053	048	038	038	10
	11	037	034 F	033 F	028 F	032 F	033 F	045	064	051			057	064 C	071	072	082	079	077	071	061	052	046	043	042	11
	MED	046	046	043	041	041	040	050	061	067	068	072	074	080	082	079	079	079	075	076	069	064	057	051	047	MED
	CNT	30	30	31	30	30	31	28	29	28	28	30	31	31	31	30	29	30	30	30	31	31	31	30	30	CNT
	1	080	080	080	076	069	U R 066	056	066	080	092	102	116	I C 125 I C	130	130	124 U R	120 U R	108	094	090	078	082	066	U F 064	1
MEXICO CITY, MEXICO	2	066	066	057	048	045	044	045	056	075	092	104	114	112	130	134	140	134	124	114	100	081	086	080	074	2
19.4N	3	070 F	074 F	065	051	047	047	048 F	062 F	053 F	076 F	090 F	108 F	122 U F	120 U F	114 U F	120	124	124 I W	096 I W	078	080	086 I C	092	082 U W	3
99.7W	4	U F	U F	074 U F	070	064	060 I B						I C	100	090	086	088	084	078	062	060 U R	086	069 U R	044	033	4
Geomag. Lat.	5	031	034	027	033	030	029	028	052	056	064	063	064	072	077	075	062	064	064	070	065	059	062	064	062	5
29.1N																										
90.0W LMT	6	060	058	052	057	043	040	036	048	067	072	078 C	088 C	088	096	106	108	110	100	088	068	066 U R	070	060	060	6
	7	060	057	056	055	053 U F	046	039	046	056	066			093	102	096	088	080	085	084	066	064	060	050	049	7
	8	049	045	046	043	041	038	038	053	063 I C	066 I C	076 I C	085 I C	098 U C	112 U C	120 U C	124 U C	124 U C	122 U C	114 U C	102	086	074	080	076	8
	9	070	068	066	074	084	030	028	036	042	052	061	069	080	084	080 U C	080 U C	078 U C	080 U C	076 U C	072	062	058	056	051	9
	10	053 U C	050 U C	044 U C	042 U C	041 U C	037 U C	038	051 U C	050 U C	054 I A	060 U C	068 U C	079 U C	094 U C	100 U C	094 U C	094 U C	080 U C	063 U C	082 U C	072 U C	066 U C	057 U C	060 U C	10
	11	054	052	055	049	034	035	036	053	076	072	068	062	070	083	096	098	104	104	104	084	060	056	052	044	11
	MED	055	055	055	049	043	041	041	055	068	072	076	086	098	108	114	116	114	110	110	096	080	068	060	058	MED
	CNT	030	030	031	031	031	031	030	030	030	030	029	029	031	031	031	031	031	031	031	031	031	031	031	031	CNT
	1	075 C	073 C	065 C	063 C	054 C	I F 057 C	058 C	069 C	081 C	081 C	081 C	078 C	085	086	086	085	087	091	088	081	074 U F	074 F	085 F	086	1
HUANCAYO, PERU	2													076	076	076	083	079	085	082	072	066			060	2
12.0S	3	066	069	061	052 F	047 F	042 F	041 U F	073	081	080	076	069	074	085	082	081	083	087 C	090 C	085	090 D R	098	089	080	3
75.3W	4	080	095	063 U F	F	F	F	025	063	078	083	087	088	092	092	090	091	091			076	082	075	084 F	070 F	4
Geomag. Lat.	5	057 F	053 F	032 F	F	F	F	031	069	078	084	084	071	081	092	089	082	082	090	098	092	083	077			5
00.6S	6					I F			068	081	075	080	082 B	075	078	081	084	086	085	086	082	083	084	085	072	6
75.0W LMT	7	057	062 U F	057	055	051	041	036	068	087	091	086		098	093	088	090	092	094	098 C	094 C	100 C	106 C	100	085	7
	8	083	084	070	060 F	050 F	044 F	038 U F	061	076	076	075	071	071	070	072 C	080 C	082 C	086 C	C	C	F	U F	077	079	8
	9	061	055	058	F	F	F	029	071	093	087	082	081	085	081								080	080	087	9
	10	074	063	055				059	080	090	098	087	082	082	080	083	084	090	097	099	092	091	096	079	063 C	10
	11	054	047	035	032	025	021	028	065	087	096	089	078	075	072	079	076	075	082	088 C	090	083	078	079		11
	MED	071	065	057	047	048	041	039	069	086	087	087	083	084	086	087	085	088	090	090	085	084	081	085	076	MED
	CNT	24	25	24	21	18	19	24	26	27	28	28	26	29	29	28	28	27	26	25	27	24	21	23	24	CNT
		00	01	02	03	04	05	06	07	08	09	10	11	12	13	14	15	16	17	18	19	20	21	22	23	

Hourly foF2 August 1-11, 1972, with median and count
Stations in order of latitude north to south
LONGITUDE 300.0E--30.0E

Station Latitude Longitude		LOCAL TIME																						
		00	01	02	03	04	05	06	07	08	09	10	11	12	13	14	15	16	17	18	19	20	21	22	23	
	1	F 052	F	F	F 042	F 041	U F 040	F 040	F	U F 041	F 041	Y	Y	Y U 056	F 057	F 055	F	F 050	F 052	F 050	F 052	F 045	F 051	A	F	1
GODHAVN,GREENLAND	2	F U 041	F 041	F	F	F 041	F 042	F 041	F 041	R 041	R 041	R U 050	Y 050	U Y 050	061	U R 052	U F 061	058	087	R	R 056	F 057	F 049	U F 047	045	2
69.3N	3	F 048	F	U R 042	F	B	R	B	B	B	B	B	B	B	B	B	B	B	B	B	B	B	B	B	B	3
53.5W	4	B	B	B	B	B	B	B	B	B	B	B	B	B	B	B	B	B	B	B	B	B	B	B	B	4
Geomag. Lat.	5	B	B	B	B	B	B	B	B	B	B	B	B	B	B	B	B	B	B	B	B	B	B	B	B	5
79.9N	6	B	B	B	B	B	B	B	B	B	B	B	B	B	B	B	B	B	B	B	B	B	B	B	B	6
45.0W LMT	7	B	B	B	B	B	B	B	B	B	B	B	B	B	B	B	B	B	B	B	B	B	B	B	B	7
	8	B	B	B	B	B	B	B	B	B	B	B	B	B	B	B	B	B	B	B	B	B	B	B	B	8
	9																					B	B	U R 041	U R 047	9
	10	041	F	041	041	B	B	B	B	B	B	U R 053	B	B	R	055	U F 058	U F 061	R 058	055	056	054	F 064	F 045	F 042	10
	11	F 042	F U 046	U F 041	F	F 041	F 041	F D 041	R 041	A	Y	Y	056	054	F	R	053	R	051	Y	F 057	F 055	F 055	F	050	11
	MED	F 044	F 043	U F 041	F 041	F 041	F 040	F 041	F 041	F 048	F 050	F 053	F 058	F 056	F 057	F 055	F 055	F 055	F 056	F 054	F 055	F 053	F 052	F 047	F 046	MED
	CNT	18	10	12	5	7	11	15	14	14	13	14	16	15	13	13	19	18	21	21	23	22	20	17	19	CNT
	1	F 056 J S	F 050	A	A A	A S	A F	F	F	F	053	057	F 053	050	U F 049	051	F 051	F 055	050	049	050	053	048	050	048	1
KIRUNA,SWEDEN	2	046		043 F	038	046	048	050	052	057	061	063	064	064	063	060	060	060	056	058	057	060	059 S	056 F	054 J S	2
67.8N	3	055	054 S		051	053 B	058 B	066 B	073 B	073 B	075 B	076 B	073 B	076 B	066 B	069 B	068 B	073 B	070 B	065 B	063 B	069 B	069 B		060 B	3
20.4E	4	053 B	051 B	049 B	048 B	B	B	B	B	B	B	B	B	B	B	B	B	B	B	B	B	B	B	B	B	4
Geomag. Lat.	5	B	B	B	B	B	B	B	B	B	B	B	B	B	B	B	B	B	B	B	B	B	B	B	B	5
65.2N	6	B	B	B	B	B	B	B	B	B	B	B	B	B	B	B	B	B	B	B	B	B	B	B	B	6
15.0E	7	B	B	B	B	B	B	B	B	B	B	B	B	B	B	B	B	B	B	R	B	B	A	B	S	7
	8	S	S	B	B	B	B	B	B	B	B	B	B	B	B	058 B	058 B	059 B	063 B	060 B	B	B	B	B	R	8
	9	R	B	B	B	B	B	B	B	B	B	B	B	B	B	B	B	B	B	B	B	B	B	A	A	9
	10	A	A	A	S 030	S	041	042	043	050	051	056	058	059	060	058	060	052	053	Z 051	051	044	U A 041	040	A	10
	11	041	A	F	F 038	A	B	045	050	Z 051	050	051	053	054	054	052	056	050	052	048	F 043	047	S 048	A	A	11
	MED	050	051	042	038	041	045	050	053	056	058	059	062	062	062	060	059	057	056	055	053	047	048	042	049	MED
	CNT	009	006	006	017	018	021	021	023	024	025	025	025	025	024	026	026	025	025	024	023	017	014	009	006	CNT
	1	065 F	060	052	F R	047	046	A	F	049	F 059	061	061	059	054 F	052 F	054 F	054	052	R 053	049	052	F 052	R 047	F 049 R	1
SODANKYLA,FINLAND	2	050	046	D R 039	046	047	049	048	052	058	065	063	068	067	068	069	068	064	063	057	060	058	062	061 R	056	2
67.4N	3	055	056	056	049	054 R	058 A	063 B	069 B	076 B	077 B	075 B	076 B	076 B	076 B	070 B	069 B	069 B	072 B	073 B	068 B	064 B	069 B	071 B	065 B	3
26.6E	4	063 B	056 B	053 B	050 B	050 B	B	B	B	B	B	B	B	B	B	B	B	B	B	B	B	B	B	B	B	4
Geomag. Lat.	5	B	B	B	B	B	B	B	B	B	B	B	B	B	B	B	B	B	B	B	B	B	B	B	B	5
63.7N	6	B	B	B	B	B	B	B	B	B	B	B	B		B											6
30.0E LMT	7	R	R	F	R	B						R	R	055 C		055 R	062	062	063 B	067 B	062 B	061 B	053 B	048 B	047 R	7
	8	050 F	044	044	046 B	B	051 B	053 B	055 B	055 B	060 B	060 B	060 D R	054 B	B	059 B	059 B	061 B	B	C	C	B	B	B	058 A	8
	9	057 A	053 A	055 A									042	R	065	062	R	058	052	053	054	053 F	045	043	A	9
	10	A	A U	R 048	030 047	034 A	037 042	042 B	044 047	048 052	052 053	061 052	063 053	063 053	065 055	062 057	058 055	064 058	052 056	053 052	054 051	044	048	047	042	10
	MED	047	045	045	041	041	043	048	052	057	060	062	064	063	065	063	062	061	059	057	056	056	052	047	046	11 MED
	CNT	021	023	024	026	022	026	024	025	024	026	025	026	027	024	027	027	027	026	026	026	025	026	025	022	CNT
		00	01	02	03	04	05	06	07	08	09	10	11	12	13	14	15	16	17	18	19	20	21	22	23	

Hourly foF2 August 1-11, 1972, with median and count
Stations in order of latitude north to south
LONGITUDE 300.0E--30.0E

Station Latitude Longitude		LOCAL TIME																							
		00	01	02	03	04	05	06	07	08	09	10	11	12	13	14	15	16	17	18	19	20	21	22	23
	1	062	060		041	040	044	048	045	053	061	059	053	052	053	054	055	054	054	052	053	054	049	048	046
	2	041	037	043	045	050	050	050	054	059	060	063	063	064	067	064	063	062	059	060	060	062	063	065	061
	3	061	051	053	049	051	058	067	073	079	076	082	080	080	070	071	070	075	076	070	067	072	080	073	071
	4	062	060	050	048																				
	5																								
	6	033																		045			039	041	042
	7	039	036	035									054	058	057	060	063	063	070	065	063	057	052	053	
	8			045	043	045	050	054	059	058	058	059	056	060	062	060	062	060	064	067	066	061	054	055	050
	9	043				047						045								047	045			031	027
	10		025	023	027	034	040	041	044	050	053	061	061	061	061	064	064	057	060	058	061	056	044	043	042
	11	047		048	042	039	041	045	049	052	051	054	055	056	057	055	058	054	054	052	048	048			050
	MED	040	037	036	032	038	043	048	053	057	060	061	061	061	063	063	062	060	060	060	060	057	053	048	044
	CNT	028	023	024	024	027	026	026	026	024	026	026	024	025	026	026	027	027	027	029	028	025	024	025	025
	1										042	045	045		055	055	053	052	054	055	055				
	2						042	045		045	045	052			056	060	058	061	060	061	061		045		
NARSSARSSUAQ, Greenland	3		043	039		042					058													050	040
61.2N	4																								
45.4W	5																								
Geomag. Lat.	6											C	C	C	C	C	C	C	C	C	B				
71.2N	7																								
45.0W LMT	8			035																					
	9																						031		
	10			026										035	069	069									
	11					034	038							058	059	062	059	050	050		049				
	MED	039	040	035	030	034	041	047	050	053	056	055	056	058	060	061	061	060	057	057	054	054	043	046	
	CNT	6	6	7	6	9	12	13	14	17	21	20	20	19	20	22	20	22	19	20	21	13	9	7	3
	1				048			049	053	056	062	070	071	068	062	057	057	057	056		055				
	2					038	043	048	050	056	067	063	064	064	070	070	068	066	064	065					
NURMIJARVI, FINLAND	3									076	080		080	080	074	077	068	068	073		070	068			
60.5N	4				045		047																		
24.6E	5																								
Geomag. Lat.	6					034												047	051	053	049				
57.8N	7						035			045			053	058		066	062	068	068	073	068	068		053	
30.0E LMT	8							048	054	061	060	061	057	061	062	063	064	062	065	066	069	070			
	9						044	048	047	052	050	052		057		049	055	056	052	058	047				
	10			023		025	032	038	043	040	052	062	063	066	062	062	063	066	058	066	062	066			
	11						043	046	047	050	055	052	054	053	052	054		056	056	054	055	054	050		
	MED		036	028	032	029	037	046	050	056	060	064	067	066	067	067	064	062	061	065	066	066	056	057	053
	CNT		001	002	005	005	016	023	023	026	024	026	023	027	027	026	026	029	028	025	019	009	003	005	001
		00	01	02	03	04	05	06	07	08	09	10	11	12	13	14	15	16	17	18	19	20	21	22	23

Hourly foF2 August 1-11, 1972, with median and count
Stations in order of latitude north to south

LONGITUDE 300.0E--30.0E

Station Latitude Longitude		LOCAL TIME																						
		00	01	02	03	04	05	06	07	08	09	10	11	12	13	14	15	16	17	18	19	20	21	22	23	
		S	S	S	J S		J S											J S	S		S	A	A			
	1				047	052	050	047	050	060	068	068	065	061	058	058	057	057		057				046	042	1
UPPSALA,SWEDEN	2	037	034	032	035	041	046	049	054	062	062	S	064	068	068	S	064	S	S	S	S	S	S	J S 071	S	2
		S	S	S			S	S				S						J S	S		S	J S	J S	J S	S	
59.8N	3				047	048			075	084	083		081	078	075	068	070	073	078	077		073	079	072		3
		S	S			V		R	R	B	B	B	B	B	B	B	B	B	B	B	B	B	B		B	
17.6E	4			049	043	045	037																	030		4
Geomag. Lat.		B	B	R	R	B	B	B										F	B	S		F	F	F	V	
	5								035	037	040	040	042	042	042	041	040	043			035				034	5
58.5N		F	F	F														S					F	F	F	
15.0E LMT	6				031	029	031	037	039	041	042	043	044	045	045	045	048		048	047	048	040				6
		F							S		S	S	J S	S	S	S	S	S	S	S	S	S	S	S	S	
	7		042	035	031	032	036	043		048			051													7
												S			S			S	S	J S	S	S	S	S	S	
	8	049	043	038	036	040	045	053	058	060	061		063	061		064	061			072						8
		S													S								F	F	F	
	9		042	037	035	040	043	045	049	048	052	053	056	059		058	052	052	059	050	050	038		027		9
		F	F	F	F					J S						S					S		S			
	10			022	022	030	038	041	044	046	052	060	063	060	059		064	060	064	060		059		046	033	10
			J S	F	F				J S	S							J S			S	S		J S			
	11	026	025			044	043	045	052		052	053	053	053	056	055	055	058	058			054	051	044	033	11
																						U	U			
	MED	038	037	035	032	035	041	046	051	057	062	065	063	065	066	064	061	061	061	063	056	063	061	045	042	MED
	CNT	020	020	019	027	030	029	023	021	021	023	024	029	028	025	025	027	024	019	018	007	012	007	014	019	CNT
					F						U R								F	U F	F	F	U F	U F	U F	
	1	059	054	050	045	044	046	055	060	069	079	077	070	069	067	063	060	063	064	054	054	058	060	050	044	1
			F	U F	F			F	F	I A	I A		I A					I A			C	U R	U R	U R		
KALININGRAD,USSR	2	040	040	038	040	043	049	051	059	066	066	070	065	073	072	069	067	068	067	068		067	068	070	061	2
			F													H						U S		U S	U S	
54.7N	3	058	054	047	047	043	056	064	078	084	090	087	080	075	077	069	066	071	078	079	069	073	074	065	060	3
					F	F			C	C	C	E G	E G	A		F	I A	F								
20.6E	4	062	057	051	045	041	041	040				044	045		052	053	053	052	053	049	048	045	041	037	031	4
Geomag. Lat.		I A	I A		F	F	F	E G	E G	E G	E G	A	E G	E G	E G	E G	E G	E G	E G	E G		F	R	R	R	
53.1N	5	021	020	022	025	024	028	034	038	036	040		041	042	041	041	040	039	037	034	034	028				5
			C	F	U F	I C	I C	I C	C	G	C	G	C	G	C	G	C	U C	C	C	C	U C	C	U C	C	
15.0E LMT	6	020			029	034	037	038										050				044		035		6
		U C	C	U C	C	U C	C	U C	C	G	C	U C	C	U C	C	U C	C	U C	C	U C	C	U C	C	U C	C	
	7	036		028		033		044				061		064		068		072		078		073		057		7
		U C				H			H													U C			F	
	8	050	045	045	041	040	049	060	060	064	067	064	071	067	065	066	067	065	069	079	081	074	068	060	056	8
		F		I C				U C	U C			U C		U C	U S										U S	
	9	049	045	041	036	040	044	047	053	054	062	068	062	060	063	063	056	054	056	055	052	048	042	043	026	9
		U C		F	U S	F																				
	10	019	019	017	020	034	043	044	045	053	057	064	068	061	057	060	066	064	066	072	073	071	058	049	042	10
						U F		H	F					U R									U R			
	11	037	035	032	024	035	041	048	048	055	055	053	056	051	060	056	056	059	060	058	059	056	054	049	044	11
	MED	043	042	039	036	036	044	051	058	062	066	068	068	068	066	066	064	064	064	067	068	068	062	056	049	MED
	CNT	031	029	030	030	031	030	031	028	028	028	029	029	029	029	030	028	031	029	030	028	031	028	030	027	CNT
		J S			N	N		R	N			J S								R	U R	U F	U F	U F	F	
	1	060	056	049	045	042	048	058	067	070	081	077	073	071	072	066	061	068	069		060	064	060	050		1
		F						U N	S	N	N				A	S	S	S	S	S	S	U S	R	R	C	
MIEDZESZYN,POLAND	2	047	048	046	045	046	049	058	063	066		071	068	074		073	070	070	069	070	070	069				2
		C	U S				R						R			R			J R	J R	R		S			
52.2N	3	060	055	050	050	046	055	068	076	087	091	092		078	078	076	068	070	079	083		078	074	068	063	3
						F				C	C	C	C	C	C	C										
21.2E	4	061	057	052	047	042	042	046	043								056	058	058	052	052	046	045	039	035	4
Geomag. Lat.		N	E S	U F	F	E G	E G	E G	E G	A	A	E G	E G	E G	E G	E G	C	E G		R		R		U S		
50.7N	5	020	016	018	023	024	029	033	039			042	043	043	043	042		039	040	038	033	031	024	018	016	5
		E S	E S	E S	F	C	F	E G	E G		E G	E G	A	A		I C				U N						
15.0E LMT	6	016	016	016	022		038	040	040	048	043	049			052	050	050	051	053	052	048	050	050	043	040	6
		R			R		N		R			N		U R		S					J R	C	C	C	C	
	7	039	037	032	029	034	040	045	048	051	059	070	064	068	071	071	070	073	081	081	083					7
		C	C	C	C	C	C	C	C		A			N	C	C	C				U R	D R		R	R	
	8									070		068	073	069				072	071	085	084	073	068		059	8
		R											U N		S											
	9	052	049	044	040	041	047	051	055	060	067	071	068	067	064	068	063	056	062	059	053	052	047	048	030	9
					F	S							J S			S				S	S	S				
	10	024	025	024	022	036	045	044	050	054	063	063	061	063	060	061	066	066	068	074	077	073	062	050	044	10
											C					R				C	J R				C	
	11	040	040	039	033	036	041	050	048	054		056	057	055	060		060	061	063		062	059	058	050		11
	MED	048	044	042	038	040	045	052	056	063	070	070	070	070	070	069	068	068	069	070	073	071	063	054	050	MED
	CNT	027	027	027	026	023	026	025	027	025	024	029	026	027	025	026	028	029	027	026	027	027	026	023	026	CNT
		00	01	02	03	04	05	06	07	08	09	10	11	12	13	14	15	16	17	18	19	20	21	22	23	

Hourly foF2 August 1-11, 1972, with median and count
Stations in order of latitude north to south

LONGITUDE 300.0E--30.0E

Station Latitude Longitude		LOCAL TIME 00	01	02	03	04	05	06	07	08	09	10	11	12	13	14	15	16	17	18	19	20	21	22	23	
	1	059	054	050	049	041	048	051	057			065		068	062	060	068		068		065	058	057	046	042	1
		U F	U F	A	F				U R	A			A									A			A	
DE BILT,NETHERLAND	2	042	045		040	043	053	057	058		059	062		062	065	069	067	065	067	067	069		069	061		2
			S	S											S						J S		A		
52.1N	3	059	050	047	044	046	052	064	072	075	077	072	070	069	069	069	067	072	078	075	078	078		066	067	3
						F	F	G	B	B	B	A	A		G					U S		S	U S	U F	B	
5.2E	4	058	058	052	045	036	038							051		054	057	055	053	053	049		047	036		4
		B	A	U F	U F	B		G	G	G	G	G	G	G	A	A	G		R	F	A	F	B	N	B	
Geomag. Lat.	5			027	028		030										034	043	045	039		030				5
53.7N		B	B	B	F	F						G	G	G											S	
00.0E LMT	6				020	034	036	036	040	041					048	048	050	052	050	050	049	050	045	044	040	6
					F	F	F					S		A	H			B	S	S	S	S	S	S	U S	
	7	037	034	029	027	034	042	044	045	052	052	052	057		056	063	065		071	072	070	062	058	058	055	7
					F	F	F														R	U R	R			
	8	058	048	043	040	040	053	062	063	068	069	070	071	065	069	066	068	070	082	088	086	076		066	056	8
			S	S	F	F							U R							S	S		U S	S		
	9	054	050	045	045	038	043	050	052	060	062	063	062	068	067	059	057	059	057	054	052	050	056		027	9
		R	F	F	R						S										S	S	S	U S	U S	
	10	028	028	028	024	032	047	052	052	052	052	057	057	052	055	063	060	063	065	068		064	050	048	046	10
				U R	U R																					
	11	043	039	034	030	032	040	046	055	056	054	053	055	060	060	060	065	062	060	068	065	063	058	052	048	11
																						S	S		S	
	MED	048	045	043	040	038	046	052	056	062	064	064	064	066	065	064	065	064	067	068	065	067	058	055	050	MED
	CNT	028	027	026	030	030	030	030	030	026	028	027	025	028	028	029	030	028	030	024	016	020	023	025	028	CNT
	1	060				042	049	054	055	J C 063	065	063	065	068	063	C 064	068	066	068	064	067	U S 063	U S 056	U S 052	U F 049	1
		U F		F U F	F	F			U C		U A	A	A	C	A	A	C		C	J C	A	J A	U C		F	
SLOUGH,ENGLAND	2	043	040	039	042	041	052	054	054	055	052			064			072	067	066	073		075	069	066	059	2
		S		J C	F	F					J C	C								C					C	
51.5N	3	061	054	050	045	044	050	058	066	075	074	071	068	076	071	069	067	072	075	071	081	085	081	066	066	3
						J C		F	B	B	A	A	H	G	G						F	F	F		F	
0.6W	4	063	061	058	058	033	036	038					050			052	056	056	056	055	051	049	051	039	023	4
		A	A	F	F		G	G	G	G	G	G	G	A	G	U C	F	U C	G	G	A	A	F	F	V	
Geomag. Lat.	5			020	023	022										049	046	045					022	019	017	5
54.3N		F	F	U F	F	F	G	G		G	G	G	G	A	G	G	A									
00.0E LMT	6	018	017	018	018	024			043						047	049		053	051	050	049	052	049	042	042	6
					F	F	G	G										B						J S		
	7	040	036	031	028	030			044	052	054	052	056	062	057	062	065		070	068	068	057	061	062	057	7
		S							V	V		A					J C							J C		
	8	054	051	044	043	040	050	058	064	067	074		072	071	070	066	073	073	084	088	089	085	076	072	064	8
				F	F	F							J C			J F						J A	F			
	9	062	050	050	047	069	041	049	051	057	061	065	071	068	068	063	060	061	058	057	053	053	061	048	030	9
					F	F	G	G					H						A				F	F		
	10	031	030	030	028	027			056	058	060	060	056	053	054	060	060	062	065	065	072	068	059	050	047	10
					F		G								C					C		S	J S	S		
	11	044	042	040	035	028		048	054	055	056	056	056	067		063	068	065	064	074	068	064	065	057	047	11
	MED	050	048	044	042	039	043	052	056	061	065	065	067	068	067	066	067	066	068	072	074	071	065	057	052	MED
	CNT	030	029	029	029	030	030	029	029	029	028	026	029	028	028	030	029	029	029	031	027	030	031	031	030	CNT
	1	056	053	050	048	042	046	050	059	072	068	066	S 071	065	064	066	070	068	070	062	A	061	S	S	U S 044	1
								U A				R		A	A	A	R						U R			
DOURBES,BELGIUM	2	042	043	042	044	042	056	054	044	056	060	059	069				068	068	067	069	072	072	064	061	061	2
				U R							U R					R					R	R	R	J R	R	
50.1N	3	057	053	048	046	044	052	063	072	075	078	072	070	072	074		067	075	073	071				064		3
		R							B	B	R	E G	E G		R										N	
4.6E	4		058	057	043	036	037	038				044	045	051		052	060	056	057	057	051	046	046	039	028	4
								E G	E G	E G E G		E G E G		E G		A										
Geomag. Lat.	5	014	017	022	027	022	031	033	033	038	042	042	044	044	050		048	045	042	040	039	034	021	019	018	5
52.7N								E G	E G	E G E G		G	G	A	R								R			
00.0E LMT	6	017	017	014	018	031	035	037	042	043	042	046	048	050		047	050	053	051	052	046	048	048	043	042	6
								N			R							B					U S			
	7	042	036	032	031	031	042	044	045	054		058	054	062	060	059	062		073	071	070	061	059	058	054	7
																			R			R				
	8	047	048	043	042	042	052	067	067	068	070	075	074	068	073	069	069	073	082	087	090	079	071	067	060	8
													R									U S	U S	U S		
	9	055	051	045	045	039	044	049	053	060	061	064	066	070	073	068	062	064	060	054	051	052	055	050	031	9
																							S			
	10	031	030	028	027	032	046	052	054	054	053	055	056	051	055	060	061	063	064	067	075	067	053	045	044	10
											R					R					R				
	11	044	043	038	034	033	044	047	055	058		054	056	064	064	058	066	064	058	070	064	062	060	055	049	11
	MED	047	046	044	042	039	045	052	056	062	065	066	067	067	068	066	066	068	067	069	074	068	060	054	049	MED
	CNT	030	030	031	030	031	030	029	030	030	028	028	030	028	028	028	030	029	030	030	024	028	028	029	030	CNT
		00	01	02	03	04	05	06	07	08	09	10	11	12	13	14	15	16	17	18	19	20	21	22	23	

Hourly foF2 August 1-11, 1972, with median and count
Stations in order of latitude north to south

LONGITUDE 300.0E--30.0E

Station Latitude Longitude		LOCAL TIME 00	01	02	03	04	05	06	07	08	09	10	11	12	13	14	15	16	17	18	19	20	21	22	23	
PRUHONICE, Czechoslovakia 50.0N 14.6E Geomag. Lat. 49.9N 00.0E LMT	1	060	052	047	044	042		060	066	078	073		063		068	062	068	071	072	062	063		053	047	044	1
		A	R	R		C	C	A	C	A			R					C	C	C			R		
	2				044						066	068		074	069	072	068				068	068	066		060	2
			R	C					C		S				R			R	R	A	A	C			
	3	060			047	050	060	068		070		080	072	070		068	069						069	066	060	3
							B	B	B	B	B	B	B	B	B	A		A								
	4	058	055	050	043	034											062		065	055	048	042	042	034	025	4
		B	B	B	B	B	B	B	B	A	B	B	B	B	B	A	B	B			A	B	B	B	B	
	5																		043	038						5
		B	B	B	B			B	B	B	B	B	B	B	B	A	B		R			C	R			
	6					037	035											054		051	045			040	043	6
		A						C	C	C	C		R					C		R			R			
	7		034	031	027	035	042					065		061	067	068	070		078		062	060		055	054	7
									C									R	R		S	C		R		
	8	051	050	044	042	050	055	062		068	070	087	072	073	068	071	070		080	085	080		063	060	054	8
				R			C	C	C		R		R				C			A				R	C	
	9	053	050		042	042				064		065		062	070	064		061	060		050	051	052			9
								R	A	A		A		R								S	R			
	10	027	026	024	026	041	055				056		059		059	062	060	064	064	064	070		053	047	042	10
							R	R		B	B	B	B	B	B		C	C	C	C	C		R		C	
	11	040	039	035	031	038	050		053							060						056		050		11
	MED	048	043	041	040	041	052	060	064	068	069	068	070	068	069	068	068	064	065	064	068	060	060	052	048	MED
	CNT	017	021	021	023	019	011	012	009	014	016	015	015	014	017	018	019	016	017	017	015	013	015	018	018	CNT
FREIBURG, GERMANY 48.1N 7.6E Geomag. Lat. 49.4N 00.0E LMT	1	062	056	052	048	042	048	056	067	074	068	072	075	070	069	068	072	073	075	068	069	065	052	049	048	1
									A	A																
	2	047	045	045	042	048	059	055			064	067	074	074	073	074	075	077	069	074	077	075	071	065	064	2
			A																	A						
	3	062		052	048	048	053	063	075	082	084	084	073	073	078	068	071	076	078		084	084	081	075	066	3
			A				A	E	G	C	A	E	G	E	G	E	G									
	4	062		056	047	036		036			044	047	048	053	056	054	064	058	059	060	053	046	046	041	032	4
		W	W						E	G	E	G	E	G	A		A		C	C	C					
	5	017	019	023	023	023	030	037	034	034	039	043		054	054		051	049				038	026	024	024	5
										C	E	G	E	G	E	G										
	6	022	021	018	018	032	036	039	048		044	045	046	054	052	053	053	056	053	052	049	050	053	045	044	6
	7	045	039	036	034	033	044	046	048	059	059	057	060	064	071	064	069	073	077	075	074	065	063	058	056	7
													A	A												
	8	051	054	047	047	046	056	069	070	071	083	081			070	074	074	076	084	086	092	075	069	066	060	8
										H			C								A					
	9	055	052	048	047	042	047	055	056	068	068	067		068	075	072	066	068	067	059		049	053	050	032	9
																							A			
	10	032	030	028	028	034	054	058	059	054	054	056	057	055	057	061	063	065	066	068	072	065		048	045	10
	11	045	044	040	036	033	049	050	061	062	056	057	057	062	066	065	068	068	062	072	068	064	061	056	051	11
	MED	047	047	046	042	042	049	056	061	068	068	068	068	070	070	068	069	068	068	074	079	071	062	054	051	MED
	CNT	031	025	029	029	031	027	028	027	026	030	030	028	030	031	030	031	031	030	028	027	031	030	030	029	CNT
ST. JOHNS, Newfoundland 47.6N 52.7W Geomag. Lat. 58.5N 60.0W LMT	1		F	F	F	S	S				R	D	R	R	R		D	R			S	S	S	D	C	D	S	S	S	
					043	046	045	045	046	047		051						055	050	056	057	060	060	063	059	059	056	059	054	1
			S	S		S	S	F		M	D	R						D	R					S	D	S	D	S	D	S	S	
	2	054	053	044	042	041	048	049			050	057	060	060	050	064	067	069	067	071	074	068	063	056	058	059	2
		S	S	S	S				D	R	D	R	D	R	D	R					S	S	S	S	S	F				
	3	055	052	051	044	040	048	054	059	059	055	050	053	056	058	058	059	061	064	064	068	065	059	054	043	3
		B	B	B	B	B	B	B	B	B	B	B	B	B	B	B	B	B	B	B	B	B	B	B	B	
	4																									4
		B	B	B	B	B	B	B	B	B	B	B	B	B	B	B	B	B	D	R	F	F	F	R	A	
	5																		042	039			034			5
		B	B	B	B	B	B	B	B	B	B	B	B	B	B	B							F	D	R	S	
	6																067	062	054	056	051	038	030	028	030	6
		F	F	F		F			B	B	B	B	B	B	B	B	B	B				S	D	S	S		
	7	030	034	034	030	030	036	040											058	059	064	069	059	054	045	7
																					D	D	S	D	S	S	S			
	8	042	041	036	030	032	049	055	059	065	060	062	061	068	069	070	071	072	073	076	070	068	057	053	050	8
		S	D	R	B	B	F		B	B	B	B	B	B	B	B				S		F	F	F	S	
	9	041	035			034	037										054	054	056	057	043	031	026			9
		F	S	D	R	A	F			D	R								S	S	S	S	S	F	F	
	10		021	020			022	035	044	049	048	056	059	065	063	065	061	065	071	074	071	076					10
												B								S	D	S	D	S	S	S	S			
	11	031	029	030	027	026	036	044	049	053		063	062	067	067	070	070	067	070	073	071	060	044	040	032	11
		S	S		U				U	U			U	U						S	U	S	D	S	U	S	U	S	
	MED	042	038	036	032	030	040	048	053	060	060	062	064	065	065	065	065	067	068	071	072	067	058	056	049	MED
	CNT	023	024	024	022	026	028	026	022	017	019	017	020	019	025	024	028	028	028	027	024	027	023	021	022	CNT
		00	01	02	03	04	05	06	07	08	09	10	11	12	13	14	15	16	17	18	19	20	21	22	23	

Hourly foF2 August 1-11, 1972, with median and count
Stations in order of latitude north to south

LONGITUDE 300.0E--30.0E

Station Latitude Longitude		LOCAL TIME																						
		00	01	02	03	04	05	06	07	08	09	10	11	12	13	14	15	16	17	18	19	20	21	22	23	
GRAZ, AUSTRIA 47.1N 15.5E Geomag. Lat. 46.9N 15.0E LMT	1	C	C	C	C	C	C	C	C	C	C	C	J R 078	J R 076	J R 080	J R 069	067	J R 074	J R 076	J R 074	R	D R 057	A	A	J R 046	1
	2	A	J F 047	J F 048	J F 047	046	049	048		J R 064	M 060	R	R	J R 077	J R 076	J R 077	C	C	J R 074	D R 070	J R 073	J R 076	J R 072	J R 063	J R 067	2
	3	J R 063	D F 058	J F 060	J F 050	J R 048	F 050	D R 056	068	J R 078	J R 079	R 085	R	D R 071	J R 077	J R 078	J R 076	D R 068	J R 077	J R 079	J R 078	J R 080	R	J R 063	J R 063	3
	4	D R 057	D R 057	D R 057	052	D R 042	042	048	R	B	A	B	B	R	B	058	U R 055	R	D R	R	D R	J F	J F	J F	J F	4
	5	D F 035	B	B	J F 025	U R 025	U R 027	U R 032	U M 035	A	C	B	B	B	R	B	R	R	060	D R	060	053	048	050	044	5
	6	R	R	D F 024	R	R	037	B	R	R	R	B	A	R	057	A	R	R	052	050	040	040	D R	R	J R	J R	6
	7	043	D R 040	J R 041	036	J R 033	A	045	U R 047	J R 052	J R 061	J R 064	R	D R 067	064	J R 073	D R 071	D R 072	J R 075	J R 083	J R 078	048 075	048 068	048 058	045 057	7
	8	D R 052	D R 052	C	D R 047	047	052	D R 057	J R 085	D R 072	J R 072	J R 078	A	J R 072	J R 076	D R 071	D R 071	J R 078	D R 068	D R 084	090	085	R	D R 059	D R 057	8
	9	051 U M	050	D R 046 D R	D R 043	U R 043 J R	045	052	D R 060	J R 063	J R 068	D V 069	D R 072	068	067	J R 075	D R 068	R	D R 069	D R 067	056	A	J M 050	055	J R 044	9
	10	031	031 D R	026 D R	024	028	043	055	055	051	A	R	A	060	058	057	J R 061	J R 063	J R 064	D R 067	J R 069	068	D R 058	F 051	V 048	10
	11	047	042 D R	039	039	033	039	050	050	056	R	058	D R 057	D R 058	R	B	C	R	D R	J R	063	R D R	058	056	051	11
	MED	051	049	047	046	043	045	052	057	065	070	073	J R 073	071	J R 076	071	070	069	067 068	059 072	063 079	J R 077	058 068	056	051	MED
	CNT	024	025	025	025	026	026	025	023	021	023	022	019	025	021	024	024	022	025	024	023	024	019	025	028	CNT
BUDAPEST, HUNGARY 46.7N 21.2E Geomag. Lat. 46.5N 15.0E LMT	1	064	061	055	051	J S 048	052	057	071	071	085	075	080	082	A	076	070	076	077	S 077	071	064	A	053	A	1
	2	A	051	U C 051	U C 048	C	C	C	067	068	072	068	078	078	083	078	080	079	075	073	070	071	068	S 065	064	2
	3	J S 059	J S 058	056	051	A	053	058	069	079	S 088	082	088	S 080	076	080	C	C	C	S	S	A	S			3
	4	064	059	C 057	052	045	S 043	045	F 055	B	A	045	F 056	057	058	F 064	058	C	064	A	063	S	F	074 F	069 U F	4
	5	034		C	023	C	E G 027	E G 033	E G 039	E G 039	E G 041	E G 042	E G 043	E G 043	054	054	052	052	053	047	041	056 042	033	048	047	5
	6	029 R	027 A	026	022	026	040 E G	040 R	045	E G 041	E G 046	A	A	054	060	054	A	A	059	A	048	J S 052	S	S 050	J S 046	6
	7	047		043	040	032	036		050	059 H	072	067	067 C	069	074	078	074	074	076	082 D S	080 S	D S 069	068	J S 066	S 059	7
	8	053	050	050	049 S	049 J S	059	059	070	075	077	S		073	075	073	073	077	074	080 S		S	S	J S 062	U S 057	8
	9	052	050	048	045	043	046	054	064	064	067	070	072	064	070	075	070	066	070	070	057 D S	S	S	A	043	9
	10	032	028	026	026 C	030 C	043 U C	050	050 F	056	058	059	059	060	061	061	065	066	066	071	068	071	J S 062	054	S 050	10
	11	047	043	042	035	037	043	051	053	059	064	057	058	063	059	070	064	068	068	064	066	061	059	055	S 050	11
	MED	050	050	046	044	044	046	056	060	067	072	071	073	073	072	073	070	071	069	072	069	070	068	059	054	MED
	CNT	025	025	027	028	023	029	028	028	029	026	024	026	028	028	025	028	026	031	027	023	022	022	026	020	CNT
BEOGRAD, YUGOSLAVIA 44.8N 20.5E Geomag. Lat. 43.7N 15.0E LMT	1	C	C	C	C	C	C	C	C	C	C	C	C	C	C	C	C	C	C	C	C	C	C	C	C	1
	2	C	C	C	C	C	C	C	C	C	C	C	C	C	C	C	C	C	C	C	C	C	C	C	C	2
	3	C	C	C	C	C	C	C	C	C	C	C	C	C	C	C	C	C	C	C	C	C	C	C	C	3
	4													C				J S					J S	D S		4
	5	044	S D S	025	028	D S 031	027	034	040	A	R	R	045	046	060 061	064 060	059 057	072 059	067 057	066 055	065 043	058	D S 052	D S 047	052	5
	6	029	D S 027	026	021	028	039	N 042	N 046	048	A	A	062	057	R	A	056	A	061	A	A	046	036	J S 028	028	6
	7	J S 048	048	044	041	J S 034	040	047	050	059	J R 073	H 066	065	072	076	080	077	073	077	082	083	056	053	053	J S 050	7
	8	056	J S J S 052	052	048	049	060	064	072	073	082	082	082	077	J S 076	075	078	081	080	087	098	078	J S 070	065	D S 056	8
	9	055	053	049	047	047	048	055	065	067	066	075	076	066	J S 074	078	075	070	073	072	057	078	070	065	056	9
	10	036	D S 031	029	D S 025	031	045	048	J R 049	056	057	057	058	060	063	060	063	066	066	072	075	057 D S	055 J S	064	046	10
	11	050	J S J S 046	044	040	038	044	051	056	058	063	060	062	064	060	072	066	072	072	065	065	066	J S 064	S 055	J S 051	11
	MED	050	048	045	044	044	047	055	058	067	072	075	072	072	075	074	074	072	070	072	077	J S 060	058	D S 050	J S	MED
	CNT	022	020	022	020	022	022	022	021	021	021	020	022	022	021	022	022	022	023	022	022	068	065	058	052	CNT
		00	01	02	03	04	05	06	07	08	09	10	11	12	13	14	15	16	17	18	19	20	21	22	23	

Hourly foF2 August 1-11, 1972, with median and count
Stations in order of latitude north to south

LONGITUDE 300.0E--30.0E

Station Latitude Longitude		LOCAL TIME																						
		00	01	02	03	04	05	06	07	08	09	10	11	12	13	14	15	16	17	18	19	20	21	22	23	
	1	F	F	F	F				S			S										S J				1
						052	048	055		080	077		084	086	082	083	083	083	083	091	086		062	050	048	
		A	A	S	U F					A		S								S	J S	S		F		
ROME, ITALY	2				052	052	057	054	064		062		072	078	086	085	085	086	082		081		069		065	2
		F	J	U	S	A							A						A	A		J S		J S	S	
41.8N	3		061	062	056		049	058	070	077	088	083		080	083	080	083	076			087	084	084	082		3
			U S		J					W	C	U F	U F	U F	U F			J	J		S	S	U S	S	S	
12.5E	4	068	065	064	061	051	042	046	054			066	066	063	061	067	060	076	076	067			054			4
Geomag. Lat.		J	W				C	C	W	W	W	W	A				J	J		S		J	J	C	C	
42.5N	5	052		029	036	028								055	070	063	062	064	065		059	053	051			5
		C	C	C	C	C	C	C	C	A	A	A	A	U S		J		J			A	A			U S	
15.0E LMT	6													060	060	054	054	062	059	056			055	054	050	6
																C	C	C	C	C	S	J	S		J	
	7	047	049	045	043	039	035	048	051	055	059	069	064	070	070							080		068	061	7
								J	J S											J S	S	U S				
	8	058	056	057	056	053	052	065	075	077	076	088	087	078	079	084	081	083	079	084		093	085	067	063	8
														U S						J	S	J	J	J	S	
	9	061	055	052	048	047	044	051	070	070	068	082	082	075	080	088	084	078	078	078		062	062	061		9
		A			U F														A	S	S	S	J			
	10		044	040	037	031	036	055	055	055	052	057	054	058	062	060	062	067					062	055	052	10
		J						J	J			A							J	U S	U S	S	J			
	11	050	049	049	045	041	041	050	061	059	065		061	061	065	078	080	077	073	070	068		064	063	056	11
	MED	055	051	050	049	047	045	054	062	069	073	075	073	078	079	078	079	076	078	078	086	084	064	062	058	MED
	CNT	025	026	027	028	028	028	028	028	024	025	025	027	029	030	029	028	028	022	018	018	013	018	024	024	CNT
	1	F	F	F		F	F		H												R	S		V	F	1
		027		028	025	020	022	022	053	064	072	075	080	090	088	092	091	086	090	083	050	032	029	025	029	
		N	F	F	I C	I C		C	C	C	C	C	C	C	C	C	C									
JOHANNESBURG,	2				032	032	030											079	089	079	031	030	032	029	030	2
Rep. of S. Afr.			N	S		F	F	S														J S			N	
26.1S	3	030		032	030			034	048	067	079	087	085	090	093	093	080	069	078	074	041	035	030	024	023	3
							H								F	F					J S		F		F	
28.1E	4	026	026	026	028	022	018	021	050	077	086	102	110	095	100	104	099	106	110	092	083	065	044	046	042	4
		F	F	U F				H							S	S				J S				N		
Geomag. Lat.	5	041	040	036	036	056	016	016	053	078	116	108	130	140	119	098	085	084	084	063	042	045	038	022	022	5
26.9S		I A						F															A	A		
30.0E LMT	6	023	024	026	028	016	018	023	053	063	071	075	085	076	074	087	093	101	090	079	059	038			030	6
				U F		F	F	F						S	S	U C	U C	U C	U C	U C	U C	U C	U C	U C	U C	
	7	027	026	031	030		021	022	056	078	083	077	090	095	097	094	101	099	110	080	041	030	020	023	022	7
		U C	U C	U C	U C													H		R			S			
	8	024	024	027	027	024	025	025	054	070	078	071	072	087	077	084	067	073	074	063	057	045	033	024	023	8
							N		H										S		J R					
	9	023	025	028	029	026	026	027	059	066	077	072	116	108	100	084	086	115	097	066	043	044	038	031	031	9
				N		C	C	C	C	C	C	C				S								F	F	
	10	033	036	029	029								078	095	099	096	084	085	083	072	047	042	037	036	027	10
		F			F			M				H	N	H					R				N		
	11	030	030	032	031	025	024	022	053	084	080	088	078	079	084	081	084	087	076	059	045	044	030	028	030	11
	MED	029	029	030	030	026	026	027	055	074	080	086	087	090	089	090	086	086	083	074	055	041	034	031	030	MED
	CNT	025	020	025	026	022	024	023	024	024	024	024	024	024	024	024	025	027	027	027	027	027	026	025	025	CNT
	1			F					N						U R		R				J S	J S			N	1
		022	023	025	026	025	023	021	019	047	064	063	078	088	092	094	095	091	094	089	051	034	025	022	029	
		S		F	F		F	F							U C				S	R				J S		
HERMANUS,	2	031	036			045		029	029	056	066	064	080	094	098	093	089	084	095	070	032	036	029	030	033	2
Rep. of S. Afr.		N	F	F	F	F	F										U C				U S					
34.4S	3	033		034	033			036	035	060	072	076	082	086	094	100	091	079	081	071	042	040	026	021	021	3
								H		S	M		U R		S	M		U S	S			U S	I S		J S	
19.2E	4	024	023	024	025	024	020	019	027	053	067	099	106	097	097	110	100	104	099	095	078	044	037	030	034	4
		F	F	F		J S	F		F				I S	S	I S					R	I S	M	N		
Geomag. Lat.	5		022	026	027	051		018	028	060	078	087	120	131	118	105	100	090	077	065	061	057	025	024	022	5
33.3S						F	I A	M	I A												M					
30.0E LMT	6	020	023	027	029	019	019	019	020	056	083	087	080	074	089	090	093	099	094	076	058	029	016	017	019	6
									H			R	U C		I S	U S		U C							
	7	020	020	022	023	021	019	017	023	053	066	073	091	101	102	104	100	095	101	090	059	030	027	021	018	7
		N							N	C			I C				U C	U C	N							
	8	023	022	024	026	027	023	020	025	057	069	074	079	084	084	080	090	082	075	067	056	038	029	023	021	8
												I C	U C	U C			U C	I S			U S	U S	I C	U C	I C	
	9	022	022	023	027	028	028	027	027	059	063	080	098	102	100	090	094	095	096	071	040	044	037	026	028	9
		U C	M	U C	C	C	C	M		C	C				U C	U C	U C	U C							V	
	10	030	030	024				025	028			067	076	089	106	095	090	089	081	070	057	038	031	028	026	10
					S			N					H	U C	U C		U S	U C		U C	J S					
	11	027	030	030	033	032	030	021	027	060	073	078	075	086	082	093	105	089	078	063	052	030	025	024	027	11
	MED	026	027	028	029	029	028	027	031	060	071	076	081	086	092	093	094	089	081	073	056	040	030	028	026	MED
	CNT	030	030	029	027	029	026	031	031	030	030	031	031	031	031	031	031	031	031	031	031	031	031	031	031	CNT
		00	01	02	03	04	05	06	07	08	09	10	11	12	13	14	15	16	17	18	19	20	21	22	23	

Hourly foF2 August 1-11, 1972, with median and count
Stations in order of latitude north to south

LONGITUDE 300.0E--30.0E

Station Latitude Longitude		LOCAL TIME																						
		00	01	02	03	04	05	06	07	08	09	10	11	12	13	14	15	16	17	18	19	20	21	22	23	
		F	F	F				F	H			H													F	
	1	027	027	026	026	026	026	026	039	060	069	067	097	069	072	072	068	049	047	035	026	020	021	024	024	1
		F	F	F	F		F	H	H			H		F		H		H	H		F	J F	F	F	H	
PORT STANLEY	2	025	025	026	026	027	026	021	032	047	062	064	057	067	068	084	061	052	048	041	027	020	022	025	025	2
Falkland I.				F	F	F			H				H	D H			H					H	F			
51.7S	3	026	025	025	026	026	026	025	036	055	060	058	064	086	071	068	064	046	041	035	035	026	027	027	027	3
				F	F	F	E A	E A	H		U H			U H	C						F		F	F	F	
57.8W	4	023	021	022	021	028	016	018	042	061	071	088	107	104		058	065	067	057	037	028	066				4
Geomag. Lat.		F	U F	U F	F	F	B	A		F		H					H		U F			H	F	F	F	
40.3S	5		020	020					035	051	055	083	114	118	073	104	083	075	048	050	056	044	035	038	037	5
		F	F	F	F	F	N	N											U H			F	F	F	F	
60.0W LMT	6	036	036	033	035	032			043	061	088	109	080	089	087	082	077	058	045	035	032	023	023	025	026	6
		F	F	F	F	U F	F	F	H	H	H			B	H		H		H		F				F	
	7	026	025	026	025	023	020	018	040	058	078	078	097			070	065	053	053	037	028	024	024	026	026	7
		F	F	F	F	F	F		H							H		H	H	H						
	8	027	028	027	027	029	020	019	042	055	060	064	072	071	078	067	064	057	043	029	031	020	022	024	024	8
			F	F	F	F		F	H	H	H	H			H	H	H		H	H	H	F			F	
	9	025	024	023	022	022	026	021	038	050	064	102	105	079	068	077	078	071	052	036	030	025	029	030	031	9
					F	F	F	F	H	H					J C	H	H	H	H							
	10	033	033	032	032	031	030	026	040	056	079	068	097	083	085	060	068	056	044	041	037	029	029	029	029	10
								F	H							H			H			H				
	11	028	028	026	027	026	025	022	038	060	068	076	073	063	070	060	065	063	041	032	038	022	026	027	028	11
					F																					
	MED	030	031	029	029	030	030	027	043	060	069	072	081	082	075	070	069	063	052	040	034	028	028	029	029	MED
	CNT	030	031	031	030	030	029	029	031	031	031	031	031	030	029	031	031	031	031	030	031	030	030	028	030	CNT

Hourly Values of Ionospheric Data from Eight Locations for the Period July 26 through August 14, 1972

by

S. M. Ostrow
National Oceanic and Atmospheric Administration
Boulder, Colorado

In Figure 1, hourly values of foF2 and fmin from eight ionosphere stations are presented for the period July 26 through August 14, 1972. The data are plotted against Universal Time, and the time of local midnight at each station is indicated by a carat. The graphs are similar to f-plots. Vertical lines drawn from the bottom of each graph indicate values of fmin, and dots connected by a continuous line represent values of foF2. Reasons for missing data and pertinent information about some of the measurements are indicated by standard symbols (see Piggott and Rawer, 1961, "URSI Handbook of Ionogram Interpretation and Reduction", for explanation of the symbols and format of the graphs). Monthly median values are also given for purposes of comparison with the daily/hourly data.

The geographic and geomagnetic coordinates of the eight ionosphere stations are listed in Table 1, together with the computed dip and computed ground L values. With the exception of Maui, the stations are all in Greenland or North America. The stations were selected to illustrate the changes in ionospheric behavior from high to low geomagnetic latitudes. These are a representative sample of the ionospheric data available at World Data Center-A for Solar-Terrestrial Physics at Boulder, Colorado. Formats in which the data are held include ionogram film, tabulations of daily, hourly and median values of characteristics, and f-plots. Depending on the originating laboratory, ionospheric data for a given location and month may arrive at the Data Center in less than a month or take more than a year, but most of the data have been received by about six months after the month of observation.

These graphs indicate that a complex pattern of global ionospheric behavior is associated with the solar-geophysical events that occurred during this time period. The most obvious feature of these graphs is the lengthy periods of high absorption produced by particle precipitation at high latitudes, the effects of which decrease with decreasing geomagnetic latitude, becoming negligible at low latitudes. Effects shown by the foF2 data, while less striking, indicate that important F2 layer changes are associated with the events in this period. The changes in diurnal patterns of foF2 at Mexico City and Maui suggest that F2-layer effects at lower latitudes during disturbed periods may deserve more study than they have received in previous years.

Table 1

Station	Geographic		Geomagnetic		Computed	
	Lat.	Long.	Lat.	Long.	Dip	L
Thule	77.50°N	69.20°W	89.00°N	357.52°E	85.6°	264.41
Godhavn	69.30°N	53.50°W	79.92°N	32.67°E	81.6°	20.62
Narssarssuaq	61.20°N	45.40°W	71.21°N	36.79°E	77.5°	7.38
Churchill	58.80°N	94.20°W	68.69°N	322.63°E	83.4°	8.59
St. John's	47.60°N	52.70°W	58.50°N	21.24°E	72.0°	3.43
Wallops Is.	37.90°N	75.50°W	49.31°N	352.12°E	69.9°	2.54
Mexico City	19.40°N	99.70°W	29.16°N	326.54°E	46.3°	1.27
Maui	20.80°N	156.50°W	20.86°N	268.11°E	38.8°	1.13

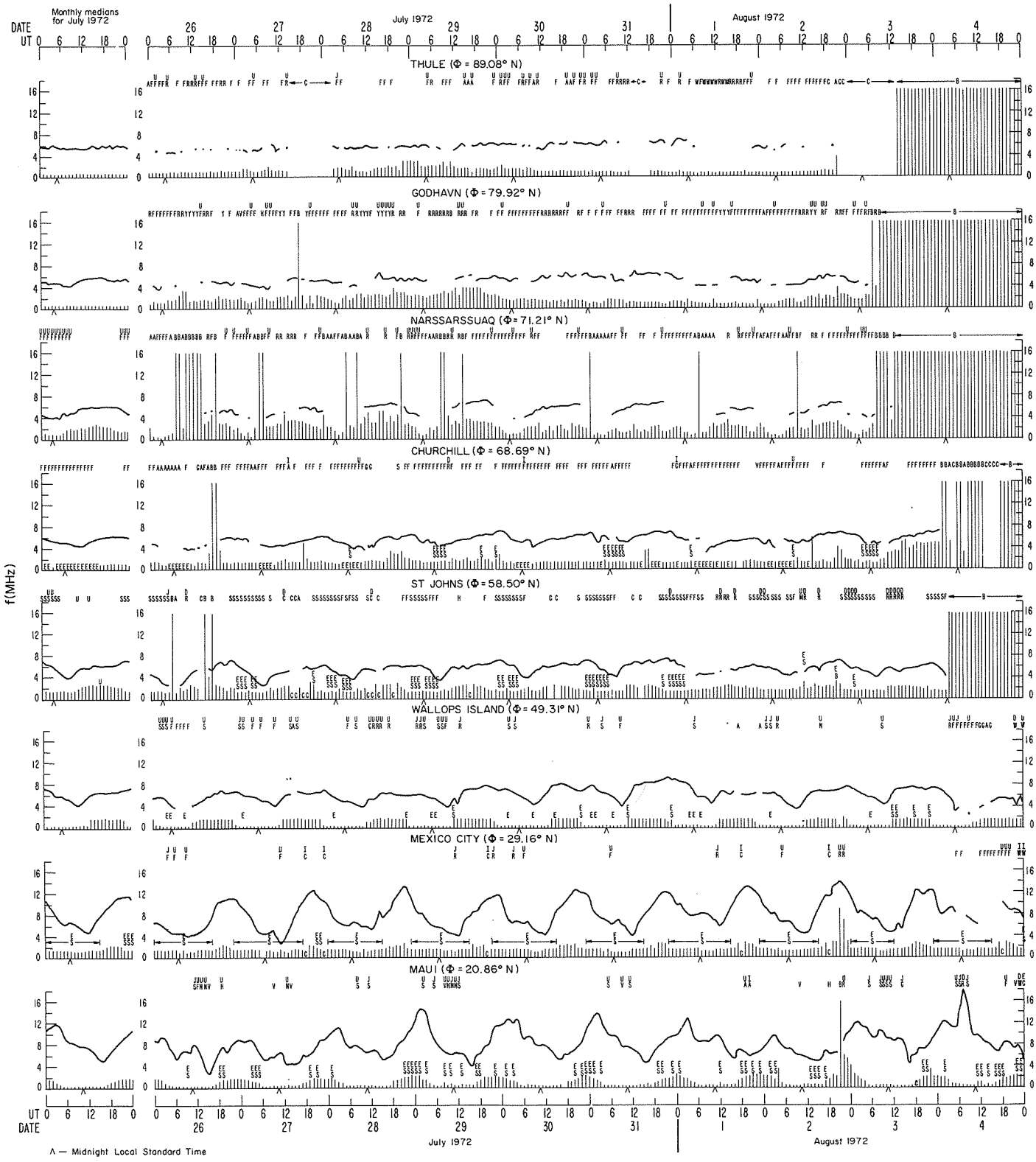
Monthly medians for July 1972
DATE
UT
July 1972
August 1972
THULE (Φ = 89.08° N)
GODHAVN (Φ = 79.92° N)
NARSSARSSUAQ (Φ = 71.21° N)
CHURCHILL (Φ = 68.69° N)
ST JOHNS (Φ = 58.50° N)
WALLOPS ISLAND (Φ = 49.31° N)
MEXICO CITY (Φ = 29.16° N)
MAUI (Φ = 20.86° N)
f(MHz)
Λ — Midnight Local Standard Time

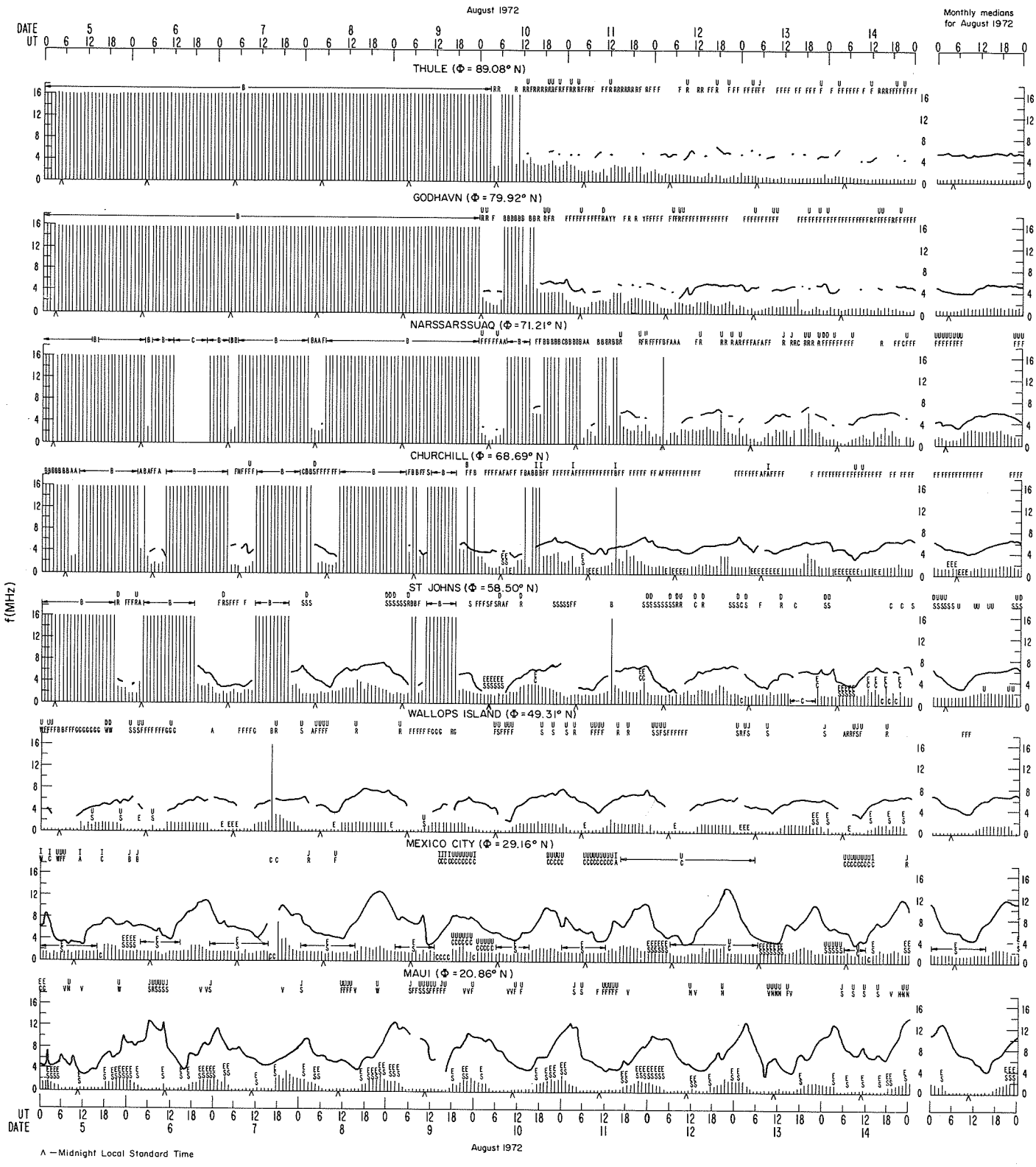
August 1972
Monthly medians for August 1972
DATE
UT
THULE (Φ = 89.08° N)
GODHAVN (Φ = 79.92° N)
NARSSARSSUAQ (Φ = 71.21° N)
CHURCHILL (Φ = 68.69° N)
ST JOHNS (Φ = 58.50° N)
WALLOPS ISLAND (Φ = 49.31° N)
MEXICO CITY (Φ = 29.16° N)
MAUI (Φ = 20.86° N)
f(MHz)
^ — Midnight Local Standard Time
August 1972

6. Supplementary Information on Geomagnetic Data

Magnetograms specially interchanged for the August events held at WDC-A.

In addition to those magnetograms which usually come in to the Data Center on a regular basis (see WDC-A Data Catalog, UAG-20), we received the following special data reports for the August 1972 events:

August 4-7, 1972

Korets	N51 E27	
Lvov I	N50 E24	
Lvov II	N50 E24	
Khaborovsk	N49 E135	
Sr. Majdan	N49 E25	
Yablonitsa	N48 E24	
Yuzhno-Sakhalinsk	N47 E143	
Alma-Ata	N43 E77	
Bada		
Mozgon		

August 3-10, 1970

Alibag	N19 E73	(H component only)
Annamalainagar	N11 E80	
Trivandrum	N08 E77	

High-Resolution Geomagnetic Micropulsation Records from the United Kingdom for August 1972 Events.

During the Retrospective World Interval July 26 - August 14, 1972, a network of eight 3-component Rubidium magnetometers were in operation in the United Kingdom at locations occupied by units of the Institute of Geological Sciences. These sites are shown in Figure 1. Also, a similar magnetometer system was then in operation at St. Johns, Newfoundland, under a cooperative program. The magnetometer systems have been described in an internal publication of the Institute of Geological Sciences, Geomagnetism Unit Report No. 7 by W. F. Stuart.

Records of component variations from the nine IGS stations during the disturbed interval of August 1972 are available to any interested experimenter from the office of Dr. W. F. Stuart, Geomagnetism Unit, Institute of Geological Sciences, Geophysical Laboratories, 6 South Oswald Road, Edinburgh, U.K. (EH9 2HX). As illustrated in Report No. 7, these records are analog traces recorded on strip charts. They are not band limited and consequently provide a means of viewing the micropulsation activity with high resolution as superposed on the overall geomagnetic variations of longer period.

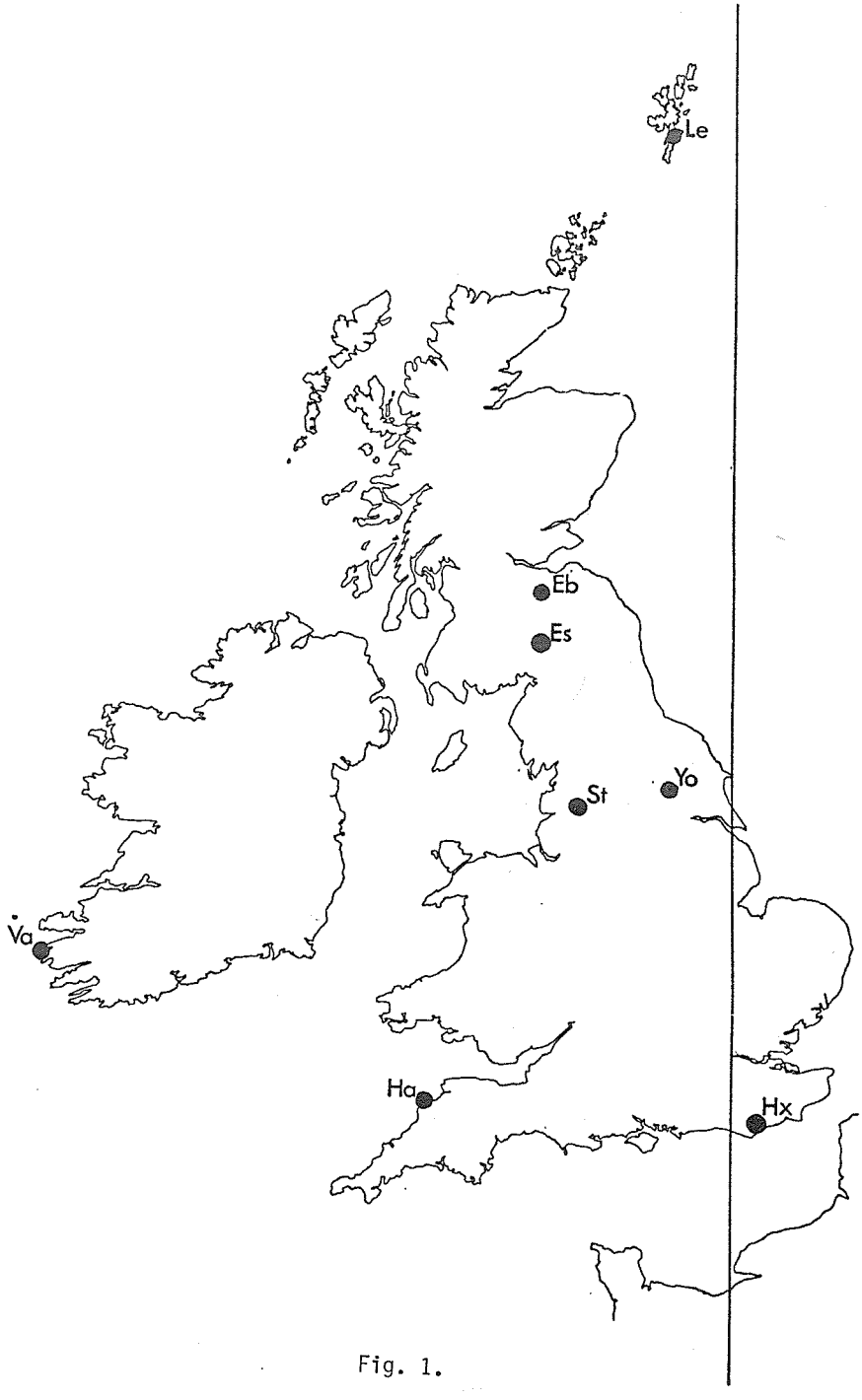

Fig. 1.

APPENDIX II

Symposia, Reports and Publications on the August 1972 Retrospective World Interval

A non-exhaustive list of talks and publications on this period follows. These are in addition to the contributions made in the present Report.

American Geophysical Union, Dec. 4-7, 1972, San Francisco, California, "Special Sessions on August 1972 Solar Event" [*EOS, Nov. 1972, Trans. A.G.U., 53, 1051-1062*].

Talks

SOLAR EVENTS AND FORBUSH DECREASES

Author & Affiliation	Title
J. A. McKinnon, G. R. Heckman, J. A. Sutorik, Space Environment Services Center, NOAA, Boulder, CO 80302	Summary of Solar, Interplanetary, and Terrestrial Events Related to Activity in McMath Region 11976.
J. Virginia Lincoln, Hope I. Leighton, World Data Center A for Solar-Terrestrial Physics, EDS, NOAA, Boulder, CO 80302	Preliminary Compilation of Data for Retrospective World Interval July 26-August 14, 1972.
Patrick S. McIntosh, Environmental Research Laboratories, NOAA, Boulder, CO 80302	Sunspot Proper Motions Related to Cosmic Ray Flares.
William C. Livingston, Kitt Peak National Observatory, Tucson, AZ 85717 (Sponsor, J. M. Wilcox)	Solar Magnetic Fields of McMath 11976.
Stephen A. Schoolman, Sara F. Martin, Lockheed Solar Observatory, Palo Alto, CA (Sponsor: Dr. B. M. McCormac)	Hα Multi-Slit Spectra.
Donald J. Michels, Richard Tousey, U. S. Naval Research Laboratory, Washington, DC 20390	Extreme Ultraviolet Images of the Sun During the Passage of Region 331.
Richard Tousey, Martin J. Koomen, U. S. Naval Research Laboratory, Washington, DC 20390	Changes Produced in the Outer White Light Corona by Region 331.
Richard Hansen, Charles Garcia*, Robert Lee, Joseph Rush, Einar Tandberg-Hanssen, Eric Yasukawa*, High Altitude Observatory, P.O. Box 1470, Boulder, CO 80302; *Hilo, Hawaii 96720	The Flare Spray of 12 August 1972.
D. J. Forrest, E. L. Chupp*, A. N. Suri, P. R. Higbie, C. Tsai, P. Dunphy, Dept. of Physics, Univ. of N.H., Durham, N.H. 03824 (*Now at Max-Planck-Inst. for Extraterrestrial Phys., Munich, Germany. Alexander von Humboldt Fellow and Fulbright Fellow.)	Solar Gamma Ray Line Observations Associated with Solar Flares in Early August 1972.
Kenneth P. Dere, Donald M. Horan, Robert W. Kreplin, Naval Research Lab., Washington DC 20390 (Sponsor: Robert W. Kreplin)	Soft X-Ray Flares from McMath Region 11976.
Dayton W. Datlowe, Dept. of Physics, UCSD, P.O. Box 109, La Jolla, CA 92037. Laurence E. Peterson, Dept. of Physics, UCSD, P.O. Box 109, La Jolla, CA 92037	Observations of Large Solar X-ray Bursts during August 1972.
J. P. Castelli, W. R. Barron, J. Aarons, Radio Astronomy Branch, Ionospheric Physics Lab., Air Force Cambridge Res. Laboratories, Bedford, MA 01730	Solar Radio Burst Spectra and Flux Densities for the Proton Flares of Early August 1972.
Hugh R. Anderson, Dept. of Space Science, Rice University, Houston, TX 77001	Cosmic Ray Total Ionization Rate in July 1972.
J. A. Lockwood, Department of Physics, University of New Hampshire, Durham, NH 03824	Cosmic Ray Neutron Monitor Observations during the August 1972 Event.
Robert L. Chasson, Dennis S. Peacock, Robert E. Gold, Dept. of Physics, Univ. of Denver, Denver, CO 80210	Cosmic Ray Modulation in Denver 4-10 August 1972.

T. Mathews, R. B. Hicks, Dept. of Physics, The University of Calgary, Calgary 44, Alberta, T2N 1N4 — Primary Cosmic Ray Energy Spectra during a Forbush Decrease.

SOLAR CHARGED PARTICLES

J. A. Lezniak, W. R. Webber, Physics Department, University of New Hampshire, Durham, NH 03824 — Pioneer 9 Cosmic Ray Observations During August 1972.

W. R. Webber, E. C. Roelof, Physics Department, University of New Hampshire, Durham, NH 03824
F. B. McDonald, B. J. Teegarden, J. H. Trainor, Goddard Space Flight Center, Greenbelt, MD 20771 — Pioneer 10 Cosmic Ray Observations During August 1972.

James A. Van Allen, Dept. of Physics and Astronomy, University of Iowa, Iowa City, Iowa 52240 — Observations of Solar Energetic Particles at 1.0 and 2.2 A.U. During Early August 1972.

J. D. Sullivan, P. B. Price, H. J. Crawford, Dept. of Physics, Univ. of California, Berkeley, CA 94720 — Composition of Heavy Nuclei from McMath Plage 11976 on August 4, 1972.

John W. Kohl, C. O. Bostrom, The Johns Hopkins Univ., Applied Physics Laboratory, Silver Spring, MD 20910 — Observations of the August '72 Solar Events by the Solar Proton Monitor on Explorer 41.

G. A. Paulikas, J. B. Blake, E. F. Martina, The Aerospace Corporation, El Segundo, CA 90245 — Energetic Solar Proton Observations 3-10 August 1972.

V. Domingo, D. Köhn, D. E. Page, B. G. Taylor, K-P. Wenzel, Space Science Dept. (ESLAB), European Space Research and Technology Centre, The Netherlands — MeV Electrons, Protons and Alphas, August 2-11, 1972.

G. K. Yates, L. Katz, AF Cambridge Research Labs, L. G. Hanscom Field, Bedford, MA 01730.
B. Seller, A. F. Hanser, Panametrics, Inc., Waltham, MA 02154 — Interplanetary Particle Fluxes in August 1972.

J. B. Reagan, W. L. Imhof, J. R. Kilner, Space Sciences Laboratory, Lockheed Palo Alto Research Laboratory, Palo Alto, CA 94304 — Characteristics of the 4 August 1972 Solar Particle Event as Observed Over the Earth's Polar Caps.

G. H. Nakano, J. B Reagan, W. L. Imhof, Space Sciences Laboratory, Lockheed Palo Alto Research Laboratory, Palo Alto, CA 94304 — Angular Distributions of Solar Particles pertaining to McMath Region 11976, August 1972.

Patricia R. Moore, David L. Reasoner, William J. Burke, Frederick J. Rich, Space Science Dept., Rice University, Houston, TX 77001 — Effects of the August, 1972 Solar Flares Observed on the Lunar Surface.

R. A. Medrano, J. W. Freeman, Jr., H. K. Hills, Dept. of Space Science, Rice Univ., Houston, TX 77001 — Penetrating Particles on the Night Side of the Moon Associated with the August, 1972, Solar Flares.

M. B. Baker, A. J. Masley, P. R. Satterblom, Space Sciences Dept., McDonnell Douglas Astronautics Co., 5301 Bolsa Avenue, Huntington Beach, CA 92647 — Polar Riometer Observations of the August 1972 Solar Proton Events.

A. J. Masley, M. B. Baker, Space Sciences Dept., McDonnell Douglas Astronautics Co., 5301 Bolsa Avenue, Huntington Beach, CA 92647 — August 1972 Solar Particle Intensities.

H. J. A. Chivers, W. I. Axford, S. Maagoe, Dept. of Applied Physics and Information Science, Univ. of California, San Diego, La Jolla, CA — Polar Cap Absorption Observed at McMurdo Antarctica.

Raymond J. Cormier, AFCRL (LII), L. G. Hanscom Field, Bedford, MA 01730 (Sponsor: Kurt Toman) — Riometer Observations during the August 1972 Polar Cap Absorption Events.

INTERPLANETARY MEDIUM AND MAGNETOSPHERE

J. Wolfe, H. Collard, D. McKibbin, J. Mihalov, Space Science Division, NASA Ames Research Center, Moffett Field, CA 94035	Preliminary Interplanetary Solar Wind Profile for the August 2-7, 1972, Solar Events.
Thomas A. Croft, Center for Radar Astronomy, Stanford University, Stanford, CA 94305	Wide Variations in Solar Wind Density on August 3-14, 1972.
John W. Armstrong, William A. Coles, John K. Harmon, Steffen Maagoe, Barney J. Rickett, David G. Sime, Department of Applied Physics and Information Science, University of California at San Diego, La Jolla, CA 92037	The Solar Wind Velocity During August 1-15, 1972.
J. D. Mihalov, Space Science Division, NASA Ames Research Center, Moffett Field, CA 94035	Studies of Interplanetary Shocks During August 1972 using Radially Aligned Pioneer Spacecraft.
Frederick L. Scarf, TRW Systems Group, Redondo Beach, CA 90278	Pioneer 9 Plasma Wave Measurements during the Disturbances Related to McMath Region 11976.
Murray Dryer, Space Environment Lab., NOAA/ERL, Boulder, CO 80302. Edmund J. Weber, Kitt Peak Observatory, Tucson, AZ 85717. Aharon Eviatar, A. L. Frohlich, A. Jacobs, Joachim H. Joseph, Tel-Aviv University, Ramat-Aviv, Israel	Interplanetary Shock Wave Propagation Beyond Earth during August 1972: A Progress Report.
Helmut Rosenbauer, Heiner Gruenwaldt, Michael D. Montgomery*, Max-Planck Insitute for Extraterrestrial Physics, Garching, Germany. (*Presently on leave from Los Alamos Scientific Laboratory)	Extreme Solar Wind Conditions observed after the Activity related to McMath Region 11976.
D. S. Colburn, B. F. Smith, C. P. Sonett, Space Science Division, NASA Ames Research Center, Moffett Field, CA 94035	Pioneer 9 Magnetic Field Observations During the Solar Storm of Early August 1972.
Edward J. Smith, Jet Propulsion Lab., Pasadena, CA. Douglas E. Jones, Brigham Young Univ., Provo, Utah. Leverett Davis, Jr., Calif. Instit. of Tech., Pasadena, CA. Paul J. Coleman, Jr., Univ. of Calif., Los Angeles, CA. Charles P. Sonett, Palmer Dyal, David Colburn, Ames Research Center, Moffett Field, CA.	Response of the Distant Interplanetary Magnetic Field: Pioneer 10.
Andrei Konradi, NASA/Manned Spacecraft Center, Houston, TX 77058. Carry L. Semar, Lockheed Electronics Co., Houston, TX 77058	Dynamics of proton pitch angle distributions and energy spectra during the geomagnetic storm of 4 August 1972.
R. A. Hoffman, Paul H. Smith, NASA-Goddard Space Flight Center, Greenbelt, MD 20771	Proton Ring Current Energy Density Measurements from Explorer 45.
Laurence J. Cahill, Jr., Space Science Center, Univ. of Minnesota, Minneapolis, MN 55455	Storm Time Distortions of the Magnetosphere During the Magnetic Storm of August, 1972.
Roger R. Anderson, Donald A. Gurnett, Dept. of Physics and Astronomy, Univ. of Iowa, Iowa City, IA 52240	Plasmawave Observations During the August 4, 1972, Magnetic Storm.
F. S. Mozer, Physics Dept. and Space Sciences Laboratory, University of California, Berkeley, CA 94720. R. R. Brown, Physics Department, University of California, Berkeley, CA 94720	Electric Field and Precipitating Particle Measurements During a Major Magnetic Storm.
H. Robert Willard, Ward J. Helms, U. of Washington, Dept. of Electrical Engineering, Seattle, WA 98195. Harold B. Liemohn, Battelle Northwest, Richland, WA	Southern Polar Region Micropulsation Activity During the 11976 Event.
S. M. Silverman, R. F. Krassa, J. P. Turtle, AFCRL Geopole Observatory, Air Force Cambridge, Research Laboratory, Bedford, MA 01730	Measurements at the AFCRL Geopole Observatory During August 1972.

E. I. Loomer and G. Jansen van Beek, Div. of Geomagnetism, Earth Physics Branch, Energy Mines and Resources, Ottawa K1A OE4, Canada — Magnetic Storm Aug. 4, 1972.

AERONOMY

J. N. Bradbury, W. L. Imhof, R. G. Johnson, J. B. Reagan, Space Sciences Laboratory, Lockheed Palo Alto Research Laboratory, Palo Alto, CA 94304 — Satellite Measurements of Radiowave Absorption during the Solar Particle Event of 4 August 1972.

Richard B. Fritz, Space Environment Lab., ERL/NOAA, Boulder, CO 80302 — Electron Content Enhancement Due to August 7th Flare.

S. Rangaswamy, DBA Systems, Inc., 9301 Annapolis Road, Lanham, MD 20801. P. E. Schmid, Trajectory Analysis and Geodynamics Division, Goddard Space Flight Center, Greenbelt, MD 20771 — Total Electron Content Variations During the Geomagnetic Storms of 4 thru 7 August 1972.

Michael Mendillo*, John A. Klobuchar, Radio Astronomy Branch, Ionospheric Physics Lab., Air Force Cambridge Research Laboratories, Bedford, MA 01730 (*NRC/NAS Postdoctoral Research Associate). D. H. Chung, Boston College, Weston Observatory, Weston, MA 02193 — Ionospheric and Geomagnetic Observations During the August 72 Solar-Terrestrial Events.

G. M. Lerfald, Space Environment Lab., NOAA/ERL, Boulder, CO 80302 — HF Doppler Observations at Boulder, Colorado, August 1-10, 1972.

Jules Aarons, Radio Astronomy Branch, Ionospheric Physics Lab., Air Force Cambridge Research Laboratories, Bedford, MA 01730 — F-Layer Irregularities During the August Events.

Ward J. Helms, University of Washington, Department of Electrical Engineering, Seattle, WA 98195 — Response of the Midlattitude D-region to Solar X-rays on August 2, 1972.

Murray J. Baron, Radio Physics Laboratory, Stanford Research Institute, Menlo Park, CA 94025. Howard F. Bates, Geophysical Institute, University of Alaska, College, Alaska 99701 — D- and E-Region Electron Density Measurements in the Auroral Zone during the August 1972 Storm.

Charles L. Rino, Radio Physics Laboratory, Stanford Research Institute, Menlo Park, CA 94025 — Electric Fields Inferred from Plasma Drifts Measured in the Auroral Zone During the August 1972 Storm.

Joe R. Doupnik, Department of Applied Physics and Information Science, University of California at San Diego, La Jolla, CA 92037 — Directly Measured Electrical Current Densities in the Auroral Zone During the August, 1972 Storm.

Asgeir Brekke, Department of Applied Physics and Information Science, University of California at San Diego, La Jolla, CA 92037 — Neutral Wind Measurements in the Polar Ionosphere During the Storm August 04 - August 09, 1972.

E. R. Young, Geophysics Program, Univ. of Wash., Seattle, WA 98195. J. B. Berndt, Pacific Northwest Labs., Battelle Memorial Inst., Richland, WA 99352 (Sponsor: K. C. Clark) — Tilting Filter Measurements of Hβ from Richland, Wash., 3-9 August 1972.

L. L. Smith, R. J. Hoch, Battelle Northwest Labs., Box 999, Richland, WA 99352 — Photometric Auroral Observations from the Battelle Observatory, Richland, Washington, for the Period August 3-9, 1972.

Ernest H. Rogers, David F. Nelson, Space Physics Laboratory, The Aerospace Corporation, Los Angeles, CA 90009. Richard C. Savage, OL-F, Hq. Air Weather Service, USAF — Auroral Activity in the Southern Hemisphere, 1 August-17 August 1972.

R. B. Bennett, Dept. of Physics, Centr. Wash. State Col. Ellensburg, WA 98926 (Sponsor: K. C. Clark). K. C. Clark, Physics, Univ. of Wash., Seattle, WA 98195. R. J. Hoch, Pacific Northwest Labs., Battelle Memorial Inst. Richland, WA 99352 — Atomic Nitrogen Emission in Mid Latitude Auroras of 3-9 August 1972.

Robert E. Smith, Gary R. Swenson, Space Environment Branch, Marshall Space Flight Center, AL 35812	Ground Based OI 6300Å Doppler Temperature Measurements During 4 August 1972 Storm Period.
Joseph H. King, National Space Science Data Center, Goddard Space Flight Center, Greenbelt, MD 20771	Solar Proton Fluxes for Solar Cycle 20

Solar Physics Division, American Astronomical Society, Jan. 8-9, 1973, Las Cruces, N. M.

Author & Affiliation	Title
Varda Bar* and David M. Rust, Sacramento Peak Observatory, AFCRL, Sunspot, New Mexico (*on leave from Tel-Aviv University, Tel-Aviv, Israel)	Magnetic Fields of the Loop Prominences of August 2, 7, and 11, 1972.
S. Biswas*, D. L. Bertsch, C. E. Fichtel, C. J. Pellerin, D. V. Reames, NASA/Goddard Space Flight Center. (*NASA-NAS Senior Postdoctoral Resident Research Associate on leave from Tata Institute of Fundamental Research, Bombay, India)	Measurements of Solar Protons, Helium and Heavy Nuclei in the Aug. 4, 1972 Solar Event.
D. W. Datlowe, L. E. Peterson, *K. Tanaka, *H. Zirin, University of Calif., San Diego. (*Big Bear Solar Observatory, Hale Observatories, Calif. Inst. of Techn., Carnegie Inst. of Wash.)	X-ray Observations from the August 2, 1972 Flare.
Gabriel L. Epstein, NASA-GSFC-Spectrometer Group, Sunspot, NM 88344, Robert W. Hobbs and Stephen P. Maran, Laboratory for Solar Physics, NASA-Goddard Space Flight Center, Greenbelt, MD 20771, and Harrison P. Jones, NASA-GSFC, Laboratory for Solar Physics, New Mexico Station, 800 Yale Blvd., N.E., Albuquerque, NM 87106	Observations of the Solar Flare of 7 August 1972.
M.A.I. Van Hollebeke, F. B. McDonald, NASA/Goddard Space Flight Center.	The Solar Particle Events of August, 1972.
W. Livingston, Kitt Peak National Observatory	Magnetic Observations Related to the 3B Flare of 4 August.
H. H. Malitson, R. G. Stone, Radio Astronomy Branch, Goddard Space Flight Center	Type II Emission at Hectometric Frequencies.
Werner M. Neupert, Laboratory for Solar Physics, NASA-Goddard Space Flight Center, Greenbelt, MD 20771	Spatial Distribution of Soft X-Ray and EUV Emission Associated with a Flare of Importance IB on August 2, 1972.
Stephen A. Schoolman, Lockheed Solar Observatory, Burbank, CA	Hα Profiles from the 2 August Events.
K. Tanaka, H. Zirin, Big Bear Solar Observatory, Hale Observatories, Calif. Inst. of Techn., Carnegie Inst. of Wash.	Motions and Heating of the August Flares.
H Zirin, K. Tanaka, Big Bear Solar Observatory, Hale Observatories, Calif. Inst. of Techn., Carnegie Inst. of Wash.	The Flares of August.

American Geophysical Union, Apr. 16-20, 1973, Washington, D. C. [*EOS, April 1973, 54*].

Author & Affiliation	Title
R. B. Jurgens, G. M. Lerfald, NOAA Environmental Research Laboratories, Space Environment Laboratory, Boulder, CO 80302	Ionospheric Disturbances Observed at Boulder, Colorado, During July 26 - August 13, 1972, Storm Period.

E. J. Maier, Goddard Space Flight Ctr., Greenbelt MD 20771	Storm time changes in the temperature and composition of the night time ionosphere at 1400 km.
H. R. Hart, Jr., R. L. Fleischer, R. T. Woods*, General Electric Res. and Dev. Center, Schenectady, NY 12305 (*Also at State University of New York at Albany, Albany, New York 12222)	Apollo 16 and 17 Low Energy Cosmic Ray Experiments.
Robert F. Theis, Larry H. Brace, Goddard Space Flight Ctr., Greenbelt, MD 20771	ISIS-II Observations during the August 4, 1972 Storm.
T. L. Aggson, Goddard Space Flight Center, Greenbelt, MD 20771 (Sponsor: Jerome R. Bohse)	Direct Electric Field Measurements in the Magnetosphere.
J. B. Reagan, W. L. Imhof, Space Sciences Laboratory, Lockheed Palo Alto Research Laboratory, Palo Alto, CA 94304. L. J. Lanzerotti, C. G. Maclennan, Bell Telephone Research Laboratories, Murray Hill, NJ 07971	Comparisons of Interplanetary and Polar Cap Fluxes During the 4-11 August Solar Particle Events.
R. L. Dowden, N. R. Thomson, L.E.S. Amon, Physics Department, University of Otago, Dunedin, New Zealand. D. A. McPherson, H. C. Koons, M. H. Dazey, The Aerospace Corp., P.O. Box 92957, Los Angeles, CA 90009	Experimentally Observed Dependence of Whistler Propagation on Pulse Length.
Laurence J. Cahill, Jr., Space Science Center, University of Minnesota, Minneapolis, MN 55455. Thomas L. Skillman, Fields and Particles Branch, Goddard Space Flight Center, Greenbelt, MD 20771	Inward Movement of the Magnetopause on 4 August 1972.
Leverett Davis, Jr., Calif. Instit. of Tech., Pasadena, CA. Edward J. Smith, Jet Propulsion Lab., Pasadena, CA. Douglas E. Jones, Brigham Young Univ., Provo, UT. Paul J. Coleman, Jr., Univ. of Calif., Los Angeles, CA. Charles P. Sonett, Palmer Dyal, David Colburn, ARC, Moffett Field, CA.	Pioneer 10 Observations of Interplanetary Shocks from the August 1972 Flares.

Seventh ESLAB Symposium, ESRO, 22-25 May 1973 Saulgau, German Federal Republic

Author & Affiliation	Title
E. L. Chupp, D. J. Forrest, A. N. Suri, U. of New Hampshire	Gamma ray observations during the August 1972 solar activity.
H. Grünwaldt, M. D. Montgomery, H. Rosenbauer, MPI, Garching	An observational summary of the large scale solar wind disturbances of May-June and August 1972 (HEOS-2 results)
J. D. Mihalov, NASA, Ames	Solar plasma and magnetic field measurements in interplanetary space during August 2-15, 1972.
M. B. Gattaneo, P. Cerulli-Irelli, L. Diodato, A. Egidi, G. Moreno, Rome	HEOS-2 observations of interplanetary shocks on August 4, 1972.
J. A. Lezniak, E. C. Roelof, W. R. Webber, U. of New Hampshire	Relation of coronal magnetic structure to the interplanetary proton events of August 2-9, 1972.
M. van Hollebeke, F. B. McDonald, NASA, Goddard	Propagation of the solar particle through the major disturbances in the event of August, 1972.
D. E. Page, V. Domingo, K. P. Wenzel, ESLAB	MeV electrons, protons and alpha particles observed, August 2-12, 1972 (HEOS-2 results).
L. J. Lanzerotti, Bell Labs.	Proton, alpha and electron observations in August, 1972.
G. K. Yates, L. Katz, AFCRL	Interplanetary particle fluxes observed by OV5-6 satellite.

G. Kremser, G. Pfotzer, E. Kirsch, H. Specht, W. Riedler, K. Zirm	Balloon-borne measurements of proton fluxes during the events of August 2-15, 1972.
P. Stauning, DSRI, Lyngby	Riometer data August 1-16, 1972

URSI Conference on Incoherent Scatter, June 12-16, 1973, Tromso, Norway

Author and Affiliation	Title
Robert D. Hunsucker, Geophysical Institute, College, Alaska	Simultaneous Riometer and Incoherent Scatter Radar Observations of the Auroral D-Region.

The Second General Scientific Assembly of the International Association of Geomagnetism and Aeronomy, IUGG, Kyoto, 9-21 September 1973.

Author and Affiliation	Title
Lincoln, J. V., Journal Review, World Data Center A for Solar Terrestrial Physics, NOAA, Boulder, CO 80302	Report UAG-28, Collected Data Reports on August 1972 Solar-Terrestrial Events.
Liemohn, H. B.	Photometric Observations.
Hakura, Y., Ohshio, M., Yamashita, F., Enome, S., Tanaka, H., Nagai, M. and Nakajima, H.	Radio, X-Ray and Proton Characteristics of Major Solar Flares in August 1972.
Dodge, J. C.	Dynamic Spectra and Positions of Decametric and Metric Solar Radio Bursts Throughout 1-11 August 1972.
Kellogg, P. J., Cartwright, D. G. and Lai, J. C.	Kilometric Wave Observations of Solar Events in August 1972.
Rosenbauer, H., Grunwaldt, H. and Montgomery, M. D.	An Observational Summary of the Large Scale Solar Wind Disturbances of Aug. 72 (HEOS-2 Results)
Croft, T. A.	Variations in Solar Wind Density During August 3-13, 1972.
Watanabe, T., Kakinuma, T., Kojima, M. and Shibasaki, K.	Solar Wind Structure Estimated from Observations of Interplanetary Scintillation of Radio Sources in August 1972.
Dryer, M., Weber, E. J., Eviatar, A., Froilich, A. L., Jacobs, A. and Joseph, J. H.	Interplanetary Shock Wave Propagation Beyond Earth During August 1972.
Smith, E. J., Jones, D. E., Davis, Jr., L., Coleman, P. J., Sonett, C. P., Dyal, P. and Colburn, D.	Pioneer 10 Observations of Interplanetary Shocks from the August 1972 Flares.
Fujimoto, K., Kodama, M., Kondo, I., Mori, S., Murakami, K., Nagashima, K., Wada, M. and Yasue, S.	Morphology of Cosmic Ray Variation in August 1972.
Medrano, R. A., Bland, C. J. and Freeman, Jr., J. W.	The Solar Energetic Particle "Square Wave" During the August 1972 Solar Storm.
Temny, V. V., Zertzalov, A. A., Vaisberg, O. L. and Berezin, Yu. E.	Measurements of Solar Plasma Protons and α -Particles on Prognoz-1 Satellite During the Active Period of August 1972.
Lanzerotti, L. J. and Maclennan, C. G.	Interplanetary Protons, Alpha Particles, and Electrons in the Solar Events of August 1972.
Bostrom, C. O.	Convection of Energetic Solar Particles and Entry into the Magnetotail During the August 4, 1972 Event.

Kremser, G., Riedler, W. and Kirsch, E.	Short Time Behaviour of Solar Particle Fluxes During the August 1972 Events.
Lazutin, L. L., Vashenjuk, E.V., Borovkov, L. P. and Javkov, V. A.	Pitch-Angle Anisotropy of the Solar Protons with Energy 100 Mev at the Boundary of the Atmosphere in Apatity During Superevent August 4-5, 1972.
Bezrukukh, V. V., Gringauz, K. I., Zastenker, G. N. and Khokhlov, M.Z.	Some Solar Wind Characteristics and Shock Wave, Magnetopause and Plasmapause Location during Flare Events in August 1972.
Bulashevitch, Yu. P., Ivanov, N. A., Ajubasheva, S. I., Krasnobaeva, A. G., Shapiro, V. A., Utkin, V. I. and Uchov, H. V.	Geophysical Observation in the Ural Region of the USSR during the 2-8 August 1972 Solar Wind.
Williams, D. J., Barfield, J. N., Fritz, T. A., Hoffman, R. A. and Smith, P. H.	Explorer 45 Observations during the August 1972 Solar Events.
Cahill, L. J.	Observation of the Magnetopause at L=5 during the August, 1972, Magnetic Storm.
Sarma, Y. S.	Micropulsation Activity at Choutuppal (Hyderabad), India, during the Retrospective World Interval, July 26 - August 14, 1972.
Martin, I. M., Rai, D. B., Trivedi, N. and da Costa, J. M.	Particle Precipitation in the Region of Brazilian Magnetic Anomaly Associated with the Storm of August 4-5, 1972.
Trivedi, N., da Costa, J. M. and Rai, D. B.	Configuration and Perturbations of Magnetosphere over Brazilian Magnetic Anomaly during Storm of August 4-5, 1972.
Anderson III, C. W. and Lanzerotti, L. J.	Effects of the 4 August 1972 Magnetic Storm on Bell System Long-Haul Communication Routes.
Matuura, N., Nakata, Y., Koizumi, T., Yamaoka, M., Ondoh, T., Nagai, M. and Takechi, A.	Storm Effects on the Ionosphere.
Watt, T. M. and Regan, J. B.	Observation of D and E Region Ionization Densities from Chatanika, Alaska during the Solar Storm of August, 1972.

Reports

Lincoln, J. Virginia and Hope I. Leighton	1972	Preliminary Compilation of Data for Retrospective World Interval July 26 - August 14, 1972, World Data Center A for Solar-Terrestrial Physics, Report UAG-21, November 1972.
Croft, Thomas A.	1972	Traveling Regions of High Density Observed in the Solar Wind on August 3 and 9, 1972, Stanford Electronics Laboratories, Radioscience Laboratory, Center for Radar Astronomy Scientific Report No. 7, Stanford University, Stanford, CA, November 1972.
McKinnon, J. A.	1972	August 1972 Solar Activity and Related Geophysical Effects, NOAA Tech. Memorandum ERL SEL-22, Boulder, Colo., December 1972.

Journal Articles

In Report of Ionospheric and Space Research in Japan, 26, 287-322, December 1972 under title "Some Observational Results for the Solar-Terrestrial Events in August 1972".

Moriyama, F.	Solar Observation at Mitaka
Kubota, J., Kurokawa, H. and Kureizumi, T.	A Large Flare of August 2, 1972
Maeda, K. Oda, N. and Nakayama, K.	Monochromatic Observation of a Flare on August 4, 1972
WDC-C2 for Solar Radio Emissions, Toyokawa	Radio Features of Four Major Solar Events
Wada, M.	Cosmic Ray Intensity Variance during August 1-10, 1972
	Observational Record of Cosmic Ray Variations at Various Stations (Antarctica, Japan and Hong Kong)
Kakioka Magnetic Observatory	Magnetograms at Kakioka on August 4-10, 1972 with K-indices and Storm Tables for Three Stations in Japan
Koizumi, T.	Ionospheric Variations during August 1-10, 1972
Naito, Y., Araki, T. and Kato, S.	Sudden Phase Anomalies Observed at Uji
Ichinose, T. and Ogawa, T.	HF Doppler Observation Associated with Magnetic Storm of August 4 to 6, 1972
Takechi, A.	The Variations of the Night Airglow Intensities during August 6-13, 1972

Albertson, V. D. and Thorson, Jr., J. M.	1973	Power System Disturbances during a K-8 Geomagnetic Storm: August 4, 1972, IEEE Transactions on Power Apparatus and Systems, to be published.
Beckmann, B	1973	Solar-terrestriche Zusammenhänge im Retrospektiven Weltinterval 26 Juli - 14 August 1972, Kleinheubacher Ber., 16, 275-285.
Brown, Robert R.	1973	Observations of Narrow Microburst Trains in the Geomagnetic Storm of August 4-6, 1972, JGR, 78, 1727-1729.
Chapman, F.	1973	Sunspots, earth currents and pipeline corrosion - and their interrelation with earthquake activity, Gas Industries, 17, No. 5.
Croft, Thomas A.	1973	Traveling Regions of High Solar Wind Density Observed in Early August 1972, JGR, 78, 3159.
Chupp, E. L., Forrest, D. J., Higbie, P. R., Suri, A. N., Tsai, C. and Dumphy, P. P.	1973	Solar Gamma Ray Lines observed during the Solar Activity of August 2 to August 11, 1972, Nature (Friday), 241, 333-335
Fürst, E., Hachenberg, O. and Hirth, W.	1973	The Solar Outburst on August 7, 1972 at 17 GHz and 35 GHz, Solar Physics, 28, 533-537.
Gribbin, John and Plagemann, Stephen	1973	Discontinuous change in earth's spin rate following great solar storm of August 1972, Nature, 243 (Friday), 26-27.
Hakura, Y., Ishii, T., Asakura, T. and Tirajima, Y.	1972	Polar Cap Phase Anomalies of VLF Waves in August 1972, Report of Iono. & Space Res., Japan, 26, 280.
Mathews, T. and Lanzerotti, L. J.	1973	Detection of Relativistic Solar Particles before the Hα Maximum of a Solar Flare, Nature (Friday), 241, 335-337.

News & Views - "J.J.Q."	1973	Record Solar Activity in August 1972, Nature (Friday), 241, 307.
Ondoh, T., Nagayama, M. and Nishizaki, R.	1972	VLF Emission Observed by ISIS-2 during the Geomagnetic Storm of August 9, 1972, Report of Iono. & Space Res., Japan, 26, 285.
Pomerantz, M. A. and Duggal, S. P.	1973	Record-breaking Cosmic Ray Storm stemming from Solar Activity in August 1972, Nature (Friday) 241, 331-333.

APPENDIX III

[The summary of solar radio data for the August 1972 period by H. Tanaka (page 4) includes a condensed table of outstanding events and two illustrative charts of the morphology of activity during the period. Since these are rather new types of data summaries and may not be well known outside of the solar radio scientific community, we reproduce in this Appendix the corresponding detailed explanations, adapted from the IAU "Quarterly Bulletin on Solar Activity" (in press). The charts and the table are also repeated here for convenience. The table covers the whole period July 1 to August 11, 1972, whereas the table on page 6 begins during August 2; the earlier data were not available when Part I of this report went to press. ----Ed.]

Explanation of Solar Radio Summary Charts and Table
(adapted from text for IAU "Quarterly Bulletin on Solar Activity")

Distinctive Events

Distinctive radio events are included in the Table when the reported peak flux near 10 cm (8 - 11.1 cm) is more than 20 flux units, or when Type IV on meter wavelengths is reported from spectral observations, or when a flare of importance $\geq$ 2N is reported.

Column 1. Date

Columns 2-5. Times of start, end, maximum and also durations are given to nearest minute.

Column 6. Peak flux density near 10-cm wavelengths is given in 10^{-22} WM^{-2}Hz^{-1}.

Column 7. Integrated 10-cm flux, i.e., [Mean flux] × [Duration in 10 minutes]. Unit is 6×10^{-20} JM^{-2}Hz^{-1}.

Columns 8-9. The same as Columns 6 and 7 except the values are at peak or maximum flux in the frequency spectrum indicated in the Column 14 'Spectrum'.

Columns 10-12. Reported intensity classes on dm, m and Dm wavelengths, checked by single frequency observations in some possible cases. Intensity classes are quite roughly defined as follows.

	Class 1	Class 2	Class 3
dm and m	5 - 50	50 - 500	> 500
Dm	5 - 20	20 - 80	80 - 300

Column 13. Shape of time profile. S=Simple, C=Complex, PR=Precursor, PI=Post-burst Increase.

Column 14. Frequency spectrum of the event. On dm, m, and Dm wavelengths, reported spectral types are entered. On microwaves more than about 1 GHz, symbols are introduced which are explained by the following examples.

P5 means that the spectrum shows a peak at 5 GHz.

0.6\ means that the flux falls toward high frequency, and the flux at 0.6 GHz is entered in the Columns 8-9 'Flux at f_p'. It does not imply that no data are available below 0.6GHz.

U1/9 means that the flux is minimum at 1 GHz and rises up to 9 GHz. The flux at 9 GHz then enters in the Columns 8-9 'Flux at f_p'.

/9 means the same case, but the frequency of minimum flux is not known. All we know is that the flux is maximum at 9 GHz and no observations are available at higher frequencies.

2-5 means that all we know is the flux is flat between 2 and 5 GHz.

Column 15. The first station name in the first line shows the origin of the selected data for f_p and the following station names are entered arbitrarily. The station name with underline shows the origin of 10-cm values.

Columns 16-17. Serial numbers of corresponding flares in Solar Geophysical Data, NOAA, USA, and in the Quarterly Bulletin on Solar Activity. For the latter, 1204 means 4th event on 12th.
Columns 18-19 and 21. Values in Q.B.S.A. have priority over those in S.G.D..
Column 20. From S.G.D..

Important bursts defined as having the following features are selected and underlined.

1. [10-cm peak flux] > 500,
2. [10-cm integrated flux] > 500,
3. accompanied by m-Dm Type IV burst or outstanding particle event.

Activity Chart

This chart is the summary of solar activity near the boundary of chromosphere and corona observed by centimetric solar radio emissions, where the activity of active regions and the outstanding events are shown synoptically.

Active Regions

The intensity and activity of each active region are expressed by the 'flux density on 3 cm' and the 'ratio of flux density 3cm/8cm' respectively.

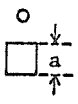

o Flux density on 3 cm <10 units. The unit is $10^{-22}WM^{-2}Hz^{-1}$.

Flux density on 3 cm ≥10 units. The area is proportional to the flux density, or more precisely, Flux = 278 a^2 units, where the side length 'a' is measured in unit of the length of one day on the chart. The square is open when the flux ratio 3cm/8cm is 0.7 or less.

Flux ratio 3cm/8cm is 0.8
0.9
1.0
1.1 or more.

Approximate heliographic latitude and the number of McMath region are shown in the chart, which are based on the maps of sunspots and calcium as well as the 'Region of Solar Activity' in Solar Geophysical Data, NOAA, USA. Radio data are based on the 1'-beam interferometers at Toyokawa.

10-cm Radio Bursts

Outstanding radio bursts listed on the table of 'Distinctive Events' are mapped in the following way.

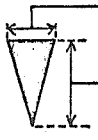

Duration of the burst with extended time scale, the size length of one day = 100 minutes.
The height is proportional to $\sqrt{Flux}$, where the size length of one day = 1000 units.
Minor burst of short duration becomes a short bar.

Emissive Regions at 169 MHz

The lower chart is the summary of radio frequency activity in the lower corona based on the observations by the interferometer at Nancay.

1. 169 MHz. The beam-width is 3'.8. Daily distributions of intensity are plotted giving diagrams of evolution. Equal intensity levels have been drawn for intensities proportional to 0.6, 1, 1.5, and 2. The first level corresponds to the sun without any radio storm center. In each noisy radio region, the smoothed intensity around noon is given in $10^{-22}WM^{-2}Hz^{-1}$.

Observing Stations

1. Code names are consistent with those in "Solar-Geophysical Data", NOAA, USA.

SOLAR ACTIVITY CHART

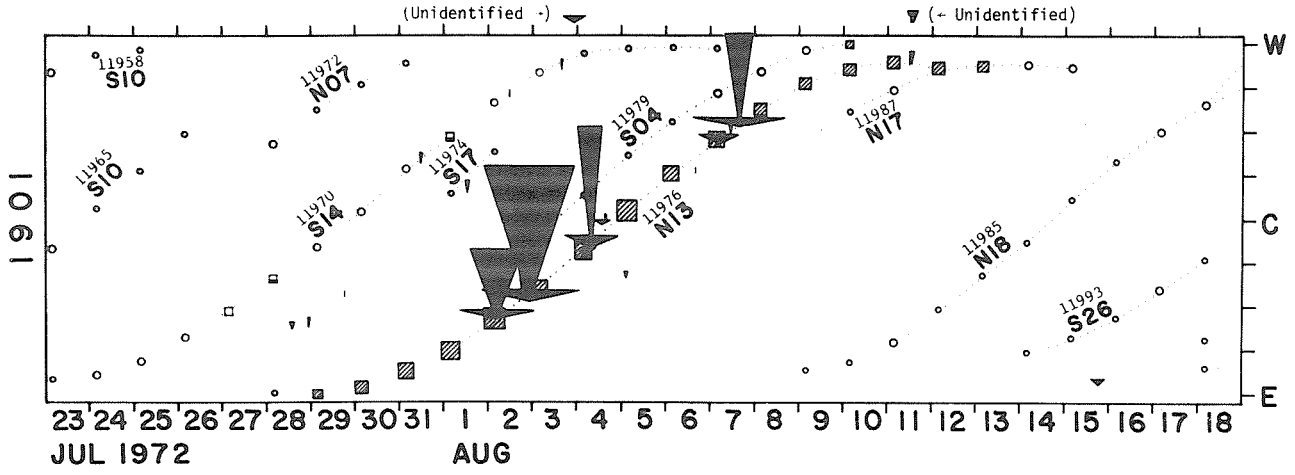

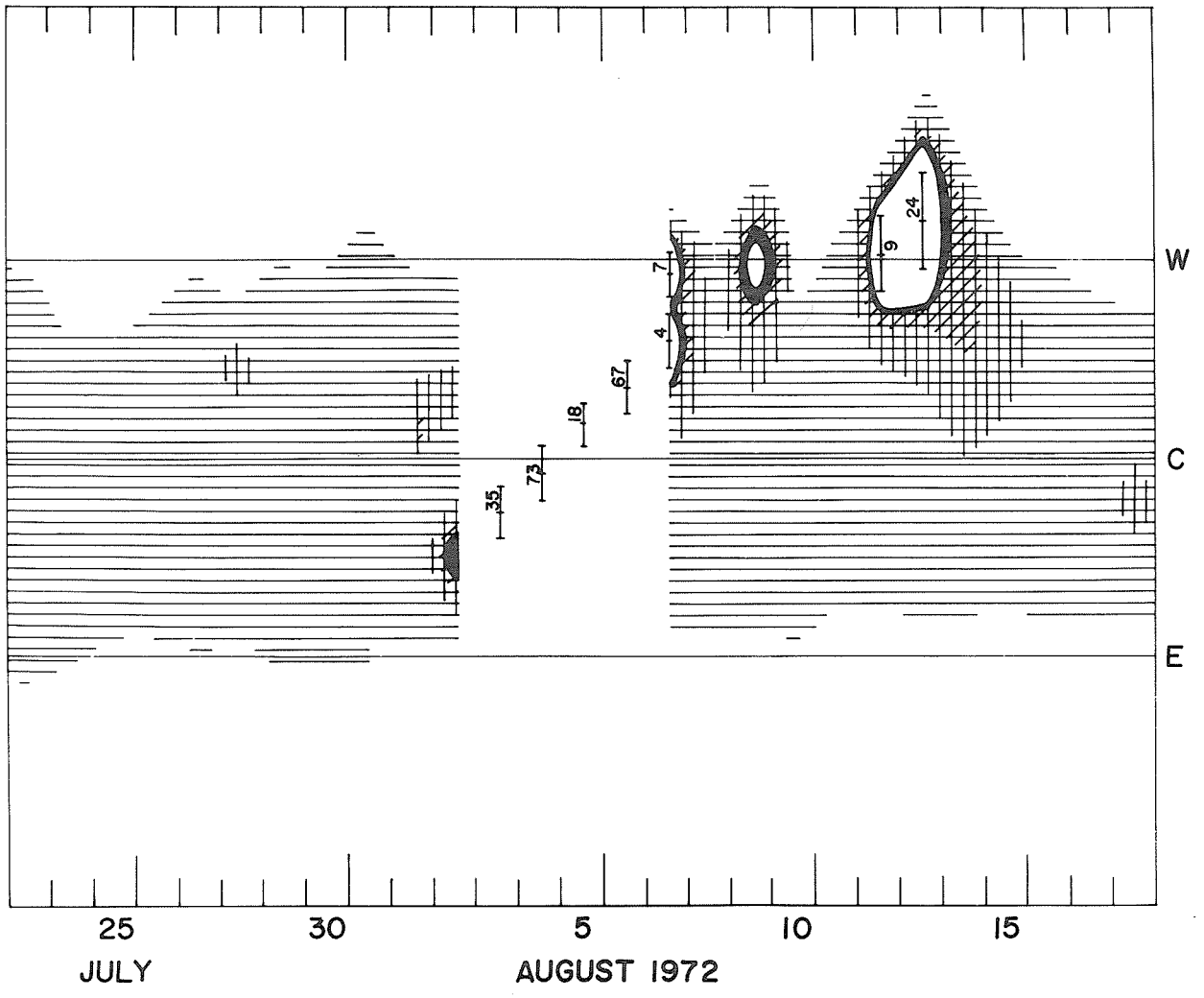

SUMMARY TABLE OF RADIO EVENTS WITH ASSOCIATED FLARES

Date 1972	Radio Burst Start U.T.	End U.T.	Max. U.T.	Dur. Min.	10cm Flux Peak	10cm Flux Intg.	Flux at fp Peak	Flux at fp Intg.	Intens. dm	Intens. m	Intens. Dm	Shape	Spectrum	Station	NOAA Group	QBSA No.	Flare Lat.Lon.	MCMA Reg.	Imp.
Jul. 8	0245	0247	0246	2	33	3						S	P4	TYKW,MANI,CRON	*CRON		S10 E23	11949	-N
10	0717	0719	0718	2	74	2	275	21				C	P2	TYKW,BERL,CRON,CANR	No Report				
11	1340	1850	1410	310	14	190	38					S	I\3	PENN,OTTA,BOUL	45216	1101	S10 W25	11949	1N
	1359	1411							3				VP	HARV					
	1422	1438							2				IV	HARV					
15	0254	0258	0255	4	80	6	140	19				S	P6	MANI,TYKW,CRON,IRKU	No Report (but by radio, W98% 11949)				
28	1320	1332	1325	12	26	14	36	3				S	U1.5P4	BOUL,SGMR,SAOP,BERL,PENN,HUAN,OTTA,BORD,CANR	45410	2803	S20 E49	11974	-N
	1322	1328																	
28	2348	2354	2352	6	74	3			1	2	2		IIIGG	HARV,BOUL					
	2352	2354								3		C	P3	TYKW,MANI,PENN,BOUL,CRON	*BOUL		S17 E46	11974	-F
													IIIG,V	CULG,IRKU					
29	1844	1845	1845	1	20	1	36	3				S	0.6\3	SGMR,OTTA,CANR,BOUL,PENN	45436		S19 E34	11974	--B
	1837	1847							2	3	3		IIIGG,V	BOUL,HARV					
31	1111	1118	1112	7	62	11	145 (at 9GHz)	25				S	P3U5P9	SGMR,CANR,BERL,SLOU,BORD,CRIM,GORK	45459	3101	S13 W16	11970	1B
Aug. 1	1148	1156	1150	8	79	16						S	P3	SGMR,OTTA,GORK,CANR,BERL	45471	0104	S20 W04	11974	-B
	1148	1151								3	3		IIIGG,DP,RS	WEIS,SGMR,SAOP,HUAN					
2	0303	0310	0308	7	15														
	0310	0510	0405	120	2600	6600						P.R.							
	0510	0800D	0510	170D	55	510						C	P4	TYKW,MANI,CRON,IRKU	45482	0203	N13 E35	11976	1B
	0300	0825										P.I.			45482	0204	N14 E34	11976	2N
	0312	0315							2	2			IS,CONT	CULG,WEIS					
	0326	0722								1			V	CULG					
	0326	0450								2			IIIS,U	CULG					
										1			UNCLF	CULG					

Date 1972 Aug.	Start UT	End UT	Max UT	Dur. min.	10 cm Flux Peak	10 cm Flux Integr	Flux at fp Peak	Flux at fp Integr	Intensity dm	Intensity m	Intensity Dm	Burst Shape	Spectrum	Stations	SGD Group No.	SGD QBSA No.	Lat.	Long.	McMath Region	Imp.
2	0303	0310	0308	7	15							P.R.								
	0310	0510	0405	120	2600	6600						C	P4	TYKW,MANI,CRON,IRKU						
	0510	0800D	0510	170D	55	510						P.I.			45482	0203	N13	E35	11976	1B
	0300	0825							2	2			IS,CONT	CULG,WEIS	45482	0204	N14	E34	11976	2N
	0312	0315								1			V	CULG						
	0326	0722								2			IIIS,U	CULG						
	0326	0450								1			UNCLF	CULG						
2	1045	1047	1045	2	30	2	65	6				S	P9	GORK,OTTA,SGMR,BERL,SLOU,CANR,CRIM	45487	0205	S12	W42	11970	1N
2	1838	1849	1840	11	610	190	960					S	P5U15/37	SLOU,OTTA,SGMR,CANR,HUAN	45491	0206	N14	E26	11976	1B
	1839	1843					(at 37GHz)		2				IV	HARV,BOUL,PENN						
2	1959	2320	2148	201	9700	38000						C	P4	OTTA,TYKW,SGMR,BOUL	45492	0207	N13	E27	11976	2B
			2144				9300	32000					2.5\35	SGMR,TYKW,HUAN						
	2320	0300	2320	220	97	880						P.I.								
	1959	2003	(3rd)							2	2		IIIG	HARV						
	2021	2100							1	3	3		IIIS	HARV,CULG						
	2021	0728							3	3	3		IVorCONT	HARV,SGMR,BOUL,CULG						
	2243	2339	(3rd)						1	2			IIIGG	HARV,CULG						
3	1502	1507	1504	5	66	12	185	63				S	P9	SGMR,OTTA,CANR,PENN,BERL	45503	0301	S12	W57	11970	1N
	1503	1505							2				IIIGG	HARV,SLOU,BOUL,HUAN						
3	2203	2253	2214	50	20	25	48	63				C	1.5/9	TYKW,OTTA,PENN,HUAN	No Flare Patrol					
	2241	2243							3	2	2		IIIGG	HARV						
4	0525	0537	0529	12	62	34						C	1.5/4	TYKW,MANI,GORK,CRON,CRIM	45508	0401	N15	E09	11976	-N
	0537	0607		30	20	57						P.I.								
4	0607	0619		12	30							P.R.								
	0619	0715	0636	56	7600	11000	25000					C	P20	SLOU,TYKW,MANI,CRON,GORK,IRKU	45509	0402	N14	E08	11976	3B
	0715	0920		125D	65	380						P.I.								
	0706	0713	0707	7	110	32	145	59				S	2\9.5	TYKW						
	0717	0739	0719	22	1800	290						C	P4	TYKW,GORK						
	0743	0803	0753	20	105	90						C	3\9.5	TYKW,GORK						
	0805	0826	0810	21	95	63	580	230				C	1\9.5	TYKW						
	0834	0847	0840	13	50	26	220	200				S	1\9.5	TYKW						
	0605	0606								1			IIIG	CULG						
	0610	0714							1	3			IIIGG	CULG,WEIS						
	0621	1245							3	3			IVorCONT	WEIS,CULG						
	0622	1156								3			IIIGG	WEIS,CULG						
4	1307	1348	1318	41	9	16	32					S	1\U3/5	PENN,SGMR,BORD,CANR	45512	0403	N13	W01	11976	-N
	1313	1330					(at 1GHz)			3	2		IIIGG,DP	WEIS,HARV						
	1315	1338							3	3			IVP	HARV						
4	1513	1518	1514	5	35	6	36	11				C	P4	SGMR,OTTA,BOUL,BERL,PENN,CANR	45513		N13	W01	11976	--N
	1514	1518								3	3		IIIGG,DP	WEIS,HARV						
5	0231	0243	0233	12	26	7	35	5				C	1\9.5	TYKW,CRON,MANI,IRKU	*TEHR		N14	E19	11976	-F
	0226	0243								3	2	1	IIIGG	CULG						
6	1613	1615	1614	2	25	2						C	NarrowB.	OTTA,BOUL,SGMR,CANR,PENN	45564		N17	W19	11976	--F
7	0251	0253	0252	2	66	4	430D	54				C	3/10	TYKW,MANI,CRON,IRKU	45569	0701	N15	W30	11976	-N
7	0346	0516	0355	90	49	180	195	400				C	1.5/10	TYKW,MANI,GORK,IRKU,CRON	45570	0702	N15	W30	11976	1B
7	1055	1102	1057	7	67	24	90					C	P9	BERL,OTTA,SGMR,GORK,SLOU,CANR,CRIM	45577	0704	N14	W34	11976	1N
7	1430	1505		35	17							P.R.								
	1505	1610	1528	65	4500	7100	15000	12000				C	3/9.5	HUAN,OTTA,SGMR,CANR,BOUL	45580	0707	N14	W36	11976	3B
			1522				27000	45000					P9	SGMR,SLOU						
	1610	1940		210	50	360						P.I.								
	1647	1656	1651	9	26	10	38	18				S	1\3	PENN,OTTA,CANR						
	1511	1530								3	2		IIIGG,V	WEIS,HARV,SGMR						
	1519	1614								3	3		II	HARV,WEIS,BOUL						
	1508	1807							3	3	3		IV,CONT	HARV,BOUL,SGMR						
	1756	1802								2	2		IIIGG	HARV						
11	1210	1212	1210	2	23	1	58	3				S	P7	SGMR,OTTA,CANR,GORK,HUAN,PENN	No Report					
11	1217	1221	1218	4	99	17						C	1.5/3	OTTA,SGMR,BERL,PENN,GORK	45643	1105	N12	W90	11976	1B
11	1231	1248	1236	17	70	36						C	0.6-9	OTTA,SGMR,GORK,BORD,PENN	45643	1105	N12	W90	11976	1B
			1239				123	31					P9	SGMR,OTTA,GORK,PENN,SLOU						
	1239	1243								2	2		IIIG	BOUL,WEIS						
	1239	1251								1	1		II	BOUL,WEIS						
	1248	1254								3	2		II	BOUL,SGMR						
	1247	1355								2	2		IV	BOUL,SGMR						
11	1313	1340	1320	27	84	76						S	P3	OTTA,SGMR,BOUL,PENN,SLOU	No Report					
	1315	1318								2			II	BOUL,BORD,BERL						
	1247	1355	(Common to the above event)							2	2		IV	BOUL,SGMR						
	1345	1350							3				UNCLF	HARV						

ALPHABETICAL INDEX

	Page
Airglow	
Doppler broadening	802
Intensity	802
Temperature	803
6300A OI	802
Stations:	
Marshall Space Flight Center	802
Roma, Southern Africa	806, 807
Atmospheric densities: May - June 1967; July - August 1972	791
Aurora	
Auroral backscatter	796, 797, 799
Doppler shift	797
E-layers	492
5577Å green line intensity	795
Radio aurora	796, 799
SAR arcs (stable auroral red arcs)	806, 807
Stations:	
Scandanavia	796
Slope Point, New Zealand	799
Cosmic Rays	142, 415, 423, 430, 448, 465, 469, 476, 479, 484, 486
Anisotropy	415
Asymptotic directions	419
1300 UT August 4	394
1600 UT August 7	394
Balloon measurements	460
Cut-off rigidity	448, 465, 485, 486
Energy spectrum	465, 469
Forbush decreases	442, 475, 618, 638
FD-1	415, 433, 446, 449, 450, 465, 469
FD-2	420, 433, 446, 449, 450, 467, 469, 486
FD-3	421, 433, 449, 450, 467
Ground-level events	16, 18, 442
GLE-1	420, 430, 450
GLE-2	421, 430, 449, 450
Intensity - time profiles	430
Ionization chamber	
Hong Kong	478
Mt. Norikura	478
Sapporo	478
Tokyo-Itabashi	478
Yakutsk	472
Meson telescopes	
Ahmedabad	486
Embudo Cave	449
Hobart	425
Lindau	459
London	425
Mt. Chacaltaya	449
Mt. Norikura	481
Nagoya	482
Socorro	449
Takeyama	478
Yakutsk	470
Modulation wave August 5-8, 1972	450
Muon Monitor	
Denver	452
Neutron Monitors	
Ahmedabad	486
Apatity	463
Athens	456
Brisbane	424
Calgary	416
Denver	452

	Page
Cosmic Rays (continued)	
Neutron Monitor Stations (continued)	
Dumont d'Urville	416
Durham	416
Gulmarg	486, 487
Hafelekar	459
Hermanus	442, 456
Huancayo	416, 442
Irkutsk	466
Iwate University	485
Kerguelen	416
Khabarovsk	466
Kiel	416, 424, 456, 463
Kiruna	416
Leeds	416, 456
Lindau	459
Magadan	466
Mawson	424
McMurdo	416, 430
Mexico City	475
Morioka	485
Mt. Norikura	477, 671
Mt. Washington	416
Mt. Wellington	424
Norilsk	466
Novosibirsk	466
Oktyomtsy	469
Oulu	416, 424
Pic-du-Midi	416
Potchefstroom	442, 456
Predigtstuhl	638
Rome	416, 424, 456
Sanae	442, 456
South Pole	416, 430, 445
Sulphur Mt.	416
Swarthmore	416, 430, 449
Syowa	477
Thule	416, 430, 633
Tixie Bay	416, 466
Tokyo-Itabashi	477
Utrecht	416, 456
Yakutsk	416, 466, 469
Primary energy spectrum	415
Primary rigidity August 7, 1972	450
Rigidity	465
Rigidity spectrum	469, 479
Earth's spin rate	792
Length of day change	793
Electric voltage between ionosphere and earth	810
Geomagnetic	
Forecasts	12
Indices:	
AE	689, 703-705
Stations:	
Barrow	686
College	686, 702
Dixon Island	686, 702
Ft. Churchill	686
Great Whale River	686, 702
Leirvogur	686, 702
Meanook	702
Narssarssuaq	686, 702
Nurmijarvi	702
Sitka	686, 702
Sodankyla	686
Tixie Bay	686, 702
AL	688, 703-705
AO	690
Ap	607, 619, 791

	Page
Geomagnetic (continued)	
Indices (continued)	
ASY	445, 703-705
Stations:	702
Honolulu Tangerang	
Kakioka Tashkent	
San Juan	
AU	687, 703-705
C	758
Cp	810
Dst	671, 699, 734
K	391, 529, 609, 715, 758
Kp	456, 649, 669, 722, 791
Micropulsations	632
Pulsations	609, 734, 745, 765, 767-771, 772, 773-775
Hissagrams	749
Stations:	
Campbell Island	800
College	777
Kakioka	750
Lindau	780
Loparskaya	728, 729, 730
Lovozero	727
Macquarie	778
Narmijarvi	777
Onagawa	750
Sodankyla	777
Thule	777
Telluric earth currents	800
Variations	
Addis Ababa	740
Ahmedabad	718, 719
Alibag	743, 761
Annamalainagar	743
Baker Lake	723
Borok	745
Boulder	570
Budkov	731
Cambridge Bay	723
Campbell Island	800
Chambon-la-Foret	739
Fort Churchill	723
Garchy	739, 740
Genoa - Mt. Capellino	733
Hermanus	807
Hyderabad	755-757, 761
Kem	727
Kiruna	609, 614, 615
Loparskaya	728, 729
Lovozero	730
Manila	763
Meanook	723
Murmansk	727
NOAA	490
Onagawa	573, 748
Roburent	733
São José dos Campos	628
Sydney	538
Tahiti	738
Thule	630, 631
Thumba	744
Trivandrum	743
Victoria	723
Interplanetary magnetic field	417
Interplanetary plasma wave	379
Interplanetary scintillations	371
Scintillation index (SI)	532

	Page
Ionosphere	
Electron density	490, 492, 497, 604, 617, 618
Faraday Rotation	
La Trobe Univ., Australia	529
Legon, Ghana	525
NASA/GSFC	526
foF2	391, 506, 539, 549, 560, 564, 609, 709, 711, 714, 733
Hourly values for August 1-11, 1972 (64 stations by latitude)	832
f-plots	558, 559, 658-662
July 26 - August 14, 1972 (8 stations by latitude)	857
HF	566, 576, 582, 588, 603, 618, 636, 637, 641, 642, 644, 651
Incoherent backscatter	
Chatanika, Alaska	492
Millstone Hill, Mass.	497
Incoherent scatter	490, 492, 497
Ionograms	
Ahmedabad	720, 721
Izmiran	712, 713, 714
Ionosondes	
Brisbane	543
Canberra	542
Cocos Island	536
Geopole	653
Godhavn	653
Godthåb	653
Hobart	538
Khabarovsk	557
Kiruna	609
Lycksele	609
Mundaring	545
Narssarssuaq	653
Norfolk Island	546
Salisbury	536
Sdr. Strømfjord	653
Sofia, Bulgaria	603
Thule	653
Torshavn	653
Townsville	544
Vanimo	536
Wallops Island	505
Ionospheric currents	725
LF	588, 595, 603, 616, 618, 622, 623-626, 627
MF	616, 619
Observatories:	
Boulder	568
Delhi	595
Doshisha Univ. (Kyoto)	572, 573
Hiraiso	622, 641, 642
Inubo	668
Izmiran	709
Lindau	616, 644
Lüchow	636, 637
Manila	562
Narssarssuaq	532
Neustrelitz	576
Ottawa	646
Port Stanley	561
Prague	588
Sagamore Hill	532
São José dos Campos	627
Scandanavia	796
Seattle	601
Slough	561
Sofia	603, 618
South Uist	561
Thule	633
Thumba	502
Uji (Kyoto)	584

	Page
Ionosphere (continued)	
Quality Figures	637
Radar	
Coherent backscatter	502
Echoes	502
Riometer Absorption	651, 666
Stations:	
Ahmedabad	235
Amderma	649
Campbell Island	800
College	490
Dixon Island	649
Geopole	653-656
Godhavn	653-656, 667
Godthåb	653-656
Goose Bay	667
Heiss Island	649
Kiruna	609, 611, 613
Lindau	581
Loparskaya	728, 729, 730
McMurdo	673, 674
Mirny	649
Molodehnaya	649
Narssarssuaq	653-656
Norilsk	649
North Pole -19	649
Sdr. Strømfjord	653-656
Shepherd Bay	673, 674
Thule	653-656, 667
Torshavn (Faroes)	653-656
Vostok	649
SFA	576, 590, 592
SPA	584, 627, 668
SWF	505, 577, 582, 588, 590, 591 592, 644, 646, 720, 721
TEC	508, 511, 525, 526, 529
VHF	796
VLF	389, 584, 588, 595, 601, 602, 603, 609, 627, 628, 633, 668, 669, 684
Lunar Surface Observations	356, 361
1969-99A Apollo 12	361
1971-8A Apollo 14	356, 361
1971-63A Apollo 15	361
PCA	549, 609, 618, 649, 668
Loparskaya	727
Rocket, August 4	354
Satellite and Space Probe Observations:	
International Designation Name	
1959-α1 Vanguard 2	784
1960-ξ1 Explorer 8	784
1966-44A Explorer 32	784
1966-70A OV3-3	784
1966-110A ATS-1	765
1967-34A NNSS	511
1967-48A NNSS	511
1967-92A NNSS	511
1967-111A ATS-3	508, 525, 532
1968-12A NNSS	511
1968-17A SOLRAD 9	298
1968-66A Explorer 39	784
1968-81D LES 6	532
1968-100A Pioneer 9	378, 381, 417, 456, 463, 490, 706, 759
1969-46B OV5-6	348
1969-53A IMP-5 (Explorer 41)	330, 334, 338, 417, 671
1969-69A ATS-5	508, 532
1970-67A NNSS	511
1971-19A IMP-6 (Explorer 43)	288, 330, 334, 417, 669
1971-24A ISIS-2	389
1971-58A SOLRAD 10	298

	Page
Satellite and Space Probe Observations (continued)	
International Designation Name (continued)	
1971-83A OSO-7	291, 325
1971-89A	676
1972-05A HEOS-2	342
1972-92A ESRO-4	319
Satellite drag	784
Solar	
Activity Chart	5
Activity Table	6
Alphas	332, 340, 345, 349, 676, 681
Calcium plage data (MM11976)	16
Coronal mag. fields	
Hale Observatory	74
Electrons	335, 337, 338, 343, 344, 357, 358, 382, 676, 679
Evolution of active region	48, 77, 81, 85, 95, 121
Flares	490, 508, 560, 595, 668, 708
1966 August 28	23
September 2	23
1972 August 1	18, 103, 465
August 2	18, 30, 103, 118, 122, 415, 460, 465, 469, 549
August 4	18, 30, 46, 71, 95, 103, 134, 139, 415, 460, 465, 469, 492, 549, 603
August 6	30
August 7	18, 30, 38, 46, 56, 155, 415, 465, 469, 497, 526, 549, 603
August 11	18, 46, 160, 161
Flare Patrol Observations (33 stations by longitude)	818
Flare spectra	103, 161
August 2	120
August 4	145
August 7	150
Forecasts	12, 33, 77
Gamma rays	142, 325
Hα Faculae evolution curves	28
Flare activity integral curves	84
Observatories:	
Big Bear	121
Catania	69
IZMIRAN	139
Kwasan Obs.	119
Manila	57, 58, 59
Meudon	49
Okayama Astrophysical Obs.	134
Swedish Astrophysical Station	161
Indices	
Active region index	19
Comprehensive flare index	19
Comprehensive region index	19
Interval between proton flares	811
K faculae evolution curves	23, 28
Observatories:	
Manila	60
Meudon	49
Line profiles	147, 148, 150
Magnetograms	
Kitt Peak	95
Mt. Wilson	82
Pulkovo Obs.	82
Rome Astronomical Obs.	82
San Fernando Obs.	85
Magnetic Fields	30, 35, 77, 81, 139
Evershed streams	35
Inferred neutral line	30
Isogauss maps	
August 2	97
August 3	98
August 4	99, 100, 102
Synoptic maps	78, 79

	Page
Solar (continued)	
McMath Regions	
8362	811
8461	811
8817	811
9503	811
9740	811
9946	811
11976	30, 46, 68, 95, 134, 161, 168, 811
12246	181
11976 compared to others of Cycle 20	20
Observatories:	
Abastumani	145
Alma-Ata	103
Big Bear	121
Catania	23
Haute Provence	46
Kuchino Astrophysical Obs.	103
Meudon	46
Rome	23
San Miguel, Argentina	150
Sternberg Astronomical Institute, Moscow	103
Swiss Federal Observatory	160, 35
Tel Aviv	121
Prominences	40, 70, 118
August 8	64
August 11	65, 160
August 13	66, 67
Spectra	40
Protons	331, 332, 335, 337, 339, 343, 344, 349, 350-353, 361, 417, 490, 618, 671, 676, 677, 679, 681, 810
Radio	
Bursts	
August 1	211
August 2	129, 170, 171, 186-190, 211, 220, 240, 263
August 4	191-192, 212, 221, 231, 232, 236, 240, 264, 265
August 7	171, 193-194, 212, 266, 288
August 10	213
August 11	160
Contour maps of % Flux	202
Drift curves 2800 MHz	175
East-West Solar Scans	216
Flux	180, 230, 269, 279
Quiet time	173
Observatories:	
Ahmedabad	234
Fort Davis	256
Hiraiso	230, 239
Kokubunji	241
Manila	183, 231
Nobeyama	241
Ottawa	169
Penn. State (PSURAO)	202
Penticton	169
Sagamore Hill	129, 183, 202, 213
Slough	210
Toyokawa	215, 241, 824
Tremsdorf (HHI)	260
Trieste	279
Univ. of Colorado	242, 283
Weissenau	269
Polarization	216, 237, 240, 279
Spectra	
July 31	184
August 1	244
August 2	241
August 4	237, 241, 272

	Page
Solar Radio (continued)	
Spectra (continued)	
August 7	195, 273
August 8	250
August 11	252, 253, 274
August 12	284
November 25	275
Spectral diagram of bursts	
August 4	267
August 7	268
Spectral Events	
July 29	222
July 31	222
August 2	222, 256, 257
August 4	222, 256
August 7	259
Scintillation sources	375
Shock wave, August 3	375
Synoptic maps	48
Transits of active region MM11976	24-27
Wind	371, 386, 388, 759
Velocity	417, 465
X-rays	129, 142, 160, 292, 293, 298, 321, 322, 323, 326, 327, 328, 335, 601, 622
Integral curves of flare activity	84
Sunspots	35, 582
Evolution	82
29 July - 10 August	30
30 July - 10 August	36
30 July - 6 August	124, 125
5-11 August	63
Evolution curves of spot areas	29
Integrated proton intensity	675
Numbers	17, 580, 675
Observatories:	
Baguio	61, 62
Boulder	30
Culgoora	30
Dusseldorf	579
Kwasan	119
Manila	61, 62
Ondrejov	156-158
Sacramento Peak	30
Whistlers	390, 593, 684
Halley Bay	684
Panska Vés	588

AUTHOR INDEX

	Page
Aarons, J.	532
Abe, M.	747
Abston, C. A.	686
Afanasyeva, L. T.	727
Agarwal, P. D.	744
Akasofu, S.-I.	702
Allen, J. H.	686
Altschuler, M. D.	74
Anderson, K. A.	334
Apostolakis, A.	454
Apostolov, E. M.	603
Araki, T.	584
Armstrong, J. W.	371
Asakura, T.	668
Badillo, V. L.	183, 231
Baker, M. B.	672
Barfield, J. N.	764
Barron, W. C.	183
Bates, H. F.	492
Bazilevskaya, G. A.	460
Beckmann, B.	635
Bednárová-Nováková, B.	752
Bell, M. B.	168
Belon, A. E.	492
Bemalkhedkar, M. M.	487
Bernes, C.	161
Bhargava, B. N.	743
Bhonsle, R. V.	234
Blomster, K. A.	415
Böhme, A.	260
Bolshakova, O. V.	745
Borg, H.	609
Bossolasco, M.	733
Bostrom, C. O.	330
Brunelli, B. E.	727
Bumba, V.	77, 80, 155
Burke, W. J.	356
Caneva, A.	733
Carman, E. H.	805
Cartwright, D. G.	288
Castelli, J. P.	183
Chapman, G. A.	85
Charakhchyan, A. N.	460
Charakhchyan, T. N.	460
Chasson, R. L.	450
Chiba, T.	484
Chirkov, N. P.	465
Chuang, L. S.	476
Chung, D-H.	508
Chupp, E.	325
Cole, D. G.	536
Cole, T. W.	222
Coles, W. A.	371
Cook, F. E.	536
Cormier, R. J.	666
Covington, A. E.	168
Crawford, H. J.	354
Croft, T. A.	381
Croom, D. L.	210
Czechowsky, P.	796
Datlowe, D. W.	291
Davis, D. J., Jr.	795
Decker, W. J.	202
Degaonkar, S. S.	234, 717
Dere, K. P.	298
Dodge, J. C.	242
Dodson, H. W.	16
Domingo, V.	342
Driatsky, V. M.	647
Duggal, S. P.	430
Dutt, J. C.	423
Elena, A.	733
Énomé, S.	215
Essex, E. A.	529
Evans, J. V.	497
Eyfrig, R.	635, 643
Filippov, V. A.	469
Fontenla, J. M.	150
Forrest, D.	325
Freeman, Jr., J. W.	361
Fujii, S.	622
Fujii, Z.	479
Fujimoto, K.	479
Gautier, T. N.	505
Gigolashvili, M. Sh.	145
Givishvili, G. V.	708
Godoli, G.	23, 68
Goncharova, E. E.	549
Gribbin, J.	792
Hakura, Y.	668
Halenka, J.	731
Hanser, F. A.	348
Harmon, J. K.	371
Harris, L.D.J.	210
Hartmann, G. K.	511
Heacock, R. R.	772
Hedeman, E. R.	16
Heeran, M. P.	805
Helms, W. J.	601, 766
Hennessey, J. J., S.J.	562
Hessler, V. P.	772
Heyden, F. J., S.J.	56
Hills, H. K.	361
Horan, D. M.	298
Houminer, Z.	375
Hoyng, P.	319
Humble, J. E.	423
Hunsucker, R. D.	490, 492
Ichinose, T.	571
Imhoh, W. L.	676
Ishii, T.	668
Jacchia, L. G.	784
Jäger, F. W.	3
Jain, C. L.	502
Jakunina, G. V.	103
Jensen, V. N.	651
Jiricer, F.	588
Jurgens, R. B.	566
Kalisher, A. L.	745
Kamide, Y.	702
Kananen, H.	415
Kato, S.	584
Katz, L.	348
Kawasaki, K.	702
Kawasaki, S.	476
Kellogg, P. J.	288
Keys, J. G.	799
Khlistov, A. I.	103
Khromova, T. P.	103
Kiryukhina, A. I.	40, 103
Kisselbach, V. J.	458
Kivinen, M.	772
Klobuchar, J. A.	508
Knuth, R.	574
Kodama, M.	476
Kohl, J. W.	330

	Page
Köhn, D.	342
Kondo, I.	479
Kondo, M.	747
Koster, J. R.	525
Krassa, R.F.K.	630
Kreplin, R. W.	298
Krüger, A.	260
Kubota, J.	118
Kurchenko, Yu. A.	465
Kureizumi, T.	118
Kurokawa, H.	118
Kusoffsky, U.	161
Kuzmin, A. I.	469
Lai, J. C.	288
Lanzerotti, L. J.	338
Lastovicka, J.	588
Leighton, H. I.	813
Lerfald, G. M	566
Leshchenko, L.N.	708
Liemohn, H. B.	766
Lin, R. P.	334
Lincoln, J. V.	813
Livingston, W. C.	95
Loginov, G. A.	727
Loomer, E. I.	722
Lozada, O. T.	475
Lundin, R.	609
Luzov, A. A.	465
Maagoe, S.	371
Maclennan, C. G.	338
Maeda, K.	134
Maeda, R.	640
Martin, E.	532
Martres, M. J.	46
Masley, A. J.	672
Matveyeva, E. T.	745
Mavromichalaki, H.	454
Maxwell, A.	255
McIntosh, P. S.	30
McNamara, L. F.	536
Medrano, R. A.	361
Mendillo, M.	508
Mirmovich, E. G.	557
Mitra, S. N.	595
Mitropolskaja, O. N.	103
Miyazaki, Y.	476
Mogilevsky, E. I.	139
Moore, P. R.	356
Morris, L. D.	686
Moughan, V. F.	676
Moussas, X.	454
Muhleisen, R.	809
Mullen, E. G.	795
Münch, J. W.	780
Murakami, K.	476
Nagashima, K.	479
Naito, Y.	584
Nakano, Y.	476
Nakayama, K.	134
Nesterov, G. T.	603, 618
Nikolayev, V. N.	465
Nikulin, I. F.	103
Oda, N.	134
Novikov, A. M.	465
Odintsova, I. N.	708
Ogawa, T.	571
Ogita, N.	445
Ohle, K. -H.	574
Olesen, J. K.	772
Ondoh, T.	389
Ostrow, S.	857
Ouchi, C.	622
Page, D. E.	342
Peterson, L. E.	291
Petrova, G. A.	727
Pfister, H. J.	35
Piggott, W. R.	684
Plagemann, S. H.	792
Pomerantz, M. A.	430
Porfirjeva, G. A.	103
Poros, D. J.	699
Price, P. B.	354
Prikhodko, A. N.	469
Prokudina, V. S.	103
Rafael, F., Jr.	562
Rangaswamy, S.	526
Rao, U. R.	486
Rastogi, R. G.	717
Razdan, H.	487
Reagan, J. B.	676
Reasoner, D. L.	356
Reid, J. S.	772
Reppin, C.	325
Rich, F. J.	356
Roederer, J. R.	1
Rickett, B. J.	371
Riddle, A. C.	283
Roquet, J.	737
Roschina, E. M.	103
Röttger, J.	643
Sahai, Y.	627
Saito, T.	747
Sakurai, K.	229
Sakurai, T.	747
Salcedo, J. E.	762
Sales, M.A.O.	627
Samsonov, I. S.	465, 469
Santin, P.	279
Sastry, T.S.G.	717
Sawant, H. S.	234
Scarf, F. L.	378
Schmid, P. E.	526
Schmidt, G.	511
Schwentek, H.	579
Sciuto, V.	23, 68
Seibold, J. R.	150
Serido, Y.	479
Sellers, B.	348
Selzer, E.	737
Sekgeyev, A. V.	465
Shafer, G. V.	469
Shapley, A. H.	1, 8
Shchepetnov, R. V.	745
Shea, M. A.	8, 394
Shimizu, M.	134
Silverman, S. M.	630
Sime, D. G.	371
Simon, P.	12
Sitnik, G. F.	103
Skripin, G. V.	469
Slowey, J. W.	784
Smart, D. F.	394
Smith, R. E.	802
Smith, R. W.	561
Srivastaua, B. J.	754
Stauning, P.	651
Stevens, G. A.	319

	Page
Stoker, P. H.	441
Stozhkov, Yu. I.	460
Suda, J.	155
Suessmann, P.	635
Sugiura, M.	699
Sullivan, J. D.	354
Suri, A.	325
Swenson, G. R.	802
Swinson, D. B.	448
Taagholt, J.	651
Takahashi, H.	484
Tamura, T.	747
Tanaka, H.	4, 215
Tanaka, K.	121
Tanaka, Y.	389
Tanskanen, P. J.	415
Tauriainen, A.	511
Taylor, B. G.	342
Terajima, Y.	668
Tetruashvili, E. I.	145
Thambyahpillai, T.	423
Thomas, T. W.	684
Timpe, C.	616
Todikov, G. G.	465
Torelli, M.	811
Trfska, P.	588
Trotter, D. E.	74
Tsai, C.	325
Turtle, J. P.	630
Ueno, H.	479
Ulyev, V. A.	647
Upolnikov, A. A.	465, 469
Urbarz, H.	269
van Beek, G. J.	722
van Beek, H. F.	319
van Sabben, D.	10
Vasiliev, K. N.	708
Velinov, P.	618
Vette, J. I.	4
Vondrak, R. R.	361
Wada, M.	476
Wakai, N.	622
Waldmeier, M.	160
Watkins, B. J.	492
Wefer, F. L.	202
Wegener, H.	635
Wenzel, K. -P.	342
Wescott, L. R.	505
Willard, H. R.	766
Williams, D. J.	330
Yamashita, F.	239
Yanchukovsky, V. L.	465
Yasuhara, F.	702
Yates, G. K.	348
Yeboah-Amankwah, D.	525
Yoshida, S.	445
Yudovitch, L. A.	549
Zappala, R. A.	23, 68
Zevakina, R. A.	549
Zianddin, S.	645
Zirin, H.	121
Zlobec, P.	279

Publication Notice

WORLD DATA CENTER A for SOLAR-TERRESTRIAL PHYSICS REPORT UAG
(Prepared by World Data Center A for Solar-Terrestrial Physics, NOAA, Boulder, Colorado)

These reports are for sale through the National Climatic Center, Federal Building, Asheville, NC 28801, Attn: Publications. Subscription price: $9.00 a year; $2.50 additional for foreign mailing; single copy price varies. These reports are issued on an irregular basis with 6 to 12 reports being issued each year. Therefore, in some years the single copy rate will be less than the subscription price, and in some years the single copy rate will be more than the subscription price. Make checks and money orders payable to: Department of Commerce, NOAA.

Upper Atmosphere Geophysics Report UAG-1, "IQSY Night Airglow Data" by L. L. Smith, F. E. Roach and J. M. McKennan of Aeronomy Laboratory, ESSA Research Laboratories, July 1968, single copy price $1.75.

Upper Atmosphere Geophysics Report UAG-2, "A Reevaluation of Solar Flares, 1964-1966" by Helen W. Dodson and E. Ruth Hedeman of McMath-Hulbert Observatory, The University of Michigan, August 1968, single copy price 30 cents.

Upper Atmosphere Geophysics Report UAG-3, "Observations of Jupiter's Sporadic Radio Emission in the Range 7.6-41 MHz, 6 July 1966 through 8 September 1968" by James W. Warwick and George A. Dulk, Department of Astro-Geophysics, University of Colorado, October 1968, single copy price 30 cents.

Upper Atmosphere Geophysics Report UAG-4, "Abbreviated Calendar Record 1966-1967" by J. Virginia Lincoln, Hope I. Leighton and Dorothy K. Kropp, Aeronomy and Space Data Center, Space Disturbances Laboratory, ESSA Research Laboratories, January 1969, single copy price $1.25.

Upper Atmosphere Geophysics Report UAG-5, "Data on Solar Event of May 23, 1967 and its Geophysical Effects" compiled by J. Virginia Lincoln, World Data Center A, Upper Atmosphere Geophysics, ESSA, February 1969, single copy price 65 cents.

Upper Atmosphere Geophysics Report UAG-6, "International Geophysical Calendars 1957-1969" by A. H. Shapley and J. Virginia Lincoln, ESSA Research Laboratories, March 1969, single copy price 30 cents.

Upper Atmosphere Geophysics Report UAG-7, "Observations of the Solar Electron Corona: February 1964-January 1968" by Richard T. Hansen, High Altitude Observatory, Boulder, Colorado and Kamuela, Hawaii, October 1969, single copy price 15 cents.

Upper Atmosphere Geophysics Report UAG-8, "Data on Solar Geophysical Activity October 24-November 6, 1968", Parts 1 and 2, compiled by J. Virginia Lincoln, World Data Center A, Upper Atmosphere Geophysics, ESSA, March 1970, single copy price (includes Parts 1 and 2) $1.75.

Upper Atmosphere Geophysics Report UAG-9, "Data on Cosmic Ray Event of November 18, 1968 and Associated Phenomena" compiled by J. Virginia Lincoln, World Data Center A, Upper Atmosphere Geophysics, ESSA, April 1970, single copy price 55 cents.

Upper Atmosphere Geophysics Report UAG-10, "Atlas of Ionograms" edited by A. H. Shapley, ESSA Research Laboratories, May 1970, single copy price $1.50.

Upper Atmosphere Geophysics Report UAG-11, "Catalogue of Data on Solar-Terrestrial Physics" compiled by J. Virginia Lincoln and H. Patricia Smith, World Data Center A, Upper Atmosphere Geophysics, ESSA, June 1970, single copy price $1.50.

Upper Atmosphere Geophysics Report UAG-12, "Solar-Geophysical Activity Associated with the Major Geomagnetic Storm of March 8, 1970", Parts 1, 2 and 3, compiled by J. Virginia Lincoln and Dale B. Bucknam, World Data Center A, Upper Atmosphere Geophysics, NOAA, April 1971, single copy price (includes Parts 1-3) $3.00.

Upper Atmosphere Geophysics Report UAG-13, "Data on the Solar Proton Event of November 2, 1969 through the Geomagnetic Storm of November 8-10, 1969" compiled by Dale B. Bucknam and J. Virginia Lincoln, World Data Center A, Upper Atmosphere Geophysics, NOAA, May 1971, single copy price 50 cents.

Upper Atmosphere Geophysics Report UAG-14, "An Experimental Comprehensive Flare Index and its Derivation for 'Major' Flares 1955-1969" by Helen W. Dodson and E. Ruth Hedeman, McMath-Hulbert Observatory, University of Michigan, July 1971, single copy price 30 cents.

Upper Atmosphere Geophysics Report UAG-15, "Catalogue of Data on Solar-Terrestrial Physics" prepared by Research Laboratories, NOAA, Boulder, Colorado, July 1971, single copy price $1.50. (Supersedes Report UAG-11, June 1970.)

Upper Atmosphere Geophysics Report UAG-16, "Temporal Development of the Geographical Distribution of Auroral Absorption for 30 Substorm Events in each of IQSY (1964-65) and IASY (1969)" by F. T. Berkey, V. M. Driatskiy, K. Henriksen, D. H. Jelly, T. I. Shchuka, A. Theander and J. Yliniemi, September 1971, single copy price 70 cents.

Upper Atmosphere Geophysics Report UAG-17, "Ionospheric Drift Velocity Measurements at Jicamarca, Peru (July 1967 - March 1970)" by Ben B. Balsley, Aeronomy Laboratory, National Oceanic and Atmospheric Administration, Boulder, Colorado, and Ronald F. Woodman, Jicamarca Radar Observatory, Instituto Geofisico del Perú, Lima, Peru, October 1971, single copy price 35 cents.

Upper Atmosphere Geophysics Report UAG-18, "A Study of Polar Cap and Auroral Zone Magnetic Variations" by K. Kawasaki and S. I. Akasofu, Geophysical Institute, University of Alaska, June 1972, single copy price 20 cents.

Upper Atmosphere Geophysics Report UAG-19, "Reevaluation of Solar Flares 1967" by Helen W. Dodson and E. Ruth Hedeman of McMath-Hulbert Observatory, The University of Michigan, and Marta Rovira de Miceli, San Miguel Observatory, Argentina, June 1972, single copy price 15 cents.

Report UAG-20, "Catalogue of Data on Solar-Terrestrial Physics", prepared by Environmental Data Service, NOAA, Boulder, Colorado, October 1972, single copy price $1.50. (Supersedes Report UAG-15, July 1971.)

Report UAG-21, "Preliminary Compilation of Data for Retrospective World Interval July 26 - August 14, 1972" compiled by J. Virginia Lincoln and Hope I. Leighton, World Data Center A for Solar-Terrestrial Physics, November 1972, single copy price 70 cents.

Report UAG-22, "Auroral Electrojet Magnetic Activity Indices (AE) for 1970" by Joe Haskell Allen, National Geophysical and Solar-Terrestrial Data Center, Environmental Data Service, November 1972, single copy price 75 cents.

Report UAG-23, "U.R.S.I. Handbook of Ionogram Interpretation and Reduction", Second Edition, November 1972, edited by W. R. Piggott, Radio and Space Research Station, Slough U.K., and K. Rawer, Arbeitsgruppe für Physikalische Weltraumforschung, Freiburg, G.F.R., November 1972, single copy price $1.75.

Report UAG-24, "Data on Solar-Geophysical Activity Associated with the Major Ground Level Cosmic Ray Events of 24 January and 1 September 1971", Parts 1 and 2, compiled by Helen E. Coffey and J. Virginia Lincoln, World Data Center A for Solar-Terrestrial Physics, December 1972, single copy price (includes Parts 1 and 2) $2.00.

Report UAG-25, "Observations of Jupiter's Sporadic Radio Emission in the Range 7.6-41 MHz, 9 September 1968 through 9 December 1971", by James W. Warwick, George A. Dulk and David G. Swann, Department of Astro-Geophysics, University of Colorado, February 1973, single copy price 35¢.

Report UAG-26, "Data Compilation for the Magnetospherically Quiet Periods February 19-23 and November 29 - December 3, 1970", compiled by Helen E. Coffey and J. Virginia Lincoln, World Data Center A for Solar-Terrestrial Physics, May 1973, single copy price 70 cents.

Report UAG-27, "High Speed Streams in the Solar Wind" by D. S. Intriligator, University of Southern California, Department of Physics, Los Angeles, California, 90007, June 1973, single copy price 15 cents.

USCOMM-NOAA-ASHEVILLE,NC-7-73-1625

Publication Notice

WORLD DATA CENTER A for SOLAR-TERRESTRIAL PHYSICS REPORT UAG
(Prepared by World Data Center A for Solar-Terrestrial Physics, NOAA, Boulder, Colorado)

These reports are for sale through the National Climatic Center, Federal Building, Asheville, NC 28801, Attn: Publications. Subscription price: $9.00 a year; $2.50 additional for foreign mailing; single copy price varies. These reports are issued on an irregular basis with 6 to 12 reports being issued each year. Therefore, in some years the single copy rate will be less than the subscription price, and in some years the single copy rate will be more than the subscription price. Make checks and money orders payable to: Department of Commerce, NOAA.

Upper Atmosphere Geophysics Report UAG-1, "IQSY Night Airglow Data" by L. L. Smith, F. E. Roach and J. M. McKennan of Aeronomy Laboratory, ESSA Research Laboratories, July 1968, single copy price $1.75.

Upper Atmosphere Geophysics Report UAG-2, "A Reevaluation of Solar Flares, 1964-1966" by Helen W. Dodson and E. Ruth Hedeman of McMath-Hulbert Observatory, The University of Michigan, August 1968, single copy price 30 cents.

Upper Atmosphere Geophysics Report UAG-3, "Observations of Jupiter's Sporadic Radio Emission in the Range 7.6-41 MHz, 6 July 1966 through 8 September 1968" by James W. Warwick and George A. Dulk, Department of Astro-Geophysics, University of Colorado, October 1968, single copy price 30 cents.

Upper Atmosphere Geophysics Report UAG-4, "Abbreviated Calendar Record 1966-1967" by J. Virginia Lincoln, Hope I. Leighton and Dorothy K. Kropp, Aeronomy and Space Data Center, Space Disturbances Laboratory, ESSA Research Laboratories, January 1969, single copy price $1.25.

Upper Atmosphere Geophysics Report UAG-5, "Data on Solar Event of May 23, 1967 and its Geophysical Effects" compiled by J. Virginia Lincoln, World Data Center A, Upper Atmosphere Geophysics, ESSA, February 1969, single copy price 65 cents.

Upper Atmosphere Geophysics Report UAG-6, "International Geophysical Calendars 1957-1969" by A. H. Shapley and J. Virginia Lincoln, ESSA Research Laboratories, March 1969, single copy price 30 cents.

Upper Atmosphere Geophysics Report UAG-7, "Observations of the Solar Electron Corona: February 1964-January 1968" by Richard T. Hansen, High Altitude Observatory, Boulder, Colorado and Kamuela, Hawaii, October 1969, single copy price 15 cents.

Upper Atmosphere Geophysics Report UAG-8, "Data on Solar Geophysical Activity October 24-November 6, 1968", Parts 1 and 2, compiled by J. Virginia Lincoln, World Data Center A, Upper Atmosphere Geophysics, ESSA, March 1970, single copy price (includes Parts 1 and 2) $1.75.

Upper Atmosphere Geophysics Report UAG-9, "Data on Cosmic Ray Event of November 18, 1968 and Associated Phenomena" compiled by J. Virginia Lincoln, World Data Center A, Upper Atmosphere Geophysics, ESSA, April 1970, single copy price 55 cents.

Upper Atmosphere Geophysics Report UAG-10, "Atlas of Ionograms" edited by A. H. Shapley, ESSA Research Laboratories, May 1970, single copy price $1.50.

Upper Atmosphere Geophysics Report UAG-11, "Catalogue of Data on Solar-Terrestrial Physics" compiled by J. Virginia Lincoln and H. Patricia Smith, World Data Center A, Upper Atmosphere Geophysics, ESSA, June 1970, single copy price $1.50.

Upper Atmosphere Geophysics Report UAG-12, "Solar-Geophysical Activity Associated with the Major Geomagnetic Storm of March 8, 1970", Parts 1, 2 and 3, compiled by J. Virginia Lincoln and Dale B. Bucknam, World Data Center A, Upper Atmosphere Geophysics, NOAA, April 1971, single copy price (includes Parts 1-3) $3.00.

Upper Atmosphere Geophysics Report UAG-13, "Data on the Solar Proton Event of November 2, 1969 through the Geomagnetic Storm of November 8-10, 1969" compiled by Dale B. Bucknam and J. Virginia Lincoln, World Data Center A, Upper Atmosphere Geophysics, NOAA, May 1971, single copy price 50 cents.

Upper Atmosphere Geophysics Report UAG-14, "An Experimental Comprehensive Flare Index and its Derivation for 'Major' Flares 1955-1969" by Helen W. Dodson and E. Ruth Hedeman, McMath-Hulbert Observatory, University of Michigan, July 1971, single copy price 30 cents.

Upper Atmosphere Geophysics Report UAG-15, "Catalogue of Data on Solar-Terrestrial Physics" prepared by Research Laboratories, NOAA, Boulder, Colorado, July 1971, single copy price $1.50. (Supersedes Report UAG-11, June 1970.)

Upper Atmosphere Geophysics Report UAG-16, "Temporal Development of the Geographical Distribution of Auroral Absorption for 30 Substorm Events in each of IQSY (1964-65) and IASY (1969)" by F. T. Berkey, V. M. Driatskiy, K. Henriksen, D. H. Jelly, T. I. Shchuka, A. Theander and J. Yliniemi, September 1971, single copy price 70 cents.

Upper Atmosphere Geophysics Report UAG-17, "Ionospheric Drift Velocity Measurements at Jicamarca, Peru (July 1967 - March 1970)" by Ben B. Balsley, Aeronomy Laboratory, National Oceanic and Atmospheric Administration, Boulder, Colorado, and Ronald F. Woodman, Jicamarca Radar Observatory, Instituto Geofisico del Perú, Lima, Peru, October 1971, single copy price 35 cents.

Upper Atmosphere Geophysics Report UAG-18, "A Study of Polar Cap and Auroral Zone Magnetic Variations" by K. Kawasaki and S. I. Akasofu, Geophysical Institute, University of Alaska, June 1972, single copy price 20 cents.

Upper Atmosphere Geophysics Report UAG-19, "Reevaluation of Solar Flares 1967" by Helen W. Dodson and E. Ruth Hedeman of McMath-Hulbert Observatory, The University of Michigan, and Marta Rovira de Miceli, San Miguel Observatory, Argentina, June 1972, single copy price 15 cents.

Report UAG-20, "Catalogue of Data on Solar-Terrestrial Physics", prepared by Environmental Data Service, NOAA, Boulder, Colorado, October 1972, single copy price $1.50. (Supersedes Report UAG-15, July 1971.)

Report UAG-21, "Preliminary Compilation of Data for Retrospective World Interval July 26 - August 14, 1972" compiled by J. Virginia Lincoln and Hope I. Leighton, World Data Center A for Solar-Terrestrial Physics, November 1972, single copy price 70 cents.

Report UAG-22, "Auroral Electrojet Magnetic Activity Indices (AE) for 1970" by Joe Haskell Allen, National Geophysical and Solar-Terrestrial Data Center, Environmental Data Service, November 1972, single copy price 75 cents.

Report UAG-23, "U.R.S.I. Handbook of Ionogram Interpretation and Reduction", Second Edition, November 1972, edited by W. R. Piggott, Radio and Space Research Station, Slough U.K., and K. Rawer, Arbeitsgruppe für Physikalische Weltraumforschung, Freiburg, G.F.R., November 1972, single copy price $1.75.

Report UAG-24, "Data on Solar-Geophysical Activity Associated with the Major Ground Level Cosmic Ray Events of 24 January and 1 September 1971", Parts 1 and 2, compiled by Helen E. Coffey and J. Virginia Lincoln, World Data Center A for Solar-Terrestrial Physics, December 1972, single copy price (includes Parts 1 and 2) $2.00.

Report UAG-25, "Observations of Jupiter's Sporadic Radio Emission in the Range 7.6-41 MHz, 9 September 1968 through 9 December 1971", by James W. Warwick, George A. Dulk and David G. Swann, Department of Astro-Geophysics, University of Colorado, February 1973, single copy price 35¢.

Report UAG-26, "Data Compilation for the Magnetospherically Quiet Periods February 19-23 and November 29 - December 3, 1970", compiled by Helen E. Coffey and J. Virginia Lincoln, World Data Center A for Solar-Terrestrial Physics, May 1973, single copy price 70 cents.